INTERNATIONAL JOURNAL OF HEAT AND MASS TRANSFER

VOLUME 1 1960-61

ol.
1
960

BOARD OF EDITORS

A. J. EDE
East Kilbride, Scotland

CARL GAZLEY, Jr.
Santa Monica, Calif.

U. GRIGULL
Leverkusen, Germany

J. P. HARTNETT
Minneapolis, Minn.

A. V. LUIKOV
Minsk, B.S.S.R.

D. B. SPALDING
London

Assisted by an Honorary Editorial Advisory Board

Co-chairmen

E. R. G. ECKERT
Minneapolis, Minn.

O. A. SAUNDERS
London

PERGAMON PRESS LTD.

OXFORD · LONDON · NEW YORK · PARIS

AIMS AND SCOPE OF THE JOURNAL

To provide a central vehicle for exchange of basic ideas in heat and mass transfer between research workers and engineers located throughout the world.

The emphasis will be placed on original research, both analytical and experimental, of permanent interest to researchers and engineers in the field of heat and mass transfer. The highest priority will be given to those contributions which increase our basic understanding of transfer processes and of their application to engineering problems. The Journal will not consider for publication any paper which has been published elsewhere.

When outstanding new advances are made in existing areas of heat and mass transfer or when new areas have been developed to a definitive stage, special review articles will be considered by the editors.

To encourage exchange of ideas, a section of the Journal will be devoted to discussions of previously published papers. Brief notes are also invited and should not exceed 750 words.

As a service to our readers an international bibliography of recent papers in heat and mass transfer listed by title, author and source will appear in each issue of the Journal. Reviews of new books on heat and mass transfer will also be contained in the Journal.

The Journal will appear every two months.

GENERAL INFORMATION FOR AUTHORS

1. There is no length limitation on submitted manuscripts. All manuscripts will be referred to acknowledged experts in the subject. Only those receiving favourable recommendations from the referees will be accepted for publication.

2. To insure rapid publication and to minimize editorial costs, the preferred language will be English. Whenever possible, authors are requested to submit their manuscripts in that language. However, the editors recognize that some manuscripts will be submitted in other languages, and the Journal is prepared to publish such papers.

3. A short abstract (100–300 words) should immediately precede the introduction. Abstracts should be most informative, giving a clear indication of the nature and range of the results contained in the paper.

4. The introduction should define clearly the nature of the problem being considered. Reference should be made to previously published pertinent papers, accenting the major original contributions. Wherever possible, the practical application of the results should be cited.

5. In order to render their papers understandable to the widest possible circle of readers, authors of analytical papers are asked to relegate the algebraic details to separate sections, highlighting the main ideas in the body of the text. Specialized mathematical techniques should either be explained in the paper or made accessible by suitable references.

6. Because there is considerable variation in nomenclature and unit systems from country to country, authors are required to include a complete list of symbols which they have used in their manuscripts, and of the units in which the corresponding quantities are measured. Wherever possible, equations should be written in dimensionless form.

7. Communications should be in the form of typescript, with the lines double spaced on one side of good grade paper, allowing a reasonable left-hand margin. Three typescripts (an original and 2 carbon copies) should be submitted to facilitate refereeing.

8. All necessary illustrations should accompany the typescript but should not be inserted in the text. All photographs, charts and diagrams are to be referred to as "Figures", and should be numbered consecutively in the order in which they are referred to in the text. Brief captions should be provided to make the figures as informative as possible.

   (a) *Photographs* should be glossy prints. Each should have, lightly written on the back, the author's name, the figure number, and an indication of which is the top of the picture.

   Where lines or lettering are to appear on the photograph, two prints should be supplied, one appropriately marked and the other unmarked.

   (b) *Charts and diagrams* should be boldly drawn in India ink on opaque paper or thin card. All relevant measurements must be included. The following standard symbols should be used on line drawings as they are readily available to the printers:

   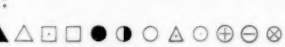

   (c) *Captions to figures* should be typed consecutively on a separate page or pages at the end of the paper. Each caption should give the Figure number.

9. References in the text should be indicated by using arabic numerals in square brackets. They should appear in numerical order through the text. The references should be quoted in order at the end of the paper. References to journal articles should take the following form:

   1. E. RUCKENSTEIN, *Chem. Engng Sci.* **10**, 22 (1959).

   In the full reference the following should be included: the names and initial of all authors, the abbreviated title of the journal as in the *World List of Scientific Periodicals* (Butterworths, London, Third Edition, 1952), the volume number, the first page number of the article, and the year of publication. References to books should be in the following form:

   2. MAX JAKOB, *Heat Transfer* Vol. 1, p. 63. John Wiley, New York (1959).

   The reference should include the following: the names and initials of all authors, the title, edition, volume number and chapter or page number (if relevant), the publisher's name, place of publication and the date. In the case of a contribution to a multi-author work, the editor's name should be quoted after the title.

10. Galley proofs will be sent to the author (or the first mentioned author in papers of multiple authorship) for correction. Fifty reprints of the paper will be supplied free; an order form for additional reprints will accompany the proofs. There will be no page charge for publication.

Vol. 1 1960

CONTENTS

Volume 1, *Number* 1

	Page	
E. R. G. Eckert and O. A. Saunders	1	An International Journal in the Field of Heat and Mass Transfer
Sinclaire M. Scala and Guido L. Vidale	4	Vaporization Processes in the Hypersonic Laminar Boundary Layer
D. T. Kokorev	23	Experimental Methods Applied to the Determination of some Temperature Radiation Parameters
C. M. Usiskin and E. M. Sparrow	28	Thermal Radiation Between Parallel Plates Separated by an Absorbing–Emitting Nonisothermal Gas
Y. Mikhailov	37	Highly Intensive Heat and Mass Transfer in Dispersed Media
S. I. Kosterin and Yu. A. Koshmarov	46	Turbulent Boundary Layer on a Flat Plate in a Stream of Dissociating Gas
P. Grassmann and W. Straumann	50	Ein instationäres Verfahren zur Messung der Wärmeleitfähigkeit von Flüssigkeiten und Gasen
G. F. C. Rogers and Y. R. Mayhew	55	Evaluation of Bulk Velocity and Temperature for Turbulent Flow in Tubes
B. le Fur	68	Convection de la chaleur en régime laminaire dans le cas d'un gradient de pression et d'une température de paroi quelconques, le fluide étant à propriétés physiques constantes
Robert and Madeleine Goulard	81	One-dimensional Energy Transfer in Radiant Media
Ernst Schmidt	92	Wärmetransport durch natürliche Konvektion in Stoffen bei kritischem Zustand
E. R. G. Eckert J. P. Hartnett and T. F. Irvine, Jr.	102	Heat Transfer Bibliography
	113	Titles of Papers from Recent Issues of *Inzhenerno-Fizicheskii Zhurnal*

Volume 1, *Numbers* 2/3

V. I. Petrovichev	115	Heat Transfer to Mercury in a Circular Tube and Annular Channels with Sinusoidal Heat Load Distribution
N. Z. Azer and B. T. Chao	121	A Mechanism of Turbulent Heat Transfer in Liquid Metals
T. Mizushina, S. Iuchi, T. Sasano and H. Tamura	139	Thermal Contact Resistance Between Mercury and a Metal Surface

	Page	
V. K. ERMOLIN	147	Local and Average Heat Transfer Coefficients at an Air Stream in a Tube with a Pointed Inlet
G. N. DULNEV	152	The Theory of Thermal Regular Regime and its Application to the Determination of Thermal Characteristics
E. M. SPARROW and R. SIEGEL	161	Application of Variational Methods to the Thermal Entrance Region of Ducts
R. G. DEISSLER and M. PERLMUTTER	173	Analysis of the Flow and Energy Separation in a Turbulent Vortex
D. B. SPALDING	192	A Standard Formulation of the Steady Convective Mass Transfer Problem
R. G. GOLDSTEIN and E. R. G. ECKERT	208	The Steady and Transient Free Convection Boundary Layer on a Uniformly Heated Vertical Plate
K. NISHIKAWA and K. YAMAGATA	219	On the Correlation of Nucleate Boiling Heat Transfer
L. S. DZUNG	236	A Cooling Problem of Pebble-Bed Nuclear Reactors
H. ZIEBLAND and J. T. A. BURTON	242	The Thermal Conductivity of Heavy Water between 75° and 260°C at Pressures up to 300 ATM
E. R. G. ECKERT, J. P. HARTNETT and E. M. SPARROW	255	Heat Transfer Bibliography

Vol. 1 1960

Volume 1, *Number* 4

S. I. ANISIMOV and T. L. PERELMAN	269	On the Investigation of Heat Transfer in the Presence of Chemical Conversions
A. V. RALKO	273	The Experimental Investigation of Heat and Mass Transfer in the Presence of Chemical Conversions
S. I. CHENG and H. H. CHIU	280	Mixing and Chemical Reaction in an Initially Non-uniform Temperature Field
P. D. LEBEDEV	294	Heat and Mass Transfer During the Drying of Moist Materials
P. D. LEBEDEV	302	Heat and Mass Transfer Between Moist Solids and Air
HENRY BARROW	306	Convection Heat Transfer Coefficients for Turbulent Flow Between Parallel Plates with Unequal Heat Fluxes
A. L. LOEFFLER, JR. and R. G. DEISSLER	312	Decay of Temperature Fluctuations in Homogeneous Turbulence Before the Final Period
P. W. MCFADDEN and R. J. GROSH	325	An Analysis of Laminar Film Boiling with Variable Properties
E. R. G. ECKERT, J. P. HARTNETT and E. M. SPARROW	336	Heat Transfer Bibliography

Int. J. Heat Mass Transfer. Vol. 1, pp. 1–3. Pergamon Press 1960. Printed in Great Britain.

AN INTERNATIONAL JOURNAL IN THE FIELD OF HEAT AND MASS TRANSFER

E. R. G. ECKERT and O. A. SAUNDERS
Co-chairmen, Editorial Advisory Board

IT is appropriate for a new journal to introduce itself in its first issue to the reader and to the interested public, to explain the reasons for its origination, and to outline the width of the segment of physical sciences that it hopes to cover.

Looking back in time one finds that it took fairly long before heat transfer had established itself as a coherent body of knowledge. That was undoubtedly due to the complexity of the physical processes involved in heat transfer. These processes are relatively simplest in heat conduction and, correspondingly, the basic laws, their mathematical formulation, and the methods for obtaining solutions were achieved at first in this field [1]. A similar process in the field of heat convection had to await the establishment of a basic understanding of viscous flow phenomena which was started by O. Reynolds' studies on turbulence (1883) and by L. Prandtl's paper on boundary layer theory (1904). A systematic approach to radiative heat transfer finally could be developed only after the laws for black body radiation had been conclusively formulated by M. Planck in 1900. Engineering needs, on the other hand, made the establishment of relations from which heat transfer could be predicted imperative. Such relations were very restricted in their applicability, and the corresponding investigations were reported in the journals which dealt with the respective engineering activity. This situation, that heat transfer papers are dispersed in a large number of magazines, still exists today and makes it extremely difficult for anybody to keep informed, especially since the number of papers has grown in recent years almost at an exponential rate. This fact alone makes it very desirable to have a journal in which essential progress in our understanding of heat transfer processes is continuously recorded.

There is, however, a still more important reason that suggests a heat transfer journal. Through the developments which have been sketched above, a well-grounded and fairly complete basic understanding of the various heat transfer processes has been obtained in recent years. In this situation, a magazine covering the complete field of heat transfer can do much to stimulate progress by demonstrating the basic unity and interrelation of the various heat transfer processes. This interrelation is very clear between heat conduction and convection, since many processes which we term "heat convection" consist essentially in the superposition of heat conduction on the transport of energy by a moving fluid. The similarity is less obvious, but nevertheless existent, between radiative heat exchange and conduction or flow processes. According to modern physics, the following model can be accepted for a radiative process: Photons are released from atoms by thermal agitation. They travel on straight paths until they are intercepted by other atoms. Those again may release new photons and in this way energy is transported from higher to lower energy levels. Such a process has a strong similarity with the model of conductive energy transport in a gas that kinetic theory provides. Here the molecules move on straight paths until they come sufficiently close to other molecules for interactions to take place. Energy transport is here provided by the molecules. In particular, the character of such an energy transport process, either by photons or by molecules, depends on the "mean free path length" of the carriers of energy. In radiation heat transfer processes that have been studied in connection with

engineering applications, the mean free path length is by several orders of magnitude greater than in normal heat conduction. Recent developments—like space flight—have, however, advanced interest in heat transfer at very low densities where mean molecular path lengths are of the same order as those encountered in radiation. Counterparts of the free molecular regime, where mean path lengths are large compared to any other dimension involved, and of the mixed regime, where both dimensions are of the same order of magnitude, exist in radiative exchange among solids with a non-absorbing medium in between and in radiative exchange between solids and absorbing gases. As a consequence of this analogy, analytic methods as well as experimental procedures are very similar for radiative heat exchange and for investigations under rarefied gas conditions. Fig. 1 demonstrates

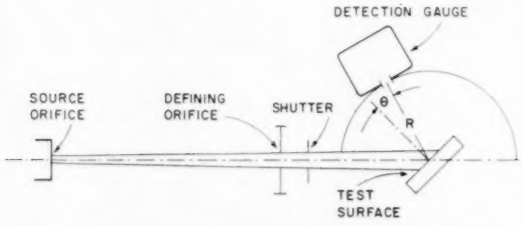

FIG. 1. Apparatus to measure the space distribution of the scattering for molecules impinging on a solid surface (from Hurlbut [3]).

this. The illustrated device might easily be taken as an apparatus to measure the angular distribution of the reflectivity of surfaces for impinging radiation, whereas actually it measures angular distribution of the scattering of molecules impinging on a solid surface.*

Considerable attention has recently been directed toward combined processes in which conduction, convection and radiation are jointly and relatedly active in transferring heat, as well as processes in which heat transfer is connected with some other physical phenomena like mass transfer, reaction kinetics, electric or magnetic interactions, and a heat transfer journal should be a good place to publish the results of such studies.

There is also a very real economic reason suggesting a basic approach to engineering heat exchange problems, an approach as it can be undertaken when a coherent science of heat transfer has been established. Experimental investigations under conditions as they are actually expected become more and more involved and expensive in many new engineering developments. One can mention in this connection cooling problems in nuclear power plants and in rockets, where elaborate safety precautions are required, or in missiles and satellites, where conditions with temperatures of several hundred thousand degrees or close to absolute zero occur on objects with considerable dimensions. It is fortunate, indeed, when analytic procedures are available to predict heat transfer under such conditions and when experiments can be restricted to selected check runs. An example which indicates how well heat transfer coefficients under new conditions can today be predicted from the available basic stock of knowledge is demonstrated in Fig. 2. Local Nusselt numbers as a dimensionless presentation of heat transfer coefficients, measured in gas flow through a tube at

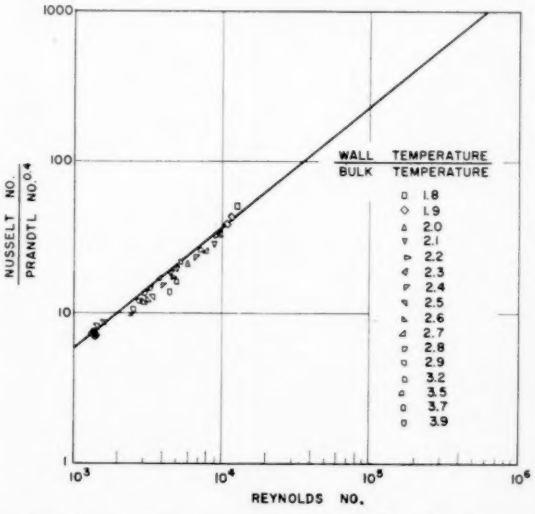

FIG. 2. Heat transfer coefficients for helium flowing in a tube with surface temperatures up to 5900°R (from a paper by Taylor and Kirchgessner [4]).

* The similarity between radiation and conduction processes has been pointed out very clearly in the book by R. C. L. Bosworth [2].

Vol. 1 1960

temperatures up to 5900°R, are presented as experimental points and compared with the line which is the result of low temperature measurements and theory. Experiments under such high temperatures have to be considered as a real achievement and it is satisfying to observe how well they confirm the prediction.

The title of the journal includes also mass transfer. The close similarity between Fick's diffusion law and Fourier's heat conduction equation, as well as the fact that turbulent mass and heat exchange are caused, according to our present understanding, by the same mechanism, suggests a common consideration of both processes very strongly. Differences in the boundary conditions and in the dependence of properties on the state parameters have, of course, to be considered.

It is hoped that the papers in the new magazine will also be of direct value to engineers engaged in the design of heat transfer appliances. Engineers in all parts of the wide field of applied heat transfer are finding more and more in common in their problems and each can help his colleagues toward a better understanding of them. To give only a few examples, the industrial furnace designer and the rocket engineer are concerned with the same basic problem of radiant gas heat exchange; the electrical engineer depends very largely on improved convection or conduction for increasing the output of electric equipment; the use of liquid metals for heat exchange, pioneered by nuclear power engineers, is not without interest in more conventional engineering; developments of the regenerator, at present of particular interest to the gas turbine engineer, might find many new applications elsewhere.

The international character of the journal, finally, should be very helpful in furthering the science under consideration, because science by its very nature has an international character and thrives best when the exchange of ideas is furthered on a world-wide basis. It is our wish that beyond this goal the journal, in its way, contributes also to a general improvement of understanding between the nations.

REFERENCES

1. J. FOURIER, *The Analytical Theory of Heat* (1822).
2. R. C. L. BOSWORTH, *Heat Transfer Phenomena.* Associated General Publications, Sidney; John Wiley, New York (1952).
3. F. C. HURLBUT, Institute of Engineering Research, University of California, Report No. HE 150–118; *J. Appl. Phys.* **28**, 844 (1957).
4. M. F. TAYLOR and T. A. KIRCHGESSNER, 1959 Semi-annual Meeting of the American Rocket Society, San Diego, California, preprint 850–59. Natl. Aeronautics and Space Agency, Tech. Note D–133 (1959).

Int. J. Heat Mass Transfer. Vol. 1, pp. 4–22. Pergamon Press 1960. Printed in Great Britain.

VAPORIZATION PROCESSES IN THE HYPERSONIC LAMINAR BOUNDARY LAYER*

S. M. SCALA† and G. L. VIDALE‡

Space Sciences Laboratory, Missile and Space Vehicle Department,
General Electric Company, Philadelphia 24, Pa., U.S.A.

(*Received* 31 *October* 1959)

Abstract—The net aerodynamic heat transfer into the surface of a vaporizing material depends critically on the blocking action due to the thickening of the boundary layer and on the heat absorbing capacity of the chemical species injected into the boundary layer during the vaporization process.

An analysis of the phenomenon of vaporization is presented for hypersonic flight conditions, and numerical solutions are presented for mass transfer at the stagnation point of an axially-symmetric vehicle. These results were obtained by solving the pertinent boundary layer equations for diffusion, convection and thermal exchange, subject to the appropriate physicochemical constraints arising from the kinetics of vaporization.

In addition, a universal solution is given, in terms of the most significant independent parameters, which defines the flight regimes where the vaporization process is diffusion controlled, kinetically limited, or both.

Utilizing the general correlation formula derived herein, one may estimate the rate of vaporization of an arbitrary material, subject to hypersonic flight conditions, provided only that one has an independent knowledge of certain minimum physicochemical data.

Résumé—Le transfert de chaleur aérodynamique à la surface d'un matériau qui se vaporize dépend principalement de l'action de blocage consécutive à l'épaississement de la couche limite et de la capacité thermique des composés chimiques injectés dans la couche limite pendant la vaporisation.

Une analyse du phénomène de vaporisation dans les conditions du vol hypersonique est présentée et des solutions numériques sont données pour le transport de masse au point d'arrêt d'un obstacle de révolution. Ces résultats ont été obtenus en résolvant les équations de la couche limite pour la diffusion, la convection et l'échange thermique, en tenant compte des conditions physico-chimiques particulières imposées par la cinétique de la vaporisation.

De plus, une solution universelle est donnée en fonction des paramétres indépendants le plus significatifs qui définissent les régimes de vol dans lesquels le processus de vaporisation est commandé par la diffusion, limité par la cinétique, ou les deux ensemble.

En se servant de la formule générale établie ici, on peut calculer la fraction vaporisée d'un matériau arbitraire, soumis aux conditions du vol hypersonique, à condition de disposer seulement de la connaissance d'un minimum de données physico-chimiques.

Zusammenfassung—Die aerodynamische Wärmeübertragung auf die Oberfläche eines verdampfenden Stoffes hängt empfindlich von dem Widerstand der anwachsenden Grenzschicht und der Wärmekapazität des Stoffes ab, der während der Verdampfung in die Grenzschicht gelangt. Für Überschallflug wurde der Verdampfungsvorgang untersucht und für die Stoffübertragung am Staupunkt eines axialsymmetrischen Körpers Lösungen mitgeteilt. Die Ergebnisse wurden erhalten durch die Lösung entsprechender Grenzschichtgleichungen für Diffusion, Konvektion und Wärmeaustausch unter Berücksichtigung des physikochemischen Vorgangs, der von der Kinetik der Verdampfung herrührt. Zusätzlich wurde eine allgemeine Lösung angegeben in Ausdrücken der wichtigsten Parameter, welche die Bereiche definiert, in denen der Verdampfungsvorgang durch die Diffusion oder Kinetik oder durch beides begrenzt ist. Die hier abgeleiteten allgemeinen Beziehungen ermöglichen die Abschätzung der Verdampfungsgeschwindigkeit für einen beliebigen Stoff bei Überschallflug, sofern man eine Mindestkenntnis gewisser physikochemischer Daten besitzt.

* This analysis is based on work performed under the auspices of the U.S. Air Force Ballistic Missiles Division, Contract No. AF 04(647)-269.

† Manager, High Altitude Aerodynamics. ‡ Physical chemist.

Vol.
1
1960

Abstract—Конвективный перенос тепла к поверхности испаряющегося материала характеризуется критической зависимостью интенсивности переноса от тормозного действия, связанного с утолщением пограничного слоя, а также теплопоглощающей способностью химических веществ, вводимых в пограничный слой во время процесса испарения.

Анализ процесса испарения проводится для условий сверхзвукового обтекания. Даны численные решения массопереноса в критической точке осесимметричного тела. Эти результаты получены при решении соответствующих уравнений пограничного слоя для диффузии, конвекции и теплообмена, которые подчиняются соответствующим химико-физическим процессам, обусловленным кинетикой испарения.

Кроме того, даётся общее решение, выраженное через важнейшие параметры. Это решение относится к таким режимам обтекания, в которых процессы испарения определяются или диффузией, или кинетикой, или и тем и другим одновременно.

Используя корреляционную формулу, полученную в данной работе, можно вычислить скорость испарения вещества, подвергающегося сверхзвуковому обтеканию, имея определённый минимум физикохимических данных.

INTRODUCTION

In a paper on heat transfer, which considered mass transfer due to vaporization processes, Nusselt [1] credited Stefan with first having recognized the importance of diffusion in problems involving evaporation. Stefan [2] pioneered in the theory of multicomponent diffusion. Hence, at least several of the aerophysical aspects of evaporation and sublimation have been known for approximately 75 years.

Until recently, the major effort in developing the technology of simultaneous vaporization and diffusion processes has come from chemical engineers [3, 4] engaged in the analysis of mass transfer equipment, and from physicists who have been interested in low density gas dynamics [5–7] and interfacial non-equilibria [8, 9, 10]. In many important practical cases, experimental data have been successfully correlated in the form of equations involving the usual dimensionless groups, such as the Reynolds, Schmidt and Prandtl numbers, so that effective working relationships are now available in standard texts [11].

One of the current major technological problems consists in the development of an efficient thermal shield for hypersonic vehicles. A metallic skin which behaves primarily as a heat sink cannot tolerate high heat fluxes, nor can it absorb sustained hypersonic aerodynamic heating. Hence, interest has focused on other forms of heat absorption schemes involving some form of mass transfer from the surface [12–18].

The analysis presented is a general study in which the physicochemical processes in the gaseous boundary layer are considered in detail, and results having wide utility are presented for the phenomenon of stagnation point vaporization in hypersonic flow.

SYMBOLS

$a_{\text{B.L.}}$ = resistance of boundary layer, reciprocal of the right-hand side of equation (52);

$a_{\text{V.M.}}$ = resistance of vaporizing material, $\sqrt{(2\pi R M_k T_i)}/\alpha P \bar{M}$;

A = number of atoms on surface per square centimeter;

$\bar{c}_p$ = $\sum_n C_n (c_p)_n$, frozen specific heat of the mixture;

$(c_p)_n$ = specific heat of the nth species at constant pressure;

C_n = mass fraction of the nth species;

D_{kn} = diffusion coefficient of the kth species;

D_n^T = thermal diffusion coefficient of the nth species;

E_v = activation energy for removing surface atom from the surface;

f = similarity stream function;

F = partition function for the surface molecule in its normal state for all degrees of freedom;

F^* = partition function of the activated complex in the surface layer, after removing term for motion along reaction coordinate;

h = enthalpy including chemical;

$\boldsymbol{h}$ = Planck's constant;

ΔH_{vap} = enthalpy of vaporization;
$\vec{j}_i$ = $\rho_i \vec{V}_i$;
$\boldsymbol{k}$ = Boltzmann's constant;
K = frozen coefficient of thermal conductivity;
$\boldsymbol{K}$ = equilibrium constant;
l = $\rho\mu/\rho_i\mu_i$
Le = $\rho\bar{c}_p D_{kn}/K$, Lewis number;
Le^T = $\bar{c}_p D_n^T/K$, thermal Lewis number;
$\bar{M}$ = $\sum_n X_n M_n$, mean molecular weight of gas;
M_n = molecular weight of nth species;
$\dot{m}_i$ = interphase mass transfer rate, $(\rho v)_i$;
Pr = $\bar{c}_p\mu/K$, frozen Prandtl number;
P = pressure;
Q = heat transfer;
r_0 = radius of cross-section of body;
R = universal gas constant;
R_B = nose radius of body;
T = temperature;
u = velocity in x-direction;
v = velocity in y-direction;
v_n = absolute velocity of nth species;
$\vec{V}_n$ = diffusion velocity of nth species;
x = co-ordinate along surface of body;
X_n = mole fraction of species n;
y = co-ordinate normal to surface of body;
Ψ = stream function;
α = vaporization coefficient
α_{vap} = vaporization coefficient defined for non-equilibrium vaporization;
Γ = fraction of ablating material which enters the gas phase;
ϵ = emissivity;
η, ξ = similarity variables;
$\theta = T/T_e$ = non-dimensional temperature;
Θ = $\{\bar{c}_p/(\bar{c}_p)_e\}\theta$;
κ = transmission coefficient;
μ = coefficient of viscosity;
τ = $\mu(\partial u/\partial y)$;
ρ = density;
λ = mean free path;
$(du_e/dx)_s$ = $1/R_B\sqrt{\{2(P_e - P_\infty)/\rho_e\}}$, stagnation point velocity gradient.

Subscripts

A = atoms;
e = outer edge of boundary layer;
i = interface;
M = air molecules;
k = vaporizing species;
n = nth species;
s = stagnation point;
η = denotes differentiation with respect to η;
∞ = infinity, upstream of shock;
0 = sea-level standard.

EXAMINATION OF THE PROBLEM

An analysis of surface melting or sublimation requires a detailed consideration of the vaporization processes at the interface between the condensed and gaseous phases. Because of current technological interest, the following discussion is focused upon a hypersonic environment.

Upon exposure to a hypersonic stream, a surface will at first behave as a heat sink until the surface temperature approaches some critical value. Above this temperature, molecular vibrations will be sufficiently violent to cause a considerable number of particles, at favorable sites, to detach from the surface. During the microscopic collison processes which follow, a number of these particles condense on the surface, while others are transported away by convection and diffusion in the fluid stream. The result is a net interphase mass transfer.

Vaporizing species generally are present in maximum concentration at the surface, which acts as a chemical source. The vaporizing species then diffuse into the gaseous boundary layer and are diluted by the main stream components as they are swept downstream by macroscopic convection. When the diffusion thermo-effect is neglected, the driving force for the diffusion process at any point in a boundary layer is related to the local gradient of the partial pressure of the diffusing species. At the surface, therefore, the driving pressure differential is proportional to $(P_k)_i - (P_k)_e$.

During hypersonic flight, the components of dissociated air which enter the outer edge of the

Vol. 1 1960

boundary layer are generally not the same species as the gaseous products of vaporization. Hence, the partial pressure of the latter species vanishes asymptotically at some finite distance from the surface, which coincides with the outer edge of the diffusion boundary layer unless dissociation of the injected species occurs. Thus, the driving force for the diffusion of each vaporizing species (other than oxygen or nitrogen) is simply the partial pressure of the vaporizing species at the surface $(P_k)_i$, which is related to the mass fraction $(C_k)_i$ by:

$$(C_k)_i = \frac{(P_k)_i \, M_k}{P_e \bar{M}} \tag{1}$$

It is noted that certain materials yield oxygen or nitrogen as vaporization or pyrolysis products, so that when the behavior of these materials is analyzed, additional compatibility equations must be derived at the surface [19]. When pure sublimation occurs (no liquid phase exists), the mathematical solution to the ablation problem consists of the determination of four unknowns: the interface temperature T_i; the interphase mass transfer $\dot{m}_i$; the interphase energy transfer Q_i; and the mass fraction of vaporizing species at the interface $(C_k)_i$.

There are several additional variables when a two-phase boundary layer forms, that is, when the solid melts to form a liquid phase boundary layer, which flows and vaporizes under the influence of the environmental conditions. Analysis indicates [18] that only two non-trivial unknowns are added to the above four required for the solution to the problem. All other variables of interest are derived quantities. The two additional unknowns are the surface viscous shear stress τ_i and the tangential velocity of the interface u_i.

For the gas phase, the six unknowns may be related functionally through the following equations:

$$\dot{m}_i = \dot{m}_i \, [(C_k)_i, \, T_i] \tag{2}$$

$$Q_i = Q_i(T_i, \, \dot{m}_i, \, u_i) \tag{3}$$

$$\tau_i = \tau_i \, (T_i, \, \dot{m}_i, \, u_i) \tag{4}$$

$$(C_k)_i = (C_k)_i \, (T_i, \, \alpha, \, \dot{m}_i) \tag{5}$$

It is noted that for practical materials u_i is generally so small that it has no influence on the solutions to the gas phase boundary layer equations and is merely determined *a posteriori*.

The functional relationships given in equations (3) and (4) represent the dependence of the heat flux and skin friction on the mass transfer rate. These functions are considered at length in reference [17] and will not be discussed here. Relations (2) and (5) depend critically on the physicochemical properties of the vaporizing species. The relationship given by equation (2) can be obtained directly from boundary layer solutions and is derived later, while equation (5) is a boundary condition which must be obtained from a consideration of the chemical kinetics of the vaporization reaction. In a later section it will be shown that kinetic theory yields as the net interphase mass transfer:

$$\dot{m}_i = \frac{\alpha P \bar{M}}{\sqrt{(2\pi R M_k T_i)}} \, \{(C_k)_{\text{eq}} - C_k\}_i \tag{6}$$

and consequently, $(C_k)_i$ must always be smaller than $(C_k)_{\text{eq},i}$ when a finite mass transfer occurs. It is clear then that equation (6) is the specific representation of the functional relationship given by equation (5). It is only when equations (2) and (6) are equated, that one obtains an *a posteriori* knowledge of the deviation of $(C_k)_i$ from $(C_k)_{\text{eq},i}$. Thus, an *a priori* assumption to the effect that $(C_k)_i = (C_k)_{\text{eq},i}$ violates the microscopic condition represented by equation (6). However, it may be considered as a zeroth order approximation which holds for certain restricted conditions. These conditions will, in fact, be determined in a later section, where it will be shown that $(C_k)_i$ may differ appreciably from $(C_k)_{\text{eq},i}$ during high altitude flight.

BOUNDARY LAYER CONSIDERATIONS

It is assumed here that the gas in the hypersonic laminar boundary layer is a ternary mixture of the products of dissociated air and the vaporizing species. Thus, at any point in the fluid, the mean mass motion depends on the contribution of the air atoms A, the air molecules M, and the vaporizing species k. At the surface of the condensed phase, the interphase mass transfer by convection and diffusion in the gas phase is expressed by:

$$\dot{m}_i = \left(\sum_n \rho_n \underset{\rightarrow}{v_n}\right)_i = \left(\rho_A \underset{\rightarrow}{v_A} + \rho_M \underset{\rightarrow}{v_M} + \rho_k \underset{\rightarrow}{v_k}\right)_i \tag{7}$$

When the gas phase atom recombination rates are of the same order of magnitude as the rates of diffusion, heterogeneous atom recombination occurs, and the surface then acts as a sink for atoms and as a source of molecules, which requires the mass balance:

$$(\rho_A \underset{\rightarrow}{v_A})_i = -(\rho_M \underset{\rightarrow}{v_M})_i \tag{8}$$

Introduction of the latter into equation (7) yields the simple result:

$$\dot{m}_i = (\rho_k \underset{\rightarrow}{v_k})_i \tag{9}$$

Noting that by definition, the summation of the diffusion fluxes is zero, i.e.

$$\sum_n \underset{\rightarrow}{j_n} = \sum_n \rho_n \underset{\rightarrow}{V_n} = 0 \tag{10}$$

the introduction of the latter into *either* equation (8) or equation (9) followed by rearrangement, yields the identical constraint:

$$\dot{m}_i = (\underset{\rightarrow}{j_k})_i \{1 - (C_k)_i\}^{-1} \tag{11}$$

The diffusion flux of a particular species depends rigorously upon the concentration gradients of all the species present in the gas. However, for a good first approximation, the diffusion flux of a species present in moderate amount is given by Fick's law, so that:

$$\underset{\rightarrow}{j_k} = -\rho D_{kn} \frac{\partial C_k}{\partial y} \tag{12}$$

Thus equation (11) becomes:

$$\dot{m}_i = -\left[\rho D_{kn} \frac{\partial C_k}{\partial y} (1 - C_k)^{-1}\right]_i \tag{13}$$

This expression relates the interphase mass transfer $\dot{m}_i$ to the concentration gradient $(\partial C_k/\partial y)_i$ which depends strongly on the surface concentration $(C_k)_i$; this relationship can be obtained by solving the boundary layer equations.

Conditions in the gas phase are assumed to be quasi-steady, since a transient response in the overall mass transfer rate is dependent primarily on the temperature response of the condensed phase to a particular heating cycle, and not on gas phase processes. It is also assumed that the third species k has the same transport properties as air molecules. For convenience, it is further assumed that the surface is fully catalytic, while gas phase reactions are frozen. Note that it has been shown [13, 16] that the relationship between heat transfer and mass transfer is virtually the same for frozen and equilibrium stagnation point boundary layers, provided only that the surface is fully catalytic.

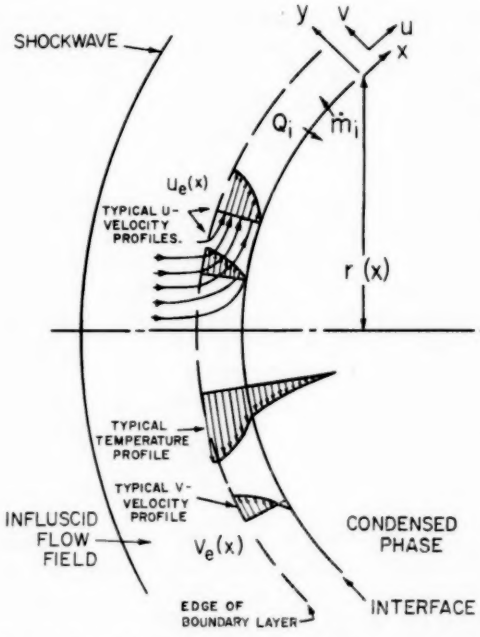

FIG. 1. Co-ordinate system and profiles for vaporizing boundary layer.

The governing equations may then be written for a body-oriented co-ordinate system (see Fig. 1); conservation of atomic species A:

$$\rho u \frac{\partial C_A}{\partial x} + \rho v \frac{\partial C_A}{\partial y} = \frac{\partial}{\partial y}\left(\rho D_{An} \frac{\partial C_A}{\partial y} + \frac{D_A^T}{T} \frac{\partial T}{\partial y}\right) \tag{14}$$

Conservation of vaporizing species k:

$$\rho u \frac{\partial C_k}{\partial x} + \rho v \frac{\partial C_k}{\partial y} = \frac{\partial}{\partial y}\left(\rho D_{kn} \frac{\partial C_k}{\partial y} + \frac{D_k^T}{T} \frac{\partial T}{\partial y}\right) \tag{15}$$

Vol. 1 1960

where two diffusion equations are required for a three component gas, since the global conservation of mass replaces the third diffusion equation.

Global continuity:

$$\frac{\partial}{\partial x}(\rho u r_0) + \frac{\partial}{\partial y}(\rho v r_0) = 0 \tag{16}$$

Conservation of momentum:

$$\rho u \frac{\partial u}{\partial x} + \rho v \frac{\partial u}{\partial y} = -\frac{\partial P}{\partial x} + \frac{\partial}{\partial y}\left(\mu \frac{\partial u}{\partial y}\right) \tag{17}$$

$$\frac{\partial P}{\partial y} = 0 \tag{18}$$

Conservation of energy:

$$\rho \bar{c}_p \left(u \frac{\partial T}{\partial x} + v \frac{\partial T}{\partial y}\right) = u \frac{\partial P}{\partial x} + \mu \left(\frac{\partial u}{\partial y}\right)^2 + \frac{\partial}{\partial y}\left(K \frac{\partial T}{\partial y}\right) + \sum_j \left[(c_p)_j \left(\rho D_{jn} \frac{\partial C_j}{\partial y} + \frac{D_j^T}{T} \frac{\partial T}{\partial y}\right)\right] \frac{\partial T}{\partial y} \tag{19}$$

Equation of state:

$$P = \rho \frac{R}{\bar{M}} T \tag{20}$$

where

$$\bar{M} = \sum_n X_n M_n \tag{21}$$

is the mean molecular weight of the gas.

On introducing the following similarity variables which include the Mangler and Dorodnitsyn transformations [20]:

$$\eta = \frac{\rho_e u_e}{\sqrt{(2\xi)}} \int_0^y \frac{\rho}{\rho_e} r_0 \, dy \tag{22}$$

$$\xi = \int_0^x \rho_i \mu_i u_e r_0^2 dx \tag{23}$$

and defining a stream function:

$$\Psi = (2\xi)^{1/2} f(\eta) \tag{24}$$

such that:

$$\rho u r_0 = \frac{\partial \Psi}{\partial y}, \qquad \rho v r_0 = -\frac{\partial \Psi}{\partial x} \tag{25}$$

the boundary layer equations are reduced to ordinary non-linear differential equations at a stagnation point.

The conservation of atomic species may be written:

$$\left\{\frac{l}{Pr} Le\,(C_A)_\eta\right\}_\eta + f(C_A)_\eta = 0 \tag{26}$$

and the conservation of the kth species becomes:

$$\left\{\frac{l}{Pr} Le\,(C_k)_\eta\right\}_\eta + f(C_k)_\eta = 0 \tag{27}$$

which implies that thermal diffusion can be neglected in first approximation. The conservation of momentum becomes:

$$(lf_{\eta\eta})_\eta + ff_{\eta\eta} + \tfrac{1}{2}\left(\frac{\rho_e}{\rho} - f_\eta^2\right) = 0 \tag{28}$$

and the dominant terms in the energy equation are:

$$\left(\frac{l\bar{c}_p}{Pr}\theta_\eta\right)_\eta + f\bar{c}_p\theta_\eta = 0 \tag{29}$$

which implies that the conduction and convection terms are more important than the diffusion terms in the frozen energy equation, when the specific heats of the species in the gas are nearly equal.

These equations constitute a coupled ninth-order system of non-linear ordinary differential equations with split boundary conditions, with a functional behavior shown in Fig. 2. However, since it is assumed that the vaporizing species

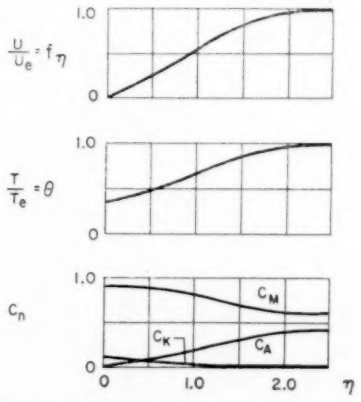

FIG. 2. Gas phase boundary layer profiles.

have the same thermochemical behavior as the air molecules, it is not necessary to consider the diffusion equation for the kth species explicitly during the solution, as demonstrated below. And, it is seen that the system of equations reduces to a set previously solved in a binary mixture analysis [17] (in which the transport and thermodynamic properties of the gas were variable, i.e. they were calculated in terms of the local temperature and composition of the gas).

Before listing the boundary conditions applicable to the analysis of this problem, it will be shown how the dimensionless concentration gradient $(C_k)_{\eta,i}$ may be related to the non-dimensional temperature gradient, $(\theta_\eta)_i$.

Upon defining the function.

$$\Theta = \frac{\bar{c}_p}{(\bar{c}_p)_e}\,\theta \tag{30}$$

and noting that $\bar{c}_p$ is a slowly varying function of η, for moderately high surface temperatures,

$$\Theta_\eta \cong \frac{\bar{c}_p}{(\bar{c}_p)_e}\,\theta\eta \tag{31}$$

and hence equation (29) becomes:

$$\left(\frac{l}{Pr}\,\Theta_\eta\right)_\eta + f\,\Theta_\eta = 0 \tag{32}$$

In order to obtain an equivalent form of the diffusion equation for the kth species, we note that to a very good approximation, the Lewis numbers are nearly unity in which case we may write:

$$\left(\frac{l}{Pr}\,(C_k)_\eta\right)_\eta + f\,(C_k)_\eta = 0 \tag{33}$$

Since equations (32) and (33) are identical in form, it is only necessary to ensure that they have identical boundary conditions.

At this point, the boundary conditions are:

$$\begin{aligned} \eta = 0:\ & C_k(0) = (C_k)_i \\ & \theta(0) \;\; = \theta_i \\ & \Theta(0) \;\; = \frac{(\bar{c}_p)_i}{(\bar{c}_p)_e}\,\theta_i = \Theta_i \end{aligned} \tag{34}$$

$$\begin{aligned} \eta = \infty:\ & \lim_{\eta\to\infty} C_k = (C_k)_e \\ & \lim_{\eta\to\infty} \theta \;\; = \lim_{\eta\to\infty} \Theta = 1{\cdot}0 \end{aligned} \tag{35}$$

Introducing the new variables:

$$\Theta^* = \Theta - 1 \tag{36}$$

$$C_k = \Theta_i^*\left[1 - \frac{(C_k)_i - C_k}{(C_k)_i - (C_k)_e}\right] \tag{37}$$

we obtain the new boundary conditions:

$$\eta = 0: \quad \Theta^*(0) = \frac{(\bar{c}_p)_i}{(\bar{c}_p)_e}\,\theta_i - 1 = \Theta_i^* \tag{38}$$

$$C_k^*(0) = \Theta_i^*$$

$$\eta = \infty: \quad \lim_{\eta\to\infty} \Theta^* = \lim_{\eta\to\infty} C_k^* = 0 \tag{39}$$

so that the boundary conditions are identical in terms of the new variables, while the differential equations become:

$$\left(\frac{l}{Pr}\,\Theta_\eta^*\right)_\eta + f\,\Theta_\eta^* = 0 \tag{40}$$

$$\left\{\frac{l}{Pr}\,(C_k^*)_\eta\right\}_\eta + f\,(C_k)_\eta^* = 0 \tag{41}$$

and hence one can now conclude that:

$$\Theta_\eta^* = (C_k)_\eta^* \tag{42}$$

i.e. the two derivatives obey the same equations, and have the same boundary conditions. We are now in a position to determine the eigenvalue $(C_k)_{\eta,i}$ in terms of the temperature gradient $(\theta_\eta)_i$.

Differentiating equation (37) and introducing equation (36) we obtain:

$$(C_k)_\eta^* = \frac{\Theta_i^*}{(C_k)_i - (C_k)_e}\,(C_k)_\eta = \Theta_\eta^* = \Theta_\eta \tag{43}$$

and upon introducing equations (30) and (31) and rearranging equation (43) we find the general relationship between the dimensionless temperature and concentration gradient:

$$(C_k)_\eta = \frac{(C_k)_i - (C_k)_e}{\{\bar{c}_p/(\bar{c}_p)_e\}\,\theta - 1}\,\frac{\bar{c}_p}{(\bar{c}_p)_e}\,\theta_\eta \tag{44}$$

Since the mass fraction of the vaporizing species other than oxygen or nitrogen vanishes at the outer edge of the boundary layer, then by definition $(C_k)_e = 0$, and thus at the wall one

Vol. 1 1960

obtains for vaporizing species (other than oxygen or nitrogen):

$$(C_k)_{\eta,i} = \frac{(C_k)_i\,(\theta_\eta)_i}{\theta_i - (\bar{c}_p)_e/(\bar{c}_p)_i} \tag{45}$$

Thus, solving the binary mixture equations (26), (28), (29) and obtaining the eigenvalue $(\theta_\eta)_i$ as a function of the flight conditions, the dimensionless wall temperature θ_i, and the dimensionless mass transfer rate $-f_i$, also solves equation (27) implicitly by means of the relationship given in equation (45).

The results obtained are now combined with equation (13). The similarity transformation requires:

$$\left(\frac{\partial}{\partial y}\right)_i = \sqrt{\left\{2\,\frac{\rho_i}{\mu_i}\left(\frac{du_e}{dx}\right)_s\right\}}\left(\frac{\partial}{\partial \eta}\right)_i \tag{46}$$

and equation (13) becomes:

$$\dot{m}_i = -\frac{\sqrt{\{2(\rho_i/\mu_i)(du_e/dx)_s\}}\,\rho_i(D_{kn})_i(C_k)_{\eta,i}}{\{1-(C_k)_i\}} \tag{47}$$

Since $$D_{kn} = \frac{\mu}{\rho}\,\frac{Le}{Pr}$$

equation (47) also may be written:

$$\dot{m}_i = -\sqrt{\left\{2\rho_i\mu_i\left(\frac{du_e}{dx}\right)_s\left(\frac{Le}{Pr}\right)_i\right\}}\,\frac{(C_k)_{\eta,i}}{\{1-(C_k)_i\}} \tag{48}$$

and since the mass transfer rate also may be written in terms of the non-dimensional stream function:

$$\dot{m}_i = -\sqrt{\left\{2\,\rho_i\mu_i\left(\frac{du_e}{dx}\right)_s\right\}} f_i \tag{49}$$

the compatibility condition becomes:

$$\frac{\dot{m}_i}{\sqrt{\{2\,\rho_i\mu_i\,(du_e/dx)_s\}}} = -f_i = -\frac{(Le/Pr)_i(C_k)_{\eta,i}}{1-(C_k)_i} \tag{50}$$

where $(C_k)_{\eta,i}$ is given by equation (45).

When the correlated eigenvalues and properties [17] are substituted into equation (50) one obtains the typical results shown in Fig. 3.

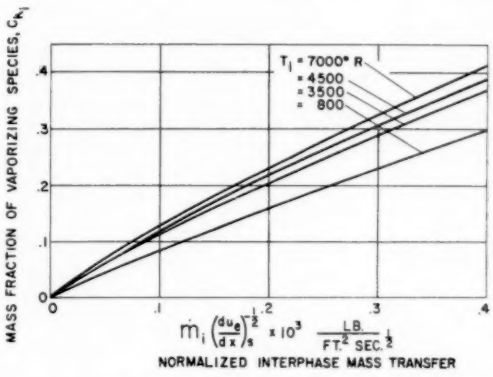

FIG. 3. Mass transfer of vaporizing species at 100,000 ft altitude and Mach No. 20.

Since the normalized interphase mass transfer

$$\dot{m}_i \Big/ \sqrt{\left\{\left(\frac{du_e}{dx}\right)_s\right\}}$$

appears to be almost a linear function of the mass fraction of vaporizing species at the interface, $(C_k)_i$, and since du_e/dx is inversely proportional to the nose radius R_B, this suggests that a useful form for representing all of the data, for the full range of hypersonic flight conditions, is the function $\dot{m}_i\sqrt{(R_B)}/(C_k)_i$.

Results are shown in Fig. 4 for the evaluation of the function $\dot{m}_i\sqrt{(R_B)}/(C_k)_i$ for various flight speeds, altitudes and surface temperatures at a value of $(C_k)_i = 0{\cdot}4$. It is seen that the interphase mass transfer function correlates directly with the boundary layer density. That is, a decrease in altitude (an increase in free stream density), causes a logarithmic increase in $\dot{m}_i\sqrt{(R_B)}/(C_k)_i$. Either an increase in flight speed, or a decrease in wall temperature acts to increase the mass transfer function since the density of the boundary layer rises for each of these effects.

When the results of a large number of individual calculations at various flight speeds, altitudes and wall temperatures are correlated, the result is:

$$\frac{\dot{m}_i}{(C_k)_i}\left[\frac{R_B}{P_\infty/P_0}\right]^{1/2} = 0{\cdot}40 + 0{\cdot}115 \times 10^{-3}(h_e - h_i) \tag{51}$$

when the enthalpies h_e and h_i are expressed in British thermal units per pound, R_B in feet and

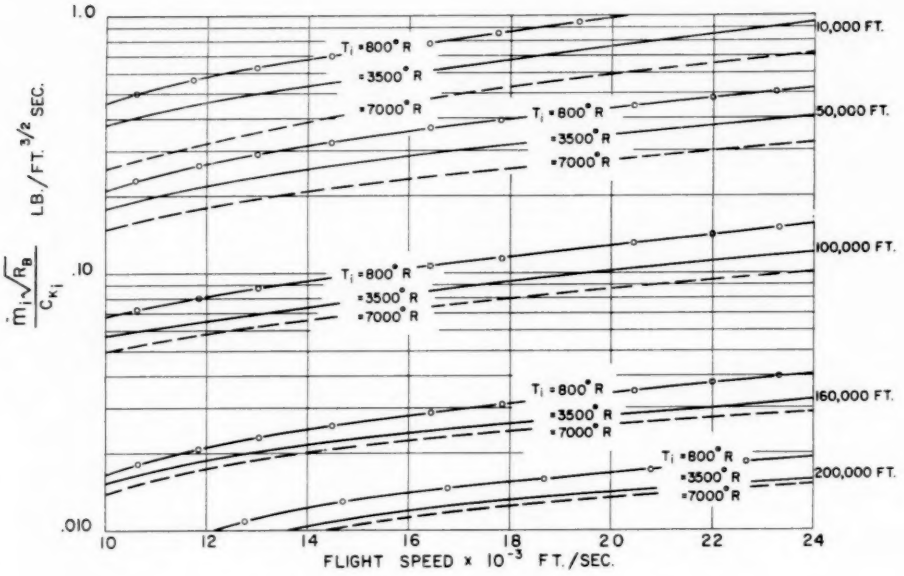

FIG. 4. Mass transfer rate vs. flight speed.

$\dot{m}_i$ in pounds per square feet seconds. Equation (51) represents all of the data within 25 per cent error.

For routine calculation, it is convenient to express the interphase mass transfer function in terms of altitude, flight speed and surface temperature. An equation which represents all of the data within a 15 per cent error may be written as the product of three factors.

$$\frac{\dot{m}_i\sqrt{R_B}}{(C_k)_i} = [1{\cdot}2333 - 6{\cdot}6667 \times 10^{-5}T_i] \times \times [10^{-(4{\cdot}3243 + 3{\cdot}9668 \times 10^{-6}\ \text{Alt.})}] \times \times [V_\infty{}^{(0{\cdot}9976 - 1{\cdot}201 \times 10^{-6}\ \text{Alt.})}] \quad (52)$$

Here T_i is expressed in degrees Rankine, the altitude in feet, the flight speed V_∞ in feet per second and the other symbols have the same dimensions as in equation (51).

Obviously, for best results, the data appearing in Fig. 4 should be used directly.

ANALYSIS OF THE VAPORIZATION PROCESS

A. *Vaporization in equilibrium systems*

1. *General considerations.* In an equilibrium system, the net rate of vaporization is identically zero, and the condensation rate and the forward rate of vaporization must be equal. Furthermore, from statistical theory it may be shown [21], that in a system in chemical equilibrium,

$$(\dot{m}_k)_i \underset{\rightarrow}{=} (\dot{m}_k)_i \underset{\leftarrow}{=} \alpha\,(P_k)_{eq}\sqrt{\left(\frac{M_k}{2\pi RT_i}\right)} \quad (53)$$

Thus, the forward rate of evaporation for an equilibrium system may be calculated precisely if each quantity appearing in the right-hand side of equation (53) is known.

Most refractory substances yield several different gaseous molecules during vaporization. Carbon, for example, produces the following equally important species [22]:

$$C(s) \rightleftharpoons C(g) \quad (54a)$$

$$2C(s) \rightleftharpoons C_2(g) \quad (54b)$$

$$3C(s) \rightleftharpoons C_3(g) \quad (54c)$$

Different values of M_k, α and $(P_k)_{eq}$ will be associated with each reaction, so that a different equation (53) must be written for each. In most cases an increase in temperature leads to a more extensive polymerization of the equilibrium vapor [23]. Particular care must be taken

Vol. 1 1960

therefore in extrapolating low temperature vapor pressure data, because other more complex molecular species, whose presence is not suspected, may become the major constituents of the equilibrium vapor at high surface temperatures.

Let us discuss in greater detail the above three quantities which appear on the right-hand side of equation (53). It is clear that once the vaporizing species has been identified, its molecular weight M_k is immediately known, and hence the molecular weight requires no further discussion.

2. *The evaporation or condensation coefficient.* The evaporation or condensation coefficient α is defined here for an equilibrium system as the fraction of gaseous molecules of species k which condenses on collision with the surface. Obviously α cannot be greater than unity. No general theory has been developed for obtaining the quantity α from fundamental molecular data, and relatively little reliable experimental data have been obtained even for vaporization reactions of the simple type illustrated by equation (55) below.

It might be expected that α is a function of the temperature of the system, of the crystallographic face under consideration, and of its previous history, as well as the vaporization reaction under investigation. In general, however, in many simple vaporizations the average effective value of α lies between 0·1 and 1, and is not affected appreciably by the temperature. Values of α less than 0·1 are observed when considerable molecular rearrangement occurs during the vaporization process. Detailed discussions of the dependence of the α of individual substances on temperature and on the crystallographic face can be found in the literature [24–31].

Finally, it must be pointed out that contamination of the surface, caused either by the presence of impurities within the material or by reaction products from the gas phase, may lead to large decreases in the rate of vaporization [32] and thus to smaller effective values of α.

3. *Simple vaporization reactions.* The simplest class of vaporization reactions is represented by:

$$a\,A\ (\text{condensed}) \rightleftharpoons A_a\ (\text{g}) \qquad (55)$$

where A_a may be any gaseous atomic or molecular species having the same empirical formula as the condensed phase. The reactions given in equations (54) are typical.

For vaporization reactions of the type shown in equation (55), the vapor pressure $(P_k)_{eq}$ is identical with the equilibrium constant $\boldsymbol{K}$, and $\boldsymbol{K}$ can be calculated directly from fundamental thermodynamic quantities which are generally available.

Familiar substances which boil at moderate temperatures, such as water, nitrogen or mercury, have a $(P_k)_{eq}$ which is known precisely at all temperatures up to the critical point. On the other hand, the vapor pressure of substances which boil at temperatures higher than 2000°C is subject to uncertainty, particularly if several complex molecular species are important components of the equilibrium vapor as in the case of graphite. For such materials, the probable error in $(P_k)_{eq}$ is generally no smaller than $\pm$ 20 per cent and may become as great as a factor of 10 [33].

4. *Complex vaporization reactions.* In more complex types of vaporization reactions, the empirical formula of the vapor molecules differs from that of the condensed phase, and a new condensed phase may appear at the interface. In such cases the choice of an appropriate value of $(P_k)_{eq}$ and of α presents greater difficulties. Two examples of such types of reaction are discussed briefly here.

The first example is characterized by an equation of the form:

$$XY(\text{s}) \rightleftharpoons X(\text{g}) + Y(\text{s}) \qquad (56)$$

In this type of reaction the equilibrium vapor pressure P_X is again identical with the equilibrium constant $\boldsymbol{K}$, which is again only a function of the temperature. During the course of the vaporization process, however, a layer of Y builds up at the interface, and eventually the net rate of vaporization may become controlled by the rate of diffusion of gaseous X through condensed Y. Great care must be exercised therefore in choosing the value of α, since α will depend on the thickness of the layer of Y and on

the diffusion coefficient of X(g) in Y. Illustrative of this type of vaporization reaction are:

$$SiC(s) \rightleftharpoons C(s) + Si(g) \quad (57)$$

$$CaCO_3(s) \rightleftharpoons CaO(s) + CO_2(g) \quad (58)$$

The second example is characterized by:

$$XY(s) \rightleftharpoons X(g) + Y(g) \quad (59)$$

which is another commonly encountered type of vaporization reaction. In such cases the equilibrium condition is:

$$P_X P_Y = \boldsymbol{K} \quad (60)$$

If no excess X or Y are present from other sources in the equilibrium gas, then $P_X = P_Y$ and

$$(P_X)_{eq} = (P_Y)_{eq} = \sqrt{\boldsymbol{K}} \quad (61)$$

In the more general case, when excess X or Y are present, equation (60) must be utilized since the simplification to (61) does not apply.

In such a case severe difficulties are encountered in determining α. Even when the macroscopic forward rates of vaporization of X and Y are equal, so that no buildup of a new phase is encountered, it is probable that the stoichiometric composition of the surface layer is not identical with the composition of the bulk condensed phase. Thus, the extent and nature of the chemisorbed layer of X and of Y may affect greatly the value of α.

As apparent from equation (60), although the product of $(P_X)_{eq}$ and $(P_Y)_{eq}$ is well defined, the individual values of $(P_X)_{eq}$ and $(P_Y)_{eq}$ are not, so that equilibrium vapor at any given temperature does not have a definite composition.

The composition of the chemisorbed layer will vary as the ratio of the pressure of X(g) to Y(g) varies from zero to infinity. Therefore, the values of α at any given temperature will vary also with the gas phase composition, and X(g) and Y(g) must have different values of α. In such cases the vaporization coefficient becomes an indeterminate quantity, and this approach is not applicable. A more fruitful approach in this instance is to rely on reaction rate theory, or perhaps use the concept of α which will be introduced as α_{vap}. An example of such a reaction is:

$$MgO(s) \rightleftharpoons Mg(g) + \tfrac{1}{2}O_2(g) \quad (62)$$

B. *Vaporization in non-equilibrium systems*

1. *General considerations.* In general, the net rate of a vaporization reaction is the difference between the rates of the forward and reverse reactions:

$$(\dot{m}_k)_i = (\underset{\rightarrow}{\dot{m}_k})_i - (\underset{\leftarrow}{\dot{m}_k})_i \quad (63)$$

The system cannot truly be in equilibrium when net vaporization takes place and thus the rate equations discussed in Section A are not necessarily applicable. Two major assumptions must be made in order to obtain a rate equation during non-equilibrium vaporization:

(a) Not only is the forward rate of vaporization assumed to be independent of the partial pressure of foreign gases, it is also assumed to be independent of the partial pressure of the vaporizing species.

(b) The fraction of incident molecules which condense on colliding with the surface is independent of the partial pressure of foreign components and of the vaporizing species.

As a consequence of assumption (a), the forward rate of vaporization is exactly the same as that obtained during equilibrium vaporization.

$$(\underset{\rightarrow}{\dot{m}_k})_i = \alpha\,(P_k)_{eq}\sqrt{\left\{\frac{M_k}{2\pi RT_i}\right\}} \quad (64)$$

where the α appearing in equation (64) is the equilibrium condensation coefficient. In general, the rate of condensation is given by:

$$(\underset{\leftarrow}{\dot{m}_k})_i = \alpha\,(P_k)_i\sqrt{\left(\frac{M_k}{2\pi RT_i}\right)} \quad (65)$$

where α is the fraction of sticky collisons, and $(P_k)_i$ is evaluated one mean free path from the surface and is not necessarily the equilibrium vapor pressure appearing in equation (53). As a consequence of assumption (b), the α appearing in equation (65) is equal to the equilibrium condensation coefficient, and hence, on substituting equations (64) and (65) into equation (63), the net rate of vaporization is obtained:

$$(\dot{m}_k)_i = \alpha\sqrt{\left(\frac{M_k}{2\pi RT_i}\right)}\{(P_k)_{eq} - P_k\}_i \quad (66)$$

2. *The evaporation or condensation coefficient.* Before proceeding with a discussion of equation

Vol. 1 1960

(66), one should consider the errors introduced in the calculated rates of vaporization of non-equilibrium systems by the assumptions that the rate of vaporization and the condensation coefficient α are independent of the gas phase composition.

Attempts have been made in recent years to develop a theory which relates the forward rate of vaporization to the partial pressure of the vapor. This was done by relating the concentration of active sites for the vaporization process to the rate of diffusion of molecules on a surface [34, 35]. Difficulties are encountered in giving an adequate physical description of even an idealized surface, and these theories are still qualitative in nature. For some types of cubic crystals, it has been estimated, for example, that the forward rate of vaporization may vary by a factor of 3 as the partial pressure is varied from zero to the equilibrium pressure [34]. The best experimental work on this subject has been done by Hock and Neumann [26], on single crystals of potassium. In this case a definite dependence on partial pressure has been obtained for both the rate of vaporization and the condensation coefficient. The observed total variation in the rate of vaporization was approximately a factor of 2. No such variation was observed for molten potassium [27]. Less precise experiments indicate that the vaporization rate of other metals has a dependence upon partial pressure which is no larger than that found for potassium. Thus, the errors introduced by the assumptions that the effective condensation coefficient and the rate of vaporization are independent of the partial pressure, are of the same magnitude as those which enter into the determination of α under equilibrium conditions.

In some cases it has been found that the presence of small amounts of some foreign molecular species can lead to a large change in the rate of vaporization, by acting as a catalyst for the vaporization process. This situation is most likely encountered in vaporizations having a low value of α, where there is an appreciable excess activation energy of vaporization so that catalytic effects can become most important. The best known example of this type is the increased rate of vaporization of ammonium chloride in the presence of moisture [36].

3. *Vaporization into a vacuum.* The experimental determination of the net rate of vaporization is generally carried out in a vacuum. Therefore, some authors have found it convenient to define the evaporation coefficient, as the ratio of the experimentally determined net rate of vaporization to the Langmuir expression for the forward rate of vaporization

$$\alpha_{\text{vap}} = \frac{(\dot{m}_k)_i \text{ (vacuum)}}{(P_k)_{\text{eq}} \sqrt{\{M_k/2\pi RT_i\}}} \tag{67}$$

Thus, α_{vap} is intended as a measure of the error in the Langmuir expression

$$(\dot{m}_k)_i = (P_k)_{\text{eq}} \sqrt{\left\{\frac{M_k}{2\pi RT_i}\right\}} \tag{68}$$

Note the tacit assumption by these authors that the forward rate of vaporization and the net rate of vaporization are identical, if the material vaporizes into a vacuum. It is clear that at high rates of vaporization, the vacuum is partially destroyed in the immediate vicinity of the surface so that care must be exercised in the use of equation (67). That is, the reverse reaction (condensation) may not necessarily be negligible.

The subscript "vap" has been added to α in equation (67) to emphasize that this definition of the vaporization coefficient is not necessarily equivalent to the equilibrium condensation coefficient α. It is considered that the use of α, which is rigorously defined for equilibrium vaporization, is preferable to the use of α_{vap} defined for non-equilibrium vaporization, since only for equilibrium vaporization systems is the forward rate of vaporization related unambiguously to the rate of condensation through the equilibrium constant. When α is defined by means of equilibrium vaporization processes, it has physical meaning in that it is the "sticking coefficient" of the equilibrium vapor, whereas α_{vap} is merely a measure of the error in the Langmuir expression and cannot be directly related to the fraction of sticky collisions during non-equilibrium vaporization. While α must lie between zero and unity, α_{vap} can exceed unity. Under the special conditions when the forward rate of vaporization is independent of the partial pressure of the foreign and vaporizing species, α_{vap} and α are identical.

In view of the discussion presented in Section B(1), one may, within the framework of assumptions (a) and (b), use α_{vap} and a interchangeably, although it is clear that both α_{vap} and the "sticking fraction" will actually have some dependence on P_k.

4. *Complex vaporization into a boundary layer.* For net vaporization into a boundary layer, as will be discussed in the following section, the partial pressure P_k, evaluated at one mean free path from the surface, depends partially on the rate of convection and diffusion into the boundary layer.

For simple vaporization reactions no added complications are anticipated. As an example of what may occur in a complex (but not overcomplicated) vaporization reaction, consider equation (59). In the simplest case, already discussed, where no chemical reactions take place to remove either species X or Y from the gas phase and where no X or Y is normally present in the boundary layer, under equilibrium conditions, equation (61) still applies.

If a chemical reaction occurs which consumes either X or Y, or if species X or Y are components of the free stream which enter the boundary layer, the quasi-equilibrium gas composition may exist nevertheless. Hence, equation (60) still is valid, but in such a case $P_X \neq P_Y$ since P_X and P_Y are affected by the presence of the free stream components and the products of reaction. A further relationship between P_X and P_Y can be established by introducing the equilibrium constant of the chemical reaction.

If preferential diffusion occurs due to unequal diffusion coefficients or due to unequal concentration gradients, but if a quasi-equilibrium vaporization process is still assumed, again equation (60) applies while (61) does not. Now, in addition to the equilibrium constants, an added relationship between P_X and P_Y must be sought in the conservation of mass at the interface (chemical source–sink considerations) [19].

Finally, for a non-equilibrium vaporization process, one must have a precise knowledge of the forward rate of vaporization since the process is no longer diffusion controlled.

C. *Summary of available experimental data*

Experimentally determined values of a and α_{vap} are given in Tables 1 and 2 for a number of materials. Since data on the rate of vaporization

Vol. 1 1960

Table 1

Substance	Gaseous molecule	α_{vap}	Temperature (°C)	Reference
White phosphorus	P_4	~1		[23]
Red phosphorus	P_4	10^{-6}		[23]
Arsenic	As_4	5×10^{-4}		[23]
Iodine	I_2	0·037–0·005	−56–35	[30]
Rhombic sulfur	S_8	0·7	16–32	[24, 25]
Potassium (liquid)	K	1	67–119	[27]
Potassium (solid)	K	1·7–0·9	50–63	[26]
Many metals, solid and liquid	atoms	~1		[32, 43]
Graphite	C	0·4	2400	[22]
	C_2	0·3	2400	[22]
	C_3	0·1	2400	[22]
	C_5	$<10^{-3}$	2400	[22]
Arsenolite	As_4O_6	~1		[46]
Claudetite	As_4O_6	10^{-6}		[46]
Water and ice	H_2O	~1		[47]
Potassium chloride	KCl	0·72	407–469	[29]
Potassium perrhenate	$KReO_4$	0·7	780–853	[48]
Many organic acids alcohols and hydrocarbons		0·36–1		[31, 47, 49, 50]

are available only for a limited number of substances (most of which appear in the tables) no effort has been made to select materials of interest for hypersonic flight, and further, no distinction is made between α and α_{vap} in these tables.

Table 2

Substance	Products of vaporization	α_{vap}	T (°C)	Reference
Na_2CO_3	$Na(g) + O_2(g) + CO_2(g) + Na_2O(g)$	0·02	881–1107	[51]
BN	$B(s) + N_2(g)$	$\sim 10^{-4}$		[52]
AlN	$Al(g) + N_2(g)$	$\sim 10^{-4}$		[52]
Mg_3N_2	$Mg(g) + N_2(g)$	"very low"		[53]
NH_4Cl	$NH_3(g) + HCl(g)$	0·003–0·0004	118–221	[28] [54]
TaC	$Ta(l) + C(g)$	~ 1		[54]
WC	$W(l) + C(g)$	~ 1		

The rates of vaporization from which the value of the vaporization coefficient was computed were usually obtained under vacuum conditions, and so are generally α_{vap} for which no attempt has been made to determine the effect of the partial pressure of the vaporizing species. Since α is temperature dependent, the temperature at which the experiments were conducted is listed for most of the substances.

Table 1 lists values of α for simple vaporization reactions of the type illustrated by equation (55). Table 2 deals with complex reactions which are listed individually in the table.

It should be apparent from the scarcity of data that much remains to be done in this field.

D. *Vaporization kinetics*

When adequate data are not available for $(P_k)_{eq}$ and for α, it becomes necessary to obtain the forward rate of vaporization $\dot{m}_k$ from kinetic expressions containing other molecular parameters. A large number of general expressions have been proposed which require more or less detailed data about the system in question, and which are only partially successful in predicting the few accurately known rates of vaporization. Only the most widely used expressions are given here. The following three equations:

$$(\dot{m}_k)_i = AM_k\nu \exp\left(-\frac{E_v}{RT}\right) \text{ [37, 38]} \quad (69)$$

$$(\dot{m}_k)_i = 2\,AM_k\nu \frac{E_v}{RT} \exp\left(-\frac{E_v}{RT}\right) \text{ [39]} \quad (70)$$

$$(\dot{m}_k)_i = AM_k\kappa \frac{kT}{h} \frac{F^*}{F} \exp\left(-\frac{E_v}{RT}\right) \text{ [40, 41, 42]} \quad (71)$$

all rest on three basic assumptions:

(a) Each molecule at a surface is exactly equivalent to every other, so that any molecule will have an equal probability of vaporizing.
(b) The activation energy of vaporization is equal to the enthalpy of vaporization.
(c) The vaporization reaction is a kinetically simple one-stage reaction.

The first two equations contain other added assumptions and may be considered as special cases of the third one, but they contain fewer parameters and are relatively easy to apply. Generally, they cannot be expected to yield anything more than an estimate of the order of magnitude.

The last expression, given in equation (71), has been used with considerable success to calculate the rate of vaporization of potassium chloride, benzene and sulfur. It is difficult to apply, however, since the partition functions F are sensitive functions of many uncertain parameters. Furthermore, it is difficult to estimate the reliability of the three assumptions mentioned above.

As a consequence of the first assumption all of these equations predict that the forward rate of vaporization is independent of the partial pressure of the foreign components of the vaporizing species. Attempts [34] to refine these models in order to make them consistent with known behavior of surfaces have not yielded any quantitative results as yet.

E. *Conclusions*

It is concluded that the value of the vaporization coefficient may vary over very wide limits, and that it is unsafe to assume that it is close to unity for refractory substances except when dealing with a highly restricted group of substances. In most cases the rate of vaporization

may be predicted to within one order of magnitude only when detailed knowledge of the mechanism and the rate of the evaporization process are available.

The following factors tend to favor a large value of α, ($\alpha > 0{\cdot}1$):

(a) The presence of a liquid rather than solid phase.

(b) The necessity of little molecular rearrangement during vaporization.

(c) The absence of impurities at the vaporizing surface.

THE RATE-DETERMINING STEP CONTROLLING MASS TRANSFER

The curves shown in Fig. 5 are helpful in visualizing the effects considered in the preceeding sections. Kinetic theory (equation (6)), predicts that the interphase mass transfer is a decreasing function of the mass fraction of vaporizing species $(C_k)_i$ (evaluated at one mean free path from the surface). Thus, when $(C_k)_i$, is identically equal to $(C_k)_{eq.i}$ the gas is in equilibrium with the surface and the net interphase mass transfer is zero. This is shown in Fig. 5 by the curves labelled "kinetic theory".

Boundary layer theory, equation (51), or equation (52) predicts that the interphase mass transfer is an increasing function of the vaporizing species $(C_k)_i$, which is evaluated at one mean free path from the surface. This result also is shown in Fig. 5 by the curves labelled "boundary layer theory".

In the steady state, the vaporized gas is transported away from the interface by convection and diffusion at a rate equal to the net rate of vaporization. Thus, the intersections of the curves shown in Fig. 5(a) and 5(b) represent the condition of microscopic compatability between kinetic theory and boundary layer theory.

In Fig. 5(a) it is seen that for a given material, at a given surface temperature, the vaporization process will be either diffusion controlled, rate controlled, or in the transition regime between the two, depending upon the slope of the boundary layer theory solution which is a unique function of environmental conditions. In Fig. 5(b), it is seen that, for given conditions, the vaporization process will be again either diffusion controlled, rate controlled, or in the transition regime depending on the slope of the kinetic theory expression, which depends primarily on the magnitude of α.

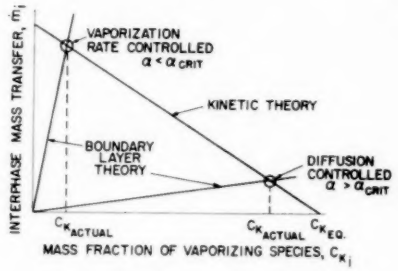

(a)

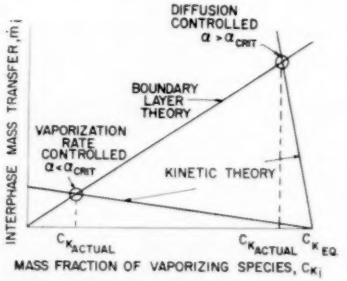

(b)

FIG. 5. Relationship between interphase mass transfer and equilibrium mass fraction.
(a) Effect of environment on net rate of vaporization.
(b) Effect of vaporization coefficient on net rate of vaporization.

In either case the magnitude of $(C_k)_i$ obtained at the point of intersection determines whether the slowest, and hence the rate-determining, step of the vaporization process is diffusion or the vaporization rate.

It is perhaps interesting to draw an analogy between the mass transfer process and ohmic flow. One may write the boundary layer solution in the form:

$$(C_k)_i = a_{B.L.}\, \dot{m}_i \sqrt{R_B} \qquad (72)$$

where $a_{B.L.}$ represents the resistance of the boundary layer to the diffusion and convection

of the vaporizing species. Similarly, the kinetic theory expression may be written:

$$(C_k)_i = (C_k)_{\text{eq},i} - a_{\text{V.M.}}\,\dot{m}_i \tag{73}$$

where $a_{\text{V.M.}}$ represents the resistance of the material to the vaporization process. Upon eliminating $(C_k)_i$ between equations (72) and (73), one obtains:

$$(C_k)_{\text{eq},i} = \dot{m}_i\,(a_{\text{B.L.}}\sqrt{R_B} + a_{\text{V.M.}}) \tag{74}$$

Equation (74) shows that the boundary layer diffusion and convection process, and the vaporization process may be thought of as two resistances in series. The interphase mass transfer $\dot{m}_i$ is analogous to the current and the equilibrium mass fraction $(C_k)_{\text{eq},i}$ is analogous to the driving force. Then $(C_k)_i$ is the voltage drop due to the boundary layer resistance, and the total resistance is the sum of the two resistances $a_{\text{B.L.}}\sqrt{R_B}$ and $a_{\text{V.M.}}$ The boundary layer resistance, $a_{\text{B.L.}}\sqrt{R_B}$, appears as an increasing function of body size, while the resistance of the material to vaporization, is independent of body size. It is seen also that since the magnitude of $a_{\text{V.M.}}$ is inversely proportional to the vaporization coefficient, the two limiting values of the interphase mass transfer are:

$$\lim_{a \to \infty} \dot{m}_i = \frac{(C_k)_{\text{eq},i}}{a_{\text{B.L.}}\sqrt{R_B}} \tag{75}$$

$$\lim_{a \to 0} \dot{m}_i = \frac{(C_k)_{\text{eq},i}}{a_{\text{V.M.}}} \tag{76}$$

That is, as a approaches infinity, the rate-determining step of the vaporization process is diffusion and convection in the boundary layer. As a approaches zero, the vaporization process becomes kinetically controlled. For intermediate values of a, the overall process is governed by the kinetics of the vaporization process and the resistance of the boundary layer.

The parameter a has been singled out for special attention in equations (75) and (76) because, as shown previously, the vaporization coefficient is generally the most difficult physical quantity to evaluate with sufficient accuracy. While equations (75) and (76) are mathematically correct, it is not necessary to go to the limits zero and infinity, since the process becomes practically diffusion controlled or kinetically controlled for finite values of a. The problem consists of the determination of the conditions which define the two limiting regimes and the transition regime. Therefore, two critical values of a can be defined, one at each end of the transition regime. However, the larger of these is of greater practical interest and will be defined here by the following expression:

$$\begin{cases} a &= a_{\text{crit}} \\ (C_k)_i &= 0{\cdot}9\,(C_k)_{\text{eq},i} \end{cases} \tag{77}$$

a_{crit} is therefore the value of a for which the resistance of the vaporization process $a_{\text{V.M.}}$ is 10 per cent of the total resistance

$$a_{\text{V.M.}} + a_{\text{B.L.}}\sqrt{R_B}.$$

When $a = a_{\text{crit}}$ it may be assumed that

$$(C_k)_i = (C_k)_{\text{eq},i}$$

without introducing an error greater than 10 per cent in the calculated value of $\dot{m}_i$, and the vaporization process is an "equilibrium" process. For higher values of a, the "equilibrium" assumption will lead to errors smaller than 10 per cent and so if this accuracy is sufficient, the quantity a need not be used for determining the net interphase mass transfer, since equation (52) suffices.

The value of a_{crit} is, of course, a function of the other parameters, which are the precise environmental conditions, the molecular weight of the vaporizing species M_k, the surface temperature T_i, the mean molecular weight of the gas at the surface $\bar{M}_i$ and the geometric scale factor $\sqrt{R_B}$.

It is therefore of considerable interest to determine the value of a_{crit} for various flight conditions as a function of these other parameters. This is done by introducing the relation given in equation (1) into equation (6) and obtaining

$$\dot{m}_i\sqrt{(R_B)} = \left[\frac{a\sqrt{R_B}}{\sqrt{(2\pi R)}}\,\frac{P\bar{M}}{\sqrt{(M_k T)}}\,\{(C_k)_{\text{eq}} - C_k\}\right]_i \tag{78}$$

On letting $\{C_k/(C_k)_{eq}\}_i = 0{\cdot}9$ and rearranging equation (78), one obtains:

$$(\alpha\sqrt{R_B})_{crit} = 9\left(\frac{\dot{m}_i\sqrt{(R_B)}}{(C_k)_i}\right)\sqrt{(2\pi R)}\,\frac{\sqrt{(M_kT_i)}}{Pe\bar{M}_i} \quad (79)$$

which is a completely general equation.

If one now selects a particular altitude and flight speed, the value of the stagnation pressure P_e is obtained from normal shock tables for dissociated air, and the value of

$$\{\dot{m}_i\sqrt{(R_B)}/(C_k)_i\}$$

is known from the boundary layer solution presented previously. Thus, a general relationship between $(\alpha\sqrt{R_B})_{crit}$ and the environmental conditions (altitude and flight speed) can be obtained for any specified value of the mean molecular weight $\bar{M}_i$ and of M_kT_i.

Notice that the value of $\{\dot{m}_i\sqrt{(R_B)}/(C_k)_i\}$ calculated earlier does depend somewhat on $(C_k)_i$ and T_i. This dependence appears to be small, however (see Fig. 3), and is neglected here.

Fig. 6 shows this general relationship graphically, and is a plot of $(\alpha\sqrt{R_B})_{crit}$ vs. flight altitude. The effect of varying the average molecular weight $\bar{M}_i$, $23 \leqslant \bar{M}_i \leqslant 33$ is shown approximately by the width of the bands shown

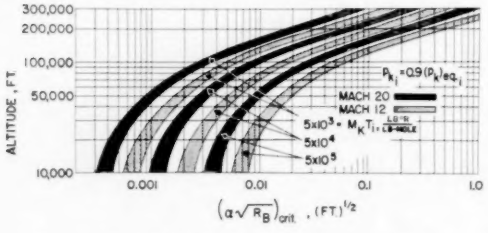

FIG. 6. Critical limit of vaporization coefficient.

in Fig. 5. Separate bands are drawn for each of three different values of M_kT_i; these three values were chosen to cover the region of greatest interest where the values of particular interest are usually $5 \leqslant M_k \leqslant 100$, and

$$1000° \leqslant T_i \leqslant 5000°\text{R}.$$

Finally, the effect of flight velocity is shown by plotting two bands for each of the three values of M_kT_i, one band being for a Mach number of 12, and the other for a Mach number of 20.

The curves have been plotted for constant M_kT_i and Mach number as a matter of convenience. In considering the behavior of a particular material during the flight of a hypersonic vehicle along a given trajectory, the value of T_i, M_k, $\bar{M}_i$ and the velocity will change with altitude. The time dependent behavior of a single material on a particular flight path will cut across the curves of Fig. 6. These curves show the value of $(\alpha\sqrt{R_B})_{crit}$ defined by $\{C_k/(C_k)_{eq}\}_i = 0{\cdot}9$ for the full range of hypersonic flight conditions.

When $\alpha > \alpha_{crit}$, $\{C_k/(C_k)_{eq}\}_i > 0{\cdot}9$, and the vaporization may be considered to be "equilibrium" vaporization since the process is diffusion controlled. When $0{\cdot}012\ \alpha_{crit} < \alpha < 0{\cdot}9\ \alpha_{crit}$, then $0{\cdot}1 < \{C_k/(C_k)_{eq}\}_i < 0{\cdot}9$, and the net rate of vaporization is determined both by diffusion and by the kinetics of the vaporization process, and the value of α must appear explicity in the equations.

When $\alpha < 0{\cdot}012\ \alpha_{crit}$, then

$$\{C_k/(C_k)_{eq}\}_i < 0{\cdot}1$$

and the boundary layer resistance can be neglected with respect to the material resistance and the net rate of vaporization may be considered equal to the forward rate of vaporization:

$$\dot{m}_i = \frac{ap\bar{M}}{\sqrt{(2\pi RM_kT_i)}}\,(C_k)_{eq,i} \quad (80)$$

An approximate formal expression for the curves shown in Fig. 6 is obtained as follows:

The introduction of equation (48), followed by some dimensional analysis shows that $(\alpha\sqrt{R_B})_{crit}$ varies inversely as the Schmidt number, inversely as the square root of the stagnation pressure, directly as the square root of M_kT_i, and directly as the fourth root of the stagnation temperature,

$$(\alpha\sqrt{R_B})_{crit} \sim \left(\frac{Le}{Pr}\right)_i\sqrt{\left(\frac{M_kT_i}{P_e}\right)}\,(T_e)^{1/4} \quad (81)$$

One can anticipate, as verified by the results shown in Fig. 6 that the region is which $(C_k)_i$ deviates from $(C_k)_{eq,i}$ is one in which the stagnation pressure is low and the product

Vol. 1 1960

$M_k T_i$ is large. Thus, at low altitudes—10,000 ft or less—for instance, the ratio $\{C_k/(C_k)_{eq}\}_i$ deviates from unity only for very low flight speeds and very large values of $M_k T_i$. At higher altitudes, this ratio may deviate from unity even at higher flight speeds (Mach number ~ 20). Notice that if the nose radius is small, this also will increase the tendency for the ratio $\{C_k/(C_k)_{eq}\}_i$ to deviate from unity. The ratio $(Le/Pr)_i$ has been evaluated as a function of flight conditions, using the properties of dissociated air, for which the ratio is of the order of 2. Actually, this ratio depends critically on the molecular weight of the injected species. For light particles, i.e. $M_k \sim 5$, the ratio $(Le_k/Pr)_i$ can exceed 5: however, this effect is minimized by the reduction in $M_k T_i$. Since the curves shown in Fig. 4 were determined using the transport properties of dissociated air, which ignores the effect of foreign gases, an additional correction for extremely light or heavy gases would involve multiplying a_{crit} obtained from Fig. 6 by the ratio $(Le_k/Le_{air})_i$.

An analysis has recently been performed in which the relationship between the interphase mass transfer and the vaporization coefficient has been established for the non-equilibrium vaporization of a refractory oxide at high altitude [55]. The dependence of the effective mass fraction at the surface upon $a\sqrt{R_B}$ is shown in Fig. 7. Note that three vaporization regimes are clearly demarcated, which are the specific representation of Fig. 5(b).

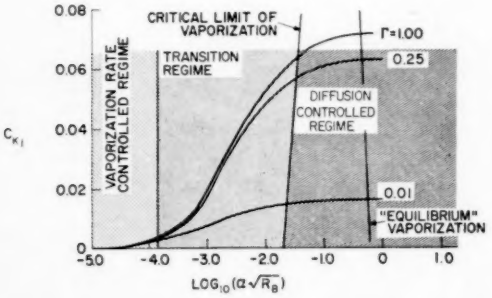

FIG. 7. Dependence of the non-equilibrium mass fraction of injected species upon the vaporization coefficient.

Altitude = 200,000 ft $P_e/P_0 = 0{\cdot}192$
V_∞ = 23,600 ft/sec $\epsilon_t/R_B = 0{\cdot}50$ ft$^{1/2}$

CONCLUSIONS

When a material is subjected to severe heating conditions, the net rate of interphase mass transfer during vaporization may be diffusion controlled, kinetically limited or both, depending on the magnitude of the vaporization coefficient a.

The flight regimes where the vaporization process is diffusion controlled, kinetically limited or both, are defined by a universal solution, utilizing the most significant independent parameters.

One may estimate the rate of vaporization of an arbitrary material, subject to hypersonic flight conditions, utilizing the numerical solutions or the general correlation formula derived herein (provided only that one has an independent knowledge of certain minimum physicochemical data).

In addition, an extensive summary is given of the available experimental data regarding forward rates of vaporization.

ACKNOWLEDGEMENTS

This work could not have been presented without the assistance of a number of personnel at the General Electric Company, Missile and Space Vehicle Department, including Mr. P. Gordon who programmed the equations for digital computation on an IBM 704, and Mr. L. Gilbert who assisted in numerical computations and in drawing the figures.

REFERENCES

1. W. NUSSELT, *Z. angew. Math. Mech.* **10**, 105 (1930). Translated as NACA TM 1367, March (1954).
2. M. J. STEFAN, *Ann. Phys., Lpz.* **17**, 550 (1882).
3. A. P. COLBURN and T. B. DREW, *Trans. Amer. Inst. Chem. Engrs.* **33**, 197 (1937).
4. T. H. CHILTON, *Industr. Engng. Chem.* **26**, 1183 (1934).
5. M. KNUDSEN, *Ann. Phys., Lpz.* **28**, 999 (1909).
6. I. LANGMUIR, *Phys. Rev.* **2**, 329 (1913).
7. T. K. SHERWOOD and N. E. COOKE, *Mass Transfer at Low Pressures.* MIT Report sponsored by OOR, 1 December 1955; ASTIA Report 80230.
8. R. W. SCHRAGE, *A Theoretical Study of Interphase Mass Transfer.* Ph.D. Thesis, Columbia University (1953).
9. R. D. SCHULTZ and A. O. DEKKER, *Advances in the Kinetics of Decomposition, Fusion and Sublimation of Solids.* Aerojet-General Corporation Report No. 961 (1955).
10. P. D. CROUT, *J. Math. Phys.* **15**, 1 (1936).
11. R. E. TREYBAL, *Mass Transfer Operations.* McGraw-Hill, New York (1955).

12. J. R. BARON, *The Binary Mixture Boundary Layer Associated with Mass Transfer Cooling at High Speeds*. MIT Naval Supersonic Laboratory Report TR No. 160 (1956).
13. S. M. SCALA, *J. Aero. Sci.* **25**, 461 (1958).
14. M. R. DENNISON and D. A. DOOLEY, *Combustion in the Laminar Boundary Layer of Chemically Active Sublimators*. Publication No. C–110, Aeronutronic Systems, Inc. (1957).
15. M. W. RUBESIN and C. C. PAPPAS, *An Analysis of the Turbulent Boundary Layer—Characteristics on a Flat Plate with Distributed Light Gas Injection*. NACA TN 4149 (1958).
16. L. LEES, *Third AGARD Colloq. Palermo 1958*, p. 451. Pergamon Press, London (1958).
17. S. M. SCALA, *Transpiration Cooling in the Hypersonic Laminar Boundary Layer*. To be published.
18. S. M. SCALA and G. W. SUTTON, *1958 Heat Transfer and Fluid Mechanics Institute*, p. 231. Stanford University Press (1958).
19. S. M. SCALA, *J. Aero. Sci.* **27**, 1 (1960).
20. L. LEES, *J. Amer. Rocket Soc.* **26**, 259 (1956).
21. E. H. KENNARD, *Kinetic Theory of Gases*. McGraw-Hill, New York (1938).
22. R. J. THORN and G. H. WINSLOW, *J. Chem. Phys.* **26**, 186 (1957).
23. L. BREWER and J. S. KANE, *J. Phys. Chem.* **59**, 105 (1955).
24. R. S. BRADLEY, *Proc. Roy. Soc.* A **205**, 553 (1951).
25. E. RIDEAL and P. M. WIGGINS, *Proc. Roy. Soc.* A **210**, 291 (1951).
26. F. HOCK and K. NEUMANN, *Z. phys. Chem.* **2**, 241 (1954).
27. K. NEUMANN, *Z. phys. Chem.* **2**, 215 (1954).
28. H. SPINGLER, *Z. phys. Chem.* B **52**, 90 (1942).
29. R. S. BRADLEY and P. VOLANS, *Proc. Roy. Soc.* A **217**, 508 (1953).
30. T. H. STERN and N. W. GREGORY, *J. Phys. Chem.* **61**, 1226 (1957).
31. J. BIRKS and R. S. BRADLEY, *Proc. Roy. Soc.* A **198**, 226 (1949).
32. S. DUSHMAN, *Scientific Foundations of Vacuum Techniques*. John Wiley, New York (1949).
33. R. E. HONIG, *J. Chem. Phys.* **22**, 1610 (1954).
34. J. P. HIRTH and G. M. POUND, *J. Chem. Phys.* **26**, 1216 (1957).
35. W. K. BURTON, N. CABRERA and F. C. GRANK, *Phil. Trans.* A **243**, 299 (1951).
36. W. H. RODEBUSH and J. C. MICHALEK, *J. Amer. Chem. Soc.* **51**, 748 (1929).
37. J. FRENKEL, *Kinetic Theory of Liquids*, p. 5. Clarendon Press, Oxford (1946).
38. B. TOPLEY and J. HUME, *Proc. Roy. Soc.* A **120**, 211 (1928).
39. M. POLYANI and E. WIGNER, *Z. phys. Chem.* A **139**, 439 (1928).
40. S. S. PENNER, *J. Phys. Colloid Chem.* **52**, 949 (1948).
41. S. S. PENNER, *J. Phys. Chem.* **45**, 475 (1952).
42. R. D. SCHULTZ and A. O. DEKKER, *J. Chem. Phys.* **23**, 2133 (1955).
43. M. KNUDSEN, *Ann. Phys., Lpz.* **47**, 697 (1915).
44. P. GOLDFINGER, *Mém. Soc. Sci. Liège* **15**, 378 (1955).
45. W. A. CHUPKA and M. G. INGHRAM, *J. Phys. Chem.* **59**, 100 (1955).
46. I. N. STRANSKY, *Research* **4**, 15 (1951).
47. R. LITTLEWOOD and E. RIDEAL, *Trans. Faraday Soc.* **52**, 1598 (1956).
48. K. NEUMANN and V. COSTEANU, *Z. phys. Chem.* A **185**, 65 (1939).
49. R. S. BRADLEY and G. C. S. WAGHORN, *Proc. Roy. Soc.* A **206**, 65 (1951).
50. R. S. BRADLEY and A. D. SHELLARD, *Proc. Roy. Soc.* A **198**, 239 (1949).
51. K. MOTZFELDT, *J. Phys. Chem.* **59**, 139 (1955).
52. M. HOCH and D. WHITE, *The Vaporization of Boron Nitride and Aluminum Nitride*. Report No. MCC 1023–TR–214. Ohio State University Research Foundation (1956).
53. J. R. SOULEN, P. STHAPITANONDA and J. L. MARGRAVE, *J. Phys. Chem.* **59**, 132 (1955).
54. M. HOCH, P. E. BLACKBURN, D. P. DINGLEDY and H. L. JOHNSTON, *J. Phys. Chem.* **59**, 97 (1955).
55. S. M. SCALA, *1959 Heat Transfer and Fluid Mechanics Institute*, p. 181. Stanford University Press (1959).

Vol. 1 1960

Int. J. Heat Mass Transfer. Vol. 1, pp. 23–27. Pergamon Press 1960. Printed in Great Britain.

EXPERIMENTAL METHODS APPLIED TO THE DETERMINATION OF SOME TEMPERATURE RADIATION PARAMETERS

D. T. KOKOREV
Institute of Chemical Engineering, Moscow, U.S.S.R.

(*Received* 16 *November* 1959)

Abstract—The analytical determination of integral angular radiation factors is very complicated for most practical cases. The known graphical and analytical methods do not present a satisfactory solution of problem as a whole.

In this work the writer makes an attempt to solve the problem experimentally. Analytical relations were obtained, which make it possible to establish simple experimental methods of determining angular radiation factors for a general case of a spatial problem, which plays an important role in the solution of engineering problems of heat transfer by radiation. In addition, it was possible to find the optical characteristics of grey surfaces: the average factors of absorption, reflection and radiation.

Résumé—Des formules analytiques, fondées sur la théorie moderne du rayonnement thermique, ont été établies. Ces formules conduisent à des méthodes expérimentales simples permettant de déterminer le coefficient géométrique moyen de rayonnement dans le cas de problèmes très généraux et de surfaces grises.

Zusammenfassung—Auf der Grundlage der modernen Theorie der Temperaturstrahlung wurden analytische Formeln abgeleitet, mit deren Hilfe man zu einfachen experimentellen Methoden bei der Bestimmung des mittleren Flächenverhältnisses im allgemeinen Falle und bei grau strahlenden Oberflächen gelangt.

Abstract—Аналитическое определение интегральных угловых коэффициентов излучения для большинства практических случаев сопряжено с непреодолимыми трудностями. Известные графические и графоаналитические способы также не приводят к удовлетворительному решению вопроса в целом.

В данной работе предпринята попытка решить задачу экспериментальным путём. С этой целью найдены аналитические соотношения, которые позволили создать простые экспериментальные методы определения угловых коэффициентов излучения в общем случае пространственной задачи, что весьма важно для теплотехнических расчётов лучистого теплообмена. Кроме этого, оказалось возможным находить оптические характеристики серых поверхностей: интегральных коэффициентов поглощения, отражения и излучения.

THE average geometrical factor is of great importance when the modern analytical methods of heat transfer theory by radiation are being applied to the solution of engineering problems.

$$\phi_{ik} = \frac{1}{\pi F_i} \int_{F_i} \int_{F_k} \cos \theta_{ik} \cdot d\omega_{ik} \cdot dF_k \qquad (1)$$

This coefficient expresses physically the relation of radiant heat flow Q_{ak} emitted by a black surface i and which is incident upon the surface k, to the total radiating heat flow emitted by the surface Q_{0i} into the semispace in the direction of k.

θ_{ik} in the formula (1) is the angle between the direction of the radiation and the normal to the platform dF_k situated at the surface k; $d\omega_{ik}$ is an elementary solid angle with the opening angle at dF_i. The application of the integral formula (1) is rather complicated in practice.

The involved graphical and analytical methods of approximative evaluation of ϕ_{ik} [1–10] do not give a satisfactory solution to the problem.

The experimental method set forth below

simplifies not only the determination of ϕ_{ik} but also of some other optical parameters as well.

Let us consider an unenclosed radiating system of two arbitrarily situated thin and reciprocally concaved plates (1) and (2) shown in Fig. 1. Suppose that the internal surfaces of the plates (1) and (2) are grey ($0 < A_1, A_2 < 1$) and their external surfaces are black ($A_1^1 = A_2^1 = 1$) where A_1, A_2, A_1^1, A_2^1 are the total absorption coefficients.

It is assumed that we have a constant energy source with a continuous and uniform heat flow supply along the external surface of the plate.

If the plates (1) and (2) are placed (Fig. 1) into a medium permeable to heat rays then a stationary thermal regime will be established

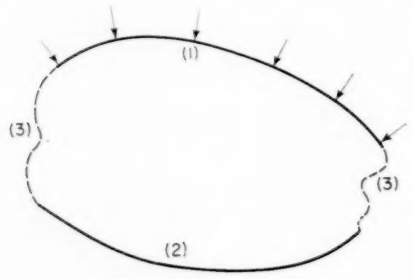

FIG. 1.

between them as a result of heat transfer by radiation and under the conditions of such a thermal regime the plates will have absolute temperatures $T_1 = \text{const.}$ and $T_2 = \text{const.}$

Using equation (1)

$$\frac{E_r(M)}{A(M)} - \int_F R(N)\frac{E_r(N)}{A(N)}K(M,N)dF_M = \int_F E_0 \cdot K(M,N)dF_M - E_0(M), \qquad (2)$$

where E_r and E_0 are the densities of incident and black radiation, respectively, A and R grey body absorption and reflection coefficients, $K(M,N)\,dF_M$ an elementary geometrical factor. The indices M and N at the values entering the equation (2) indicate that these values correspond to the points at the boundary surface of the radiating body under consideration at given points M and N.

If a closed radiating system consists of a finite number n of optically uniform grey surfaces at

$$\phi_{ik} = \phi(M_i, F_k), \quad (i,k = 1,2,3,\ldots) \qquad (3)$$

where $\phi(M_i,F_k)$ is a radiating local geometrical factor then the equation (2) converts into a final system of linear algebraic equations of the following type [12, 13].

$$E_{ri} = A_i \sum_{k=1}^{n} A_k \cdot \Phi_{ik}E_{ik}, \qquad (4)$$

where

$$\Phi_{ik} = \phi_{ik} + \sum_{j=1}^{n} R_j \Phi_{ij}\phi_{jk} \quad (i,k = 1,2,3,\ldots) \qquad (5)$$

$$E_{ik} = E_{0k} - E_{0i}$$

when E_{0k} and E_{0i} are densities of black radiation ($E_0 = \sigma_0 T^4$) relative to the surfaces k and i.

The parameter Φ_{ik} expresses the optical and geometrical properties of any pair of grey surfaces i and k depending on all the grey surfaces entering the given system. If the surfaces are black then $\Phi_{ik} = \phi_{ik}$.

The radiating system under consideration differs from those described by the equations (3) and (4) not only by the fact that this system is an unenclosed one, but also by the fact that the plate (2) is absorbing a radiating energy by one of its surfaces (internal) and radiates by both—internal and external.

The first difference is not an important one, since an unenclosed system may be easily converted into a closed one by an imaginary cover (3) (Fig. 1), the optical properties of which may depend upon the surrounding conditions. For example, in the system under consideration this cover has black body properties ($A_3 = 1$) at absolute zero ($T_3 = 0$).

The second difference is more important since it leads to a different expression for E_{r2} than follows from the equations (3) and (4).

So, taking all this into account we can find the following expression for the density of the total radiation of the plate

$$E_{r2} = A_2 \sum_{k=1}^{3} A_k \Phi_{2k} E_{k2} - E_{02} \qquad (6)$$

In the case of the steady-state thermal regime for a given radiating system $E_{r2} = 0$, and therefore equation (6) becomes

$$A_2A_1\Phi_{21}E_{12} + A_2^2\Phi_{22}E_{22} + A_2A_3\Phi_{23}E_{32} = E_{02} \qquad (7)$$

But as we have

$$A_3 = 1,$$
$$E_{22} = E_{02} - E_{02} = 0,\ E_{03} = 0,$$
$$E_{32} = E_{03} - E_{02} = -E_{02},$$

then from the equation (7) we get

$$A_1 \cdot A_2 \cdot \Phi_{21} E_{12} - A_2 \Phi_{23} E_{02} = E_{02} \qquad (8)$$

The conditions of the system being closed relative to the surface (2) are determined by the expression

$$\sum_{k=1}^{3} A_k \cdot \Phi_{2k} = 1 \qquad (9)$$

The solution of the equations (8) and (9) taken together relative to Φ_{21} gives:

$$\Phi_{21} = \frac{1}{A_1 \cdot A_2} (1 + A_2 - A_2^2 \Phi_{22}) \frac{E_{02}}{E_{01}} \qquad (10)$$

or, as $E_{02} = \sigma_0 T_2^4$ and $E_{01} = \sigma_0 T_1^4$, so

$$\Phi_{21} = \frac{1}{A_1 A_2} (1 + A_2 - A_2^2 \Phi_{22}) \left(\frac{T_2}{T_1}\right)^4 \qquad (11)$$

The function Φ_{22} depends not only upon the process of radiating flow reflections from the grey surface of the plate (2) upon itself as it has a concave form, but also on the geometrical configuration and optical properties of the radiating system as a whole. This function is determined from the equations (5) for $i = 1{\cdot}2$ and $k = 2$.

$$\left.\begin{aligned} \Phi_{12} - \sum_{j=1}^{3} R_j \phi_{1j} \Phi_{j2} &= \phi_{12} \\ \Phi_{22} - \sum_{j=1}^{3} R_j \phi_{2j} \Phi_{j2} &= \phi_{22} \end{aligned}\right\} \qquad (12)$$

i.e.

$$\Phi_{22} = \frac{\gamma_2(\phi_{22} + \gamma_1 R_1 \phi_{12} \phi_{22})}{1 - \gamma_1 \gamma_2 R_1 R_2 \phi_{12} \phi_{21}} \qquad (13)$$

where

$$\gamma_1 = \frac{1}{1 - R_1 \phi_{11}},\quad \gamma_2 = \frac{1}{1 - R_2 \phi_{22}} -$$

are the reflection coefficients of the surfaces (1) and (2), respectively.

Introducing Φ_{22} from (13) into (11) we get:

$$\Phi_{21} = \frac{1}{A_1 A_2} \left[1 + A_2 - A_2^2 \frac{\gamma_2(\phi_{22} + \gamma_1 R_1 \phi_{12} \phi_{21})}{1 - \gamma_1 \gamma_2 R_1 R_2 \phi_{12} \phi_{21}}\right] \cdot \left(\frac{T_2}{T_1}\right)^4 \qquad (14)$$

Thus, taking into account the known properties of geometrical factors, one may write

$$\Phi_{21} F_2 = \Phi_{12} F_1 \qquad (15)$$

where F_1 and F_2 are the heat transfer areas of the plates (1) and (2), and hence

$$\Phi_{12} = \frac{F_2}{F_1 A_1 A_2} \left[1 + A_2 - A_2^2 \frac{\gamma_2(\phi_{22} + \gamma_1 R_1 \phi_{12} \phi_{21})}{1 - \gamma_1 \gamma_2 R_1 R_2 \phi_{12} \phi_{21}}\right] \left(\frac{T_2}{T_1}\right)^4 \qquad (16)$$

If (1) and (2) are the plane plates, then

$$\phi_{11} = \phi_{22} = 0,\ \gamma_1 = \gamma_2 = 1,$$

and consequently

$$\Phi_{12} = \frac{F_2}{F_1 A_1 A_2} \left(1 + A_2 - A_2^2 \frac{R_1 \phi_{12} \phi_{21}}{1 - R_1 R_2 \phi_{12} \phi_{21}}\right) \left(\frac{T_2}{T_1}\right)^4 \qquad (17)$$

$$\Phi_{21} = \frac{1}{A_1 A_2} \left(1 + A_2 - A^2 \frac{R_1 \phi_{12} \phi_{21}}{1 - R_1 R_2 \phi_{12} \phi_{21}}\right) \left(\frac{T_2}{T_1}\right)^4 \qquad (18)$$

Suppose that the opposite internal surfaces (1) and (2) are black, i.e. $A_1 = A_2 = 1$, and so $\gamma_1 = \gamma_2 = 1$. From equations (12) and (16) we get

$$\left.\begin{aligned} \Phi_{12} = \phi_{12} &= \frac{F_2}{F_1} \left(2 - \phi_{22}\right) \left(\frac{T_2}{T_1}\right)^4 \\ \Phi_{21} = \phi_{21} &= (2 - \phi_{22}) \left(\frac{T_2}{T_1}\right)^4 \end{aligned}\right\} \qquad (19)$$

for the concave surfaces and

$$\left.\begin{aligned} \Phi_{12} = \phi_{12} &= 2 \frac{F_2}{F_1} \left(\frac{T_2}{T_1}\right)^4 \\ \Phi_{21} = \phi_{21} &= 2 \left(\frac{T_2}{T_1}\right)^4 \end{aligned}\right\} \qquad (20)$$

for the plane surfaces.

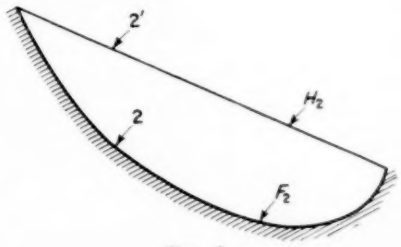

FIG. 2.

The geometrical factor ϕ_{22} characterizes the concavity of the surface (2) and may be expressed through the areas F_2 and H_2 (Fig. 2), where F_2 is the effective area of the concave surface (2), and H_2 is the area of its closing surface. From the condition of closeness

$$\left.\begin{aligned}\phi_{22} + \phi_{22'} &= 1,\\ \phi_{2'2} &= 1.\end{aligned}\right\} \tag{21}$$

But as

$$F_2\phi_{22'} = H_2\phi_{2'2} = H_2, \tag{22}$$

then

$$\phi_{22} = 1 - \frac{H_2}{F_2} \tag{21'}$$

Introducing ϕ_{22} from (21) into (19) we get:

$$\left.\begin{aligned}\phi_{12} &= \frac{H_2 + F_2}{F_1}\left(\frac{T_2}{T_1}\right)^4\\ \phi_{21} &= \left(1 + \frac{H_2}{F_2}\right)\left(\frac{T_2}{T_1}\right)^4\end{aligned}\right\} \tag{22'}$$

From the last formulae we can see that it is possible to determine ϕ_{12} and ϕ_{21} if F_1, F_2, H_2, T_1, T_2 are known. The first, the second and the third ones are usually given and it is quite possible to determine T_1 and T_2 experimentally, as shown by the writer [14].

And now using the equations (15) and (16) we can get the expressions which determine the absorption (reflection) coefficient of the grey surfaces experimentally. Let us analyse the following cases:

Assume that the inside surface of the plate (1) shown in Fig. 1 is black ($A_1 = 1$) and the outside surface of the plate (2) is grey ($0 < A_2 < 1$). If the outside surface of the plate (2) is black, then on the basis of the equation (15) the absorption coefficient A_2 becomes:

$$A_2 = \frac{T_2^4}{\phi_{21}T_1^4 - T_2^4} \tag{23}$$

The plate (2) being black from both surfaces ($A_2 = A_2^1 = 1$) and the inside surface of the plate (1) being grey ($0 < A_1 < 1$) then as it was mentioned above, we get on the basis of the equation (15)

$$A_1 = \frac{2 - \phi_{12}\phi_{21}}{\phi_{21}[(T_1/T_2)^4 - \phi_{12}]} \tag{24}$$

The internal opposite surfaces of the plates (1) and (2) are black ($A_1 = A_2 = 1$) and the outside surface of the plate (2) is grey ($0 < A_2^1 < 1$) Then the equation (6) must be rearranged to the following form:

$$E_{r2} = \sum_{k=1}^{3} A_k\Phi_{2k} \cdot E_{k2} - A_2^1E_{02} \tag{25}$$

Since

$$E_{r2} = 0,\ A_1 = A_2 = 1,$$

then

$$\Phi_{21}E_{12} - \Phi_{23}E_{02} = A_2^1E_{02} \tag{26}$$

Thus

$$\sum_{k=1}^{3} A_k\Phi_{2k} = \sum_{k=1}^{3} \phi_{2k} = \phi_{21} + \phi_{22} + \phi_{23} = 1 \tag{27}$$

or

$$\Phi_{21} = \phi_{21},\ \Phi_{23} = \phi_{23},\ \Phi_{22} = \phi_{22} = 0. \tag{28}$$

Taking this into account we get from the equation (26)

$$A_2^1 = \phi_{21}\left(\frac{T_1}{T_2}\right)^4 - 1 \tag{29}$$

In accordance with the known expressions

$$R = 1 - A \text{ and } \sigma = \sigma_0 A \tag{30}$$

where σ and σ_0 are the radiation coefficients of the grey and black bodies, respectively. The formulae (23), (24) and (29) lead to the explicit dependence

$$\sigma,\ R = f(T_1 \cdot T_2)$$

Consequently, from formulae (23), (24) and (29) it is possible to determine A, R and σ if ϕ_{12}, ϕ_{21}, T_1, T_2 are known. ϕ_{12} and ϕ_{21} may be given, and T_1, T_2 may be easily found experimentally. Therefore it is better to deal with the radiating system of two round and flat plates with the equal diameters.

It the plates are placed in parallel with the normal through their centres then (15):

$$\phi_{12} = \phi_{21} = \left[\sqrt{\left\{1 + \left(\frac{h}{d}\right)^2\right\}} - \frac{h}{d}\right]^2 \tag{31}$$

where $d = d_1 = d_2$ and h are their diameters and the distance between them, respectively.

Vol. 1 1960

The distance between them is taken out in accordance with the design of the apparatus.

The experimental method of determination of A, R and σ, which is described by the writer [16], was created on the basis of the previously given expressions.

The further analysis, which is not adduced here, gives the possibility of receiving the analogous expressions and the corresponding methods of the experimental determination of the radiation optical and geometrical parameters Φ_{ik}, γ_{ik} and others.

Finally we may note that the derived formulae for ϕ_{ik}, ϕ_{ki} and A are based on the assumption that the given radiating system is in an empty space of an infinite length.

However, the real condition does not correspond to this. The laboratory room where the plates (1) and (2) are placed is limited by the walls, the ceiling and the floor, and is filled with air. Because of this the surfaces of the heated plates (1) and (2) will take part not only in the convective heat transfer with air, but also in the heat transfer by radiation with floor, ceiling and the walls of the room. The above mentioned factors cannot effect the temperature of the surface (1), since the conditions $T_1 = \text{const.}$ are provided by the heater.

On the contrary, the heat transfer by convection between the plate (2) and air, and the heat transfer by radiation of the above mentioned and other bodies, except the plate (1), lead to the fact that the temperature T_2 will turn out to be different and will not correspond to the conditions of the derivation of formulae for ϕ_{ik}, ϕ_{ki}, A, R and σ.

Nevertheless, we can choose such a temperature field for the plate (2), that the influence of the external factors on it and, consequently, on the accuracy of the determination of ϕ_{ik}, ϕ_{ki}, A becomes irrelevant.

This phenomenon is explained by the fact that the heat loss by the plate (2) because of convection at a certain temperature is compensated by the inflow of heat to it as the barriers of the room also emit radiation. For example, the investigations showed [14] that this compensation takes place at $T_2 = 323° - 333°\text{K}$ when the experiment is performed at the room conditions. T_1 and T_2 are determined by the experiment as average values on the surfaces F_1 and F_2.

REFERENCES

1. H. GRÖBER, *Die Grundgesetze der Wärmestrahlung und ihre Anwendung auf Dampfkessel mit Innenfeuerung*. Springer Verlag, Berlin (1917).
2. W. NUSSELT, *Z. Ver. dtsch. Ing.* **78**, (1928).
3. SEIBERT, *Forsch. Arb. Ingwes.* No. 324 (1930).
4. KESSLER, *Z. bayer. (Dampfk) RevisVer.* **29**, 115 (1925).
5. H. C. HOTTEL, *Heat Transfer* by V. MACADAMS. Russian translation, Moscow (1936).
6. T. T. USENKO, *Izv. Gozn. Inst.* No. 3 (1920).
7. V. N. TIMOFEEV, *Izv. VTI*, No. 9 (1934).
8. G. L. POLYAK, *Izv. Akad. Nauk SSSR, OTN*, No. 3 (1937).
9. G. L. POLYAK, *Izv. Energet. Inst. Akad. Nauk SSSR* **3** (1937).
10. S. P. SYROMYATNIKOV, *Teplovaya Rabota Paravoznoj Topki*. Transjeldozirdat (1953).
11. U. A. SURINOV, *Izv. Akad. Nauk SSSR, OTN*, No. 7 (1948).
12. U. A. SURINOV, *Izv. Akad. Nauk SSSR, OTN*, No. 7 (1953).
13. U. A. SURINOV, *Dokl. Akad. Nauk SSSR* **33**, No. 2 (1952).
14. D. T. KOKOREV, *Trud. Mosk. inst. Khim. Mash.* **12** (1957).
15. M. V. KIRPICHEV and others, *Kotelnye Ustanovki*, Vol. 1. Energoizdat, Moscow (1947).
16. D. T. KOKOREV, *Trud. Mosk. inst. Khim. Mash.* **12** (1957).

Int. J. Heat Mass Transfer. Vol. 1, pp. 28–36. Pergamon Press 1960. Printed in Great Britain.

THERMAL RADIATION BETWEEN PARALLEL PLATES SEPARATED BY AN ABSORBING–EMITTING NONISOTHERMAL GAS

C. M. USISKIN* and E. M. SPARROW†
NASA, Lewis Research Center, Cleveland, Ohio, U.S.A.

(*Received* 9 *January* 1959)

Abstract—A complete formulation, including the local details of gas absorption–emission processes, has been made for thermal radiation in a parallel plate enclosure. The temperature is permitted to vary continuously between the plates, and the emissive power of the gas may have an arbitrary dependence on temperature. Thermal conductivity effects have been omitted. Solutions of the governing integral equations have been carried out for values of the single governing parameter kL (k = absorption coefficient, L = spacing) in the range 0·1 to 2·0. Temperature distributions and heat transfer results are given. For moderate values of kL, the temperature is quite uniform across the gas.

Résumé—Une formulation complète comprenant les caractéristiques détaillées et locales d'absorption et d'émission d'un gaz a été établie pour le rayonnement dans un enceint formée par façon continue entre les plaques et le pouvoir émissif du gaz peut dépendre d'une façon quelconque de la température. Les effets de conductibilité thermique ont été négligés. Des solutions aux équations intégrales du problème ont été calculées pour des valeurs du paramètre déterminant, kL, comprises entre 0,1 et 2 (k coefficient d'absorption, L écartement des plaques). Les distributions de températures et des résultats sur le le transfert de chaleur sont donnés. Pour des valeurs modérées de kL la température est pratiquement uniforme dans le gaz.

Zusammenfassung—Für die thermische Strahlung in einem Hohlraum mit parallelen Wänden wird die vollständige Formulierung angegeben einschließlich der örtlichen Einzelheiten der Absorption und Emission des Gases. Die Temperatur soll sich innerhalb der Wände kontinuierlich ändern und das Emissionsvermögen des Gases soll beliebig von der Temperatur abhängen. Wärmeleitung wird nicht in Betracht gezogen. Die maßgebenden Integralgleichungen wurden für einen Bereich des einzigen maßgebenden Parameters kL = 0,1 bis 2,0 gelöst (k = Absorptionskoeffizient, L = Abstand). Temperaturverteilungen und Wärmeübertragung sind angegeben. Für mittlere Werte kL ist die Temperatur einheitlich innerhalb des Gases.

Abstract—В статье дано решение задачи лучистого теплообмена между двумя параллельными пластинами с учётом излучения и поглощения газа, находящегося между ними. При этом предполагается непрерывное изменение температуры между пластинами, а лучеиспускательная способность газа является любой функцией температуры. Решения основных интегральных уравнений даны для значения параметра kL от 0·1 до 2·0, где k—коэффициент лучепоглощения, L—линейный размер системы. Приведены результаты расчётов температурного поля и потоков тепла. Для других значений kL температура газа принимается постоянной в плоскости сечения системы.

NOMENCLATURE

e_b = emissive power of black wall, σT^4;
e_g = emissive power of gas element, see equation (2);
k = absorption coefficient (logarithmic decrement of radiation);
L = spacing between plates;
q = net rate of heat transfer per unit area to wall;
r = distance between emitting and receiving elements;
S = internal heat source per unit volume;

* Present address: RCA, Princeton, New Jersey.
† Present address: Professor of Mechanical Engineering, University of Minnesota, Minneapolis, Minnesota.

Vol. 1 1960

T = absolute temperature;
X = dimensionless normal co-ordinate, x/L; X_0, dimensionless co-ordinate of absorbing volume, x_0/L;
x = distance measured normal to lower plate; x_0, distance of absorbing volume from lower plate;
y = radial co-ordinate in plane of walls;
δ = infinitesimal diameter of absorbing sphere;
θ = angle between surface normal and direction of absorbing volume (see Fig. 3);
λ = integration variable;
Φ = dimensionless emissive power $(e_g - e_b)/(S/2k)$;
ϕ = dimensionless emissive power $(e_g - e_{b1})/(e_{b2} - e_{b1})$.

Differentials

dA_s = wall surface area;
dA_τ = surface area of radiating gas strip (see Fig. 2);
$d\omega$ = solid angle;
$d\tau$ = gas volume;

Subscripts

1 = lower wall;
2 = upper wall.

INTRODUCTION

THE high temperature levels achieved in modern propulsion systems (as well as in furnaces) demand that heat transfer calculations include radiation effects of absorbing–emitting gases which may lie between heat transfer surfaces. In general, the gas would be non-uniform in temperature and may contain heat sources. The general problem would involve heat transfer by convection and conduction as well as by radiation. However, it appears that even the simpler situation of purely radiant interchange between surfaces separated by a non-isothermal, absorbing–emitting gas has not yet been fully solved. It is to this latter problem to which we turn our attention here.

Specifically, consideration is given to a system composed of two parallel plates, each infinite in extent, which are separated by a gap of thickness L. The configuration is shown schematically in Fig. 1. The plate temperatures T_1 and T_2 are specially uniform, but may differ from one another. The gas filling the gap will be permitted to take a full part in the radiative heat exchange, absorbing energy and also re-emitting. The gas temperature will, in general, vary across the gap. Further, there may be a heat source in the gap.

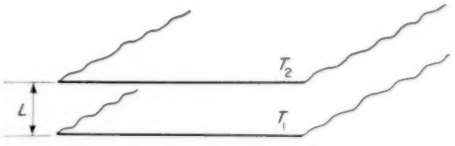

FIG. 1. Parallel plate enclosure.

Within the framework of the limiting assumptions, our aim is to make a complete formulation of the problem in which the details of local absorption and emission processes are accounted for. Applying conservation of energy to an infinitesimal gas volume element, we are led to an integral equation for the emissive power (temperature). Solutions have been carried out for several values of the governing parameter kL (k = absorption coefficient), yielding temperature distributions and heat flux rates. Among the results of practical interest, there is quantitatively displayed the manner in which the heat transfer decreases as the gas becomes more absorbant.

Heat transfer by conduction through the gas can be included in the formulation. But, its introduction into the problem introduces mathematical non-linearities which significantly complicate the solution of the governing integral equation. In the present study, conduction has not been accounted for. It is interesting to note that the techniques used in setting up the present problem also apply to other geometries.

From a review of the literature on radiation in a parallel plate enclosure, it would appear that previous investigations have given incomplete consideration to the role of the gas. For example, Jakob [1] (p. 105) computes the absorption in a gas layer as radiant energy passes from a hotter to a colder wall. But, the gas is not permitted to re-radiate, as it must under steady state conditions. By ignoring the emission of the gas, Jakob circumvents the problem of computing the temperature distribution of the

gas; and as a consequence, his analysis does not permit a complete computation of the net heat transfer. A practical procedure has been proposed by Wohlenberg [1] (p. 132) for computing the net heat transfer in a gas-filled parallel plate enclosure. He ignores the local absorption–emission processes, supposing the gas to be isothermal and to radiate as a whole according to Stephan–Boltzmann's law.

An important engineering approach in the study of non-isothermal radiating gas bodies has been made by Hottel and Cohen [2]. They provide interchange factors between *finite*-sized rectangular gas volumes situated at various orientations with respect to one another. Similar information is also given for surface-to-volume radiation. Such factors are useful when a radiation problem is formulated by subdividing the gas body into a group of finite volumes elements, each of which possesses a uniform temperature different from its neighbors. The approach of the present analysis differs from Hottel and Cohen in that the temperature is permitted to vary continuously throughout the gas and energy conservation is therefore applied to *infinitesimal* volume elements.

Readers who are interested primarily in results are invited to pass over the Analysis section.

ANALYSIS

Conservation of energy

We now proceed to study the purely radiative exchange in the parallel plate system of Fig. 1. Attention is focused on an infinitesimal volume element dV, and the conservation of energy principle is applied. According to this law, the energy content of the element must remain constant in the steady state; and as a consequence, inflow must equal outflow. Energy arrives at the element dV due to radiation emitted at both bounding walls and due to radiation emitted in the remainder of the gas body. In addition, there may be an internal heat source S which also supplies an energy input into dV. For simplicity, it will be supposed that the walls behave as black bodies so that there is no indirect energy transfer due to reflections at the surface. The analysis can be extended to include the effects of non-black walls.

Then, we can write the conservation principle for dV as:

$$\left.\begin{array}{l} \text{energy absorbed in } dV \text{ from emission of gas body} \\ + \text{ energy absorbed in } dV \text{ from emission of lower wall} \\ + \text{ energy absorbed in } dV \text{ from emission of upper wall} \\ + \text{ internal heat generation} \\ = \text{ energy emitted by } dV \end{array}\right\} \quad (1)$$

Our task is to evaluate the various terms of this expression. In the derivation that follows, it will be assumed that the gas occupying the enclosure is gray, so that the absorption coefficient* k is independent of wavelength. Further, k will be taken as independent of temperature. In principle, extension can be made to the situation where k depends on wavelength and/or temperature, with the net result of enormously increasing the difficulty of obtaining solutions to the problem. We will select a spherical element of diameter δ for our infinitesimal volume dV. Separate examination of the terms comprising equation (1) will be made in the ensuing paragraphs.

Energy absorbed in dV from emission of gas body

The derivation of this quantity is facilitated by reference to Fig. 2. We focus attention on the volume dV located at a distance x_0 from the

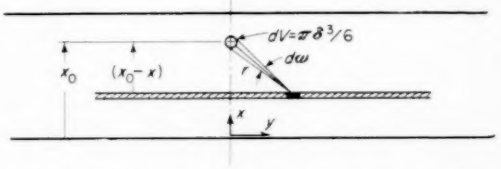

FIG. 2. Diagram for deriving absorption at dV due to gas emission.

lower surface. The first step is to determine the energy absorbed in dV due to the emission of the cross-hatched gas layer situated at a distance $(x_0 - x)$ below dV. Since the temperature depends only on x, the emission per unit volume of such a layer is spatially uniform.

* Jakob uses the alternate designation: logarithmic decrement of radiation.

Vol. 1 1960

It will be supposed that the emission from a gas volume $d\tau$ can be written as

$$4ke_g\, d\tau \tag{2}$$

which includes as a special case the conventional representation [2]

$$4k\sigma T^4\, d\tau \tag{2a}$$

Under the assumption that an infinitesimal element of the gas radiates uniformly in all directions, it follows that the energy leaving the shaded volume through a solid angle $d\omega$ is

$$4ke_g(dA_\tau\, dx)\,\frac{d\omega}{4\pi} \tag{3}$$

where $d\tau = dA_\tau\, dx$. Of this amount, there arrives at dV

$$\frac{ke_g}{\pi}\, dA_\tau\, dx\, d\omega\, e^{-k\tau} \tag{4}$$

the exponential factor accounting for the absorbing effects of the intervening gas.

Since we are dealing with infinitesimal bodies, the rays arriving at dV from the shaded volume form a *parallel* bundle. As is shown in the Appendix, the energy absorbed (per unit of arriving energy) by a sphere of diameter δ on which there impinges a bundle of parallel rays is

$$\frac{2}{3}\,k\delta \tag{5}$$

So, of the energy leaving the shaded volume, the amount

$$\frac{2}{3\pi}\,k^2\delta\, e_g\, dA_\tau\, dx\, d\omega\, e^{-k\tau} \tag{6}$$

is absorbed in the spherical volume dV.

Now, we proceed to compute the absorption in dV due to energy emitted by the entire cross-hatched strip. From geometrical considerations, making use of symmetry, we have

$$d\omega = \frac{\pi\delta^2/4}{r^2},\quad dA_\tau = 2\pi y\, dy,\quad r^2 = y^2 + (x - x_0)^2$$

Introducing these relations into (6), we integrate from $y = 0$ to $y = \infty$ and thereby obtain the contribution of the entire strip to the absorption in dV. The result of the integration can be rephrased in the following form

$$2k^2e_g\, dV\left[\int_{k(x_0 - x)}^{\infty}(e^{-\lambda}/\lambda)d\lambda\right] dx \tag{7}$$

where the bracketed quantity is called the exponential integral and has been tabulated to high accuracy in reference [3].

The entire gas body can be considered as being made up of a series of cross-hatched strips. Each strip contributes an amount of energy to dV depending on the distance $(x_0 - x)$ and upon the local temperature (i.e. the local value of e_g). The energy absorbed in dV from all the emitting gas strips is found by adding up (integrating) the contributions of each strip. Then, the final expression for the energy absorbed at dV due to the emission of the entire gas body is

$$2k^2\, dV\left\{\int_0^{x_0} e_g\left[\int_{k(x_0-x)}^{\infty}(e^{-\lambda}/\lambda)d\lambda\right] dx + \right.$$
$$\left. + \int_{x_0}^{L} e_g\left[\int_{k(x-x_0)}^{\infty}(e^{-\lambda}/\lambda)d\lambda\right] dx\right\} \tag{8}$$

Energy absorbed in dV from emission of walls

Consideration is first given to the energy emitted at the lower wall, and attention is directed to Fig. 3. Since it has been assumed that

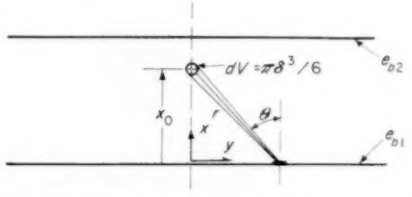

FIG. 3. Diagram for deriving absorption at dV due to surface emission.

the wall is black, the energy leaving the darkened segment of surface area dA_s in the direction θ in a solid angle $d\omega$ is

$$\frac{e_{b1}}{\pi}\, dA_s \cos\theta\, d\omega \tag{9}$$

This energy travels a distance r before encountering the spherical element dV. As a consequence

of absorption in the intervening gas, there arrives at dV

$$\frac{e_{b1}}{\pi}\, dA_s \cos\theta\, d\omega\, e^{-kr} \tag{10}$$

As already discussed in the preceding section, the sphere (diameter δ) absorbs $2k\delta/3$ of this amount. So, the contribution of the surface area dA_s to dV is

$$\frac{2}{3\pi}\,\delta\, ke_{b1}\, dA_s \cos\theta\, d\omega\, e^{-kr} \tag{11}$$

Since dA_s is a typical element of the lower wall, the contribution of the entire wall may be found by integrating equation (11). Introducing the relations

$$d\omega = \frac{\pi\delta^2/4}{r^2}, \quad dA_s = 2\pi y\, dy,$$

$$r^2 = y^2 + x^2, \cos\theta = x_0/r$$

integration over the range $y = 0$ to $y = \infty$ gives, after rearrangement

$$2k\, e_{b1}\, dV \left[\exp(-kx_0) - kx_0 \int_{kx_0}^{\infty} (e^{-\lambda}/\lambda)d\lambda\right] \tag{12}$$

Equation (12) represents the energy absorption in dV due to black body emission at the lower surface. In an analogous way, the contribution to dV from black body radiation at the upper surface can be written as

$$2k\, e_{b2}\, dV \left[\exp\{-k(L - x_0)\} - k(L - x_0) \int_{k(L-x_0)}^{\infty} (e^{-\lambda}/\lambda)d\lambda\right] \tag{13}$$

Internal heat generation

There may be an internal heat source in the gas due to chemical reactions, electric currents, etc. Suppose that the heat generation rate per unit volume is denoted by S; so within dV, there is generated

$$S\, dV \tag{14}$$

Within the framework of our model, S can be a function of x; but it will be taken as a constant here.

Governing equation for the temperature (e_g) *distribution*

We are now in a position to evaluate the conservation equation (1) using the results of the preceding paragraphs. Gathering together the successive terms respectively represented by equations (8), (12), (13) and (14) and equating to the emission as given by equation (2) with $d\tau = dV$, we arrive at

$$\left.\begin{aligned}
&\int_0^{x_0} e_g(x) \left[\int_{k(x_0-x)}^{\infty} (e^{-\lambda}/\lambda)d\lambda\right]dx + \\
&\quad + \int_{x_0}^{L} e_g(x) \left[\int_{k(x-x_0)}^{\infty} (e^{-\lambda}/\lambda)d\lambda\right]dx + \\
&\quad + e_{b1}\left[\frac{\exp(-kx_0)}{k} - \right. \\
&\qquad \left. - x_0 \int_{kx_0}^{\infty} (e^{-\lambda}/\lambda)d\lambda\right] + \\
&\quad + e_{b2}\left[\frac{\exp\{-k(L - x_0)\}}{k} - \right. \\
&\quad \left. - (L - x_0) \int_{k(L-x_0)}^{\infty} (e^{-\lambda}/\lambda)d\lambda\right] + \\
&\qquad + S/2k^2 = \frac{2}{k}\, e_g(x_0)
\end{aligned}\right\} \tag{15}$$

This integral equation governs the variation of the emissive power e_g with x. Since, in general, e_g would be a specific function of temperature, it follows that equation (15) can as be regarded as the governing equation for the temperature distribution.

It is evident that equation (15) is linear in e_g. This suggests a rather convenient reduction of the general problem which includes different wall temperatures ($e_{b1} \neq e_{b2}$) and a non-zero heat source to two simpler problems. One of these is the case of different wall temperatures in the *absence* of a heat source; while the second is the case of an internal heat source with *identical* wall temperatures. The solution of the general case is simply a linear sum of the two. These separate situations are discussed separately below.

Different wall temperatures; no heat source

In the absence of a heat source, it is convenient to introduce the dimensionless emissive power ϕ as follows

Vol. 1 1960

$$\phi = \frac{e_g - e_{b1}}{e_{b2} - e_{b1}} \tag{16}$$

Substituting into equation (15) and integrating by parts, we find the following integral equation for ϕ

$$\left.\begin{aligned}&\int_0^{X_0} \phi(X)\left[\int_{kL(X_0-X)}^{\infty}(e^{-\lambda}/\lambda)d\lambda\right]dX + \\ &+\int_{X_0}^{1}\phi(X)\left[\int_{kL(X-X_0)}^{\infty}(e^{-\lambda}/\lambda)d\lambda\right]dX + \\ &+\frac{\exp\{-kL(1-X_0)\}}{kL} - \\ &-(1-X_0)\int_{kL(1-X_0)}^{\infty}(e^{-\lambda}/\lambda)d\lambda = \\ &\qquad\qquad \frac{2}{kL}\phi(X_0)\end{aligned}\right\} \tag{17}$$

where $X = x/L$. It may be observed that only a single parameter, kL, appears in the integral equation.

It is thus seen that use of the dimensionless emissive power ϕ removes the need to consider specific values for the wall temperature and reduces the problem to a dependence on one dimensionless parameter, kL.

Of practical interest is the calculation of the heat transfer between the walls. In the steady state, the *net* energy transferred from the hotter wall must be identical to the *net* energy transferred to the cooler wall. Focusing attention on the lower wall, we write

$$\left.\begin{aligned}&\text{net heat transferred to lower wall} \\ &= \text{radiation absorbed from emission of gas body} \\ &+ \text{radiation absorbed from emission of upper wall} - \text{energy emitted}\end{aligned}\right\} \tag{18}$$

To evaluate the gas radiation term, we first find the contribution from the elementary cross-hatched strip of Fig. 2 and then integrate over all strips. The radiation from the upper wall is evaluated in a straightforward way taking proper account of absorption in the intervening gas. After a lengthy calculation, equation (18) is evaluated to be

$$\left.\begin{aligned}\frac{q}{e_{b2}-e_{b1}} &= 2kL\int_0^1 \phi e^{-kLX}\,dX - \\ &-2(kL)^2\int_0^1 \phi X\left[\int_{kLX}^{\infty}(e^{-\lambda}/\lambda)d\lambda\right]dX + \\ &+e^{-kL}(1-kL)+(kL)^2\int_{kL}^{\infty}(e^{-\lambda}/\lambda)d\lambda\end{aligned}\right\} \tag{19}$$

where q is the net rate of heat transfer per unit area to the lower wall (or from the upper wall). Since $e_{b2} - e_{b1}$ is the net heat transfer in the absence of an absorbing gas, equation (19) immediately gives the fractional reduction in the heat transfer due to the absorbing–emitting medium.

Uniform internal heat source; same wall temperatures

For this situation, we denote the black body emission common to both walls by e_b. Then, a dimensionless emissive power variable is introduced according to the definition

$$\Phi = \frac{e_g - e_b}{S/2k} \tag{20}$$

Under the transformation, it can be shown using integration by parts that equation (15) simplifies to

$$\left.\begin{aligned}&\int_0^{X_0}\Phi(X)\left[\int_{kL(X_0-X)}^{\infty}(e^{-\lambda}/\lambda)d\lambda\right]dX + \\ &+\int_{X_0}^{1}\Phi(X)\left[\int_{kL(X-X_0)}^{\infty}(e^{-\lambda}/\lambda)d\lambda\right]dX + \\ &\qquad +\frac{1}{kL} = \frac{2}{kL}\Phi(X_0)\end{aligned}\right\} \tag{21}$$

It is interesting to observe that the transformation completely removes the need to consider specific values of the source strength S. The only parameter in the problem is kL. Solution of equation (21) gives the distribution of emissive power (temperature) across the gap, and in particular, the maximum temperature.

The general solution

Since the equations are linear, the general solution can be written in terms of ϕ and Φ. However, care must be taken to dimensionalize

them first. Then, the general solution appears in the form

$$e_g = (e_{b2} - e_{b1})\phi + e_{b1} + \frac{S}{2k}\Phi + e_b$$

where the lower and upper walls have the emmissive powers $(e_b + e_{b1})$ and $(e_b + e_{b2})$, respectively.

RESULTS FOR NO-SOURCE CASE

The governing equation for the no-heat source case, equation (17), has been solved for values of kL equal to 0·1, 0·5, 1 and 2. The solutions were accomplished numerically on a desk calculator using an iterative scheme augmented by the intuition of the operator. Numerical integrations were carried out using the trapezoidal rule and the stability of the solutions was checked by perturbation.

Based on these solutions, the variation of the dimensionless emissive power ϕ across the gap has been plotted in Fig. 4. Utilizing these distributions, the heat transfer has been evaluated

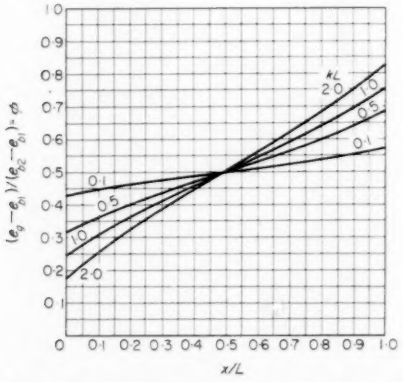

FIG. 4. Distribution of emissive power in a radiating gas between parallel plates (no internal heat source).

from the equation (19) and is shown on Fig. 5. As already noted, the ratio $q/(e_{b2} - e_{b1})$ directly gives the reduction in heat transfer due to the presence of the absorbing–emitting gas.

Turning first to Fig. 4, it may be observed that the curves are relatively flat over a large part of the gap, with the flattening becoming more marked with decreasing values of kL. Consequently, for moderate values of kL, the bulk of the gas body is at a relatively uniform temperature. Under these conditions, the neglect of the temperature dependency of k seems to be vindicated.

The relative uniformity of the temperature in the bulk of the gas suggests that heat conduction effects, which depend on temperature gradients, will be confined to the neighborhood of the walls provided that the thermal conductivity is small. So, there appears to be a boundary layer phenomenon somewhat similar to the situation in fluid dynamics.

The solutions of equation (17), as displayed in Fig. 4, have the property that $e_g \neq e_b$ at the walls ($X = 0$ and $X = 1$). This is completely consistent with our model. In the present problem, where heat conduction is omitted, temperature continuity is not required at the walls. The values taken on by e_g at $X = 0$ and $X = 1$ are simply those required to satisfy energy conservation.

The flattening trend displayed on Fig. 4 with decreasing kL has its analogue in the heat conduction problem in rarefied gases. In that instance, the temperature distribution across the gap passes through a sequence of shapes with decreasing gas density which are qualitatively similar to the curves of Fig. 4. The two phenomena have a qualitatively similar explanation. In the rarefied conducting gas, a decrease in density leads to an increase in mean free path for molecular collisions. For the absorbing–emitting gas, a decrease in kL leads to an increase

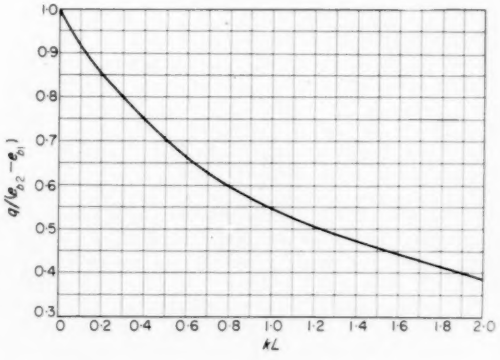

FIG. 5. Heat transfer between parallel plates separated by a radiating gas (no internal heat source).

Vol. 1 1960

in the mean free path (relative to the gap spacing) for photon collisions.

Next, we turn to Fig. 5. The finding that the heat transfer q decreases with increasing kL is quite expected. For instance, it is physically reasonable that increasing the gap spacing L for a gas of given k must increase the resistance to radiative heat flow. A similar conclusion applies when the absorption coefficient is increased for a gap of fixed spacing L. The results of Fig. 5 should be useful in choosing an "insulating gas" to diminish the radiative heat exchange between two surfaces.

RESULTS FOR THE HEAT SOURCE CASE

Solutions of the integral equation (21) which governs the uniform internal heat source case have been carried out numerically for values of kL equal to 0·1, 0·5, 1 and 2. The distribution of the dimensionless emissive power Φ obtained from these solutions is plotted in Fig. 6. In

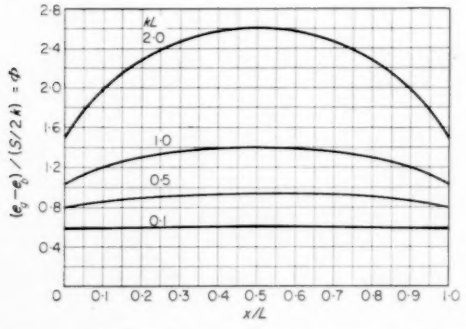

FIG. 6. Distribution of emissive power in a heat generating and radiating gas between parallel plates.

common with the findings of the previous section, it is seen that the curves are relatively flat over a major portion of the gap. The tendency towards flatness increases with decreasing kL. So, for moderate kL there is again an essentially isothermal zone over the major portion of the gas, and the neglect of the temperature dependence of k is vindicated.

It is interesting to study the separate effects of the various physical parameters L, k, and S on the energy (temperature) distribution. Fig. 6 is well suited to study the effect of changing the gap spacing L. For fixed values of k, S and e_b, the only parameter which changes from curve to curve is L. As expected, the temperature level increases as the spacing increases. For small gap spacings, the gas body is essentially isothermal.

Next, we proceed to display the effect of changing k while holding S, L and e_b fixed. Fig. 6 is inadequate, since k appears both as a parameter on the curves and as part of the ordinate variable. To illustrate the effect, we consider the special case where $S/2ke_b = 1$ when $kL = 1$. (Then, as k changes and the other quantities are held fixed, $S/2ke_b$ must change in a corresponding manner.) Fig. 7 has been constructed

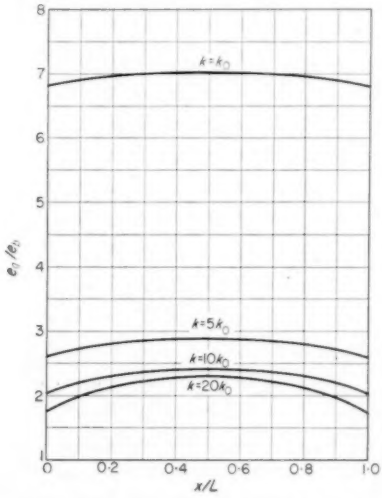

FIG. 7. Effect of k on distribution of emissive power in a heat generating gas for fixed S, L and e_b and $k_0 = S/20e_b$, $L = 2e_b/S$.

on this basis, the distribution of e_g being plotted against x/L with k decreasing by a factor of 20 from the lowest to the highest curve. From the figure, we note the interesting result that the temperature level *increases* as the absorption coefficient k decreases and that this effect is more accentuated at lower values of k. This suggests that the gas temperature may be minimized by using a gas with a high absorption coefficient.

Finally, we can show the effect of changing the source strength S while holding k, L and e_b fixed. For purposes of illustration, consideration is given to the situation where $kL = 1$. Fig. 8,

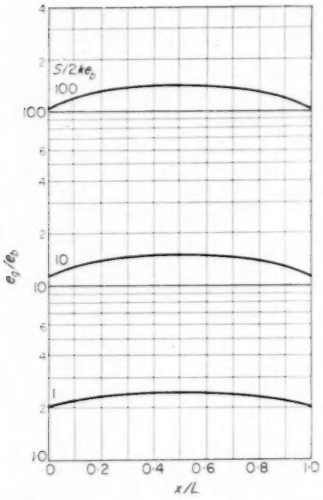

FIG. 8. Effect of heat source S on distribution of emissive power for fixed k, L, and e_b and $kL = 1$.

drawn for values of $S/2ke_b$ of 1, 10 and 100 shows the variation of e_g with distance across of gap. The level of the curves is seen to increase linearly with the source strength, as might have been expected from the linearity of the problem.

CONCLUDING REMARKS

Within the framework of the simplifying assumptions, it has been possible to give an exact formulation for the problem of radiation between two plane walls separated by a non-isothermal absorbing–emitting gas. Numerical solutions have shown the quantitative response of the temperature distribution and heat transfer rate to changes in such parameters as absorption coefficient k, gap spacing L, and heat source S.

For moderate values of kL, the temperature of the gas body is nearly uniform over a large part of the gap, in some measure justifying the neglect of the temperature dependence of k.

Further work involving a more complicated model is clearly indicated. Heat conduction effects would appear to be important in the region near the wall. A more refined treatment might well account for the temperature dependence of k and might consider the non-gray characteristics of real gases. Finally, a variable heat source might also be included.

APPENDIX

Absorption of Parallel Radiation by a Sphere

According to a Nusselt's derivation (reproduced in [1], pp. 100–101), the energy absorbed by a sphere of diameter δ from a parallel bundle of rays of intensity J is

$$J\left\{1 + \frac{2}{(k\delta)^2}\left[[e^{-k\delta}(1 + k\delta) - 1\right]\right\} \quad \text{(A1)}$$

Now, we wish to find the limit of equation (A1) for an infinitesimal sphere. First, the exponential term is expanded in series

$$e^{-k\delta} = 1 - k\delta + \frac{(k\delta)^2}{2} - \frac{(k\delta)^3}{6} + \cdots$$

and then introduced into (A1). After cancellation and retaining only first order infinitesimals, we find that the absorbed energy is

$$J\left(\frac{2}{3}\right)k\delta \quad \text{(A2)}$$

ACKNOWLEDGEMENT

The writers gratefully acknowledge the valuable suggestions of Dr. E. R. G. Eckert, consultant in heat transfer.

REFERENCES

1. M. JAKOB, *Heat Transfer*, Vol. II. John Wiley, New York (1957).
2. H. C. HOTTEL and E. C. COHEN, *A.I. Ch. E. Journal*, **4**, 3 (1958).
3. ANON., *Tables of Sine, Cosine and Exponential Integrals* Vol. I. Federal Works Agency, Work Projects, Administration, Sponsored by National Bureau of Standards (1940).

Vol. 1 1960

Int. J. Heat Mass Transfer. Vol. 1, pp. 37–45. Pergamon Press 1960. Printed in Great Britain.

HIGHLY INTENSIVE HEAT AND MASS TRANSFER IN DISPERSED MEDIA

Y. MIKHAILOV

Institute of Energetics and Electrical Engineering,
Academy of Sciences of the Latvian S.S.R., Riga, U.S.S.R.

(*Received* 24 *September* 1959)

Abstract—A solution is given for a system of differential equations for heat and mass transfer in a dispersed medium in the presence of phase conversions (the evaporation of liquid or steam condensation). The mass transfer is thought to occur under the effect of mass transfer potential gradient $\nabla\theta$, a temperature gradient ∇t and a total pressure gradient ∇p. Solutions are obtained for the heat and mass transfer potentials (t, θ, p) applicable to a one-dimensional problem (an infinite plate and a sphere with boundary conditions of the third order. The solutions are given in the criterion form using heat and mass transfer similarity criteria. An analysis is given of the effect of the separate similarity criteria (Bi_q, Bi_m, Pn, Lu_p) on the fields of heat and mass transfer potentials. The effect of molar (filtration) transfer on heat and mass transfer is shown.

Résumé—La solution du système différentiel régissant le transfert de chaleur et de masse dans un milieu dispersé a été donné en présence de changement de phase (évaporation du liquide et condensation de vapeur). Le transfert de masse est supposé se produire sous l'effet du gradient de potentiel de transfert de masse $\nabla\theta$, du gradient de température ∇t et du gradient de pression totale ∇p. Les solutions pour les potentiels de transfert de chaleur et de masse (t, θ, p) sont obtenues dans le cas du problème unidimensionnel (plaque infinie et sphère) et avec des conditions aux limites de 3ème espèce. Les solutions sont données sous forme de critère par application des critères de similarité relatifs au transfert de chaleur et de masse. Une analyse a été faite sur l'influence des critères de similarité particuliers (Bi_q, Bi_m, Pn, Lu_p) sur champs de potentiel de transfert de chaleur et de masse.

Zusammenfassung—Die Differentialgleichungen für Wärme- und Stoffübertragung im dispersen Medium wurden bei gleichzeitiger Phasenumwandlung gelöst (Flüssigkeitsverdampfung oder Dampfkondensation). Es wurde angenommen, dass die Stoffübertragung stattfindet unter der gleichzeitigen Wirkung des Potentialgradienten der Stoffübertragung $\nabla\theta$, dem Temperaturgradienten ∇t und dem Gradienten des Gesamtdruckes ∇p. Die Lösungen für die Potentiale der Wärme- und Stoffübertragung (t, θ, p) werden angegeben für das eindimensionale Problem (unendliche Platte und Kugel) bei Randbedingungen dritter Art. Die Lösungen sind in Form von Kenngrössen mitgeteilt. Der Einfluss der besonderen Kenngrössen (Bi_q, Bi_m, Pn, Lu_p) auf die Potentialfelder der Wärme- und Stoffübertragung wurde untersucht.

Abstract—В статье дано решение системы дифференциальных уравнений тепло- и массопереноса в дисперсной среде при наличии фазовых превращений (испарение жидкости или конденсация пара). Предполагается, что перенос массы вещества происходит под действием градиента потенциала массопереноса $\nabla\theta$, градиента температуры ∇t и градиента общего давления. ∇p. Получены решения для потенциалов переноса тепла и массы вещества (t, θ, p) применительно к одномерной задаче (неограниченная пластина и шар) при граничных условиях третьего рода. Решения даны в критериальной форме с использованием критериев подобия тепломассопереноса. Дан анализ влияния отдельных критериев подобия (Bi_q, Bi_m, Pn, Lu_p) на поля потенциалов тепломассопереноса. Показано влияние молярного (фильтрационного) переноса массы на тепло- и массоперенос.

In order to intensify heat and mass transfer high temperatures and pressures are employed in modern engineering on an increasing scale. Under such conditions the mechanism of transfer of matter and energy is considerably modified. In addition to transfer due to molecular processes, molar processes of a filtrational nature start playing an important part. Let us consider

highly intensive internal heat and mass transfer in moist dispersed media, and the influence of various factors on such transfer.

The transfer of heat and that of matter in dispersed media are interconnected and interdependent. It is being effected by the action of various thermodynamic forces: heat transfer, mass transfer and filtration. On the other hand, the magnitude of the thermodynamic force is determined by the difference of the respective transfer potential. The heat transfer potential — t the potential of molecular mass transfer θ, and the potential of filtration (molar) transfer — the general or excess pressure p [1]. The system of differential equations for heat and mass exchange in the case of molecular and molar transfer can be represented as follows [2]:

$$c_q\gamma\frac{\partial t}{\partial\tau} = \nabla(\lambda_q\nabla t) + \epsilon\rho\gamma\, c_m\frac{\partial\theta}{\partial_\tau} - \sum_i c_i q_{mi}\nabla t$$

$$c_m\gamma\frac{\partial\theta}{\partial\tau} = \nabla[\lambda_m(\nabla\theta + \delta\nabla t) + \lambda_p\nabla p] \qquad (1)$$

$$c_p\gamma\frac{\partial p}{\partial\tau} = \nabla(\lambda_p\nabla p) - \epsilon\gamma\, c_m\frac{\partial\theta}{\partial\tau}$$

where λ_q is the coefficient of heat conductivity; λ_m and λ_p are the coefficients of molecular filtration conductivity of matter; c_q, c_m and c_p are the respective heat, liquid and vapour capacities of the material; ρ is the specific heat of phase transition; δ is the thermogradient coefficient; a_m is the mass transfer coefficient of potential conductivity; γ is the density of the dispersed medium; ϵ is the criterion of phase transition; τ is the time; the added term $\sum_i c_i q_{im}\nabla t$ characterizes the convective component of heat transfer in the dispersed medium.

In order to connect the dispersed medium with the surrounding medium we assume boundary conditions of the third kind, since they represent a mathematical analogy of frequently occurring convection processes. In case of highly intensive heat and mass transfer they can be expressed as follows:

$$-\lambda_q(\nabla t)_s + \alpha_q[t_c - (t)_s] - (1 - \epsilon)\rho\alpha_m[(\theta)_s - \theta_e] = 0,$$

$$\lambda_m(\nabla\theta)_s + \lambda_m\delta(\nabla t)_s + \lambda_p(\nabla p)_s + \alpha_m[(\theta)_s - \theta_e] = 0. \qquad (2)$$

$$(p)_s = p_0,$$

where α_q and α_m, respectively, denote the coefficients of heat exchange and mass transfer between the carrier of heat and the dispersed medium; indices s refer to the surface of the dispersed medium, and indices c to the surrounding medium; index 0 refers to the initial value of the respective parameter, and index e refers to its equilibrium value.

The transfer coefficients and the thermodynamic characteristics of the disperse medium are in one way or other functions of co-ordinates and time. In the first approximation the co-ordinate relation can be neglected. The system of equations (1) is thus simplified and permits evaluation of the process for each zone [3, 4].

The solution of the system of equations (1) for one-dimensional bodies under boundary conditions (2) and with constant initial distribution of transfer potentials is as follows:
for an infinite plate

$$T(X,\mathrm{Fo}) = 1 - \sum_{n=1}^{\infty}\sum_{j=1}^{3} C_{nj}\cos\nu_j\mu_n X\cdot\exp(-\mu_n^2\mathrm{Fo})$$

$$\Theta(X,\mathrm{Fo}) = 1 + \frac{1}{\epsilon\mathrm{Ko}}\sum_{n=1}^{\infty}\sum_{j=1}^{3} C_{nj}(1-\nu_j^2)\cos\nu_j\mu_n X\cdot\exp(-\mu_n^2\mathrm{Fo})$$

$$P(X,\mathrm{Fo}) = -\frac{1}{\epsilon\mathrm{Bu}}\sum_{n=1}^{\infty}\sum_{j=1}^{3} C_{nj}\sigma_j\cos\nu_j\mu_n X\cdot\exp(-\mu_n^2\mathrm{Fo})$$

Vol. 1 1960

for a sphere

$$T(X,\mathrm{Fo}) = 1 + \sum_{n=1}^{\infty}\sum_{j=1}^{3} C_{nj}\,\frac{\sin\,\nu_j\mu_n X}{X}\cdot\exp\,(-\,\mu_n^2\mathrm{Fo})$$

$$\Theta(X,\mathrm{Fo}) = 1 - \frac{1}{\epsilon\mathrm{Ko}}\sum_{n=1}^{\infty}\sum_{j=1}^{3} C_{nj}\,(1-\nu_j^2)\,\frac{\sin\,\nu_j\mu_n X}{X}\cdot\exp\,(-\,\mu_n^2\mathrm{Fo})$$

$$P(X,\mathrm{Fo}) = \frac{1}{\epsilon\mathrm{Bu}}\sum_{n=1}^{\infty}\sum_{j=1}^{3} C_{nj}\sigma_j\,\frac{\sin\,\nu_j\mu_n X}{X}\cdot\exp\,(-\,\mu_n^2\mathrm{Fo})$$

where

$$C_{n1} = 2\,\frac{(\epsilon\mathrm{Ko}\,k_1 - 1)(P_{n2} - (X_{n2}/X_{n3})\,P_{n3}) - \epsilon\mathrm{Ko}(Q_{n2} - (X_{n2}/X_{n3})\,Q_{n3})}{\mu_n\psi_n}$$

$$C_{n2} = -\,2\,\frac{(\epsilon\mathrm{Ko}k_1 - 1)(P_{n1} - (X_{n1}/X_{n3})\,P_{n3}) - \epsilon\mathrm{Ko}(Q_{n1} - (X_{n1}/X_{n3})\,Q_{n3})}{\mu_n\psi_n}$$

$$C_{n3} = 2\,\frac{(\epsilon\mathrm{Ko}k_1 - 1)(P_{n1}\,(X_{n2}/X_{n3}) - P_{n2}\,(X_{n1}/X_{n3}) - \epsilon\mathrm{Ko}(Q_{n1}\,(X_{n2}/X_{n3}) - Q_{n2}\,(X_{n1}/X_{n3})}{\mu_n\psi_n}$$

$$\psi_n = \left(P_{n1} - \frac{X_{n1}}{X_{n3}}P_{n3}\right)\left[\nu_2 A_{n2} - \frac{X_{n2}}{X_{n3}}(\nu_3 A_{n3} + b_{n2}Q_{n3})\right] + \left(Q_{n2} - \frac{X_{n2}}{X_{n3}}Q_{n3}\right)\left[\nu_1 B_{n1} - \frac{X_{n1}}{X_{n3}}\,(\nu_3 B_{n3} +\right.$$

$$\left. + b_{n1}P_{n3})\right] - \left(P_{n2} - \frac{X_{n2}}{X_{n3}}P_{n3}\right)\left[\nu_1 A_{n1} - \frac{X_{n1}}{X_{n3}}(\nu_3 A_{n3} + b_{n1}Q_{n3})\right] - \left(Q_{n1} - \frac{X_{n1}}{X_{n3}}Q_{n3}\right)\left[\nu_2 B_{n2} -\right.$$

$$\left. - \frac{X_{n2}}{X_{n3}}(\nu_3 B_{n3} + b_{n2}P_{n3})\right]$$

$$\sigma_j = (1-\epsilon)(1-\nu_j^2) - \mathrm{Lu}(1-\nu_j^2)\,\nu_j^2 - \epsilon\mathrm{KoPnLu}\,\nu_j^2$$

$$\nu_j = +\sqrt{(\Lambda_j + \tfrac{1}{3}\beta_1)},\ (j = 1, 2, 3)$$

$$\Lambda = \sqrt[3]{\{-\tfrac{1}{2}\Pi_2 + \sqrt{(\tfrac{1}{4}\Pi_2^2 + \tfrac{1}{2\,7}\Pi_1^3)}\}} + \sqrt[3]{\{-\tfrac{1}{2}\Pi_2 - \sqrt{(\tfrac{1}{4}\Pi_2^2 + \tfrac{1}{2\,7}\Pi_1^3)}\}}$$

Here the correct values of Λ_j must simultaneously satisfy the following relation:

$$\sqrt[3]{\{-\tfrac{1}{2}\Pi_2 + \sqrt{(\tfrac{1}{4}\Pi_2^2 + \tfrac{1}{2\,7}\Pi_1^3)}\}}\cdot\sqrt[3]{\{-\tfrac{1}{2}\Pi_2 - \sqrt{(\tfrac{1}{4}\Pi_2^2 + \tfrac{1}{2\,7}\Pi_1^3)}\}} = -\tfrac{1}{3}\Pi_1$$

where

$$\Pi_1 = -\frac{\beta_1^2}{3} + \beta_2,\ \Pi_2 = -\frac{2\beta_1^3}{27} + \frac{\beta_1\beta_2}{3} - \beta_3$$

$$\beta_1 = 1 + (1-\epsilon)\,\frac{1}{\mathrm{Lu}} + \frac{1}{\mathrm{Lu}_p} + \epsilon\mathrm{KoPn}$$

$$\beta_2 = (1-\epsilon)\,\frac{1}{\mathrm{Lu}} + \left(1 + \frac{1}{\mathrm{Lu}} + \epsilon\mathrm{KoPn}\right)\frac{1}{\mathrm{Lu}_p};\quad \beta_3 = \frac{1}{\mathrm{Lu}\cdot\mathrm{Lu}_p}$$

Also, for an infinite plate

$$A_{nj} = \left[1 + (1-\nu_j^2)\,K_1 + \frac{1}{\mathrm{Bi}_q}\right]\sin\,\nu_j\mu_n + \frac{\nu_j\mu_n}{\mathrm{Bi}_q}\cos\,\nu_j\mu_n$$

$$B_{nj} = (1 - \nu_j^2) \sin \nu_j\mu_n + \frac{(1 - \nu_j^2) + \epsilon \mathrm{KoPn} + \sigma_j \mathrm{Lu}_p/\mathrm{Lu}}{\mathrm{Bi}_m} (\sin \nu_j\mu_n + \nu_j\mu_n \cos \nu_j\mu_n)$$

$$P_{nj} = (1 - \nu_j^2) \cos \nu_j\mu_n - \frac{(1 - \nu_j^2) + \epsilon \mathrm{KoPn} + \sigma_j \mathrm{Lu}_p/\mathrm{Lu}}{\mathrm{Bi}_m} \nu_j\mu_n \sin \nu_j\mu_n$$

$$Q_{nj} = [1 + (1 - \nu_j^2) K_1] \cos \nu_j\mu_n - \frac{\nu_j\mu_n}{\mathrm{Bi}_q} \sin \nu_j\mu_n$$

$$b_{nj} = \nu_j \tan \nu_j\mu_n - \nu_3 \tan \nu_3\mu_n, \quad X_{nj} = \sigma_j \cos \nu_j\mu_n$$

for a sphere

$$A_{nj} = [1 + (1 - \nu_j^2) K_1] \cos \nu_j\mu_n - \frac{\nu_j\mu_n}{\mathrm{Bi}_q} \sin \nu_j\mu_n$$

$$B_{nj} = (1 - \nu_j^2) \cos \nu_j\mu_n - \frac{(1 - \nu_j^2) + \epsilon \mathrm{KoPn} + \sigma_j \mathrm{Lu}_p/\mathrm{Lu}}{\mathrm{Bi}_m} \nu_j\mu_n \sin \nu_j\mu_n$$

$$P_{nj} = (1 - \nu_j^2) \sin \nu_j\mu_n + \frac{(1 - \nu_j^2) + \epsilon \mathrm{KoPn} + \sigma_j \mathrm{Lu}_p/\mathrm{Lu}}{\mathrm{Bi}_m} (\nu_j\mu_n \cos \nu_j\mu_n - \sin \nu_j\mu_n)$$

$$Q_{nj} = \frac{1}{\mathrm{Bi}_q} \nu_j\mu_n \cos \nu_j\mu_n + \left[1 - \frac{1}{\mathrm{Bi}_q} + (1 - \nu_j^2) K_1\right] \cdot \sin \nu_j\mu_n$$

$$b_{nj} = \nu_j \cot \nu_j\mu_n - \nu_3 \cot \nu_3\mu_n, \quad X_{nj} = \sigma_j \sin \nu_j\mu_n$$

μ_n is determined by the solutions of the characteristic equation

$$\left(P_{n1} - \frac{X_{n1}}{X_{n3}} P_{n3}\right)\left(Q_{n2} - \frac{X_{n2}}{X_{n3}} Q_{n3}\right) - \left(P_{n2} - \frac{X_{n2}}{X_{n3}} P_{n3}\right)\left(Q_{n1} - \frac{X_{n1}}{X_{n3}} Q_{n3}\right) = 0.$$

The values of the characteristic roots μ_1 for a dispersed medium possessing the form of an infinite plate are given in Table 1.

The solutions are given in dimensionless form: T, Θ, P denote, respectively, the dimensionless values of temperature, molecular and molar potentials, viz.

$$T = \frac{t - t_0}{t_c - t_0}, \quad \Theta = \frac{\theta_0 - \theta}{\theta_0 - \theta_e}, \quad P = \frac{p - p_0}{p_0}.$$

where

$X = \dfrac{x}{R}$, dimensionless co-ordinate;

$\mathrm{Fo} = \dfrac{a_q \tau}{R^2}$, criterion of homochronism of temperature fields, the so-called Fourier criterion (a_q is the heat coefficient of potential transfer $a_q = \lambda_q/c_q\gamma$);

$\mathrm{Lu} = \dfrac{a_m}{a_q}$, criterion of inertia of fields of heat and mass content, the so-called Luikov criterion, a_m is the liquid coefficient of potential transfer $a_m = \lambda_m/c_m\gamma$;

$\mathrm{Lu}_p = \dfrac{a_p}{a_q}$, criterion of inertia of filtration potential field with respect to temperature field (a_p is the filtrational coefficient of potential transfer $a_p = \lambda_p/c_p\gamma$);

Vol. 1 1960

$$\mathrm{Bi}_q = \frac{\alpha_q R}{\lambda_q}$$

and $\mathrm{Bi}_m = \dfrac{\alpha_m R}{\lambda_m a_m}$, Biot criteria of heat and mass transfer;

$$\mathrm{Pn} = \frac{\delta(t_c - t_0)}{\theta_0 - \theta_e},$$ Posnov criterion;

$$\mathrm{Ko} = \frac{c_m \rho(\theta_0 - \theta_e)}{c_q(t_c - t_0)}$$ Kossovich criterion;

$$\mathrm{Bu} = \frac{\rho c_p}{c_q} \frac{p_0}{t_c - t_0},$$ Bulygin criterion;

$$K_1 = \frac{1 - \epsilon}{\epsilon} \mathrm{Lu} \frac{\mathrm{Bi}_m}{\mathrm{Bi}_q},$$ complex criterion.

An analysis of the solution shows that the infinite series which the expressions for T, Θ and P contain, converge very quickly with increase of Fo. Beginning with Fo $\approx 0{\cdot}7$ it is possible with an accuracy of 1 per cent to limit oneself to two or three terms of a series.

The solution of the system of differential equations (1) (2) gives the dependence of the process on a large number of similarity criteria of heat and mass transfer. It must be stressed, however, that not all of these criteria have equal effect on the development of the process. Some of them primarily affect heat transfer, others—mass transfer, others again—filtrational characteristics of the transfer. Some of the criteria are connected with molecular, others with molar transfer. Let us consider the effect of various similarity criteria on highly intensive internal heat and mass transfer.

The heat and mass criteria of Biot

$$\mathrm{Bi}_q = \frac{\alpha_q}{\lambda_q} R, \qquad \mathrm{Bi}_m = \frac{\alpha_m}{\lambda_m} R$$

Table 1

Bi_q	Lu			Lu_p		ϵ		Bi_m			KoPn			
	0·3*	0·7	1·0	300	1000	0·1	0·9	5	10	15	0·45	1·50	3·00	5·85
0·30	0·469	0·0779	0·0578	0·454	0·468	0·463	0·474	0·454	0·466	0·468	0·508	0·485	0·456	0·412
0·35	0·495	0·0834	0·0622	0·480	0·493	0·490	0·501	0·476	0·492	0·494	0·544	0·513	0·480	0·430
0·40	0·517	0·0884	0·0662	0·503	0·517	0·512	0·523	0·493	0·513	0·515	0·574	0·538	0·501	0·445
0·45	0·536	0·0928	0·0699	0·523	0·537	0·533	0·543	0·511	0·532	0·534	0·602	0·563	0·518	0·458
0·50	0·556	0·0968	0·0733	0·541	0·554	0·550	0·561	0·528	0·552	0·553	0·625	0·582	0·534	0·470
0·60	0·583	0·1050	0·0801	0·572	0·584	0·579	0·590	0·555	0·577	0·581	0·669	0·617	0·560	0·488
0·70	0·607	0·111	0·0858	0·596	0·607	0·603	0·614	0·578	0·599	0·605	0·709	0·646	0·581	0·504
0·80	0·627	0·117	0·0911	0·617	0·628	0·623	0·633	0·596	0·617	0·624	0·741	0·670	0·599	0·515
0·90	0·645	0·123	0·0962	0·634	0·644	0·639	0·649	0·611	0·633	0·640	0·771	0·690	0·613	0·525
1·0	0·658	0·128	0·1011	0·648	0·658	0·653	0·662	0·622	0·645	0·653	0·796	0·707	0·625	0·533
1·5	0·706	0·151	0·1197	0·699	0·707	0·702	0·709	0·656	0·686	0·700	0·885	0·765	0·666	0·558
2·0	0·733	0·170	0·1340	0·727	0·734	0·731	0·736	0·676	0·714	0·725	0·938	0·798	0·690	0·572
3·0	0·764	0·197	0·157	0·758	0·765	0·761	0·767	0·696	0·739	0·755	0·993	0·836	0·716	0·589
4·0	0·779	0·214	0·173	0·775	0·781	0·776	0·784	0·704	0·752	0·771	1·023	0·856	0·730	0·599
5·0	0·789	0·228	0·184	0·786	0·791	0·785	0·794	0·712	0·761	0·781	1·042	0·867	0·738	0·604
6·0	0·796	0·242	0·197	0·793	0·799	0·792	0·803	0·715	0·767	0·787	1·054	0·875	0·744	0·608
7·0	0·801	0·250	0·208	0·798	0·803	0·796	0·807	0·718	0·771	0·792	1·061	0·881	0·748	0·611
8·0	0·804	0·254	0·214	0·802	0·807	0·800	0·812	0·721	0·775	0·796	1·068	0·886	0·751	0·613
9·0	0·807	0·260	0·220	0·805	0·810	0·802	0·815	0·723	0·777	0·798	1·073	0·889	0·754	0·614
10	0·810	0·263	0·225	0·808	0·813	0·804	0·817	0·725	0·779	0·801	1·077	0·891	0·756	0·616
15	0·817	0·280	0·245	0·816	0·820	0·810	0·825	0·728	0·786	0·808	1·090	0·900	0·761	0·621
20	0·820	0·287	0·256	0·819	0·824	0·813	0·828	0·730	0·788	0·812	1·096	0·904	0·764	0·622
30	0·824	0·296	0·269	0·823	0·828	0·816	0·832	0·732	0·792	0·816	1·103	0·908	0·766	0·624
40	0·826	0·300	0·275	0·825	0·830	0·818	0·834	0·734	0·794	0·817	1·105	0·911	0·769	0·626
50	0·827	0·302	0·278	0·826	0·831	0·819	0·836	0·735	0·795	0·818	1·106	0·913	0·770	0·627

* μ_1 values for Lu = 0·3 simulaneously correspond to μ_1 values for Lu_p = 500, ϵ = 0·7, Bi_m = 20, KoPn = 2·25

characterize the intensity of external transfer (Bi_q for heat and Bi_m for matter), as compared to the intensity of internal transfer. One might therefore call them criteria of surface heat and mass transfer. When the Biot coefficients are small the potentials in the centre of the material differ little from the corresponding potentials on its surface. Transfer of matter and heat is slow. With increase of Bi_q and Bi_m transfer intensifies. The surface temperature rapidly approaches that of the heat carrier. In a disperse medium big temperature gradients arise effecting intensive redistribution of matter. At the same time large stresses occur inside the material, creating conditions for warping, and formation of cracks and pores.

Once the processes within the material have become quasi-regular, i.e. once the Fourier criterion has reached the value of Fo = 0·7 — 1·0, the Biot heat transfer criterion affects only the fields of the thermal characteristic (Fig. 1), and the Biot mass exchange criterion affects only the fields of molecular transfer potential or mass content (Fig. 2). The field of filtration potential becomes an automodelous one with respect to both criteria. A similar result has been found by considering molecular heat and mass transfer in moist material [5, 6]. This, as well as the fact that the Biot criteria are indifferent to the field of filtration potential indicates that the criteria of heat and mass exchange are chiefly connected with the molecular mechanism of transfer. The nature of the change of criteria with molecular transfer potential and temperature is in good accordance with experimental results obtained by Lebedev [7].

The criteria of Posnov

$$\mathrm{Pn} = \frac{\delta(t_c - t_0)}{\theta_0 - \theta_e},$$

of Kossovich

$$\mathrm{Ko} = \frac{c_m \rho(\theta_0 - \theta_e)}{c_q(t_c - t_0)},$$

of phase change (ϵ), and of Bulygin

$$\mathrm{Bu} = \frac{\rho c_p}{c_q} \frac{p_0}{t_c - t_0}$$

can be considered as belonging to the group of criteria of internal heat and mass transfer because they characterize deeper processes of phase change and transfer taking place within the material.

The Posnov criterion characterizes the relative non-uniformity of the mass content field produced by heat transfer. The Kossovich criterion is a specific form of the phase change criterion. It is equal to the ratio between specific heat consumed on evaporation of matter and specific heat consumed on heating the dispersed medium.

If there is no molar transfer in the material the nature of the effect of the criteria Pn and Ko on the potential of heat and mass transfer is

Vol. 1 1960

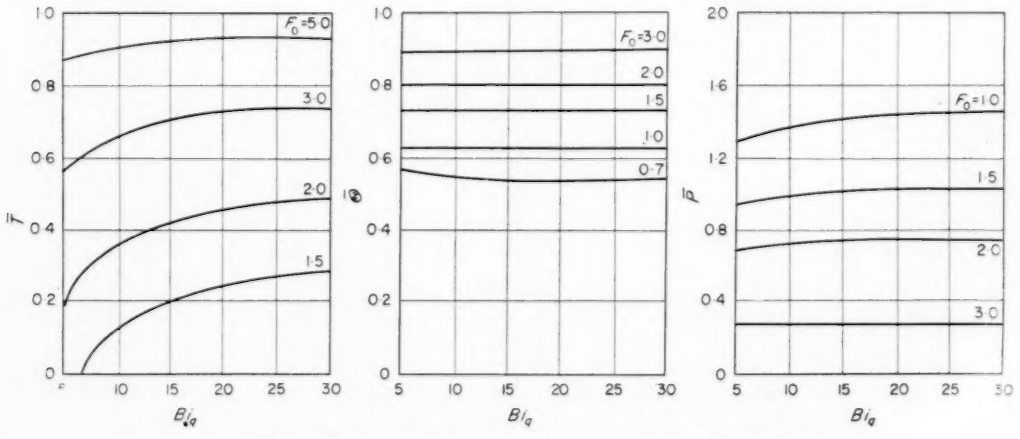

FIG. 1. Dimensionless transfer potentials as a function of Bi_q criterion

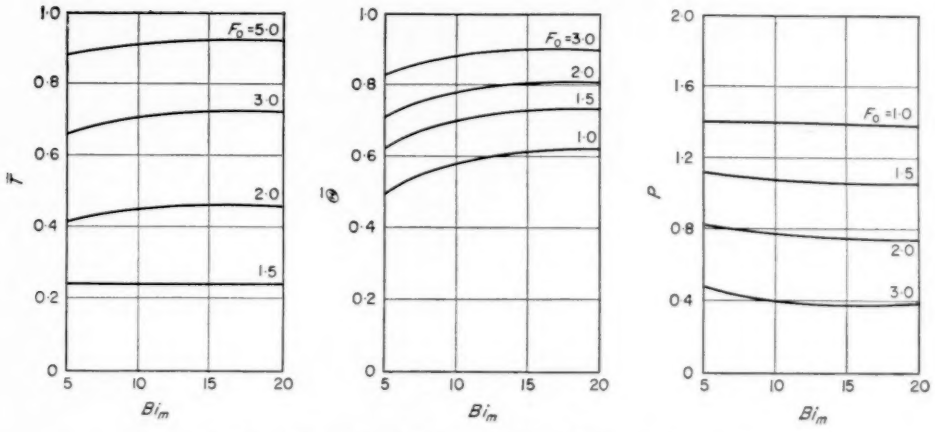

FIG. 2. Dimensionless transfer potentials as a function of Bi_m criterion

analogous to the effect on these potentials of the criteria of surface heat and mass transfer Bi_q and Bi_m. Under conditions of quasi-regular process the criterion Pn is automodelous with respect to the temperature field whilst the criterion Ko is automodelous with respect to the field of potential of molecular transfer of matter [5, 6]. The fact that molar transfer of matter starts taking place in the material changes the dependence of dimensionless potentials on the criteria Pn and Ko. At small values of Fo the temperature of the material increases visibly with increase of Pn, but in the course of time this effect diminishes and changes its sign at values of the Fourier criterion larger than two (Fig. 3). The dependence of the filtration potential on Pn, combined with the new nature of the influence on the temperature distribution shows that the Posnov criterion is connected with a molecular as well as with a molar transfer mechanism. A similar conclusion can be obtained with respect to the Kossovich criterion.

The fact that a powerful molar mechanism arises in the material has its effect first of all on redistribution of matter. The Posnov criterion which in case of molecular transfer characterizes internal processes of mass exchange must show

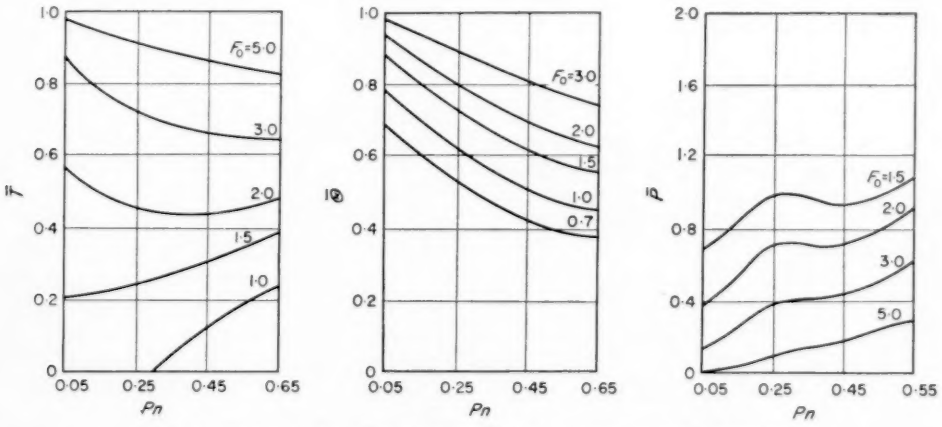

FIG. 3. Dimensionless transfer potentials as a function of Pn criterion

the appearance of a new mechanism much more clearly than the Kossovich criterion which characterizes internal processes of heat exchange. An analysis of the results of solution of the system of equations confirms this: the change of the effect of criterion Pn on the index of heat transfer of the process proves to be stronger than the change of criterion Ko with respect to the index of mass transfer.

With increase of criterion Pn the dimensionless potential of transfer of matter diminishes. This indicates that within equal intervals of time at smaller values of the Posnov criterion larger quantities of matter are being removed from the material. The effect of criterion Ko manifests itself primarily in the temperature field where the above-mentioned similarity between the Kossovich criterion and the Biot heat exchange criterion remains.

The criterion of phase change (ϵ) has the same effect on the internal process of heat and mass transfer as the Kossovich criterion. The difference lies only in the intensity of effect on the thermal characteristics: the effect of ϵ is weaker than that of Ko.

New and specific for high temperature heat and mass exchange is the Bulygin criterion Bu. Like the Kossovich criterion, the Bulygin criterion characterizes the accumulating power of the body. However, as distinct from the former, it concerns not the total heat consumed on formation of vapour but only the heat consumed on formation of vapour participating in molar transfer. The Bulygin criterion is closely linked with molar transfer and therefore affects only excess pressure distribution in the material, and not the temperature distribution and the potential of molecular transfer. The criterion Bu changes over a very wide range. The magnitude of the mean value of the filtration potential in the material is inversely proportional to the criterion and diminishes rapidly with increase of the latter.

The most essential effect on transfer potential belongs to the Luikov criterion ($\mathrm{Lu} = a_m/a_q$) which may also be called the criterion of correlation between heat and mass transfer. The Luikov criterion characterizes the inertia of the potential field of molecular transfer of matter in relation to the field of heat transfer potential. In case of purely molecular transfer mechanism the value $\mathrm{Lu} \approx 1{\cdot}0$ (with an accuracy up to 12 per cent) forms the limit for symmetry of relative relaxation speed of the above-mentioned potentials. Thus, if the criterion Lu is smaller than unity the propagation of temperature in the material occurs at higher speed than that of the mass transfer potential; if Lu is larger than unity the reverse takes place. If intensive molar transfer arises within the material, the symmetry observed in case of molecular transfer disappears, although the general trend of the process remains unchanged. Calculations show that with increase of Lu the mean dimensionless transfer potentials undergo a marked change: the temperature of the material drops, while the mean value of mass content and of filtration potential increases. The changes of the latter are particularly marked with increase of the Luikov criterion. Thus, we have at $\mathrm{Lu} = 0{\cdot}3$ $\bar{P} = 0{\cdot}7268$ and, respectively, at $\mathrm{Lu} = 0{\cdot}7$ $\bar{P} = 60{\cdot}57$, but at $\mathrm{Lu} = 1{\cdot}0$ $\bar{P} = 83{\cdot}95$.

Another criterion for inertia or correlation between heat and mass transfer is $\mathrm{Lu}_p = a_p/a_q$. It characterizes the inter-connexion between molar transfer of matter within the material, and the transfer of heat; in other words, it characterizes the inertia of the fields of filtration potential (fields of excess pressure) with respect to temperature fields. It can be seen from Fig. 4 that criterion Lu_p is automodelous with respect to $\bar{T}$ and $\bar{\Theta}$; it affects only the pressure field of the material. In connexion with the dependence of heat and mass transfer on molar similarity criteria let us consider in greater detail the dynamics of change of filtration potential.

During intensive heating of moist dispersed media very strong vapour formation occurs inside the material. This leads to the formation of a stable gradient of filtration potential—the gradient of general or excess pressure. The latter is determined by the commensurability of the time of relaxation of pressure through the skeleton of the material, and the formation within the same period of time of vapour necessary for the restitution of the original state. The distribution of filtration potential depends on the method of heating the medium and also on the values of the thermophysical and mechanical

Vol. 1 1960

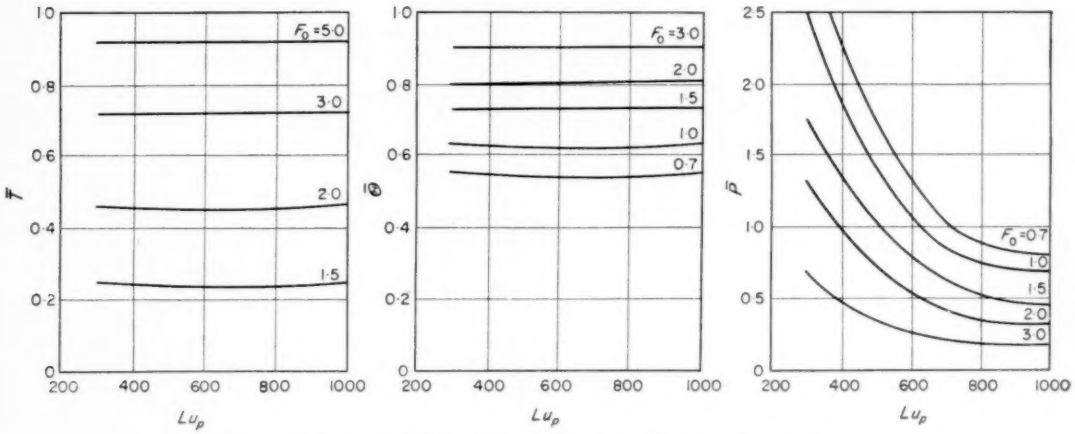

FIG. 4. Dimensionless transfer potentials as a function of Lu_p criterion

characteristics of the material. However, qualitatively speaking, in any case there is a strong increase of the potential at the beginning stage of the process. With decrease of mass content (i.e. with increase of $\bar{\Theta}$) the intensity of internal vapour formation diminishes. That, in its turn, leads to a decrease of the gradient of filtration potential. The results of analysis of the solutions of the system of equations (1) are in complete accordance with experimental results [8].

Considering the effect of various criteria on processes of heat and mass exchange simplified criterial equations can be suggested describing internal heat and mass transfer. The equations are:

$$T = T\,(\mathrm{Lu},\ \mathrm{Bi}_q,\ \mathrm{Pn},\ \mathrm{Ko},\ \epsilon,\ \mathrm{Fo},\ x/R)$$

$$\Theta = \Theta\,(\mathrm{Lu},\ \mathrm{Bi}_m,\ \mathrm{Pn},\ \mathrm{Ko},\ \epsilon,\ \mathrm{Fo},\ x/R)$$

$$P = P\,(\mathrm{Lu},\ \mathrm{Lu}_p,\ \mathrm{Bu},\ \mathrm{Pn},\ \mathrm{Ko},\ \epsilon,\ \mathrm{Fo},\ x/R)$$

A further analysis of highly intensive heat and mass transfer will most probably permit still further simplification the criterial equations by finding correlations between the separate similarity criteria in the above-mentioned expressions. There is reason to believe [6] that in the temperature expression Bi_q and Ko appear in form of the ratio $\mathrm{Bi}_q/\mathrm{Ko}$, and, similarly, in the expression for the transfer potential Bi_m and Pn appear in form of the ratio $\mathrm{Bi}_m/\mathrm{Pn}$.

REFERENCES

1. A. LUIKOV, *Heat and Mass Transfer in Processes of Drying*. Gosenergoizdat, Moscow and Leningrad (1956).
2. A. LUIKOV, *Zh. Inzh.-fiz.* No. 6, 12 (1958).
3. Y. MIKHAILOV, *Izv. Akad. Nauk Latv.SSR* No. 12, 107 (1956).
4. Y. MIKHAILOV, *Izv. Akad. Nauk Latv.SSR* No. 3, 127 (1958).
5. Y. MIKHAILOV, Collected articles in *Heat and Mass Transfer in Evaporation Processes*, p. 145. Akademiia Nauk SSSR (1958).
6. Y. MIKHAILOV, *Izv. Akad. Nauk Latv.SSR* No. 7, 129 (1957).
7. P. LEBEDEV, *Drying with Infra-red Rays*. Gosenergoizdat, Moscow and Leningrad (1955).
8. G. MAKSIMOV, *Proceedings of the All-Union Conference on Drying. Section of Energetics*, p. 20. Profizdat, (1958).

Int. J. Heat Mass Transfer. Vol. 1, pp. 46–49. Pergamon Press 1960. Printed in Great Britain.

TURBULENT BOUNDARY LAYER ON A FLAT PLATE IN A STREAM OF DISSOCIATING GAS

S. I. KOSTERIN and YU. A. KOSHMAROV

Institute of Energetics of the Academy of Sciences of the U.S.S.R., Moscow, U.S.S.R.

(*Received* 13 *October* 1959)

Abstract—This paper gives a theoretical solution of a turbulent boundary layer problem of dissociating gas on a flat plate. A half-empirical Prandtl–Kármán turbulent theory is used to solve this problem.

Résumé—Cet article donne une solution théorique du problème de la couche limite turbulente sur une plaque plane dans un écoulement de gaz dissocié. Une théorie semi-empirique de Prandtl-Kármán sui la turbulence a été utilisée pour résoudre ce problème.

Zusammenfassung—Es wird eine theoretische Lösung der turbulenten Grenzschicht eines dissoziierenden Gases an der ebenen Platte mitgeteilt. Heirzu wird eine halbempirische Theorie nach Prandtl und und Kármán herangezogen.

Abstract—В статье излагается теоретическое решение задачи о турбулентном пограничном слое диссоциирующего газа на плоской пластине. Для решения этой задачи привлекается полуэмпирическая теория турбулентности Прандтля-Кармана.

Vol. 1 1960

THE writing of this paper developed from certain studies on turbulent boundary layer on a strongly cooled flat plate flowed by the non-gradient dissociating gas with assumed existence of thermodynamic equilibrium. The problem is determined by:

(1) Prandtl numbers of laminar sublayer and in turbulent region of layer are equal to unity.
(2) Diffusion Prandtl numbers of laminar sublayer and turbulent region of a layer are also equal to unity.
(3) The wall temperature over a plate is uniform and constant.
(4) A perfect purified two-atomic gas is being discussed.

Boundary layer equations at the above-mentioned conditions can be written in the following forms:

$$\rho u \frac{\partial u}{\partial x} + \rho v \frac{\partial u}{\partial y} = \frac{\partial}{\partial y}\left(\mu \frac{\partial u}{\partial y} + \mu_T \frac{\partial u}{\partial y}\right) - \overline{\rho' v'} \frac{\partial u}{\partial y} \quad (1)$$

$$\rho u \frac{\partial H}{\partial x} + \rho v \frac{\partial H}{\partial y} = \frac{\partial}{\partial y}\left(\frac{\lambda}{c_p} \frac{\partial H}{\partial y} + \frac{\lambda_T}{c_p} \frac{\partial H}{\partial y}\right) - \overline{\rho' v'} \frac{\partial H}{\partial y} \quad (2)$$

$$\frac{\partial \rho u}{\partial x} + \frac{\partial \rho v}{\partial y} = 0 \quad (3)$$

the equations of state for the perfect dissociating gas can be written in the form (2)

$$P = \rho R T (1 + \alpha) \quad (4)$$

where $R = gR_b$; as numbers $\mathrm{Pr} = 1$, $\mathrm{Pr}_T = 1$, then the equations of energy and motion will have the same form. All this allows us to consider both velocity profiles and total enthalpies as similar.

Choosing the condition of identity for the equations of energy and motion we shall have the ratio:

$$\frac{H - H_w}{H_0 - H_w} = \frac{u}{u_0} \quad (5)$$

the ratio (5) makes it possible to establish the

dependence between velocities fields, densities, atom concentrations fields which are the results of dissociation and temperature fields.

Referring to Lighthill [2], we write the value of total enthalpy in the form:

$$\bar{H} = \bar{T}(4 + \alpha) + \alpha + \frac{u^2}{2RT_d} \tag{6}$$

where $\bar{H} = \frac{H}{RT_d}; \bar{T} = \frac{T}{T_d}$

At the presence of thermodynamic equilibrium the rate of dissociation can be determined according to formula (2):

$$\frac{\alpha^2}{1-\alpha} = \frac{1}{\bar{\rho}} \exp\left(-\frac{1}{\bar{T}}\right) \tag{7}$$

Using equations (4) to (7) we get the formulae describing the dependence between the parameters of flow at any point of the boundary layer:

$$\alpha^2 \frac{4+\alpha}{1-\alpha^2} = \frac{\bar{H}_w}{\bar{\rho}_w \bar{T}_w}\left[-\bar{R}_w^2 q^2 + \beta q + 1 - \frac{\alpha}{\bar{H}_w}\right] \exp\left\{\frac{4+\alpha}{\bar{H}_w(-\bar{R}_w^2 q + \beta q + 1 - \alpha/\bar{H}_w)}\right\} \tag{8}$$

or briefly:

$$\alpha = f(q) \tag{8a}$$

The form of the function $f(q)$ is determined by the parameters of the external flow and by the conditions on the wall

$$\bar{R}_w^2, \beta, \bar{H}_w, \bar{T}_w$$

$$\bar{T} = \bar{H}_w\left[-\bar{R}_w^2 q^2 + \beta q + 1 - \frac{f(q)}{\bar{H}_w}\right]\frac{1}{4+f(q)} \tag{9}$$

$$\frac{\rho}{\rho_w} = \bar{T}_w/(\bar{H}_w[-\bar{R}_w^2 q^2 + \beta q + 1 - f(q)/\bar{H}_w]\{1+f(q)\}/\{4+f(q)\}) \tag{10}$$

Here we have:

$$\beta = \frac{\bar{H}_0 - \bar{H}_w}{H_w}; q = \frac{u}{u_0}; \bar{R}_w^2 = \frac{u_0^2}{2H_w}$$

Velocity profile at the turbulent region of boundary layer can be defined by the approximate method.

When in equation (1) (the left-hand side of the equation) the forces of inertia of the average flow are neglected in comparison with the forces of "apparent" viscosity and using the scheme of Prandtl turbulent mixing then we shall get the following expression [1]:

$$\rho l \frac{\partial u}{\partial y} = \sqrt{\Omega} \tag{11}$$

where $\Omega = \rho_w \tau_w$† and $l = xy$

From (11) and using (10) we shall get the following formula for velocities profile:

$$\ln\eta = M\int_1^{\bar{\rho}} d\bar{\rho}/([-\bar{R}_w^2 q^2 + \beta q + 1 - f(q)/\bar{H}_w][1 - 3/\{4 + f(q)\}]) \tag{12}$$

where

$$M = \frac{\bar{T}_w}{\bar{H}_w} x\,\xi;\ \xi = \frac{u_0}{\sqrt{(\tau_w/\rho_w)}};\ \eta = \frac{y}{\delta}$$

In every actual case the form of $f(q)$ can be defined from (8), and, then it is possible to integrate the left-hand side of (12) in this way or other.

The expression $[1 - 3/\{4 + f(q)\}]$ may be taking into account for the slightest changes of the rates of dissociation as a constant value equal to Q, and for $f(q)$ we take the following approximating formula:

$$f(q) = \phi\ 1/\rho$$

where

$$\phi = f(\bar{P})$$

In this case we shall have the following formula for the profile of velocities

$$\eta = \left[\frac{a-q}{b+q}\cdot\frac{1}{C}\right]^{x\xi 1/s} \tag{13}$$

† We can find the values of integration constant Ω at conversion of velocities profile, with $\rho \to \rho_{\text{const}}$, into Prandtl logarithmic profile.

where

$$a = \sqrt{\left\{\frac{1}{\bar{R}_w^2} + \left(\frac{\beta}{2\bar{R}_w^2}\right)^2\right\}} - \frac{\beta}{2\bar{R}_w^2}$$

$$b = \sqrt{\left\{\frac{1}{\bar{R}_w^2} + \left(\frac{\beta}{2\bar{R}_w^2}\right)^2\right\}} + \frac{\beta}{2\bar{R}_w^2}$$

$$C = \frac{a+1}{b-1}$$

$$S = \sqrt{\left\{\frac{1}{\bar{R}_w^2} + \left(\frac{\beta}{2\bar{R}_w^2}\right)^2\right\}} \cdot 2\bar{R}_w^2$$

$$\xi_i = \frac{u_0}{\sqrt{(\rho_w \tau_w)}} \cdot N_w \rho_d;$$

$$N_w = \frac{\bar{\rho}_w \bar{T}_w + Q\varphi}{4\bar{T}_w Q}$$

If we neglect the forces of inertia then the equation of motion at the region of laminar sublayer is transformed to the form

$$\frac{\partial \tau}{\partial y} = 0 \tag{14}$$

where $$\tau = \mu \frac{\partial u}{\partial y}$$

The integration (14) of $y = 0$ to y will give

$$\tau_w - \mu \frac{\partial u}{\partial y} = 0 \tag{15}$$

The value of μ entering the equation (14) is the function of state parameters which generally speaking are changing through the thickness of the sublayer.

However, the determination of the values of μ in equation (15) we should produce in such a way that we might compensate the neglect of inertia forces from the point of establishing the velocities profile in sublayer. Let us make the most simple assumption

$$\mu = \mu_w = \text{const.}$$

In this case we have a linear profile of velocities

$$\frac{y}{\delta} = \xi^2 \frac{1}{\mathrm{Re}_{\delta_w}} \cdot \frac{u}{u_0} \tag{16}$$

where

$$\mathrm{Re}_{\delta_w} = \frac{u_0 \delta}{\nu_w}$$

The region where we shall have a profile (16), i.e. the thickness of the laminar sublayer, we shall define by the second empirical coefficient of the turbulent theory, i.e. by Kármán number, referring the physical parameters to the wall temperature:

$$\frac{V_* \delta_0}{\nu_w} = \omega \dagger \tag{17}$$

where $\omega = 11{\cdot}5$ and $V_* = \sqrt{(\tau_w/\rho_w)}$.

The formulae (17) and (16) give the possibility to determine the value of velocity on the external boundary of the laminar sublayer

$$\frac{u_l}{u_0} = \frac{\omega}{\xi^2} \tag{18}$$

We get the law of resistance using the formulae (18) and (12):

$$\ln\left[\xi \cdot \frac{1}{(\mathrm{Re}_\vartheta)_w} \frac{\vartheta}{\delta} \omega\right] = M \int_1^{\varphi = \omega/\xi} d\varphi / ([-\bar{R}_w^2 \varphi^2 + \beta\varphi + 1 - f(\varphi)/\bar{H}_w] [1 - 3/\{4 + f(\varphi)\}]) \tag{19}$$

where

$$\frac{\vartheta_w}{\delta} = \int_0^1 \frac{\rho}{\rho_w} \varphi(1-\varphi)\, d\eta$$

The value of ϑ_w/δ may be calculated substituting into (20) the expression for velocity profile (12) and the expression for densities profile (10).‡

Thus the formula (12) presents a relation between the coefficients of friction ξ and number $\mathrm{Re}_{\vartheta_w} = \vartheta_w u_0/\nu_w$. Taking into account this dependence it is possible to integrate the equation of motion written in the integral form and receive the distribution of friction coefficients along the plate:

$$Re_x = \int_0^{(\mathrm{Re})_{\vartheta_w}} \xi^2 \, d(\mathrm{Re})_{\vartheta_w} \tag{21}$$

† It is quite possible to make an assumption which is anologous to that we had in the reference [1]. However, it does not bring the essential accuracy.

‡ The use of velocity profile as (13) gives more simple expression for the law of resistance.

Vol. 1 1960

The counting of heat flows may be made on the basis of the existence of similarity of the profiles of velocities and enthalpies.

CONCLUSION

The above-mentioned method of calculation makes it possible to determine both friction and heat exchange in the flow of dissociating gas moving at high velocities.

NOMENCLATURE

x = distance along plate (m);
y = distance from plate (m);
u = gas velocity component, directed along plate (m/sec);
u' = velocity pulsation u;
v = gas velocity component, directed along axis y (m/sec);
v' = velocity pulsation v (m/sec);
ρ = gas density (kg sec^2/m^4);
ρ' = gas density pulsation (kg sec^2 m^{-4});
δ = boundary layer thickness (m),
δ_0 = laminar sublayer thickness (m);
ϑ = impulse loss thickness (m);
a = dissociation rate;
H = total enthalpy;
τ = friction stress (kg/m^2);
l = length of mixture path (m);
T = thermodynamical temperature (°K);
R_b = gas constant consisting of molecule A_2 (kg m/kg °C);
P = pressure (kg/m^2);
T_d = characteristic temperature (°K);
P_d = characteristic pressure (kg/m^2);
$\mathrm{Pr} = \frac{c_p \mu}{\lambda}$ = Prandtl criterion of laminar sublayer;
$\mathrm{Pr}_T = \frac{c_p \mu_T}{\lambda_T}$ = Prandtl criterion of boundary layer turbulent section;
g = gravity acceleration (m/sec^2);

Indices

w = flow parameters on wall;
0 = flow parameters on external boundary of layer.

REFERENCES

1. S. I. KOSTERIN and YU. A. KOSHMAROV, *Zh. tekh. fiz.* No. 7 (1959).
2. M. LIGHTHILL, *J. Fluid Mech.* **2**, 1 (1957).

Int. J. Heat Mass Transfer. Vol. 1, pp. 50–54. Pergamon Press 1960. Printed in Great Britain.

EIN INSTATIONÄRES VERFAHREN ZUR MESSUNG DER WÄRMELEITFÄHIGKEIT VON FLÜSSIGKEITEN UND GASEN

P. GRASSMANN und W. STRAUMANN

Institut für kalorische Apparate und Kältetechnik,
Eidgenössische Technische Hochschule, Zürich, Switzerland

(*Received* 30 *June* 1959)

Zusammenfassung—Die nachstehend beschriebene Methode zur Messung der Wärmeleitfähigkeit von Flüssigkeiten und Gasen ist eine Weiterentwicklung der bekannten instationären Drahtverfahren. Die Apparatur gestattet, auf einfachste Weise rasche und dennoch genaue Messungen auszuführen: Nach einer Heizdauer von nur wenigen Sekunden kann die Wärmeleitfähigkeit mit einer Genauigkeit von ±1 Prozent unmittelbar auf einem Registriergerät abgelesen werden.

Abstract—The method described here for measuring the thermal conductivity of liquids and gases is an extension of the well-known non-steady-state hot wire method. The equipment developed for this purpose offers a simple practical means for obtaining rapid and exact measurements: with heating for only a few seconds, the thermal conductivity with an accuracy of ±1 per cent can be read off directly from an instrument.

Résumé—La méthode décrite ici pour mesurer la conductibilité thermique des liquides et des gaz est une extension de la méthode classique du fil chaud en régime non permanent. L'équipement construit à cet effet utilise des moyens simples et pratiques pour l'obtention de mesures exactes et rapides: par un chauffage de quelques secondes seulement, la conductibilité thermique peut être lue directement sur l'instrument avec une précision de ±1%.

Abstract—Предлагается метод экспериментального определения коэффициента теплопроводности жидкости и газов, основанный на закономерностях нестационарного температурного поля неограниченной среды, создаваемого линейным источником тепла. Разработанная аппаратура позволяет получить надёжные необходимые расчётные данные после нескольких секунд нагревания. Точность определения коэффициента теплопроводности ±1%.

Vol. 1 1960

GRUNDLAGEN INSTATIONÄRER DRAHTVERFAHREN

Die mathematischen Grundlagen der instationären Drahtverfahren wurden erstmals von Pfriem [1] sowie Eucken und Englert [2] angegeben. Seither sind nach diesem Prinzip weitere Verfahren entwickelt und messtechnisch verbessert worden [3–12]. Das Prinzip sei anhand von Abb. 1 kurz erläutert: Ein dünner Draht vom Radius r_0 befindet sich senkrecht in einem unendlich ausgedehnten Medium mit der Wärmeleitfähigkeit λ und der Temperaturleitfähig keit $a = \lambda/c\rho$. Durch elektrische Heizung vom Zeitpunkt $t = 0$ an, wird eine pro Zeit- und Längeneinheit konstante Wärmemenge $\dot{q}$ im Draht entwickelt und durch Wärmeleitung ins umgebende Medium abgeführt. Die Rechnung zeigt [13], dass nach einer gewissen Anlaufzeit die Temperatur T an der Drahtoberfläche mit dem Logarithmus der Zeit linear ansteigt, und zwar in dimensionsloser Schreibweise nach der Beziehung

$$\frac{4\pi\lambda T}{\dot{q}} = \ln\frac{4at}{r_0^2} - 0{,}5772 \qquad (1)$$

Wird der Temperaturanstieg des Drahtes in verschiedenen Medien als Funktion der Zeit gemessen und in einen logarithmischen Zeitmasstab umgezeichnet, so ergeben sich nach

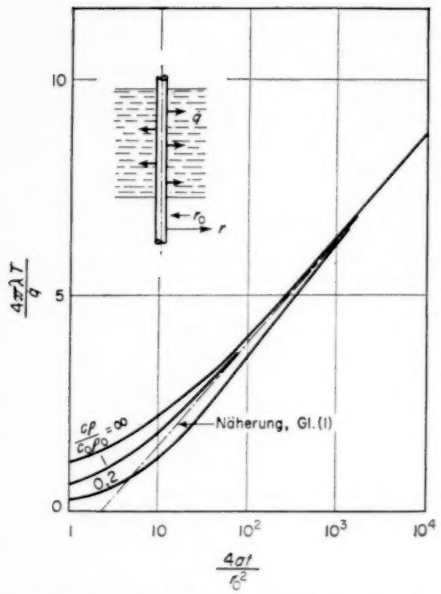

ABB. 1. Grundlage der instationären Drahtverfahren: Anstieg der dimensionslosen Temperatur an der Drahtoberfläche in Funktion der dimensionslosen Zeit. Kurven nach [14].
Draht: $c_0\rho_0$ Medium: c, ρ, λ

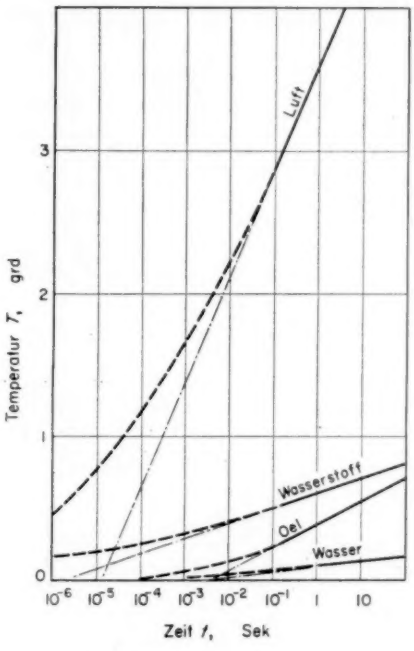

ABB. 2. Temperaturanstieg in Funktion der Zeit bei verschiedenen Medien.
Draht $\phi = 50\mu$ $\dot{q} = 0{,}1\ W/m$

Abb. 2 für den Gültigkeitsbereich der Näherung (1) Geraden. Schreibt man Gl. (1) in der Form

$$T = \frac{\dot{q}}{4\pi\lambda} \ln \frac{4\lambda}{c\rho r_0^2} + \frac{\dot{q}}{4\pi\lambda} \ln t - \frac{0{,}5772\dot{q}}{4\pi\lambda} \quad (2)$$

so erkennt man, dass die Steigung der Geraden

$$\frac{dT}{d \ln t} = \frac{\dot{q}}{4\pi\lambda} \quad (3)$$

nur eine Funktion von λ und $\dot{q}$ ist, während z.B. die Wärmekapazität $c\rho$ nur als additive Konstante eingeht. Diese vergleichsweise einfache Abhängigkeit ist eine Eigenheit der radialsymmetrischen Anordnung, worauf schon Eucken und Englert [2] hingewiesen haben.

NEUES VERFAHREN, RELATIVMETHODE

Die für die Auswertung nach Gl. (3) erforderliche Umzeichnung auf eine logarithmische Zeitachse lässt sich vermeiden, wenn man den Temperaturanstieg unmittelbar in Funktion des Logarithmus der Zeit registriert. Die logarithmische Zeitskala wird dabei durch die Erwärmung eines zweiten, gleichen Drahtes erzeugt, der sich in einem Vergleichsmedium von bekannter Wärmeleitfähigkeit befindet. Mit Vorteil verwendet man als Vergleichsmedium einen festen Körper, z.B. ein vergiessbares Kunstharz. Diese Vorrichtung sei im folgenden log-Schaltelement genannt. Bei Drähten von z.B. 10 μ Durchmesser und bei einem bestimmten Verhältnis $c_0\rho_0/c\rho$ der Wärmekapazitäten von Draht und umgebendem Medium kann die Anlaufzeit, nach deren Ablauf das logarithmische Gesetz bis auf 1% genau befolgt wird, in die Grössenordnung von Millisekunden gebracht werden.

Abb. 3 zeigt das elektrische Schaltschema. Der Draht (1) im Vergleichsmedium der Wärmeleitfähigkeit λ_A und der Draht (2) im unbekannten Medium der Wärmeleitfähigkeit λ_B sind als Widerstandsthermometer in zwei gleiche

Wheatstone-Brücken (3) und (4) geschaltet. Werden vom Zeitpunkt $t = 0$ an durch Schliessen des Schalters (5) beide Drähte durch die Stromquelle (6) geheizt, so ändern sich die Temperaturen und damit die elektrischen Widerstände R_1 und R_2 der beiden Drähte nach einer

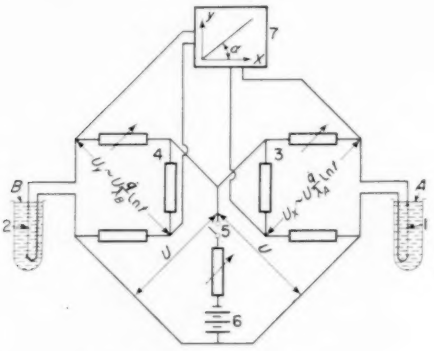

ABB. 3. Elektrisches Schema.
A Vergleichsmedium des log-Schaltelements
B unbekanntes Medium
(1) Draht des log-Schaltelements
(2) Draht im unbekannten Medium
(3) Wheatstone-Brücke des log-Schaltelements
(4) Wheatstone-Brücke
(5) Schalter
(6) Stromquelle
(7) Registriergerät

gewissen Anlaufzeit linear mit dem Logarithmus der Zeit. In den Brückendiagonalen entstehen die ebenfalls mit dem Logarithmus der Zeit linear veränderlichen Ausgleichsspannungen

$$U_y \sim U \frac{\Delta R_2}{R_2} \sim U \cdot \Delta T \sim U \cdot \frac{\dot{q}}{\lambda_B} \ln t$$

$$\text{und } U_x \sim U \cdot \frac{\dot{q}}{\lambda_A} \ln t \qquad (4)$$

Durch ein Koordinaten-Registriergerät (7) werden diese Spannungen in der Form

$$U_y = f(U_x) = \frac{\lambda_A}{\lambda_B} U_x \qquad (5)$$

aufgezeichnet, was eine Gerade mit der Steigung λ_A/λ_B darstellt. Die Wärmeleitfähigkeit erhält man nach

$$\lambda_B = \lambda_A \frac{U_x}{U_y} = \frac{\lambda_A}{\operatorname{tg} \alpha} \qquad (6)$$

durch einfaches Messen der Steigung tg α dieser registrierten Geraden.

Abb. 4 zeigt am Beispiel einiger Flüssigkeiten die Gl. (5) entsprechenden Geraden, wie sie von einem elektronischen Koordinatenschreiber aufgezeichnet wurden. Der Durchmesser der Platindrähte betrug 70 μ, die Länge 15 cm. Als Vergleichsmedium im Schaltelement diente Paraffinöl. Hier gilt das logarithmische Gesetz mit 1% Genauigkeit erst nach Ablauf von 0,1 sek. Zufolge der endlichen Einstellzeit des

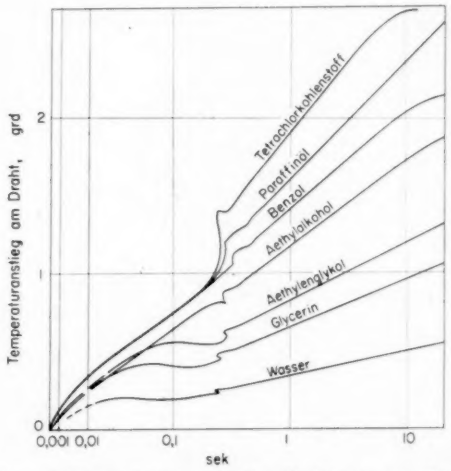

ABB. 4. Temperaturanstieg des Drahtes in verschiedenen Flüssigkeiten als Funktion des Temperaturanstiegs eines Drahtes in Paraffinöl (log-Zeitskala) Vergleichsmedium: Paraffinöl 20°C.

Geräts (automatisch abgleichende Kompensation) vermag der Schreibstift erst ab etwa 0,5 sek den veränderlichen Spannungen stetig zu folgen; die Kurvenzüge bei kleineren Zeiten stellen den Einschwingvorgang des Schreibers dar. Das Abbiegen der Geraden bei wenig viskosen Flüssigkeiten, z.B. Aethylalkohol, Benzol, zeigt das Einsetzen der freien laminaren Konvektion an. Wegen des zusätzlichen Wärmetransportes steigt dabei die Temperatur langsamer als nach dem logarithmischen Gesetz an. Damit sind hier die nutzbaren Messzeiten auf etwa 5 sek beschränkt; jedoch lässt sich die Steigung des verbleibenden Geradenstückes noch auf $\pm 1\%$ genau ausmessen.

Verwendet man ein Registriergerät höherer Empfindlichkeit und Registriergeschwindigkeit,

Vol. 1 1960

z.B. einen Elektronenstrahloszillographen, so erhält man schon nach Bruchteilen von Sekunden ein genügend langes Geradenstück. Solch kurze Zeiten werden bei Medien mit rasch einsetzender freier Konvektion, z.B. Gasen, notwendig.

Die Steigung der registrierten Geraden ist entsprechend den Wärmeleitfähigkeiten der verschiedenen Medien stark verschieden von 1. Zum genauen Ausmessen wäre jedoch eine Steigung von 1 vorteilhaft. Die Steigung kann nun leicht in die Nähe von 1 gebracht werden, indem man auf der x- und y-Achse des Registriergeräts verschiedene Empfindlichkeiten einstellt oder in den beiden Drähten zwei verschiedene Heizleistungen entwickelt oder auch von beiden Möglichkeiten Gebrauch macht. Da an beiden Drähten die gleiche Spannung liegt, erhält man verschiedene Heizleistungen durch verschiedene Widerstände, z.B. Wahl verschiedener Materialien, Drahtdurchmesser oder Längen L. Bei der Berechnung der Wärmeleitfähigkeit berücksichtigt man diese Verhältnisse durch

$$\lambda_B = \frac{\lambda_A}{\operatorname{tg}\alpha} \cdot \frac{R_1 L_1}{R_2 L_2} \cdot \frac{\text{Empfindlichkeit der } y\text{-Achse}}{\text{Empfindlichkeit der } x\text{-Achse}} \quad (8)$$

ABSOLUTMETHODE

Auch ohne Kenntnis der Wärmeleitfähigkeit im log-Schaltelement kann ein unbekanntes Medium nach der Absolutmethode gemessen werden. Die elektrische Schaltung bleibt dieselbe wie beim Relativverfahren. Nur muss dazu das log-Schaltelement z.B. mit Hilfe eines elektronischen Zeitgebers geeicht werden. Die Wärmeleitfähigkeit erhält man dann aus der Steigung der registrierten Geraden und einer apparativen Konstanten.

VERGLEICH MIT BEKANNTEN VERFAHREN

Beim beschriebenen Verfahren beträgt die Messzeit nur etwa 5 sek. Dabei muss keine elektrische Grösse wie Strom oder Spannung gemessen werden. Durch Auflegen eines Winkelmessinstrumentes mit Tangensskala auf das Registriergerät kann ohne weitere Auswertung das Resultat abgelesen werden. Eine Verfälschung der gemessenen Wärmeleitfähigkeit durch freie Konvektion ist ausgeschlossen, da man aus dem Abbiegen der registrierten Geraden das Einsetzen von Konvektion erkennt und nur das gerade Teilstück zur Winkelmessung benützt. Zwischen zwei Messungen braucht es nur eine Ruhezeit von etwa 2 Minuten, damit sich das erwärmte log-Schaltelement wieder auf Ausgangstemperatur abkühlen kann.

Somit eignet sich das Verfahren besonders für Reihenuntersuchungen, z.B. von Flüssigkeitsgemischen. Eine Anwendung ist auch denkbar zur Analyse von Flüssigkeitsgemischen auf Grund der Wärmeleitfähigkeit, wie das bei Gasen—hier allerdings durch Messen im stationären Zustand—schon üblich ist. Flüssigkeiten und Gase können auch in einem Behälter oder Apparat gemessen werden, da der Heizdraht in einer offenen Sonde ausgespannt ist, die man nur an geeigneter Stelle senkrecht in das Medium eintauchen muss. Messungen bei verschiedenen Temperaturen und Drücken können ebenfalls leicht vorgenommen werden. Immerhin ist das Verfahren auf die Messung elektrischer Nichtleiter beschränkt, solange es nicht gelingt, den Draht z.B. durch Aufdampfen eines Isolators elektrisch zu isolieren.

Im Gegensatz dazu benötigen die *Platten- und Ringspaltapparate* zur Messung im stationären Zustand lange Einstellzeiten bis zu mehreren Stunden; ausserdem sind sie in ihrer Handhabung oft umständlich. Die *stationären Hitzdrahtverfahren*, z.B. [15], verwenden ebenfalls einen dünnen Draht in der Achse einer engen Bohrung. Zur Vermeidung von Konvektion bei Flüssigkeiten darf dabei der Bohrungsdurchmesser nur etwa 2 mm betragen; dadurch treten leicht Fehler in der Justierung auf. Ausserdem muss noch der Drahtdurchmesser genau bekannt sein. Die eingangs erwähnten *instationären Hitzdrahtverfahren* arbeiten zwar auch mit kurzen Messzeiten, erfordern jedoch eine graphische Auswertung.

FEHLERQUELLEN

Wie bei allen instationären Drahtverfahren treten auch hier eine Anzahl Fehlerquellen auf. Es sind dies z.B.:

(1) Nicht konstante Heizleistung zufolge der Widerstandsänderung des Drahtes.

(2) Änderung der thermischen Konstanten bei Erwärmung des Mediums.

(3) Wärmeableitung an den Heizdrahtenden.

(4) Abweichung der gemessenen mittleren Drahttemperatur gegenüber der Temperatur an der Drahtoberfläche zufolge der endlichen Wärmekapazität des Drahtes.

(5) Wärmeabstrahlung des Drahtes.

Man kann jedoch zeigen, dass bei Drahtdurchmessern unterhalb 70 μ und Temperaturerhöhungen von höchstens 2,5 Grad diese Einflüsse teils selber sehr klein sind, teils noch dadurch kompensiert werden, dass zwei Drähte mit denselben Fehlerquellen vorhanden sind.

ANERKENNUNG

Es ist uns eine angenehme Pflicht, der Schweiz. Volkswirtschaftsstiftung für die Bereitstellung der für die Entwicklung dieses Verfahrens benötigten finanziellen Mittel zu danken.

LITERATUR

1. H. Pfriem, *Z. Ver. dtsch. Ing.* **82**, 71 (1938).
2. A. Eucken und H. Englert, *Z. ges. Kälteind.* **45**, 109 (1938).
3. J. Weishaupt, *Forsch. IngWesen* **11**, 20 (1940).
4. P. Destable, *Ann. Inst. Bâtim.* Nr. 86, **1** (1949).
5. E. F. M. van der Held und F. G. van Drunen, *Physica's Grav.* **15**, 865 (1949).
6. E. F. M. van der Held, J. Hardebel und J. Kalshofen, *Physica's Grav.* **19**, 208 (1953).
7. B. H. Vos, *Appl. Sci. Res. Hague* **A 5**, 425 (1955).
8. B. H. Vos, *Bull. Int. Inst. Refrig. Annexe* **1**, 47 (1957).
9. D. G. Gillam und O. Lamm, *Acta Chem. Scand.* **9**, 657 (1955).
10. D. G. Gillam, L. Romben, H. Nissen und O. Lamm, *Acta Chem. Scand.* **9**, 641 (1955).
11. R. A. W. Hill, *Proc. Roy. Soc.* **A 239**, 476 (1957).
12. P. H. G. Allen, Fluid thermal conductivity by a transient method. *Symp. Amer. Soc. Mech. Engrs.*, p. 350 (1959).
13. H. S. Carslaw und J. C. Jaeger, *Conduction of Heat in Solids*, Sections 13.7 II, 342 und 13.7 IV, 345 (1959).
14. J. C. Jaeger, *Aust. J. Sci. Res.* **9**, 167 (1956).
15. R. Goldschmidt, *Phys. Z.* **12**, 417 (1911).

Vol.
1
1960

Int. J. Heat Mass Transfer. Vol. 1, pp. 55–67. Pergamon Press 1960. Printed in Great Britain.

EVALUATION OF BULK VELOCITY AND TEMPERATURE FOR TURBULENT FLOW IN TUBES

G. F. C. ROGERS and Y. R. MAYHEW
Mechanical Engineering Department, University of Bristol, England

(*Received* 17 *November* 1959)

Abstract—This article describes two methods by which bulk velocities and temperatures can be found without resorting to traversing or the use of mixing chambers; in each case by only one local measurement at the section considered. Both methods depend on a knowledge of the velocity and temperature profiles at that section; knowledge which is now available for fully established turbulent flow in smooth tubes.

(a) *Axial method:* The velocity or temperature probe is placed at the axis, and the reading multiplied by an appropriate weighting factor.

(b) y_m/r *method:* The velocity or temperature probe is placed a distance from the wall at which it reads the mean value directly.

Information is presented for finding the bulk velocity and temperature by either method, and their relative merits are discussed.

When making temperature measurements in a fluid with a thermocouple it is often convenient to bring the wire out radially from a butt-welded junction, and it is then necessary to establish that no serious conduction error is introduced. Data are presented which allow estimates to be made of temperature errors for a centrally placed junction of various materials and gauges, and for various rates of flow and types of fluid including liquid metals.

Résumé—Cet article décrit deux méthodes permettant le calcul des vitesses et des températures moyennes sans nécessiter de dispositif permettant le déplacement transversal et sans utiliser de chambre de mélange; dans chaque cas, la mesure se fait en un point seulement de la section considérée. Les deux méthodes dépendent de la connaissance des profils de vitesses et de températures dans cette section; cette connaissance est maintenant valable pour un écoulement turbulent pleinement établi dans des tubes lisses.

(a) *Méthode axiale*: la sonde de vitesse ou de température est placée sur l'axe et la lecture est multipliée par un facteur de pondération convenable.

(b) *Méthode* y_m/r: la sonde de vitesse ou de température se trouve à une distance de la paroi telle que la lecture fournit directement la valeur moyenne.

Des indications sont données pour le calcul des vitesses et températures moyennes par les deux méthodes dont les qualités respectives sont discutées.

Quand on mesure les températures dans un fluide avec un thermocouple, il est souvent commode de sortir le fil radialement grâce à une connexion soudée et il est alors nécessaire d'établir que l'erreur de conduction introduite est négligeable. On présente ici des résultats permettant d'estimer l'erreur de température pour une disposition centrale des jonctions de fils et de jauges de nature variée, pour différents régimes d'écoulement et pour différentes sortes de fluides, y compris les métaux liquides.

Zusammenfassung—Dieser Aufsatz beschreibt zwei Verfahren zur Ermittlung von mittleren Geschwindigkeiten und Temperaturen ohne Messung der Geschwindigkeits- und Temperaturverteilung und ohne die Anwendung von Mischern. In jedem Falle hängt die Auswertung für einen Rohrquerschnitt von einer örtlichen Messung ab. Für beide Methoden braucht man die Kenntnis der Temperatur und Geschwindigkeitsprofile in diesem Querschnitt, wie sie für ausgebildete turbulente Strömung in glatten Rohren bekannt ist.

(a) *Axiales Verfahren*: Die Geschwindigkeits- oder Temperatursonde wird in die Rohrachse gelegt, und der Messwert wird mit einem passenden Faktor multipliziert.

(b) y_m/r *Verfahren*: Die Geschwindigkeits- oder Temperatursonde wird in einem Wandabstand gelegt, wo sie den Mittelwert direkt angibt.

Für beide Verfahren werden die notwendigen Angaben gemacht, um die mittlere Geschwindigkeit und Temperatur zu erhalten und ihre Vorzüge werden miteinander verglichen.

Bei Messung von Flüssigkeitstemperaturen mit einem Thermoelement werden oft die Drähte radial von der Lötstelle nach aussen geführt und es ist dann wichtig festzustellen, dass keine grossen Messfehler durch Wärmeleitung entstehen. Zur Abschätzung von Temperaturmessfehlern für axiale Lötstellen aus verschiedenen Drahtmaterialien und Durchmessern und für verschiedene Strömungsgeschwindigkeiten und Flüssigkeiten, einschliesslich flüssiger Metalle, werden Zahlenwerte angegeben.

Abstract—В статье описываются два метода, с помощью которых можно определить осредненные по объёму скорости и температуры, не прибегая к перемещению соответствующих датчиков или использованию камер смешения. В каждом случае они сводятся только к одному локальному замеру в рассматриваемом сечении. Оба метода требуют знания профилей скорости и температуры в этом сечении. Для полностью установившегося турбулентного потока в гладких трубах эти профили хорошо известны.

(*а*) *Осевой метод:* Датчик скорости или температуры помещается на оси, а его показание умножается на соответствующий коэффициент веса.

(*б*) *Метод* y_m/r *:* Датчик скорости или температуры помещается на расстоянии от стенки, на котором он непосредственно даёт среднее значение.

Даётся описание обоих методов и рассматриваются их относительные преимущества.

При измерениях температуры в потоке с помощью термопары часто бывает удобно вывести проводники от спая по радиусам. В этом случае необходимо убедиться, что не вносится серьёзная погрешность, связанная с теплопроводностью проводников. Приведены данные, позволяющие оценить температурные погрешности для различных по материалу и диаметру проводов термопар с центральным расположением спая, при различных скоростях потока и различных субстанциях, включая жидкие металлы.

In experimental heat transfer work it is often necessary to measure bulk velocities and temperatures of fluids flowing through tubes. Bulk velocity can be obtained either by radial traversing (e.g. with pitot or hot wire probe) or by some kind of orifice meter. Bulk temperature can be obtained by radial traversing or by means of a mixing chamber. (It must be remembered that when a bulk temperature is obtained by traversing, both velocity and temperature traverses are necessary if the correct weighted-mean value is to be obtained.) Orifice meters or mixing chambers, while giving bulk values directly, can only be used at entry to and exit from a test length, since they would completely upset the flow when mounted at an intermediate section. Traverses are impractical in tubes of small diameter, and are at best laborious, and they cannot normally be justified unless the purpose of an investigation is the study of the velocity and temperature profiles themselves.

This article describes two further methods by which bulk velocities and temperatures can be found; in each case by only one local measurement at the section considered. Both methods depend on a knowledge of the velocity and temperature profiles at that section: knowledge which is now available for fully established turbulent flow in smooth tubes.

(a) *Axial method.* The velocity or temperature probe is placed at the axis, and the reading multiplied by an appropriate weighting factor u_m/u_r or $(t_m - t_w)/(t_r - t_w)$, respectively.

(b) y_m/r *method.* The velocity or temperature probe is placed a distance from the wall y_{mu} or y_{mt}, respectively, at which it reads the mean value directly.

Information is presented in Sections 1 and 2 for finding bulk velocity and temperature by either method, and their relative merits are discussed.

When making temperature measurements in a fluid with a thermocouple, the wire is often laid axially along an isothermal, before being taken out radially, to reduce conduction error. Sometimes it is more convenient, however, to bring the wire out radially from a butt-welded junction, and it is then necessary to establish that no serious conduction error is introduced. Data are presented in Section 3 which allow estimates to be made of temperature errors for a centrally placed junction of various wire materials and gauges, and for various rates of flow and types of fluid including liquid metals.

Vol. 1 1960

NOMENCLATURE

d = thermocouple wire diameter;
D = tube diameter;

h = convection heat transfer coefficient;
I_1 = integral defined by equations (3) and (4);
I_2 = integral defined by equations (11) and (12);
q = heat flow per unit area and unit time;
r = tube radius;
r^+ = dimensionless radius $(= r\sqrt{(\tau_w/\rho)}/\nu)$;
t = temperature at any radius;
Δt = temperature relative to wall $(= t - t_w)$;
Δt^+ = dimensionless temperature relative to wall $(= \Delta t \rho c_p \sqrt{(\tau_w/\rho)}/q_w)$;
u = velocity at any radius;
u^+ = dimensionless velocity $\{= u/\sqrt{(\tau_w/\rho)}\}$;
y = distance from wall;
y^+ = dimensionless distance from wall $(= y\sqrt{(\tau_w/\rho)}/\nu)$;
y_{mt}, y^+_{mt} = wall distance at which $t = t_m$;
y_{mu}, y^+_{mu} = wall distance at which $u = u_m$.

Greek symbols

μ = dynamic viscosity;
ν = kinematic viscosity;
ρ = density;
τ = shear stress.

Dimensionless groups

P = Prandtl number $(= c_p\mu/k)$;
R_d = Reynolds number based on thermocouple wire diameter $(= ud/\nu)$;
R_m = Reynolds number based on mean velocity $(= 2u_m r/\nu)$;
R_r = Reynolds number based on axial velocity $(= 2u_r r/\nu)$;
ϵ_M/ϵ_H = ratio of eddy diffusivities for momentum and heat transfers.

Suffixes

d = refers to the thermocouple wire;
f = refers to the fluid;
m = mean value;
r = at axis of tube;
w = at wall.

1. MEASUREMENT OF MEAN VELOCITY

1.1. *Axial method*

For a tube, the mean or bulk velocity is defined by the equation

$$\rho\, u_m\, \pi r^2 = \rho \int_0^r u\, 2\pi(r - y)dy \qquad (1)$$

in which it is assumed that ρ is independent of y. Hence the ratio of mean to axial velocity is obtained as

$$\frac{u_m}{u_r} = \frac{2}{u_r\, r^2} \int_0^r u(r - y)dy \qquad (2)$$

To find the integral, it is necessary to know the function $u = f(y)$. It has been found [1] that if the velocity and distance from the wall are expressed in dimensionless form by $u^+ = u/\sqrt{(\tau_w/\rho)}$ and $y^+ = y\sqrt{(t_w/\rho)}/\nu$, respectively, it is possible to deduce a universal velocity profile, Fig. 1, which fits experimental results over a wide range of Reynolds numbers. Introducing u^+ and y^+ into equation (2), the ratio u_m/u_r becomes

$$\frac{u_m}{u_r} = \frac{u^+_m}{u^+_r} = \frac{2}{u^+_r r^{+2}} \int_0^{r+} u^+ (r^+ - y^+)dy^+ = \frac{2}{u^+_r r^{+2}} I_1 \qquad (3)$$

Using the equatons in Fig. 1, I_1 can be expanded to give

$$I_1 = \int_0^5 y^+(r^+ - y^+)dy^+ + \int_5^{30} (-3{\cdot}05 + 5 \ln y^+)(r^+ - y^+)dy^+ + \int_{30}^{r+} (5{\cdot}5 + 2{\cdot}5 \ln y^+)(r^+ - y^+)\, dy^+ =$$
$$1{\cdot}25\, r^{+2}(0{\cdot}7 + \ln r^+) - 63{\cdot}9\, r^+ + 573 \qquad (4)$$

In this way values of u_m/u_r can be found for various values of r^+.

It is normally more convenient to relate u_m/u_r to the Reynolds number based either on axial velocity $R_r = 2u_r r/\nu$, or on mean velocity $R_m = 2u_m r/\nu$. It can easily be shown that

$$R_r = 2u^+_r r^+ \qquad (5)$$

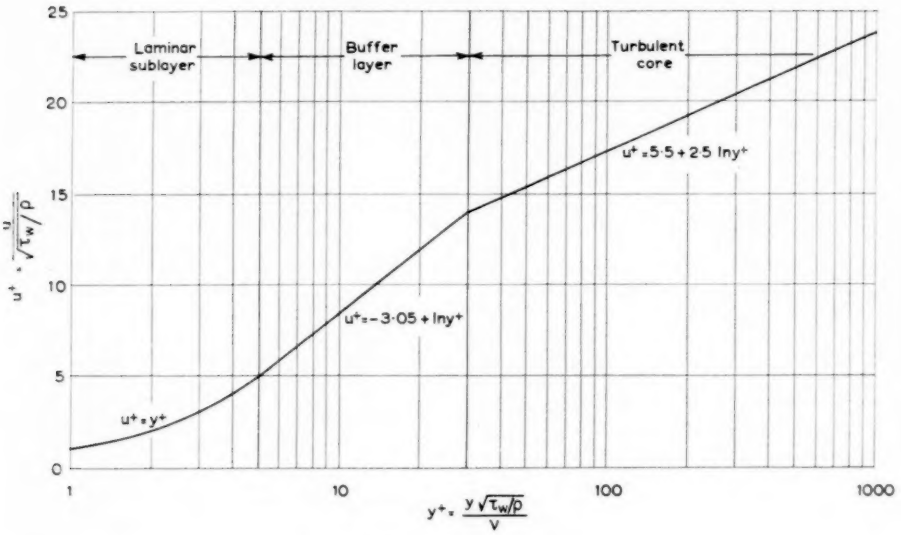

FIG. 1. Universal velocity profile.

Vol. 1 1960

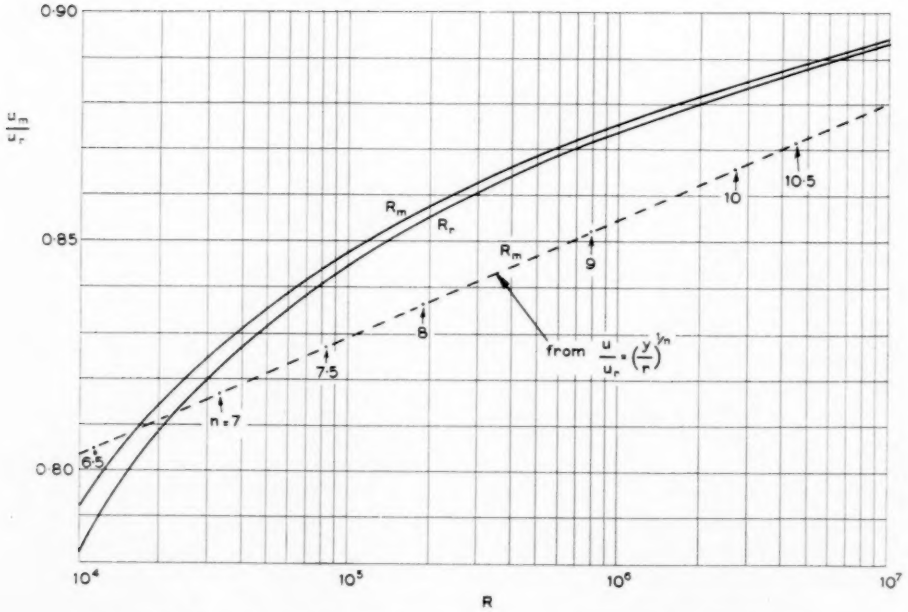

FIG. 2. Ratio u_m/u_r against Reynolds number $R_r = 2u_r r/\nu$ and $R_m = 2u_m r/\nu$.

and

$$R_m = 2u_m^+ r^+ = R_r \frac{u_m}{u_r} \tag{6}$$

Thus with these equations, and u^+ taken from Fig. 1, it is possible to relate u_m/u_r with R_r or R_m: these relations are shown in Fig. 2. If the axial velocity u_r is measured in an experiment, it is then possible to calculate the value of R_r, and the appropriate mean velocity $u_m = u_r\,(u_m/u_r)$ can be found by means of Fig. 2.

It is interesting to compare the result with that obtained for fully developed laminar flow when a parabolic velocity profile can be assumed: the value of u_m/u_r is then 0·5 and is independent of Reynolds number.

1.2. *y_{mu}/r method*

The mean velocity can also be found by placing the probe at the appropriate wall distance y_{mu}. For various values of r^+, corresponding values of u_m^+ have been obtained from equation (3) and corresponding values of R_m from (6). It is found that y_{mu} is always in the turbulent core, and to find it, it is necessary to use the appropriate equation from Fig. 1. Thus

$$y_{mu}^+ = \exp\left(\frac{u_m^+ - 5{\cdot}5}{2{\cdot}5}\right) \tag{7}$$

and hence the correct placing of the velocity probe is found as

$$\frac{y_{mu}}{r} = \frac{y_{mu}^+}{r^+} = \frac{1}{r^+} \exp\left(\frac{u_m^+ - 5{\cdot}5}{2{\cdot}5}\right)$$

Values of y_{mu}/r against R_m are plotted in Fig. 3.

Again for comparison, the value of y_{mu}/r for fully developed laminar flow is 0·293.

1.3. *Conclusions*

Mean velocity deduced from an axial measurement is to be preferred to that deduced from a measurement at y_{mu}. Firstly, at the axis a larger and more easily read deflexion of the measuring instrument is obtained and wall interference is less serious. Secondly, near the axis u does not vary appreciably with y, and neither location nor instrument width are as critical. The advantage of the y_{mu} method is that several pitot tubes, connected by a piezometer ring, can be spaced around the circumference so that the effect of any slight asymmetry in the flow is minimized.

How critical the location is with the y_{mu}/r method can be shown by the following argument. From the velocity profile, $u^+ = 5{\cdot}5 + \ln y^+$, in the turbulent core,

$$\frac{du^+}{dy^+} = \frac{2{\cdot}5}{y^+}$$

or

$$\frac{dy^+}{r^+} = 0{\cdot}4\,\frac{du^+}{u^+}\,\frac{y^+}{r^+}\,u^+$$

Putting $y^+ = y_{mu}^+$, $u^+ = u_m^+$, and placing a limit of 1 per cent on $\delta u^+/u_m^+$, the maximum permissible deviation is found to be

$$\frac{\delta y}{r} = \frac{\delta y^+}{r^+} = 0{\cdot}004\,\frac{y_{mu}^+}{r^+}\,u_m^+ \tag{8}$$

The results are plotted in Fig. 3.

Jakob [2] presented an analysis similar to that in Sections 1.1 and 1.2, but based on the simpler and earlier velocity profile $u/u_r = (y/r)^{1/n}$ where n is a function of Reynolds number. The results, for comparison with the curves based on the universal velocity profile, have been added as dotted curves in Figs. 2 and 3.

2. MEASUREMENT OF MEAN TEMPERATURE

2.1. *Axial method*

For a tube, the mean or bulk temperature is defined by the equation

$$\rho c_p\,u_m\,(t_m - t_w)\,\pi r^2 = \rho c_p \int_0^r u(t - t_w)\,2\pi\,(r - y)dy \tag{9}$$

in which it is assumed that ρ and c_p are independent of y, and u_m is given by equation (3). Writing Δt for $(t - t_w)$, the ratio of mean to axial temperature becomes

$$\frac{\Delta t_m}{\Delta t_r} = \frac{2}{u_m \Delta t_r r^2}\int_0^r u\Delta t\,(r - y)dy \tag{10}$$

To evaluate the integral, it is necessary to know the functions $u = f(y)$ and $t = g(y)$. For the velocity profile it is again possible to use the dimensionless presentation of Fig. 1, while for

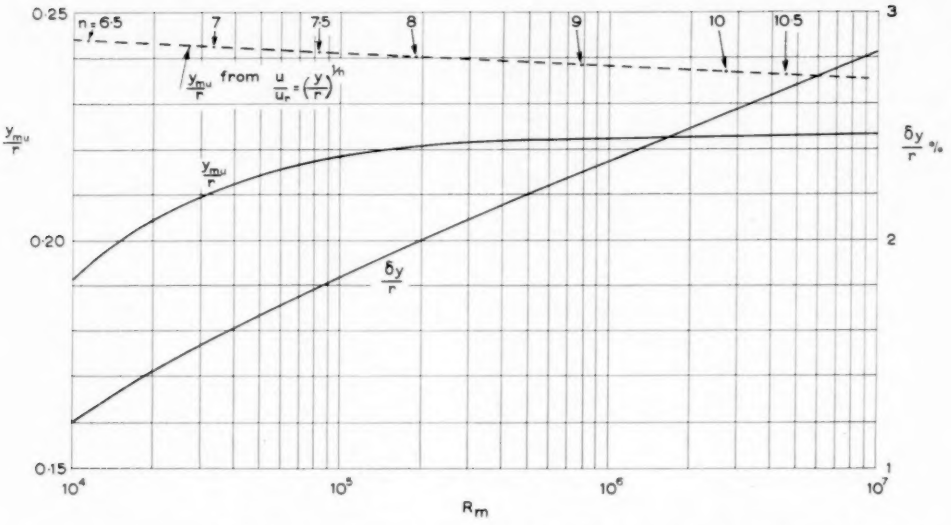

FIG. 3. Position y_{mu}/r of velocity probe and permissible location error $\delta y/r$ (for 1 per cent error in u_m) against R_m.

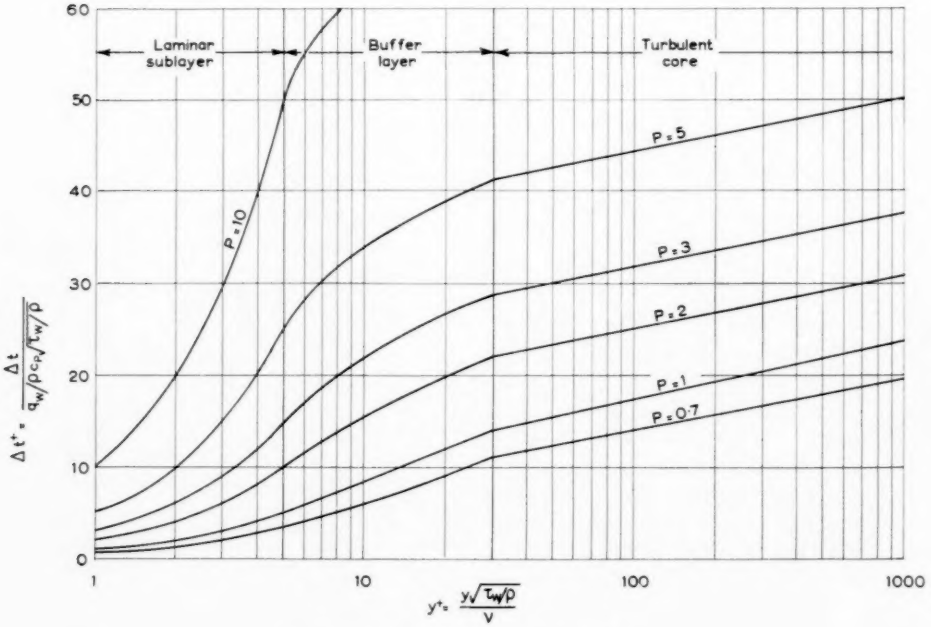

FIG. 4. Universal temperature profile.

Laminar sublayer $\Delta t^+ = Py^+$;
Buffer layer $\Delta t^+ = 5[P + \ln(0{\cdot}2Py^+ - P + 1)]$;
Turbulent core $\Delta t^+ = 5[P - 1{\cdot}691 + \ln(5P + 1) + 0{\cdot}5 \ln y^+]$ (For $P < 0{\cdot}1$ use equation 13)

Vol. 1 1960

the temperature profile the dimensionless presentation of Fig. 4, due to Squire [3] (extension of von Kármán [1]), can be used. It will be seen that no single equation in terms of y^+ represents the temperature profile, but that a family of curves is necessary for which the Prandtl number is the parameter. Introducing the dimensionless temperature, velocity and wall distance into equation (10), and substituting for u_m from equation (3), the ratio $\Delta t_m/\Delta t_r$ becomes

$$\frac{\Delta t_m}{\Delta t_r} = \frac{\Delta t_m^+}{\Delta t_r^+} = \frac{1}{\Delta t_r^+ I_1}\int_0^{r^+} u^+ \Delta t^+ (r^+ - y^+)\, dy^+ = \frac{I_2}{\Delta t_r^+ I_1^+} \qquad (11)$$

where

$$\left.\begin{aligned} I_2 = {} & \int_0^5 y^+ P y^+ (r^+ - y^+)\, dy^+ + \\ & + \int_5^{30} (-3{\cdot}05 + 5 \ln y)\, 5\,[P + \\ & + \ln (0{\cdot}2 P y^+ - P + 1)]\,(r^+ - y^+) dy^+ + \\ & + \int_{30}^{r^+} (5{\cdot}5 + 2{\cdot}5 \ln y^+)\, 5\,[P - 1{\cdot}691 + \\ & \quad + \ln (5P + 1) + 0{\cdot}5 \ln y^+] \times \\ & \quad \times (r^+ - y^+) dy^+ \end{aligned}\right\} (12)$$

I_2 must be solved by numerical integration for a series of values of r^+ and P. Since a value of R_m can be found for every value of r^+ as explained in Section 1.1, $\Delta t_m/\Delta t_r$ can finally be determined as a function of R_m and P. This procedure is extremely laborious, but Martinelli [4] obtained values of $\Delta t_m/\Delta t_r$ by a method equivalent to the one presented here, and his results are reproduced in Fig. 5. For comparison, $\Delta t_m/\Delta t_r$ for fully developed laminar flow is approximately 0·6.

It will be seen that the curves in Fig. 5 extend to the low Prandtl numbers which are associated with liquid metals. Equation (12) does not apply when P is much less than 0·1, and the case of liquid metals deserves special mention. Low P (i.e. high thermal conductivity k) implies a steeper temperature gradient in the turbulent core, and the equation for $y^+ > 30$ given in Fig. 4 is no longer applicable. (The equation is derived on the assumption that the thermal diffusivity ν/P is negligible compared with the eddy diffusivity ϵ and this is no longer true for the turbulent core when P is small.) The appropriate equation which must be used to replace the term

$$5[P - 1{\cdot}691 + \ln (5P + 1) + 0{\cdot}5 \ln y^+]$$

in the third integral of equation (12), for the limits $30 < y^+ < r^+$, is as follows

$$\left.\begin{aligned} \Delta t^+ = {} & 1{\cdot}25 \times \\ & \times \ln \left[\frac{(5/Pr^+) + (y^+/r^+)\,\{1 - (y^+/r^+)\}}{(5/Pr^+) + (30/r^+)\,\{1 - (30/r^+)\}}\right] + \\ & + \frac{1.25}{\sqrt{\{1 + (20/Pr^+)\}}} \times \\ & \times \ln \left[\frac{\{(2y^+/r^+) - 1\} + \sqrt{\{1 + (20/Pr^+)\}}}{\{(2y^+/r^+) - 1\} - \sqrt{\{1 (+ 20/Pr^+)\}}} \times \right. \\ & \left. \times \frac{\{(60/r^+) - 1\} - \sqrt{\{1 + (20/Pr^+)\}}}{\{(60/r^+) - 1\} + \sqrt{\{1 + (20/Pr^+)\}}}\right] + \\ & + 5\,[P + \ln (5P + 1)]. \end{aligned}\right\} (13)$$

2.2. y_{mt}/r method

The mean temperature can be found by placing the probe at the appropriate wall distance y_{mt}, which in general is not the same as y_{mw}. y_{mt}/r $(= y_{mt}^+/r^+)$ can be found by substituting the appropriate value of Δt_m^+ in the equation for the turbulent core

$$\Delta t_m^+ = 5\,[P - 1{\cdot}691 + \ln (5P + 1) + 0{\cdot}5 \ln y_{mt}^+].$$

(For fluids of $P < 0{\cdot}1$ equation (13) would have to be used.) Δt_m^+ at any value of R_m can be obtained from both Δt_r^+ and the ratio $\Delta t_m/\Delta t_r$ taken from Fig. 5. Unfortunately Martinelli's data presented in Fig. 5 are not sufficiently detailed to enable reliable and consistent curves to be obtained for y_{mt}/r. Nevertheless these calculations have been made for fluids having Prandtl numbers greater than 0·7 and certain conclusions can be drawn from them.

(a) y_{mt}/r is not very sensitive to Reynolds number R_m.

(b) y_{mt}/r varies significantly with P, being approximately 0·31 at $P = 1$, 0·22 at $P = 10$, and 0·15 at $P = 40$.

(c) An analysis to reveal the permissible tolerance of positioning, analogous to that presented for velocity u_m in Section 1.3, has been carried out. For an error of $\delta\Delta t/\Delta t_m = 1$ per cent this gave

$$\frac{\delta y}{r} = \frac{\delta y^+}{r^+} = 0{\cdot}004\,\frac{y^+_{mt}}{r^+}\,\Delta t^+_m \qquad (14)$$

At $P = 1$, positioning is sensitive to $\delta y/r$ of 2–3 per cent (depending somewhat on R_m), and it becomes less sensitive at higher values of P; at $P > 50$ the probe will give a reading to better than 2 per cent anywhere between the axis and the buffer layer.

2.3. *Conclusions*

Mean temperature deduced from axial measurement is to be preferred to that deduced from a measurement at y_{mt}, for the same

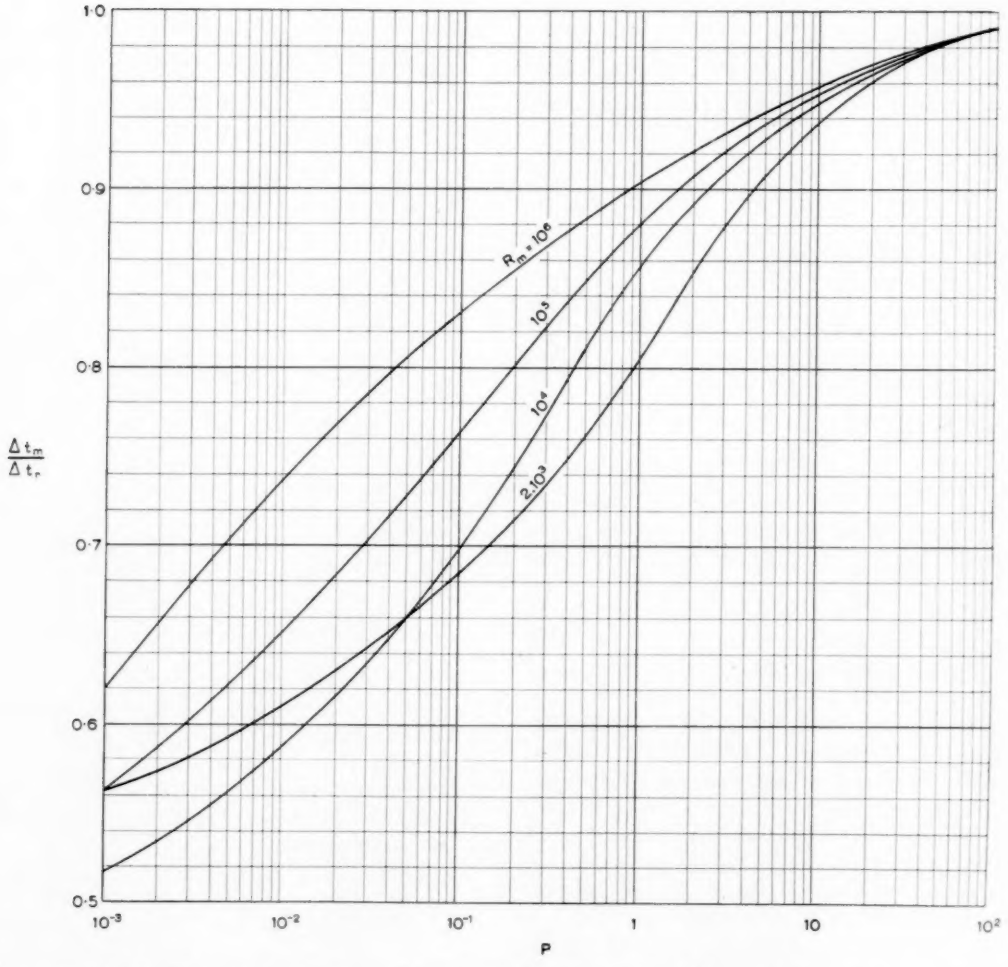

FIG. 5. Ratio $\Delta t_m/\Delta t_r$ against Prandtl number P, for several values of Reynolds number R_m (from Martinelli [4]).

Vol. 1 1960

reasons given in Section 1.3 when discussing the measurement of mean velocity. Only an approximate guide to positioning for the y_{mt}/r method can be given at present.

It must be remembered that the universal temperature profile has been derived by von Kármán using two principal assumptions.

(a) The ratio q/τ is independent of y (i.e. $q/\tau = q_w/\tau_w$.
(b) The ratio of eddy diffusivities for momentum and heat transfer, ϵ_M/ϵ_H, is equal to unity.

Assumptions (a) and (b) provide the basis for the simple Reynolds Analogy between momentum and heat transfer. The importance of assumption (b) has been tested by a few spot calculations to see its effect on the results of this section. By taking the lowest experimental value of ϵ_M/ϵ_H for flow in tubes ($0{\cdot}7 < \epsilon_M/\epsilon_H < 1$), and using a temperature profile modified to take account of variations in ϵ_M/ϵ_H, it was found that ϵ_M/ϵ_H has little effect on the ratio $\Delta t_m/\Delta t_r$.

It must be remembered that there are more serious deficiencies in the theory presented here. First, the universal velocity profile itself is an approximation and it fits well only in isothermal flow. ("Isothermal flow" implies a small value of $\Delta t = t - t_w$ so that it is reasonable to assume constant fluid properties over the flow cross-section.) In non-isothermal flow ν may vary appreciably across the tube. To allow for such variation in generalized and condensed form for all kinds of fluids is impossible. Deissler [5, 6] has done some work of this kind, allowing for variations of fluid properties with temperature, for air, supercritical water, and fluids of $P = 1$.

Secondly, the universal profiles are only good approximations for flow in hydraulically smooth tubes. The best check as to whether a tube is smooth is by comparing measured friction factors with those obtained from published data. Alternatively, a fairly safe criterion is that the surface roughness should be less than that corresponding to $y^+ = 5$, i.e. the roughness should lie within the laminar sublayer.

3. THERMOCOUPLE CONDUCTION ERROR

In order to reduce the error due to conduction along the wire when measuring temperature with a thermocouple, it is usual to lay the wire along an isothermal before taking it out radially, as shown in Fig. 6 (a). Often, particularly with tubes of small diameter, it is more convenient to use a centrally placed butt junction with taut wires emerging radially, an arrangement which gives rigidity and accurate location without elaborate supports that may interfere with the flow. It is necessary, however, to be able to estimate whether the observed couple temperature t_c reads the axial temperature t_r with negligible error, i.e. whether $(t_r - t_c)$ is small compared with $(t_r - t_w)$ (see Fig. 6 b).

So that a fair idea of the errors may be obtained, half the wire—from wall to junction—is treated as a "fin" projecting from a surface at t_w into a fluid at t_r, as shown in Fig. 6 (c).

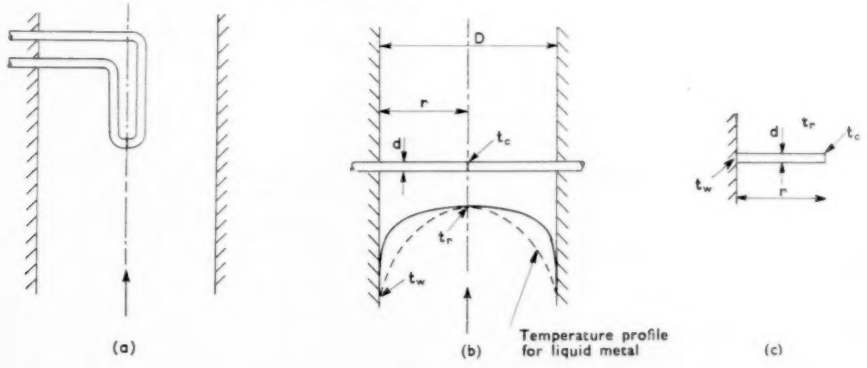

FIG. 6.

Simple fin theory shows, e.g. in Ref. [7], that

$$\frac{t_r - t_c}{t_r - t_w} = \frac{1}{\cosh mr} \tag{15}$$

where

$$mr = \left(\frac{h \times \text{fin circumference}}{k_d \times \text{fin cross-sectional area}}\right)^{1/2} r = \left(\frac{4h}{k_d d}\right)^{1/2} r \tag{16}$$

The principal assumptions in the derivation of equation (15) are:

(a) The fluid temperature t_r is uniform along the "fin".

(b) The heat transfer coefficient h is constant over the "fin" surface.

(c) The heat flow from the tip of the "fin" is negligible, i.e. $dt/dy = 0$ at $y = r$.

Assumption (a) is obviously not satisfied in a tube, but since for most fluids in turbulent flow the temperature profile is very flat across the turbulent core, this assumption is far off the mark only in a very thin layer near the wall. The only exceptions are liquid metals, for which t varies significantly in the core, and they are dealt with later.

Assumption (b) is also not satisfied in the tube because h depends mainly on the velocity u. But again the velocity profile is very flat in the turbulent core and this assumption is valid except in a very thin layer near the wall.

Assumption (c) is true only if the two metals forming the junction have the same thermal conductivity, because otherwise conditions are asymmetrical. With metals of different conductivity there will be a slight flow of heat from the better to the worse conductor but, because of the flatness of the temperature profile near the centre of the tube, this will be very small.

In the following, all three assumptions will be taken as adequate for determining the circumstances in which the error $(t_r - t_c)$ is negligible, even though they may not be quite satisfactory in estimating accurately errors when they are significant.

To evaluate equation (16) it is necessary to know how h varies with Reynolds number and Prandtl number for a cylinder in cross-flow. For air and other gases with similar Prandtl number, the curve on p. 259 of McAdams [8] has been used. This relates the Nusselt number $N_d = hd/k_f$ to the Reynolds number $R_d = u_m d/\nu_f$. For liquids (other than liquid metals) the following relation from p. 268 of McAdams [8] has been used:

$$\frac{N_d}{P^{0.3}} = 0.35 + 0.56\, R_d^{0.52} \tag{17}$$

Substituting for $h = N_d k_f/d$ in equation (16), the following is obtained

$$mr = \left(\frac{4N_d k_f}{d^2 k_d}\right)^{1/2} r = N_d^{1/2} \left(\frac{k_f}{k_d}\right)^{1/2} \left(\frac{D}{d}\right) = \mathrm{f}(R_d, P_f) \left(\frac{k_f}{k}\right)^{1/2} \left(\frac{D}{d}\right) \tag{18}$$

For any fluid of given Prandtl number P, it is therefore possible to express $(t_r - t_c)/(t_r - t_w)$ as a function of R_d, (D/d) and (k_d/k_f). Furthermore, since the Reynolds number R_m based on the tube diameter D is equal to $R_d(D/d)$, it is possible to substitute R_m for R_d.

The results of a few calculations are shown in Figs. 7(a)–(c). Figs. 7(a) and (b) are based on data for air, but they are equally applicable to other gases because all gases have Prandtl numbers which do not depart appreciably from the value for air ($P \simeq 0.7$). Fig. 7(a) refers to a k_d/k_f ratio of 15,000 which corresponds approximately to a copper wire in air (e.g. a copper–constantan thermocouple). Fig. 7(b) refers to a k_d/k_f ratio of 1000 which corresponds to a manganin–constantan or chromel–alumel thermocouple in air, all of which metals have similar conductivities. It is clear that if errors of less than 1 per cent are desired, it is necessary to use a low conductivity couple, such as manganin–constantan, unless a very high D/d ratio can be used.

Fig. 7(c) refers to a liquid of Prandtl number 5 (e.g. water at about 90°F) and a k_d/k_f ratio of 600 (e.g. copper in water). The error is negligible except for very low D/d ratios. Manganin–constantan in water would yield a k_d/k_f ratio of about 40 and the error is then negligible for all practical values of D/d. Liquids of higher Prandtl number (e.g. oils of $P \simeq 100$) are no problem, because N_d is appreciably greater and

Vol. 1 1960

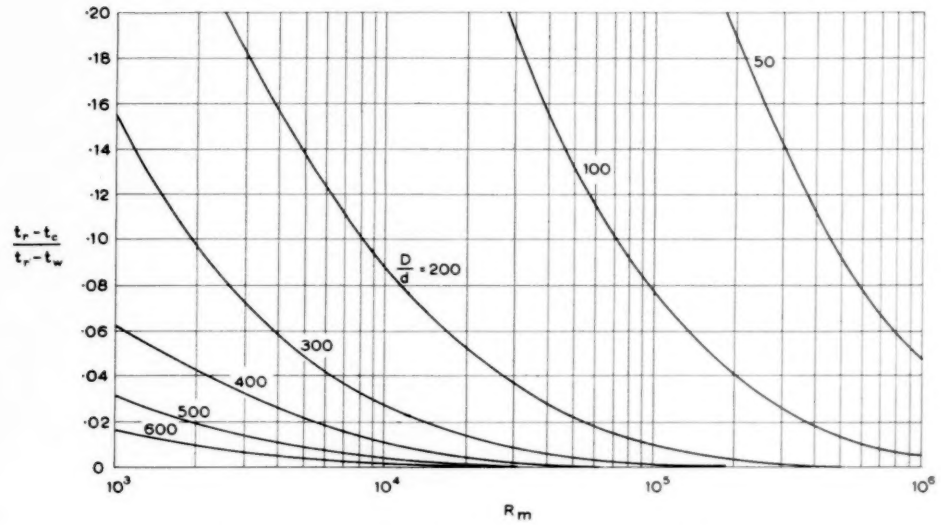

FIG. 7(a). Air and other gases ($P \simeq 0{\cdot}7$), $k_d/k_f = 15{,}000$.

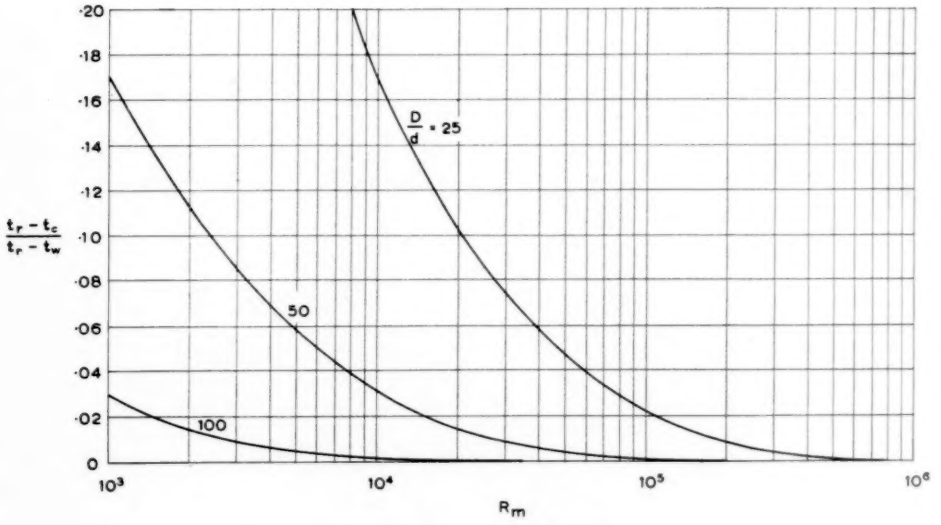

FIG. 7(b). Air and other gases ($P \simeq 0{\cdot}7$), $k_d/k_f = 1000$.

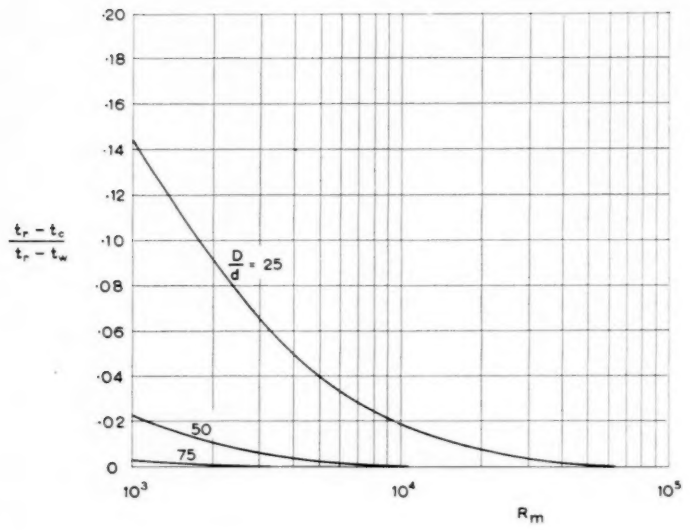

FIG. 7(c). Liquids of $P = 5$, $k_d/k_f = 600$.

Vol. 1 1960

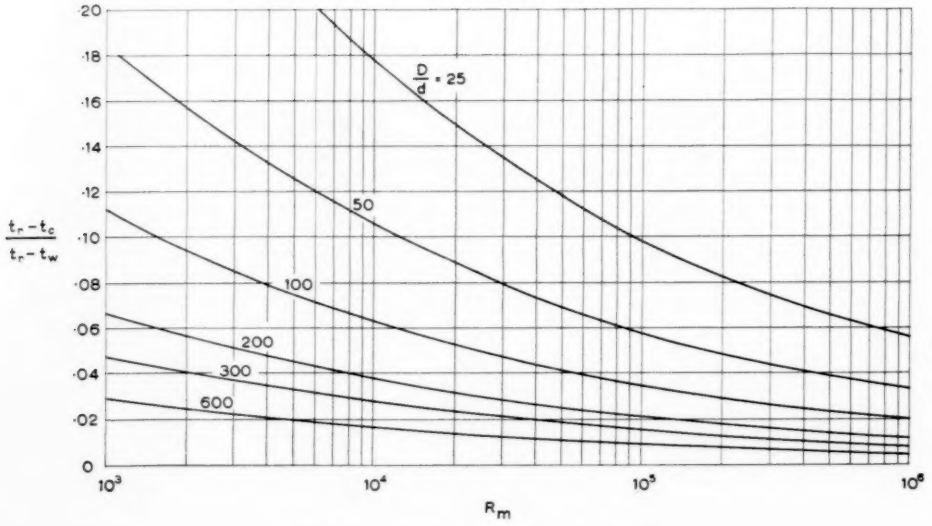

FIG. 8. Liquid metals of $P = 0{\cdot}01$, $k_d/k_f = 40$.

even the use of copper and low ratios of D/d results in negligible errors.

It is still necessary to consider liquid metals, which have very low Prandtl numbers (viz. 0·005–0·03). As already mentioned in Section 2.1, the high thermal conductivity results in a marked variation of temperature even in the turbulent core. Assumption (a) in the analysis of the "fin" is no longer valid, and a much better approximation is to assume that the fluid temperature varies linearly from t_w at the wall to t_r at the axis of the tube. With this modification it is possible to show that

$$\frac{t_r - t_c}{t_r - t_w} = \frac{1}{mr} \tanh mr \qquad (19)$$

mr is again given by equation (18), but N_d must be found from the appropriate equation for liquid metals

$$N_d = 1{\cdot}015\,(R_d\,P)^{1/2} \qquad (20)$$

taken from Eckert and Drake [9]. The results for a liquid metal of $P = 0{\cdot}01$ and $k_d/k_f = 40$ are given in Fig. 8. $k_d/k_f = 40$ corresponds approximately to copper wire in mercury. Even with liquid sodium, which has a much higher thermal conductivity than mercury, the use of copper would lead to too large an error. Manganin–constantan thermocouples would, however, be quite satisfactory. It is found that for all practical values of mr, tanh mr is virtually unity. Hence the results of Fig. 8 can easily be applied to any k_d/k_f ratio, because for any given D/d

$$\frac{t_r - t_c}{t_r - t_w} \propto \frac{1}{mr} \propto \left(\frac{k_d}{k_f}\right)^{1/2}$$

In the foregoing analysis it has been assumed that the wires are either bare, or carry a very light electrical insulation (e.g. a thin layer of enamel) of negligible thermal resistance. With liquid metals a rather heavier insulation might be necessary, in which case the estimates of error are on the low side.

REFERENCES

1. Th. von Kármán, *Trans. Amer. Soc. Mech. Engrs.* **61**, 705 (1939).
2. M. Jakob, *Trans. Amer. Inst. Chem. Engrs.* **36**, 657 (1940).
3. H. B. Squire, *Proc. Gen. Disc. Heat Transfer, London 11–13 September 1951.* Institution of Mechanical Engineers, London (1951).
4. R. C. Martinelli, *Trans. Amer. Soc. Mech. Engrs.* **69**, 947 (1947).
5. R. G. Deissler, *Trans. Amer. Soc. Mech. Engrs.* **73**, 101 (1951).
6. R. G. Deissler, *Trans. Amer. Soc. Mech. Engrs.* **76**, 73 (1954).
7. G. F. C. Rogers and Y. R. Mayhew, *Engineering Thermodynamics, Work and Heat Transfer.* Longmans, Green, London (1957).
8. W. H. McAdams, *Heat Transmission.* McGraw-Hill, New York (1954).
9. E. R. G. Eckert and R. M. Drake, *Heat and Mass Transfer.* McGraw-Hill, New York (1959).

Int. J. Heat Mass Transfer. Vol. 1, pp. 68–80. Pergamon Press 1960. Printed in Great Britain.

CONVECTION DE LA CHALEUR EN RÉGIME LAMINAIRE DANS LE CAS D'UN GRADIENT DE PRESSION ET D'UNE TEMPÉRATURE DE PAROI QUELCONQUES, LE FLUIDE ÉTANT À PROPRIÉTÉS PHYSIQUES CONSTANTES

B. LE FUR

Sorbonne, Paris, France

(*Received* 12 *October* 1959)

Résumé—L'intégration par approximations successives des équations de la couche limite laminaire permet de calculer dans le cas d'un gradient de pression quelconque les coefficients de frottement et de convection, la température effective et le facteur thermique pariétal de frottement.

Abstract—Integration by successive approximations of the laminar boundary layer equations enables one to calculate, for any pressure gradient, the friction and convection coefficients, the effective temperature and the recovery factor.

Zusammenfassung—Die Gleichungen der laminaren Grenzschicht werden durch schrittweise Verbesserung integriert. Man kann dadurch für beliebige Druckgradienten die Koeffizienten der Reibung und Wärmeübertragung, die effektive Temperatur und den Rückgewinnfaktor berechnen.

Abstract—Приведены решения уравнений переноса для ламинарного пограничного слоя методом последовательных приближений. Вычислены коэффициенты трения, теплообмена и эффективная температура для любого градиента давления.

Vol. 1 1960

NOTATIONS UTILISÉES

x = abscisse curviligne le long de la paroi,
y = ordonnée prise perpendiculairement à la paroi;
u = composante longitudinale de la vitesse;
v = composante transversale de la vitesse;
θ = température absolue;
ρ = masse volumique;
ψ = fonction de courant;
μ = viscosité;
ν = viscosité cinématique;
τ_p = tension de frottement à la paroi;
λ = coefficient de conductibilité thermique;
C_p = chaleur spécifique à pression constante;
Φ_p = densité de flux de chaleur à la paroi;
Φ_m = densité moyenne de flux de chaleur;
θ_f = température de frottement;
θ_{fm} = température moyenne de frottement;
θ_{eff} = température effective locale;
$\theta_{\overline{\text{eff}}}$ = température effective moyenne;
Pr = nombre de Prandtl;
r = facteur thermique pariétal de frottement;
r_c = facteur thermique pariétal de convection local;
$\bar{r}_c$ = facteur thermique pariétal de convection moyen;
α = coefficient de convection local;
α_m = coefficient de convection moyen;
R_x = nombre de Reynolds rapporté à x;
C_f = coefficient de frottement local;
N_x = nombre de Nusselt local rapporté à x;
N_{xm} = nombre de Nusselt moyen rapporté à x.

Indices inférieurs

e = écoulement extérieur à la couche limite;
p = conditions à la paroi;
t = conditions au point d'arrêt;
0 = fonction de départ;
1 = première approximation.

INTRODUCTION

Nous nous placerons dans le cas de la couche limite laminaire sur un obstacle bidimensionnel. Nous supposerons en outre que la vitesse extérieure u_e et la différence entre la température de la paroi θ_p et la température extérieure θ_e sont faibles, afin que la viscosité μ, la masse volumique ρ, la conductibilité thermique λ et la chaleur spécifique à pression constante C_p du fluide puissent être considérées comme constantes.

Nous introduirons ici un processus d'intégration par itération des équations de l'impulsion et de l'énergie mises sous la forme de von Mises [1]. Nous considérerons le cas général dans lequel les répartitions de vitesses $u_e(x)$ et de températures $\theta_p(x)$ sont quelconques.

Dans cet article nous n'étudierons que la première approximation.

1. TRANSFORMATION DE VON MISES

1.1. *Equations de Prandtl*

Les équations qui régissent la vitesse et la température ont été données par Prandtl sous la forme suivante:

$$\frac{\partial u}{\partial x} + \frac{\partial v}{\partial y} = 0 \tag{1}$$

$$u\frac{\partial u}{\partial x} + v\frac{\partial u}{\partial y} = -\frac{1}{\rho}\frac{\partial p}{\partial x} + \frac{\mu}{\rho}\cdot\frac{\partial^2 u}{\partial y^2} \tag{2}$$

$$\frac{\partial p}{\partial y} = 0 \tag{3}$$

$$u\frac{\partial \theta}{\partial x} + v\frac{\partial \theta}{\partial y} = \frac{u}{\rho C_p}\cdot\frac{\partial p}{\partial x} + \frac{\lambda}{\rho C_p}\cdot\frac{\partial^2 \theta}{\partial y^2} + \frac{\mu}{\rho C_p}\left(\frac{\partial u}{\partial y}\right)^2 \tag{4}$$

D'après l'équation (3), nous aurons:

$$\frac{\partial p}{\partial x} = \frac{dp_e}{dx}$$

La relation de Bernoulli nous donne:

$$\frac{dp_e}{dx} = -\rho u_e \frac{du_e}{dx}$$

D'autre part, la température totale $\theta_t = \theta_e + u_e^2/2C_p$ étant constante dans l'écoulement extérieur à la couche limite:

$$C_p \frac{d\theta_e}{dx} = -u_e \frac{du_e}{dx}$$

Les équations (2) et (4) deviennent alors:

$$u\frac{\partial u}{\partial x} + v\frac{\partial u}{\partial y} = u_e\frac{du_e}{dx} + \nu\frac{\partial^2 u}{\partial y^2} \tag{5}$$

$$u\frac{\partial \theta}{\partial x} + v\frac{\partial \theta}{\partial y} = u\frac{d\theta_e}{dx} + \frac{\lambda}{\rho C_p}\cdot\frac{\partial^2 \theta}{\partial y^2} + \frac{\nu}{C_p}\left(\frac{\partial u}{\partial y}\right) \tag{6}$$

Nous prendrons comme origine des x le point d'arrêt et nous nous limiterons au cas de l'écoulement sur l'extrados de l'obstacle pour lequel $x > 0$, étant bien entendu que l'écoulement sur l'intrados se traitera de la même façon après avoir changé l'abscisse curviligne x de signe. Les fonctions $u(x, y)$, $v(x, y)$ et $\theta(x, y)$ définies dans le quadrant $x > 0$ et $y > 0$ obéiront aux conditions aux limites suivantes:

$$\left.\begin{aligned} &\lim_{y\to 0} u(x, y) = 0 \\ &\lim_{y\to 0} v(x, y) = 0 \\ &\lim_{y\to 0} \theta(x, y) = \theta_p(x) \end{aligned}\right\} \tag{7}$$

$$\left.\begin{aligned} &\lim_{y\to \infty} u(x, y) = u_e(x) \\ &\lim_{y\to \infty} \theta(x, y) = \theta_e(x) \end{aligned}\right\} \tag{8}$$

1.2. *Equations de von Mises*

Von Mises a imaginé d'utiliser comme variables indépendantes l'abscisse x et la fonction de courant ψ définie par les relations:

$$u = \frac{1}{\rho}\frac{\partial \psi}{\partial y} \quad \text{et} \quad v = -\frac{1}{\rho}\frac{\partial \psi}{\partial x} \tag{9}$$

et telle que $\psi = 0$ lorsque $y = 0$. L'équation (1) est alors automatiquement satisfaite.

Nous aurons une correspondance biunivoque entre le quadrant $x > 0$ et $\psi > 0$ et le quadrant $x > 0$ et $y > 0$ si u est toujours positif.

Le changement de variables de von Mises permet de remplacer les dérivées particulaires $u(\partial/\partial x) + v(\partial/\partial y)$ des équations (2) et (4) par des dérivées partielles, puisque ψ est constant sur une ligne de courant.

En effet, nous avons entre les opérateurs de dérivation partielle, les relations:

$$\left(\frac{\partial}{\partial x}\right)_y = \left(\frac{\partial}{\partial x}\right)_\psi - \rho v \left(\frac{\partial}{\partial \psi}\right)_x$$

et

$$\left(\frac{\partial}{\partial y}\right)_x = \rho u \left(\frac{\partial}{\partial \psi}\right)_x$$

Les équations (5) et (6) deviennent en sous-entendant les indices x et ψ:

$$u\frac{\partial u}{\partial x} - u_e\frac{du_e}{dx} - \mu\rho u\frac{\partial}{\partial \psi}\left(u\frac{\partial u}{\partial \psi}\right) = 0 \quad (10)$$

$$u\frac{\partial \theta}{\partial x} - u\frac{d\theta_e}{dx} - \frac{\mu\rho u}{Pr}\frac{\partial}{\partial \psi}\left(u\frac{\partial \theta}{\partial \psi}\right) = \frac{\mu\rho u^2}{C_p}\left(\frac{\partial u}{\partial \psi}\right)^2 \quad (11)$$

où $Pr = \mu C_p/\lambda$ est le nombre de Prandtl.

1.3. *Equations en $Z(x, \psi)$ et en $T(x, \psi)$*

Prenons comme variables dépendantes:

$$Z(x, \psi) = u_e^2(x) - u^2(x, \psi)$$

et

$$T(x, \psi) = \theta(x, \psi) - \theta_e(x)$$

L'équation (10) devient

$$\frac{\partial Z}{\partial x} - \mu\rho u\frac{\partial^2 Z}{\partial \psi^2} = 0 \quad (12)$$

avec les conditions aux limites:

$$\left.\begin{aligned} &\lim_{x\to 0} Z(x, \psi) = 0 \\ &\lim_{\psi\to 0} Z(x, \psi) = u_e^2(x) \\ &\lim_{\psi\to\infty} Z(x, \psi) = 0 \end{aligned}\right\} \quad (13)$$

L'équation (11) devient, si on la divise par u:

$$\frac{\partial T}{\partial x} - \frac{\mu\rho}{Pr}\frac{\partial}{\partial \psi}\left(u\frac{\partial T}{\partial \psi}\right) = -\frac{\mu\rho}{2C_p}\cdot\frac{\partial u}{\partial \psi}\cdot\frac{\partial Z}{\partial \psi} \quad (14)$$

avec les conditions aux limites:

$$\left.\begin{aligned} &\lim_{x\to 0} T(x, \psi) = 0 \\ &\lim_{\psi\to 0} T(x, \psi) = \theta_p(x) - \theta_e(x) \\ &\lim_{\psi\to\infty} T(x, \psi) = 0 \end{aligned}\right\} \quad (15)$$

Une fois que les équations (12) et (14) auront été résolues avec les conditions aux limites (13) et (15), u et θ seront des fonctions paramétriques de l'ordonnée y, le paramètre étant la fonction de courant ψ.

En effet, l'on aura:

$$y = \int_0^\psi \frac{d\psi}{\rho u} = \int_0^\psi \frac{d\psi}{\rho\sqrt{(u_e^2 - Z)}}$$

2. ÉQUATION DIFFÉRENTIELLE DE L'IMPULSION

2.1. *Première approximation*

Pour résoudre l'équation (12) nous utiliserons le processus d'itération suivant, où l'indice i varie de 0 à l'infini:

$$\frac{\partial Z_{i+1}}{\partial x} - \mu\rho u_0\frac{\partial^2 Z_{i+1}}{\partial \psi^2} = \mu\rho(u_i - u_0)\frac{\partial^2 Z_i}{\partial \psi^2} \quad (17)$$

en prenant comme fonction de départ:

$$u_0 = \left(\frac{2\tau_{p1}}{\mu\rho}\right)^{1/2}\psi^{1/2} \quad (18)$$

premier terme du développement en série de $u_1(x, \psi)$.

τ_{p1} est la tension de frottement

$$\mu\left(\frac{\partial u_1}{\partial y}\right)_p = -\frac{\mu\rho}{2}\left(\frac{\partial Z_1}{\partial \psi}\right)_p$$

obtenue en intégrant l'équation à laquelle satisfait la première approximation $Z_1(x, \psi)$.

Les conditions aux limites seront:

$$\lim_{x\to 0} Z_i(x, \psi) = 0;\ \lim_{\psi\to 0} Z_i(x, \psi) = u_e^2(x);\ \lim_{\psi\to\infty} Z_i(x, \psi) = 0 \quad (19)$$

La première approximation est donc solution de l'équation:

$$\frac{\partial Z_1}{\partial x} - \mu\rho u_0\frac{\partial^2 Z_1}{\partial \psi^2} = 0 \quad (20)$$

Vol. 1 1960

ou

$$\frac{\partial Z_1}{\partial x} - (2\mu\rho\tau_{p1})^{1/2}\psi^{1/2}\frac{\partial^2 Z_1}{\partial \psi^2} = 0 \qquad (19)$$

avec les conditions aux limites (19).

Lighthill [2] a résolu cette équation en faisant le changement de variable:

$$t = \int_0^x (2\mu\rho\tau_{p1})^{1/2}\,dx \qquad (22)$$

On obtient l'équation suivante:

$$\frac{\partial Z_1}{\partial t} - \psi^{1/2}\frac{\partial^2 Z_1}{\partial \Psi^2} = 0 \qquad (23)$$

Comme la fonction $Z(t, \psi)$ n'est définie que lorsque $t > 0$, on utilisera le calcul symbolique.

Soit $\mathcal{Z}_1(p, \psi)$ l'image de la fonction $Z_1(t, \psi)$ dans la transformation de Carson:

$$\mathcal{Z}_1(p, \psi) = p\int_0^\infty e^{-pt}Z_1(t, \psi)dt$$

l'équation (23) devient, en tenant compte de la première condition du système (19):

$$p\mathcal{Z}_1 - \psi^{1/2}\frac{\partial^2 \mathcal{Z}_1}{\partial \psi^2} = 0 \qquad (24)$$

avec les conditions aux limites:

$$\lim_{\psi\to 0}\mathcal{Z}_1(p, \psi) = \zeta(p);\ \lim_{\psi\to\infty}\mathcal{Z}_1(p, \psi) = 0 \quad (25)$$

$\zeta(p)$ étant l'image de la fonction $u_e^2(t)$.

Faisons le changement de variables:

$$\left.\begin{aligned} z &= \tfrac{4}{3}\,p^{1/2}\psi^{3/4}\delta \\ U_1(p, z) &= z^{-2/3}\mathcal{Z}_1(p, \psi) \end{aligned}\right\} \qquad (26)$$

on aura:

$$\psi^{1/2} = \left(\frac{3}{4}\right)^{2/3} p^{-1/3}z^{2/3}$$

$$\frac{\partial}{\partial\psi} = \left(\frac{4}{3}\right)^{1/3} p^{2/3}z^{-1/3}\frac{\partial}{\partial z}$$

L'équation (24) devient après avoir divisé par $pz^{2/3}$ et changé de signe:

$$\frac{\partial^2 U_1}{\partial z^2} + \frac{1}{z}\frac{\partial U_1}{\partial z} - \left(1 + \frac{4}{9z^2}\right)U_1 = 0 \quad (27)$$

Les conditions aux limites (25) deviennent:

$$\lim_{z\to 0} z^{2/3}U_1(p, z) = \zeta(p);\ \lim_{z\to\infty} z^{2/3}U_1(p, z) = 0 \qquad (28)$$

La solution de l'équation (27) avec les conditions (28) sera donc:

$$\left.\begin{aligned} U_1(p, z) &= 2^{-2/3}\frac{3}{\pi}^{1/2}\Gamma(1/3)\zeta(p)K_{2/3}(z), \\ K_\lambda(z) &= \frac{\pi}{2\sin\lambda\pi}\,[I_{-\lambda}(z) - I_\lambda(z)] \end{aligned}\right\} \qquad (29)$$

étant la fonction de Bessel modifiée de seconde espèce. On a donc:

$$\mathcal{Z}_1(p, \psi) = \frac{2^{2/3}\,\Gamma(1/3)}{3^{1/6}\pi}\,p^{1/3}\zeta(p)\psi^{1/2}K_{2/3}\left[\tfrac{4}{3}\,p^{1/2}\psi^{3/4}\right] \quad (30)$$

2.2. *Tension de frottement à la paroi*

Le développement limité de $Z_1(t, \psi)$ au voisinage de $\psi = 0$ est:

$$Z_1(t, \psi) = u_e^2(t) - 2\frac{\tau_{p1}(t)}{\rho\mu}\,\psi + 0\,(\psi^{3/2}) \qquad (31)$$

En prenant les images terme à terme, on obtiendra le développement limité de $\mathcal{Z}_1(p, \psi)$ au voisinage de $\psi = 0$:

$$\mathcal{Z}_1(p, \psi) = \zeta(p) - 2\xi_1(p)\psi + 0(\psi^{3/2}) \quad (32)$$

avec $$\xi_1(p) \subset \frac{\tau_{p1}(t)}{\rho\mu}$$

Le développement limité de $\mathcal{Z}_1(p, z)$ en puissances de $z^{2/3}$ est

$$\mathcal{Z}_1(p, z) = \zeta(p) - 2^{-5/3}3^{4/3}p^{-2/3}\,\xi_1(p)z^{4/3} + 0(z^2) \quad (33)$$

Le développement en série de puissances de $z^{2/3}$ de l'expression (30) est:

$$\mathcal{Z}_1(p, z) = 2^{-2/3}\Gamma(1/3)\zeta(p)z^{2/3}\left\{\sum_{r=0}^{\infty}\frac{(z/2)^{-2/3+2r}}{r!\,\Gamma(1/3 + r)} - \sum_{r=0}^{\infty}\frac{(z/2)^{2/3+2r}}{r!\,\Gamma(5/3 + r)}\right\}$$

Egalons les termes en $z^{4/3}$ dans (33) et (34), on obtiendra:

$$\xi_1(p) = \frac{\Gamma(1/3)}{2^{2/3}3^{1/3}\Gamma(2/3)}\,p^{2/3}\zeta(p) \qquad (35)$$

Prenons l'original de cette relation:

$$\int_0^t (t-t')^{-1/3}\tau_{p1}(t')dt' = \frac{\mu\rho\Gamma(1/3)u_e^2(t)}{2^{2/3}3^{1/3}} \quad (36)$$

On voit enfin que $\tau_{p1}(x)$ doit être solution de l'équation intégrale:

$$\int_0^x \left(\int_{x'}^x [\tau_{p1}(z)]^{1/2}dz\right)^{-1/3} [\tau_{p1}(x')]^{3/2}dx' = \frac{(\mu\rho)^{2/3}\Gamma(1/3)u_e^2(x)}{2\cdot 3^{1/3}} \quad (37)$$

Cette équation peut être résolue facilement pour certaines fonctions $u_e(x)$, par exemple si $u_e(x)$ est une puissance de x.

On peut résoudre plus aisément le problème inverse, c'est à-dire déterminer l'expression de $u_e(x)$, connaissant $\tau_{p1}(x)$.

3. ÉQUATION DIFFÉRENTIELLE DE L'ÉNERGIE

3.1. *Première approximation*

Pour résoudre l'équation (14) nous utiliserons un processus d'itération analogue à celui du paragraphe 2.1:

$$\left.\begin{aligned}\frac{\partial T_{i+1}}{\partial x} - \frac{\mu\rho}{Pr}\frac{\partial}{\partial\psi}\left(u_0\frac{\partial T_{i+1}}{\partial\psi}\right) = \\ -\frac{\mu\rho}{Pr}\frac{\partial}{\partial\psi}\left[(u_0-u_i)\frac{\partial T_i}{\partial\psi}\right] - \\ -\frac{\mu\rho}{2C_p}\cdot\frac{\partial u_0}{\partial\psi}\cdot\frac{\partial Z_{i+1}}{\partial\psi} + \\ +\frac{\mu\rho}{2C_p}\cdot\frac{\partial(u_0-u_i)}{\partial\psi}\cdot\frac{\partial Z_i}{\partial\psi}\end{aligned}\right\} \quad (38)$$

Les conditions aux limites seront:

$$\begin{aligned}&\lim_{x\to 0} T_i(x,\psi) = 0;\\ &\lim_{\psi\to 0} T_i(x,\psi) = \theta_p(x) - \theta_e(x);\\ &\lim_{\psi\to\infty} T_i(x,\psi) = 0\end{aligned} \quad (39)$$

La première approximation sera donc solution de l'équation:

$$\frac{\partial T_1}{\partial x} - \frac{\mu\rho}{Pr}\cdot\frac{\partial}{\partial\psi}\left(u_0\frac{\partial T_1}{\partial\psi}\right) = -\frac{\mu\rho}{2C_p}\cdot\frac{\partial u_0}{\partial\psi}\cdot\frac{\partial Z_1}{\partial\psi} \quad (40)$$

ou

$$\frac{\partial T_1}{\partial x} - \frac{(2\mu\rho\tau_{p1})^{1/2}}{Pr}\cdot\frac{\partial}{\partial\psi}\left(\psi^{1/2}\frac{\partial T_1}{\partial\psi}\right) = -\frac{(2\mu\rho\tau_{p1})^{1/2}}{4C_p}\psi^{-1/2}\frac{\partial Z_1}{\partial\psi} \quad (41)$$

avec les conditions aux limites (39).

Lighthill [2] a résolu l'équation sans second membre, nous allons traiter maintenant le cas général pour lequel l'échauffement dû au frottement n'est plus négligeable.

Faisons le changement de variable (22), on aura:

$$\frac{\partial T_1}{\partial t} - \frac{1}{Pr}\frac{\partial}{\partial\psi}\left(\psi^{1/2}\frac{\partial T_1}{\partial\psi}\right) = -\frac{\psi^{-1/2}}{4C_p}\cdot\frac{\partial Z_1}{\partial\psi} \quad (42)$$

Soit $T_1(p,\psi)$ l'image de la fonction $T_1(t,\psi)$, l'équation (42) devient en tenant compte de la première condition du système (39):

$$pT_1 - \frac{1}{Pr}\frac{\partial}{\partial\psi}\left(\psi^{1/2}\frac{\partial T_1}{\partial\psi}\right) = -\frac{\psi^{-1/2}}{4C_p}\cdot\frac{\partial Z_1}{\partial\psi} \quad (43)$$

avec les conditions aux limites suivantes:

$$\lim_{\psi\to 0} T_1(p,\psi) = \delta(p);\ \lim_{\psi\to\infty} T_1(p,\psi) = 0 \quad (44)$$

$\delta(p)$ étant l'image de la fonction $\theta_p(t) - \theta_e(t)$.

Faisons le changement de variables:

$$\left.\begin{aligned}s = Pr^{1/2}z = \tfrac{4}{3}(pPr)^{1/2}\psi^{3/4}\\ V_1(p,s) = s^{-1/3}\,T_1(p,\psi)\end{aligned}\right\} \quad (45)$$

On aura:

$$\psi^{1/2} = \left(\frac{3}{4}\right)^{2/3}(pPr)^{-1/3}s^{2/3}$$

$$\frac{\partial}{\partial\psi} = \left(\frac{4}{3}\right)^{1/3}(pPr)^{2/3}s^{-1/3}\frac{\partial}{\partial s}$$

L'équation (44) devient après avoir divisé par $ps^{1/3}$ et changé de signe:

$$\frac{\partial^2 V_1}{\partial s^2} + \frac{1}{s}\cdot\frac{\partial V_1}{\partial s} - \left(1+\frac{1}{9s^2}\right)V_1 = H_1(p,s) \quad (46)$$

avec

$$H_1(p,s) = \frac{Pr^{1/2}}{3C_p}s^{-4/3}\frac{\partial}{\partial z}\left[z^{2/3}\,U_1(p,z)\right]$$

Vol. 1 1960

Remplaçons $U_1(p, z)$ par son expression (29) et utilisons les relations de récurrence des fonctions de Bessel modifiées de seconde espèce:

$$H_1(p, s) = -\frac{2^{1/3}}{3^{1/2}}\Gamma(1/3)\frac{Pr^{1/6}}{\pi s^{2/3}}\cdot\frac{\zeta(p)}{2C_p}K_{1/3}(sPr^{-1/2}) \tag{47}$$

Les conditions aux limites auxquelles devra obéir $V_1(p, s)$ seront:

$$\lim_{s\to 0} s^{1/3}V_1(p, s) = \delta(p);\ \lim_{s\to\infty} s^{1/3}V_1(p, s) = 0 \tag{48}$$

Nous utiliserons la méthode de variation des constantes pour intégrer l'équation (46). L'intégrale générale est donc de la forme:

$$V_1(p, s) = B_1^-(p, s)I_{-1/3}(s) + B_1^+(p, s)I_{1/3}(s) \tag{49}$$

avec

$$\left.\begin{aligned} B_1^-(p, s) &= b_1^-(p) - \frac{\pi}{3^{1/2}}\int_0^s sH_1(p, s)I_{1/3}(s)ds \\ B_1^+(p, s) &= b_1^+(p) + \frac{\pi}{3^{1/2}}\int_0^s sH_1(p, s)I_{1/3}(s)ds \end{aligned}\right\} \tag{50}$$

La première condition du système (48) nous impose:

$$b_1^-(p) = 2^{-1/3}\Gamma(2/3)\delta(p) \tag{51}$$

Pour pouvoir satisfaire à la deuxième condition du système (48), il faut, d'après les développements asymptotiques de $I_{-1/3}(s)$ et de $I_{1/3}(s)$, que:

$$\lim_{s\to\infty} B_1^-(p, s) + \lim_{s\to\infty} B_1^+(p, s) = 0$$

donc

$$b_1^+(p) = -2^{-1/3}\Gamma(2/3)\delta(p) - \int_0^\infty sH_1(p, s)K_{1/3}(s)ds \tag{52}$$

avec:

$$\left.\begin{aligned} \int_0^\infty sH_1(p, s)K_{1/3}(s)ds = \\ -\frac{2^{1/3}\Gamma(1/3)}{3^{1/2}\pi}Pr^{1/6}\frac{\zeta(p)}{2C_p}\times \\ \times\int_0^\infty s^{1/3}K_{1/3}(sPr^{-1/2})K_{1/3}(s)ds \end{aligned}\right\} \tag{53}$$

Cette dernière intégrale est de la forme:

$$I(\alpha, \beta) = \int_0^\infty s^\lambda K\mu(\alpha s)K\nu(\beta s)ds$$

qui existe lorsque $\mu + \nu < \lambda + 1$; elle s'exprime à l'aide d'une fonction hypergéométrique:

$$I(\alpha, \beta) = \frac{G(\lambda, \mu, \nu)}{\alpha^{1+\lambda-\nu}}\,{}_2F_1\left(\frac{1+\lambda-\mu-\nu}{2},\ \frac{1+\lambda+\mu-\nu}{2};\ 1+\lambda;\ 1-\frac{\beta^2}{\alpha^2}\right) \tag{54}$$

avec

$$\left.\begin{aligned} G(\lambda, \mu, \nu) &= 2^{\lambda-2}\times \\ &\times\big[\Gamma[(1+\lambda-\mu-\nu)/2]\times \\ &\times\Gamma[(1+\lambda+\nu-\mu)/2]\times \\ &\times\Gamma[(1+\lambda+\mu+\nu)/2]\times \\ &\times\Gamma[(1+\lambda+\mu-\nu)/2]\big]\Gamma(1+\lambda) \end{aligned}\right\} \tag{55}$$

Dans notre cas $\lambda = \frac{1}{3}$, $\mu = \nu = \frac{1}{3}$.

Si nous posons $\alpha = Pr^{-1/2}$ et $\beta = 1$.

$$\left.\begin{aligned} \int_0^\infty sH_1(p, s)K_{1/3}(s)ds = \\ -2^{-1/3}\Gamma(2/3)Pr^{2/3}\frac{\zeta(p)}{2C_p}\times \\ \times\,{}_2F_1(\tfrac{1}{3},\ \tfrac{2}{3};\ \tfrac{4}{3};\ 1-Pr) \end{aligned}\right\} \tag{56}$$

Si nous posons $\alpha = 1$ et $\beta = Pr^{-1/2}$

$$\left.\begin{aligned} \int_0^\infty sH_1(p, s)K_{1/3}(s)ds = \\ -2^{-1/3}\Gamma(2/3)Pr^{1/3}\frac{\zeta(p)}{2C_p}\times \\ \times\,{}_2F_1\left(\tfrac{1}{3},\ \tfrac{2}{3};\ \tfrac{4}{3};\ \frac{Pr-1}{Pr}\right) \end{aligned}\right\} \tag{57}$$

Nous aurons enfin:

$$b_1^+(p) = -2^{-1/3}(\Gamma 2/3)\left[\delta(p) - r(Pr)\frac{\zeta(p)}{2C_p}\right] \tag{58}$$

où $r(Pr)$ est une fonction du nombre de Prandtl qui est donnée par:

$$r(Pr) = Pr^{2/3}\,{}_2F_1(\tfrac{1}{3},\ \tfrac{2}{3};\ \tfrac{4}{3};\ 1-Pr) \tag{59}$$

la série étant convergente lorsque $0 < Pr < 2$; ou par:

$$r(Pr) = Pr^{1/3}\,{}_2F_1\left(\tfrac{1}{3},\ \tfrac{2}{3};\ \tfrac{4}{3};\ \frac{Pr-1}{Pr}\right) \quad (60)$$

la série étant convergente lorsque $\frac{1}{2} < Pr < \infty$.

La solution de l'équation (44) avec les conditions (45) sera donc:

$$\left.\begin{aligned} T_1(p,\psi) = &\left\{2^{-1/3}\Gamma(2/3)\delta(p) + \right.\\ &+\frac{2^{1/3}}{3}\,\Gamma(1/3)Pr^{1/6}\,\frac{\zeta(p)}{2C_p}\int_0^s \sigma^{1/3}\times\\ &\left.\times K_{1/3}(\sigma Pr^{-1/2})\,I_{1/3}(\sigma)d\sigma\right\} s^{1/3}I_{-1/3}(s) -\\ &-\left\{2^{-1/3}\Gamma(2/3)\left[\delta(p) - r(Pr)\times\frac{\zeta(p)}{2C_p}\right] + \right.\\ &+\frac{2^{1/3}}{3}\,\Gamma(1/3)Pr^{1/6}\,\frac{\zeta(p)}{2C_p}\int_0^s \sigma^{1/3}\times\\ &\left.\times K_{1/3}(\sigma Pr^{-1/2})I_{-1/3}(\sigma)d\sigma\right\} s^{1/3}I_{1/3}(s) \end{aligned}\right\} \quad (61)$$

avec

$$s = \tfrac{4}{3}(pPr)^{1/2}\psi^{3/4}$$

3.2. *Densité de flux de chaleur à la paroi et facteur thermique pariétal de frottement*

Le développement limité de $T_1(t, \psi)$ au voisinage de $\psi = 0$ est:

$$T_1(t,\psi) = \theta_p(t) - \theta_e(t) - \frac{Pr}{C_p}\,\Phi_{p1}(t)\left(\frac{2}{\mu\rho\tau_{p1}(t)}\right)^{1/2}\psi^{1/2} + 0(\psi) \quad (62)$$

$\Phi_{p1} = -\lambda(\partial\theta_1/\partial y)_p$ étant la densité de flux de chaleur à la paroi dans le cas de la première approximation.

Le développement limité de $T_1(p, \psi)$ au voisinage de $\psi = 0$ sera donc:

$$T_1(p,\psi) = \delta(p) - \frac{2^{1/2}Pr}{C_p}\,\chi_1(p)\psi^{1/2} + 0(\psi) \quad (63)$$

avec

$$\chi_1(p) \subset \frac{\Phi_{p1}(t)}{[\mu\rho\tau_{p1}(t)]^{1/2}}$$

Le développement limité de $T_1(p, s)$ en puissances de $s^{2/3}$ sera:

$$T_1(p,s) = \delta(p) - \frac{3^{2/3}}{2^{5/6}}\cdot\frac{Pr^{2/3}}{C_p}\,p^{-1/3}\chi_1(p)s^{2/3} + 0(s^{4/3}) \quad (64)$$

Le coefficient de $s^{2/3}$ dans le développement en série de puissances de $s^{2/3}$ de l'expression (61) de $T_1(p, s)$ est:

$$\lim_{s\to 0}\, s^{-2/3}[T_1(p,s) - \delta(p)] = \frac{b_1^+(p)}{2^{1/3}\Gamma(4/3)}$$

Egalons-le au coefficient correspondant du développement (64) en remplaçant $b_1^+(p)$ par son expression (58):

$$\chi_1(p) = C_p\,\frac{3^{1/3}2^{1/6}\Gamma(2/3)}{\Gamma(1/3)}\,Pr^{-2/3}p^{1/3}\times \left[\delta(p) - r(Pr)\,\frac{\zeta(p)}{2C_p}\right] \quad (65)$$

Lorsque la paroi est thermiquement isolée, $\Phi_{p1} = 0$ et donc $\chi_1(p) = 0$. D'après (65) il faut que:

$$\delta(p) = r(Pr)\,\frac{\zeta(p)}{2C_p}$$

En prenant l'original de cette relation, on trouve que la température θ_f de la paroi est:

$$\theta_f = \theta_e + r(Pr)\,\frac{u_e^2}{2C_p} \quad (66)$$

On voit donc que le facteur thermique pariétal de frottement $r = [2C_p(\theta_f - \theta_e)]/u_e^2$ est égal à la fonction $r(Pr)$ introduite dans le paragraphe 3.1, dont nous redonnerons les expressions:

$$r = Pr^{2/3}\,{}_2F_1(\tfrac{1}{3},\ \tfrac{2}{3};\ \tfrac{4}{3};\ 1 - Pr) \quad (67)$$

lorsque $0 < Pr < 2$, et

$$r = Pr^{1/3}\,{}_2F_1\left(\tfrac{1}{3},\ \tfrac{2}{3};\ \tfrac{4}{3};\ \frac{Pr-1}{Pr}\right) \quad (68)$$

lorsque $\frac{1}{2} < Pr < \infty$.

On remarquera que dans le cadre de la première approximation étudiée ici, le *facteur thermique pariétal de frottement est indépendant du gradient de pression.*

Vol. 1 1960

Dans le cas de la plaque plane, Pohlhausen [3] a obtenu l'expression suivante du facteur thermique pariétal de frottement:

$$r = 8\,Pr\int_0^\infty [f''(\eta)]^{Pr}\left(\int_0^\eta [f''(\eta')]^{2-Pr}d\eta'\right)d\eta \quad (69)$$

la fonction $f(\eta)$ étant solution de l'équation de Blasius:

$$f''' + ff'' = 0 \quad (70)$$

avec $\psi = \rho f(\eta)\sqrt{(2\nu u_e x)}$ et $\eta = y\sqrt{(u_e/2\nu x)}$.

Nous avons porté sur le Tableau 1 les valeurs de r obtenues à l'aide des formules (67) et (68) pour différentes valeurs de Pr ainsi que les valeurs exactes données par l'expression (69).

On voit que les valeurs données par la formule (67) sont extrêmement voisines des résultats exacts.

Lorsque $Pr = 1$, les dérivées première, seconde et troisième de l'expression (67) sont égales respectivement à $\frac{1}{2}$, $-\frac{2}{7}$ et $\frac{3}{7}$. L'expression empirique $Pr^{1/2}$ utilisée généralement a ses trois premières dérivées égales respectivement à $\frac{1}{2}$, $-\frac{1}{4}$ et $\frac{3}{8}$, ce qui explique qu'elle soit voisine des valeurs exactes lorsque Pr n'est pas trop différent de 1.

Lorsque Pr tend vers 0, l'expression (67) est équivalente à:

$$\frac{\Gamma^3(1/3)}{2\pi\sqrt{3}}\,Pr^{2/3} = 1{,}7666\,Pr^{2/3} \quad (71)$$

Lorsque Pr tend vers l'infini, l'expression (68) est équivalente à:

$$\frac{\Gamma^3(1/3)}{2\pi\sqrt{3}}\,Pr^{1/3} = 1{,}7666\,Pr^{1/3} \quad (72)$$

Sur la Fig. 1, nous avons porté log r en fonction de log Pr.

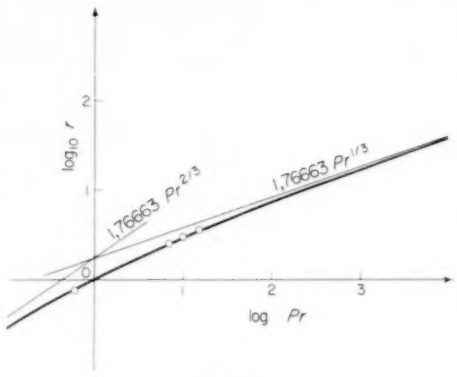

FIG. 1.
○ Pohlhausen

Si l'on prend l'original de la relation (65) en tenant compte de (66), on aura:

$$\left.\begin{aligned}\Phi_{p1}(t) = C_p\frac{3^{1/3}2^{1/6}}{\Gamma(1/3)}(\mu\rho)^{1/2}Pr^{-2/3}[\tau_{p1}(t)]^{1/2}\times\\ \times\int_0^t (t-t')^{-1/3}d\,[\theta_p(t') - \theta_f(t')]\end{aligned}\right\} (73)$$

La densité de flux de chaleur à la paroi est donnée par une intégrale de Stieltjes:

$$\left.\begin{aligned}\Phi_{p1}(x) = C_p\frac{3^{1/3}}{\Gamma(1/3)}(\mu\rho)^{1/3}Pr^{-2/3}[\tau_{p1}(x)]^{1/2}\times\\ \times\int_0^x\left(\int_{x'}^x [\tau_{p1}(z)]^{1/2}dz\right)^{-1/3} d[\theta_p(x') - \theta_f(x')]\end{aligned}\right\} (74)$$

La densité moyenne de flux de chaleur prise de 0 à x est par définition:

$$\Phi_{m1}(x) = \frac{1}{x}\int_0^x \Phi_{p1}(x)dx$$

d'où

$$x(t)\Phi_{m1}(t) = \int_0^t \frac{\Phi_{p1}(t)}{[2\mu\rho\tau_{p1}(t)]^{1/2}}\,dt \supset \frac{\chi_1(p)}{2^{1/2}p} \quad (75)$$

Tableau 1

Pr	0,6	0,7	0,8	0,9	1,0	1,1	7	10	15
Pohlhausen	0,770	0,835	0,895	0,950	1,000	1,050	2,515	2,965	3,535
Première approximation	0,771	0,835	0,894	0,948	1,000	1,049	2,478	2,888	3,424
$Pr^{1/2}$	0,775	0,837	0,894	0,949	1,000	1,049	2,646	3,162	3,873

On a donc:

$$\Phi_{m1}(t) = C_p \frac{3^{4/3} Pr^{-2/3}}{2^{4/3}\Gamma(1/3)} \cdot \frac{1}{x(t)} \times \times \int_0^t (t-t')^{2/3} d[\theta_p(t') - \theta_f(t')] \quad (76)$$

La densité moyenne de flux de chaleur est donnée aussi par une intégrale de Stieltjes:

$$\left.\begin{aligned} \Phi_{m1}(x) &= C_p \frac{3^{4/3}(\mu\rho)^{1/3}}{2\Gamma(1/3)} \cdot \frac{Pr^{-2/3}}{x} \times \\ &\times \int_0^x \left(\int_{x'}^x [\tau_{p1}(z)]^{1/2} dz \right)^{2/3} d[\theta_p(x') - \theta_f(x')] \end{aligned}\right\} \quad (77)$$

3.3. *Température effective locale et coefficient de convection local*

Lorsque la température θ_p est uniforme et lorsque la distribution de vitesse $u_e(x)$ est quelconque, la formule (74) nous montre qu'il n'y a aucune raison pour que Φ_{p1} s'annule en un point où la température de frottement θ_f est égale à θ_p, puisque la fonction $\Phi_{p1}(x)$ dépend de l'histoire de la couche limite. En effet, la formule (73) devient:

$$\left.\begin{aligned} \Phi_{p1}(t) = C_p \frac{3^{1/3} 2^{1/6}}{\Gamma(1/3)} (\mu\rho)^{1/2} Pr^{-2/3} [\tau_{p1}(t)]^{1/2} \times \\ \times \left\{ (\theta_p - \theta_t) t^{-1/3} + (1-r) \times \right. \\ \left. \times \int_0^t (t-t')^{-1/3} d[u_e^2(t')] \right\} \end{aligned}\right\} \quad (78)$$

Pour pouvoir définir un coefficient de convection local, nous allons introduire une température effective locale $\theta_{\text{eff}}(x)$ telle que Φ_{p1} s'annule en un point d'abscisse x, lorsqu'on fait varier θ_p. On aura donc:

$$\theta_{\text{eff}}(t) = \theta_t + \frac{r-1}{2C_p} t^{1/3} \int_0^t (t-t')^{-1/3} d[u_e^2(t')] \quad (79)$$

d'où:

$$\left.\begin{aligned} \theta_{\text{eff}}(x) = \theta_t + \frac{r-1}{2C_p} \left[\int_0^x [\tau_{p1}(z)]^{1/2} dz \right]^{1/3} \times \\ \times \int_0^x \left(\int_{x'}^x [\tau_{p1}(z)]^{1/2} dz \right)^{1/3} d[u_e^2(x')] \end{aligned}\right\} \quad (80)$$

On définira un facteur thermique pariétal local de convection:

$$r_c = 2C_p \frac{(\theta_{\text{eff}} - \theta_e)}{u_e^2} \quad (81)$$

On remarquera que lorsque $Pr = 1$, on a toujours $\theta_{\text{eff}} = \theta_t$ et $r_c = 1$ et que, lorsque u_e est uniforme, on a $\theta_{\text{eff}} = \theta_f$ et $r_c = r$. Le coefficient de convection local sera par définition:

$$\alpha = \frac{\Phi_{p1}}{\theta_p - \theta_{\text{eff}}} \quad (82)$$

3.4. *Température effective moyenne et coefficient moyen de convection*

On peut également définir une température effective moyenne $\theta_{\overline{\text{eff}}}(x)$ telle que $\Phi_{m1}(x)$ s'annule lorsqu'on fait varier θ_p. On aura d'après (76):

$$\theta_{\overline{\text{eff}}}(t) = \theta_t + \frac{r-1}{2C_p} t^{-2/3} \int_0^t (t-t')^{2/3} d[u_e^2(t')] \quad (83)$$

d'où

$$\left.\begin{aligned} \theta_{\overline{\text{eff}}}(x) = \theta_t + \frac{r-1}{2C_p} \left[\int_0^x [\tau_{p1}(z)]^{1/2} dz \right]^{-2/3} \times \\ \times \int_0^x \left(\int_{x'}^x [\tau_{p1}(z)]^{1/2} dz \right)^{2/3} d[u_e^2(x')] \end{aligned}\right\} \quad (84)$$

On définira de même un facteur thermique pariétal moyen de convection:

$$\bar{r}_c = 2C_p \frac{(\theta_{\overline{\text{eff}}} - \theta_e)}{u_e^2} \quad (85)$$

Le coefficient de convection moyen sera donc:

$$\alpha_m = \frac{\Phi_{m1}}{\theta_p - \theta_{\overline{\text{eff}}}} \quad (86)$$

3.5. *Comparaison avec la méthode de Lighthill*

Lighthill dans son mémoire déjà cité [2] a supposé que dans l'équation de l'énergie (6) le terme $u(d\theta_e/dx)$ dû au gradient de pression et le terme $\lambda(\partial^2\theta/\partial y^2)/\rho C_p$ dû au frottement étaient négligeables et ne s'est donc intéressé qu'à l'équation:

$$\frac{\partial\theta}{\partial x} - \frac{\mu\rho}{Pr} \cdot \frac{\partial}{\partial\psi} \left(u \frac{\partial\theta}{\partial\psi} \right) = 0$$

Vol. 1 1960

avec les conditions aux limites:

$$\lim_{x \to 0} \theta(x, \psi) = 0; \lim_{\psi \to 0} \theta(x, \psi) = \theta_p(x);$$

$$\lim_{\psi \to \infty} \theta(x, \psi) = \theta_t$$

Pour résoudre cette équation, cet auteur a remplacé u par le premier terme du développement en puissances de $\psi^{1/2}$ de la *solution exacte* $u(x, \psi)$ de l'équation (10).

Il obtient alors une expression de Φ_p analogue à la relation (74), mais dans laquelle $\theta_p - \theta_f$ est remplacée par $\theta_p - \theta_t$, et τ_{p1} par la valeur exacte τ_p de la tension de frottement à la paroi.

L'hypothèse de Lighthill revient à supposer que l'épaisseur Δ (Fig. 2) de la couche limite thermique est beaucoup plus faible que l'épaisseur δ de la couche limite dynamique; elle ne se justifie donc que pour des *nombres de Prandtl élevés*.

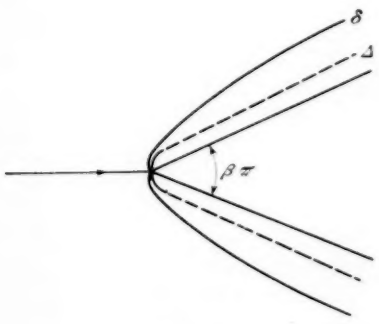

FIG. 2.

4. CAS PARTICULIER DES DIÈDRES À TEMPÉRATURE UNIFORME

4.1. *Coefficient de frottement local*

La vitesse extérieure u_e à la couche limite sur un dièdre d'angle $\beta\pi$ attaqué dans le plan bissecteur (Fig. 2) est de la forme

$$u_e(x) = cx^m$$

où c est une constante et $m = \beta/(2 - \beta)$. L'équation intégrale (37) nous donne:

$$\tau_{p1}(x) = c^{3/2} \frac{3^{1/4}(\mu\rho)^{1/2}}{2^{7/4}} (m + 1)^{1/2} [Q(m)]^{3/4} x^{(3m-1)/2} \quad (87)$$

avec:

$$Q(m) = \frac{\Gamma(1/3)\Gamma\{(11m + 3)/(3m + 3)\}}{\Gamma(2/3)\Gamma\{(9m + 1)/(3m + 3)\}} \quad (88)$$

Le coefficient de frottement local $C_f = 2\tau_{p1}/\rho u_e^2$ s'exprimera sous la forme:

$$C_f R_x^{1/2} = \frac{3^{1/4}(m + 1)^{1/2}}{2^{3/4}} [Q(m)]^{3/4} \quad (89)$$

où $R_x = u_e x/\nu$ est le nombre de Reynolds.

On a porté sur le Tableau 2 les valeurs de $C_f R_x^{1/2}$ données par l'expression (89) pour différentes valeurs de m, ainsi que les valeurs exactes calculées par Hartree [4]:

$$C_f R_x^{1/2} = f''(0)\sqrt{\{2(m + 1)\}} \quad (90)$$

$f(\eta)$ étant solution de l'équation:

$$f''' + ff'' + \beta(1 - f'^2) = 0 \quad (91)$$

avec

$$\psi = \rho f(\eta)\sqrt{\left(\frac{2\nu u_e x}{m+1}\right)} \text{ et } \eta = y\sqrt{\left(\frac{m+1}{2} \cdot \frac{u_e}{\nu x}\right)}$$

Le cas de la plaque plane correspond à $m = 0$, on a alors:

$$C_f R_x^{1/2} = \frac{3^{5/8}[\Gamma(1/3)]^{3/4}}{2^{3/2}\pi^{3/4}} = 0{,}62340 \quad (92)$$

Tableau 2

m	$-1/9$	$-0{,}0904$	$-0{,}0654$	0	1/9	1/3	1	4	∞
β	$-0{,}25$	$-0{,}1898$	$-0{,}14$	0	0,20	0,50	1	1,6	2
Première approximation	0	0,201	0,341	0,623	0,946	1,396	2,272	4,436	$2{,}200\, m^{1/2}$
Valuers exactes		0	0,328	0,664	1,023	1,514	2,465	4,811	$2{,}386\, m^{1/2}$

La valeur exacte calculée par Howarth [5] est 0,66412; on a donc une erreur par défaut de 6,1% lorsqu'on s'arrête à la première approximation. Nous avons porté sur la Fig. 3 la variation de $C_f R_x^{1/2}$ en fonction de $\beta = 2m/(m+1)$.

La différence entre les valeurs approchées données par (89) et les valeurs exactes augmente lorsque le gradient de pression croît. La valeur de m pour laquelle on aurait constamment $\tau_{p1} = 0$ est plus faible que la valeur exacte $-0{,}0904$.

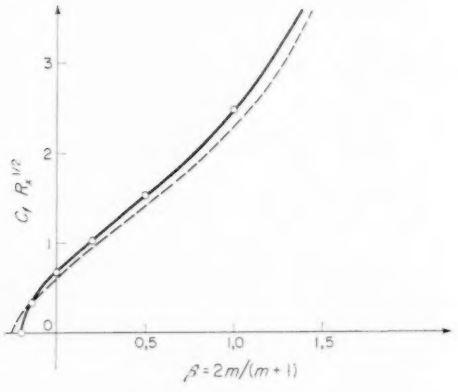

FIG. 3.
—○— Hartree
— — Première approximation

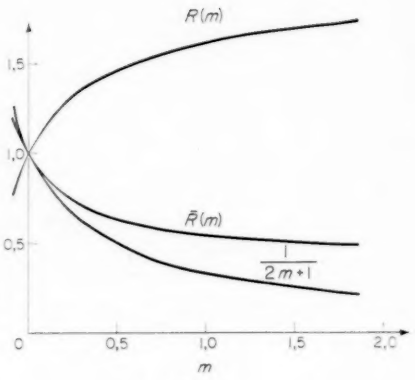

FIG. 4.

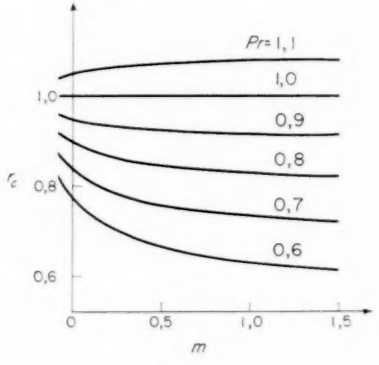

FIG. 5.

4.2. *Coefficient de convection local*

La température effective locale est donnée par la formule (80) qui devient:

$$\theta_{\text{eff}}(x) = \theta_t + \frac{r-1}{2C_p} R(m) u_e^2 \qquad (93)$$

où:

$$R(m) = \Gamma(2/3) \frac{\Gamma[(11m+3)/(3m+3)]}{\Gamma[(10m+2)/(3m+3)]} \qquad (94)$$

La courbe représentative de la fonction $R(m)$ a été portée sur la Fig. 4. Le facteur thermique pariétal de convection local est constant et égal à:

$$r_c = 1 + (r-1)R(m) \qquad (95)$$

On a porté sur la Fig. 5 les courbes donnant la variation de r_c en fonction de m pour différentes valeurs de Pr. On voit que la première approximation donne des valeurs de r_c très voisines des valeurs exactes données sur la Fig. 2 de l'article de Brun [6].

Le coefficient de convection local est donné par (74) et (82):

$$\alpha = C_p(\mu\rho)^{1/2} Pr^{-2/3} \times \times \frac{3^{3/4}(m+1)^{1/2}[Q(m)]^{1/4}}{2^{5/4}\Gamma(1/3)} c^{1/2} x^{(m-1)/2} \qquad (96)$$

Le nombre de Nusselt local $N_x = \alpha x/\lambda$ sera donné par la formule:

$$N_x \cdot R_x^{-1/2} = Pr^{1/3} \frac{3^{3/4}(m+1)^{1/2}}{2^{5/4}\Gamma(1/3)} [Q(m)]^{1/4} \qquad (97)$$

Par contre la méthode de Lighthill nous donne:

$$N_x \cdot R_x^{-1/2} = Pr^{1/3} \frac{3^{2/3}(m+1)^{1/2}}{2^{5/6}\Gamma(1/3)} [f''(0)]^{1/3} \qquad (98)$$

Vol. 1 1960

Tableau 3

m	$-1/9$	$-0{,}0904$	$-0{,}0654$	0	1/9	1/3	1	4	∞
β	$-0{,}25$	$-0{,}1988$	$-0{,}14$	0	0,20	0,50	1	1,6	2
Valeurs exactes		0,220	0,284	0,332	0,378	0,440	0,570	0,939	$0{,}429\ m^{1/2}$
Première approximation	0	0,220	0,265	0,332	0,395	0,478	0,643	1,091	$0{,}505\ m^{1/2}$
Lighthill		0	0,262	0,339	0,405	0,491	0,661	1,121	$0{,}519\ m^{1/2}$

où N_x est égal à $\Phi_p x/\lambda(\theta_p - \theta_t)$ puisque l'on ne tient compte ni de l'échauffement dû au gradient de pression ni de celui dû au frottement.

Avec les mêmes hypothèses, Eckert [7] a obtenu la relation:

$$N_x \,.\, R_x^{-1/2} = \sqrt{\left(\frac{m+1}{2}\right)}\left[\int_0^\infty \exp\left(-Pr\int_0^\eta f(\eta')d\eta'\right)d\eta\right]^{-1} \quad (99)$$

Nous avons porté sur le Tableau 3 les valeurs de $N_x \,.\, R_x^{-1/2}$ lorsque $Pr = 1$ obtenues à l'aide des formules (97) et (98) et les valeurs exactes données par (99).

Lorsque $m = 0$, la formule (97) devient:

$$N_x \,.\, R^{-1/2} = Pr^{1/3}\frac{3^{7/8}}{2^{3/2}\pi^{1/4}[\Gamma(1/3)]^{3/4}} = 0{,}33165\ Pr^{1/3},$$

tandis que la formule (98) devient:

$$N_x \,.\, R_x^{-1/2} = Pr^{1/3}\frac{3^{2/3}[0{,}66412]^{1/3}}{2\Gamma(1/3)} = 0{,}33872\ Pr^{1/3}$$

Lorsque $Pr = 1$, Pohlhausen [3] a montré que pour la plaque plane $N_x \,.\, R_x^{-1/2}$ était égal à $C_f R_x^{1/2}/2$ soit 0,33206. La formule (97) conduit à une erreur par défaut de 0,1% tandis que la formule (98) conduit à une erreur par excès de 2%.

Dans le cas général de $m \neq 0$, la formule (97) diffère d'autant plus des résultats exacts que m est plus grand, mais donne toujours des valeurs plus voisines que la formule de Lighthill.

Nous avons porté sur la Fig. 6 la variation de $N_x \,.\, R_x^{-1/2}$ en fonction de β lorsque $Pr = 1$.

D'autre part, comme on l'a vu au paragraphe 3.2, le facteur thermique pariétal de frottement est indépendant de m dans le cadre de la première approximation, tandis que Eckert et Drewitz [8] ont trouvé en intégrant directement l'équation de l'énergie (6) que r variait avec m mais faiblement.

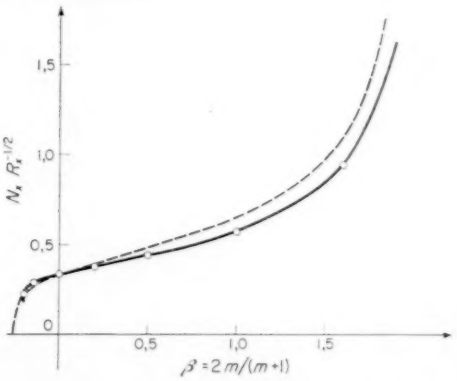

FIG. 6. $Pr = 1$.
○ Eckert
— — Première approximation

4.3. *Coefficient de convection moyen*

La température effective moyenne est donnée par la formule (84) qui devient:

$$\theta_{\overline{\text{eff}}}(x) = \theta_t + \frac{r-1}{2C_p}\,\bar{R}(m)u_e^2 \quad (100)$$

où:

$$\bar{R}(m) = \Gamma(5/3)\,\frac{\Gamma\{(11m+3)/(3m+3)\}}{\Gamma\{(13m+5)/(3m+3)\}} = \frac{m+1}{5m+1}\,R(m) \quad (101)$$

La courbe représentative de la fonction $\bar{R}(m)$ a été portée sur la Fig. 4.

Le facteur thermique pariétal de convection moyen est constant et égal à:

$$\bar{r}_e = 1 + (r - 1)\bar{R}(m) \qquad (102)$$

On a porté sur la Fig. 7 les courbes donnant la variation de $\bar{r}_e$ en fonction de m pour différentes valeurs de Pr.

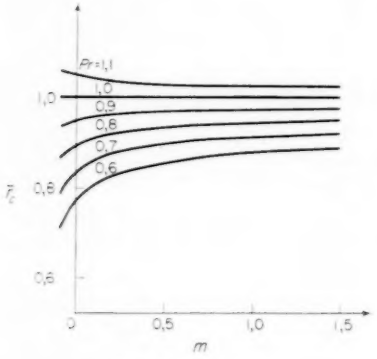

FIG. 7. $Pr = 1{,}1$.

La température moyenne de frottement est par définition:

$$\theta_{fm} = \frac{1}{x}\int_0^x \theta_f dx = \theta_t + \frac{r-1}{2C_p}\cdot\frac{u_e^2}{2m+1} \qquad (103)$$

On voit sur la Fig. 4 que la fonction $1/(2m + 1)$ est voisine de la fonction $\bar{R}(m)$, surtout lorsque m est faible.

On vérifie donc dans le cas des dièdres que l'on ne fait pas une grande erreur en supposant que la température effective moyenne est égale à la température moyenne de frottement, comme Brun l'a fait remarquer.

Le coefficient de convection moyen rapporté à la température effective moyenne est obtenu grâce à (77) et à (86):

$$\alpha_m = C_p(\mu\rho)^{1/2}Pr^{-2/3} \times \times \frac{3^{3/4}[Q(m)]^{1/4}}{2^{1/4}\Gamma(1/3)(m+1)^{1/2}}\, c^{1/2}x^{(m-1)/2} \qquad (104)$$

On trouve donc que le nombre de Nusselt moyen $N_{xm} = \alpha_m x/\lambda$ sera donné par la formule:

$$N_{xm} \cdot R^{-1/2} = \frac{2}{m+1} N_x \cdot R_x^{-1/2} \qquad (105)$$

$N_x \cdot R_x^{-1/2}$ étant obtenu par la formule (97).

5. CONCLUSION

La première approximation donne dans le cas de la plaque plane des expressions du coefficient de convection et du facteur thermique pariétal très voisines des résultats exacts.

Par contre, le cas où le gradient de pression n'est plus nul nécessiterait de poursuivre l'itération plus loin à moins que l'on ne s'intéresse qu'à un ordre de grandeur.

La méthode de calcul exposée ici permet donc d'obtenir, dans le cas général la valeur de la densité de flux de chaleur avec une erreur de l'ordre de 15% dans le cas le plus défavorable.

Je remercie M. le Professeur E. Brun pour les conseils qu'il m'a donnés au cours de cette étude que j'ai effectuée sous sa direction.

Vol. 1 1960

BIBLIOGRAPHIE

1. R. VON MISES, *Z. angew. Math. Mech.* **7**, 425 (1927).
2. M. J. LIGHTHILL, *Proc. Roy. Soc.* A **202**, 359 (1950).
3. E. POHLHAUSEN, *Z. angew. Math. Mech.* **1**, 115 (1921).
4. D. R. HARTREE, *Proc. Camb. Phil. Soc.* **33**, 223 (1937).
5. L. HOWARTH, *Proc. Roy. Soc.* A **164**, 547 (1938).
6. E. A. BRUN, *Selected Combustion Problems* Vol. II, p. 185. AGARD. Pergamon Press, London (1956).
7. E. ECKERT, *Forschungsh. Ver. dtsch. Ing.* 416 (1942).
8. E. ECKERT et O. DREWITZ, *Luftfahrtforsch.* **19**, 189, (1942).

Int. J. Heat Mass Transfer. Vol. 1, pp. 81–91. Pergamon Press 1960. Printed in Great Britain.

ONE-DIMENSIONAL ENERGY TRANSFER IN RADIANT MEDIA†

R. and M. GOULARD

Advanced Development Laboratories, Bendix Products Division, South Bend, Indiana, U.S.A.

(*Received* 26 *October* 1959)

Abstract—The equations of one-dimensional radiative energy transfer are extended from their classical astrophysics form to include walls of arbitrary radiative properties. The concepts of emissivity and penetration length are examined. As an application, the case of the steady infinite flat layer is considered, with conduction and radiation present. The wall conditions are so chosen as to give a good model of a low-speed high-temperature boundary-layer. It is found that the effect of the "long-range" process of radiation is to smooth out the temperature profiles and relieve the sharp temperature gradients at the cool wall. As a result, the application of the exact method yields a lower value of both components of the total heat flux (radiation plus convection) than calculated previously by assuming a temperature profile on the basis of conduction only. Such coupling of convective and radiative fluxes is governed by the magnitude of a non-dimensional parameter, depending on the physical properties and the flow geometry of the problem.

Résumé—Les équations de la transmission unidimensionnelle d'énergie par rayonnement ont été étendues, à partir de leur forme classique en astrophysique, de façon à traiter le cas de parois à propriétés de rayonnement quelconques. Les notions d'émissivité et de longueur de pénétration sont examinées. Le cas d'une couche infinie, plane et permanente, en présence de conduction et de rayonnement, est traité à titre d'application. Les conditions de paroi sont choisies de façon à donner un bon modèle de couche limite à basse vitesse et à haute température. On trouve que l'effet à grande distance du processus de rayonnement est d'adoucir les profils de température et de mettre en relief les importants radients de température à la paroi froide. Il en résulte que l'application de la méthode exacte fournit pour les deux composantes du flux de chaleur total (rayonnement + convection) une valeur plus basse que celle calculée précédemment en supposant le profil de température dû à la seule conduction. Une telle combinaison des flux de convection et de rayonnement est déterminée par la grandeur d'un paramètre sans dimensions dépendant des propriétés physiques et de la géométrie de l'écoulement du problème.

Zusammenfassung—Die Gleichungen für die eindimensionale Energieübertragung durch Strahlung wird von ihrer klassischen Form der Astrophysik erweitert, um auch Wände mit beliebigen Strahlungseigenschaften einzuschließen. Die Begriffe der Emission und der Durchdringungslänge werden untersucht. Zur Anwendung wird eine unendliche flache Schicht im Beharrungszustand betrachtet, in der Leitung und Strahlung stattfindet. Die Wandbedingungen werden so gewählt, dass ein brauchbares Modell für eine Hochtemperaturgrenzschicht bei kleinen Geschwindigkeiten entsteht. Es zeigt sich, dass die Wirkung der Strahlung die Temperaturprofile ausgleicht und den steilen Temperaturgradienten an der kalten Wand abflacht. Die Anwendung der exakten Methode ergibt geringere Werte für beide Komponenten des gesamten Wärmestroms (Strahlung und Konvection), als sie sich bei der Annahme eines Temperaturprofiles für reine Leitung bisher ergeben hat. Das Zusammenwirken der Wärmeströme durch Konvektion und Strahlung wird durch eine dimensionslose Kenngrösse bestimmt, die von den Stoffwerten und der geometrischen Anordnung abhängt.

Abstract—Классические уравнения одномерного лучистого переноса энергии, используемые в астрофизике распространяются на случай лучистого теплообмена в ограниченном пространстве с произвольными радиационными характеристиками стенок. Рассматриваются понятия степени черноты тела и глубины проникновения. В качестве примера рассматривается случай стационарного неограниченного плоского слоя при наличии теплопроводности и лучистого теплообмена. Условия на стенках выбраны таким образом, чтобы получить хорошую модель низкоскоростного высокотемпературного пограничного слоя. Установлено, что влияние „дальнодействующего"

† The work described in this paper was supported by the United States Army Rocket and Guided Missile Agency, under contracts Nos. DA-11-022-ORD-2642 and DA-11-022-ORD-8130.

процесса излучения заключается в сглаживании температурных профилей и уменьшении „остроты" температурных градиентов на холодной стенке. Применение точного метода даёт более низкую величину обеих составляющих полного потока тепла (лучистой и конвективной) нежели это вычислялось прежде, когда предполагалось, что температурный профиль определяется только теплопроводностью. Для данной задачи сочетание конвективного и лучистого потоков регулируется величиною безразмерного параметра, зависящего от физических свойств и геометрии потока.

NOTATION

$A(B)$, equation (34);
B, B_ν, Planck's function (equations (6) and (7));
C, variable coefficient (equation (11));
c, velocity of light;
E, E_ν, radiative energy;
$E_n(t)$, equation (19);
h, Planck's constant;
k, conduction heat transfer coefficient;
I, I_ν, specific intensity (equation (1));
j_ν, emission coefficient;
L, plane layer thickness;
$\mathbf{L}$, direction of incident radiation;
l, penetration length;
N_{r-c}, equation (37);
$\mathbf{n}$, unit vector normal to surface $d\sigma$ (Fig. 1);
q, radiative energy flux;
r, reflectivity;
ds, elementary length along $\mathbf{L}$;
t, integration variable (also: time, in equation (1));
T, absolute temperature;
tr, transparency;
V, flight velocity;
y, vertical co-ordinate (Fig. 2);
α, absorptivity;
ε, emissivity;
ϑ, spherical co-ordinate of $\mathbf{L}$ (Fig. 1);
κ, absorption coefficient;
μ, equation (9);
ν, frequency;
σ, Stefan's constant;
$d\sigma$, surface element (Fig. 1);
ρ, density;
τ, τ_ν, optical thickness (equation (8));
ϕ, spherical co-ordinate of $\mathbf{L}$ (Fig. 1);
$d\omega$, solid angle (Fig. 1).

Subscripts

g, gas;
w, wall;
ν, frequency;
0, lower wall;
2, L, upper wall.

Superscript

*, floating boundary.

INTRODUCTION

ENERGY transfer by radiation has been for a long time a familiar problem to the physicists concerned with high-temperature gases. Its important role in specialized subjects of applied physics, such as blast waves, plasma physics and astrophysics has been the object of many studies and these different domains have attained a high degree of organization [1, 2, 11, 15].

Technological progress has, meanwhile, steadily increased the demand for engineering designs capable of withstanding higher and higher temperatures. The associated problems of radiative energy transfer are becoming, therefore, increasingly important in the field of combustion [4, 5] and propulsion. They are also to be considered, now, in very high speed aerodynamics [16] and new reactor concepts.

A major difference between the two classes of problems just described is due to the existence of solid boundaries in most engineering systems using radiative media. In this paper, the mathematical expressions of radiant energy transfer developed in astrophysics will be extended to include wall effects in simple one-dimensional geometries. A typical application will be made to a steady infinite flat layer, with wall conditions so chosen as to give a good model of a low-speed high-temperature boundary layer.

A. ONE-DIMENSIONAL RADIATION FLUX

Specific intensity I_ν and flux q_ν

The fundamentals of the theory of radiation transfer in gases can be found in standard textbooks of astrophysics [1, 2]. Two important quantities to be used extensively in this paper will be redefined here. The notation adopted is that of Kourganoff [3].

Vol. 1 1960

Let dE_ν be the amount of radiative energy in the frequency interval $\nu, \nu + d\nu$ transmitted through an elementary surface $d\sigma$ at a point P during a time interval dt within a solid angle $d\omega$ (see Fig. 1). The normal **n** to the surface and

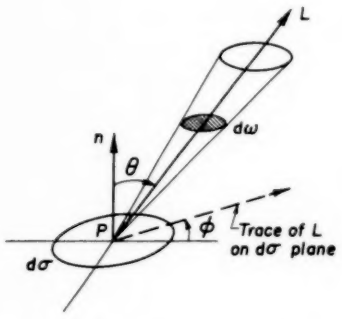

FIG. 1. Radiation intensity symbols.

the direction **L** of the solid angle form an angle θ. I_ν, the *specific intensity* in the direction **L** is defined as:

$$I_\nu = \lim. \left| \frac{dE_\nu}{\cos\theta \, d\sigma \, d\omega \, d\nu \, dt} \right|_{d\sigma,\, d\omega,\, d\nu,\, dt \to 0} \tag{1}$$

Accordingly, I_ν depends on the location of P and on the direction **L**. Because of the introduction of $\cos\theta$ in equation (1), the specific intensity I_ν is usually independent of the angle θ between the direction **L** and the normal **n** to the elementary surface. It should be pointed out that this definition is *not* the one most frequently used in engineering ([17], equation 13–6), where $\cos\theta$ does not appear in the definition of the intensity. As a result, "engineering" radiation intensities vary with θ (e.g. Lambert's law). In this paper, the "astrophysics" definition of the intensity will be used (equation (1)).

The flux q_ν of radiative energy across the surface $d\sigma$, in the frequency interval $d\nu$, is obtained simply by summing up the quantity

$$\frac{dE_\nu}{d\sigma \, dt \, d\omega} = I_\nu \cos\theta \, d\omega$$

for all the directions **L** ($d\omega = \sin\theta \, d\theta \, d\phi$). It is convenient to split the net flux q_ν into the contribution q_ν^+ coming from the side of the normal unit vector **n** and the contribution q_ν^- from the opposite side:

$$q_\nu^+ = \int_0^{\pi/2} \int_0^{2\pi} I_\nu(\theta, \phi) \cos\theta \sin\theta \, d\theta \, d\phi \tag{2}$$

$$q_\nu^- = -\int_{\pi/2}^{\pi} \int_0^{2\pi} I_\nu(\theta, \phi) \cos\theta \sin\theta \, d\theta \, d\phi \tag{3}$$

Equation of radiative energy transfer

The intensity, on a length ds, along the direction **L**, is attenuated by absorption and scattering away from the direction **L**, while it is reinforced by the energy emitted by the particles along **L** and the scattering of photons from other directions into the direction **L**.

The intensity I_ν is therefore determined by the equation:

$$\frac{dI_\nu}{ds} = -\kappa_\nu \rho I_\nu + \rho j_\nu \tag{4}$$

where κ_ν and j_ν are, respectively, the absorption and emission coefficients [3]. It is further shown in [2, 3], that, provided the gradients of temperature are not too considerable and the densities not too small, "local thermodynamic equilibrium" can be assumed and equation (4) can be written:

$$-\frac{1}{\rho\kappa_\nu} \frac{dI_\nu}{ds} = I_\nu - B_\nu \tag{5}$$

where B_ν is Planck's function [2]:

$$B_\nu(T) = \frac{2h}{c^2} \frac{\nu^3}{\exp(h\nu/kT) - 1} \tag{6}$$

with

$$B = \int_0^\infty B_\nu \, d\nu = \frac{\sigma}{\pi} T^4 \tag{7}$$

Specific intensity in one-dimensional problems

A glance at equations (2) and (5) shows that all radiation problems but those with the simplest geometry, will be difficult to solve. In this study, only one-dimensional geometries will be discussed.

It is convenient to define at this point the *optical thickness* τ_ν such that:

$$d\tau_\nu \equiv \rho\kappa_\nu \, dy \tag{8}$$

where y is the privileged direction of the one-dimensional problem illustrated on Fig. 2. If θ is the angle between the direction **L** and the negative (downward) y-direction, then:

$$dy = -\mu\, ds \text{ where } \mu \equiv \cos\theta \qquad (9)$$

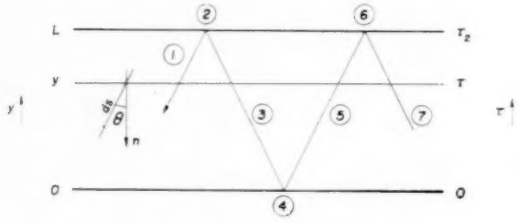

FIG. 2. Multiple reflexions in a plane layer.

Equation (5) can then be rewritten:

$$\mu \frac{dI}{d\tau_\nu} = I_\nu - B_\nu \qquad (10)$$

The solution $I_\nu(\tau_\nu)$ of equation (10) is simply obtained by the variable coefficient method:

$$I_\nu = C(\tau_\nu) \exp(\tau_\nu/\mu) \qquad (11)$$

The function $C(\tau_\nu)$ is, after substitution of equation (11) into equation (10):

$$C(\tau_\nu) = C(\tau_\nu^*) - \int_{\tau_\nu^*}^{\tau} \frac{B_\nu(t)}{\mu} \exp(-t/\mu)\, dt \qquad (12)$$

where τ_ν^* is an arbitrary value, to be determined by the boundary value of the problem. For instance, the radiation directed upwards in Fig. 2 will be determined by the condition at the lower wall: $\tau_\nu^* = 0$. After substitution, equation (11) becomes:

$$I_\nu^- = \int_0^{\tau_\nu} B_\nu(t) \exp\{-(t-\tau_\nu)/\mu\} \frac{dt}{\mu} + I_\nu^-(0) \exp(\tau_\nu/\mu) \qquad (13)$$

Similarly, the radiation directed downwards will be determined by the conditions at the upper wall:

$$I_\nu^+ = \int_{\tau_\nu}^{\tau_{\nu 2}} B_\nu(t) \exp\{-(t-\tau_\nu)/\mu\} \frac{dt}{\mu} + I_\nu^+(\tau_{\nu 2}) \exp\{(\tau_\nu - \tau_{\nu 2})/\mu\} \qquad (14)$$

Radiation flux in one-dimensional problems

Since we confine ourselves to one-dimensional problems, equations (2) and (3) can be integrated with respect to ϕ. One obtains:

$$q_\nu^+ = 2\pi \int_0^1 I_\nu(\mu)\, \mu d\mu \qquad (15)$$

$$q_\nu^- = 2\pi \int_0^{-1} I_\nu(\mu)\, \mu d\mu \qquad (16)$$

It is then a simple matter to substitute equations (13) and (14) into (15) and (16). The result is:

$$q_\nu^- = 2\pi \int_0^{\tau_\nu} B_\nu(t)\, E_2(\tau_\nu - t)\, dt + 2q_\nu^-(0)\, E_3(\tau_\nu) \qquad (17)$$

$$q_\nu^+ = 2\pi \int_{\tau_\nu}^{\tau_{\nu 2}} B_\nu(t)\, E_2(t - \tau_\nu)\, dt + 2q_\nu^+(\tau_{\nu 2})\, E_3(\tau_{\nu 2} - \tau_\gamma) \qquad (18)$$

where the dependence on μ appears through the functions:

$$E_n(t) \equiv \int_0^1 \mu^{n-2} e^{-t/\mu}\, d\mu \qquad (19)$$

These functions are conveniently tabulated by Kourganoff [3]. The net flux q_ν is the difference between equations (17) and (18).

To obtain the total flux, it is necessary to integrate the flux expressions for all wavelengths. To simplify the discussion, the medium under study will be assumed to be *gray*: by definition, the absorption coefficient κ_ν will then be independent of the frequency ν and so will be the optical thickness τ_ν. The only wavelength-dependent function left in the expressions derived above, will be Planck's function (equation (6)). It can therefore be integrated separately (equation (7)), and the subscript ν will be dropped from the rest of the paper.

B. WALL EFFECTS†

The second terms, on the right-hand side of the expressions (17) and (18) of q^- and q^+,

† Part B of this paper is a condensation of a more detailed study made by the Senior Author in Report No. A–59–8, School of Aeronautical Engineering, Purdue University, Lafayette, Indiana.

Vol. 1 1960

account for the contribution of the wall to the radiative flux. Whenever walls are non-existent, as it is the case in star photospheres, this term disappears and the expressions (17) and (18) take their classical Milne formulation [3].

In general, however, the contribution from the wall is determined by its absorptivity α_w, its emissivity ϵ_w, its transparency tr_w and its reflectivity r_w. The relations between these quantities are:

$$\alpha_w + tr_w + r_w = 1 \tag{20}$$

$$\alpha_w = \epsilon_w \tag{21}$$

The flux *downwards* q^+ in the slab geometry shown on Fig. 2, is at a given station τ, made of several components:

(1) the flux from the gas slab $\tau - \tau_2$

$$2\pi \int_{\tau}^{\tau_2} B(t)\, E_2(t-\tau)\, dt$$

(2) the flux from the upper wall, attenuated

$$2\pi\epsilon_2\, B(\tau_2)\, E_3(\tau_2 - \tau)$$

(3) the flux from the gas slab $0 - \tau_2$, after reflection on the upper wall and attenuation

$$\left\{ 2\pi \int_0^{\tau_2} B(t)\, E_2(t-\tau_2)\, dt \right\} 2r_2\, E_3(\tau_2 - \tau)$$

(4) the flux from the lower wall, after two attenuations and one reflection:

$$2\pi\, \epsilon_0\, B(0)\, E_3(\tau_2 - 0)\, r_2\, 2E_3(\tau_2 - \tau)$$

(5) the flux from the gas slab $0 - \tau_2$, after two reflections and two attenuations:

$$\left\{ 2\pi \int_0^{\tau_2} B(t)\, E_2(t)\, dt \right\} \times \times\, r_0\, 2E_3(\tau_2)\, r_2\, 2E_3(\tau_2 - \tau)$$

(6) the flux from the upper wall twice reflected and three times attenuated

$$2\pi\, \epsilon_2\, B(\tau_2)\, E_3(\tau_2) r_0\, 2E_3(\tau_2) r_2\, 2E_3(\tau_2 - \tau)$$

(7) . . . ., etc., . . .

It is to be noted that the contribution from the upper wall in (6) is equal to its contribution in (2), except for the attentuation factor:

$$4r_0 r_2\, E_3^2(\tau_2)$$

due to two additional reflections. The contribution of the wall along a ray which has been reflected $2n$ times, is similarly attenuated by a factor:

$$[4r_0 r_2\, E_3^2(\tau_2)]^n$$

The total contribution of the upper wall is therefore equal to:

$$2\pi\, \epsilon_2\, B(\tau_2)\, E_3(\tau_2 - \tau) \left[\sum_{n=0}^{n=\infty} \{4r_0 r_2\, E_3^2(\tau_2)\}^n \right]$$

which can be rearranged $\{4r_0 r_2\, E_3^2(\tau_2) < 1\}$ as:

$$\frac{2\pi}{1 - 4r_0 r_2\, E_3^2(\tau_2)}\, \epsilon_2\, B(\tau_2)\, E_3(\tau_2 - \tau) \tag{22}$$

Using the same method to account for the other contributions to the flux, the expression of the *net* flux across station τ is therefore:

$$\begin{aligned} q = q^+ - q^- = {} & 2\pi \int_{\tau}^{\tau_2} B(t)\, E_2(t-\tau)\, dt - \\ & - 2\pi \int_0^{\tau} B(t)\, E_2(\tau - t)\, dt + \\ & + \frac{2\pi}{1 - 4r_0 r_2\, E_3^2(\tau_2)} \Big\{ \epsilon_2 B(\tau_2) E_3(\tau_2 - \tau) - \\ & - \epsilon_0\, B(0)\, E_3(\tau) + \\ & + \epsilon_0\, B(0)\, E_3(\tau_2)\, 2r_2\, E_3(\tau_2 - \tau) - \\ & - \epsilon_2\, B(\tau_2)\, E_3(\tau_2)\, 2r_0\, E_3(\tau) + \\ & + 2r_2\, E_3(\tau_2 - \tau) \int_0^{\tau_2} B(t)\, E_2(t-\tau_2)\, dt - \\ & - 2r_0\, E_3(\tau) \int_0^{\tau_2} B(t)\, E_2(t)\, dt + \\ & + 4r_0 r_2\, E_3(\tau_2)\, E_3(\tau_2 - \tau) \int_0^{\tau} B(t)\, E_2(t)\, dt - \\ & - 4r_0 r_2\, E_3(\tau_2)\, E_3(\tau) \int_0^{\tau_2} B(t)\, E_2(t - \tau_2)\, dt \Big\} \end{aligned} \tag{23}$$

This lengthy expression is the most general form of the flux through a one-dimensional non-scattering medium†. Among its many

† A completely general form, including non isotropic scattering, is under preparation by R. Viskanta, School of Mechanical Engineering, Purdue University.

applications to special cases are familiar formulas.

(a) Slab of very large thickness (star photosphere or blast waves):

$$\epsilon_0 = \epsilon_2 = r_0 = r_2 = 0 \quad \tau_2 \to \infty$$

$$q = 2\pi \int_{\tau}^{\infty} B(t)\, E_2(t-\tau)\, dt - 2\pi \int_{-\infty}^{\tau} B(t)\, E(t)\, dt$$

equation (11–4) of [3].

(b) Transparent medium between two gray parallel plates:

$$\kappa \sim 0 \to \tau \sim 0\,,\ E_3(\tau) \sim E_3(0) = \tfrac{1}{2}\,,\ \epsilon = 1 - r$$

$$q = \sigma (T_2^4 - T_0^4) \frac{1}{1/\epsilon_2 + 1/\epsilon_0 - 1}$$

equation (4–5) of [5].

(c) Absorbing medium between two black body plates at same temperature T_w:

$$r_0 = r_2 = 0\,,\ \epsilon_0 = \epsilon_2 = 1$$

$$q = 2\pi \int_{\tau}^{\tau_2} B(t)\, E_2(t-\tau)\, dt - 2\pi \int_{0}^{\tau} B(t)\, E_2(t)\, dt + 4\pi\, B(\tau_2)\, E_3(\tau_2 - \tau) - 4\pi\, B(0)\, E_3(\tau)$$

Assume also $\tau \ll 1$; then $E_2 \simeq 1$, $E_3 \simeq 1/2 - t$:

$$q = 2\int_{y}^{L} \sigma T^4 \rho\kappa dy - 2\int_{0}^{y} \sigma T^4 \rho\kappa dy + \sigma(T_2^4 - T_0^4) - 2\sigma T_2^4 \rho\kappa (L - y) + 2\sigma T_0^4 \rho\kappa y$$

At the lower wall, $y = 0$, $\tau = 0$, and since $T_0 = T_2 = T_w$,

$$q_w = 2\int_{0}^{L} \sigma T^4 \rho\kappa dy - 2\sigma T_w^4\, \rho\kappa L$$

and, since $2\rho\kappa L = \epsilon$ (equation (27)), this is equivalent to:

$$q_w = \sigma (\epsilon_g T_g^4 - a_g T_w^4)$$

equation (4–57) of [5].

C. PHYSICAL PROPERTIES

With these expressions of fluxes and intensities available, it is now possible to describe the physical properties of the medium, in a form more directly applicable to transfer problems.

Emissivity ε of a constant-temperature gas layer†

A simple application of equation (23) consists of the constant-temperature slab, with a transparent upper wall and either a cool [$B(0) \simeq 0$], black-body ($r_0 = 0$) lower wall, or a transparent lower wall. The expression of the radiant flux on either face of the slab, is therefore:

$$q = 2\pi \int_{0}^{\tau_2} B(t)\, E_2(t)\, dt \tag{24}$$

and

$$q = 2\sigma T^4 \int_{0}^{\tau_2} E_2(t)\, dt = -2\sigma T^4 \int_{0}^{\tau_2} d\,[E_3(t)]$$

and since $E_3(0) = \frac{1}{2}$, [see (31a)]

$$q = \sigma T^4\, [1 - 2\, E_3(\tau_2)] \tag{25}$$

If, furthermore, the medium is optically thin (i.e. $\tau \ll 1$), $E_3(\tau)$ can be written in good approximation (31a):

$$E_3(\tau) \simeq \tfrac{1}{2} - \tau$$

Hence:

$$q = \sigma T^4 \{1 - 2(\tfrac{1}{2} - \tau_2)\} = 2\tau_2 \sigma T^4 = 2\rho\kappa L \sigma T^4 \quad (\tau_2 \ll 1) \tag{26}$$

where L is the physical thickness of the layer corresponding to τ_2. It is then natural to call the quantity $2\rho\kappa L$ the emissivity ϵ of the gas layer:

$$\frac{\epsilon}{L} \equiv 2\rho\kappa \tag{27}$$

This convenient ratio has been tabulated, for instance, in [6] for high-temperature air. The coefficient κ can be obtained directly from this relation.

† This derivation of the relationship between ϵ and κ was suggested by W. Glauz, School of Engineering Sciences, Purdue University. It avoids the difficulty met in [6], in which the contribution of grazing rays in the slab (very large $\rho\kappa s$), is used in an "optically thin" approximation (small $\rho\kappa s$).

Vol. 1 1960

Penetration length l

In the case studied above, equation (25) shows that, if there is a transparent or no upper wall a black-body radiation flux to the lower wall will be achieved only for $\tau_2 \to \infty$ (where $E_3 \to 0$). The intensity variation along a beam of arbitrary angle (arbitrary fixed μ) is, at the lower wall ($\tau = 0$) according to equation (14):

$$I^+ = \frac{\sigma T^4}{\pi} \int_0^{\tau_2} \exp(-t/\mu) \frac{dt}{\mu} = \frac{\sigma T^4}{\pi} \{1 - \exp(-\tau_2/\mu)\} \quad (28)$$

and, for optically thin layers (τ_2 1),

$$I^+ = \frac{\sigma T^4}{\mu\pi} \tau_2 = \rho\kappa L \frac{\sigma T^4}{\pi\mu} \quad (29)$$

It can be concluded from these two equations that both I and q depend on the absorption properties of the medium, only through the optical thickness τ. The optical thickness is therefore a useful dimensionless concept and is refered to often as the Bueger number (N_{Bu}) in the Russian literature [7].

A useful index of the absorption properties of a substance is also the physical thickness l corresponding to an optical thickness unity:

$$l \equiv \frac{1}{\rho\kappa}$$

This "penetration length" l has been discussed in [8]. It is shown in Fig. 3 for high-temperature air in terms of temperature and density ratios, using the values of ϵ from [6].

If the characteristic dimension L of the problem under study is much less than l, then

$$\tau = \frac{L}{l} \ll 1$$

and the "optically thin" layer approximation of equation (29) can be used. We note that in equation (29), the contributions of all the infinitesimal layers forming a layer of finite thickness L, are *additive*. Physically, this means that in optically thin layers, the energy radiated in any part of the layer is *not* absorbed by the other parts. This is a great simplification in some transfer problems in re-entry aerodynamics, where for most altitudes ($\rho \ll \rho_0$), velocities ($V < 35{,}000$ ft/sec), and vehicle sizes ($L < 100$ cm): $L \ll l$ as illustrated in Fig. 3.

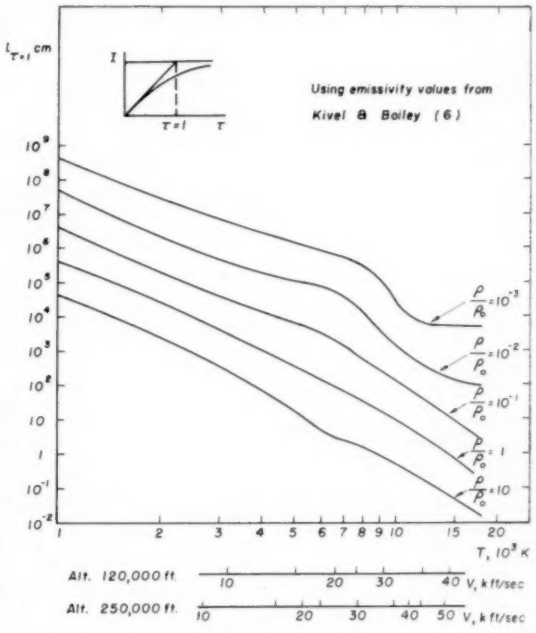

FIG. 3. Length of penetration $l = 1/\rho\kappa$ in aerodynamic problems.

On the contrary, if $l \ll L$, intermediate absorption takes place and at the limit, l plays the role of a mean free path (Rosseland), leading to a differential form for the flux expression q. This is often a considerable mathematical simplification which is justified in many cases [5, 7, 10], including high temperature ($T > 10{,}000$°K), large size ($L \sim 10^4$ cm) blast waves in air [11].

D. THE PLANE-LAYER PROBLEM

The determination of the temperature profile and energy flux across an infinite plane layer of uniform thickness and arbitrary wall temperature, is a classical problem of conduction heat transfer [4], even when chemical reactions occur in the layer or at the walls [14]. The energy conservation equation to solve is then in purely differential form.

The energy conservation equation

This problem is greatly complicated, however, when radiation contributes appreciably to the energy transfer. In this case a complex integral term, equation (23), is added to the convection flux. Unless this new term can be reduced to a differential form, as for some cases discussed in Section C, no closed solution is available to this class of problems.

In this paper, a numerical solution to the steady-state plane-layer problem is presented. The solution can be applied to the fluid-layer problem (Couette flow) if the velocity gradients are not too large (no energy dissipation term in the energy equation). Such a simple model, showing a close analogy with the boundary-layer problem in high-temperature flow, is considered here. The upper wall is transparent (emissivity $\epsilon_2 = 0$, reflectivity $r_2 = 0$), and the lower wall is an opaque gray surface (emissivity ϵ_0, reflectivity $r_0 = 1 - \epsilon_0$). Equation (23) reduces, in this case, to:

$$q = 2\pi \int_{\tau}^{\tau_2} B(t)\, E_2(t-\tau)\, dt - 2\pi \int_0^{\tau} B(t)\, E_2(\tau - t)\, dt - 2\pi\epsilon_0\, B(0)\, E_3(\tau) - 4\pi r_0\, E_3(\tau) \int_0^{\tau_2} B(t)\, E_2(t)\, dt \tag{30}$$

The physical meaning of the four terms on the right-hand side of equation (30) is, respectively:

(a) the energy radiated past the elementary slab τ by all the elementary slabs located above ($\tau < t < \tau_2$);
(b) the energy radiated past the elementary slab τ by all the elementary slabs located below ($0 < t < \tau$);
(c) the fraction of energy radiated by the lower wall that reaches the layer τ, the other fraction being absorbed by the layer ($0 - \tau$);
(d) the fraction of the energy radiated by the slab to the lower wall, after partial reflection by the lower wall and partial absorption of the layer ($0 - \tau$).

Substitution of this value of q into the energy conservation equation for the one-dimensional steady state:

$$k \frac{\partial T}{\partial y} + q = \text{constant} \tag{31}$$

yields a non-linear integro-differential equation that is satisfied by a temperature distribution $T(y)$ to be determined.† In the general non-gray case, this same method would apply with an additional integration of the radiative terms for all wavelengths.

The solution of the aerodynamic flow problem

A further (but not essential to the solution) simplification to the aerodynamic problems in radiant media is due to the low optical thicknesses τ involved (i.e. high penetration lengths l, as seen on Fig. 3). In this case, Kourganoff ([3], p. 255) shows that

$$E_2(t) = 1 - 0(t), \qquad E_3(t) = \tfrac{1}{2} - t + 0(t^2) \tag{31a}$$

where $0(t^n)$ means "terms of order n and higher". Substituting into equations (30) and (31), one sees that the contribution of the variable part of $E_2(t)$ is a second-order term in t, which can be neglected.

The physical meaning of this simplification has already been found in the preceding section: in an optically thin layer, the energy radiated by any elementary thickness of the layer is *not* absorbed by the rest of the layer. q can then be written:

$$q = 2\pi \int_{\tau}^{\tau_2} B(t)\, dt - 2\pi \int_0^{\tau} B(t)\, dt - 2\pi\epsilon_0\, B(0)\, (\tfrac{1}{2} - \tau) - 2\pi r_0 \int_0^{\tau_2} B(t)\, dt$$

and since $r_0 = 1 - \epsilon_0$ (opaque wall),

$$q = 2\pi\epsilon_0 \int_0^{\tau_2} B(t)\, dt - \pi\epsilon_0\, B(0) - 4\pi \int_0^{\tau} B(t)\, dt + 2\pi\epsilon_0\, B(0)\tau$$

† Once the distribution $T(\tau)$ is established, $T(y)$ is easily obtained through the relation $d\tau = \rho\kappa\, dy$.

or:

$$q = 2\pi\epsilon_0 B(0)\tau - 4\pi\int_0^\tau B(t)\,dt + \text{constant}$$

After substitution into equation (31), the energy transfer equation is:

$$k\frac{\partial T}{\partial y} + 2\pi\epsilon_0 B(0)\,\tau - 4\pi\int_0^\tau B(t)\,dt = C \qquad (32)$$

where C is a constant. It is left now to determine the profile $T(y)$ which satisfies this question. It can be further simplified if the optical parameters are used:

$$dB = \frac{1}{\pi}\,4\sigma T^3\,dT \qquad (33)$$

$$d\tau = \rho\kappa dy$$

After substitution in (33):

$$A(B)\frac{dB}{d\tau} - 4\pi\int_0^\tau B(t)dt + 2\pi\epsilon_0 B(0)\tau = C \qquad (34)$$

where $A = k\pi(\rho\kappa/4\sigma T^3)$, hence a function of B through T.

This equation is of a non-linear integro-differential type for which no closed solution is available. Furthermore, in the case of most chemically-active gases such as high-temperature air, there is no closed formulation for either k, κ or ρ since the latter, at constant pressure, is a function of the compressibility Z. Both k and Z are tabulated for high-temperature air in [12]. For these two reasons, the solution of equation (34) is only possible by iteration, like most other problems of radiative transfer.

This iteration is performed without difficulty when equation (34) is integrated and the two boundary conditions of given temperatures at the walls are used. The process will converge for physical reasons, if the temperature profile used as the first approximation is that due to conduction alone, provided the optical thickness τ_2 has a physical meaning.

It is possible to convert the "optical" solution $B(\tau)$ into a "physical" solution $T(y)$ by using the definition (33) of B and τ:

$$T = \left(\frac{B\pi}{\sigma}\right)^{1/4} \text{and } y = \int_0^\tau \frac{dt}{\rho\kappa} \qquad (35)$$

Note that the correspondence $y - \tau$ is to be established only after the temperature profile $T(\tau)$ has been established, because of the dependence of κ on temperature. This point is of special importance since only a certain class of optical lengths τ have a physical correspondence y in this problem [13].

RESULTS AND CONCLUSIONS

Two numerical cases are presented on Figs. 4 and 5 for low and high values of T_0, respectively. On each diagram is shown the profile that would be obtained without radiation (which was used as the first try in the iteration) as well as the profiles obtained including radiation for lower wall emissivities $\varepsilon_0 = 0$, $\frac{1}{2}$ and 1. The following general remarks can be made:

1. *Whenever the wall effects are small* ($\varepsilon_0 = 0$, *or* $\varepsilon_0 \neq 0$ *but* $T_0 \ll T_2$)

To insure a constant total flux of energy across the gas layer, it is necessary for the convective flux variations to be compensated by opposite variations of the radiative flux.

Now, the radiation emitted by the gas layer near both limiting planes (*no wall effects considered*), is directed towards the outside, in the upper direction near the upper wall and in the lower direction near the lower wall. It is then expected that this radiative flux reversal across the layer will be compensated by an increased convective flux near the hot wall and by a decreased one near the cool wall. This is illustrated in Figs. 4 and 5 for the case $\epsilon_0 = 0$ (no wall effects): Larger temperature gradients are introduced by radiation near the hot wall (as compared to the purely conductive case) while smaller temperature gradients are found near the cool wall. *Convection to a cool wall is therefore reduced if the layer radiates.* As can be seen on Fig. 4, this conclusion also applies practically for all possible emissivities of the cool wall, because of its relatively low $B(0)$.

Although the additional radiative transfer makes for a higher total heat flux through the flow, it is therefore apparent that calculating this additional radiative flux to the cool wall by simply using the non-radiative temperature profile would lead in this case to an excessive

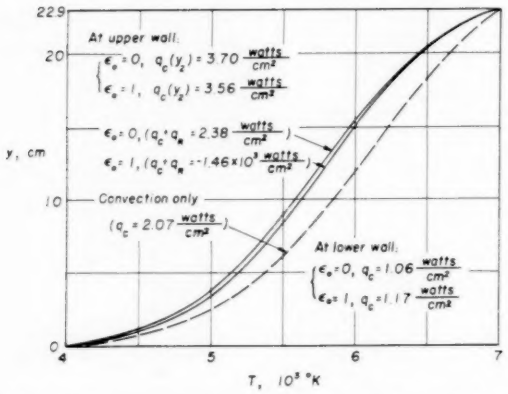

FIG. 4. Temperature profiles and fluxes of energy in air ($p = 0{\cdot}1$ atm). (Transparent upper wall, opaque lower wall.)

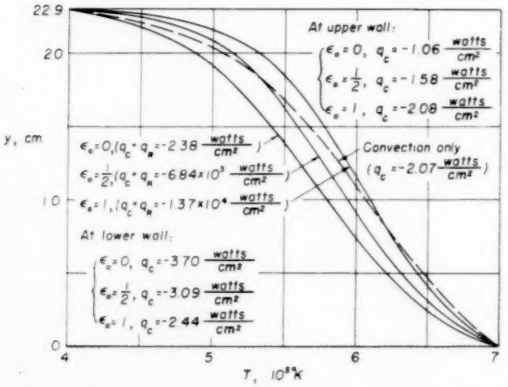
22.9
20
10
0
y, cm
At upper wall:
$\epsilon_0 = 0$, $q_c = -1.06 \frac{watts}{cm^2}$
$\epsilon_0 = \frac{1}{2}$, $q_c = -1.58 \frac{watts}{cm^2}$
$\epsilon_0 = 1$, $q_c = -2.08 \frac{watts}{cm^2}$
$\epsilon_0 = 0$, $(q_c + q_R = -2.38 \frac{watts}{cm^2})$
$\epsilon_0 = \frac{1}{2}$, $(q_c + q_R = -6.84 \times 10^3 \frac{watts}{cm^2})$
$\epsilon_0 = 1$, $(q_c + q_R = -1.37 \times 10^4 \frac{watts}{cm^2})$
Convection only
$(q_c = -2.07 \frac{watts}{cm^2})$
At lower wall:
$\epsilon_0 = 0$, $q_c = -3.70 \frac{watts}{cm^2}$
$\epsilon_0 = \frac{1}{2}$, $q_c = -3.09 \frac{watts}{cm^2}$
$\epsilon_0 = 1$, $q_c = -2.44 \frac{watts}{cm^2}$
4
5
6
7
T, 10^3 °K

FIG. 5. Temperature profiles and fluxes of energy in air ($p = 0{\cdot}1$ atm). (Transparent upper wall, opaque lower wall.)

value for both convective and radiative fluxes. If, in addition, the lower cool wall is perfectly reflective, the total heat transfer to the wall (q_c alone, in this case) is effectively reduced by the presence of radiation.

2. *Whenever the wall effects are important* ($\epsilon_0 \neq 0$ *and* $T_0 \gg T_2$)

A fraction of the energy radiated by the hot lower wall is absorbed by each gas layer $2\pi\rho\kappa\epsilon_0 B(T_0)dy$; hence, a continuous decrease of the wall flux on its path upwards on Fig. 5. This contribution can be conveniently broken down into a constant flux $\epsilon_0 B(T_0)$ across the layer, minus a flux in the downward direction

$$2\pi \int_0^\tau \epsilon_0 \, B(T_0) \, dt$$

which increases from zero at the lower wall to a maximum value at the upper wall. This arrangement is useful, because it is seen from equation (32) that only the variable part of the fluxes affects the temperature distribution.

This variable downwards flux is often larger than the variable flux due to the radiation of the gas layers themselves:

$$4\pi \int_0^\tau B(T) \, dt$$

This is especially true for the cooler layers where $\epsilon_0 B(T_0) > B(T)$ for most values of ϵ_0 and T_2; in this case, these two radiative effects, which determine alone the temperature profile in the problem, introduce a net radiative flux *downwards*. In opposition to the case where wall effects are negligible, the temperature gradients at the *cool wall* are therefore *larger* than they are without radiation (as can be seen in Fig. 5): this adjustment of the temperature profile compensates in part the net downward radiative flux at the upper cool wall by a larger upward convective flux. Another compensation comes from a reduction of the sum of these two variable fluxes as can be seen at the lower wall, where larger emissivities correspond to lower temperature gradients and convection rates than for $\epsilon_0 = 0$.

3. *In general*

An increased layer thickness will increase the role of radiation while decreasing the temperature gradient and thus the convection flux. Inversely, radiation effects will be relatively unimportant in very thin layers. The problems of the type considered here, correspond to the intermediate case where convection and radiation are of the same order of magnitude.

It is convenient to characterize these three classes of problems by writing an equation in non-dimensional form:

Vol. 1 1960

$$\frac{A(\tau_2)}{\tau_2^2}(B)\bar{A}\frac{d\bar{B}}{d\bar{\tau}} - 4\pi\int_0^{\bar{\tau}}[\bar{B}(t) - \frac{\epsilon_0}{2}\bar{B}(0)]\,dt = \text{const.} \quad (36)$$

where

$$\bar{A}(B) = \frac{A\ (B)}{A\ (\tau_2)},\ \bar{B} = \frac{B}{B\ (\tau_2)} \text{ and } \bar{\tau} = \frac{\tau}{\tau_2}$$

In equation (36), the following ratio plays a special role:

$$N_{r-c} \equiv \frac{A\ (\tau_2)}{\tau_2^2} = \left|\frac{k}{\rho\kappa y^2\ 4\sigma\ T^3}\right|_{\tau=\tau_2} \quad (37)$$

The magnitude of this non-dimensional parameter N_{r-c} (r–c for radiation–convection) determines the relative role of the convective term (the first term of equation (36)) vs. the radiative terms. For very large values of N_{r-c}, convection is the only appreciable transport process while radiation is the important process for low values of N_{r-c}.

A physical interpretation of N_{r-c} is also:

$$N_{r-c} = \frac{k\ (T_2/L)}{2\epsilon_2\sigma\ T_2^4} \quad (38)$$

In equation (38), the numerator is a typical conductive heat flux from the hot wall across the gas layer and the denominator is the radiative flux from the gas layer assumed arbitrarily at the hot-wall temperature. This parameter is of the same family as the non-dimensional quantities discussed in [7] and [9].

REFERENCES

1. S. Chandrasekhar, *Radiative Transfer*. Clarendon Press, Oxford (1950).
2. A. Unsöld, *Physik der Sternatmosphären*. Julius Springer, Berlin (1955).
3. V. Kourganoff, *Basic Methods in Transfer Problems*. Clarendon Press, Oxford (1952).
4. M. Jakob, *Heat Transfer*. John Wiley, New York (1957).
5. W. H. MacAdams, *Heat Transmission*. McGraw-Hill, New York (1957).
6. B. Kivel and K. Bailey, *Tables of Radiation from High Temperature Air*. AVCO Research Laboratory Research Report 21 (1957).
7. V. N. Adrianov and S. N. Shorin, *Izv. Akad. Nauk SSSR, otdel. tekn. nauk*, No. 5, 46 (1958).
8. Iu. P. Raizer, *Zh. eksp. teor. fiz.* **34**, No. 2, 331; translation, *Soviet Physics, JETP*, August 1958.
9. R. Goulard, *The Coupling of Radiation and Convection in Detached Shock Layers*. Bendix Products Division, Applied Sciences Laboratory, South Bend, Indiana, April 1959.
10. P. K. Konakov, S. S. Filimonov and B. A. Khrustalev, *Soviet Physics, Tech. Phys.* **2**, No. 5, 971 (1957).
11. *Blast Wave*. Los Alamos Scientific Laboratory, University of California, Los Alamos, New Mexico, LA–2000, August 47 (released March 1958).
12. F. C. Hansen, *Approximations for the Thermodynamic and Transport Properties of High Temperature Air*. NACA TN 4150.
13. R. and M. Goulard, *Energy Transfer in the Couette Flow of a Radiant and Chemically Reacting Gas*. Bendix Products Division, Applied Sciences Laboratory, South Bend, Indiana, April 1959.
14. J. O. Hirschfelder, *J. Chem. Phys.* **26**, 274 (1957).
15. W. Finkelnburg and H. Maecker, Elektrische Bogen und thermisches Plasma. *Handbuch der Physik*, Vol. XXII, Gasentladungen II, pp. 254–444. Julius Springer, Berlin (1956).
16. R. E. Meyerott, Radiation heat transfer to hypersonic vehicles, *Third AGARD Combustion and Propulsion Panel Colloquim, Palermo, Sicily*. Pergamon Press, London (1958).
17. E. R. G. Eckert and R. M. Drake, Jr., *Heat and Mass Transfer*. McGraw-Hill, New York (1959).

Int. J. Heat Mass Transfer. Vol. 1, pp. 92–101. Pergamon Press 1960. Printed in Great Britain.

WÄRMETRANSPORT DURCH NATÜRLICHE KONVEKTION IN STOFFEN BEI KRITISCHEM ZUSTAND

E. SCHMIDT
Technische Hochschule München, Germany

(*Received* 9 *January* 1960)

Zusammenfassung—Durch Versuche mit Ammoniak und mit Kohlensäure in senkrechten, unten beheizten und oben gekühlten Rohren wird gezeigt, dass bei Annäherung des Rohrinhaltes an seinen kritischen Zustand (132,4°C und 115,2 at. für NH_3 und 31°C und 75,2 at. für CO_2) ausserordentlich hohe Wärmetransportleistungen durch natürliche Konvektion, d.h. allein durch die Wirkung von Auftriebskräften erzielt werden. Im mittleren Stück eines solchen mit der Flüssigkeit im kritischen Zustand gefüllten Rohres führt die Flüssigkeit die Wärme ebenso gut fort, wie wenn man an ihre Stelle einen festen Körper setzen würde mit dem mehr als 4 000-fachen Wärmeleitvermögen des Kupfers. Diese Erscheinung ist zu erklären durch das starke Anwachsen der spezifische Wärme und des thermischen Ausdehnungskoeffizienten im kritischen Zustandsgebiet bis zum Wert unendlich im kritischen Punkt selbst. Nach Überschreiten der kritischen Temperatur fällt die Wärmetransportleistung des Mediums sehr schnell wieder ab.

Abstract—Experiments with ammonia and with carbon dioxide in vertical tubes heated at the lower and cooled at the upper end, show that near the critical point of the fluid (132·4°C and 115·2 at.* for NH_3 and 31°C and 75·2 at. for CO_2) extremely high heat transportation is achieved by natural convection, i.e. only by the effect of gravitational buoyancy. In the mean part of such a tube filled with a liquid at its critical state the transportation of heat nears that of a solid rod of the same outer diameter as the liquid and having a heat conductivity up to 4,000-fold that of solid copper. This phenomenon is due to the increase of the specific heat and of the coefficient of thermal expansion near the critical state up to infinity at this very point.

At temperatures above the critical value the heat transportation rapidly falls down again.

Résumé—Des expériences, effectuées avec de l'ammoniac et du gaz carbonique dans des tubes verticaux chauffés dans le bas et refroidis dans le haut, ont montré qu'au voisinage du point critique du fluide (132,4°C et 115,2 atmosphéres pour NH_3 et 31°C et 75 atmosphères pour CO_2) une transmission de chaleur très élevée se produit par convection naturelle, par le seul effet de la force ascensionnelle de gravitation. Dans la plus grande partie d'un tel tube, rempli d'u liquide à l'état critique, la transmission de chaleur est voisine de celle d'une barre solide de même diamètre que le tube et qui possèderait une conductivité 4000 fois plus grande que celle du cuivre. Ce phénomène est dû à l'augmentation de la chaleur spécifique et du coefficient de dilatation, jusqu'a des valeurs infinies au voisinage du point critique.

A des températures inférieures aux valeurs critiques, la transmission de chaleur s'abaisse très rapidement.

Abstract—Эксперименты с аммиаком и двуокисью углерода в вертикальных трубах, нагреваемых внизу и охлаждаемых вверху, показывают, что вблизи критической точки газа (132,4° С и 115,2атм для NH_3, и 31° С и 75,2атм для CO_2) перенос тепла путём естественной конвекции становится чрезвычайно большим. В средней части такой трубы с жидкостью, находящейся в критическом состоянии, перенос тепла близок к теплопереносу в случае твёрдого стержня, наружний диаметр которого равен диаметру трубы, а теплопроводность достигает 4000-кратной теплопроводности твёрдой меди. Этот эффект обязан возрастанию вблизи критического состояния удельной теплоёмкости и коэффициента теплового расширения, достигающих в самой критической точке бесконечности.

При температурах выше критической перенос тепла снова быстро уменьшается.

* Als Druckeinkeit ist die technische Atmosphäre (at.) benutzt. Für die Umrechnung auf andere Einheiten gilt: 1 at. = 0,980665 bar = 14,2234 Lb/in²

Vol. 1 1960

1. EINLEITUNG

Um aus einem gegebenen Raum möglichst grosse Wärmemengen herauszuholen, verwendet man in der Regel verdampfende Flüssigkeiten, die bei konstanter Temperatur den hohen Betrag der Verdampfungswärme aufnehmen. Dabei tritt eine starke Volumenzunahme auf und es entsteht ein brodelndes inhomogenes Gemisch von Flüssigkeit und Dampf, aus dem der als Transportmittel von Wärme dienende Dampf erst abgetrennt werden muss, bevor man ihn fortleiten kann. Die wichtigste Einrichtung dieser Art ist der Dampfkessel von Kraftwerken, der in den letzten Jahrzehnten für immer höhere Drücke und Temperaturen bis über den kritischen Druck des Wassers entwickelt wurde.

Im kritischen Zustand haben Dampf und Flüssigkeit gleiche Dichte, es verschwindet die unstetige Volumenzunahme und aus dem unbequem zu handhabenden Zwischenphasengemisch wird wieder eine homogene Flüssigkeit.

Bei Annäherung an den kritischen Zustand geht aber die Verdampfungswärme gegen Null. Trotzdem bleibt die Flüssigkeit ein Wärmetransportmittel von bemerkenswerten Eigenschaften, denn am kritischen Punkt wird die spezifische Wärme unendlich und in seiner Nähe hat sie Werte, die um ein Vielfaches grösser sind als die der Flüssigkeit bei niederen Drücken. Die als Verdampfungswärme auf eine bestimmte Temperatur konzentrierte Wärmekapazität wird in der Nähe der kritischen Temperatur sozusagen auf einen endlichen Temperaturbereich ausgebreitet. Entsprechend der Temperaturzunahme nimmt auch die Zähigkeit der Flüssigkeit stark ab und erreicht bei der kritischen Temperatur den kleinsten für eine Flüssigkeit möglichen Wert, was sich in einer Verminderung der Strömungswiderstände beim Fortleiten der Flüssigkeit auswirkt.

Ein weiteres für den Wärmetransport wichtiges Phänomen ist das Unendlichwerden des thermischen Ausdehnungskoeffizienten bei konstantem Druck am kritischen Punkt und das Auftreten sehr grosser Werte dieser Grösse in seiner Nähe.

Der sehr grosse Ausdehnungskoeffizient zusammen mit der kleinen Zähigkeit und dem hohen Wert der spezifischen Wärme begünstigen in besonderen Maße den Wärmetransport durch natürliche Konvektion, dessen treibende Kraft der Auftrieb der wärmeren und dadurch spezifisch leichter gewordenen Flüssigkeitsteile im Schwerefelde ist.

Die ersten Versuche, welche diese hohen Wärmetransportleistungen von Flüssigkeiten im kritischen Zustand zeigten, wurden vom Verfasser und seinen Mitarbeitern [1] im Jahre 1939 veröffentlicht. Dabei wurde von zwei senkrechten Rohren, die unten und oben durch halbkreisförmige Rohrbogen zu einem geschlossenen mit Flüssigkeit gefüllten Kanal verbunden waren, das eine geheizt, das andere gekühlt, sodass der Auftrieb der wärmeren Flüssigkeit im Schwerefelde eine Umlaufströmung hervorrief.

Noch um ein hohes Vielfaches grösser kann der Auftrieb unter dem Einfluss von Fliehkraftfeldern werden, wie sie in rotierenden Maschinen vorkommen mit bis zu mehr als dem 30 000-fachen der Schwerebeschleunigung.

Im folgenden werden Versuchsergebnisse mitgeteilt über den Wärmetransport durch natürliche Konvektion in vertikal stehenden unten beheizten und oben gekühlten Rohren, die mit einem flüssigen Medium in der Nähe seines kritischen Zustandes gefüllt sind.

2. THEORETISCHE GRUNDLAGEN

Der Wärmeübergangskoeffizient bei natürlicher Konvektion hängt, wie die Ähnlichkeitstheorie der Wärmeübertragung lehrt, wesentlich ab von der dimensionslosen Grashof–Zahl:

$$Gr = \frac{d^3 g \beta \theta}{\nu^2} \tag{1}$$

wobei

- d eine kennzeichnende Längenabmessung (m);
- g die Beschleunigung des Schwere- oder Fliehkraftfeldes (m/sec²);
- β der thermische Ausdehnungskoeffizient (1/grd);
- θ eine kennzeichnende Temperatur differenz (grd);
- $\nu = \eta/\rho$ die kinematische Viskosität (m²/sec);
- η die dynamische Viskosität (kg/m sec);
- ρ die Dichte der Flüssigkeit (kg/m³) ist.

Ausserdem spielt noch die dimensionlose Prandtl–Zahl:

$$Pr = \frac{\nu}{a} = \frac{\eta c_p}{\lambda} \tag{2}$$

eine Rolle, die eine Stoffeigenschaft ist, wobei

$a = \lambda/c_p\rho$ die Temperaturleitfähigkeit (m^2/h);
λ das Wärmeleitvermögen (kcal/m h grd);
c_p die spezifische. Wärme bei konstantem Druck bedeutet.

Benutzt man als dimensionslosen Wärmeübergangskoeffizienten die Nusselt–Zahl:

$$Nu = \frac{\alpha d}{\lambda} \tag{3}$$

wobei α der Wärmeübergangskoeffizient (kcal/m h grd) ist, so gilt für eine bestimmte Körperform mit der kennzeichnenden Längenabmessung d die Beziehung:

$$Nu = f(Gr, Pr) \tag{4}$$

in der die Funktion f in der Regel durch Versuche ermittelt werden muss. Die Prandtl–Zahl $Pr = \nu/a = \eta c_p/\lambda$ kann in der Nähe des kritischen Zustandes sehr grosse Werte annehmen, da c_p im kritischen Punkt unendlich gross ist. Auch kann sich die Grashof–Zahl sehr stark ändern, da die kennzeichnende Längenabmessung d mit der dritten Potenz eingeht, der Ausdehnungskoeffizient in der Nähe des kritischen Zustandes sehr grosse Werte annimmt und in Fliehkraftfeldern sehr hohe Vielfache der Schwerebeschleunigung vorkommen können.

Als kennzeichnende Längenabmessung wollen wir bei Rohren den lichten Durchmesser wählen, dann geht für Rohre verschiedener Länge l als weitere Veränderliche noch das Verhältnis l/d in Gleichung (4) ein und sie ist:

$$Nu = f(Gr, Pr, l/d) \tag{4a}$$

als Funktion dreier Veränderlicher zu schreiben. Für $l \gg d$ wird die Abhängigkeit von l/d vermutlich verschwinden.

In dem mit Flüssigkeit gefüllten senkrecht stehendem Rohr vollzieht sich der Wärmetransport in der Weise, dass am unteren Ende erwärmte Flüssigkeitsteile sich nach oben bewegen und dafür andere am oberen Ende gekühlte Teile herabsinken, wobei die Bewegung je nach der Grösse der Grashof–Zahl laminar oder turbulent sein wird. Da die hin und her bewegten Mengenströme und ihre Temperaturverhältnisse nicht direkt gemessen werden können und da die Gleichungen (4) und (4a) sich auf die Stellen beziehen, wo die Wärme an einer festen Oberfläche mit dem flüssigen Medium ausgetauscht wird, wollen wir im folgenden nur den Wärmetransport durch Leitung und Konvektion in dem mittleren, weder beheizten noch gekühlten Rohrstück untersuchen. Diese Wärmetransportleistung sei durch eine gleichwertige, den konvektiven Wärmetransport mit umfassende Wärmeleitfähigkeit λ_k ausgedrückt, d.h. λ_k ist die Wärmeleitfähigkeit, die ein fester, den Raum des flüssigen Mediums einnehmender Körper haben müsste, um bei demselben Temperaturgefälle ebensoviel Wärme durch Leitung zu befördern als das flüssige Medium durch Leitung und durch Konvektion transportiert. Die gleichwertige Wärmeleitfähigkeit kann man dimensionlos machen, indem man sie durch die Wärmeleitfähigkeit der ruhenden Flüssigkeit dividiert. Da das auf sehr grosse Zahlen führt, ist es anschaulicher, die gleichwertige Wärmeleitfähigkeit als Vielfaches der Wärmeleitfähigkeit des Kupfers anzugeben, die als konstanter Wert von

$$\lambda_{Cu} = 300 \text{ kcal/m h grd} = 1256{,}04 \text{ kJ/m h grd}$$
$$= 348{,}91 \text{ W/m grd}$$

angenommen sei.

Diese dimensionslose Grösse $\Lambda = \lambda_k/\lambda_{Cu}$ lässt sich in Analogie zu Gleichung (4a) durch eine Funktion ϕ von der Form

$$\Lambda = \lambda_k/\lambda_{Cu} = \phi(Gr, Pr, l/d) \tag{5}$$

darstellen.

3. VERSUCHE MIT AMMONIAK

Zur Untersuchung des konvektiven Wärmetransportes durch natürliche Konvektion in der Nähe des kritischen Zustandes wurde zusammen mit F. MAYINGER eine erste Versuchsreihe mit Ammoniak als flüssiges Medium in einem Stahlrohr von 40 mm innerem Durchmesser, 56 mm äusserem Durchmesser und 445 mm Länge des

Vol. 1 1960

inneren Hohlraumes also mit $l/d = 11{,}1$ ausgeführt. Am linken Rande von Abb. 1 ist dieses Rohr maßstäblich dargestellt. Um das untere Ende des Rohres ist eine elektrische Widerstandsheizung in Form eines Chromnickelbandes gewickelt und ein zweites Heizelement ähnlicher Art ist in den Hohlraum des Rohres hineingebaut. Am oberen Ende ist das Rohr an einen massiven Stahlzylinder angeschweisst, der durch Wasser gekühlt wird. Dazu wird auf das konisch zugespitzte Oberteil des Stahlzylinders, wie in der Abbildung angedeutet, ein Wasserstrahl gespritzt, wobei Wärmeübergangszahlen von mehr als 50 000 kcal/m² h grd erreicht werden.

Der Hohlraum des Rohres ist mit Ammoniak in solcher Menge gefüllt, dass es bei der kritischen Temperatur von 132,4 °C den Hohlraum möglichst ganz ausfüllt, wobei der kritische Druck von 115,2 at. entsteht. Bei normaler Zimmertemperatur von 20 °C wird dann nur das untere Drittel des Hohlraumes von Flüssigkeit eingenommen, die oberen zwei Drittel enthalten gesättigten Dampf. Bei unterkritischen Temperaturen verdampft die Flüssigkeit, der Dampf kondensiert am oberen Teil der Rohrwand und fliesst zur Flüssigkeit zurück.

Der Wärmefluss, den das Rohr und seine Füllung von unten nach oben befördert, wird aus der sekundlichen Kühlwassermenge und deren Temperaturzunahme ermittelt. Eine zweite Möglichkeit bietet die Messung der elektrischen Heizleistung, wobei sich wegen der Wärmeverluste von Rohr und Heizkörper etwas grössere Werte ergeben. Diese Wärmeverluste betrugen 3–8% der elektrischen Heizleistung, sie schwankten, weil der Wärmeschutz öfters abgenommen und erneuert wurde und deshalb in seiner Wirkung nicht immer gleich war.

Um die Temperaturverteilung längs des Rohres zu messen, sind Thermoelemente aus Manganin- und Konstantandraht an den in Abb. 1 angegebenen vier Stellen auf die Rohrlänge verteilt. Dabei sind an jeder Stelle zwei Thermoelemente auf dem Rohr einander gegenüberliegend angeordnet, deren Ablesungen gemittelt wurden. Die so gemessenen Temperaturen sind für verschiedene Mitteltemperaturen von etwa 68, 92, 101, 122 °C und schliesslich für die kritische Temperatur von 132,4 °C nach rechts aufgetragen und durch Kurven verbunden, welche die Temperaturverteilung längs des Rohres darstellen. In dem mittleren für die Auswertung benutzten Rohrstück AB von 25 cm Länge sind die Temperaturgradienten so klein, dass sie in der Zeichnung nicht erkennbar sind und aus den Messwerten unmittelbar entnommen werden müssen. Bei den kleinen Wärmeverlusten und der grossen Wärmeübergangszahl zwischen Flüssigkeit und innerer Rohrwand ist die Temperatur des Rohres zugleich die mittlere Temperatur der Flüssigkeit in dem entsprechenden Rohrquerschnitt.

Dicht vor dem oberen Rohrende biegen, wie die Abbildung zeigt, die Temperaturkurven um, weil die freie Konvektion gegen die Stirnwand des Hohlraumes hin auf Null zurückgeht und deshalb die Wärmeleitfähigkeit der Rohrwand nicht mehr klein gegen die wirksame Wärmeleitfähigkeit der Flüssigkeit ist. Die Rohrwand übernimmt dann einen merklichen Teil des Wärmestromes, was in ihr ein Temperaturgefälle hervorruft.

Aus dem Wärmestrom, dem mittleren Temperaturgradienten längs der Rohrstrecke AB und dem inneren Querschnitt des Rohres erhalten wir die wirksame, den Wärmetransport durch natürliche Konvektion einschliessende Wärmeleitfähigkeit λ_k des Rohrinhaltes. Die aus den Kurven der Abb. 1 und aus weiteren Versuchen mit anderen Mitteltemperaturen erhaltenen Werte von λ_k sind in Abb. 2 als ausgefüllte Kreise eingetragen und durch die ausgezogene Kurve λ_{k1} verbunden. Die zugehörige Wärmestromdichte in Watt je cm² der Rohrfüllung ist durch die ausgezogene Kurve q_1 angegeben. Die mit λ_{k2} bezeichnete gestrichelte Kurve gilt für einen Versuch gleicher Art aber bei doppelt so grosser Heizleistung, die durch die gestrichelte Gerade q_2 dargestellt ist. In beiden Fällen wächst die Wärmestromdichte mit steigender Temperatur, da bei ungefähr konstant bleibender Temperatur des Kühlmittels, höhere Mitteltemperatur des Rohrinhalts nur durch Vergrössern der Heizleistung zu erreichen ist. Die nicht unerhebliche Streuung der Versuchswerte ist auf die geringe Grösse von weniger als 1 °C des Unterschiedes der Temperaturen der Punkte A und B zurückzuführen.

Am Randmaßstab links erkennt man bei unterkritischen Temperaturen von 80 bis 120 °C,

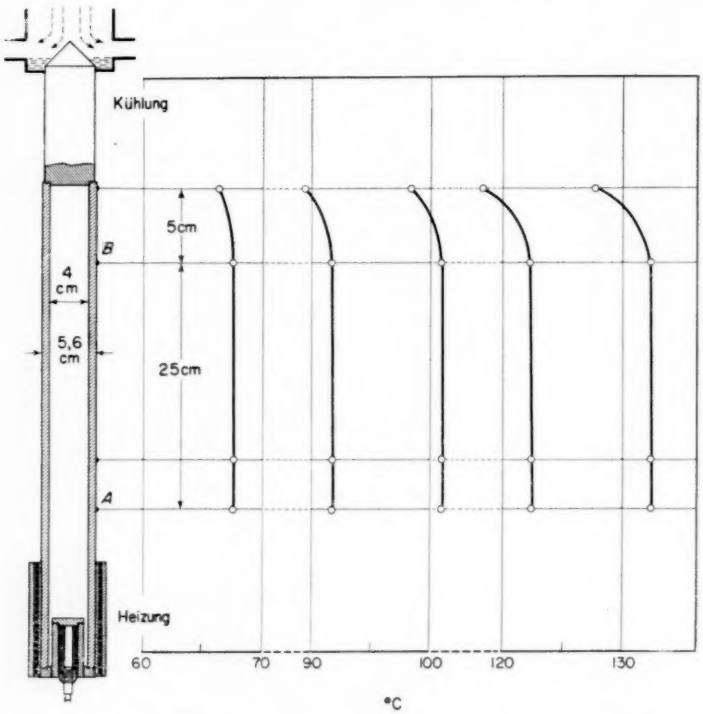

ABB. 1. Temperaturverteilung längs eines senkrechten unten geheizten und oben gekühlten Rohres von 4 cm lichter Weite, das mit Ammoniak von dem kritischen Zustand entsprechender Menge gefüllt ist, bei verschiedenen mittleren Temperaturen des Inhalts.

dass durch Verdampfen und Wiederkondensieren und damit verbundenes Hochwerfen der nur den unteren Teil des Hohlraumes einnehmenden Flüssigkeit sehr hohe wirksame Wärmeleitfähigkeiten des Mediums von etwa $7 \cdot 10^4$ kcal/m hr grd auftreten; das ist, wie die zweite Ordinatenskala zeigt, mehr als das 200-fache des Wärmeleitvermögens von Kupfer. Mit der Annäherung der mittleren Temperatur der Flüssigkeit an den kritischen Zustand wächst die wirksame Wärmeleitfähigkeit in einer steilen Spitze auf mehr als das 800-fache der Wärmeleitfähigkeit von Kupfer. Die zweite mit $\lambda_{k,2}$ bezeichnete Kurve ist durch die als leere Kreise eingetragenen Messpunkte einer Versuchsreihe mit etwa doppelt so grosser Wärmestromdichte q_2 gelegt. Abgesehen von den etwa um den Faktor 1,4 bis 1,8 grössenen Werten im Zweiphasenbereich bei unterkritischer Temperatur zeigen beide Kurven denselben Verlauf mit der gleichen steilen Spitze bei der kritischen Temperatur des Ammoniaks. Bei überkritischen Temperaturen sinkt das Wärmeleitvermögen steil ab auf erheblich kleinere Werte als im Zweiphasenbereich, weil hier kein Verdampfen mehr stattfinden kann.

Um den Einfluss einer Änderung des Rohrdurchmessers zu untersuchen, wurde eine zweite Apparatur gebaut mit einem Rohr von 2 cm lichter Weite und 3,8 cm äusserem Durchmesser, bei 34 cm Länge des Hohlraumes. Am linken Rande von Abb. 3 ist dieses Rohr maßstabgerecht dargestellt und ebenso wie in Abb. 1 sind in Abb. 3 die Kurven des Temperaturverlaufes längs des Rohres für Mitteltemperaturen der Meßstrecke von etwa 69, 101 und 132°C wiedergegeben. Ausserdem ist noch eine Kurve des überkritischen Gebietes von

Vol. 1 1960

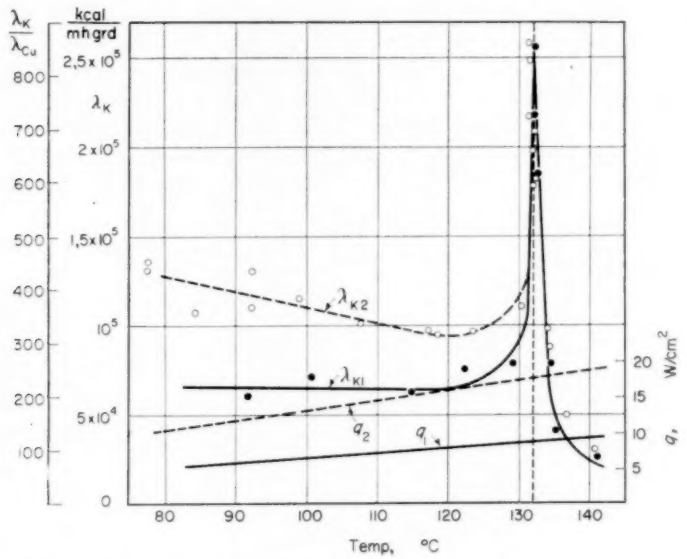

ABB. 2. Wirksame Wärmeleitfähigkeit λ_k eines mit Ammoniak von kritischer Menge gefüllten Rohres von 4 cm lichter Weite in Abhängigkeit von der mittleren Rohrtemperatur.

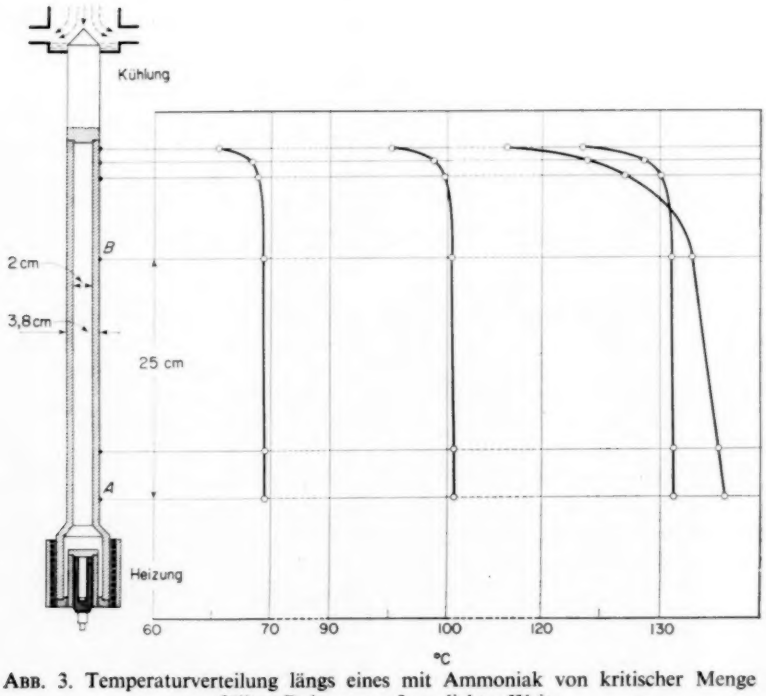

ABB. 3. Temperaturverteilung längs eines mit Ammoniak von kritischer Menge gefüllten Rohres von 2 cm lichter Weite.

erheblich geringerer Steigung eingetragen, bei der die Temperatur im Messbereich von 133 auf 136°C ansteigt.

Das Ergebnis der Auswertung dieser Kurven und weiterer Messreihen sind in Abb. 4 wiedergegeben. Der Verlauf von λ_k ist ähnlich dem Verlauf der λ_{k2}—Kurve in Abb. 2, nur sind die

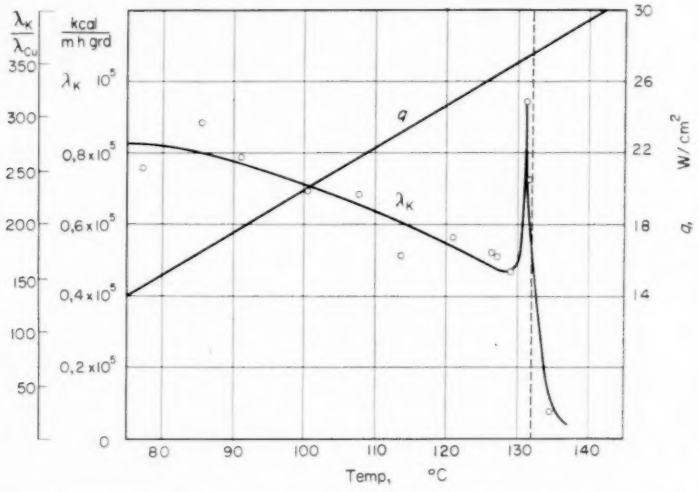

ABB. 4. Wirksame Wärmeleitfähigkeit λ_k des Inhaltes eines mit Ammoniak von kritischer Menge gefüllten Rohres von 2 cm lichter Weite in Abhängigkeit von der mittleren Rohrtemperatur.

Werte von λ_k etwa 40% niedriger, obwohl die Wärmestromdichte, wie die mit q bezeichnete Kurve zeigt, um rund 50% grösser ist. Das spitze Maximum ist weniger hoch als bei dem Rohr von 40 mm lichter Weite und tritt schon etwas unterhalb der kritischen Temperatur ein. Diese Unterschiede sind vermutlich dadurch verursacht, dass sich in dem Rohr um 0,2 g mehr Ammoniak befand als die dem Rohrvolumen entsprechende kritische Menge von 46,0 g, was nach Abschluss der Versuche festgestellt wurde.

In jedem Falle ist die Grashof–Zahl unter sonst gleichen Verhältnissen bei dem 2 cm Rohr um den Faktor $2^3 = 8$ kleiner als bei dem Rohr von 4 cm lichter Weite. Leider lässt sich der Zahlenwert von *Gr* nicht genau angeben, da der Ausdehnungskoeffizient in der Nähe des kritischen Punktes sehr grosse Werte erreicht bis zum Wert unendlich, und es an genügend genauen Versuchswerten in diesem Zustandsgebiet fehlt. Ausserdem kann man einen gewünschten Zustand in grosser Nähe des kritischen Punktes wegen der experimentellen Schwierigkeiten nur mit beschränkter Genauigkeit einstellen. Die relativ hohen Wärmetransportleistungen schon bei unterkritischen Temperaturen sind darauf zurückzuführen, dass der Inhalt des Rohres sich in zwei Phasen trennt, wovon die Flüssigkeit unten verdampft und der Dampf oben kondensiert. Dazu kommt, dass der aufsteigende Dampf Flüssigkeit mitreisst, die abgekühlt zurückfliesst, wodurch zusätzliche Wärme befördert wird.

4. VERSUCHE MIT KOHLENSÄURE

Um zu zeigen, dass die bei Ammoniak in der Nähe seines kritischen Zustandes beobachteten Erscheinungen nicht etwa individuelle Eigenschaften dieses Stoffes sind, wurden zusammen mit E. HAHNE auch Versuche mit Kohlensäure durchgeführt, deren kritischer Zustand bei 31°C und 75,2 at. liegt. Dafür bauten wir die in Abb. 5 dargestellte Apparatur, bestehend aus einem Rohr *a* von 40 mm lichter Weite bei 60 mm Aussendurchmesser und 2 m Länge. Von dem Rohr sind die unteren 200 mm mit einer elektrischen Heizwicklung *b* versehen, am oberen Ende wird das Rohr von einem ebenfalls 200 mm hohen Kühlmantel *c* umgeben.

Vol. 1 1960

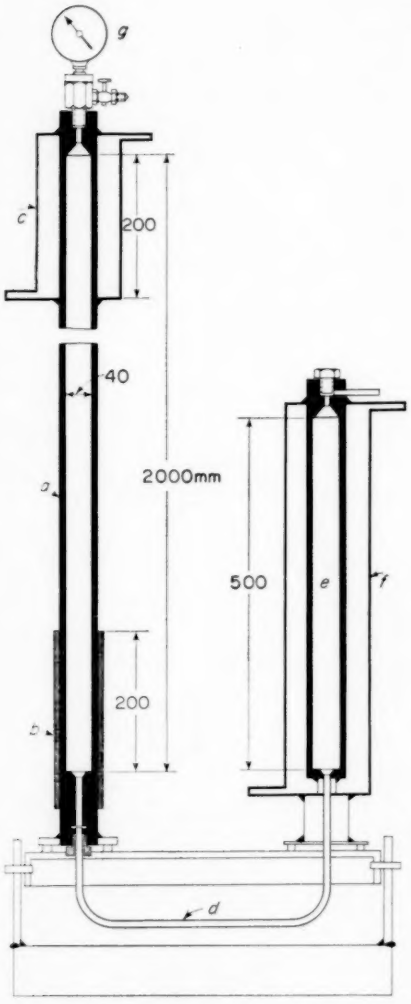

ABB. 5. Versuchsanordnung zur Messung des Wärmetransportes durch Kohlensäure nahe ihrem kritischen Zustand im senkrechten Rohr: *a* Versuchsrohr mit Kohlensäurefüllung; *b* elektrische Heizwicklung; *c* Wasserkühlung; *d* Verbindungsrohr; *e* Ausgleichsbehälter mit Kohlensäurefüllung; *f* Wassermantel mit regelbarer Temperatur; *g* Manometer.

Um bei unterkritischen Temperaturen die Entstehung zweier Phasen zu vermeiden, ist das Versuchsrohr durch das dünne Verbindungsrohr *d* mit einem ebenfalls mit flüssiger Kohlensäure gefüllten Ausgleichsbehälter *e* verbunden, der mit Hilfe des Wassermantels *f* beliebiger durch einen Thermostaten geregelter Temperatur gehalten werden kann. Durch entsprechendes Einregeln des Thermostaten kann man Kohlensäure aus dem Ausgleichsbehälter in das Versuchsrohr drücken, so dass dieses auch bei unterkritischen Temperaturen stets ganz mit Flüssigkeit gefüllt bleibt und die Trennung in eine flüssige und eine dampfförmige Phase mit dem Wärmetransport durch Verdampfen und Kondensieren vermieden wird.

Das Rohr ist, wie Abb. 6 zeigt, mit Thermoelementen versehen, die den Temperaturverlauf längs des Rohres zu messen erlauben. Dabei waren an jedem Messquerschmitt vier Thermoelemente auf den Rohrumfang verteilt angebracht, deren Angaben gemittelt wurden. Als Meßstrecke wird das mittlere Stück *AB* des Rohres von 750 mm Länge betrachtet. Die gemessenen Temperaturen sind als Abszisse aufgetragen und liefern die Kurven des Temperaturverlaufs längs des Rohres, die als geknickte Linienzüge eingetragen und mit den Buchstaben *a* bis *g* bezeichnet sind. Bei der Ablesung der Temperaturen ist zu beachten, dass der Bereich von 29,5 bis 31,5°C in fünfmal grösserem Maßstab aufgetragen ist als die Temperaturen unterhalb 29,5°C und oberhalb 31,5°C. Die Zahlen am unteren Ende jedes Linienzuges geben die Wärmeleistung des jeweiligen Versuches in Watt, ermittelt aus dem vom Kühlwasser abgeführten Wärmestrom. Die Wärmeleistung der Kurven ist von der gleichen Grössenordnung, nur die Kurve g wurde bei einer um den Faktor 4 kleineren Leistung aufgenommen.

Ermittelt man in gleicher Weise wie bei den Versuchen mit Ammoniak die wirksame Wärmeleitfähigkeit λ_k der Flüssigkeit und trägt sie über der mittleren Temperatur der Versuchsstrecke auf, so erhält man die Kurve der Abb. 7. Dabei sind die Punkte *a–g* aus der mittleren Neigung im Messbereich *AB* der mit denselben Buchstaben bezeichneten Kurven der Abb. 6 bestimmt.

Anders als bei den Kurven der Abbildungen 2–4 steigt hier die Wärmeleitfähigkeit im unterkritischen Bereich mit der Temperatur monoton an, weil keine 2 Phasen vorhanden sind und ein Wärmetransport durch Verdampfen und Kondensieren nicht stattfindet. Der steile Anstieg

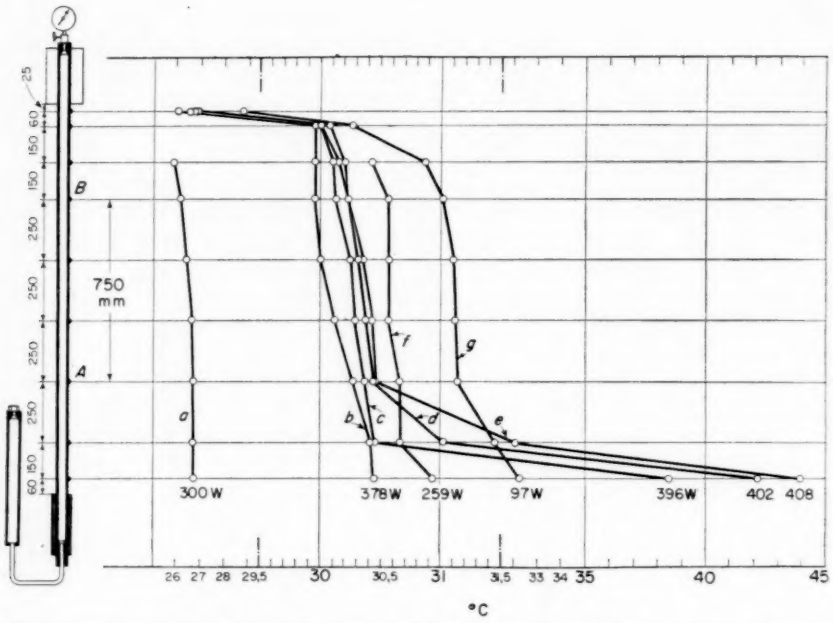

ABB. 6. Temperaturverteilungen längs des mit Kohlensäure in kritischer Menge gefüllten Rohres bei verschiedenen mittleren Temperaturen des Inhaltes.

Vol. 1 1960

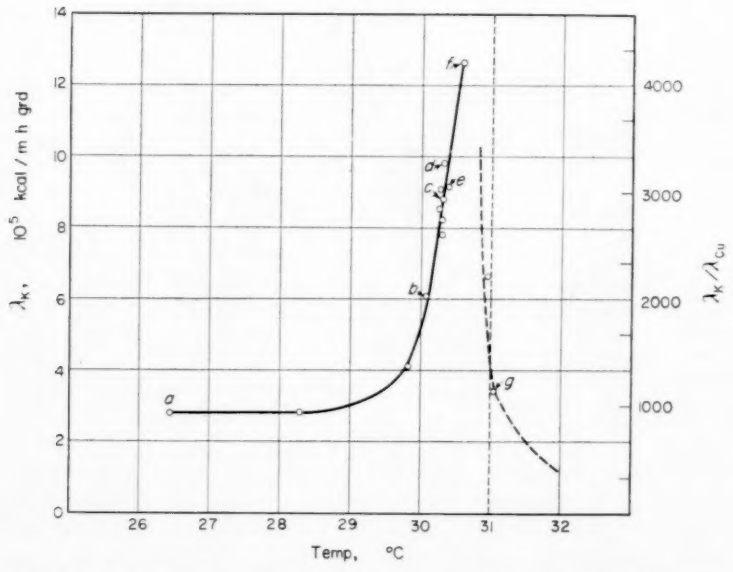

ABB. 7. Wirksame Wärmeleitfähigkeit λ_k des Inhaltes eines mit Kohlensäure von kritischer Menge gefüllten Rohres von 4 cm lichter Weite und 2 m Länge.

von λ_k mit Annäherung an die kritische Temperatur ist hier noch ausgeprägter als bei den Versuchen mit Ammoniak in kleineren Rohren und führt im Punkt F zu dem mehr als 4 000-fachen Wärmeleitvermögen von Kupfer, wie die Skala λ_k/λ_{Cu} der Ordinatenachse angibt. Das Maximum scheint aber noch nicht erreicht zu sein, da ebenso wie bei Abb. 4 offenbar etwas mehr Kohlendioxyd im Rohr war als der kritischen Dichte entspricht. Bei überkritischen Temperaturen sinkt die Wärmetransportleistung wieder rasch auf bescheidene Werte.

Die Genauigkeit dieser Angaben darf aber nicht zu hoch eingeschätzt werden, denn die Temperaturdifferenzen am Rohr, auf die sie sich stützt, sind nur von der Grössenordnung $\frac{1}{10}$°C. Zweifellos sind aber die Werte um ein Vielfaches grösser als bei den Versuchen mit Ammoniak, was aber wahrscheinlich nicht auf die Verschiendenheit der stofflichen Eigenschaften von Ammoniak und Kohlensäure zurückzuführen ist, vielleicht ist die grössere Rohrlänge von Einfluss. In der Hauptsache wird der Unterschued aber wohl dadurch hervorgerufen, dass bei dem längeren Rohr die Meßstrecke weiter von den geheizten und gekühlten Rohrenden entfernt war als bei den kürzeren Rohren der Ammoniakversuche. Hätte man hier die Meßstrecke nach oben oder unten verlängert, so wäre man in Gebiete grösserer Temperaturgradienten hineingekommen und hätte wesentlich kleinere Werte von λ_k erhalten.

LITERATUR

1. E. SCHMIDT, E. ECKERT und U. GRIGULL, *Jahrbuch der Deutschen Luftfahrtforschung* Bd. II, S. 53/58. (1939) AAF Translation Nr. 527, Air Material Command, Wright Field, Dayton, Ohio.

Int. J. Heat Mass Transfer. Vol. 1, pp. 102–112. Pergamon Press 1960. Printed in Great Britain.

HEAT TRANSFER BIBLIOGRAPHY*

E. R. G. ECKERT, J. P. HARTNETT and T. F. IRVINE, JR.
Department of Mechanical Engineering, Institute of Technology,
University of Minnesota, Minneapolis 14, Minnesota, U.S.A.

APPLICATIONS

R. ALAMI and P. AGERON, *Extraction and Utilization of Heat from Nuclear Reactors* (*Evacuation et Recuperation de la Chaleur des Reacteurs Nucleaires*), Vol. 3. Paris, Dunod (1958).

M. A. BASIN, R. H. MACNEAL and J. H. SHIELDS, Direct-analog method of analysis of influence of aerodynamic heating on static characteristics of thin wings. *J. Aero. Space Sci.* **26,** No. 3, 145 (1959).

J. A. CYPHERS, R. D. CESS and E. V. SOMERS, Heat transfer character of wire-and-tube heat exchangers. *Amer. Soc. Heat. Refrig. Air Cond. Engrs. J.* **1,** 86 (1959).

N. F. DOW, Heat protection for re-entry vehicles. *Astronautics* **4,** No. 3, 28, 82, 84 and 86 (1959).

G. M. DUSINBERRE, Calculation of transients in a cross-flow heat exchanger, *J. Heat Transfer* **1,** 61 (1959).

A. J. EGGERS, JR., *A Discussion on Methods for Reducing Aerodynamic Heating in Supersonic Flight.* NACA RM A55F21a (1955).

A. J. EGGERS, JR., *A Method for Simulating the Atmospheric Entry of Long-range Ballistic Missiles.* NACA Report 1378; supersedes NACA RM A55I15 (1958).

H. HAUSENBLAS, The mean temperature difference in hairpin heat exchangers, *Brennst.-Wärmekr.* **11,** 114 (1959).

W. M. KAYS and A. L. LONDON, *Compact Heat Exchangers—A Summary of Basic Heat Transfer and Flow Friction Design Data.* McGraw-Hill, New York (1958).

N. H. KEMP and F. R. RIDDELL, *Heat Transfer to Satellite Vehicles Re-entering the Atmosphere.* AVCO Research Laboratory, Research Report 2; formerly Research Note 21 (1956).

A. LAPIN and W. T. SCHURIG, Heat transfer coefficients for finned exchangers. *Industr. Engng. Chem.* **51,** No. 8, 941 (1959).

J. MILLS, An analogue solution of the heating of a power cable buried in the soil. *J. Instn. Engrs. Aust.* **30,** No. 3, 91 (1958).

S. E. NEICE, J. A. CARSON and B. E. CUNNINGHAM, *Experimental Investigation of the Simulation of Atmospheric Entry of Ballistic Missiles.* NACA RM A57I26 (1957).

L. V. NESINA, Calculations for heat exchange in water reservoirs. *Trud. gl. Geofiz. Observ.* No. 59 (121), 29 (1956); *Ref. Zh. Mekh.* No. 11, Rev. 12822 (1957). (In Russian).

B. OSWALD, How is DOD moving on reliability? *Missile and Rockets.* 1 June, 21 (1959).

R. G. RAGSDALE, *Heat-transfer and Friction Measurements with Variable Properties for Airflow Normal to Finned and Unfinned Tube Banks.* NASA Memo. No. 10–9–58E (1958).

T. C. REEVES, Quantitative criteria for thermal evaluation of electronic equipment. *Elect. Mfg.* **60,** 110 (1957).

T. C. REEVES, Design plan for forced air cooling. *Elect. Mfg.* **63,** No. 6, 63 and 73 (1959).

A. N. REZNIKOFF, The temperature field produced in a chip under the action of frictional forces on the front face of a tool. *J. Tech. Phys., Moscow* **3,** No. 1, 182 (1958).

N. N. RYKALIN, *Calculation of the Heat Transfer Processes in Welding* (*Berechnung der Wärmevorgänge beim Schweissen*). VEB Verlag, Technik, Berlin (1957).

H. O. SLONE and J. B. ESGAR, *Gas to Blade Heat-transfer Coefficients and Turbine Heat-rejection Rates for a Range of One-spool Cooled-turbine Engine Designs.* NACA RM E56A31 (1956).

E. W. STEPHENS, *Free-flight Investigation of Rocket-propelled Model to Determine Aerodynamic Heating on Thin, Unswept, Untapered,*

* This bibliographic material was prepared at the Heat Transfer Laboratory, University of Minnesota.

Vol. 1 1960

Multispar, Aluminum-alloy Wing at Mach Numbers up to 2·22. NASA Memo. No. 12–15–58L (1959).

A. G. SWANSON and C. B. RUMSEY, *Aerodynamic Heating of a Wing as Determined from a Free Flight Rocket-model Test to Mach Number* 3·64. NACA RM L56F11a (1956).

O. W. WITZELL, W. E. FONTAINE and W. J. PAPANEK, Convective films evaluated for wire tube heat exchangers. *Amer. Soc. Heat. Refrig. Air Cond. Engrs. J.* **1,** 35 (1959).

Storage tank heating coils for transient conditions. *Brit. Chem. Engng.* **4,** No. 4, 206 (1959).

BOOKS

Short Notes Contributed to Pressure Measurements Meeting sponsored by AGARD Wind Tunnel and Model Testing Panel. AGARD Report No. 163 (1958).

W. HRYNISZAK, *Heat Exchangers, Applications to Gas Turbine.* Academic Press, New York (1958)

K. KONDO, S. NISHIMURA, T. UEHARA, M. SIBAHAYASI, E. SUGINO, M. HIRATA, S. YAMAZAKI, T. HARA, J. OKUSHI and Y. MIYAI, *Hydrodynamics, Aerodynamics, Hydraulics and Lubrication, Heat and Heat Transfer. Non-holonomic Character of Hydroaerodynamical Forces.*

F. KREITH, *Principles of Heat Transfer.* International Textbook Company, Scranton, Pa. (1958).

H. SCHENCK, JR., *Heat Transfer Engineering.* Prentice-Hall, Engelwood Cliffs, N.J. (1959).

BOUNDARY LAYERS

R. M. L. BAKER, The transitional aerodynamic drag of meteorites. *Astrophys. J.* **129,** No. 3, 826 (1959).

L. V. BALDWIN, *Slip-flow Heat Transfer from Cylinders in Subsonic Airstreams.* NACA TN No. 4369 (1958).

A. BANDETTINI and W. E. ISLER, *Boundary-layer transition Measurements on Hemispheres of Various Surface Roughnesses in Wind Tunnel at Mach Numbers from* 2·48 *to* 3·55. NASA MN 12–25–58 (1959).

I. E. BECKWITH and J. J. GALLAGHER, *Experimental Investigation of the Effect of Boundary-layer Transition on the Average Heat Transfer to a Yawed Cylinder in Supersonic Flow.* NACA RM L56E09 (1956).

I. E. BECKWITH, *Theoretical Investigation of Laminar Heat Transfer on Yawed Infinite Cylinders in Supersonic Flow and a Comparison with Experimental Data.* NACA RM L55F09 (1955).

M. H. BERTRAM and W. V. FELLER, *A Simple Method for Determining Heat Transfer, Skin Friction, and Boundary Layer Thickness for Hypersonic Laminar Boundary-layer Flows in a Pressure Gradient.* NASA Memo. 5–24–59L (1959).

T. J. BLACK and A. J. SARNECKI, *The Turbulent Boundary Layer with Suction or Injection.* Cambridge University, ARC 20, 501 FM 2745 (1958).

M. H. BLOOM and S. RUBIN, *High-speed Viscous Corner Flow.* Polytechnic Institute of Brooklyn, Dept. of Aeronautical Engineering and Applied Mechanics, PIBAL Report No. 530, WADC TN 59–312 (1959).

D. E. BOURNE, Eddy diffusivities in forced and free convection boundary layers. *J. Aero. Space Sci.* **26,** No. 7, 459 (1959).

W. E. BRINK, *Approximate Method for Calculation of Laminar Boundary Layer with Heat Transfer on Cone at Large Angle of Attack in Supersonic Flow.* NACA TN No. 4380 (1958).

Investigation of the Effects of an Axial Magnetic Field on the Flow of an Ionized Gas. Chicago Midway Laboratories, Quarterly Progress Report, 15 May to 1 September, 1959 (1959).

P. M. CHUNG, *Shielding Stagnation Surfaces of Finite Catalytic Activity by Air Injection in Hypersonic Flight.* NASA TN D–27 (1959).

D. C. COLLIS and H. J. WILLIAMS, *Molecular and Compressibility Effects on Forced Convection of Heat from Cylinders.* Aero Res. Lab., Melbourne, Australia, Report A11C (1958).

D. G. DE COURSIN, R. E. LARSON and N. C. HELM, *Experimental Investigation of Laminar Heat Transfer with Nonuniform Surface Temperature at* $M = 4{\cdot}3$. WADC TR 59–285, ASTL AD 216300 (1959).

D. F. DURGIN, An "insulating" boundary-layer experiment. *J. Aero. Space Sci.* **26,** No. 7, 450 (1959).

A. J. EDE and O. A. SAUNDERS, Heat transfer from a flat surface to a parallel stream of water.

Proc. Inst. Mech. Engrs. **172,** No. 23, 743 (1958).

A. J. EGGERS, JR., C. F. HANSEN and B. E. CUNNINGHAM, *Theoretical and Experimental Investigation to the Effect of Yaw on Heat Transfer to Circular Cylinders in Hypersonic Flow*. NACA RM A55E02 (1955).

S. FELDMAN, *A Numerical Comparison between Exact and Approximate Theories of Hypersonic Inviscid Flow past Slender Blunt-nosed Bodies*. AVCO Everett Research Laboratory, Research Report 71 (1959).

W. V. FELLER, *Heat Transfer to Bodies at Angles of Attack*. NACA RM L57D19c (1957).

W. V. FELLER, *Investigation of Equilbrium Temperatures and Average Laminar Heat-transfer Coefficients for the Front Half of Swept Circular Cylinders at a Mach Number of* 6·9. NACA RM L55F08a (1955).

A. FERRI, *Some Heat Transfer Problems in Hypersonic Flow*. Polytechnic Institute of Brooklyn, Dept. of Aeronautical Engineering and Applied Mechanics, WADC TN 59–308; PIBAL Report No. 473 (1959).

B. J. GARLAND and L. T. CHAUVIN, *Measurements of Heat Transfer and Boundary-layer Transition on an* 8*-inch Diameter Hemisphere-cylinder in Free Flight for a Mach Number Range of* 2·00 *to* 3·88. NACA RM L57D04a (1957).

K. GLASSMAN and J. E. A. JOHN, An unusual aerodynamic stagnation-temperature effect. *J. Aero. Space Sci.* **26,** No. 6, 387 (1959).

H. GORTLER, Über eine Analogie zwischen den Instabilitäten laminarer Grenzschichtströmungen an konkaven Wänden und an erwärmten Wänden. *Ingen.-Arch.* **28,** 71 (1959).

R. J. GRIBBEN, Laminar boundary-layer with suction and injection. *Phys. Fluids* **2,** No. 3, 305 (1959).

J. R. HALL, K. C. SPEEGLE and R. O. PILAND, *Preliminary Results from a Free-flight Investigation of Boundary-layer Transition and Heat Transfer on a Highly Polished* 8*-inch Diameter Hemisphere-cylinder at Mach Numbers up to* 3 *and Reynolds Numbers Based on a Length of* 1 *foot up to* $17{\cdot}7 \times 10^6$, NACA RM L57D18c (1957).

H. A. HASSAN, On heat transfer to laminar boundary layers. *J. Aero. Space Sci.* **26,** No. 7, 464 (1959).

H. T. HO and R. F. PROBSTEIN, *A Series Solution to the Laminar Heat Transfer Problem at Hypersonic Speeds*. WADC TN 58–263 Brown Univ. Div. of Eng.; ASTIA AD 202 333 (1958).

H. HOSHIZAKI and H. J. SMITH, The effect of helium injection at an axially symmetric stagnation point. *J. Aero. Space Sci.* **26,** No. 6, 399 (1959).

R. R. JOHN and W. L. BADE, Stagnation point heat transfer in a subsonic jet of arc-heated air. *J. Amer. Rocket Soc.* **29,** No. 7, 523 (1959).

J. J. JONES, *Experimental Investigation of the Heat Transfer Rate to a Series of* 20° *Cones of Various Surface Finishes at a Mach Number of* 4·95. NASA Memo. 6–10–59L (1959).

J. J. JONES, *Shock-tube Heat-transfer Measurements on Inner Surface of a Cylinder* (*Simulating a Flat Plate*) *for Stagnation-temperature Range* 4,100° *to* 8,300°R. NASA TN D–54 (1959).

N. H. KEMP, P. H. ROSE and R. W. DETRA. Laminar heat transfer around blunt bodies in dissociated air. *J. Aero. Space Sci.* **26,** No. 7, 421 (1959).

S. J. KLINE and P. W. RUNSTADLER, Visual studies of the wall layers in the turbulent boundary layer. *J. Appl. Mech.* E **26,** No. 2, 166 (1959).

W. D. KROLL, *Aerodynamic Heating and Fatigue*. National Bureau of Standards, NASA Memo. 6–4–59W (1959).

G. M. LOW, *Boundary Layer Transition at Supersonic Speeds*. Presented at Symposium on High-speed Aerodynamics and Structures, Buffalo, New York. NACA RM E56E10 (1956).

H. J. MERK, Mass transfer in the laminar boundary layer along a flat plate calculated by means of the integral method. *Appl. Sci. Res., Hague* A **8,** No. 4, 261 (1959).

H. J. MERK, Mass transfer in laminar boundary layers calculated by means of a perturbation method. *Appl. Sci. Res., Hague* A **8,** No. 4, 237 (1959).

R. X. MEYER, *Rate of Heat-transfer near the Stagnation Point of a Blunt Body of Revolution*

Vol. 1 1960

in the Presence of a Magnetic Field. Physical Research Laboratory, Space Technology Laboratories, Los Angeles (1958).

R. J. MONAGHAN, *A Survey and Correlation of Data on Heat Transfer by Forced Convection at Supersonic Speeds.* Aeronautical Research Council, Ministry of Supply, R & M No. 3033, ARC Technical Report. Her Majesty's Stationery Office, London (1958).

D. E. NESTLER, *Survey of Theoretical and Experimental Determination of Skin Friction in Compressible Boundary Layers—V—The Effects of Slip Flow.* Missile and Space Vehicle Department, General Electric Company, Technical Information Series, Document No. R59SD343 (undated, apparently 1959).

R. A. OMAN and R. A. SCHEUING, On slip-flow heat transfer to a flat plate. *J. Aero. Space Sci.* **26,** No. 2, 126 (Reader's Forum) (1959).

R. O. PILAND and K. A. COLLIE, *Aerodynamic Heating of Rocket-powered Research Vehicles at Hypersonic Speeds.* NACA RM L55E10c (1955).

R. O. PILAND, K. A. COLLIE and W. E. STONEY, *Turbulent and Laminar Heat-transfer Measurements on a* 1/6 *Scale* NACA RM-10 *Missile in Free Flight to a Mach Number of* 4·2 *and to a Wall Temperature of* 1400°R. Appendix A: *Estimated Errors.* NACA RM L56C05 (1956).

E. RESHOTKO and I. E. BECKWITH, *Compressible Laminar Boundary Layer over a Yawed Infinite Cylinder with Heat Transfer and Arbitrary Prandtl Number.* NACA Report 1379; supersedes TN 3986 (1958).

L. ROBERTS, *Theoretical Study of Stagnation-point Ablation.* NACA TN No. 4392 (1958).

P. H. ROSE, Shock tube research in hypersonic aerodynamics. *J. Instrum. Soc. Amer.* (1958).

P. H. ROSE, R. F. PROBSTEIN and M. C. ADAMS, Turbulent heat transfer through a highly cooled, partially dissociated boundary layer. *J. Aero. Space Sci.* **25,** No. 12, 751 (1958).

P. H. ROSE and F. R. RIDDELL, *An Investigation of Stagnation Point Heat Transfer in Dissociated Air.* AVCO Research Laboratory, Research Report 7 (1957).

D. E. ROSNER, Steady-state surface temperatures in dissociated high-speed gas flows. *J. Aero. Space Sci.* **26,** No. 6, 384 (1959).

L. A. ROZIN, The growth of a laminar layer on a flat plate set impulsively into motion. *Appl. Math. Mech., Leningr.* **22,** No. 3, 568 (1958).

N. SANDS and J. R. JACK, *Preliminary Heat-Transfer Studies of two Bodies of Revolution at Angle of Attack at Mach Number of* 3·12. NACA TN No. 4378 (1958).

S. M. SCALA, Hypersonic stagnation point heat transfer to surfaces having finite catalytic efficiency. In *Proceedings of the Third U.S. National Congress of Applied Mechanics* pp. 99–806. The American Society of Mechanical Engineers, New York (1958).

J. F. SCHMIDT, *Laminar Skin-friction and Heat-transfer Parameters for a Flat Plate at Hypersonic Speeds in Terms of Free-stream Flow Properties.* NASA TN D-8 (1959).

N. SCHOLZ, Zur rationellen Berechnung laminarer und turbulenter kompressibler Grenzschicheten mit Wärmeübertragung. *Z. Flugwiss.* **7,** No. 2, 33 (1959).

M. SIBULKIN, Estimation of turbulent heat transfer at the sonic point of a blunt-nosed body. *Jet Propulsion* **28,** No. 8, 548 (1958).

A. M. O. SMITH and D. W. CLUTTER, The smallest height of roughness capable of affecting boundary-layer transition. *J. Aero. Space Sci.* **26,** 229 (1959).

E. M. SPARROW, R. EICHHORN and J. L. GREGG, Combined forced and free convection in a boundary layer flow. *Phys. Fluids* **2,** No. 3, 319 (1959).

E. M. SPARROW and J. L. GREGG, Effect of a nonisothermal free stream on boundary-layer heat transfer. *J. Appl. Mech.* E **26,** No. 2, 161 (1959).

K. F. STETSON, *Boundary Layer Transition on Blunt Bodies with Highly Cooled Boundary Layers.* IAS Report No. 59–36, AVCO Research Laboratory, Research Report 41 (1959).

H. S. TAN, Nose drag in free-molecule flow and its minimization. *J. Aero. Space Sci.* **26,** No. 6, 360 (1959).

LU TING, *Boundary Layer over a Flat Plate in the Presence of Shear Flow.* Dept. of Aeronautical Engineering and Applied Mechanics, Polytechnic Institute of Brooklyn, PIBAL Report No. 524, WADC TN 59–334 (1959).

T. TSUBOUCHI and S. SATO, On the heat transfer coefficients of cylindrical bodies. *Rep. Inst.*

Speed Mech., Sendai B **9,** Nos. 81/90, 135 (1958).

R. VAGLIO-LAURIN, *Turbulent Heat Transfer on Blunt-nosed Bodies in Two-dimensional and General Three-dimensional Hypersonic Flow.* WADC TN 58–301; Polyt. Inst. Brooklyn, Dept. Aero. Engng. Appl. Mech.; ASTIA AD 206 050 (1958).

C. T. WALKER and C. E. ADAMS, Thermal effects of acoustic streaming near a cylindrical obstacle. *J. Acoust. Soc. Amer.* **31,** No. 6, 813 (1959).

K. T. YANG, Unsteady laminar boundary layers over an arbitrary cylinder. *J. Appl. Mech.* E **26,** No. 2, 171 (1959).

A further note on the calculation of heat-transfer through the arisymmetrical laminar boundary layer on a circular cylinder. *Quart. Appl. Math.* **12,** Pt. 2, 257 (1959).

CHANGE OF PHASE

M. ALTMAN, F. W. STAUB and R. H. NORRIS, *Local Heat Transfer and Pressure Drops for Refrigerant-22 Condensing in Horizontal Tubes.* Reprint by American Institute of Chemical Engineers, New York, preprint 113 (1959).

E. K. AVERIN and G. N. KRUZHILLIN, Influence of surface tension and viscosity on the conditions of heat exchange when water boils. *Izv. Akad. Nauk SSSR, otdel tekh. nauk* No. 10, 131 (1955); *Ref. Zh. Mekh.* No. 4, Rev. 4254 (1958). (In Russian).

L. V. BALDWIN, *Slip-flow Heat Transfer from Cylinders in Subsonic Airstreams.* NACA TN No. 4369 (1958).

S. G. BANKOFF, *On the Mechanism of Subcooled Nucleate Boiling.* JPL Memo. 30–8, Jet Propulsion Laboratory, California Institute of Technology (1959).

L. D. BERMAN, Experimental investigation on steam condensation in the media of uncondensible gases. *Teploenergetika* No. 6, 43 (1957). (In Russian).

V. M. DEMENT'EV, Voprosy aerodinamoki kipyaschchego sloya. *Teploenergetika* **6,** No. 1, 50 (1959).

W. R. GAMBILL and N. D. GREENE, Boiling burnout with water in vortex flow. *Chem. Engng. Progr.* **54,** No. 10, 68 (1959).

E. GOTTESMAN, Efficiency of evaporative water cooling towers. *Appl. Sci. Res., Hague* A **8,** No. 1, 28 (1958).

P. GRASSMANN, Wärme- und stoffaustausch zwischen zwei fluiden Phasen. *Chem.-Ing.-Tech.* **31,** 148 (1959).

S. K. HELLMAN, S. KAMINSKY and R. W. KUPP, *Third Compilation of Current Work on Transient Boiling.* Report 3 (Enclosure A), Vitro Engineering Company, Homestead, Pa., WAPD–V(FBE)–26 (1959).

D. P. JORDAN and G. LEPPERT, Nucleate boiling characteristics of organic reactor coolants. *Nuclear Sci. Engng.* **5,** No. 6, 349 (1959).

E. L. KNUTH, Nonstationary phase changes involving a condensed phase and a saturated vapor. *Phys. Fluids* **2,** No. 1 (1959).

H. P. LOW, *Stoffaustauch zwischen Rieselfilm und gegenströmendem Dampf bei Zweistoffgemischen.* Doctor's thesis, Eidgenössischen Technischen Hochschule Zürich. Referent, P. GRASSMANN (1958).

Z. L. MIROPOL'SKII, M. E. SHITSMAN, I. L. MOSTINSKII and A. A. STAVROSKII, Vliyanie vkhodnykh uslovii na kriticheskie teplovye potoki pri kipenii vody v trubakh. *Teploenergetika* **6,** No. 1, 80 (1959).

P. G. POLETAVKIN and N. A. SHAPKIN, Heat transfer at surface boiling of water. *Teploenergetika* No. 5, 49 (1958). (In Russian).

L. ROBERTS, *An Approximate Analysis of Unsteady Vaporization near the Stagnation Point of Blunt Bodies.* NASA TN D–41 (1959).

S. L. SOO, C. I. TIEN and V. KADAMBI, Determination of turbulence characteristics of solid particles in a two-phase stream by optical autocorrelation. *Rev. Sci. Instrum.* **30,** No. 9, 821 (1959).

B. E. STANISEWSKI, *Nucleate Boiling Bubble Growth and Departure.* Division of Sponsored Research, MIT, Cambridge, Mass. TR No. 16 (1959).

B. A. ZENKEVICH, The experimental data generalization on the critical heat fluxes in forced flowing of subheated water. *Atomnaia Energiia,* **6,** No. 2, 169 (1959).

N. ZUBER, *Hydrodynamic Aspects of Boiling Heat Transfer.* A dissertation submitted for the degree Doctor of Philosophy in Engineering, University of California (1959).

Vol. 1 1960

CHANNEL FLOW

M. Abramowitz, W. F. Cahill and C. Wade, Jr., Heat transfer in laminar flow through tube. *J. Res. Nat. Bur. Stand.* **62,** No. 3, 101 (1959) (RP2937).

D. C. Boque, Entrance effects and prediction of turbulence in non-Newtonian flow. *Industr. Engng. Chem.* **51,** No. 7, 874 (1959).

W. B. Bush, *On One-dimensional Channel Flow in the Presence of a Magnetic Field.* Physical Research Laboratory, Space Technology Laboratories, Los Angeles (1959).

W. G. Brown and P. Grassman, Der Einfluss des Auftriebs auf Wärmeübergang und Druckgefälle bei erswungeter Strömung in lotrechten Rohren. *Forsch. IngWes.* **25**, Nr. 3, (1959).

R. D. Cess, Approximation of the eigenvalues for heat transfer in turbulent tube flow. *J. Aero. Space Sci.* **25,** No. 12, 751 (1958).

Ning Hsing Chen, Heat transfer and pressure drop. *Chem. Engng.* **66,** 141 (1959).

G. B. Darling, Heat transfer to liquids in intermittent flow. *Petroleum* **22,** 177 (1959).

R. G. Deissler and M. F. Taylor, *Analysis of Turbulent Flow and Heat Transfer in Non-circular Passages.* NACA TN No. 4384, 35 (1958).

R. G. Deissler, W. F. Weiland and W. H. Lowdermilk, *Analytical and Experimental Investigation of Temperature Recovery Factors for Fully Developed Flow of Air in Tube.* NACA TN No. 4376, 35 (1958).

W. L. Friend and A. B. Metzner, Turbulent heat transfer inside tubes and the analogy among heat, mass and momentum transfer. *J. Amer. Inst. Chem. Engrs.* **4,** No. 4, 393 (1958).

S. Globe, Laminar steady-state magnetohydrodynamic flow in an annular channel. *Phys. Fluids* **2,** No. 4, 404 (1959).

P. Griffith and G. Wallis, *Slug Flow.* Division of Sponsored Research, MIT, Cambridge, Mass., TR No. 15 (1959).

T. J. Hanratty, E. M. Rosen and R. L. Kabel, Effect of heat transfer on flow field at low Reynolds numbers in vertical tubes. *Industr. Engng. Chem.* **50,** No. 5, 815 (1958).

J. Harbedol, Stromings- en temperatuureffecten in de wervelbuis. *Ingenieur Berl.* **71,** No. 25, 21 (1959).

V. P. Isachenko and F. Salomzoda, Teplootdacha i gidravlicheskoe soprotivienie poperechnc omyvaemogo puchka trub. *Teploenergetika* **5,** No. 11, 69 (1958).

H. Ito, Friction factors for turbulent flow in curved pipes. *J. Basic Engng.* D **81,** No. 2, 123 (1959).

L. M. Mack, *The Compressible, Viscous, Heat-conducting Vortex.* Jet Propulsion Laboratory, California Institute of Technology (1959).

S. H. Maslen, *On Fully Developed Channel Flows: Some Solutions and Limitations, and Effects of Compressibility, Variable Properties, and Body Forces.* NACA TN No. 1319 (1959).

A. B. Metzner and P. S. Friend, Heat transfer to turbulent non-Newtonian fluids. *Industr. Engng. Chem.* **51,** No. 7, 879 (1959).

B. S. Petookhov and V. Kirillov, On heat exchange at turbulent flow of liquid in pipes. *Teploenergetika* No. 4, 63 (1958). (In Russian).

H. F. Poppendiek, *Heat Transfer in a Liquid Metal Flowing Turbulently through a Channel with a Step Function Boundary Temperature.* NASA Memo. 2–5–59W (1959).

H. F. Poppendiek, Turbulent liquid-metal heat transfer in channels. *Nucl. Sci. Engng.* **5,** No. 6, 390 (1959).

S. A. Regirer, The influence of thermal effects on the viscous resistance of a steady uniform flow of liquid. *Appl. Math. Mech., Leningr.* **22,** No. 3, 580 (1958).

H. Reichardt, *Gesetzmässigkeiten der geradlinigen turbulenten Couetteströmung.* Mitteilungen aus dem Max-Planck-Institut für Strömungsforschung und der Aerodynamischen Versuchsanstalt, Herausgegeben von W. Tollmien und H. Schlichting. Nr. 22, Göttingen (1959).

J. Schenk and J. van Laar, Heat transfer in non-Newtonian laminar flow in tubes. *Appl. Sci. Res., Hague* A **7,** No. 6, 449 (1958).

L. H. Soo, Friction and heat transfer of compressible flow into an infinite lattice of flat plates. *Z. angew. Math. Phys.* **10,** No. 3, 291 (1959).

E. M. Sparrow and A. L. Loeffler, Longitudinal laminar flow between cylinders arranged in regular array. *J. Amer. Inst. Chem. Engrs.* **5,** No. 3, 325 (1959).

E. M. Sparrow and R. Siegel, Thermal entrance

region of a circular tube under transient heating conditions. *Proceedings of the Third U.S. National Congress on Applied Mechanics* pp. 817–26. American Society of Mechanical Engineers, New York (1958).

E. M. SPARROW and R. SIEGEL, A variational method for fully developed laminar heat transfer in ducts. *J. Heat Transfer* C **81,** No. 2, 157 (1959).

M. A. STYRIKOVICH and Z. L. MIROPOL'SKII, The temperature regime of the work of horizontal and slipping steam-generating tubes at high pressures. *Hydrodynamics and Heat-exchange during Evolution of Steam in High-pressure Boilers* pp. 229–234. Akad. Nauk SSSR, Moscow (1955); *Ref. Zh. Mekh.* No. 3, Rev. 3020 (1958). (In Russian).

H. L. WEISSBERG, Laminar flow in the entrance region of a porous pipe. *Phys. Fluids* **2,** No. 5, 510 (1959).

CONDUCTION

M. A. BIOT, Further developments of new methods in heat flow analysis. *J. Aero. Space Sci.* **26,** No. 6, 367 (1959).

C. M. CARMICHAEL and A. D. MISENER, On maintaining an object at a uniform temperature. *Canad. J. Phys.* **37,** No. 7, 890 (1959).

H. S. CARSLAW and J. C. JAEGER, *Conduction of Heat in Solids* (2nd Ed.). Oxford University Press, London (1959).

A. DEMETRIADES, *Heat Conduction in a Circular Cylinder Rotating with its Axis Normal to the Direction of Flight.* Guggenheim Aeronautics Laboratory, California Institute of Technology, Pasadena, Pub. No. 461. *J. Amer. Rocket Soc.* **29,** 653 (1959).

R. J. DUFFIN, A variational problem relating to cooling fins. *J. Math. Mech.* **8,** No. 1, 47 (1959).

P. FORTESCUE and W. B. HALL, Heat transfer experiment on the fuel elements (Calder Hall Reactor). *J. Brit. Nuclear Energy Conf.* **2,** 83 and 242 (1959).

A. FRIEDMAN, Generalized heat transfer between solids and gases under nonlinear boundary conditions. *J. Math. Mech.* **8,** No. 2, 161 (1959).

T. R. GOODMAN, *The Heating of Slabs with Arbitrary Heat Inputs.* AFOSR TN 58–524, Allied Research Assoc. Inc., Report (1958).

R. HOFMANN, Zur Losung spezieller Wärmeleitungeprobleme. *Z. angew. Math. Phys.* **10,** No. 3, 233 (1959).

M. J. LAUBITZ, Thermal conductivity of powders. *Canad. J. Phys.* **37,** No. 7, 798 (1959).

B. L. MCFARLAND, Comparison between the linear and nonlinear steady-state behavior of a heated tube. *J. Appl. Phys.* **29,** No. 12, 1682 (1958).

T. P. NEWCOMB, The flow of heat in a parallel-faced infinite solid. *Brit. J. Appl. Phys.* **9,** 370 (1958).

T. P. NEWCOMB, The radial flow of heat in an infinite cylinder. *Brit. J. Appl. Phys.* **9,** No. 11, 456 (1958).

J. S. THOMSEN, *Physical Interpretation of the Relaxation Method in Heat Conduction.* Reprint from *J. Amer. Inst. Chem. Engrs.* June (1959).

V. VON VODKKA, Stationäre Temperaturverteilung in den Wand Vielschichtigee Röhrenlertungen. *J. Phys. Soc., Japan* **14,** No. 7, 959 (1959).

N. A. YARYSLEV, Application of Academician V. G. Galerkin's method to the solution of some problems in the theory of a regular thermal regime. *Investigations in the Field of Thermal Measurements and Appliances* pp. 187–197. Leningrad (1957); *Ref. Zh. Mekh.* No. 3, Rev. 3027 (1958). (In Russian).

P. M. YAVORSKY, R. J. FRIEDRICH and E. GORIN, Heat transfer and thermal stresses in carbonization of briquets. *Industr. Engng. Chem.* **51,** No. 7, 833 (1959).

FLOW WITH SEPARATED REGIONS

J. ACKERAT, Über die Temperaturverteilung hinter augestromten Zylindern. Presented at the Fall Meeting of the Swiss Physical Society at Bern on 24 August 1952. NASA. Tech. Trans. F–2 (1959); trans. from Eidgenossische Technische Hochschule, Institut für Aerodynamik, Mitteilungen 21, p. 5–21 (1954).

M. H. BLOOM and A. PALLONE, *Shroud Tests of Pressure and Heat Transfer over Short Afterbodies with Separated Wakes.* WADC TN 58–185, Polyt. Inst. Brooklyn, Aero. Lab., ASTIA AD 155–690 (1958).

Vol. 1 1960

D. C. COLIS and M. J. WILLIAMS, *Two-dimensional Forced Convection from Cylinders at Low Reynolds Numbers*. Aero. Res. Lab., Melbourne, Austral., Report A–105 (1957).

A. J. HANAWALT, A. J. BLESSING and C. M. SCHMIDT, Thermal analysis of stagnation regions with emphasis of heat-sustaining nose shapes at hypersonic speeds. *J. Aero. Space Sci.* **26,** 257 (1959).

A. A. LONDON, J. W. MITCHELL and W. A. SUTHERLAND, *Heat Transfer and Flow Friction Characteristics of Crossed-rod Matrices*. Department of Mechanical Engineering, Stanford Univ., Stanford, California, TR No. 41 (1959).

J. M. F. VICKERS, Heat transfer coefficients between fluid jets and normal surfaces, behaviour of laminar impacted jets. *Industr. Engng. Chem.* **51,** No. 8, 967 (1959).

S. YAGI and N. WAKAO, Heat and mass transfer from wall to fluid in packed beds. *J. Amer. Inst. Chem. Engrs.* **5,** No. 1, 79 (1959).

LOW-DENSITY HEAT TRANSFER

S. H. MASLEN, On heat transfer in slip flow. *J. Aero. Space Sci.* **25,** No. 6, 400 (1958).

R. F. PROBSTEIN and N. H. KEMP, *Viscous Aerodynamic Characteristics in Hypersonic Rarefied Gas Flow*. AVCO Research Laboratory, Research Report 48 (1959).

J. V. BECK, *Study of Thermal Discontinuities and Associated Temperature Disturbances in a Solid Subject to a Surface Heat Flux—III—Effect of Sensors in Low Conductivity Material upon Temperature Distribution and its Measurement*. Research and Advanced Development Division, AVCO Corporation, Wilmington, Mass. (1959).

J. S. CAMMERER, Messung von Temperaturen und Wärmemengen mittels elektronischer Zählgerlte. *Allg. Warmetechn.* **9,** Nr. 3, 49 (1959).

I. G. DONALDSON, Temperature errors introduced by temperature measuring probes. *Brit. J. Appl. Phys.* **10,** No. 6, 252 (1959).

H. W. DEEM, Stretching the scale of temperature measurement. *Battelle Tech. Rev.* **8,** No. 7, 4 (1959).

J. P. FUNK, Improved polythene shielded net radiometer. *J. Sci. Instrum.* **36,** No. 6, 267 (1959).

W. GRACEY, *Measurement of Static Pressure on Aircraft*. NACA Report 1364; supersedes TN 4184 (1958).

A. S. GUPTA, Effect of bouyancy forces on certain viscous flows with suction. *Appl. Sci. Res., Hague* A **8,** 309 (1959).

D. A. JONES, Anisotropic field plotting in the electrolytic tank. *Rev. Sci. Instrum.* **30,** No. 7, 577 (1959).

C. E. MOELLER, Welding a thermocouple junction. *Instrum. Control Syst.* **32,** No. 6, 895 (1959).

J. L. MONTEITH, Solarmeter for field use. *J. Sci. Instrum.* **36,** 341 (1959).

J. A. RIETDIJK and A. VALSTAR, On a thermometer with recovery factor. *Appl. Sci. Res., Hague* A **7,** No. 4, 251 (1958).

P. H. ROSE, *Development of the Calorimeter Heat Transfer Gage for Use in Shock Tubes*. AVCO Research Laboratory, Research Report 17 (1958).

M. SIBULKIN, A total temperature probe for high-temperature boundary-layer measurements. *J. Aero. Space Sci.* **26,** No. 7, 458 (1959).

NATURAL CONVECTION

A. ACRIVOS, Combined laminar free and forced-convection heat transfer in external flows. *J. Inst. Chem. Engrs.* **4,** No. 3, 285 (1958).

D. R. DAVIS, On the calculation of eddy viscosity and heat transfer in a turbulent boundary layer near a rapidly rotating disk. *Quart. Appl. Math.* **12,** Pt. 2, 211 (1959).

D. DROPKIN and S. GLOBE, Effect of spin on natural convection in mercury heated from below. *J. Appl. Phys.* **30,** No. 1, 84 (1959).

R. M. FAND and J. KAYE, *The Effect of High Intensity Stationary and Progressive Sound Fields on Free Convection from a Horizontal Cylinder*. Wright Air Development Center. WADC TN 59–18, ASTIA AD 209532 (1959).

F. R. HAMA and J. CHRISTIAENS, *Experiment on the Axisymmetric Free-convection Field along a Vertically-suspended Wire*. AFOSR TN 58–444; Inst. Fluid Dynam. Appl. Math., Univ. Maryland, TN BN–138; ASTIA AD 158 249 (1958).

F. R. HAMA, J. V. RECESSO and J. CHRISTIAENS, The axisymetric free-convection temperature field along a vertical thin cylinder. *J. Aero. Space Sci.* **26,** No. 6, 335 (1959).

J. P. HOLMAN and T. P. MOTT-SMITH, *The Effect of High Constant Pressure Sound Fields on Free Convection Heat Transfer from a Horizontal Cylinder*. U.S. Air Force Wright Development Center, WADC TN 58–352 (1958).

N. IBL, *Studies of Mass Transfer during Electrolysis with Natural Convection*. Reprint from the *Proceedings of the Eighth Meeting of the International Committee of Electrochemical Thermodynamics and Kinetics, Madrid*, 1958 pp. 174–189. Butterworths, London (1958).

N. IBL and R. H. MILLER, Studies of natural convection at vertical electrodes. Reprint from *J. Electrochem. Soc.* **105,** No. 6, 346 (1958).

P. N. KUBANSKII, The influence of acoustical streaming on convective heat exchange. *Akust. Zh.* **5,** No. 1, 51 (1959).

L. I. KUDRIASHEV and A. IA. IPATENKO, Influence of the free motion on the heat transmission factor in a flow around a sphere in the region of small Reynolds numbers. *Zh. Tekh. Fiz.* **24,** No. 3, 309 (1959).

G. A. OSTROUMOV, Problem of thermoelectric convection. *Zh. Tekh. Fiz.* **26,** No. 3, 636 (1956); *Ref., Zh. Mekh.* No. 3, Rev. 3040 (1958). (In Russian).

G. A. OSTROUMOV, *Free Convection under the Conditions of the Internal Problem*. NACA TM 1407 (1958); Translation of *Svobodnaya Convectzis v Ousloviakh Vnoutrennei Zadachi*. State Publishing House Technico-Theoretical Lit., Moscow and Leningrad (1952).

B. S. PETUKHOV and L. D. NOL'DE, Teploobmen pri vyazkostno-gravitatsionnom techenil zhidkosti v trubakh. *Teploenergetika* **6,** No. 1, 72 (1959).

I. G. SEVRUK, Transient heat convection within a spherical film. *Appl. Math. Mech., Leningr.* **22,** 3, 587 (1958).

E. A. SIDEROV, Accounting for the effect of unstable conditions on convective heat exchange. *Teploenergetika* No. 4, 79 (1958). (In Russian).

R. K. SOBERMAN, Onset of convection in liquids subjected to transient heating from below. *Phys. Fluids* **2,** No. 2, 131 (1959).

K. STEWARTSON, On the free convection from a horizontal plate. *Z. angew. Math. Phys.* **9a,** No. 3, 276 (1958). (In English).

F. KREITH, J. H. TAYLOR and J. P. CHONG, Heat and mass transfer from a rotating disk. *J. Heat Transfer* **81,** No. 2, 95 (1959).

W. B. WELSH, JR. and J. P. HARTNETT, Velocity measurements in the boundary layer and in the main flow between two coaxial disks rotating with equal velocities in air. Paper from *Proceedings of the Third U.S. National Congress of Applied Mechanics* pp. 847–855. The American Society of Mechanical Engineers, New York (1958).

R. A. WOODING, An experiment on free thermal convection of water in saturated permeable material. *J. Fluid Mech.* **3,** No. 6, 582–600 (1958).

CHIA-SHUN YIH, Thermal instability of viscous fluids. *Quart. Appl. Math.* **17,** No. 1, 25–42 (1959).

About breakdown in laminar flow viscous liquid in natural convection. *Teploenergetika* No. 12, 66 (1957). (In Russian).

Vol. 1 1960

PROPERTIES

F. BOSNJAKOVIC, W. SPRINGE, K. F. KNOCHE and P. BURGHOLTE, Mollier enthalpy–entropy charts for high-temperature plasmas. Reprint from *Thermodynamic and Transport Properties of Gases, Liquids and Solids* pp. 465–472. The American Society of Mechanical Engineers, New York (1959).

C. F. HANSEN and S. P. HEIMS, *Review of Thermodynamic, Transport and Chemical Reaction Rate Properties of High-temperature Air*. NACA TN No. 4359 (1958).

R. W. POWELL and A. R. CHALLONER, New measurements of the thermal conductivities of several liquid refrigerants of the fluorochloro derivatives types. *Properties of Liquids Thermal Conductivity*. Personal communication of a paper presented at the Tenth International Conference on Refrigeration, held 19–26 August 1959 in Copenhagen (1959).

C. A. SCHAEFER and G. THODOS, Thermal conductivity of diatomic gases: liquid and gaseous states. *J. Amer. Inst. Chem. Engrs.* **5,** No. 3, 367 (1959).

K. L. WRAY and T. J. CONNOLLY, *Thermal Conductivity of Clear Fused Silica at High Temperatures.* AVCO Research Laboratory, Research Report 44 (1959).

RADIATION

V. N. ADRIANOV, Application of the electric analogue method to the problem of radiant heat transfer. *Izv. Akad. SSSR, otdel tekh. nauk Energetikai Avtomatika* No. 1, 20 (1959). (In Russian).

V. N. ADIANOV and S. N. SHORIN, Radiant heat transfer in a flowing radiating medium. *Izv. Akad. Nauk SSSR, otdel tekh. nauk* No. 5, 46 (1958). (In Russian).

A. BOGGESS, III and D. DUNKELMAN, Ultraviolet reflectivities of Mars and Jupiter. *Astrophys. J.* **129,** Nos. 1 and 2, 236 (1959).

P. HAMMERLING, J. D. TEARE and B. KIVEL, *Theory of Radiation from Luminous Shock Waves in Nitrogen.* AVCO Everett Research Laboratory, Research Report 49, AFDMD–TR–59–3 (1959).

R. V. JONES, The detection of thermal radiation using linear expansion. *Proc. Roy. Soc.* A **249,** No. 1256, 100 (1959).

L. P. KADANOFF, *Radiative Transport within an Ablating Body.* AVCO Everett Research Laboratory, Research Report 61 (1959).

J. KECK, B. KIVEL and T. WENTINK, *Emissivity of High-temperature Air.* AVCO Research Laboratory, Research Report 21 (1957).

B. KIVEL and K. BAILEY, *Tables of Radiation from High-temperature Air.* AVCO Research Laboratory, Research Report 21 (1957).

D. A. LABUNTSOV, Heat emission in pipes during laminar flow of a liquid with axial heat conduction taken into account. *Soviet Res. in Phys.* **3,** No. 1, 33 (1958); translation of *Dokl. Akad. Nauk SSSR* (N.S.) **118,** No 6, 1118 (1958).

M. A. MIKHEEV, V. A. BAUN, K. D. VOSKRENSKII and O. S. FEDUNSKII, Heat emission of smelted metals. *Reactor Construction and the Theory of Reactors* pp. 139–151. Izd-vo Akad. Nauk SSSR, Moscow (1955).

D. OLF and S. S. PENNER, Errata: Relations between gas absorptivities and emissivities. *J. Appl. Phys.* **30,** No. 6, 953 (1959).

U. P. OPPENHEIM, Experimental verification of theoretical relations between total gas absorptivities and total gas emissivities for CO. *J. Appl. Phys.* **30,** No. 6, 803 (1959).

A. A. TOWNSEND, The effects of radiative transfer on turbulent flow of a stratified fluid. *J. Fluid Mech.* **4,** No. 4, 361 (1958).

W. WADE and F. W. CASEY, *Measurements of Total Hemispherical Emissivity of Several Stably Oxidized Nickel–Titanium Carbide Cemented Hard Metals from* 600°F *to* 1,600°F. NASA Memo. 5–13–59L (1959).

Radiant heat exchange in a gas-filled enclosure; allowance for nonuniformity of gas temperature. *J. Amer. Inst. Chem. Engrs.* **4,** No. 1 (1958).

Spectral Emittance of Uncoated and Ceramic-coated Inconel and Type 321 *Stainless Steel.* NASA Memo. 4–9–59W (1959).

TRANSFER MECHANISMS

G. K. BATCHELOR, Diffusion in a fluid in turbulent motion. *Cienc. y Téc.* **126,** No. 631, 3–11 (1958). (In Portuguese).

D. B. CONGER, Heat flow towards a moving cavity. *Quart. Appl. Math.* **12,** Pt. 2, 222 (1959).

P. GRASSMANN and G. ANDERES, Abhängigkeit des Stoffaustausches von der Austauschrichtung. *Chem.-Ing.-Tech.* **31,** 154 (1959).

P. S. KLEBANOFF and K. D. TIDSTROM, *Evolution of Amplified Waves Leading to Transition in a Boundary Layer with Zero Pressure Gradient.* National Bureau of Standards, NASA TN D–195 (1959).

S. I. KOSTERIN, I. A. KOZHINOV and A. I. LEONTIEV, The effect of pressure fluctuations in a gas flow upon convective heat exchange. *Teploenergetika* **6,** No. 3, 66 (1959).

S. S. KUTATELADZE, *Basis of the Theory of Heat Exchange* p. 385. Mashgiz, Moscow and Leningrad (1957); *Ref. Zh. Mekh.* No. 4, Rev. 4276 (1958). (In Russian).

N. NESS, On the continuity of the Schmidt number at the interface between the laminar sub-layer and the outer turbulent region. *J. Aero. Space Sci.* **26,** No. 6, 396 (1959).

L. A. VULIS and A. T. TROFIMENKO, Thermal problems for a laminar stream spreading along a wall. *Zh. Tekh. Fiz.* **26,** No. 12, 2709 (1956); *Ref. Zh. Mekh.* No. 10, Rev. 11668 (1957).

C. S. YIH, Inhibition of hydrodynamic instability by an electric current. *Phys. Fluids* **2,** No. 2, 125 (1959).

TRANSPIRATION AND MASS TRANSFER

MAC C. ADAMS, W. E. POWERS and S. GEORGIEV, *An Experimental and Theoretical Study of Quartz Ablation at the Stagnation Point.* AVCO Everett Research Laboratory, Research Report 57 (1959).

E. BAUER and M. ZLOTNICK, Evaporation into a boundary layer—II. Dissociation in evaporation. *Phys. Fluids* **2,** No. 2, 236 (1959).

H. A. BETHE and H. C. ADAMS, A theory for the ablation of glassy materials. *J. Aero. Space Sci.* **26,** No. 6, 321 (1959).

L. A. DE VRIES, Simultaneous transfer of heat and moisture in porous media. *Trans. Amer. Geophys. Un.* **39,** No. 5, 909 (1958).

T. R. GOODMAN, Aerodynamic ablation of melting bodies. *Proceedings of the Third U.S. National Congress of Applied Mechanics* pp. 735–745. The American Society of Mechanical Engineers, New York (1958).

P. GROOTENHUIS, The mechanism and application of effusion cooling. *J. Ry. Aero. Soc.* **63,** No. 578, 73 (1959).

A. A. HAYDAY, *Mass Transfer Cooling in a Laminar Boundary Layer in Steady Two-dimensional Stagnation Flow.* AFOSR TN 58–337; Heat Transf. Lab. Univ. Minn. Inst. Tech. TN 19; ASTIA AD 154–241 (1958).

J. T. HOWE and W. A. MERSMAN, *Solutions of the Laminar Compressible Boundary-layer Equations with Transpiration which are Applicable to the Stagnation Regions of Axisymmetric Blunt Bodies.* NASA TN D–12 (1959).

E. L. KNUTH, Multicomponent diffusion and Fick's law. *Phys. Fluids* **2,** No. 3, 339 (1959).

B. M. LEADON, C. J. SCOTT and G. E. ANDERSON, *Mass Transfer Cooling of a* 20° *Porous Cone at* $M = 5$. AFOSR TN 57–461; Univ. Minnesota, Institute of Technol. Dept. Aero. Engng., Rosemount Aero. Lab. Res. Rep. 143; ASTIA 136–452 (1957).

L. LEES, *Ablation in Hypersonic Flows.* Paper presented at the Seventh Anglo-American Conference, sponsored jointly by the Royal Aeronautical Society and the Institute of the Aeronautical Sciences, 5–7 October, New York (1959).

L. LEES, Similarity parameters for surface melting of blunt nosed body in high velocity gas stream. *J. Amer. Rocket Soc.* **29,** No. 5, 345 (1959).

H. J. MERK, The macroscopic equations for simultaneous heat and mass transfer in isotropic, continuous and closed systems. *Appl. Sci. Res., Hague* A **8,** No. 1, 73 (1958).

S. S. PAPELL and A. M. TROUT, *Experimental Investigation of Air Film Cooling Applied to an Adiabatic Wall by Means of an Axially Discharging Slot.* NASA TN D–9 (1959).

H. T. RICHARDS, *Evaluation of Transpiration-cooled Turbine Blades with Shells of "Poroloy" Wire Cloth.* NASA Memo. 1–29–59E (1959).

L. ROBERTS, *Mass Transfer Cooling Near Stagnation Point.* NACA TN No. 4391 (1958).

C. J. SCOTT, *The Application of Constant Property Solutions to Mass Transfer Cooling Calculations.* AFOSR TN 59–201; Univ. Minn., Inst. of Technol., Rosemount Aero. Lab. Engng. Memo. 76; ASTIA AD 211 527 (1958).

A. SIMON, Alternative neutral burnout equation. *Phys. Fluids* **2,** 336 (1959).

J. R. STALDER and M. INOUYE, *A Method of Reducing Heat Transfer to Blunt Bodies by Air Injection.* NACA RM A56B27a (1956).

G. W. SUTTON, A comparison of several approximate theories of melting ablation. *J. Aero. Space Sci.* **26,** No. 6, 397 (1959).

W. J. THOMAS and P. HOUSTON, Simultaneous heat and mass transfer in cooling towers. *Brit. Chem. Engng.* **4,** 217 (1959).

S. W. YUAN and A. BARGZOTTI, *Experimental Investigation of Transpiration Cooling in Turbulent Pipe Flow.* ONR 839 16, Polyt. Inst. Brooklyn, Aero. Lab. Rep. 479 (1958).

Vol. 1 1960

Int. J. Heat Mass Transfer. Vol. 1, pp. 113–114. Pergamon Press 1960. Printed in Great Britain.

TITLES OF PAPERS FROM RECENT ISSUES OF *INZHENERNO-FIZICHESKII ZHURNAL*

(JOURNAL OF ENGINEERING PHYSICS)

Vol. II, No. 8 **August 1959**

D. K. KOLLEROV: The foundations of the theory of the thermal decomposition of materials in particle form.
V. I. BLINOV: Pulsation of diffusion flames.
H. A. LENIGER: Drying of solid foodstuffs in air.
N. U. KOIDA: Application of similarity theory to the filtration of liquids.
S. A. REGIRER: The non-steady flow of a conducting liquid in a magnetic field.
V. V. SKOROKHOD: The electrical conductivity of conductor–nonconductor dispersions.
I. G. NEKRASHEVICH and I. A. BAKUTO: On the mechanism of electrode pitting during an electric discharge.
V. F. STEPHANCHUK: The designing of an adiabatic-isothermal expansion nozzle.
F. F. KHARAKHORIN: The liquid–vapour equilibrium in the system ethane–ethylene.
G. V. OVECHKIN, A. B. USTINOVICH and V. D. SHAFOROSTOVA: The effect of sodium concentration in a plasma on the relative intensity of a selected pair of spectral lines of magnesium and copper.
A. M. SAMSON: Non-stationary luminescence from a sheet of infinite thickness.
M. G. MARKEVICH: Some aspects of the geometry of solid bodies.

Notes

R. I. ARTIM: Nucleation of a new phase in dilute binary solutions.
M. A. KOVNER: Calculation of the thermodynamic functions of benzene and toluene and their fully deuterated analogues from spectroscopic data.
N. I. KUZNETSOV and M. P. KHALIMANOVICH: The effect of manufacturing inaccuracies on the motion of a symmetrical gyroscope.
A. A. GUSAK: The theory of the mechanisms known as parallelograms.

Vol. II, No. 9 **September 1959**

E. D. FEDOROVICH: Heat transfer of a plate in a turbulent boundary layer of an incompressible liquid at $Pr \ll 1$.
Y. MALAK and I. SHMID: Investigation of the heat exchange in a homogenous boiler-type atomic reactor.
F. F. KHARAKHORIN: Liquid–vapour equilibrium in the systems nitrogen–helium and helium–methane.
G. D. RABINOVICH and G. N. SLOBODICH: An experimental investigation of the process of heat exchange between a pulsed gas flow and solid particles suspended in it.
A. P. KASHURICHEV: A method of investigating the process of thermal decomposition of solid fuels.
I. L. LIUBOSHITS: Contact mass transfer in a layer of granular material.
V. D. DUNSKY: The thickness of the heat insulating layer in a vertical cyclone furnace.
I. N. FRANTSEVICH, D. F. KALINOVICH, I. I. KOVENSKY and M. D. SMOLIN: Donor–acceptor interactions of the components of a binary iron–chrome alloy.
L. O. MELESKO: An investigation of the kinetics of crystallization of betol, salipyrine and antipyrine.
A. P. PRISHIVALKO: The accuracy of determination of optical constants of absorbing materials by the reflection method.
I. L. KAROL and A. Y. PRESSMAN: The dispersion of a heavy aerosol, having distributed particle size, in a turbulent atmosphere at large distances from an instantaneous point source.

Notes

A. I. RYCHKOV and N. A. SHAKHOVA: Calculation of the rate of pseudo-liquefication of suspensions with fixed or distributed particle size.
E. M. ORGRYZKIN: The mechanism of the effect of an oxygen jet on a liquid bath.
K. V. ELSHIN: Natural convection in an oil tank.
L. I. KISELEVSKY and N. S. SVENTITSKY: The effect of polarity on the entry of electrode material into the light source during spectral analysis.

Vol. II, No. 10 **October 1959**

G. L. BABUKHA and M. M. NAZARCHUK: A method of calculating the heating of a suspension having distributed particle size.
M. A. GOLDSHTIK: A thermoanemometer with automatic compensation for changes in flow temperature.
V. S. BURAKOV and A. A. YANKOVSKY: An investigation of the effect of sulphur on the intensity of the spectral lines of iron.
V. S. VOLKENSHTEIN and N. N. MEDVEDEV: The determination of coefficients of temperature conductivity and heat conductivity of solids and liquids.
A. S. KASPEROVICH: Tne use of the method of electrothermal analogies in calculating the behaviour of circuits containing indirectly heated thermistors.
L. S. STERMAN, V. G. MOROZOV and S. A. KOVALEV: Investigation of heat transfer during the boiling of water and ethanol in pipes (under pressure).
A. A. ANDREYEVSKY: Heat transfer to a single pipe in a transverse liquid flow at low Prandtl numbers.

Notes

N. N. INOZEMTSEV: The effect of initial temperature and pressure on the normal rate of flame propagation of various hydrocarbon–air mixtures.
N. N. SIROTA and A. V. SHIBAEVA: Etch contrasting of dislocations in monocrystals of silicon.
P. I. KUDRYASHOV, A. S. CHERKASOV, B. Y. SVESHNIKOV and G. A. TISHCHENKO: Boro-glycerine organic phospors.
G. V. PLYATSKO: The temperature field in a hollow cylinder with variable boundary conditions.
G. P. STELMAKH: An approximate calculation of particle velocity in the suspended state.
A. I. MOCHALIN: The combined utilization of the Dirac delta-function and integral transforms.
M. M. FARZETDINOV: Heat transfer through a revolving cylindrical body enclosed within a solid mass.
F. L. YUDITSKY: The wear resistance of graphite piston rings in a water vapour environment.
V. D. KUZNETSOV and V. N. KASHCHEYEV: The hardness of metals and their wear in a stream of abrasive particles.

Criticism and Bibliography

L. D. BERMAN: Remarks on the article of A. A. POLUSHKIN entitled: "The criteria of similarity of heat and mass exchange in processes of evaporation of liquids".
A. A. POLUSHKIN: On the remarks of L. D. BERMAN.

Vol. 1 1960

Vol. II, No. 11 **November 1959**

E. V. SHISHOV: The use of thermocouples placed across streamlines to record the temperature of supersonic flows.
A. Y. PRESSMAN: The role of turbulent vertical dispersion in the settling of non-homogeneous aerosols from the atmosphere.
A. V. LUIKOV: An investigation of heat and mass transfer in binary gas mixtures.
V. A. BAUM and A. S. OKHOTIN: A method of calculating the performance of solar batteries.
N. I. GAMAYUNOV: A new method for determining coefficients of heat and mass transfer.
Y. CIBOROWSKI: A graphic method of determining the degree of sublimation condensation.
F. I. MURASHKEVICH: The dust-removal efficiency of a turbulent scrubber.
B. V. LVOV: Analytical applications of atomic absorption spectra.
A. I. RYCHKOV: The relationship between the heat exchange of a liquid during boiling and its internal pressure $[(\partial E/\partial V)_T]$.

Notes

A. S. PLESHANOV: A mathematical theory concerning normal rates of flame propagation.
I. S. KOCHENOV and V. L. ROMODANOV: The coefficient of resistance during the flow of liquid under suction through a porous wall.
F. S. VORONIN: The effects of compressibility on the coefficient of friction resistance in turbulent gas flow.
E. A. SIDOROV: The calculation of resistance and convection heat exchange under turbulent non-stationary conditions.
V. N. OLEINIKOV and M. F. KAZANSKY: The investigation of means of gamma-rays of a non-stationary hydrothermal field during the drying of a macroporous body.
B. I. TIMCHUK: An investigation of heat transfer in molten metals during phase transformations.
L. I. BERGER and N. N. SIROTA: Some properties of alloys of the system: $InAs–In_2Se_3$.
M. A. YAKOVLEV: The kinetics of the decay of induced thermal e.m.f.s in industrial iron.
A. I. MOCHALIN: The problem of heat conduction in an infinite cylinder.
L. N. GRIGORYEV and A. G. USMANOV: Heat transfer in boiling azeotropic mixtures.
I. I. PETROVSKY: Germanium diodes with "negative resistance".

Translated by T. BODDINGTON

Int. J. Heat Mass Transfer. Vol. 1, pp. 115–120. Pergamon Press 1960. Printed in Great Britain.

HEAT TRANSFER TO MERCURY IN A CIRCULAR TUBE AND ANNULAR CHANNELS WITH SINUSOIDAL HEAT LOAD DISTRIBUTION

V. I. PETROVICHEV

Moscow Institute of Physical Engineering,
Moscow, U.S.S.R.

(*Received* 18 *November* 1959)

Abstract—To calculate the maximum wall temperature for a turbulent mercury flow in circular tubes with $l/d = 44{\cdot}6$ and 67 for a sinusoidal heat load distribution along the axis the following formula was derived

$$\theta_{\max} = \frac{(t_s)_{\max} - t_a}{t_b - t_a} = 0{\cdot}22\, Pe^{0{\cdot}27}$$

at $Pe = 400$–3900, which can be used for the estimation of heat transfer in tubes with sinusoidal heat distribution sources.

The experimental data were obtained on heat transfer to mercury when $q = q_0 \cdot \sin \pi x/l$ in annular channels with $d_m = 5{\cdot}4$ mm and $3{\cdot}5$ mm which can be used for comparative estimation.

The experimental data qualitatively agree with the solution of the present problem on an electric integrator

Résumé—Pour calculer la température maximum de paroi relative à un écoulement turbulent de mercure dans des tubes circulaires pour lesquels $l/d = 44{,}6$ et 67, dans le cas d'une distribution sinusoïdale des charges thermiques sur l'axe, on a établi la formule suivante

$$\theta_{\max} = \frac{(t_s)_{\max} - t_a}{t_b - t_a} = 0{,}22\, Pe^{0{,}27}$$

pour $Pe = 400$–3900. Cette formule peut être utilisée pour le transfert de chaleur dans des tubes avec des apports de chaleur à variation sinusoïdale.

Les résultats expérimentaux obtenus sur le transfert de chaleur avec du mercure pour $q = q_0 \cdot \sin \pi x/l$ dans des conduits annulaires $d_m = 5{,}4$ mm et $3{,}5$ mm peuvent être utilisés à titre de comparaison.

Les résultats expérimentaux concordent bien avec ceux que l'on obtient par le calcul à l'aide des machines électriques.

Zusammenfassung—Zur Berechnung der maximalen Wandtemperatur einer turbulenten Quecksilberströmung im Kreisrohr mit $l/d = 44{,}6$ und 67 bei sinusförmig längs der Achse verteiltem Wärmestrom wird die Gleichung

$$\theta_{\max} = \frac{(t_s)_{\max} - t_a}{t_b - t_a} = 0.22\, Pe^{0{,}27}$$

für Pe 400 bis 3900 abgeleitet.

Versuchswerte über den Wärmeübergang an Quecksilber mit $q = q_0 \cdot \sin \pi x/l$ in ringförmigen Kanälen mit $d_m = 5{,}4$ mm und $3{,}5$ mm können als Vergleich dienen.

Die Versuchswerte stimmen qualitativ mit der Lösung dieses Problems durch den elektrischen Integrator überein.

Abstract—Для вычисления максимальной температуры стенки при турбулентном течении ртути в круглых трубах с $l/d = 44{,}6$ и 67 при синусоидальном распределении тепловой нагрузки вдоль оси получена расчётная формула

$$\theta_{\max} = \frac{(t_s)_{\max} - t_a}{t_b - t_a} = 0{,}22\, Pe^{0{,}27}$$

при $Pe = 400 - 3900$, которой удобно пользоваться для оценочных расчётов теплоотдачи в трубах при синусоидальном тепловыделении.

H

Получены экспериментальные данные по теплоотдаче ртути при $q = q_0 \cdot \sin \pi x/l$ в кольцевых каналах $d_m = 5{,}4$ mm и 3,5 mm, которые могут быть использованы для сравнительных оценок.

Экспериментальные данные качественно согласуются с расчётом данной задачи на электроинтеграторе [6].

It is known from analytical investigations [1–4] that boundary conditions for a turbulent flow have greater effect on the heat transfer from liquids with low Prandtl numbers, i.e. from liquid metals, because of their high "molecular" thermal conductivity.

Having in view the modern development of physical power plants where heat sources are distributed sinusoidally, investigation of the influence on heat transfer of such heat load distribution along the length of a channel is of great interest. One may suppose that the influence of the sources of heat distribution along the length of a channel will also affect the heat transfer from liquid metals to a greater extent in comparison with the transfer from agents with Prandtl numbers of the order $Pr \gg 1$.

The calculation of heat transfer for a sinusoidal heat load distribution along the length of a channel for laminar flow of a heat transfer agent in a circular tube and between parallel planes was made by Dzung [5]. In a previous paper [6] we calculated the heat transfer for a turbulent flow of liquid metal when $Pr = 0{\cdot}025$ in a circular tube for various ratios of l/d. The purpose of this investigation is to check the results given in reference [6] and to perform some more calculations.

EXPERIMENTAL METHODS

The experimental installation for the investigation of heat transfer in mercury for a sinusoidal heat load distribution along the length of a channel represents (as shown in Fig. 1) a circulation contour which consists of a mercury container, a centrifugal pump, a Venturi nozzle, a differential manometer, a water cooler, a regulating valve and an experimental heat exchanger. All the parts of the installation in contact with mercury are made of stainless steel. For each series of

Vol. 1 1960

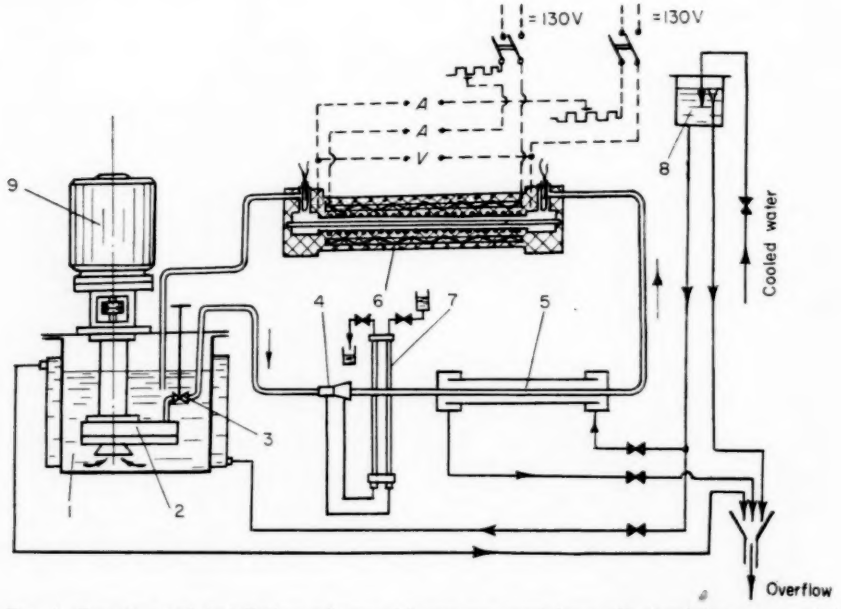

FIG. 1. Experimental installation scheme: (1) mercury container; (2) circulating pump; (3) regulating valve; (4) Venturi nozzle; (5) water cooler; (6) experimental heat exchanger; (7) differential manometer; (8) tank with a constant cooling water level.

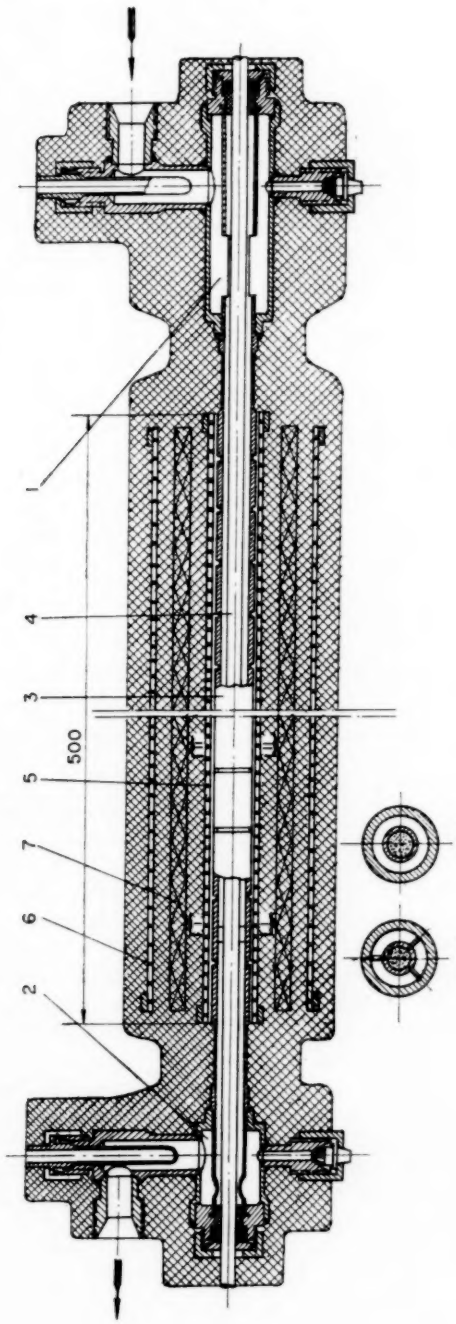

FIG. 2. Experimental heat exchanger N2 (1) inlet chamber; (2) outlet chamber; (3) outside tube; (4) displacer; (5) electric heater; (6) compensating electric heater; (7) heat measuring apparatus.

experiments the mercury was filtered and purified by nitric acid, alkali and alcohol before being poured into the installation. Visual observations of the mercury surface in the container during the experiments pointed to the absence of any contamination.

The tests were carried out with two different experimental heat exchangers. The experimental heat exchanger $N1$ was made in the form of a steel tube 600 mm length, with an outside diameter of 14 mm and an inside diameter of 9 mm. The tube has inlet and outlet chambers for mercury at each end, from the cross-cut ends of which it is possible to clean the inside of the tube surface and visual observation of its state can be carried out. The tube was divided into twelve parts by circular grooves to decrease axial heat losses, which could happen for low Pe numbers. An electric heater was wound over the outside tube surface and it provided for heating according to the sinusoidal law.

Control of the winding accuracy was performed by measuring its resistance along the length by a Wheatstone bridge to within 0·01 Ω for a total resistance of the heater equal to 20 Ω. A compensating heater also wound according to the sinusoidal law, was mounted above the main heater to compensate for heat losses. Three sections of heat measuring apparatus were mounted between the heaters to control the compensation of heat losses.

The electric heaters are fed by a direct current of 130 V from a constant current source. The stability of mercury cooling is possible due to the tank with cooling water at a constant level. The wall temperature is measured by twelve copper–constantan thermocouples placed in the middle of each part of the tube (twelve in all). Mercury intake temperature and the temperature at which mercury leaves the heat exchanger are also measured by copper–constantan thermocouples placed in the wells of the chambers.

The electromotive force of the thermocouples is measured by a potentiometer. The maximum heat unbalance between the electrical power supplied to the experimental heat exchanger and mercury heating does not exceed 3–4 per cent. The experimental heat exchanger $N2$ has the same length of 600 mm and is made of the same material, but as shown in Fig. 2, it was divided into twenty-four parts and differs from the first heat exchanger in having a tube of larger diameter (d_i = 13·5 mm and d_e = 17·5 mm, l/d = 44·6). The experimental heat exchanger inlet and outlet chambers were designed in such a way, that it is possible to insert displacers with an outside diameter of 8·1 mm and 10 mm into the tube, forming an annular clearance with the ratio d_2/d_1 = 1·68 and 1·35 for the mercury flow through it. The displacers are put into the experimental heat exchanger in jackets at both sides. This prevents deformations when thermal expansion occurs and allows the displacers to be regulated in order to measure the influence of possible eccentricity. Three narrow stops are placed into one section of the displacers at an angle of 120° to avoid eccentricity. The winding of the heater and the whole measuring scheme is the same as with the experimental heat exchanger $N1$. Thus, the heat exchanger $N2$ allowed heat transfer to mercury for two geometries to be measured: in a circular tube with l/d = 44·6 and in annular clearances with the ratios l/d = 110 and 170.

The experiments were performed at an average mercury temperature of 40° to 60°C and at a maximum heat flow at the centre of the tube 50×10^3 kcal/m² hr.

RESULTS

Experiments were held with the same experimental heat exchangers and the same thermocouples on determination of heat transfer to mercury in a circular tube with boundary conditions q_s = const. to control the correctness of the work of the installation. In this case a new electric heater with a constant space between the turns of the wire was wound over the tube. The experimental data for the heat exchanger $N1$ are exact to ±5 per cent and coincide with those given by Johnson [8] on heat transfer from mercury with q_s = const. For the experimental heat exchanger $N2$ the values are somewhat higher due to different intake conditions.

If we have a sinusoidal heat load distribution along the length of the channel, then the value of the maximum wall temperature is of particular interest. The results are therefore given in the form of a relationship between the maximum dimensionless wall temperature

Vol. 1 1960

and the number Pe. The distribution of the wall temperature along the channel was found for each experiment. An average liquid temperature distribution along the length may be found from the heat balance equation. Thus, we can find the local temperature differences and calculate the local dimensionless heat transfer coefficient Nu_x with the help of the temperature distribution throughout the wall and in the liquid. It must be emphasized that the temperature throughout the wall in the maximum region has a gently sloping form. An exact definition of the position of this maximum is therefore not quite easy and strictly we may only speak of the value of the maximum.

The results of heat transfer measurements to turbulent mercury flow in a circular tube with sinusoidal heat load distribution along the length of the tube are shown in Fig. 3 in the form of the dependence

$$\frac{(t_s)_{\max} - t_a}{t_b - t_a} = f(Pe)$$

for $l/d = 44{\cdot}6$ and 67. Consequently from the examination of this figure all the experimental

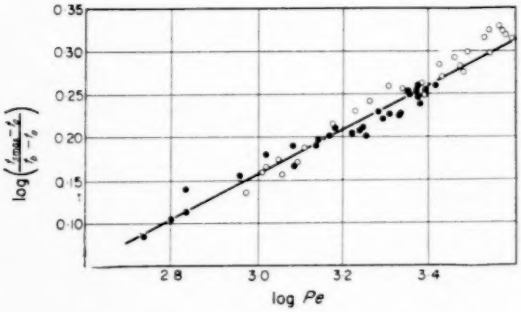

FIG. 3. Heat transfer to mercury in the circular tube at $q = q_0 \cdot \sin \pi x/l$; ○ $l/d = 44{\cdot}6$; ● $l/d = 67$.

points within these co-ordinates may be represented with an exactness equal to ± 7 per cent by a single dependence

$$\theta_{\max} = \frac{(t_s)_{\max} - t_a}{t_b - t_a} = 0{\cdot}22\, Pe^{0{\cdot}27}$$

The same dependence for the channels with an annular section ($l/d = 110$ and 170) is depicted in Fig. 4. An equivalent hydraulic diameter

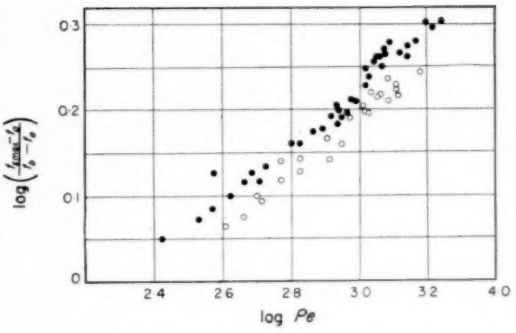

FIG. 4. Heat transfer to mercury in the annular channels at $q = q_0 \cdot \sin \pi x/l$; ○ $d_m = 5{\cdot}4$ mm, $l/d = 110$; ● $d_m = 3{\cdot}5$ mm, $l/d = 170$.

$d_m = d_2 - d_1$ is taken here for a determinative value in numbers Pe. So one can draw the conclusion that $\theta_{\max}$ in annular channels at $q = q_0 \cdot \sin \pi x/l$ in a first approximation will be uniform for both annular clearances ($d_m = 5{\cdot}4$ mm and $3{\cdot}5$ mm). Thus we can see that for annular clearances at $q = q_0 \cdot \sin \pi x/l$ besides the ratio l/d, the equivalent diameter d_m influences the heat transfer. Strictly speaking, the equivalent diameter cannot be applied to the calculation of heat transfer from a liquid metal in an annular clearance.

Fig. 5 gives a comparison of the local number Nu_x for a circular tube of the present investigation with the solution of the problem on an electric integrator [6]. The solution was derived for two approximations of a turbulent thermal diffusivity coefficient in previous works [1, 2, 7].

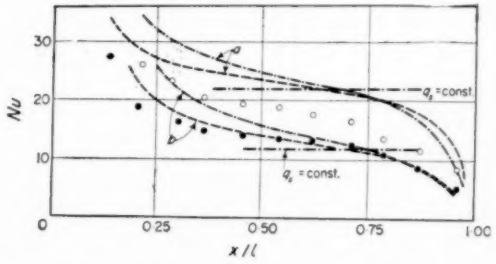

FIG. 5. Comparison of local mercury heat transfer in circular tubes for $q = q_0 \cdot \sin \pi x/l$ with the solution on an electric integrator [6] for $Re = 100 \times 10^3$, $Pr = 0{\cdot}025$, (a) with $a_T = \nu_T$, (b) a_T according to [7], ○ $l/d = 44{\cdot}6$, $Pe = 2480$; ● $l/d = 67$, $Pe = 2440$; – – – for $l/d = 67$; — · — · for $l/d = 44{\cdot}6$.

Fig. 5 shows that the data of the experimental investigation are qualitatively in agreement with the solution and are placed between two extreme limits of approximation a_T. The experimental data for $l/d = 44{\cdot}6$ are somewhat higher in comparison with the calculated values and it can be explained, perhaps, by the different intake condition of the experimental heat exchanger $N2$, which differs from that of the heat exchanger $N1$, which has a rounded entrance.

While winding the electric heater sinusoidally the space between the turns of the wire and the edges was made comparatively larger and it essentially influences the accuracy of the determination of local values along the length of a channel. But the heat flow values and the wall temperatures decrease at the edges and these regions are therefore of less interest for the investigation. We are interested more in the region of a maximum heat flow and a maximum wall temperature (i.e. the regions at the centre of the tube) where the space between the turns of the wire is of the order of thickness of the wall tube and the error due to it does not exceed 3 per cent. The estimation of heat expansion over the tube wall gives evidence of the fact that even at Peclet numbers greater than 100 the error due to expansion does not exceed 0·1 per cent.

REFERENCES

1. R. C. Martinelli, *Trans. Amer. Soc. Mech. Engrs.* **69** (1947).
2. R. Lyon, *Chem. Engng. Progr.* **47** (1951).
3. R. A. Seban and T. T. Shimazaki, *Trans. Amer. Soc. Mech. Engrs.* **73** (1951).
4. S. S. Kutateladze, V. G. Borishansky, I. I. Novikov and O. S. Fedynsky, *Zhidkometallicheskie teplonositeli* (*Fluid Metaltic Heat Carriers*). Atomizdat, Moscow (1953).
5. L. S. Dzung, *Second United Nations International Conference on the Peaceful Uses of Atomic Energy*, Paper Nos. 253, 254. Geneva (1958).
6. V. I. Petrovichev and L. S. Kokorev, *Inzh.-fiz zh.* No. 12 (1959).
7. M. A. Mikheev, V. A. Baum, K. D. Voskresensky and O. S. Fedynsky, *Reaktorostroenie i teorija* (*Reactor Construction and Theory*). U.S.S.R. Academy of Sciences, Moscow (1955).
8. H. A. Johnson and W. J. Clabaugh, *Trans. Amer. Soc. Mech. Engrs.* **76**, No. 4 (1954).

Vol. 1 1960

Int. J. Heat Mass Transfer. Vol. 1, pp. 121–138. Pergamon Press 1960. Printed in Great Britain.

A MECHANISM OF TURBULENT HEAT TRANSFER IN LIQUID METALS

N. Z. AZER† **and B. T. CHAO**‡

†University of Alexandria, UAR (Egypt) and ‡University of Illinois, Urbana, Ill.

(*Received April* 1959; *revised* 15 *February* 1960)

Abstract—A simplified mechanism of turbulent heat transfer, based on a modification of Prandtl's mixing-length hypothesis, has been proposed. It is assumed that there is a continuous change of momentum and energy during the flight of the eddy. Two expressions giving the ratio of eddy diffusivities for heat and momentum were obtained for fully developed pipe flow. One is for fluids of Prandtl number ranging from 0·6 to 15 and the other for liquid metals. Both correctly predict the influence of Reynolds number, Prandtl number and radial location across the pipe on the diffusivity ratio when compared to trends revealed by limited published data.

Computation of Nusselt number and temperature profile in liquid metals were carried out under conditions of constant wall flux using the deduced expression for diffusivity ratio. They agree well with experimental results. For practical calculation of film coefficient of heat transfer, the following interpolation formula may be used:

$$N_{Nu} = 7 + 0{\cdot}05\, N_{Pr}^{0{\cdot}25}\, N_{Pe}^{0{\cdot}77}$$

which fits the calculated data with a maximum deviation of less than 12 per cent for $N_{Pr} < 0{\cdot}1$ and $N_{Pe} < 15{,}000$. Limiting values of Nusselt number as $N_{Pr} \to 0$ and $N_{Re} \to \infty$ were discussed.

Résumé—Un mécanisme simplifié de la transmission de chaleur turbulente, fondé sur une modification de l'hypothèse de Prandtl sur la longueur de mélange, est proposé. On suppose qu'il y a une variation continue de la quantité de mouvement et d'énergie pendant la trajectoire de la masse tourbillonnaire. Deux expressions donnat le rapport des diffusivités turbulentes pour la chaleur et la quantité de mouvement ont été obtenues dans le cas d'un écoulement pleinement établi dans une conduite. L'une est valable pour les fluides dont le nombre de Prandtl varie de 0,6 à 15 et l'autre convient pour les métaux liquides. Ces deux expressions permettent de prévoir correctement l'influence du nombre de Reynolds, du nombre de Prandtl et de la distance à l'axe de la conduite sur le rapport des diffusivités, comparativement aux tendances indiquées par les quelques résultats publiés.

Le calcul du nombre de Nusselt et du profil des températures dans les métaux liquides a été effectué, dans les conditions de flux de paroi constant, en se servant de l'expression obtenue pour le rapport des diffusivités. Ce calcul est en bon accord avec les résultats expérimentaux. Pour le calcul pratique d'un coefficient de transmission de chaleur surfacique, on peut utiliser la formule d'interpolation suivante

$$N_{Nu} = 7 + 0{,}05\, N_{Pr}^{0{,}25}\, N_{Pe}^{07{,}7}$$

qui donne les résultats calculés avec un écart maximum inférieur à 12% pour $0{,}1 < N_{Pe} < 15.000$. Les valeurs limites du nombre de Nusselt quand $N_{Pr} \to 0$ et $N_{Pe} \to \infty$ sont discutées.

Zusammenfassung—Für die turbulente Wärmeübertragung wird ein vereinfachter Mechanismus vorgeschlagen, der auf einer Abwandlung der Hypothese der Mischungslänge nach Prandtl beruht. Es wird angenommen, dass sich während der Bewegung eines Ballens Impuls und Energie kontinuierlich ändern. Für voll entwickelte Rohrströmung erhält man zwei Ausdrücke für das Verhältnis der turbulenten Leitfähigkeiten für Wärme und Impuls, einen für den Bereich der Prandtlzahl von 0,6 bis 15 und den anderen für flüssige Metalle. Beide geben den Einfluss der Reynoldszahl, der Prandtlzahl und der radialen Koordinate im Rohr auf das Verhältnis der Wärmeleitfähigkeiten richtig wieder, wenn man sie mit Literaturwerten vergleicht.

Nusseltzahlen und Temperaturprofile für flüssige Metalle wurden unter der Bedingung konstanter Wärmestromdichte an der Wand berechnet, wobei der abgeleitete Ausdruck für das Verhältnis der Leitfähigkeiten verwendet wurde. Die Ergebnisse stimmen gut mit Messungen überein. Für die praktische Berechnung kann folgende Gleichung verwendet werden.

$$N_{Nu} = 7 + 0{,}05\, N_{Pr}^{0{,}25}\, N_{Pe}^{0{,}77}$$

Diese Gleichung gibt die errechneten Werte mit einer Grössenabweichung von weniger als 12% $N_{Pr} < 0{,}1$ und $N_{Pe} < 15\,000$. Auch die Grenzwerte der Nusseltzahl für $N_{Pr} \to 0$ und $N_{Re} \to \infty$ werden diskutiert.

Abstract—Предлагается упрощенный механизм турбулентного теплообмена, основанный на видоизменённой гипотезе Прандтля о длине смешения. Допускается, что происходит непрерывное изменение количества движения и энергии за время движения вихря. Для стабилизированного потока в трубе получены два соотношения между коэффициентом диффузии вихря при переносе тепла и количеством движения. Оба выражения правильно отображают влияние критериев Рейнольдса, Прандтля и радиальной координаты, что и подтверждается сравнением с имеющимися опубликованными данными.

Вычисление критерия Нуссельта и температурного профиля в жидких металлах проводилось в условиях постоянного потока тепла на стенке с использованием соотношения коэффициентов диффузии вихря. Эти данные хорошо согласуются с результатами эксперимента. Для практического расчёта коэффициента теплообмена можно использовать следующую интерполяционную формулу

$$N_{Nu} = 7 + 0{,}05\, N_{Pr}^{0{,}25}\, N_{Pe}^{0{,}77}$$

которая даёт меньше отклонения чем 12% для $N_{Pe} < 0{,}1$ и $N_{Pe} < 15\,000$. Рассмотрены предельные значения критерия Нуссельта при $N_{Pr} \to 0$ и $N_{Re} \to \infty$.

NOMENCLATURE

a, radius of the eddy (ft);
A, area per unit length of pipe (ft²/ft);
c_p, specific heat at constant pressure (B.t.u./lb °F);†
D, pipe inside diameter, $2r_w$ (ft);
g_c, mass unit conversion constant (lb ft/Lb hr²);†
h, surface conductance (B.t.u./hr ft² °F);
k, thermal conductivity of fluid (B.t.u./hr ft °F);
l, mixing length (ft);
q, rate of radial heat flow at any radius r per unit length of pipe (B.t.u./hr ft);
r, radius (ft);
r_w, inside radius of pipe (ft);
t, fluid temperature (°F);
u, axial velocity (ft/hr);
u_b, mean velocity in pipe (ft/hr);
v', fluctuating velocity in radial direction (ft/hr);
v^*, friction velocity defined by $v^* = \sqrt{(g_c \tau_w/\rho)}$ (ft/hr);
y, radial distance from pipe wall (ft);
ϵ_H, eddy diffusivity for heat transfer (ft²/hr);
ϵ_M, eddy diffusivity for momentum transfer (ft²/hr);
κ, thermal diffusivity of fluid, $= k/c_p\rho$ (ft²/hr);
μ, dynamic viscosity of fluid (lb/ft hr);
ν, kinematic viscosity of fluid (ft²/hr);
ρ, density of fluid (lb/ft³);
τ, shear stress at any radius r (Lb/ft²);
θ, time (hr).

† Lb represents pounds force, and lb pounds mass in this paper.

Dimensionless quantities

b, empirical constant in equations (17) and (20);
f, Darcy friction factor;
N_{Nu}, Nusselt number, hD/k;
N_{Pe}, Peclet number, $N_{Re}\, N_{Pr} = u_b D/\kappa$;
N_{Pr}, Prandtl number, $c_p\mu/k = \nu/\kappa$;
N_{Re}, Reynolds number, $u_b D/\nu$;
N_{St}, Stanton number, $N_{Nu}/N_{Re}N_{Pr} = h/c_p\rho u_b$;
$N_{Pe'}$, $N_{Re'}$, $N_{St'}$ refer to eddy;
U $= u/u_b$;
u^+ $= u/v^*$;
y^+, friction distance parameter defined by $y^+ = v^* y/\nu$;
Z $= r/r_w$;
α $= \epsilon_H/\epsilon_M$, ratio of eddy diffusivity of heat to momentum;

Vol. 1 1960

Subscripts

b, bulk;
c, center of pipe;
e, eddy;
w, wall.

Other symbols or subscripts that might be used are defined in the text.

1. INTRODUCTION

THE advantage of using liquid metals as heat-transfer media is primarily due to their high conductivity, relatively low viscosity and high boiling point. Among the disadvantages, one may mention the difficulty of handling. Some liquid metals are corrosive and chemically reactive. Techniques are being developed to overcome these difficulties.

After the World War II, a widespread interest has appeared in using liquid metals as a coolant in nuclear-chain reactors. In spite of the many attractions and the potentialities of its use in industrial applications, the mechanism of turbulent heat transfer, even under the simple condition of fully developed pipe flow, is not well understood. Lubarsky and Kaufman [1] made a thorough examination and re-evaluation of the experimental results on film coefficient of heat transfer reported by numerous investigators up to 1953. They observed that the bulk of data for Nusselt number were lower than those predicted by the then existing theoretical analyses. After reviewing the available literature on the subject, and performing some preliminary analysis, the writers were led to believe that a major reason for the observed discrepancy could be due to the oversimplified relation commonly assumed for eddy diffusivities of heat and momentum. An improved macroscopic theory of turbulent exchange mechanism is herein proposed which brings closer the theoretical predictions and measured data, both for heat-transfer coefficients and temperature profiles.

The governing equations for the analysis of turbulent heat transfer in circular tubes, at a large distance from the entrance, where both the velocity and temperature profiles are fully developed,† may be expressed as:

$$\frac{\tau g_c}{\rho} = (\nu + \epsilon_M)\frac{du}{dy} \tag{1}$$

$$\frac{q}{Ac_p\rho} = -(\kappa + \epsilon_H)\frac{dt}{dy} \tag{2}$$

Equations (1) and (2) are deduced from the time averaged Reynolds momentum and energy equation for axially symmetric incompressible flow in a pipe, using the following assumptions:

(a) The flow is steady on the average.
(b) All properties are constants.
(c) Axial conduction is negligible when compared to axial convection.‡
(d) Frictional heating is negligible.

The analogous nature of momentum transfer and heat transfer is evident from the foregoing pair of equations. They are linked to each other through the relationship between the two eddy diffusivities. Such a relation depends on the physical model which one selects.

Reynolds [4], who made the first important step in the analysis of turbulent exchange mechanism, postulated that energy and momentum were transferred in the same manner. Reynolds analogy, as the postulate is commonly known, implies $\epsilon_H = \epsilon_M$. Taylor [5], Prandtl [6], von Kármán [7], Martinelli [8, 9], Lyon [10] and others [2, 11, 12] all adopted this assumption in their analysis of turbulent heat transfer. Relatively recently, various experiments have been conducted to determine the diffusivity ratio α from measured temperature and velocity profiles in fluids flowing turbulently in circular tubes as well as between parallel plates [13–21]. It has been established that α is not a constant and, with even more certainty, ϵ_H cannot in general be equal to ϵ_M. In spite of the discrepancies which exist among the published data, it appears that the following has generally been agreed on:

(a) The diffusivity ratio, α, is not a constant across the tube.

(b) For air, α is greater than unity. It exhibits higher values in regions close to the wall and has

† Seban and Shimazaki's definition of fully developed temperature profile is implied, see [2].

‡ Schneider [3] has demonstrated that this is a good assumption provided that $N_{Pe} > 100$.

a decreasing trend toward the pipe center. For flow at high subsonic Mach numbers, an opposite trend has been reported [21]. The latter may be attributed to compressibility. Increasing N_{Re} tends to reduce α but in no case is it less than unity.

(c) For liquid metals, α is less than unity. The variation of α with a greater distance from the wall shows a trend opposite to that described in (b) above. At a fixed N_{Re}, α increases first relatively rapidly and then more slowly as one moves away from the wall. Increasing N_{Re} tends to increase α but in no case it is greater than unity.

Jenkins [22], Deissler [23] and recently Lykoudis and Touloukian [24] attempted to evaluate α on a theoretical basis by modifying Prandtl's mixing-length theory. All the models proposed failed to predict the behavior of α as summarized above.

2. SUGGESTED MODEL FOR THE MECHANISM OF TURBULENT EXCHANGE—MODIFIED MIXING-LENGTH THEORY

In 1925, Prandtl [25] proposed the now famous mixing-length hypothesis. It was presumed that the eddy preserved both its momentum and energy while travelling between layers of a fluid before mixing occurs. Referring to Fig. 1(a), an eddy originated at layer (1) and moving upwards preserved its velocity u_1 and temperature t_1 over an average distance l called the mixing-length till it reached layer (2) where it mixes with the bulk of fluid there and completely loses its identity. An eddy created at layer (2) and moving downwards behaves in a similar way as illustrated in Fig. 1(b). Conceivably, neither the momentum (in the u-direction) nor the energy may be conserved during its travel. In fluids of high thermal conductivity, heat transfer at the surface of the eddy may become appreciable. Thus in Fig. 2(a), an eddy created at layer (1), with velocity u_1 and temperature t_1 will attain a velocity u_1' and temperature t_1' before mixing takes place at layer (2). A similar event takes place for an eddy moving towards the wall as illustrated in Fig. 2(b). With this simple modification of Prandtl's mixing-length hypothesis, one has:

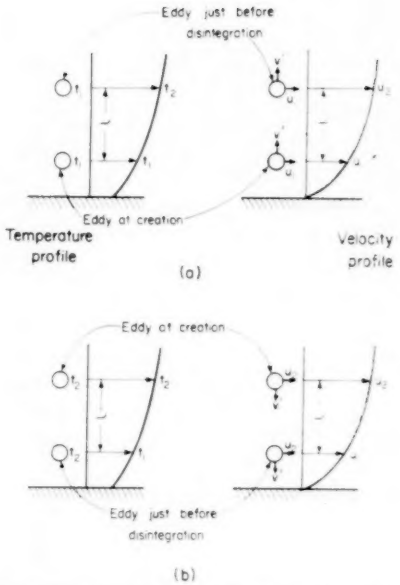

FIG. 1. Prandtl's model of turbulent mixing: (a) eddy moving upward; (b) eddy moving downward.

$$\frac{\epsilon_H}{\epsilon_M} = \frac{(t_2 - t_1')/(t_2 - t_1)}{(u_2 - u_1')/(u_2 - u_1)} = \frac{1 + (u_1' - u_1)/(u_2 - u_1')}{1 + (t_1' - t_1)/(t_2 - t_1')}$$

for an eddy moving upward (3a†)

and

$$\frac{\epsilon_H}{\epsilon_M} = \frac{(t_2' - t_1)/(t_2 - t_1)}{(u_2' - u_1)/(u_2 - u_1)} = \frac{1 + (u_2 - u_2')/(u_2' - u_1)}{1 + (t_2 - t_2')/(t_2' - t_1)}$$

for an eddy moving downward (3b)†

In order to maintain continuity, one would logically assume that there will be just as many eddies moving upward as there are moving downward. (Equations (3a) and (3b) are, in effect, identical.)

† See (33) for derivation.

Vol. 1 1960

In the foregoing equations, $(u_2 - u_1')$ and $(t_2 - t_1')$ are conceived, respectively, as the flunctuating axial component of velocity and temperature at layer (2). The corresponding fluctuating quantities at layer (1) are $(u_2 - u_1)$ and $(t_2' - t_1)$.

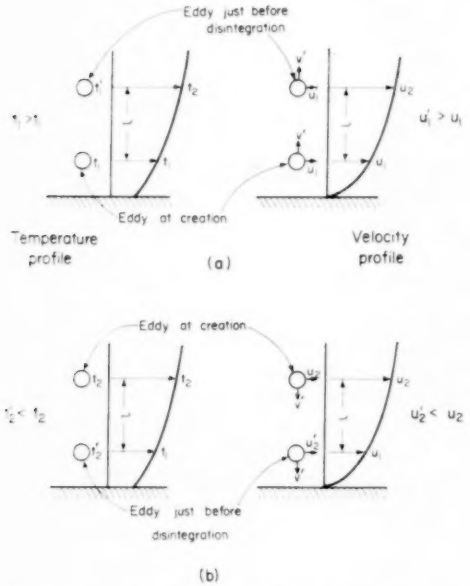

Fig. 2. Modified Prandtl's model of turbulent mixing: (a) eddy moving upward; (b) eddy moving downward.

To ascertain the influence of fluid drag and heat transfer at the surface of the eddy, it is assumed that they are both associated with its boundary layer. For simplicity, the eddy is presumed to be spherical. As it moves from layer (1) to layer (2), its average axial velocity is $\frac{1}{2}(u_1 + u_1')$ while that of the surrounding fluid is $\frac{1}{2}(u_2 + u_1)$. Application of the momentum principle yields,

$$\lambda \frac{\rho}{2}\left(\frac{u_2 - u_1'}{2}\right)^2 S \frac{l}{v'} = \rho V(u_1' - u_1) \qquad (4)$$

S being the surface area of the eddy, V its volume, l/v, the time required for an eddy to travel between layers (1) and (2) and λ the average friction coefficient defined by:

$$\lambda = \frac{\tau_e g_c}{\frac{1}{2}\rho[\frac{1}{2}(u_2 + u_1) - \frac{1}{2}(u_1 + u_1')]^2} = \frac{\tau_e g_c}{\frac{1}{2}\rho[\frac{1}{2}(u_2 - u_1')]^2}$$

For spherical eddy of radius a, $V/S = a/3$. Equation (4), upon rearrangement, becomes

$$\frac{u_1' - u_1}{u_2 - u_1'} = \frac{3}{2}\lambda\left(\frac{l}{a}\right)\frac{u_2 - u_1'}{4v'} \qquad (5)$$

To estimate the amount of heat transfer during flight, the spherical eddy is conceived to have an average temperature T_e $[=\frac{1}{2}(t_1 + t_1')]$ being immersed in an immense fluid initially at a uniform temperature T_0 $[=\frac{1}{2}(t_1 + t_2)]$. The film coefficient of heat transfer at the eddy surface is h_e. We shall now proceed to evaluate the heat transferred from the surrounding fluid to the eddy during the flight time l/v'. With this simplified model,† the differential equation of the temperature field in the surrounding fluid and its initial and boundary conditions are as follows:

$$T_\theta = \kappa\left(T_{RR} + \frac{2}{R}T_R\right), a < R < \infty$$

$$T(0, R) = T_0; T_R(\theta, a) = -h'[T_e - T(\theta, a)], h' = \frac{h_e}{k} \qquad (6)^{\ddagger}_{\ddagger}$$

The solution of equation (6) is

$$\frac{T - T_0}{T_e - T_0} = \frac{a}{R}\frac{ah'}{1 + ah'}\left\{1 - \operatorname{erf}\left[\frac{R - a}{2\sqrt{(\kappa\theta)}}\right] - \exp\left[H(R - a) + H^2\kappa\theta\right] \times \operatorname{erfc}\left[\frac{R - a}{2\sqrt{(\kappa\theta)}} + H\sqrt{(\kappa\theta)}\right]\right\} \qquad (7)$$

where

$$H = \frac{1 + ah'}{a} \qquad (7a)$$

† An alternative model would be to assume that the surrounding fluid is at a constant, uniform temperature T_0 and to calculate the total heat transferred during the time l/v, allowing the temperature of the eddy to vary.

‡ $T_\theta = \dfrac{\partial T}{\partial \theta}$, $T_R = \dfrac{\partial T}{\partial R}$ etc.

The quantity of heat flowing into the eddy during the flight time l/v' is

$$Q_e = \int_0^{\frac{l}{v'}} k(4\pi a^2) T_R(\theta, a) d\theta =$$

$$k(4\pi a^2)(T_0 - T_e)\frac{h'}{1+ah'}\left[\frac{l}{v'} + \frac{aH-1}{\kappa H^2}F(X)\right] \quad (8)$$

where $F(X) = \exp(X^2)\operatorname{erfc} X + \frac{2}{\sqrt{\pi}} X - 1$ (8a)

and $$X = H\sqrt{\left(\kappa \frac{l}{v'}\right)} \quad (8b)$$

This flow of heat results in an enthalpy change of the eddy and is reflected as a temperature increase,

$$t_1' - t_1 = \frac{Q_e}{\frac{4}{3}\pi a^3 c_p \rho} \quad (9)$$

Since $T_0 - T_e = \frac{1}{2}(t_2 - t_1')$, one obtains from equation (9):

$$\frac{t_1' - t_1}{t_2 - t_1'} = \frac{3}{2}\frac{\kappa}{a}\frac{h'}{1+ah'}\left[\frac{l}{v'} + \frac{aH-1}{\kappa H^2}F(X)\right] \quad (10)$$

Equation (10) contains the surface coefficient of the eddy h_e which has yet to be evaluated. According to the proposed model, the heat transfer is characterized by the laminar boundary layer at the eddy surface. Possible influences of curvature behind it are to be ignored, and Pohlhausen's expression [26] for flat plate may thus be used. Hence, for $N_{Pr} = 0{\cdot}6$ to 15,

$$N_{St'} N_{Pr}^{2/3} = \frac{\lambda}{2} \quad (11)$$

with $$\frac{\lambda}{2} = \frac{0{\cdot}664}{N_{Re}^{1/2}}$$

λ being the skin-friction drag coefficient. For the present calculation, the characteristic length in N_{Re} and N_{Nu} is taken as πa which is one-half of the circumference of a great circle of the eddy. Admittedly, such a selection as well as the model used for heat transfer and drag calculation is somewhat arbitrary. It is hoped that the major inaccuracies so introduced could be adequately compensated by including one empirical constant in the analysis which will be described shortly.

With the foregoing characteristic length, the Reynolds and average Nusselt number of the eddy are:

$$N_{Re'} = \left(\frac{u_2 + u_1}{2} - \frac{u_1 + u_1'}{2}\right)\frac{\pi a}{\nu}$$

$$= \frac{u_2 - u_1'}{2}\frac{\pi a}{\nu} \quad (12)$$

$$N_{Nu'} = \frac{h_e(\pi a)}{k} \quad (13)$$

It follows that the average Stanton number of the eddy is:

$$N_{St} = \frac{N_{Nu'}}{N_{Re'} N_{Pr}} \quad (14)$$

Equation (11) is known to be valid for relatively high N_{Pr} fluids as indicated. Since, in this paper, one is primarily concerned with heat transfer in liquid metals, it is necessary to deduce a similar expression for fluids of much smaller N_{Pr}. Using the well-known approximate procedure of solving the integral momentum and energy equation of the boundary layer, one obtains:

$$N_{St'} N_{Pr}^{1/2} = 1{\cdot}64\frac{\lambda}{2} = \frac{1{\cdot}06}{N_{Re'}^{1/2}} \quad (15)\dagger$$

Of particular interest is the fact that N_{Pr} which occurs in equation (11) is raised to the power $\frac{2}{3}$ while in equation (15) it is raised to the power $\frac{1}{2}$. Inasmuch as it has not been possible to use a single expression for the Stanton number, two separate expressions for the eddy diffusivity ratio will be given.

2.1. *Eddy diffusivity ratio for fluids of Prandtl number ranging from* 0·6 *to* 15

If one introduces the Peclet number of the eddy $N_{Pe'}$ $(=N_{Re'} N_{Pr})$ into equation (8b), there results:

$$X = \left(\frac{\pi}{2N_{Pe'}}\right)^{1/2}\left(1 + \frac{N_{Nu'}}{\pi}\right)\left(\frac{l}{a}\frac{u_2 - u_1'}{v'}\right)^{1/2} \quad (16)$$

As pointed out earlier, due to the arbitrariness of the selected shape of the eddy, model for the

† A detailed derivation is given in [33].

Vol. 1 1960

heat transfer process, etc., it was decided to replace the constant 0·664 in the Pohlhausen equation by an empirical constant b, the value of which is to be determined later. Accordingly, one writes equation (11) in the modified form:

$$N_{St'}\, N_{Pr}^{2/3} = \frac{b}{N_{Re'}^{1/2}} \tag{17}$$

Introducing this relation into equations (10) and (16) and inserting the results into equation (3), yield:

$$\left.\begin{aligned}\frac{\epsilon_H}{\epsilon_M} = \\ \frac{1 + \frac{3}{4}b(l/a)\,[(u_2 - u_1')/v']\,N_{Re'}^{-1/2}}{1 + \frac{3}{4}\{1/[0{\cdot}318N_{Pe'} + (1/b)(N_{Re'}^{1/2}\,N_{Pr}^{2/3})]\}} \\ \{(l/a)[(u_2 - u_1')/v'] + 0{\cdot}203bN_{Pr}^{4/3}\,N_{Re'}^{3/2} \\ F(X)/\,(1 + 0{\cdot}318bN_{Pr}^{1/3}\,N_{Re'}^{1/2})^2\}\end{aligned}\right\} \tag{18}$$

in which $F(X)$ is given by equation (8a) and

$$X = \left(\frac{\pi}{2}\right)^{1/2}\left(\frac{b}{\pi N_{Pr}^{1/6}} + \frac{1}{N_{Pe'}^{1/2}}\right)\left(\frac{l}{a}\,\frac{u_2 - u_1'}{v'}\right)^{1/2} \tag{19}$$

2.2. *Eddy diffusivity ratio for liquid metals*

Following the same argument expounded in the preceding section, one modifies equation (15) as

$$N_{St'}\, N_{Pr}^{1/2} = 1{\cdot}64\,\frac{b}{N_{Re'}^{1/2}} \tag{20}$$

The corresponding expressions for equation (18) and (19) are, for this case,

$$\left.\begin{aligned}\frac{\epsilon_H}{\epsilon_M} = \\ \frac{1 + \frac{3}{4}b(l/a)\,[(u_2 - u_1')/v']\,N_{Re'}^{-1/2}}{1 + \frac{3}{4}\{1/[0{\cdot}318N_{Pe'} + (0{\cdot}609/b)\,N_{Pe'}^{1/2}]\}} \\ \{(l/a)\,[(u_2 - u_1')/v'] + 0{\cdot}333bN_{Pe'}^{1/2}F(X)/ \\ (1 + 0{\cdot}522bN_{Pe'}^{1/2})^2\}\end{aligned}\right\} \tag{21}$$

and,

$$X = \left(\frac{\pi}{2}\right)^{1/2}\left(0{\cdot}522b + \frac{1}{N_{Pe'}^{1/2}}\right)\left(\frac{l}{a}\,\frac{u_2 - u_1'}{v'}\right)^{3/2} \tag{22}$$

Equations (18) and (21) contain common unknowns, namely, the ratio of fluctuating velocities $(u_2 - u_1')/v'$, the ratio of mixing-length to radius of the eddy l/a, the Reynolds number of the eddy $N_{Re'}$ and empirical constant b. The following two sections are devoted to their discussion and evaluation.

2.3. *Ratio of fluctuating velocities*

Referring to Fig. 2(a), $u_2 - u_1'$ and v' are, respectively, the fluctuating velocities in the axial and radial direction. Both are complicated functions of space and time; their exact nature is not known. Customarily, they are treated on a statistical basis and expressed in terms of their root-mean square values. These two quantities are so interpreted in this paper.

Numerous experiments have been conducted by various investigators, notably Laufer [27], Reichardt [28], and Wattendorf [29], to study the structure of turbulence in two-dimensional channels. Laufer [30] also carried out one of the most detailed investigations on turbulence in fully developed pipe flow. When the ratio of either fluctuating velocity to the friction velocity $v^*[=\sqrt{(g_c\tau_w/\rho)}]$ were plotted against the dimensionless radial location y/r_w, it was found that, up to a region very close to the wall, both were almost independent of the Reynolds number. Laufer's measurements also indicate that $(u_2 - u_1')/v^*$ and v'/v^* vary almost linearly with radial location, showing an increase towards the wall till a maximum is reached in the buffer zone, followed by a rapid drop as the wall is approached. Laufer's results may be closely approximated by the following expressions:

$$\frac{u_2 - u_1'}{v^*} = 1{\cdot}95\left(1 - 0{\cdot}64\,\frac{y}{r_w}\right) \tag{23}$$

and

$$\frac{v'}{v^*} = 1{\cdot}08\left(1 - 0{\cdot}36\,\frac{y}{r_w}\right) \tag{24}$$

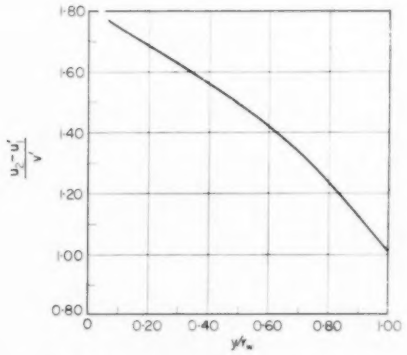

FIG. 3. Variation of fluctuating velocity ratio with radial location across pipe.

It follows that,

$$\frac{u_2 - u_1'}{v'} = 1{\cdot}81\,\frac{1 - 0{\cdot}64\,y/r_w}{1 - 0{\cdot}36\,y/r_w} \qquad (25)$$

which is shown graphically in Fig. 3. Laufer's data were obtained for air, it will be assumed that they remain valid for other fluids.

2.4. *Reynolds number of the eddy $N_{\mathrm{Re}'}$ and the ratio l/a*

Eliminating $(u_2 - u_1')$ from equations (23) and (12) gives,

$$N_{\mathrm{Re}'} = \frac{\pi}{2}\frac{a}{\nu}\left[1{\cdot}95v^*\left(1 - 0{\cdot}64\,\frac{y}{r_w}\right)\right] \qquad (26a)$$

which can be shown to equal

$$N_{\mathrm{Re}'} = 1{\cdot}53\,\frac{a}{l}\,\frac{l}{r_w}\left(1 - 0{\cdot}64\,\frac{y}{r_w}\right)N_{\mathrm{Re}}\sqrt{\left(\frac{f}{8}\right)} \qquad (26b)$$

For $N_{\mathrm{Re}} > 10^5$, Nikuradse [31] reported the following expression for the ratio of mixing length to pipe radius,

$$\frac{l}{r_w} = 0{\cdot}14 - 0{\cdot}08\left(1 - \frac{y}{r_w}\right)^2 - 0{\cdot}06\left(1 - \frac{y}{r_w}\right)^4 \qquad (27)$$

which will be extrapolated for use at lower N_{Re} since no other information is available.

Next, we shall consider the ratio l/a. In the preliminary examination of the behaviour of equation (18), the diffusivity ratio was calculated for air of $N_{\mathrm{Pr}} = 0{\cdot}718$ with the empirical constant b retained as that originally appeared in the Pohlhausen equation, namely, 0·664. Computations were carried out for $y/r_w = 0{\cdot}5$ and for three arbitrarily selected values of $l/a = 2$, 3 and 4. The results are summarized in Table 1.

Table 1. *Prediction of ϵ_H/ϵ_M by equation* (18) *for air of $N_{\mathrm{Pr}} = 0{\cdot}718$, $b = 0{\cdot}664$, $y/r_w = 0{\cdot}5$*

N_{Re}	$\alpha = \dfrac{\epsilon_H}{\epsilon_M}$		
	$\dfrac{l}{a} = 2$	$\dfrac{l}{a} = 3$	$\dfrac{l}{a} = 4$
14,500	1·008	1·018	1·030
80,300	1·007	1·016	1·029

It is seen that the calculated ratio ϵ_H/ϵ_M is not sensitive to variations in l/a. For simplicity we select $l/a = 2$ for subsequent calculations.

Using Nikuradse's expression for l/r_w and $l/a = 2$, the Reynolds number of the eddy may be related to the pipe Reynolds number and Darcy friction factor as:

$$\frac{N_{\mathrm{Re}'}}{N_{\mathrm{Re}}\sqrt{(f/8)}} = 0{\cdot}766\left(1 - 0{\cdot}64\,\frac{y}{r_w}\right)\left[0{\cdot}14 - 0{\cdot}08\left(1 - \frac{y}{r_w}\right)^2 - 0{\cdot}06\left(1 - \frac{y}{r_w}\right)^4\right] \qquad (28)$$

which is shown plotted in Fig. 4. It vanishes at the wall, reaches a maximum at about $y/r_w = 0{\cdot}5$ and then decreases toward the pipe center. $N_{\mathrm{Re}'}$ may be regarded as a measure of the turbulence intensity.

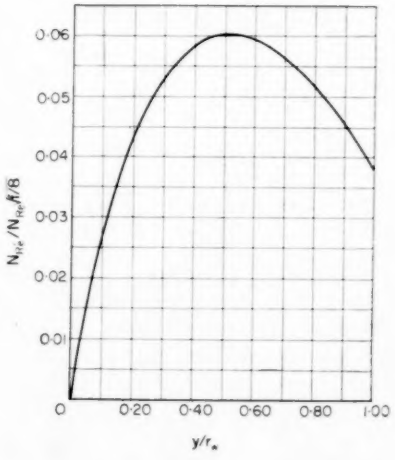

FIG. 4. Variation of $\dfrac{N_{\mathrm{Re}'}}{N_{\mathrm{Re}}\sqrt{(f/8)}}$ with radial location across pipe.

Diffusivity ratios for air as listed in Table 1 are only slightly higher than unity. Page *et al.* [18] reported experimentally determined values of α for air flowing between parallel plates. Sleicher [19] also reported data for air in turbulent pipe flow. While there are some discrepancies between Page's and Sleicher's results, the general behavior with respect to the influence of Reynolds number and location across the pipe or channel seems to be in good agreement.

Vol. 1 1960

However, Sleicher's data have been chosen for the determination of the empirical constant b in equation (18) because they were obtained for pipe flow. After a few calculations, it was found that by assigning $b = 2{\cdot}5$, the predicted value for air at $N_{Re} = 14{,}500$ and $y/r_w = 0{\cdot}35$ could be made to agree with Sleicher's data. The reason for the selection of this particular y/r_w was that the experimental data indicated a nearly constant trend beyond this location. It is pertinent that the artificial matching of the theoretical equation (18) and experimental data was done at only one point and only for $N_{Pr} = 0{\cdot}718$.

Using the expression for the ratio of fluctuating velocities given by equation (25), $l/a = 2$, and $b = 2{\cdot}5$, equations (18) and (21) finally become:

$$\frac{\epsilon_H}{\epsilon_M} = \frac{1 + 6{\cdot}77\phi\, N_{Re'}^{-1/2}}{1 + 0{\cdot}75\, F_1 F_2} \tag{29}$$

in which

$$\phi = \frac{1 - 0{\cdot}64\, y/r_w}{1 - 0{\cdot}36\, y/r_w} \tag{29a}$$

and,

(i) For fluids of N_{Pr} ranging from 0·6 to 15

$$\left.\begin{aligned} F_1 &= \frac{1}{0{\cdot}318 N_{Pe'} + 0{\cdot}4 N_{Pe'}^{1/2} N_{Pr}^{1/6}} \\ F_2 &= 3{\cdot}61\phi + \\ &\quad + \frac{0{\cdot}508 N_{Pe'}^{3/2} N_{Pr}^{-1/6}}{(1 + 0{\cdot}795 N_{Pe'}^{1/2} N_{Pr'}^{-1/6})^2} F(X) \\ X &= 2{\cdot}38\phi^{1/2}(N_{Pe'}^{-1/2} + 0{\cdot}795 N_{Pr}^{-1/6}) \end{aligned}\right\} \tag{29b}$$

(ii) For liquid metals

$$\left.\begin{aligned} F_1 &= \frac{1}{0{\cdot}318 N_{Pe'} + 0{\cdot}244 N_{Pe'}^{1/2}} \\ F_2 &= 3{\cdot}61\phi + \frac{0{\cdot}833 N_{Pe'}^{3/2}}{(1 + 1{\cdot}305 N_{Pe'}^{1/2})^2} F(X) \\ X &= 2{\cdot}38\phi^{1/2}(1{\cdot}305 + N_{Pe'}^{-1/2}) \end{aligned}\right\} \tag{29c}$$

In either case, $N_{Pe'} = N_{Re'} N_{Pr}$, $N_{Re'}$ is given by equation (28) and $F(X)$ by equation (8a).

For approximate calculations, the following may be used:

(i) For fluids of N_{Pr} ranging from 0·6 to 15

$$\frac{\epsilon_H}{\epsilon_M} = \frac{1 + 135 N_{Re}^{-0{\cdot}45} \exp\,[-(y/r_w)^{0{\cdot}25}]}{1 + 57 N_{Re}^{-0{\cdot}46} N_{Pr}^{-0{\cdot}58} \exp\,[-(y/r_w)^{0{\cdot}25}]} \tag{30a}$$

(ii) For liquid metals

$$\frac{\epsilon_H}{\epsilon_M} = \frac{1 + 135 N_{Re}^{-0{\cdot}45} \exp\,[-(y/r_w)^{0{\cdot}25}]}{1 + 380 N_{Pe}^{-0{\cdot}58} \exp\,[-(y/r_w)^{0{\cdot}25}]} \tag{30b}$$

both give a maximum deviation of less than 14 per cent.

3. COMPUTED RESULTS ON DIFFUSIVITY RATIO, α

Equations (29), (29a) and (29b) have been used to evaluate α for fluids of $N_{Pr} = 0{\cdot}718$, 1 and 10 at several N_{Re}. Results obtained for $N_{Pr} = 0{\cdot}718$ are plotted in Fig. 5. For purpose of comparison, Sleicher's experimental results are also shown.

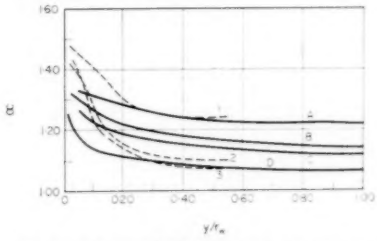

FIG. 5. Comparison of Sleicher's experimental data with calculated values of diffusivity ratio.

$N_{Pr} = 0{\cdot}718$

——— Theoretical prediction

1, A $N_{Re} = 1{\cdot}45 \times 10^4$

B $N_{Re} = 4{\cdot}34 \times 10^4$

3, C $N_{Re} = 8{\cdot}03 \times 10^4$

D $N_{Re} = 3{\cdot}96 \times 10^5$

2 $N_{Re} = 3{\cdot}85 \times 10^4$

— — — Sleicher's data.

It may be recalled that the empirical constant b in equations (18) and (21) was determined by matching the calculated value of α with Sleicher's data at only a single point. It is interesting to note that the predicted variation of α with N_{Re} and radial location does show fair agreement with experiments. While Sleicher reported values of α for y/r_w only up to 0·55, Page's data included regions close to the channel center. The latter indicate a continuous, slight decrease of α towards the channel center—a trend also revealed by the present analysis. Fig. 6 illustrates the calculated results for $N_{Pr} = 1$ and 10. The former differs from Jenkins' prediction [22] which gives $\alpha = 1$ when $N_{Pr} = 1$ irrespective of N_{Re}. No experimental data for higher Prandtl number fluids are available for comparison.

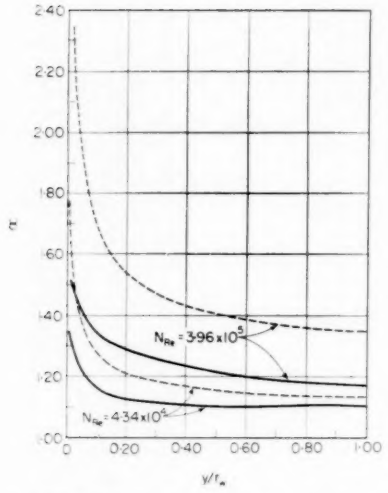

FIG. 6. Calculated variation of diffusivity ratio with radial location for two Prandtl numbers and two Reynolds numbers.
——— $N_{Pr} = 1{\cdot}0$ — — — $N_{Pr} = 10.$

One interesting consequence of the present analysis is that α, for any N_{Pr}, approaches unity as N_{Re} increases indefinitely. When this occurs, both the numerator and denominator of equation (29) become unity. It implies that at very high N_{Re}, the original Prandtl's mixing-length hypothesis becomes valid. At this point, a question which naturally arises is: Why does the previous analysis, such as that of von Kármán [7], Martinelli [9], or Lyon [10] in which α is assumed to be unity for all N_{Re} and N_{Pr}, give good prediction of heat transfer for fluids of N_{Pr} equal to or higher than that of air? The answer lies in the fact that, in such fluids, the thermal resistance is essentially confined to the laminar sub-layer and buffer region. For instance, at $N_{Re} = 10{,}000$, Martinelli [9] reported that over 99 per cent of the temperature difference occurred in the combined laminar sub-layer and buffer zone for a fluid of $N_{Pr} = 100$. The corresponding values for $N_{Pr} = 1$ and 0·01 are 71 per cent and 21 per cent, respectively. Hence, for ordinary fluids, any inaccuracy which one introduces in computing the thermal resistance of the turbulent core would have only minor effect on the prediction of Nusselt number. This is not the case for liquid metals.

It is also seen that Sleicher's data for air which showed $\alpha > 1$ at a region close to wall are not contradictory to the fact that von Kármán's analysis and others ($\alpha = 1$) give reasonably good agreement with experiment in so far as the prediction of heat transfer is concerned. In the laminar sub-layer, turbulence is, by and large, suppressed, and molecular conduction predominates.

The available experimental data of α for liquid metals are those of Isakoff and Drew [15] and Brown *et al.* [20]. Again, for the purpose of

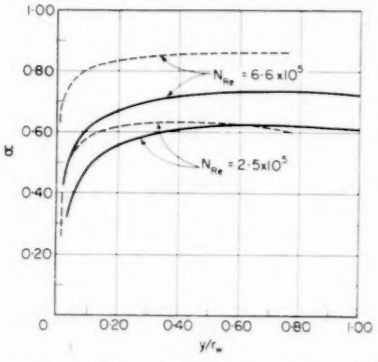

FIG. 7. Comparison of experimental data of diffusivity ratio for mercury due to Brown, Amstead and Short with calculated values.
$N_{Pr} = 0{\cdot}02$
——— Theoretical prediction — — — Brown *et al.*

comparison, numerical calculations of equations (29), (29a) and (29c) were carried out for $N_{Pr} = 0{\cdot}0239$ and 0·02 at several N_{Re}. The two N_{Pr} selected correspond to those of mercury as reported respectively in [15] and [20]. Results of computation are shown in Figs. 7 and 8. The theoretical prediction of equations (29), (29a) and (29c) is seen to be in fair agreement with the experimental measurements of Brown. It is to be emphasized that the comparison made here involves no further matching of the empirical constant which has been previously determined from results on air. At the lower N_{Re}, the agreement is considered good. At the higher N_{Re}, the theory predicts lower values. According to the present analysis one sees that, for liquid metals, increasing N_{Re} tends to increase α, a trend which is an antithesis to that for air or higher N_{Pr}

Vol. 1 1960

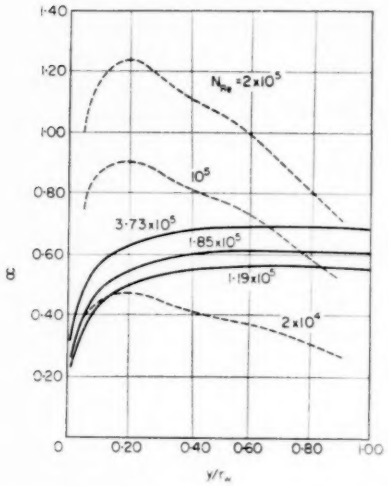

FIG. 8. Comparison of experimental data of diffusivity ratio for mercury due to Isakoff and Drew with calculated values.
$N_{Pr} = 0{\cdot}0239$
— — — Isakoff and Drew ——— Present analysis.

fluids. Fig. 7 shows that there is a slight drop in the values of α as the center of the pipe is approached—a phenomenon which may also be noticed in Brown's data. Isakoff and Drew's results do not agree with those of Brown *et al.*, and hence are not in agreement with those predicted by the present theory. Drew and Isakoff based their calculation on temperature data which showed considerable scatter. As will be pointed out in a later section, some of their reported temperature profiles fell below the limiting profile of $N_{Pr} = 0$. This led the writers to believe that Isakoff and Drew's results are most probably in error.

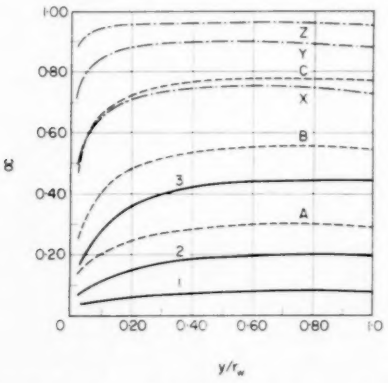

FIG. 9. Predicted variations of diffusivity ratio with radial location as influenced by Prandtl numbers and Reynolds numbers
——— $N_{Pr} = 0{\cdot}001$ 1, A, X $N_{Re} = 4{\cdot}34 \times 10^4$
— — — $N_{Pr} = 0{\cdot}01$ 2, B, Y $N_{Re} = 3{\cdot}96 \times 10^5$
— - — $N_{Pr} = 0{\cdot}1$ 3, C, Z $N_{Re} = 3{\cdot}24 \times 10^6$.

Equations (29), (29a) and (29c) have also been used to calculate for $N_{Pr} = 0{\cdot}001$, $0{\cdot}01$ and $0{\cdot}1$ and for $N_{Re} = 4{\cdot}34 \times 10^4$, $3{\cdot}96 \times 10^5$ and $3{\cdot}24 \times 10^6$. Fig. 9 summarizes the results obtained. For a given N_{Pr}, α increases with increase in N_{Re}. In the limit, as $N_{Re} \to \infty$, $\alpha \to 1$ for any N_{Pr}. As the distance from wall increases, α also increases, first rapidly and then slowly till it assumes a more or less constant value. For the highest Prandtl number investigated, namely $0{\cdot}1$, there is less variation of α with respect to radial location across the pipe, particularly when the Reynolds number is large.

4. NUSSELT NUMBER AND TEMPERATURE PROFILE FOR FULLY DEVELOPED PIPE FLOW WITH CONSTANT WALL FLUX

The case to be considered concerns the turbulent flow of liquid metals in smooth, circular pipes with constant wall flux. The fluid properties are regarded as constants. This problem was first considered by Martinelli [9] who recognized the importance of molecular conduction in the turbulent core for the transfer of heat in fluids of very low Prandtl number, such as molten metals. Martinelli's analysis was later modified by Lyon [10] who showed that the Nusselt number could be expressed as:

$$\frac{1}{N_{Nu,\,b}} = 2\int_0^1 \frac{(\int^z UZdZ)^2}{Z[1+\alpha(\epsilon_M/\nu)N_{Pr}]}\,dZ \qquad (31)$$

In the above expression, the Nusselt number is based on temperature difference between the wall and the bulk of the fluid. Lyon integrated equation (31) numerically, using point values of velocity and ϵ_M/ν as evaluated directly from Nikuradse's data [31]. Like Martinelli, Lyon assumed that $\alpha = 1$ in his calculations. He approximated his results of calculation for

Nusselt number by the following interpolation formula:

$$N_{\mathrm{Nu},b} = 7 + 0{\cdot}025N_{\mathrm{Pe}}^{0{\cdot}8} \tag{32}$$

which has been recommended for use in the *Liquid Metals Handbook* [32]. The results of experiments are on the average, about 50 per cent lower than the prediction of equation (32). It is clear from equation (31) that, for a given N_{Pr}, the Nusselt number depends on a, ϵ_M/ν and the velocity profile whose effect is reflected in the integral $\int_0^z UZdZ$. The latter two quantities will be discussed separately in the following sections.

4.1. *The integral* $\int_0^z UZdZ$

For an incompressible fluid of constant properties flowing turbulently in a pipe with fully developed velocity and temperature profiles, Seban and Shimazaki [2] showed that, for constant wall flux, the axial temperature gradient is independent of the radial position in the pipe. Under such circumstance, it can be readily shown that the radial q-distribution is given by:

$$\frac{q}{q_w} = 2\int_0^z UZdZ = \frac{\displaystyle\int_{y/r_w}^1 u^+(1 - y/r_w)\,d(y/r_w)}{\displaystyle\int_0^1 u^+(1 - y/r_w)\,d(y/r_w)} \tag{33}$$

If the logarithmic velocity profile proposed by von Kármán [7] were adopted, namely,

$$\left.\begin{aligned} u^+ &= y^+, && 0 \leqslant y^+ < 5\\ u^+ &= -3{\cdot}05 + 5\ln y^+, && 5 \leqslant y^+ < 30\\ u^+ &= 5{\cdot}5 + 2{\cdot}5\ln y^+, && y^+ \geqslant 30 \end{aligned}\right\} \tag{34}$$

the integrals in equation (33) could be readily evaluated and the result expressed in a closed form. It is,

$$\left.\begin{aligned} &\frac{q}{q_w} = \\ &\frac{\begin{aligned} &2{\cdot}75(1 - y/r_w)^2 + 1{\cdot}25\ln N_{\mathrm{Re}}/2\sqrt{(f/8)}\\ &\quad - 1{\cdot}25y/r_w(2 - y/r_w)\ln\left[y/r_w\,N_{\mathrm{Re}}/2\right.\\ &\quad \left.\sqrt{(f/8)}\right] - 0{\cdot}625(1 - y/r_w)(3 - y/r_w) \end{aligned}}{\begin{aligned} &1{\cdot}25\ln N_{\mathrm{Re}}/2\sqrt{(f/8)} - 127{\cdot}8\\ &(N_{\mathrm{Re}}\sqrt{(f/8)^{-1}} + 22{,}960[N_{\mathrm{Re}}\\ &\quad \sqrt{(f/8)}]^{-2} + 0{\cdot}875 \end{aligned}} \end{aligned}\right\} \tag{35}$$

Equation (35) ignores the influence of laminar sub-layer and buffer region. If the latter is considered additional terms will appear in the numerator of the above equation. A detailed derivation has been given [33]. For the present analysis, equation (35) may be used for the entire cross-section without sacrificing accuracy. Fig. 10 is a graphical representation of such distribution for N_{Re} ranging from 4×10^3 to $3{\cdot}24 \times 10^6$.

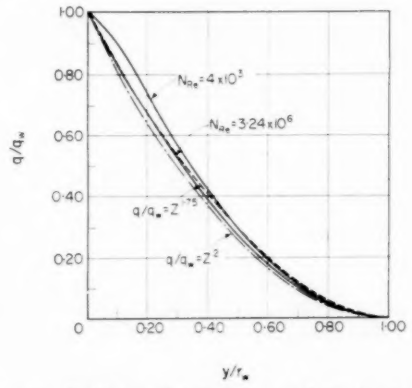

FIG. 10. Radial q-distribution in fully developed turbulent pipe flow.
——— q-distribution according to equation (35)
— - — Martinelli's distribution
- - - - Simple distribution used in the present analysis.

These correspond to the extremes of N_{Re} used by Lyon. Calculated data for all intermediate N_{Re} lie within the narrow loop bounded by the two solid curves. It is thus seen that for the realm of N_{Re} considered, the ratio q/q_w may be closely approximated by a single curve expressible by:

$$\frac{q}{q_w} = 2\int_0^z UZdZ \simeq \left(1 - \frac{y}{r_w}\right)^{1{\cdot}75} = Z^{1{\cdot}75} \tag{35a}$$

Lyon's individually computed values agree well with this simple result. This is demonstrated in Table 2.

That the q-distribution in turbulent pipe flow is insensitive to Reynolds number variation has also been confirmed experimentally by Isakoff [34].

With the foregoing simplification, equation (31) could be written as:

$$\frac{1}{N_{\mathrm{Nu},b}} = \tfrac{1}{2}\int_0^1 \frac{Z^{2{\cdot}5}}{1 + (a\,\epsilon_M/\nu)N_{\mathrm{Pr}}}\,dZ \tag{36}$$

Table 2. Comparison of the numerical values of the integral $\int_0^z ZUdZ$ *as reported by Lyon and the suggested relation given by equation* (35*a*)

$\frac{y}{r_w}$	Z	$\int_0^z ZUdZ$ due to Lyon			$\frac{Z^{1\cdot75}}{2}$
		$N_{Re} = 4{\cdot}34 \times 10^4$	$N_{Re} = 3{\cdot}96 \times 10^5$	$N_{Re} = 3{\cdot}24 \times 10^6$	
0	1	0·5022	0·4990	0·5004	0·5000
0·1	0·9	0·4287	0·4230	0·4216	0·4158
0·2	0·8	0·3490	0·3430	0·3405	0·3384
0·3	0·7	0·2735	0·2680	0·2651	0·2679
0·4	0·6	0·2047	0·2000	0·1974	0·2045
0·5	0·5	0·1444	0·1410	0·1386	0·1487
0·6	0·4	0·0936	0·0909	0·0895	0·1006
0·7	0·3	0·0532	0·0515	0·0508	0·0608
0·8	0·2	0·0238	0·0230	0·0228	0·0299
0·9	0·1	0·0060	0·0058	0·0057	0·0089
1·0	0	0	0	0	0

It is interesting to note that the corresponding expression used by Martinelli has the exponent of Z replaced by 3, since the rather crude assumption $u = u_b$, was adopted in his analysis.

4.2. *The ratio of eddy viscosity to kinematic viscosity,* ϵ_M/ν

A rational calculation of the ratio ϵ_M/ν is not possible at the present time since no precise theory of turbulence exists. Consequently, one turns to experimentally measured velocity profile for the evaluation of ϵ_M. After examining the several turbulent velocity profiles proposed by various investigators, namely, Prandtl [35] von Kármán [36], Deissler [37] Reichardt [38] Rannie [39] Ross [40] and Pai [41], the writers came to the following conclusion. The semi-empirical velocity profiles proposed by various investigators may seemingly fit well the experimental data, it does not necessarily follow that the assumed model of turbulence is precise. ϵ_M calculated from the directly measured velocity gradient across the pipe may not be in good agreement with that computed from the semi-empirical equation which is supposedly to represent the velocity distribution. A detailed analysis and discussion is given in [33]. For fluids of relatively high N_{Pr}, any error introduced in the evaluation of ϵ_M will produce only minor effect on the final result of Nusselt number calculations. This is no longer true for liquid metals. In view of these observations, it was decided to use Nikuradse's data of ϵ_M/ν [31] which were evaluated directly from the measured velocity gradient. However, no data were reported by Nikuradse for $y/r_w < 0{\cdot}02$. Extrapolation was then made with the aid of Kármán profile as given by equation (34). For those cases of N_{Re} for which no information was reported by Nikuradse, Deissler's velocity profile [37] has been used for the determination of ϵ_M.

4.3. *Result of Nusselt number calculations*

With α and ϵ_M/ν known, the Nusselt number may be evaluated from equation (36), using numerical integration. For the purpose of comparison, the Prandtl and Reynolds number selected were those used by Lyon, i.e. $N_{Pr} = 0$, 0·001, 0·01, and 0·1 and $N_{Re} = 4{\cdot}34 \times 10^4$, $3{\cdot}96 \times 10^5$ and $3{\cdot}24 \times 10^6$. For the limiting case of $N_{Pr} = 0$, equation (36) may be readily integrated to give $N_{Nu,\,b} = 7$. This limiting Nusselt number is independent of the Reynolds number, at least for the range considered in the present work. As $N_{Re} \to \infty$, the flux distribution becomes linear which has been assumed by Martinelli. Consequently, the exponent of Z in equation (36) should be replaced by 3, which gives a limiting value of 8 as $N_{Pr} \to 0$.

Calculated values of Nusselt number for the four N_{Pr} and three N_{Re} selected are listed in Table 3. Tabulated also are the results reported

Table 3. Calculated values of Nusselt number

N_{Re}	N_{Pr}	N_{Pe}	$N_{Nu,b}$	
			Lyon's theoretical result	Present theory equation (36)
	0	0	6·83	7
$4·34 \times 10^4$	0·001	43·4	7·30	7·04
	0·01	434	10·30	8·01
	0·1	4340	30·5	26·07
	0	0	7·05	7
	0·001	396	9·54	7·46
$3·96 \times 10^5$	0·01	3960	26·5	16·9
	0·1	39,600	132·0	108
	0	0	7·17	7
	0·001	3240	20·8	12·5
$3·24 \times 10^5$	0·01	32,400	100	65·2

by Lyon. A significant difference is seen to exist. For design computations, Lyon approximated his calculated results by equation (32) with a maximum deviation of 12 per cent. Lyon's expression implies that viscosity has no effect on turbulent heat transfer in liquid metals. This, however, can not be confirmed by the present results. Fig. 11 illustrates the independent effect of Prandtl and Reynolds number on the Nusselt number. For $N_{Pr} < 0·1$, and $N_{Pe} < 15{,}000$, the theoretical results of the present analysis could be represented by an interpolation formula of the form:

$$N_{Nu,\,b} = 7 + 0·05\, N_{Pe}^{0·77}\, N_{Pr}^{0·25} \qquad (37)$$

which gives a maximum deviation of less than 12 per cent.

To ascertain the accuracy of equation (37), some of Lubarsky and Kaufman's re-evaluated experimental data on mercury and lead–bismuth eutectic [1] were reproduced in Figs. 12(a, b, c)

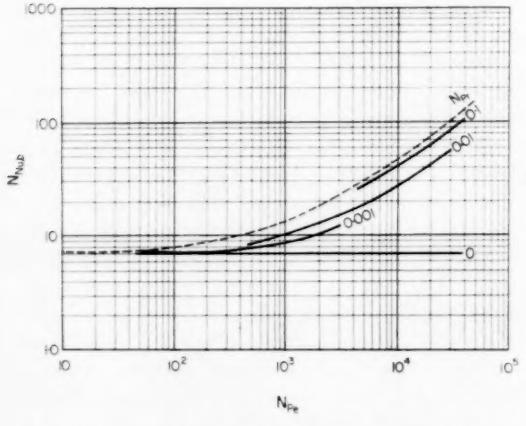

FIG. 11. Comparison of Lyon's equation and the predicted Nusselt numbers according to the present analysis.
— — — Lyon's equation $N_{Nu,b} = 7 + 0·025 N_{Pe}^{0·8}$.

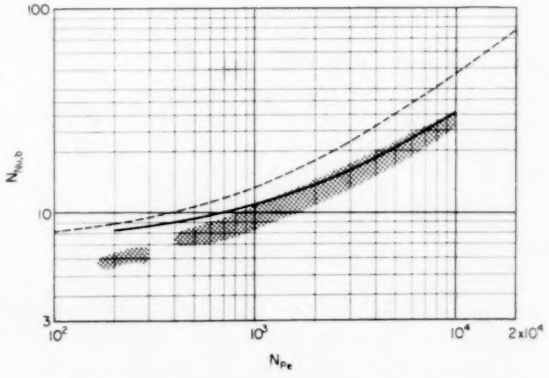

FIG. 12(a). Comparison of experimental Nusselt number for mercury due to Johnson, Clabaugh and Hartnett [1] with the present analysis.
$N_{Pr} = 0·022$
— — — Lyon
——— Present analysis, equation (37).

Vol. 1 1960

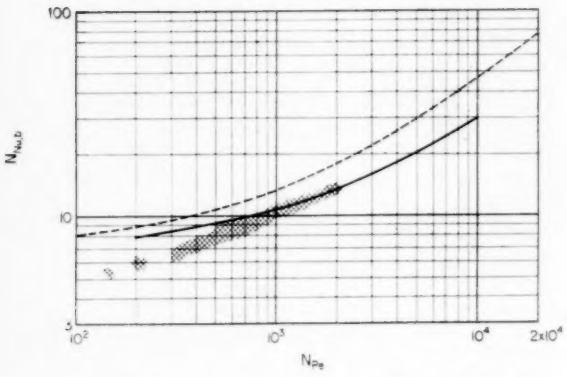

FIG. 12(b). Comparison of experimental Nusselt number for mercury due to Trefthen [1] with the present analysis.
$N_{Pr} = 0{\cdot}02$
– – – – Lyon
——— Present analysis, equation (37).

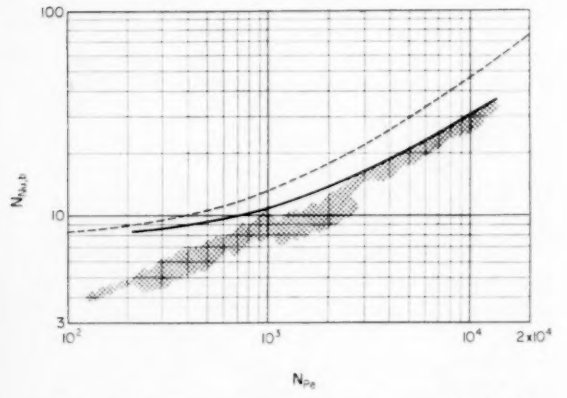

FIG. 12(c). Comparison of experimental Nusselt number for mercury due to Stromquist [1] with the present analysis.
$N_{Pr} = 0{\cdot}02$
— — — Lyon
——— Present analysis, equation (37).

and Figs. 13(a, b). Comparison is made to those predicted by equation (37) as well as to those of Lyon. The improvement over Lyon's expression is obvious. However, according to the proposed theory, the lowest possible Nusselt number is 7 but the bulk of experimental data at low Peclet numbers indicate a value considerably less than 7. It is not clear at the present time whether this indicates a deficit in the theory or is due to errors in experimental data. In a discussion of [24], Lyon pointed out that since most of the data in this range of N_{Pe} were obtained in a horizontal tube with dense fluids (mercury and lead–bismuth), the stratifying effect of thermal expansion might have been the cause.

Having carefully examined published data on liquid metal heat transfer, Lubarsky and Kaufman [1] proposed an empirical equation of the form:

$$N_{Nu,\,b} = 0{\cdot}625\, N_{Pe}^{0{\cdot}4} \qquad (38)$$

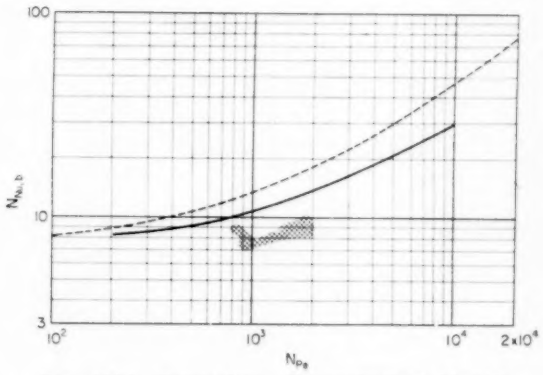

FIG. 13(a). Comparison of experimental Nusselt number for lead–bismuth eutectic due to Seban [1] with the present analysis.
$N_{Pr} = 0{\cdot}02$
— — — Lyon
——— Present analysis, equation (37).

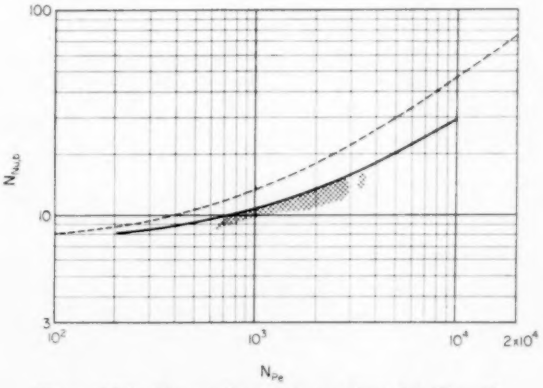

FIG. 13(b). Comparison of experimental Nusselt number for lead–bismuth eutectic due to Johnson, Hartnett and Clabaugh [1] with the present analysis.
$N_{Pr} = 0{\cdot}023$
— — — Lyon
——— Present analysis, equation (37).

which has been claimed to best fit most of the fully developed turbulent heat transfer data on liquid metals. It is shown plotted in Fig. 14 along with the theoretical relation depicted by equation (37). Like Lyon's expression, equation (38) does not involve viscosity. At the present

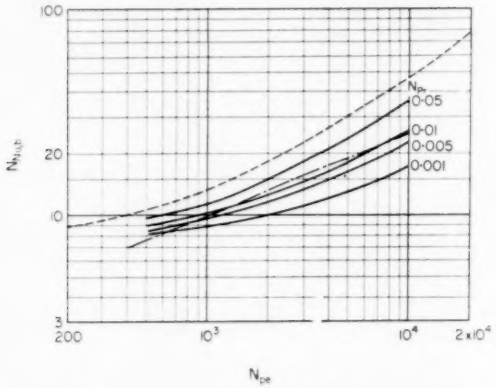

FIG. 14. Comparison of Lyon's theoretical prediction, the empirical relation due to Lubarsky and Kaufman with the present analysis.
— — — Lyon $N_{Nu,b} = 7+0{\cdot}025N_{Pe}^{0{\cdot}8}$
———— Present analysis $N_{Nu,b} = 7+0{\cdot}05N_{Pe}^{0{\cdot}77}N_{Pr}^{0{\cdot}25}$
—·—·— Lubarsky and Kaufman $N_{Nu,b} = 0{\cdot}625N_{Pe}^{0{\cdot}4}$.

time, experimental data are not available to confirm or to contradict the independent effect of N_{Pr} as indicated by equation (37).

4.4. *Temperature profile*

If the dimensionless variable Z is introduced into equation (2), followed by using the q-distribution given by equation (35a), one obtains, upon integration,

$$t_w - t = \frac{q_w}{A_w}\frac{r_w}{k}\int_z^1 \frac{Z^{0{\cdot}75}}{1+\alpha(\epsilon_M/\nu)N_{Pr}}\,dZ \qquad (39)$$

Hence, the normalized temperature profile is

$$\frac{t_w - t}{t_w - t_c} = \frac{\int_z^1 \{Z^{0{\cdot}75}\,dZ/[1+\alpha(\epsilon_M/\nu)\,N_{Pr}]\}}{\int_0^1 \{Z^{0{\cdot}75}\,dZ/[1+\alpha(\epsilon_M/\nu)\,N_{Pr}]\}} \qquad (40)$$

For the limiting case of vanishingly small Prandtl number, but finite N_{Re}, equation (40) reduces to a simple form:

$$\frac{t_w - t}{t_w - t_c} = 1 - Z^{1{\cdot}75} \qquad (41)$$

which is independent of the Reynolds number, at least for the range considered in this paper. An interesting corollary is: For a fluid of very low N_{Pr}, say 0·001 or less, one might expect that the influence of N_{Re} on both temperature profile and $N_{Nu,b}$ would be small.

On the other hand as $N_{Pe} \to \infty$, the velocity profile becomes flat, and the heat flux (q/A) distribution becomes linear. The temperature distribution is then given by:

$$\frac{t_w - t}{t_w - t_c} = \frac{\int_z^1 \{ZdZ/[1+\alpha(\epsilon_M/\nu)\,N_{Pr}]\}}{\int_0^1 \{ZdZ/[1+\alpha(\epsilon_M/\nu)\,N_{Pr}]\}} \qquad (42)$$

which has been indiscriminately used by Martinelli [9] for all N_{Re}. If, furthermore, the condition $N_{Pr} \to 0$ is introduced into equation (42), there results,

$$\frac{t_w - t}{t_w - t_c} = 1 - Z^2 \qquad (43)$$

which is a parabolic distribution.

Several temperature profiles have been calculated by numerical integration for the following cases for which experimental data are available for comparison: (i) Mercury of $N_{Pr} = 0{\cdot}0239$; $N_{Pe} = 1{\cdot}19 \times 10^5$ and $3{\cdot}73 \times 10^5$. Data reported by Isakoff and Drew [15]. (ii) Mercury of $N_{Pr} = 0{\cdot}02$; $N_{Re} = 2{\cdot}5 \times 10^5$ and $6{\cdot}6 \times 10^5$. Data reported by Brown *et al.* [20]. Results of computation are shown plotted in Figs. 15(a, b)

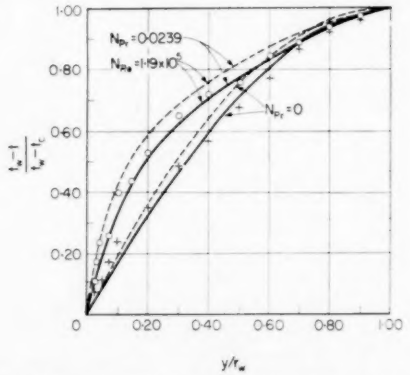

FIG. 15(a). Comparison of measured temperature distribution in mercury by Isakoff and Drew [15] with calculated profiles.
○ Isakoff and Drew $N_{Re} = 1{\cdot}19 \times 10^5$
+ Isakoff and Drew $N_{Re} = 4{\cdot}73 \times 10^4$
— — — Martinelli
———— Present analysis.

Vol. 1 1960

and Figs. 16(a, b). Included are Martinelli's theoretical predictions. In general, Martinelli's profile exhibits a steeper temperature change at the wall vicinity than that predicted by the present theory. This is to be expected since Martinelli's analysis predicts Nusselt numbers which are too high. From the plotted results, it is seen that the temperature profile as calculated from equation (40) has somewhat better agreement with measured data than Martinell's prediction. The difference, however, is not great.

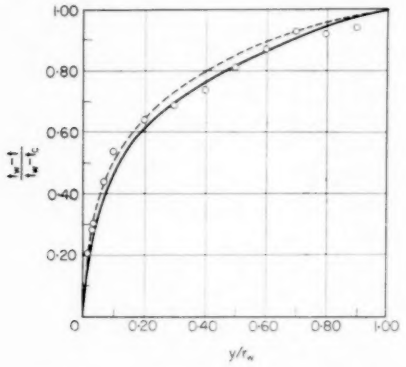

FIG. 15(b). Comparison of measured temperature distribution in mercury by Isakoff and Drew [15] with the calculated profile.
○ Isakoff and Drew $N_{Pr} = 0{\cdot}0239$, $N_{Re} = 3{\cdot}73 \times 10^5$
— — — Martinelli
——— Present analysis.

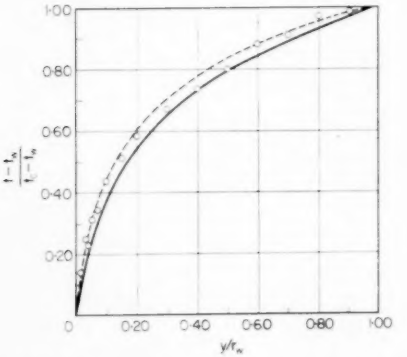

FIG. 16(a) Comparison of measured temperature distribution in mercury by Brown, Amstead and Short [20] with the calculated profile.
○ Brown *et al.* $N_{Pr} = 0{\cdot}02$, $N_{Re} = 2{\cdot}5 \times 10^5$
— — — Martinelli
——— Present analysis.

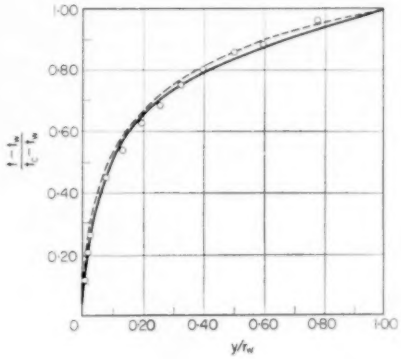

FIG. 16(b). Comparison of measured temperature distribution in mercury by Brown, Amstead and Short [20] with the calculated profile.
○ Brown *et al.* $N_{Pr} = 0{\cdot}02$, $N_{Re} = 6{\cdot}6 \times 10^5$
— — — Martinelli
——— Present analysis.

In a discussion of a recent paper [24], Sleicher pointed out that normalization of temperature profiles often made it inadequate for comparison.

It should be mentioned that the experimental data of Isakoff and Drew exhibit, in many cases, considerable scatter. Many of their data for $N_{Re} = 4{\cdot}73 \times 10^4$ fell below the limiting profile of $N_{Pr} = 0$ as shown in Fig. 15(a), which is most unlikely. As pointed out earlier, this consideration made the writers doubt seriously the accuracy of the α-values reported by Isakoff and Drew. In general, Brown's data had less scatter and showed much better agreement with the theoretical results.

Computed results on Nusselt number and temperature profile in fully developed pipe flow with constant wall temperature will be given in a subsequent paper.

REFERENCES

1. B. LUBARSKY and S. J. KAUFMAN, *Review of Experimental Investigations of Liquid Metal Heat Transfer*. NACA Report 1270 (1956); NACA TN 3336 (1955).
2. R. A. SEBAN and T. T. SHIMAZAKI, *Trans. Amer. Soc. Mech. Engrs.* **73**, 803 (1951).
3. P. SCHNEIDER, *Effect of Axial Conduction on Heat Transfer in the Entrance Regions of Parallel Plates and Tubes*. Heat Transfer and Fluid Mechanics Institute, Preprints of Papers, Stanford University, p. 41 (1956).
4. O. REYNOLDS, *Proc. Manchr. Lit. Philos. Soc.* **14**, 7 (1874).

5. G. I. TAYLOR, *Conditions at the Surface of a Hot Body Exposed to Wind*. Technical Report of the Advisory Committee for Aeronautics, Vol. 2; Reports and Memo no. 272, 423 (1916).
6. L. PRANDTL, *Phys. Z.* **29**, 487 (1928).
7. T. VON KÁRMÁN, *Trans. Amer. Soc. Mech. Engrs.* **61**, 705 (1939).
8. R. C. MARTINELLI, L. M. K. BOELTER and F. JONNASSEN, *Trans. Amer. Soc. Mech. Engrs.* **63**, 447 (1941).
9. R. C. MARTINELLI, *Trans. Amer. Soc. Mech. Engrs.* **69**, 947 (1949).
10. R. N. LYON, *Chem. Engng. Progr.* **47**, 75 (1951).
11. R. G. DEISSLER, *Analytical Investigation of Turbulent Flow in Smooth Pipes with Heat Transfer with Variable Fluid Properties for Prandtl Number of* 1. NACA TN 2242 (1950).
12. R. G. DEISSLER and C. S. EIAN, *Analytical and Experimental Investigation of Fully Developed Turbulent Flow of Air in a Smooth Tube with Heat Transfer with Variable Fluid Properties*. NACA TN 2629 (1952).
13. W. A. SHEPPARD MS Thesis, Mech. Eng. Dept., University of California (1946).
14. W. H. CORCORAN, B. ROUDEBUSH and B. H. SAGE, *Chem. Engng. Progr.* **43**, 135 (1947).
15. S. E. ISAKOFF and T. B. DREW, *General Discussion on Heat Transfer* p. 405. Institution of Mechanical Engineers, London (1951).
16. R. A. SEBAN and T. T. SHIMAZAKI, *General Discussion on Heat Transfer* p. 122. Institution of Mechanical Engineers, London (1951).
17. W. H. CORCORAN, F. PAGE, W. G. SCHLINGER and B. H. SAGE, *Industr. Engng. Chem.* **44**, 410 (1952).
18. F. PAGE, W. G. SCHLINGER, D. K. BREAUX and B. H. SAGE, *Industr. Engng. Chem.* **44**, 424 (1952).
19. C. A. SLEICHER, JR., Ph.D. Thesis in Chemical Engineering, University of Michigan (1955); *Trans. Amer. Soc. Mech. Engrs.* **80**, 693 (1958).
20. H. E. BROWN, B. H. AMSTEAD and B. E. SHORT, *Trans. Amer. Soc. Mech. Engrs.* **79**, 279 (1957).
21. H. LUDWIEG, *Z. Flugwiss.* **4**, 73 (1956).
22. R. JENKINS, *Variation of Eddy Conductivity with Prandtl Modulus and its use in Prediction of Turbulent Heat Transfer Coefficients*. Heat Transfer and Fluid Mechanics Institute, Preprints of Stanford University, p. 147 (1951).
23. R. G. DEISSLER, *Analysis of Fully Developed Turbulent Heat Transfer at Low Peclet Numbers in Smooth Tubes with Application to Liquid Metals*. NACA RM E52F05 (1952).
24. P. S. LYKOUDIS and Y. S. TOULOUKIAN, *Trans. Amer. Soc. Mech. Engrs.* 653 (1958); P. S. LYKOUDIS, *Analytical Study of Heat Transfer in Liquid Metals*. Ph.D. Thesis, School of Mechanical Engineering, Purdue University (1956).
25. L. PRANDTL, *Z. angew. Math. Mech.* **5**, 136 (1925); NACA TM 1231 (1949).
26. E. POHLHAUSEN, *Z. angew. Math. Mech.* **1**, 115 (1921).
27. J. LAUFER, *Investigation of Turbulent Flow in a Two-Dimensional Channel*. NACA Rept. 1053 (1951).
28. H. REICHARDT, *Z. angew. Math. Mech.* **13**, 177 (1933); *Ibid.* **18**, 358 (1938).
29. F. L. WATTENDORF, *J. Aero. Sci.* **13**, 200 (1936).
30. J. LAUFER, *The Structure of Turbulence in Fully Developed Pipe Flow*. NACA TN 2954 (1953).
31. J. NIKURADSE, *Ver. dtsch. Ing. Forsch.* 356 (1932).
32. R. LYON (Editor) *Liquid-Metals Handbook* (2nd Ed.). USAEC (1952).
33. N. Z. AZER, Ph.D. Thesis, University of Illinois (1959).
34. S. E. ISAKOFF, Ph.D. Thesis, Columbia University (1952).
35. L. PRANDTL, *Ergebnisse der Aerodynamischen Versuchanstalt zu Göttingen*, III series (1927).
36. T. VON KÁRMÁN, *Mechanical Similitude and Turbulence*. NACA TM 611 (1931).
37. R. G. DEISSLER, *Analytical and Experimental Investigation of Adiabatic Turbulent Flow in Smooth Tubes*. NACA TN 2138 (1950).
38. H. REICHARDT, *Z. angew. Math. Mech.* **31**, 208 (1951).
39. W. D. RANNIE, Ph.D. Thesis, California Institute of Technology (1951).
40. D. ROSS, *Proceedings of the Third Midwestern Conference of Fluid Mechanics*. University of Minnesota (1953).
41. S. I. PAI, *J. Franklin Inst.* **25b**, 337 (1953).

Vol. 1 1960

Int. J. Heat Mass Transfer. Vol. 1, pp. 139–146. Pergamon Press 1960. Printed in Great Britain.

THERMAL CONTACT RESISTANCE BETWEEN MERCURY AND A METAL SURFACE

T. MIZUSHINA, S. IUCHI, T. SASANO and H. TAMURA*
Department of Chemical Engineering, Kyoto University, Kyoto, Japan

(*Received* 18 *September* 1959; *revised* 19 *February* 1960)

Abstract—This paper reports an experimental analysis of the contact resistance in heat transfer between stagnant mercury and a solid metal surface. It is shown experimentally that there is a very small amount of contact resistance between chromium-plated copper and pure mercury.

Résumé—Cet article décrit une étude expérimentale de la résistance de contact dans la transmission de chaleur entre du mercure au repos et une surface solide métallique. On montre expérimentalement que la résistance de contact entre cuivre chromé et mercure pur est très faible.

Zusammenfassung—Diese Arbeit behandelt eine experimentelle Untersuchung des thermischen Kontaktwiderstandes zwischen ruhendem Quecksilber und einer festen Metalloberfläche. Es zeigt sich aus den Versuchen, dass ein besonders kleiner Kontaktwiderstand zwischen chromplattiertem Kupfer und reinem Quecksilber besteht.

Abstract—В настоящей статье приводятся экспериментальные данные по сопротивлению между инертной ртутью и твердой металлической поверхностью в процессе теплообмена. На основании опытных данных показывается, что термическое сопротивление между пластиной из хромовой меди и чистой ртутью мало.

NOTATION

A = cross-sectional area (m²);
A_{Hg} = equivalent cross-sectional area of mercury mass defined by equation (2) (m²);
h = heat-transfer coefficient (kcal/m² hr °C);
J_0, J_1 = Bessel functions of the first kind and zero- and first-order, respectively;
k = thermal conductivity (kcal/m hr °C);
q = heat transferred per unit time (kcal/hr);
r = radial distance from axis (m);
r_1 = radius of copper cylinder (m);
r_2 = inner radius of Dewar vessel (m);
t = temperature (°C);
Δx = clearance between solid surfaces (m);
x = vertical distance (m);
λ = variable in Bessel function;
Nu = Nusselt number;
Pe = Peclet number.

Subscripts

c = contact surface;
Hg = mercury;
w = difference between two solid walls.

INTRODUCTION

In recent years, great interest in the use of liquid metal as a heat-transfer medium has been stimulated. Martinelli [1] developed the analogy between heat and momentum transfer in the case of liquid-metal heat transfer, and derived a complicated theoretical equation. This equation was simplified by Lyon [2] as follows:

$$Nu = 7{\cdot}0 + 0{\cdot}025\, Pe^{0{\cdot}8} \qquad (1)$$

On the other hand, various investigators have accumulated experimental data, most of which unfortunately do not agree with Lyon's equation and are 30–40 per cent lower than the values predicted by the equation. Considerable numbers of experimental and theoretical investigations have been done in order to give explanations of this discrepancy.

* Present address: Showa Denko Co. Ltd., Kawasaki, Japan.

Most of these investigations can be classified as follows:

(a) Thermal contact resistance between liquid metal and a solid surface (experimental study). These are completely covered by MacDonald and Quittenton [3].

(b) Gas entrainment phenomenon (experimental study). This was discussed by MacDonald and Quittenton [3] and Chelemer [4].

(c) Direct measurement of eddy-diffusivity ratio (experimental study). Isakoff and Drew [5], Brown *et al.* [6] and Mizushina *et al.* [7] studied this subject.

(d) Modification of momentum transfer analogy, assuming special models in heat-transfer mechanism (theoretical study). Deissler [8] and Lykoudis [9] developed different theories, respectively.

(e) Vorticity-transfer theory (theoretical study). Cope [10] discussed this subject.

As mentioned above there might be many reasons for this discrepancy, among which, however, only the thermal contact resistance between liquid metal and a solid metal will be studied experimentally in this paper. Mercury purified chemically was used as a liquid metal. Chromium-plated copper, pure copper and nickel plate were used as solid metal surfaces.

EXPERIMENTAL APPARATUS AND PROCEDURE

The experimental apparatus is shown schematically in Fig. 1. *A* and *B* are copper cylinders 20·5 cm long and 3·7 cm in diameter. The two end surfaces of *A* and *B* were polished on a surface plate to make them as flat as possible and then all surfaces were carefully plated with chromium. The thickness of the chromium deposit is less than $\frac{1}{100}$ mm. In order to measure temperature distributions in the cylinders, fourteen copper–constantan thermocouples were inserted in radial direction and fixed on the centre line of the cylinders. Thus, 1·85 cm from the hot junction of each thermocouple lead is left in an isothermal region. Furthermore each thermocouple lead is wound twice around the cylinders. A melamine resin coating protects them from corrosion by mercury. The axial locations of the thermocouples are shown in Fig. 2. After the thermocouples were fixed in the cylinders, the whole cylinders were put in a 0·01°C thermostatted bath and the thermocouples were calibrated. *C* is an electric heater to supply heat to the upper end of *A*, and *E* is a water jacket to subtract heat from the lower end of *B*. *D* is an electric heater which serves as compensation for the heat loss from the main heater *C*. The cylindrical surfaces are doubly insulated thermally with cellulose–melamine resin coating and a Dewar vessel *F*. The clearance between *A* and *B* can be freely varied with a screw at the top of cylinder *A* and measured accurately to $\frac{1}{20}$ mm by a cathetometer. The parallelness of the two surfaces was ascertained by measuring the clearance between the surfaces at three different points in every run. End surfaces of cylinders *A* and *B* being in contact with mercury, were carefully cleaned physically with benzene or ethyl alcohol before each experimental run. The space between *A* and *B* was filled up carefully with 99·999 per cent pure mercury. Not even a small bubble of gas was allowed to remain in the space. In some series of runs, a copper plate or a nickel plate was inserted in the middle of mercury layer between *A* and *B* at the beginning of runs. In such cases, the plate was supported in

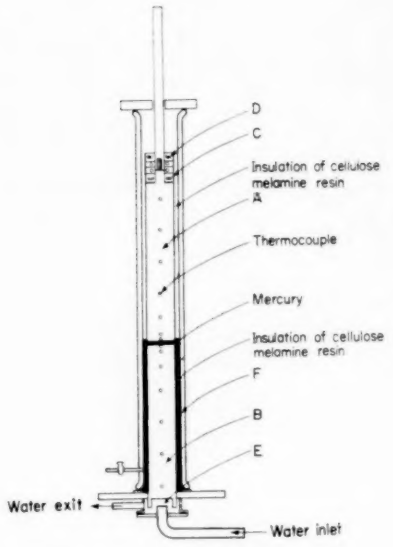

FIG. 1. Experimental apparatus.

Vol. 1 1960

a suitable distance with the needles fixed at the lower end of *A*. Since the thermal insulation was nearly complete, the full amount of the heat supplied to the upper end penetrates the whole system downwards without appreciable loss. This was confirmed by uniformity of the axial temperature gradient in the copper cylinders. The amount of the heat was measured as electric power to heater *C* with a voltmeter and an ammeter. The temperature distribution in the cylinder at the axis of cylinder was measured by

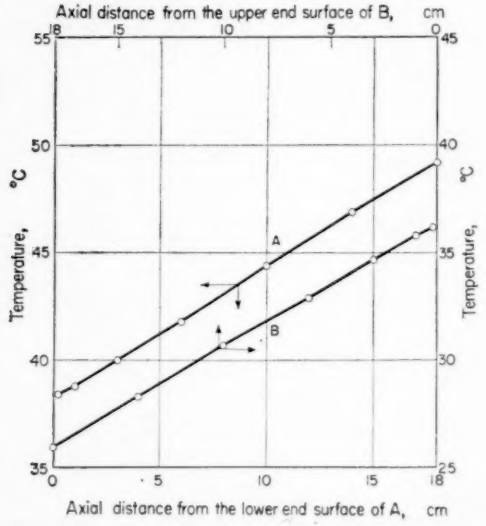

FIG. 2. A typical measurement of the axial temperature distribution in the copper cylinders *A* and *B*.

thermocouples and a potentiometer to 0·01 °C. A typical measurement of the axial temperature is shown in Fig. 2.*

Every measured value was recorded after the steady state was reached. The end-surface temperatures of *A* and *B* were obtained by extrapolation. After each run, the clearance between *A* and *B* was measured as fast as possible to prevent the effect of thermal expansion or contraction of the cylinders.

* It may be interesting to compute, as a check, the thermal conductivity of the copper from this measurement. The value obtained was 274 kcal/m hr °C, which is lower than 330 kcal/m hr °C of the generally used value. The greatest cause of this discrepancy might be an inpurity in the copper.

ANALYSIS

Suppose that there is something like a boundary layer having resistance to heat transfer between the stagnant mercury and the solid metal. The layer could be an absorbed gas layer

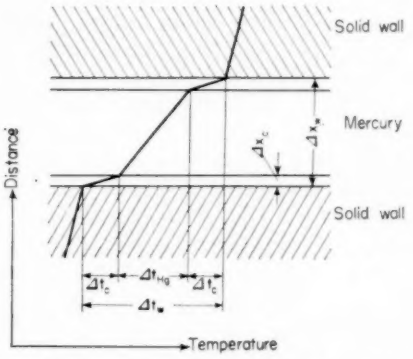

FIG. 3. A schematic representation of the temperature profile in the vicinity of the contact interface.

or a metallic oxide film or any other contaminant. At steady state, the following equations are given (see Fig. 3):

In mercury

$$q = A_{Hg} \cdot k_{Hg} \cdot (\Delta t/\Delta x)_{Hg} \tag{2}$$

In boundary layer

$$q = A_c \cdot h_c \cdot (\Delta t)_c \tag{3}$$

and

$$(\Delta t)_{Hg} = (\Delta t)_w - 2(\Delta t)_c \tag{4}$$

From equations (2), (3) and (4)

$$\frac{(\Delta t)_w}{q} = \frac{(\Delta x)}{A_{Hg} \cdot k_{Hg}} + \frac{2}{A_c h_c} \tag{5}$$

Since the thickness of the boundary layer $(\Delta x)_c$ is very small,

$$(\Delta x)_{Hg} = (\Delta x)_w - 2(\Delta x)_c \doteqdot (\Delta x)_w \tag{6}$$

As shown in Fig. 1, the cylindrical mass of mercury has a cross-sectional area larger than those of the copper cylinders. The former is $1{\cdot}37 \times 10^{-3}$ m² and the latter is $1{\cdot}075 \times 10^{-3}$ m². Thus, the heat flux curves slightly outwards in the mercury layer. Therefore, A_{Hg} in equation (2) should be an equivalent cross-sectional area

consistent with the representation of equation (2) and thus is affected by the geometrical condition. By solving a heat conduction problem, A_{Hg} for this case was given as

$$A_{Hg} = 1{\cdot}075 \times 10^{-3}\,(1 + 24{\cdot}8\,\Delta x_{Hg}) \qquad (7)$$

where A_{Hg} and Δx_{Hg} are in square metres and metres, respectively. The calculations are shown in appendix. Hence, if the values of $(\Delta t)_w$, q and $(\Delta x)_w$ or $(\Delta x)_{Hg}$, are measured, one can obtain the values of h_c and k_{Hg} by a graphical method. When the value of $(\Delta t)_w/q$ are plotted against $(\Delta x)_{Hg}/A_{Hg}$, the intercept at $(\Delta x)_{Hg}/A_{Hg} = 0$ gives $2/(A_c h_c)$ and the gradient $d(\Delta t_w/q)/d(\Delta t_{Hg}/A_{Hg})$ gives $1/k_{Hg}$.

When a thin metal plate is inserted in the mercury layer parallel to the metal surfaces, two contact surfaces are added. Denote the contact area of the inserted plate A_c', and its contact heat transfer coefficient h_c', thus

$$\frac{\Delta t_w}{q} = \frac{(\Delta x)}{A_{Hg}\,.\,k_{Hg}} + \frac{3}{A_c h_c} + \frac{2}{A_c' h_c'} + \frac{(\Delta x)_{plate}}{A_c'\,.\,k_{plate}} \qquad (8)$$

In this case the intercept at $(\Delta x)_{Hg}/A_{Hg} = 0$ gives $[2/(A_c h_c) + 2/A_c' h_c' + (\Delta x)_{plate}/(A_c'\,.\,k_{plate})]$. As the last term can be calculated and the first term is determined by the experiment without inserting a plate, one can determine the resistance $2/(A_c' h_c')$ between the mercury and the inserted plate.

RESULTS AND DISCUSSIONS

The plots in Fig. 4 show the experimental data of thermal contact resistance between pure mercury and chromium-plated copper as well as the case with a copper plate inserted. However, only the data of the former case was correlated, since the data of the latter scattered considerably.

1. *The contact resistance between chromium-plated copper and pure mercury and the thermal conductivity of mercury*

A least-squares line was put through the data as shown in Fig. 4. From the magnitude of the intercept and gradient, two unknown values of $2/(A_c h_c)$ and k_{Hg} in the equation (5) were computed as $2/(A_c h_c) = 0{\cdot}009$ hr °C/kcal and $k_{Hg} = 8{\cdot}46$ kcal/m hr °C.

Since $A_c = \pi r_1^2 = 1{\cdot}075 \times 10^{-3}$ m², the thermal contact resistance $1/h_c = 0{\cdot}48 \times 10^{-5}$ m² hr °C/kcal.

2. *Runs in which a copper plate is inserted*

In order to examine the thermal resistance between copper and mercury, the runs in which a copper plate is inserted were also performed. The experimental results are plotted in Fig. 4. In this case the last term in equation (8)

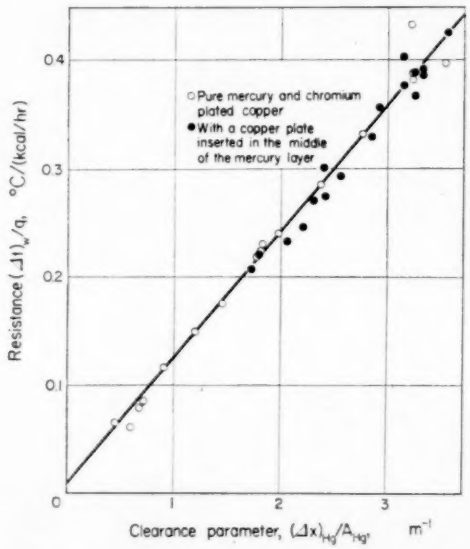

FIG. 4. The experimental data of the thermal resistance $(\Delta t)_w/q$ vs. the clearance parameter. $(\Delta x_{Hg}/A_{Hg})$

is negligible, since the thickness of the plate is very small (about 0·1 mm) and the thermal conductivity of the copper is much larger than that of mercury. If a correlating line is obtained, the intercept would correspond to twice the resistance between chromium-plated copper and mercury plus twice the resistance between copper plate and mercury. However, the data of these runs are not so different from the case of no copper plate insertion, but the former are slightly lower than the latter in thermal resistance $(\Delta t)_w/q$. It may, therefore, be said that there is no thermal contact resistance between copper plate and

Vol. 1 1960

mercury and even that the decrease of the contact resistance between mercury and chromium-plated copper occurs owing to the wetting effect by copper slightly dissolved in mercury.

3. *Other series of runs*

In addition to the data plotted in Fig. 4, several other series of runs were performed. Without the insertion of a plate, two other series of runs were performed and the following results were obtained, respectively:

$$1/h_c = 2{\cdot}15 \times 10^{-5}\ \text{m}^2\ \text{hr}\ ^\circ\text{C/kcal}, \qquad k_{\text{Hg}} = 8{\cdot}8\ \text{kcal/m hr}\ ^\circ\text{C}$$

$$1/h_c = 1{\cdot}88 \times 10^{-5}\ \text{m}^2\ \text{hr}\ ^\circ\text{C/kcal}, \qquad k_{\text{Hg}} = 8{\cdot}25\ \text{kcal/m hr}\ ^\circ\text{C}$$

In another run, a thin nickel plate was inserted in the mercury layer. The increase of thermal contact resistance $2/(A_c'h_c')$ was 0·024 hr °C/kcal. Since

$$A_c' = 1{\cdot}35 \times 10^{-3}\ \text{m}^2,$$

$$1/h_c' = 1{\cdot}62 \times 10^{-5}\ \text{m}^2\ \text{hr}\ ^\circ\text{C/kcal}.$$

A nickel surface seems not to differ from a chromium surface in its character so far as the behaviour of contact with mercury is concerned. If the thermal resistance between the copper base and the plated chromium film is appreciable, the contact resistance between mercury and the chromium-plated copper should be larger than that between mercury and the nickel plate. Since this is not the case, it may support the assumption that there is no thermal resistance between the copper base and the plated chromium film.

Thus, the magnitude of the thermal contact resistance $1/h_c$ between pure mercury and a chromium or nickel surface, is in the range of 0·48 to 2·15 $\times$ 10^{-5} m² hr °C/kcal.

Now the effects of various probable errors on the value obtained for the thermal contact resistance will be discussed.

(1) Since the accuracy in measuring the clearance between the surfaces is about $\frac{1}{200}$ mm, the resulting error in the value of the interfacial resistance can be as high as

$$(\tfrac{1}{200} \times 10^{-3})/7{\cdot}9 = 0{\cdot}6 \times 10^{-5}\ \text{m}^2\ \text{hr}\ ^\circ\text{C/kcal}.$$

However, as the probabilities of overestimation and underestimation can be assumed to be equal, a least-squares procedure may decrease the error.

(2) It is difficult to determine the positions of the thermocouple junctions accurately. However, the thermocouple holes were drilled carefully and the error in determining the position of the junction might be about 0·2 mm, which corresponds to an error of

$$0{\cdot}7 \times 10^{-6}\ \text{m}^2\ \text{hr}\ ^\circ\text{C/kcal}$$

for the contact resistance.

(3) As the thickness of the chromium deposit is less than $\frac{1}{1000}$ mm, its thermal resistance is substantially negligible.

(4) If a part of the heat supplied to the upper end of the cylinder was lost out of the system, one should estimate the magnitude of $\Delta t/q$ slightly larger, and so also the value of the contact resistance. However, since the temperature gradient in the copper cylinders was substantially uniform, this effect may be small.

(5) As the thermal contraction of the copper cylinder during the measurement of the clearance is inevitable, one might possibly overestimate the clearance. If the temperature descent of the copper cylinder during the measurement was 1 °C, the contraction of a copper cylinder of 20 cm could reach 0·003 mm, which results in an error of 0·4 $\times$ 10^{-6} m² hr °C/kcal in estimating the contact resistance.

Consequently, the possible magnitude of accumulated errors in the contact resistance may be between 10^{-6} and 10^{-5} m² hr °C/kcal. Therefore, it may be concluded that there is a thermal contact resistance between a chromium-plated copper surface and pure mercury a few times 10^{-5} m² hr °C/kcal at most.

The heat transfer coefficient of mercury flow inside a round tube of 2 cm inside diameter at Peclet number = 1000 can be calculated by Lyon's equation (1) as h = 5000 kcal/m² hr °C. If the value of the contact resistance between mercury and metal wall is assumed to be 1 $\times$ 10^{-5} m² hr °C/kcal, the value of the heat transfer coefficient will decrease to 4750 kcal/m² hr °C. On the other hand, the experimental heat transfer coefficient at the same condition is about 3900 kcal/m² hr °C. Therefore, the

thermal contact resistance plays only a part of the role in the discrepancy between theoretical prediction and the experimental data of heat-transfer.

Average temperature of the mercury layer was about 40°C and the value of k_{Hg} at this temperature is given as 7·9 kcal/m hr °C by the *Liquid Metals Handbook* [11], while Gehlhoff and Neumeier [12] gives 10 kcal/m hr °C at the same temperature. Experimental values of the present work are in the range of from 8·25 to 8·8 kcal/m hr °C, which is slightly larger than the data of *Liquid Metals Handbook*. This may partly be due to the small amount of heat loss out of the system from the upper cylinder and partly due to the heat transferred between the mercury and the cylindrical wall of the cylinders. If the former is taken into account, the estimated q must decrease and $\Delta t/q$ must increase and consequently k_{Hg} must decrease, while the latter makes the apparent magnitude of A_{Hg} somewhat larger and thus the value of k_{Hg} smaller.

CONCLUSION

There is a small amount of thermal contact resistance of the order of 10^{-5} m² hr °C/kcal but less than a few times of that between a chromium-plated surface and pure liquid mercury. Its magnitude is, however, not so large as to explain the whole amount of discrepancy between the theoretical prediction and the experimental data of heat transfer.

ACKNOWLEDGEMENTS

The writers wish to express their thanks to the Ministry of Education of Japan, and Asahi Glass Co. Ltd. for their Financial support, and to acknowledge gratefully the valuable contributions of T. Tsujino and H. Kamimura in the construction of the apparatus and the preliminary work.

REFERENCES

1. R. C. Martinelli, *Trans. Amer. Soc. Mech. Engrs.* **69**, 947 (1947).
2. R. N. Lyon, *Chem. Engng. Progr.* **47**, 75 (1951).
3. W. C. MacDonald and R. C. Quittenton, *Chem. Engng. Progr.* Symposium Series **50**, No. 9, 59 (1954).
4. H. Chelemer, Ph.D. Thesis, University of Tennessee (1955).
5. S. E. Isakoff and T. B. Drew, *General Discussion on Heat Transfer* p. 405. Institution of Mechanical Engineers, London (1951).
6. H. E. Brown, B. H. Amstead and B. E. Short, *Trans. Amer. Soc. Mech. Engrs.* **79**, 279 (1957).
7. T. Mizushina, S. Iuchi, M. Nakao and T. Sasano' Unpublished.
8. R. G. Deissler, NACA RM E52F05 1 (1952).
9. P. S. Lykoudis, Ph.D. Thesis, Purdue University (1956).
10. W. F. Cope, *General Discussion on Heat Transfer* p. 453. Institution of Mechanical Engineers, London (1951).
11. R. Lyon (Editor), *Liquid Metals Handbook* (2nd Ed.) p. 43. Atomic Energy Commission, Washington, D.C. (1952).
12. G. Gehlhoff and F. Neumeier, *Verh. d. Phys. Ges.* **21**, 201 (1919).

APPENDIX

Mathematical Estimation of A_{Hg}

As represented schematically in Fig. 5 the complicated heat flow in the mercury layer can be analysed as a problem of the steady-state heat conduction in a cylinder which has the following boundary conditions:

$$\begin{array}{lll} x = \Delta x & r \leqq r_1 & t = t_0 \\ x = 0 & r \leqq r_1 & t = 0 \end{array} \quad (9)$$

$$\begin{array}{lll} x = \Delta x & r_2 \geqq r > r_1 & \partial t/\partial x = 0 \\ x = 0 & r_2 \geqq r > r_1 & \partial t/\partial x = 0 \end{array} \quad (10)$$

$$r = r_2 \qquad \Delta x \geqq x \geqq 0 \qquad \partial t/\partial r = 0 \quad (11)$$

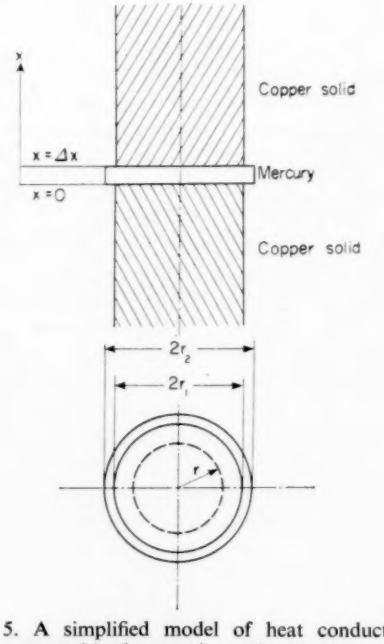

FIG. 5. A simplified model of heat conduction occurred in the experimental apparatus.

The equivalent cross-sectional area of the mercury mass is affected by the geometrical condition and takes a value between

$\pi r_1^2 = 1{\cdot}075 \times 10^{-3}\,\mathrm{m}^2$ and $\pi r_2^2 = 1{\cdot}37 \times 10^{-3}\,\mathrm{m}^2$

corresponding to the magnitude of the clearance.

It is beyond the present attempt to solve this boundary value problem quite rigorously. However, it is not difficult to solve the problem, if the temperature distribution at $x = \Delta x$ and $x = 0$ can be assumed reasonably instead of the boundary condition (10). The writers assumed the temperature distribution as follows:

$$x = \Delta x \qquad t = f_1(r) \tag{12}$$

where $f_1(r) = t_0 \; (0 < r < r_1)$

$= t_0 - Ct_0\,[1 - (2/\pi)\sin^{-1} r_1/r]$*, $(r_1 < r < r_2)$

$$x = 0 \qquad t = f_2(r) \tag{13}$$

where $f_2(r) = 0 \; (0 < r < r_1)$

$= Ct_0\,[1 - (2/\pi)\sin^{-1} r_1/r]$, $(r_1 < r < r_2)$

A correction factor C in the above equations should be determined so as to satisfy the following equation:

$$Q = Q' \tag{14}$$

where $$Q = \int_0^{r_1} 2\pi kr\,(\partial t/\partial x)_{x=0}\,dr \tag{15}$$

$$Q' = \int_0^{r_2} 2\pi kr\,(\partial t/\partial x)_{x=x}\,dr \tag{16}$$

The basic differential equation for the steady-state heat conduction in a cylinder is

$$\partial^2 t/\partial x^2 + (1/r)\partial t/\partial r + \partial^2 t/\partial r^2 = 0 \tag{17}$$

The boundary value problem denoted by equations (17), (9), (11), (12) and (13) can be separated into two somewhat simpler boundary-value problems whose solutions can be superposed to yield the solution of the original problem. Consider the following two boundary-value problems:

$$\left.\begin{aligned} &\partial^2 t_1/\partial x^2 + (1/r)\partial t_1/\partial r + \partial^2 t_1/\partial r^2 = 0 \\ &t_1 = f_1(r) \qquad (\text{at } x = \Delta x) \\ &t_1 = 0 \qquad (\text{at } x = 0) \\ &\partial t_1/\partial r = 0 \qquad (r = r_2) \end{aligned}\right\} \tag{18}$$

$$\left.\begin{aligned} &\partial^2 t_2/\partial x^2 + (1/r)\,\partial t_2/\partial r + \partial^2 t_2/\partial r^2 = 0 \\ &t_2 = 0 \qquad (\text{at } x = \Delta x) \\ &t_2 = f_2(r) \qquad (\text{at } x = 0) \\ &\partial t_2/\partial r = 0 \qquad (r = r_2) \end{aligned}\right\} \tag{19}$$

The analytical solutions of the two problems defined by equations (18) and (19) respectively, have already been solved and are described in standard text-books of heat conduction.†

$$t_1 = \frac{2}{r_2^2}\sum_{n=0}^{\infty}\frac{J_0(\lambda_n\, r/r_2)\,\sinh\,(\lambda_n x/r_2)}{[J_0\,(\lambda_n)]^2\,\sinh\,(\lambda_n \Delta x/r_2)} \int_0^{r_1} \rho\, f_1(\rho) J_0\left(\frac{\lambda_n \rho}{r_2}\right) d\rho \tag{20}$$

$$t_2 = \frac{2}{r_2^2}\sum_{n=0}^{\infty}\frac{J_0(\lambda_n\, r/r_2)\,\sinh\,[\lambda_n(\Delta x - x)/r_2]}{[J_0(\lambda_n)]^2\,\sinh\,(\lambda_n \Delta x/r_2)} \int_0^{r_2} \rho\, f_2(\rho) J_0\left(\frac{\lambda_n \rho}{r_2}\right) d\rho \tag{21}$$

where λ_n is the nth root of $J_1\,(\lambda_n) = 0$.

Substituting $f_1(r)$ and $f_2(r)$ defined by equations (12) and (13) into equations (20) and (21), the solution of the original boundary value problem is obtained as follows:

$$\left.\begin{aligned} &t = t_1 + t_2 \\ &= (t_0\, x/\Delta x) + Ct_0 \frac{\Delta x - 2x}{\Delta x}\left(\frac{r_2^2 - r_1^2}{r_2^2} - \right. \\ &\left. - \frac{4}{\pi r_2^2}\int_{r_1}^{r_2} \rho \sin^{-1}\frac{r_1}{\rho}\,d\rho\right) + \frac{2t_0 C}{r^2} \\ &\sum_{n=1}^{\infty}\frac{J_0 \dfrac{\lambda_n r}{r_2}\left(\sinh\dfrac{\lambda_n x}{r_2} - \sinh\dfrac{\lambda_n(\Delta x - x)}{r_2}\right)}{J_0(\lambda_n)]^2\,\sinh\,\lambda_n \Delta x/r_2} \\ &\times\left[\frac{r_1 r_2}{\lambda_n} J_1\left(\lambda_n \frac{r_1}{r_2}\right) + \right. \\ &\left. + \int_{r_1}^{r_2}\left(\frac{2}{\pi}\right)\rho \sin^{-1}\frac{r_1}{\rho} J_0\left(\frac{\lambda_n \rho}{r_2}\right) d\rho\right] \end{aligned}\right\} \tag{22}$$

From equation (14), (15), (16) and (22), one obtains

* When a circular region ($r \leqq r_1$) of the surface of a semi-infinite solid is kept at a constant temperature t_0 and the other region is insulated, the surface temperature distribution is given as $t_0\,(2/\pi)\sin^{-1} r_1/r$.

† For example, H. S. Carslaw and J. C. Jaeger, *Conduction of Heat in Solids* p. 188. Clarendon Press, Oxford (1950).

$$Q = \int_0^{r_1} 2\pi kr \left(\frac{\partial t}{\partial x}\right)_{x=0} dr$$
$$= \frac{\pi k t_0 r_1^2}{\Delta x}\left\{1 - 2C\left(\frac{r_2^2 - r_1^2}{r_2^2} - \frac{4}{\pi r_2^2}\int_{r_1}^{r_2} \rho \sin^{-1}\frac{r_1}{\rho}\, d\rho\right) + \frac{4\Delta x C}{r_1 r_2^2} \times \sum_{n=1}^{\infty} \frac{J_1(\lambda_n r_1/r_2)\,[1 + \cosh(\lambda_n \Delta x/r_2)]}{[J_0(\lambda_n)]^2 \sinh(\lambda_n \Delta x/r_2)} \times \left[\frac{r_1 r_2}{\lambda_n} J_1\left(\frac{\lambda_n r_1}{r_2}\right) + \left(\frac{2}{\pi}\right)\int_{r_1}^{r_2} \rho \sin^{-1}\frac{r_1}{\rho} J_0\left(\frac{\lambda_n \rho}{r_2}\right) d\rho\right]\right\} \quad (23)$$

$$Q' = \frac{\pi k r_2^2 t_0}{\Delta x}\left[1 - 2C\left(\frac{r_2^2 - r_1^2}{r_2^2} - \frac{4}{\pi r_2^2}\int_{r_1}^{r_2} \rho \sin^{-1}\frac{r_1}{\rho}\, d\rho\right)\right] \quad (24)$$

From equations (14), (23) and 24), the value of C can be determined. Let

$$Q = K\frac{\pi k r_1^2}{\Delta x} t_0 \quad (25)$$

Thus, the values of K in equation (25) are computed for $\Delta x = 0{\cdot}0035$, $0{\cdot}0040$ and $0{\cdot}0045$ m when $r_1 = 1{\cdot}85$ and $r_2 = 2{\cdot}10$. The results are shown in Table 1 in which the values of C are also shown.

Table 1. *The values of K in equation* (25), *and of C in equations* (12) *and* (13) *which satisfy equation* (14)

Δx (m)	K	C
0	1·000	—
0·0035	1·086	1·621
0·0040	1·099	1·535
0·0045	1·109	1·457

Since the assumptions of the temperature distribution of equations (12) and (13) are not reasonable when the value of Δx is too small, the calculations were limited to $\Delta x \geqslant 0{\cdot}0035$. However, from inspection of the variation of K listed in Table 1, it may be assumed that the values of K between $\Delta x = 0$ and $\Delta x = 0{\cdot}0035$ m can be correlated approximately by a linear function of Δx as follows:

$$K = 1 + 24{\cdot}8\,\Delta x \quad (26)$$

Consequently,

$$A_{Hg} = K\pi r_1^2 = (1 + 24{\cdot}8\,\Delta x)(\pi r_1^2) \quad (27)$$

where K, Δx and A_{Hg} have dimensions (−), (m) and (m²), respectively.

Vol. 1 1960

Int. J. Heat Mass Transfer. Vol. 1, pp. 147–151. Pergamon Press 1960. Printed in Great Britain.

LOCAL AND AVERAGE HEAT TRANSFER COEFFICIENTS AT AN AIR STREAM IN A TUBE WITH A POINTED INLET

V. K. ERMOLIN

The Polzunov Boiler-Turbine Institute, Leningrad

(*Received* 23 *January* 1960)

Abstract—This work adduces experimental data on local and average coefficients of heat transfer from air to the wall of a tube with a pointed inlet in the range of *Re* numbers including a transient region.

Résumé—Ce travail apporte de nouveaux résultats expérimentaux sur les coefficients locaux et moyens de transmission de chaleur, pour l'air, à la paroi d'un tube à entrée effilée, pour un domaine de nombres de Reynolds qui comprend la région de transition.

Zusammenfassung—Diese Arbeit liefert weitere Versuchswerte über den örtlichen und mittleren Wärmeübergangskoeffizient von Luft an die Wand eines Rohres mit scharfkantigem Einlauf in einem Bereich der *Re*-Zahl, der auch den Übergangszustand enthält.

Abstract—В работе приведены экспериментальные данные по локальным и средним коэффициентам теплообмена от воздуха к стенке трубы с острым входом в диапазоне чисел *Re*, включающем переходную область.

THE influence of l/d on heat transfer was discovered by some investigators who suggested that the generalized heat transfer equation should take this influence into account [1, 2].

Other investigators who examined the heat transfer process under the heating conditions of a working media came to the conclusion that the influence of l/d on heat transfer is negligible and that it should not be taken into account by the generalized equation.

The well-known method of calculation [3] for determining the influence of the tube length on heat transfer coefficients by introduction of the factor $(l/d)^{-0.054}$ into equations of such a type as $Nu = c.Re^n Pr^m$ contradicts the conditions of the experiment since an increase of l/d gives an infinite decrease of heat transfer.

Experimental data [4] were obtained when water was heated for the single case of an inlet. They are of a particular character and valid for the given conditions of the experiment.

A horizontal, cylindrical steel tube with an experimental part 1236 mm long and an inside diameter 31·66 mm is the main element of the installation for the investigation of heat transfer in a tube (Fig. 1).

The experimental tube was mounted between the reservoir (2) and a feeder of the ventilator. The tube was joined to the reservoir by means of a coupling flange through the feeder (4), the diameter of which is equal to that of the tube. Heat transfer from the coupling flange was avoided with the help both of the heat insulation packing 8 mm thick, and the bolt plugs, which eliminated direct contact of the metallic surfaces.

The room air entered the reservoir, which was divided by a fixed partition into two wells; then while passing the electric heater (3), mounted in the hoisting well of the reservoir, the air was heated, and having passed the drop well, made its way into the experimental tube, out of which it was sucked by the ventilator. The entrance to the tube from the reservoir side is a pointed one and answers the usual entrance conditions.

From the outlet the experimental tube also had a coupling flange with an insulation packing, a straight part $8d$ long, a bend of 90°, and a transition to the vertical part (10) 49·8 mm in diameter, where a double diaphragm for the measuring of air expanse was mounted. A regulating target was placed in front of the feeder.

The experimental part of the tube was placed concentrically into the casing (6), made of a tube 89/80 mm in diameter.

To receive the data on heat distribution along

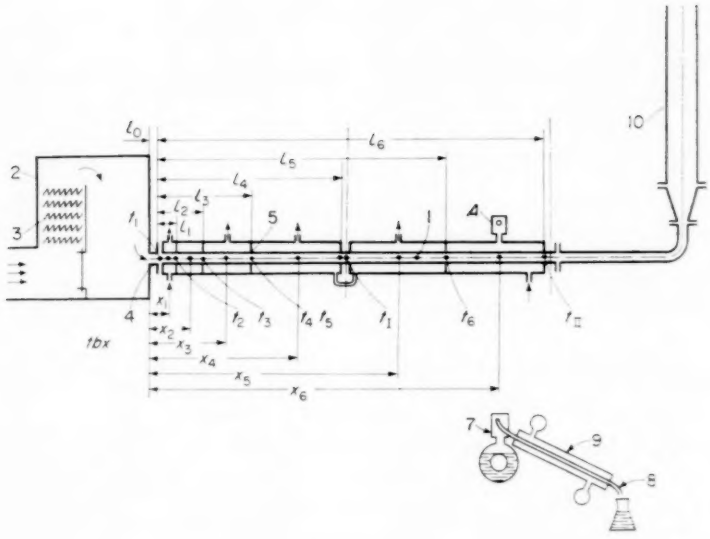

FIG. 1. The scheme of the experimental installation for the investigation of heat transfer in an annular pipe with a pointed inlet.

the length of the experimental tube the annular space between the tube and the casing was divided by transversal partitions (5) into six compartments of different length. All the compartments are joined and they are fed from both ends by the boiling water flowing out of the tank. The operation both of the tank and the casing is based on the principle of communicating vessels.

The water level in the casing was maintained constant and exceeded the mark of the upper generating line on the outside surface of the experimental part of the tube by 6–7 mm; this ensured a constant submerging of the experimental part of the tube in the casing.

The air was cooled while passing the experimental part of the tube, giving up its heat to the boiling water in the casing. The steam received from the separate parts was drawn off into the refrigerators (9), where it was condensed. In order to measure the condensate, it was drained out of each compartment through separate branches (8) into glass bulbs. The selection of steam from the compartments was carried out from the upper point of steam collectors (7) to avoid the priming of moisture by the steam.

The experimental tube was safely isolated to decrease heat transfer into the external medium.

Fig. 1 shows the tube division into the experimental parts and the geometrical characteristics are given in Table 1. The beginning of the experimental tube is $l_0 = 36$ mm distant from the entrance and therefore it is assumed that $l'_i = l_i + l_0$.

The points for measuring the balanced values which characterize the state of flow at the entrance, at a distance $l = 20d$ and at the outlet with $l = 40d$ are depicted by cross-sections 0–0, I–I and II–II, respectively.

The measurement both of the total pressure and temperature fields at the cross-sections I–I and II–II was made at two reciprocally perpendicular radii with the help of micropipes of total pressure, and with the help of microthermocouples moving by means of a micrometer screw. The temperature of the heated air in the reservoir at the tube entrance was measured by several thin thermocouples and was checked by a suction thermocouple. The measurement of the wall temperature along the tube was made by thin thermocouples (copper–constantan couples) 0·20 mm in diameter, placed at the

Vol. 1 1960

Table 1. *A diagram of the division of the experimental tube into parts*

Designation	Nos. of the experimental tube parts (1)	(2)	(3)	(4)	(5)	(6)
The distance from the entrance to the middle of the experimental section x_i (mm)	70	146	267	493	822	1122
Relative length $\frac{x_i}{d}$	2·21	4·63	8·45	15·6	26·0	35·5
The length of the tube experimental part from the beginning of the tube l_i (mm)	64	155	306	608	936	1236
Relative length $\frac{l_i}{d}$	2·02	4·9	9·67	19·2	29·6	39·1
The length of the experimental part from the entrance l'_i (mm)	100	191	342	644	972	1272
Relative length $\frac{l'_i}{d}$	3·17	6·05	10·8	20·4	30·7	40·3

points of average length in each compartment on the upper generating line of the experimental tube's outer surface. The thermoelectromotive force of all the thermocouples was measured by a potentiometer. The air discharge was registered by a twin diaphragm calibrated for cooled and for heated air.

When the installation was set into operation, the measurements were made after the achievement of a stationary regime after a time interval of 3–4 hr.

The isothermal blowing of the experimental tube with the attached stabilizing part $l = 46d$ long and a diameter equal to that of the experimental tube was carried out before the non-isothermal experiments took place. It was ascertained under these conditions for the experimental tube that the resistance factor obeys the well-known resistance law for smooth tubes which is expressed by the following equation $\zeta = 0{\cdot}316\ Re^{-0{\cdot}25}$. It proves that the experimental tube is technically smooth.

The non-isothermal experiments were carried out without the attached stabilizing part and covered a range of variation of Reynolds numbers from $3{\cdot}9 \times 10^3$ to 19×10^3 including the transition region. The air temperature at the tube entrance was maintained within the limits 340° to 421°C.

The values of average and local coefficients of heat transfer by convection were determined from the heat balance equations for the tube section under consideration according to the amount of heat transferred per hour through the tube element, considered as a result of heat transfer between the air flow and the surface of the tube element [5].

On the other hand, the heat transferred by the air to the part of the tube under consideration is spent on the evaporation of water and on heat transfer into the external medium.

The heat transfer from the experimental tube into the external medium was determined by direct measurements both of the isolation and the room air temperatures. During the whole period of the experiments the temperature of the isolation of part 0–I was 43·3°C and of part I–II it was 43·2°C.

As the casing wall temperature along the length of the tube did not vary and was equal to the temperature of boiling water under atmospheric pressure then we consider the distribution of the heat transfer over separate elements of the tube proportional to their lengths.

All the experimental data on local and average values of heat transfer coefficients were processed in the generalized equations:

$$Nu = \frac{Qd}{F\Delta tx} \tag{1}$$

and

$$Re = \frac{4G}{\pi dg\mu} \tag{2}$$

The local values of heat transfer coefficients are given in Fig. 2 as the dependence $Nu_x = c_1 Re^{n_1}$.

The local heat transfer coefficients vary in the range of the Reynolds numbers investigated at the air flow in a tube with a pointed inlet, and they have a sharp fall with the increase of the relative length to $x/d = 5$ at the beginning and then, while proceeding away from the entrance

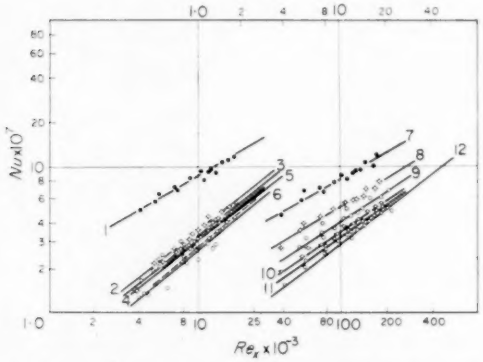

FIG. 2. The local and average values of the heat transfer coefficients for a tube with a pointed inlet without inside insertions.

they vary very slightly at the approach to a definite value for the cross-section which is $x/d \geqslant 40$ distant from the entrance. It is possible to determine local values of heat transfer coefficients for the elements of the tube situated at a distance more than $40d$ from the following equation

$$Nu = 0{\cdot}0145\ Re_f^{0{\cdot}83}\ Pr_f^{0{\cdot}4} \qquad (3)$$

The local values for cross-sections situated from the entrance at a distance less than $40d$ can be determined in accordance with the formula

$$Nu_x = 0{\cdot}0145\ Re_f^{0{\cdot}83}\ Pr_f^{0{\cdot}4}\left(1 + \kappa_x \frac{d}{x}\right) \qquad (4)$$

where κ_x for $x/d \geqslant 5$ are given in Table 2.

In Fig. 2 the experimental data for average values of heat transfer coefficients are given by the equation $Nu = c\ Re^n$.

From the experimental results obtained we can see that the average values of the heat transfer coefficients vary in the investigated range of the Reynolds numbers up to a cross-section which is situated at a distance of $40d$ from the beginning of the experimental tube. Thus with an increase of Re this distance gradually decreases. Beginning with a tube length equal to $l \geqslant 40$ the average values of heat transfer coefficients become practically constant and satisfy an equation of the following type

$$Nu = 0{\cdot}023\ Re_f^{0{\cdot}8}\ Pr_f^{0{\cdot}4} \qquad (5)$$

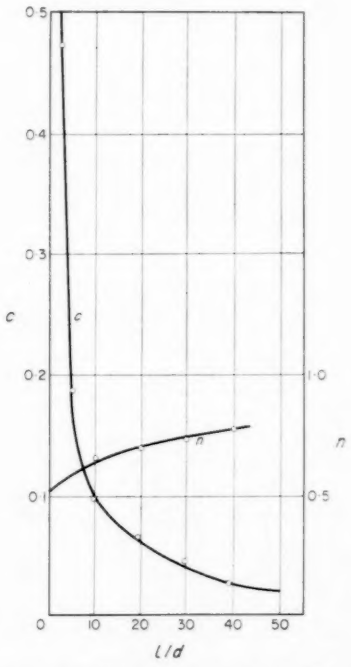

FIG. 3. The dependence of the c and n coefficients for the average values of Nusselt criterium on the relation l/d.

Table 2. The meaning of the coefficient κ_x at various Reynolds numbers

Re × 10^{-3}	4	6	8	10	12	14	16	18	20
κ_x	2·22	1·93	1·89	1·7	1·6	1·55	1·39	1·37	1·34

Vol. 1 1960

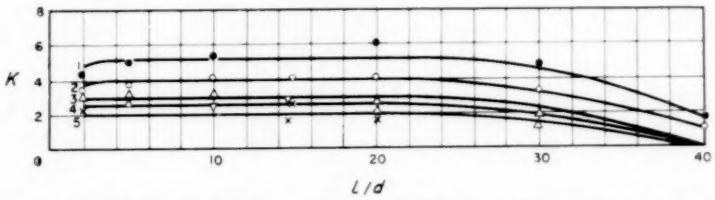

FIG. 4. The dependence of the coefficient κ at a pointed intake of gas on the relation l/d for various values of Reynolds number: (1) 4×10^3; (2) 8×10^3; (3) 12×10^3; (4) 16×10^3; (5) 20×10^3.

which gives a satisfactory approximation for the present experimental data and for the theoretical formula which is valid at $0{\cdot}6 < Pr_f < 100$ [6].

The equation

$$Nu = 0{\cdot}0202\ Re^{0{\cdot}8} \tag{6}$$

was obtained for air. It is quite possible to use the numerical values of coefficients c and n for short tubes with the relative length of $l/d \leqslant 40d$ given in Fig. 3.

The influence of the tube length on the average heat transfer coefficient for tubes of $l/d \leqslant 40d$ can be accounted for by the principal heat transfer equation by an introduction of the error factor κ which is a function of the number Re (see Fig. 4). And the criterium for the average values of heat transfer coefficients will have the following form:

$$Nu = 0{\cdot}023\ Re_f^{0{\cdot}8}\ Pr_f^{0{\cdot}4}\left(1 + \kappa\frac{d}{l}\right) \tag{7}$$

REFERENCES

1. G. GRASS, *Allg. Wärmetechn.* **7**, No. 3 (1956).
2. A. CHOLLETTE, *Chem. Engng. Progr.* **44**, No. 1 (1948).
3. H. KRAUSSOLD, *Forsch. IngWes.* No. 1 (1933).
4. I. I. ALADIEV, *Izv. Akad. Nauk SSSR, otdel tekh. nauk* No. 11 (1951).
5. M. A. MICHEEV, *Osnovy teplootdachi* (*Basic Principals of Heat Transfer*). Gosenergoizdat (1956).
6. S. S. KUTATELADZE, *Osnovy teorii teploobmena* (*The Theory of Heat Exchange*). Mashgiz (1957).

Int. J. Heat Mass Transfer. Vol. 1, pp. 152–160. Pergamon Press 1960. Printed in Great Britain.

THE THEORY OF THERMAL REGULAR REGIME AND ITS APPLICATION TO THE DETERMINATION OF THERMAL CHARACTERISTICS

G. N. DULNEV

The Institute of Exact Mechanics and Optics, Leningrad, U.S.S.R.

(*Received* 21 *October* 1959)

Abstract—The basic regularities of the thermal regular regime theory developed by G. M. Condratjev and its practical application to the thermotechnical measurements are discussed in this paper.

Under the thermal regular regime of a body or a system of bodies one understood such a process of cooling or heating the system when: (1) the initial temperature distribution in the system does not influence the law of temperature change; (2) the law of temperature change is expressed in a simple mathematical form; (3) this law is general for all the points of the system.

These regularities of the thermal regular regime permitted: (a) to work out a number of methods to determine the thermal characteristics of different materials; (b) to determine the thermal inertia of thermometers and pyrometers; (c) to obtain the relations to calculate the kinetics of cooling or heating the complicated thermotechnical apparatus and equipment.

Résumé—Les conditions de régularité qui sont à la base de la théorie du régime thermique régulier développée par G. M. Condratjev et son application aux mesures thermiques de la technique sont précisées dans cet article.

Par régime thermique régulier d'un corps ou d'un ensemble de corps, on désigne un processus de refroidissement ou de chauffage du système tel que: 1° la distribution des températures initiales dans le système n'influence pas la loi d'évolution des températures; 2° la loi d'évolution des températures s'exprime dans une forme mathématique simple; 3° cette loi est générale et s'applique en tout point du système.

Ces conditions de régularité du régime thermique régulier ont permis: (a) d'établir un certain nombre de méthodes pour la détermination des caractéristiques thermiques des différents matériaux, (b) de déterminer l'inertie thermique de thermomètres et pyromètres, (c) d'obtenir les relations permettant de calculer la cinétique de refroidissement ou de chauffage dans le cas d'appareillages techniques compliqués.

Zusammenfassung—In dieser Arbeit werden die Grundzüge der Theorie des regulären thermischen Zustandes, nach G. M. Condratjev, und ihre praktische Anwendung auf wärmetechnische Messungen behandelt.

Unter dem regulären thermischen Zustand eines Körpers oder eines Systems von Körpern versteht man einen Kühlungs- oder Erwärmungsvorgang, bei dem (1.) die anfängliche Temperaturverteilung in dem System das Gesetz der Temperaturänderung nicht beeinflußt, (2.) das Gesetz der Temperaturänderung in einer einfachen mathematischen Form ausgedrückt ist, (3.) dieses Gesetz für alle Punkte des Systems gültig ist.

Diese Grundzüge des regulären thermischen Zustandes erlauben (a) eine Anzahl von Methoden zur Bestimmung der thermischen Eigenschaften verschiedener Materialien anzugeben, (b) die thermische Trägheit von Thermometern und Pyrometern zu bestimmen, (c) die Kinetik der Kühlung oder Heizung von komplizierten wärmetechnischen Apparaten zu berechnen.

Abstract—В статье рассматриваются основные закономерности теории теплового регулярного режима, разработанные Г. М. Кондратьевым, и её применение в практике теплотехнических измерений.

Тепловым регулярным режимом тела или системы тел называется такой процесс её нагревания или охлаждения при котором: (1) на закон изменения температуры не влияет начальное распределение температуры в системе, (2) закон изменения температуры

Vol. 1 1960

имеет простое математическое выражение, (3) этот закон является общим для всех точек системы.

Эти закономерности теплового регулярного режима позволили: (а) разработать ряд методов определения тепловых характеристик различных материалов, (б) определить тепловую инерцию термометров и пирометров, (в) получить расчётные соотношения для исследования кинетики охлаждения или нагревания сложных теплотехнических аппаратов и устройств.

CONDRATJEV has developed experimental methods serving to determine the thermophysical charactersitics of non-metallic materials. These methods are based on the general regularities of the unstationary temperature field of a body or system of bodies in cooling or heating processes.

It is known that the general solution of the Fourier equation for the problem of cooling of a uniform and isotropic body of any configuration is expressed by an infinite series, the terms of which have been distributed along the rapidly decreasing exponential functions of time

$$t - t_c = \sum_{i=0}^{\infty} A_i U_i \exp(-m_i \tau) \qquad (1)$$

so that the positive numbers $m_0, m_i, \ldots$ are the series of continuously increasing discrete numbers

$$0 < m_0 < m_1 < m_2 < \ldots \qquad (2)$$

$U_0, U_1, \ldots$ are the finite functions of body points co-ordinates;

$A_0, A_1, \ldots$ are also finite and constant numbers independent of time and co-ordinates. The functions of U_i satisfy the boundary conditions

$$\left(\frac{\partial U_i}{\partial n} + hU_i\right)_s = 0 \qquad (3)$$

The functions of A_i are determined from the initial conditions

$$\sum_{i=0}^{\infty} A_i U_i = f(x, y, z) \qquad (4)$$

The following symbols are assumed here: $t = t(x, y, z, \tau)$ is the temperature of a body at the point (x, y, z) at the time τ; t_c is the medium temperature; $\partial U_i/\partial n$ is the derivative of the function U_i along the external normal to the outside surface of the body S; $f(x, y, z)$ is the function which characterizes the initial distribution of temperatures; $h = \alpha/\lambda$, where α is the heat transfer coefficient and λ is the thermal conductivity coefficient. For the latter coefficients we assume that they are independent of temperature as it is generally used in the theory of heat conduction. The kinetics of cooling a body has three stages. The first one is qualified by the strong influence of the initial state of a body upon its temperature field. In general, the initial state of a body is occasional and quite independent of both the system characteristics and the conditions under which the cooling process is going on. In the course of time the influence of the initial peculiarities of the temperature field upon further change is smoothed. From the "irregular stage" the process becomes "regular" and the influence of non-uniformity of the initial temperature distribution no longer has any effect; the law of change of the temperature field has the ordinary exponential form

$$t_{reg} - t_c = A_0 U_0 \exp(-m_0 \tau) \qquad (5)$$

Condratjev gives a generalization of the above theorem for a system of bodies.†

Suppose that the thermal characteristics: thermal conductivity λ_j, thermal diffusivity a_j, specific heat c_j and also the density γ_j depend upon the co-ordinates of the points of the given part (j) of the system (if the material, for example, is non-homogeneous) but it is assumed here that λ_j, a_j, c_j, γ_j are independent of temperature in the temperature ranges observed in the system during the process.

Under these conditions the principle about the conversion from an irregular state to a regular regime, proved by Boussinesq for any uniform and isotropic body, is valid for the system of bodies as well.

So we see that the rate of change of ln

† By the system of bodies one may understand a whole complex of various solids which are in close contact. If the components of a system are liquids then we suppose that a field of temperature is uniform.

$(t - t_c)$ is the same for all the points of the system

$$\frac{\partial}{\partial \tau} \ln (t - t_c) = -m \tag{6}$$

Therefore the temperature field of a body will be expressed by co-ordinates τ, $\ln (t - t_c)$ after the regular regime has been established, and by the system of straight parallel lines with the negative angle coefficient equal to $-m$, as shown in Fig. 1. This is a typical feature of the regular

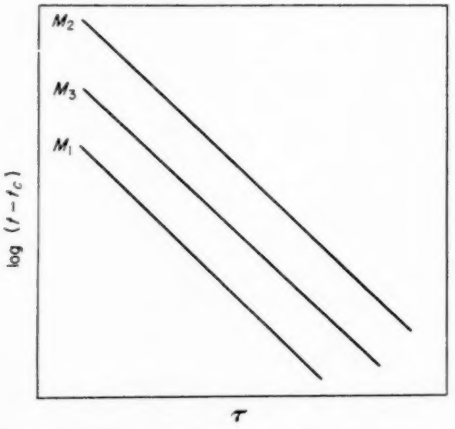

FIG. 1. The temperature field of the system at its regular cooling or heating.

regime and is only essential for it. m plays an important role in the theory of regular regime and it is known as the rate of cooling, since it characterizes the rapidity with which the body is cooled.

The theoretical and experimental researches dealing with the cooling of bodies in various mediums indicate that the rate of cooling depends upon the heat transfer coefficient, the thermal characteristics of a body, and its size and configuration.

The rate of regular cooling of a uniform and isotropic body at the final value of heat transfer coefficient is proportional to the surface of the body and inversely proportional to its total heat capacity (C).

The coefficient of proportionality is a product of the heat transfer coefficient α and the criterion ψ which is decreasing monotonously as α is increasing.

$$m = \alpha \psi \frac{S}{C} \tag{7}$$

$$\psi = \frac{t_s - t_c}{t_v - t_c} \tag{8}$$

where the criterion ψ characterizes the non-uniformity of the temperature field in a body and is numerically equal to the ratio of the average surface temperature of a body to its average volumetric temperature of superheating.

If $\alpha(\mathrm{Bi}) = 0$, then $\psi = 1$

and $\alpha(\mathrm{Bi}) \to \infty \qquad \psi \to 0$

$\lim m = m_\infty$ which corresponds to $\mathrm{Bi} = \infty$ and the thermal diffusivity of the material are directly proportional:

$$a = K m_\infty \tag{9}$$

where the coefficient of proportionality K depends only on the size and the form of a body.

The coefficient K serves as a measure of thermal inertia of a given model: the greater the value of K the smaller is m and thus the slower the cooling of a body proceeds, irrespective of what material the body is made.

K, in the theory of regular regime is called a coefficient of a body shape. This coefficient can be calculated in two ways: either at $\mathrm{Bi} \to \infty$ or considering the boundary conditions

$$U|_S = 0 \tag{10}$$

and we shall define m_∞. In many works on the regular regime theory [2–4] the value of the form coefficient has been calculated for bodies of various configurations.

The application of equation (7) was in practice restricted by the difficulty of calculating the criterion ψ. The methods of calculation used for this criterion have been developed only for bodies which have a simple configuration. Later on Condratjev and his followers Dulnev and Jaryshev proved that the equation (8) can be expressed in the more general form [5–7]:

$$M = \psi H \tag{11}$$

where $M = m/m_\infty = mK/a$ is the criterion of

Vol. 1 1960

the body's thermal inertia; $H = (\alpha/\lambda)(KS/V)$ is the generalized Biot criterion; V and S are the volume and the body's external surface, respectively.

For bodies of various configurations an approximate analytic expression for the criterion ψ has been found:

$$\psi = \frac{1}{\sqrt{(H^2 + 1{\cdot}437H + 1)}} \qquad (12)$$

The equation (12) defines the value of criterion ψ for bodies of various configurations with an exactness sufficient for practical calculations [7, 8].

If we picture the dependence between the rate of cooling of a body and the coefficient of heat transfer (Fig. 2) then the curve will be of a non-general character which is valid for the concrete

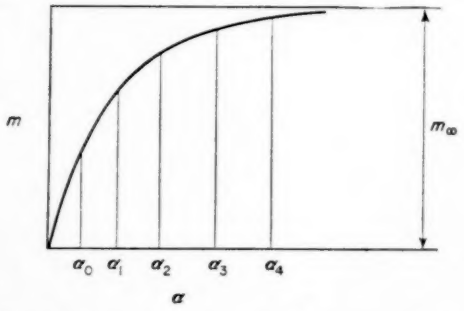

FIG. 2. The asymptotic law of m-rate increase for the regular body cooling when the heat transfer coefficient increases.

case where the configuration and the size of a body as well as the characteristics of the material are given. The dependence between the criteria M and H plotted in Fig. 3 is of a general type and it is valid with sufficient exactness for non-uniform isotropic bodies of various configurations and sizes which are made of solid or dry materials.

(a) The thermo-insulating nucleus of any arbitrary form with a metallic cover round it.†

† The "thermo-insulating nucleus" is defined as a part of a body or a system with a non-uniform temperature distribution. The "thermo-insulating cover" is a part of a body or a system with a uniform temperature distribution for the given experimental conditions.

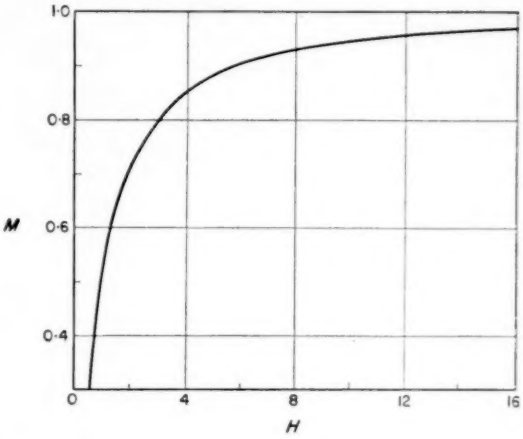

FIG. 3. The approximated universal dependence $M = M(H)$ for regular cooling or heating of a body which has any configuration.

The previous criteria are valid for these systems and to calculate them we can use formulae (11) and (12):

$$M = \frac{Km}{\lambda}\,\frac{\psi S_{\text{cov}}}{V}\left(\frac{\alpha}{m} - \frac{C_{\text{cov}}}{S_{\text{cov}}}\right) \qquad (13)$$

where C_{cov} and S_{cov} are the total heat capacity and a cover external surface; m is the rate of cooling of the whole system and the other symbols relate to the nucleus.

(b) A metallic nucleus with a thin thermo-insulating cover round it.

Suppose we neglect the heat capacity of the cover (C_{cov}) in comparison with the heat capacity C of the nucleus then the regular thermal regime can be expressed by:

$$m\,\frac{C}{S}\left(\frac{1}{\alpha} + \sum_i \frac{\delta_i}{\lambda_i}\right) = 1 \qquad (14)$$

where m is the cooling rate of the whole system; C and S are the heat capacity and a nucleus surface; λ_i and δ_i are the thermal conductivity coefficient and the thickness of the ith layer of the cover;‡ α is the heat transfer coefficient of the system.

(c) The simplest two-component bodies are spherical and plane bi-calorimeters.

‡ A cover may consist of several layers.

We shall define "bi-calorimeters of regular regime" as systems consisting of a metallic nucleus with a layer of close-fitting heat insulating material, which has finite heat capacity. In the spherical bi-calorimeter the nucleus (1) and the sphere cover (2) are arranged concentrically (see Fig. 4). In the plane bi-calorimeter the flat-parallel plate has a heat insulating material of thickness δ_2 round it (see Fig. 5).

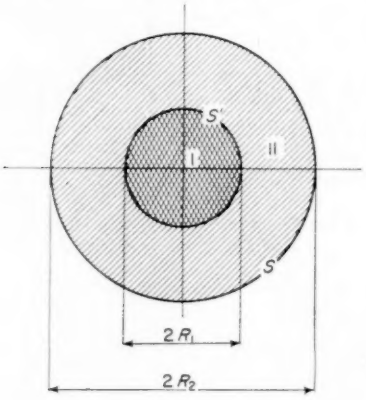

FIG. 4. A spherical bi-calorimeter.

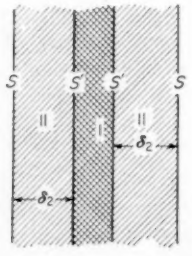

FIG. 5. A plane bi-calorimeter of a symmetric type.

Let us introduce the following values: $\phi = C_1/S^1$ is the nucleus constant; $l = R_1/R_2$ is the ratio of nucleus and cover radii; $P_1 = \delta_2/\lambda_2$ is the thermal resistance of the heat insulating layer and some new criteria such as

$$B = l\phi P_1 m$$

$$N = \frac{1 + l + l^2}{3l} \frac{C_1}{C_{\text{cov}}}$$

$$S^2 = \frac{B}{N}$$

$$\Pi = l \frac{m\phi}{\alpha}$$

Then a regular regime for all kinds of spheres with a metallic nucleus will be described by equation [2]:

$$1 - lA - NS^2 = \Pi\left\{\frac{(1-l)^2}{N}\frac{A}{S^2} + \frac{l}{N} + l - A\right\} \quad (15)$$

where $A = A(S)$ is a dimensionless parameter an expression of which is given in [2].

Note that $0 \leqslant N \leqslant \infty, 0 \leqslant l \leqslant 1, 0 \leqslant B \leqslant 1$. When we have such a case as $N \geqslant 2$, which is more frequently used, it is quite possible to reduce equation (15) to a simpler approximate form

$$B \approx \frac{1 - l\Pi - (1 + l + l^2)/3(\Pi/N)}{1 + (l - \Pi)/N} \quad (16)$$

The dependence $B = f(N,l)$ for all kinds of N and l has been plotted in Fig. 6. Analogous

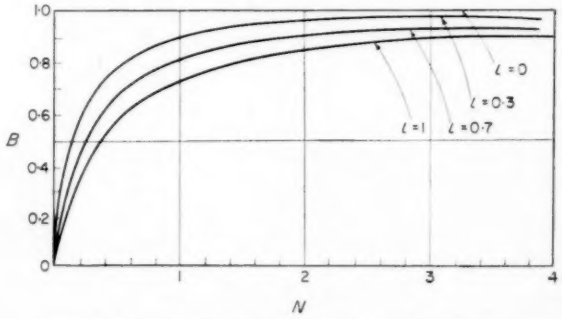

FIG. 6. The dependence $B = f(N,e)$ for the spherical bi-calorimeter at $\alpha \to \infty$.

formulae have been derived for a plane bi-calorimeter [2]. Here we shall take only the formula for the case $\alpha = \infty$. The criteria B and N for the plane bi-calorimeter are of the type

$$B = \phi P.m,\ N = \frac{C_1}{C_{\text{cov}}} \quad (17)$$

The graphical relation between criteria B and N has been presented in Fig. 6 and the curve corresponds to a plate for which $l = 1$.

In 1954 Condratjev and Dulnev gave a generalization of the thermal regular regime

Vol. 1 1960

theory for heating both of bodies and of systems under the action of the energy sources inside the body or at its boundary [11].

The theory is based on the following assumptions: (a) the capacity of energy sources (or sinks) is constant in time; (b) the ambient temperature is also constant; (c) the heat transfer coefficient and material thermal properties are independent of the temperature.

Analysing the exact solution of the problem† of body heating under the action of the internal energy sources one may come to the following conclusion as to why in some time the process becomes regular, when the temperature at any point of the body is changing according to the simple exponential law, i.e.

$$\ln (t_\infty - t) = -m\tau + G^*(x,y,z) \qquad (18)$$

where m is the rate of heating and G^* is the co-ordinate function.

The analysis of the heating of a body of any arbitrary configuration under the influence of an energy source will bring us to the conclusion that the rate of heating has the following dependence on the heat transfer coefficient:

$$m = a\psi^* \frac{S}{C} \qquad (19)$$

where

$$\psi^* = \frac{(t_\infty - t)_S}{(t_\infty - t)_V} \qquad (20)$$

the indexes S and V mean the average of the corresponding values along the body surface and its volume.

(a) The rate of heating either a body or a system is independent of the sources of power and their location in the system and is numerically equal to the rate of cooling (the sources of power are equal to zero).

(b) The rate of heating is independent of the co-ordinates.

(c) The shape coefficient K of a body which is heated by energy sources has the same physical meaning as the shape coefficient K' of a body which is heated in the medium. K and K' are equal.

† Later on we shall speak about the body heating under the influence of energy sources. All conclusions are valid for the case of a body cooling under the influence of energy sinks.

(d) The criteria ψ^* and ψ have a different physical meaning, but numerically they are equal.

(e) The temperature t_j at any point j of a body which is in a stage of regular regime, is subordinated to the following equation:

$$\frac{1}{m(t_j)_\infty} \frac{dt_j}{d\tau} + \frac{1}{(t_j)_\infty} - t_j = 1 \qquad (21)$$

where $(t_j)_\infty$ is the stationary temperature at the point j. Taking into account the first four results we can use the theory given above of a regular regime to calculate the numerical values of m and ψ^*.

Now we can show that a stationary temperature $(t_j)_\infty$ of any point j of the system depends upon the sources of power in the following way [8]:

$$(t_j) = t_e = \sum_{i=1}^{n}{}_\infty P_i F_{ij} \qquad (22)$$

where P_i is a total output, at i-region of the bodies system; n is a number of the system regions; F_{ij}, some coefficients which are independent of either temperature or the sources' output. To determine these coefficients it is necessary to solve an ordinary system of equations for the stationary temperature field.

If we consider the heating of a body under the influence of many energy sources we can obtain an approximated solution of a problem supposing that the temperature field becomes regular from time $\tau = 0$. In this case the temperature at any j-point will be determined by the approximated formula

$$t_j \approx \{1 - \exp(-m\tau)\} \sum_{i=1}^{n} P_i F_{ij} \qquad (23)$$

The peculiarity of the above discussed regular regime lies in the fact that after the regular regime has already started the peculiarities of the initial state do not influence the temperature field. The same phenomenon of the regularization of thermal regime takes place in other cases. For example, if the temperature of the external medium t_e changes at a constant velocity $w \neq 0$ then after a lapse of time the temperatures of all the points of the system will change with a constant velocity equal to w. Such a regular

regime was called a regular regime of the second kind and its regularities for bodies and systems of bodies have been studied in detail [12–14].

The regularization of the temperature field of a body for the oscillating change of the external temperature has not yet been thoroughly studied.† In this case we also observe the following regularity: the temperature at any point of the system is in the range of a mean value and has the same oscillating period for the ambient temperature [2, 10, 14].

An analysis of various cases of temperature field regularization made it possible to calculate the general thermal determination of a regular regime. Under the expression the "regular thermal regime" of a body or a system of bodies one may understand such a regime for the change of a system's temperature having the following properties:

(a) In the course of time a system's initial state does not influence the regularity of temperature change.

(b) The regularity of a temperature change with space–time has a simple mathematical expression.

(c) This rule is general for all points of the system.

The practical application of the regular regime theory: The regular regime theory is useful in solving various problems of practical value; in particular this theory is the basis of a technique for the determination of the thermal characteristics of materials.

(a) *The determination of the material's thermal characteristics*

The high speed methods based on this theory are fit for tests with any substance. Here we give only some of these methods.

The experimental part of the work according to any method of regular regime lies in the determination of the cooling rate m either of a body or of a system. For this purpose we generally use a differential thermocouple, one junction of which is in the body and the other in the medium. Observing the temperature change in space with time when a body is cooled in a liquid or a gas it is not difficult to define the rate of cooling, m, graphically:

$$\ln (t - t_c) = f(\tau).$$

The thermocouple junction can be at any point of a body since according to the theory the rate is independent of co-ordinates.

If the experiment is carried out in conditions of intensive heat transfer and $\alpha \geqslant 25\lambda V/KS$, it is possible to consider the heat transfer coefficient, assumed equal to infinity; using formulae (24) and (9) we find the rate of cooling and the thermal diffusivity of the material.

Cooling at very low values of the heat transfer coefficient and with a body of small size the temperature distribution in the body will be uniform. The criterion ψ is near unity and taking formula (8) we shall find the heat capacity of the material. The possible sizes of a sample will be evaluated as:

$$\frac{KS}{V} \leqslant \frac{0{\cdot}03\lambda}{a}$$

Thus the error in the determination of the thermal capacity caused by non-uniformity of the temperature field will not exceed 2 per cent [10, 16]. If we know the rate of a body's cooling at two different heat transfer coefficients, using formulae (11) and (12), we shall find the thermal characteristics of the material either (λ and c) or (a and λ), and the samples may be of any configuration [15].

In the cases discussed above it is not necessary to put samples into the apparatus. The exception is made only for dry substances and fibrous materials, which are usually put into metallic jars with thin walls. In this case we calculate using the formula (13), which takes into account the cover effect upon the rate of cooling.

Bi-calorimeters based on the regular regime theory are being practised on a large scale to measure the thermal properties of solids and liquids (see item 4). Three types of bi-calorimeters have been developed: plane, spherical and cylindrical. All three have a massive metallic nucleus in the centre with a thermocouple placed into it. The material under test is put between the metallic nucleus and the metallic cover of the apparatus (Fig. 7).

† The so called regular regime of the third kind.

Vol. 1 1960

The preheated apparatus is intensively cooled in a liquid and the rate of cooling is determined according to formula (24).

Then the thermal conductivity of the material under test is determined by formulae (17) and (18) (see [9, 10, 16]).

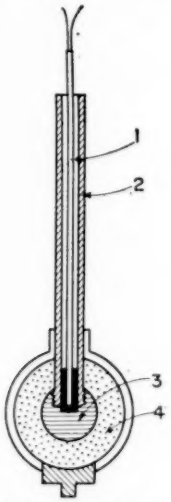

FIG. 7. A spherical bi-calorimeter. (1) A porcelain two-channel tube for a thermocouple. (2) An ebonite and textolite tube joined with the metallic nucleus (3). (4) A heat insulator under the test.

The application of bi-calorimeters for testing heat protective properties of clothing and fabrics has to be studied separately. The apparatus used for this has a simple mounting: the bi-calorimeter enveloped in a fabric has air freely flowing through it (this can be quiet or flowing, rarefied, dry or humid, etc.). The methods for the determination of heat protective properties of clothing and fabrics based on the regular regime theory, which is of a high speed by its nature, make it possible to collect information about the behaviour of different fabrics, depending on meteorological data, in a short space of time [2].

(b) *Determination of the heat transfer coefficient and total emissivity by the regular regime methods*

A new method for the determination of the heat transfer coefficient of various bodies, and total emissivity of any coverings has been developed using formulae (9) and (20). A model of high thermal conductivity material has been made to achieve this aim. Observing its process of cooling it is possible to determine the coefficient of heat transfer depending on temperature for a very short time. The total emissivity was measured analogically [10, 18, 19].

(c) *Determination of thermal inertia of thermometers and pyrometers*

This problem is of great importance for meteorology, experimental physics and engineering measurements. Therefore from the very start of exact thermometrics attention was drawn to it and became a subject of numerous investigations which are not finished even now. The theory of a regular thermal regime made it possible to analyse the notion of a constant of heat inertia and gave a new method for its experimental determination. It is rather easy to show that the value of ϵ is a convenient measure of the thermal inertia characteristic of an arrangement; $\epsilon = m^{-1}$, where m is the rate of cooling. Using equations (9), (10) and (20) we can find the dependence of the thermal inertia constant ϵ upon the heat transfer coefficient and this dependence is called the characteristic curve of heat inertia.

Recently Soviet scientists successfully completed investigations on heat inertia of various engineering arrangements based on an application of the regular regime theory [2, 10, 19].

(d) *Thermal calculations*

The theory of a regular thermal regime permits us to make approximate thermal calculations for various complex arrangements. For example, using the formulae of Section 4[2] it is possible to calculate the heat insulation of different units (aggregates) operating in unsteady state conditions [2].

Formulae (9) and (10) serve to elucidate the influence of the shape and size of a body upon the rate of its cooling or heating which is of special importance for the theory of thermal treatment.

The theory of regular regime, developed for bodies and systems with energy sources, has been used on a large scale for the last few years in the study of unstable processes in a complicated apparatus such as in a radio-electronic technique, which is a complex of cables set in piles.

REFERENCES

1. T. BOUSSINESQ, *Théorie Analytique de la Chaleur*, Tom. I et II (1901).
2. G. M. CONDRATJEV, *Regulyarnyi Teplovoi Rezhim* (*Regular Heat Cycle*). Gostekhteoretizdat (1954).
3. G. M. CONDRATJEV, *Zh. prikl. fiz.* **5**, 3 (1928).
4. G. M. CONDRATJEV, *Issledovanija v Oblasti Teplovykh Izmerenij i Priborov* (*Thermal Measurement and Equipment Research*). No. 21. LITMO (1957).
5. G. N. DULNEV and G. M. CONDRATJEV, *News Acad. Sc. USSR* (techn. depart.). News high educ. inst. (Instrument building). No. 3 (1955).
6. N. A. JARYSHEV, *Issledovanija v Oblasti Teplovykh Izmerenij i Priborov* (*Thermal Measurement and Equipment Research*). No. 37. LITMO (1959).
7. G. N. DULNEV and D. A. KIKNADZE, *Priborostroenie* No. 1 (1959).
8. G. N. DULNEV, *Teploobmen v Ogranichennykh Sistemakh Tel* (*Heat Transfer in Finite Systems of Bodies*). Doctoral dissertation, Energetics Institute, U.S.S.R. Academy of Sciences, Moscow (1958).
9. G. M. CONDRATJEV, *Kriterial'nye Velichiny Teorii Regulyarnogo Teplovogo Rezhima. Teorija Rodobija i Modelirovanya* (*Standard Quantities in the Theory of Regular Heat Cycles. Theory of Similarity and Modelling*). U.S.S.R. Academy of Sciences, Moscow (1951).
10. G. M. CONDRATJEV, *Teplovye Izmerenija* (*Thermal Measurements*). Mashgiz (1957).
11. G. N. DULNEV and G. M. CONDRATJEV, *News Acad. Sc. USSR* (techn. depart.). News high educ. inst. (Instrument building). No. 7 (1956).
12. G. P. IVANTSOV, *J. tech. ph.* **4**, 3 (1934).
13. G. M. CONDRATJEV, *Teploperedacha i Teplovoye Modelirovanie* (*Heat Transfer and Thermal Modelling*). U.S.S.R. Academy of Sciences, Moscow (1959).
14. A. V. LYKOV, *Teorija teploperedachi* (*The Theory of Heat Conduction*). Gostekhizdat (1952).
15. G. N. DULNEV, *Priborostroenie* No. 3 (1958).
16. A. F. BEGUNKOVA, *Issledovanija v Oblasti Teplovykh Izmerenij i Priborov* (*Thermal Measurement and Equipment Research*). No. 12. Mashgiz (1954).
17. G. N. DULNEV and E. M. SEMIASHKIN, *Issledovanija v Oblasti Teplovykh Izmerenij i Priborov* (*Thermal Measurement and Equipment Research*). No. 21. Leningrad (1957).
18. E. M. SEMIASHKIN, *Priborostroenie* No. 1 (1958).
19. N. A. JARYSHEV, *Issledovanija v Oblasti Teplovykh Izmerenij i Priborov* (*Thermal Measurement and Equipment Research*). No. 37. Leningrad (1959).

Vol. 1 1960

Int. J. Heat Mass Transfer. Vol. 1, pp. 161–172. Pergamon Press. 1960. Printed in Great Britain.

APPLICATION OF VARIATIONAL METHODS TO THE THERMAL ENTRANCE REGION OF DUCTS

E. M. SPARROW* and R. SIEGEL
Lewis Research Center,
National Aeronautics and Space Administration, Cleveland 35, Ohio

(*Received* 25 *November* 1959)

Abstract—A variational method is presented for solving eigenvalue problems which arise in connection with the analysis of convective heat transfer in the thermal entrance region of ducts. Consideration is given to both situations where the temperature profile depends upon one cross-sectional co-ordinate (e.g. circular tube) or upon two cross-sectional co-ordinates (e.g. rectangular duct). The variational method is illustrated and verified by application to laminar heat transfer in a circular tube and a parallel-plate channel, and good agreement with existing numerical solutions is attained. Then, application is made to laminar heat transfer in a square duct as a check, an alternate computation for the square duct is made using a method indicated by Millsaps and Pohlhausen. The variational method can, in principle, also be applied to problems in turbulent heat transfer.

Résumé—Une méthode variationnelle est présentée pour la résolution des problèmes de valeurs propres qui se présentent dans l'analyse de la transmission de chaleur par convection dans la région d'entrée des conduites. On considère les deux cas dans lesquels le profil des températures dépend soit d'une seule coordonnée dans la section droite (c'est-à-dire tuyaux circulaires) ou de deux coordonnées (tuyaux rectangulaires). La méthode est vérifiée par application à la transmission de chaleur laminaire dans un tuyau circulaire et dans un canal à faces planes parallèles, on obtient un bon accord avec les solutions numériques existantes. Une application est faite ensuite à la transmission de chaleur laminaire dans une conduite carrée. A titre de contrôle, un calcul différent pour la conduite carrée est effectué en utilisant la méthode indiquée par Millsaps et Pohlhausen. Cette méthode variationnelle peut également être appliquée aux problèmes de transmission de chaleur turbulente.

Zusammenfassung—Zur Lösung von Eigenwertproblemen des konvektiven Wärmeübergangs beim thermischen Einlauf in Kanäle wird eine Variations-methode mitgeteilt. Es wird sowohl der Fall betrachtet, dass das Temperaturprofil von einer Querschnittskoordinate (z.B. Kreisrohr), als auch jener, bei der es von zwei Querschnittskoordinaten (rechtwinkliger Kanal) abhängt. Die Variations-methode wird erläutert und auf den laminaren Wärmeübergang im Kreisrohr und im ebenen Spalt angewandt, wobei mit den bestehenden numerischen Lösungen eine gute Übereinstimmung gefunden wird. Sodann wird die Methode auf den laminaren Wärmeübergang im quadratischen Kanal angewendet und mit einer Iterationsrechnung nach Millsaps und Pohlhausen verglichen. Prinzipiell kann die Variations-methode auch auf Probleme des turbulenten Wärmeübergangs angewendet werden.

Abstract—Даётся вариационный метод решения задачи отыскания собственных значений уравнения, основанный на анализе конвективного теплообмена во входной области каналов. Рассматриваются два случая: один, когда температурный профиль зависит от одной координаты поперечного сечения (например, круглая труба), и второй — от двух координат поперечного сечения (например, канал прямоугольного профиля). Вариационный метод иллюстрируется и подтверждается применением его к случаям теплообмена при ламинарном потоке в круглой трубе и в плоско-параллельном канале; получается хорошее совпадение с существующими численными решениями. Затем, этот метод применяется к теплообмену в условиях ламинарного потока в канале с квадратным профилем. В последнем случае для контроля провели расчёт по указанному Миллсапсом и Польхаузеном методу. В принципе вариационный метод можно также применить и к задачам теплообмена в условиях турбулентного потока.

* At present, Professor of Mechanical Engineering, University of Minnesota Minneapolis 14, Minnesota.

NOMENCLATURE

A_{ni}, constants in eigenfunction equation (8);
a, half-height of parallel plate channel; half-length of side of square duct;
C_n, coefficients in temperature distribution;
c_p, specific heat at constant pressure;
d, tube diameter, $2r_0$;
e, f, g, functions of cross-section co-ordinates in equations (4a) and (10a);
I_0, I_1, I_2, integrals used in the variational procedure;
J, variational expression, $I_1 - \beta_n^2 I_2$;
k, thermal conductivity;
N, normal direction;
n, index number of eigenvalue;
Pr, Prandtl number, ν/α;
p, number of terms in eigenfunction equation (8);
Q, heat transfer rate per unit length;
q, heat transfer rate per unit area;
Re, tube Reynolds number, $\bar{w}d/\nu$;
Re_a, channel Reynolds number, $\bar{w}a/\nu$;
R_n, nth eigenfunction;
R_{ni}, functions in eigenfunction equation (8);
r, radial co-ordinate; r_0, tube radius;
T, static temperature; T_w, wall temperature; T_b, bulk temperature; T_0, entering temperature;
w, axial velocity distribution; $\bar{w}$, average velocity;
x, cross-section co-ordinate; $X = x/a$;
y, cross-section co-ordinate; $Y = y/a$;
z, axial co-ordinate; $Z = z/a$;
α, thermal diffusivity, $k/\rho c_p$;
β_n^2, nth eigenvalue;
η, η_1, η_2, cross-section co-ordinates;
ν, kinematic viscosity;
ρ, density;
ϕ, fully developed temperature distribution in square duct;

Subscript:
fd, denotes fully developed condition.

INTRODUCTION

In a previous paper [1], it was shown that variational methods could be successfully applied to the computation of the fully developed heat transfer characteristics for forced-convection flow in passages. Here, attention is directed to the thermal entrance region of flow passages. Our aim is to formulate and apply a variational procedure which may be used to determine entrance-region heat-transfer results. To illustrate the method and to establish confidence in its predictions, variational calculations are first carried out for the circular tube and the parallel-plate channel, and comparisons are made with exact (numerical) solutions available in the literature. Then, the variational method is applied to the square duct, for which there are no entrance-region calculations in the literature and for which an exact solution has not been possible.† In all the examples considered, the flow is laminar and fully developed, while the heat input is uniform along the length of the passage. However, the variational method may also be applied to the isothermal-wall boundary condition and to turbulent flow.

Vol. 1 1960

DESCRIPTION OF THE VARIATIONAL METHOD

General remarks

As early as 1885, it was demonstrated by Graetz [2] that the temperature solution in the thermal entrance region of a passage could be formulated as an eigenvalue problem. His analysis was concerned only with fully developed laminar flow in a circular tube having uniform wall temperature. Later, it was found [3–7] that the eigenvalue formulation would provide entrance-region results for both fully developed laminar and turbulent flows in circular tubes and parallel-plate channels for either uniform wall temperature or uniform wall heat flux. The same sort of formulation will apply to other non-circular ducts, as will be shown in a succeeding section.

† added in proof: A paper, which appeared after this work was completed, gives some approximate results for rectangular ducts with boundary conditions different from those treated here. This work by S. C. R. Dennis, A. McD. Mercer, and G. Poots, appeared in *Quart. Appl. Math.* **17**, 285 (1959).

To illustrate the way in which eigenvalues arise in the entrance-region heat transfer analysis, consider the problem of laminar flow in a circular tube with uniform wall heat flux. As shown in [6], the longitudinal variation of the wall temperature corresponding to the prescribed wall heat flux q may be written as

$$\frac{T_w - T_0}{qr_0/k} = \frac{11}{24} + \frac{4z/r_0}{Re\ Pr} + \\ + \sum_{n=1}^{\infty} C_n R_n(r_0) \exp\left(-\frac{\beta_n^2}{Re\ Pr}\ \frac{z}{r_0}\right) \quad (1)$$

where T_0 is the temperature of the fluid entering the tube and z is the distance measured from the entrance of the heated section. In the expression, β_n^2 and R_n, respectively, represent the eigenvalues and eigenfunctions of the following equation:

$$\frac{r_0}{r}\ \frac{d}{d(r/r_0)}\left[\frac{r}{r_0}\ \frac{dR_n}{d(r/r_0)}\right] + \\ + R_n\beta_n^2\left[1 - \left(\frac{r}{r_0}\right)^2\right] = 0 \quad (2)$$

$$dR_n/dr = 0 \text{ at } r = 0 \text{ and } r = r_0$$

Solutions of this homogeneous equation with homogeneous boundary conditions are possible only for a discrete, though infinite number of β_n^2 values. Each β_n^2 which permits a solution is called an eigenvalue, and the function R_n associated with the eigenvalue is called an eigenfunction. Equation (2) is a special case of the general Sturm–Liouville type. From Sturm–Liouville theory, it is noted in [6] that:

$$C_n = -\frac{\int_0^1 [r/r_0 - (r/r_0)^3]\ [(r/r_0)^2 - \\ - \tfrac{1}{4}(r/r_0)^4 - 7/24]\ R_n\, d(r/r_0)}{\int_0^1 [r/r_0 - (r/r_0)^3] R_n^2\, d(r/r_0)} \quad (3)$$

From this, it is seen that once the eigenfunctions R_n are known, the coefficients C_n of equation (1) may be evaluated. So it is apparent that a knowledge of the eigenvalues and eigenfunctions of equation (2) holds the key to the temperature solution (1). Since the β_n^2 are all positive, it is seen that the series contribution to equation (1) dies away for large values of z. Thus, the series is only important in the entrance region and consequently, the eigenvalue problem is of interest only in connection with entrance-region heat transfer results. For the uniform wall temperature problem, the knowledge of eigenvalues is not only necessary in the entrance region, but also in the fully developed domain.*

Our goal here is to present and apply a variational procedure for solving eigenvalue problems which may arise in connection with entrance-region heat transfer computations. The variational method is especially advantageous for the lower eigenvalues, and because of this, it serves to compliment the approximate techniques of [8–10] which work best for higher eigenvalues.

Consideration will be given to two general types of eigenvalue problems which may be of heat transfer interest. The first type arises when the temperature profile depends only on one cross-sectional co-ordinate, for example, the radial position in a circular tube or the distance from the center line of a parallel-plate channel. We will call this the one-dimensional eigenvalue problem. The second type arises when the temperature profile depends upon two cross-section co-ordinates, as in a rectangular duct. We will call this the two-dimensional eigenvalue problem. Separate presentations and examples will be given for each of the two types of problems.

The one-dimensional eigenvalue problem

We direct our attention to the Sturm–Liouville eigenvalue problem, which will include as special cases all heat transfer situations in which the temperature depends on only one cross-section co-ordinate. The Sturm–Liouville problem with which we are concerned is to find the eigenvalues† β_n^2 and eigenfunctions R_n of the following equation:

$$\frac{d}{d\eta}\left(e\ \frac{dR_n}{d\eta}\right) + fR_n + \beta_n g\ R_n = 0 \quad (4a)$$

with the condition that on the boundary surface

$$R_n = 0 \text{ or } dR_n/d\eta = 0 \quad (4b)$$

The functions e, f and g may depend upon the

* The first eigenvalue, at least, is necessary in the fully developed region.

† Only positive eigenvalues will arise in the problems of interest here.

independent variable η. Now, according to the calculus of variations (e.g. [11]), there corresponds to equation (4) the following variational expression J:

$$J \equiv I_1 - \beta_n^2 I_2 \tag{5}$$

$$I_1 = \int_a^b [e(dR_n/d\eta)^2 - fR_n^2]d\eta \tag{6}$$

$$I_2 = \int_a^b g R_n^2 \, d\eta \tag{7}$$

The variational expression J has a very special property, namely, that it takes on a stationary value, i.e. $\delta J \equiv 0$, when evaluated using a β_n^2 and an R_n which satisfy equations (4a) and (4b). This characteristic suggests a procedure for obtaining approximate solutions for the eigenvalues and eigenfunctions of equations (4a) and (4b) by using the variational expression J. The procedure is based on the Ritz method. According to this approach, a set of functions R_{n1}, R_{n2}, . . . is selected, each of which satisfies the boundary condition (4b). With these, the nth eigenfunction R_n is written as

$$R_n = A_{n1}R_{n1} + A_{n2}R_{n2} + \ldots = \sum_{i=1}^{p} A_{ni}R_{ni} \tag{8}$$

where the A_{n1}, A_{n2}, . . . are constants which remain to be determined. As explained later in detail, these unknown constants are found by imposing the condition that J take on a stationary value. An additional condition which must be satisfied by the eigenfunctions is that they are mutually orthogonal with respect to the weighting function g, i.e.

$$I_0 = \int_a^b g R_n R_m \, d\eta = 0, \qquad m = n-1, n-2, \ldots, 1 \tag{9}$$

Thus, for the nth eigenfunction, there are $n-1$ orthogonality equations. As a consequence, it is necessary to have at least n terms in the eigenfunction expression (8) to insure that the variational procedure can be fully carried through. For each eigenfunction, the variational procedure may be reapplied successively using an increasing number of terms in the series (8) until convergence to a desired accuracy is achieved. The convergence is hastened by choosing the form of the R_{ni} in accordance with any intuition or knowledge one may have about the problem. We now turn to describing the detailed steps by which the variational procedure is applied.

First eigenvalue: We begin by writing an expression for R_1 in the form of equation (8), selecting each function R_{1i} in the series to satisfy the boundary conditions. With this, the integrals I_1 and I_2, equations (6) and (7), are evaluated, and the variational expression J, equation (5), is constructed. For the first eigenfunction, the orthogonality condition (9) need not be considered, since there are as yet no other eigenfunctions. To find a stationary value of J, the expression is differentiated successively with respect to each A_{1i} and each resulting equation is set equal to zero. This provides a set of p linear, homogeneous (right-sides equal zero), algebraic equations involving the A_{11}, A_{12}, . . ., A_{1p}. A solution to such a homogeneous set is possible only if the determinant of the coefficients is equated to zero, and from this, there arises a polynomial of which β_1^2 is the smallest root. Then, returning to the p homogeneous algebraic equations, it is possible to find $p-1$ of the constants A_{1i}. The last coefficient is found by some other condition such as normalizing, i.e. setting $I_2 = 1$, or else by assigning some arbitrary value to R_1 at some particular value of η. As has already been noted, the procedure can then be repeated using a larger number of terms in the series (8) until a desired accuracy is attained.

Higher eigenvalues: The variational method for higher eigenvalues follows a path similar to that outlined for the first eigenvalue, except that the orthogonality condition (9) must now be incorporated into the procedure. This condition requires that the eigenvalues and eigenfunctions be found in ascending order; since the computation for the nth eigenfunction R_n assumes that all preceeding eigenfunctions are known. By employing the orthogonality conditions (9), it is possible to solve for $n-1$ of the A_{ni} in terms of all the others. Then, turning to the expression for J, these particular A_{ni} may be eliminated by direct substitution. Thus, the number of A_{ni} remaining in J is reduced to $p-(n-1)$. The stationary value of J is found by differentiating successively with respect to each of the remaining A_{ni} and equating each of the resulting equations to zero. From these $p-(n-1)$ linear homogeneous equations, the

Vol. 1 1960

eigenvalue β_n^2 can be found in a manner identical to that described in connection with the computation of the first eigenvalue. Then, the constants A_{ni} are computed using these $p-(n-1)$ equations and the orthogonality conditions. Because these equations are homogeneous, there will still be one undetermined A_{ni} and this can be found by imposing additional conditions as previously described. The process can then be repeated, taking additional terms in the series (8) until a suitable result for β_n^2 and R_n is achieved.

To help fix these ideas, illustrative examples will be given in a later section.

The two-dimensional eigenvalue problem

For the situation where the temperature depends upon two cross-sectional co-ordinates, the two-dimensional eigenvalue problems which lend themselves to solution by the variational technique are given by the following equation [12]:

$$\frac{\partial}{\partial\eta_1}\left(e\frac{\partial R_n}{\partial\eta_1}\right)+\frac{\partial}{\partial\eta_2}\left(e\frac{\partial R_n}{\partial\eta_2}\right)+fR_n+\beta_n^2gR_n=0 \tag{10a}$$

with the condition that on the bounding surface

$$R_n=0 \quad \text{or} \quad \partial R_n/\partial N=0 \tag{10b}$$

In this equation, the functions e, f and g may depend on both co-ordinates η_1 and η_2. In a manner parallel to the one-dimensional case, there exists a variational expression J which corresponds to the eigenvalue problem defined by equations (10a) and (10b). Rephrasing the findings of [12], J may be written as

$$J=I_1-\beta_n^2I_2 \tag{11}$$

$$I_1=\int_{\text{area}}\int\left[e\left\{\left(\frac{\partial R_n}{\partial\eta_1}\right)^2+\left(\frac{\partial R_n}{\partial\eta_2}\right)^2\right\}-fR_n^2\right]d\eta_1\,d\eta_2 \tag{12}$$

$$I_2=\int_{\text{area}}\int gR_n^2\,d\eta_1\,d\eta_2 \tag{13}$$

As before, the variational expression has the particular property that it takes on a stationary value when evaluated with an eigenvalue and eigenfunction of equations (10a) and (10b). This characteristic serves as a basis of an approximate method for finding the β_n^2 and R_n which is essentially identical to that which has already been described for the one-dimensional case. In applying the procedure to the two-dimensional case, it is to be remembered that the functions R_{ni} which make up the series (8) may now depend upon the two co-ordinates η_1 and η_2, instead of on the single η as before. Also, for the two-dimensional situation, the orthogonality condition takes the form

$$I_0=\int_{\text{area}}\int gR_nR_m\,d\eta_1\,d\eta_2=0, \qquad m=n-1,n-2,\ldots,1 \tag{14}$$

With these modifications, the detailed directions for using the variational method in the one-dimensional problem also apply here, and hence they need not be repeated.

An entrance-region heat transfer computation for a square duct will be carried out in a later section, and this will aid in further clarifying the application of the variational procedure to the two-dimensional case.

APPLICATION TO A CIRCULAR TUBE

As a first illustration of the application of the variational procedure, we consider the problem of laminar flow in a circular tube with uniform wall heat flux. The solution for the wall temperature as a function of position along the tube length has already been given in equation (1), while the associated eigenvalue problem is defined by equation (2). Now, for the uniform heat flux problem, it is well known that the first eigenvalue β_1^2 is zero, while R_1 is a constant usually taken as unity. It is also easy to show from equation (3) that $C_1=0$. So, with β_1^2 and R_1 known, we turn our attention to finding the second eigenvalue β_2^2 and its corresponding eigenfunction R_2.

To apply the variational method, we first compare equation (2) with the general form (4) and find that

$$\eta=r/r_0,\quad e=\eta,\quad f=0,\quad g=\eta(1-\eta^2)$$

With this, the integrals I_0, I_1 and I_2 become

$$I_0=\int_0^1\eta(1-\eta^2)R_nR_m\,d\eta=0, \qquad m=n-1,n-2,\ldots,1 \tag{15}$$

$$I_1 = \int_0^1 \eta(dR_n/d\eta)^2\, d\eta,$$
$$I_2 = \int_0^1 \eta(1-\eta^2)R_n^2\, d\eta \qquad (16)$$

The next step is to write R_2 as a sum of terms in the form of equation (8). In selecting the functions R_{2i}, we take cognizance of the boundary conditions (2) and of the fact that the eigenfunctions can have both positive and negative lobes between $\eta = 0$ and $\eta = 1$. Functions which immediately suggest themselves for the role of R_{2i} are $\cos 0\pi\eta = 1$, $\cos \pi\eta$, $\cos 2\pi\eta$, etc. So as a first approximation for R_2 in the form (8), we write:

$$R_2 = A_{21} + A_{22}\cos \pi\eta \qquad (17)$$

Then, substituting in equations (15) and (16) and carrying out the integration yields:*

$$I_0 = \frac{A_{21}}{4} + A_{22}\left(\frac{1}{\pi^2} - \frac{12}{\pi^4}\right) = 0 \qquad (18a)$$

$$I_1 = \frac{A_{22}^2\,\pi^2}{4} \qquad (18b)$$

$$I_2 = \frac{A_{21}^2}{4} + 2A_{21}A_{22}\left(\frac{1}{\pi^2} - \frac{12}{\pi^4}\right) + \frac{A_{22}^2}{8}\left(1 - \frac{3}{\pi^2}\right) \qquad (18c)$$

Now, using equations (18b) and (18c), we can construct the variational expression

$$J = I_1 - \beta_2^2 I_2$$

Then, by the orthogonality condition (18a), A_{21} can be eliminated from J, giving

$$J = \frac{A_{22}^2\pi^2}{4} - \beta_2^2\left[-4A_{22}^2\left(\frac{12}{\pi^4} - \frac{1}{\pi^2}\right)^2 + \frac{A_{22}^2}{8}\left(1 - \frac{3}{\pi^2}\right)\right] \qquad (19)$$

To find the stationary value, we take $\partial J/\partial A_{22} = 0$, and from this it follows that

$$\beta_2^2 = 28{\cdot}997 \qquad (20)$$

Considering the simplicity of the approximation and the relative ease of computation, this result is in surprisingly good agreement with the exact value [6]:

$$\beta_2^2 = 25{\cdot}6796 \qquad (21)$$

* It is to be remembered that $R_{n-1} = R_1 =$ constant.

The constants A_{21} and A_{22} remain to be determined. From the condition $\partial J/\partial A_{22} = 0$, there is obtained an algebraic equation which tells us nothing about the constants. But, from the orthogonality condition (18a), we have the ratio of A_{21} to A_{22}. With this, the eigenfunction expression (17) becomes

$$R_2 = A_{22}(0{\cdot}087482 + \cos \pi\eta) \qquad (17a)$$

As expected in accordance with what has been said in the general presentation of the variational method, there remains one undetermined constant which must be found from other conditions. To facilitate comparison with [6], we impose the condition that $R_2(0) = 1$, and with this, equation (17a) becomes

$$R_2 = 0{\cdot}080445 + 0{\cdot}91956\cos \pi\eta \qquad (17b)$$

The value of R at $r = r_0$ ($\eta = 1$) plays an important role in the wall-temperature computation, as may be seen from equation (1). The first approximation, equation (17b), gives a value $R_2(1) = -0{\cdot}83911$, as opposed to $-0{\cdot}49252$ from the exact solution. This comparison strongly suggests that a higher variational approximation be carried out for R_2.

As a logical refinement of equation (17), we add on a term $\cos 2\pi\eta$ and write

$$R_2 = A_{21} + A_{22}\cos \pi\eta + A_{23}\cos 2\pi\eta \qquad (22)$$

Proceeding as before, I_0, I_1 and I_2 are computed by integration of equation (22). From the orthogonality condition, $I_0 = 0$, there is obtained

$$A_{21} = 0{\cdot}087482\,A_{22} + 0{\cdot}303964\,A_{23} \qquad (23)$$

Using I_1 and I_2, the variational expression $J = I_1 - \beta_2^2 I_2$ is evaluated to be

$$J = 2{\cdot}46740\,A_{22} - 3{\cdot}55556\,A_{22}A_{23} + 9{\cdot}86960 = A_{23}^2 - \beta_2^2[0{\cdot}0870045\,A_{22}^2 - 0{\cdot}0121336\,A_{22}A_{23} + 0{\cdot}115501\,A_{23}^2 - 0{\cdot}25\,A_{21}^2] \qquad (24)$$

A_{21} can be eliminated from this expression by using equation (23), leaving only A_{22} and A_{23}. The stationary value of J is achieved by taking

Vol. 1 1960

$\partial J/\partial A_{22} = 0$, $\partial J/\partial A_{23} = 0$. From this, there results:

$$\left.\begin{aligned} \frac{\partial J}{\partial A_{22}} = 0 \rightarrow (4{\cdot}93480 - 0{\cdot}170182\,\beta_2^2)A_{22} + \\ + (-3{\cdot}55556 + 0{\cdot}0254293\,\beta_2^2)A_{23} = 0 \\ \frac{\partial J}{\partial A_{23}} = 0 \rightarrow (-3{\cdot}55556 + \\ + 0{\cdot}0254293\,\beta_2^2)A_{22} + (19{\cdot}7392 - \\ - 0{\cdot}184805\,\beta_2^2)A_{23} = 0 \end{aligned}\right\} \quad (25)$$

A nontrivial solution of this pair of linear, homogeneous equations is possible only if

$$\begin{vmatrix} (4{\cdot}93480 - 0{\cdot}170182\,\beta_2^2) & (-3{\cdot}55556 + 0{\cdot}0254293\,\beta_2^2) \\ (-3{\cdot}55556 + 0{\cdot}0254293\,\beta_2^2) & (19{\cdot}7392 - 0{\cdot}184805\,\beta_2^2) \end{vmatrix} = 0$$

This determinant yields a quadratic equation for β_2^2, the smallest root* of which is

$$\beta_2^2 = 25{\cdot}6956 \quad (26)$$

This is in remarkably close agreement with the value 25·6796 from the exact solution. Now, turning to the determination of the constants A_{2i}, there is first obtained from either of equations (25) the ratio A_{23}/A_{22}. Next, from equation (23), the ratio A_{21}/A_{22} is found. Finally there is imposed the condition that $R_2(0) = 1$. With this information, all three constants may be calculated and the expression for R_2 becomes

$$R_2 = 0{\cdot}109207 + 0{\cdot}746309\cos\pi\eta + \\ + 0{\cdot}144484\cos 2\pi\eta \quad (22a)$$

The value of R_2 at the tube wall ($\eta = 1$) has been already noted as playing an important role in the heat transfer results. Equation (22a) gives a value $R_2(1) = -0{\cdot}49262$, which is in excellent agreement with the result −0·49252 from the exact solution. In addition to $R_n(1)$, the solution for the wall temperature variation as given by equation (1) depends on the coefficients C_n. These constants can be computed from the quotient of integrals given in equation (3). Utilizing equation (22a) for R_2, the coefficient C_2 is computed as 0·40680, which deviates by only 0·8 per cent from the value 0·40348 given by the exact solution.

This illustration demonstrates that the variational procedure is capable of providing excellent heat transfer results. The high level of agreement indicates that there is no need to refine R_2 further. However, if an exact solution had not been available for comparison purposes, it would have been necessary to take a higher approximation for R_2 to establish the level of accuracy.

If desired, the variational method could now be applied to the computation of the next eigenfunction R_3. No essential changes in the method are necessary, except that the expression for R_3 in the form of equation (8) would likely contain additional cosine terms. Also, in the orthogonality condition (15), we would use equation (22a) for the known eigenfunction R_2, while R_1 is a constant. However, since our purpose in considering the circular tube has only been to illustrate the variational method, the computation for the higher eigenvalues will not be carried out.

APPLICATION TO A PARALLEL PLATE CHANNEL

As a second example which may serve to establish confidence in the variational procedure, we turn to the problem of laminar flow in a parallel-plate channel with uniform wall-heat flux. Corresponding to the prescribed heat flux, the variation of the wall temperature along the length is given by:

$$\frac{T_w - T_0}{qa/k} = \frac{17}{35} + \frac{z/a}{Re_a\,Pr} + \\ + \sum_{n=1}^{\infty} C_n\,R_n(a)\exp\left\{-\frac{\beta_n}{(3/2)\,Re_a\,Pr}\,\frac{z}{a}\right\} \quad (27)$$

The eigenvalues R_n and eigenfunctions β_n are found from the following homogeneous system:

$$\frac{d^2R_n}{d(y/a)^2} + R_n\beta_n^2\,[1 - (y/a)^2] = 0 \quad (28a)$$

$$dR_n/dy = 0 \text{ at } y = 0 \text{ and } y = a \quad (28b)$$

* Since the value of β_2^2 associated with the exact solution is an absolute minimum, it is clear that the best result is achieved by selecting the smallest root.

while the coefficients C_n are computed from the ratio:

$$C_n = -\frac{\int_0^1 [1-(y/a)^2][\frac{3}{4}(y/a)^2 - \frac{1}{8}(y/a)^4 - 39/280] R_n \, d(y/a)}{\int_0^1 [1-(y/a)^2] R_n^2 \, d(y/a)} \tag{29}$$

Here again is a problem ideally suited for the variational procedure. Comparing equation (28a) with the general one-dimensional form (4a), it is seen that

$$\eta = y/a, \; e = 1, \; f = 0, \; g = 1 - \eta^2 \tag{30}$$

and the integrals I_0, I_1 and I_2 become

$$I_0 = \int_0^1 (1-\eta^2) R_n R_m \, d\eta = 0, \quad m = n-1, n-2, \ldots, 1 \tag{31a}$$

$$I_1 = \int_0^1 (dR_n/d\eta)^2 \, d\eta, \quad I_2 = \int_0^1 (1-\eta^2) R_n^2 \, d\eta \tag{31b}$$

Since we are dealing with the case of uniform wall heat flux, it follows that $\beta_1^2 = 0$, $R_1 =$ constant, and $C_1 = 0$. So, attention can immediately be directed to the second eigenvalue R_2. Drawing upon our experience with the circular tube, we start out by writing R_2 in the form of equation (22). Following through the operations as before, it is found that

$$\beta_2^2 = 18{\cdot}39, \qquad R_2 = -0{\cdot}3157 + 1{\cdot}124 \cos \pi\eta + 0{\cdot}1924 \cos 2\pi\eta \tag{32}$$

The numerical solution of [7] yields a value of 18·38 for β_2^2. For $R_2(1)$, which is needed in the wall-temperature computation, [7] gives $-1{\cdot}27$ as compared to $-1{\cdot}25$ from the variational solution (32). No results for C_2 are provided in [7] and so this computation is omitted here.

From the excellent level of agreement which has been demonstrated, one can draw a real feeling of confidence in the utility of the variational procedure.

APPLICATION TO A SQUARE DUCT

For the previous examples which have been presented, there exist numerical solutions in the literature. These illustrations have been useful in establishing a feel for the accuracy which could be achieved by the variational method. Now, we turn to a situation for which there are no entrance-region calculations in the literature.

Consideration is given to a laminar flow in a square duct, Fig. 1, having a heat flux which is uniform both along the length and around the periphery. Since this physical problem is not treated elsewhere, we start from first principles.

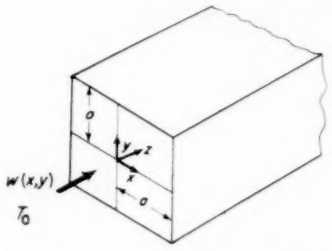

FIG. 1. Co-ordinate system for square duct.

The energy equation appropriate to the fully developed laminar flow of an incompressible, constant property fluid is

$$\rho c_p w \frac{\partial T}{\partial z} = k \left(\frac{\partial^2 T}{\partial x^2} + \frac{\partial^2 T}{\partial y^2} \right) \tag{33}$$

where axial heat conduction has been neglected compared to transverse conduction. Far down the duct, $\partial T/\partial z$ becomes a constant and the condition of fully developed heat transfer is achieved. A solution for the temperature distribution in the fully developed regime has been found by variational means in [1] as follows.

$$\frac{T - T_0}{Q/8k} = \frac{2Z}{Re_a Pr} + \phi \tag{34a}$$

$$\phi = \frac{X^2 + Y^2}{2} - 0{\cdot}16032 \, [(X^2-1)^2 + (Y^2-1)^2] - 0{\cdot}13290 \, [(X^2-1)(Y^2-1)]^2 + 0{\cdot}06803 \tag{34b}$$

where T_0 is the temperature of the fluid entering the duct, Q is the heat transfer per unit length and X, Y and Z are dimensionless co-ordinates.

Now, turning to the entrance-region, we propose a solution in the following form which will apply anywhere throughout the duct:

$$\frac{T - T_0}{Q/8k} = \frac{2Z}{Re_a \, Pr} + \phi + \sum_{n=1}^{\infty} C_n R_n \exp\left(- \frac{\beta_n^2}{Re_a \, Pr} Z \right) \tag{35}$$

Vol. 1 1960

In this equation, R_n depends on both cross-section co-ordinates X and Y. To find the governing equation for R_n, (35) is introduced into the energy equation (33), from which it follows that:

$$\frac{\partial^2 R_n}{\partial X^2} + \frac{\partial^2 R_n}{\partial Y^2} + \beta_n^2 (w/\bar{w}) R_n = 0 \qquad (36a)$$

It is also easy to show that:

$$dR/dX = 0 \text{ at } X \pm 1,$$
$$dR/dY = 0 \text{ at } Y = \pm 1 \qquad (36b)$$

So, once again we have an eigenvalue problem. The first thought about solving equation (36) is to try separation of variables, i.e. to suppose that R_n is a product of a function of X and a function of Y. However, this approach is not successful since the velocity distribution $w/\bar{w}$ is not in a product form. Hence, it is necessary to deal with equation (36a) as it stands.

The eigenvalue problem as represented by equations (36a) and (36b) is well-suited to be attacked by the variational procedure. Comparing equation (36a) with the general two-dimensional form (10a), it is seen that:

$$\eta_1 = X,\ \eta_2 = Y,\ e = 1,\ f = 0,\ g = w/\bar{w} \qquad (37)$$

With this, the integrals I_0, I_1 and I_2 as given by equations (14), (12) and (13) become

$$I_0 = 4 \int_0^1 \int_0^1 (w/\bar{w}) R_n R_m \, dX \, dY = 0,$$
$$m = n - 1, n - 2, \ldots, 1 \qquad (38a)$$

$$I_1 = 4 \int_0^1 \int_0^1 [(\partial R_n/\partial X)^2 + (\partial R_n/\partial Y)^2] dX \, dY \qquad (38b)$$

$$I_2 = 4 \int_0^1 \int_0^1 (w/\bar{w}) R_n^2 \, dX \, dY \qquad (38c)$$

Since we are dealing with the uniform heat flux case, the first eigenvalue β_1^2 is zero, while $R_1 =$ constant and $C_1 = 0$. So consideration can be immediately given to the second eigenvalue R_2. In selecting a trial function for R_2, we are guided by prior experience with the parallel-plate channel. For that configuration, an eigenvalue expression in the form of equation (22) proved to be quite satisfactory. Generalizing equation (22) to the two-dimensional case, we write

$$R_2 = A_{21} + A_{22} \cos \pi X \cos \pi Y +$$
$$+ A_{23} [\cos \pi X \cos 2\pi Y + \cos 2\pi X \cos \pi Y] \qquad (39)$$

where the constants A_{21}, A_{22} and A_{23} remain to be determined by use of the variational method. The first step is to compute the I integrals of equations (38). To carry out the integrations, a knowledge of the velocity distribution $w/\bar{w}$ is required. An accurate velocity profile has been determined by variational means [1] as follows:

$$w/\bar{w} = (X^2 - 1)(Y^2 - 1)[2{\cdot}0983 +$$
$$+ 0{\cdot}29181 (X^2 + Y^2) + 0{\cdot}87546 X^2 Y^2] \qquad (40)$$

Utilizing this expression in conjunction with equation (39), the I integrals are found to be

$$I_0 = A_{21} + 0{\cdot}082665 A_{22} -$$
$$- 0{\cdot}0432577 A_{23} = 0 \qquad (41a)$$

$$I_1 = 2\pi^2 [A_{22}^2 + 5A_{23}^2] \qquad (41b)$$

$$I_2 = -4A_{21} + 0{\cdot}83989 A_{22}^2 +$$
$$+ 2{\cdot}0001 A_{23}^2 + 1{\cdot}16410 A_{22} A_{23} \qquad (41c)$$

Then, the variational expression $J = I_1 - \beta_2^2 I_2$ is constructed. Utilizing equation (41a), it is possible to eliminate A_{21} from J, leaving only A_{22} and A_{23}. The stationary value is found by setting $\partial J/\partial A_{22} = 0$ and $\partial J/\partial A_{23} = 0$. From this, there is obtained

$$\frac{\partial J}{\partial A_{22}} = 0 \rightarrow (39{\cdot}478 - 1{\cdot}6251 \beta_2^2) A_{22} -$$
$$- (1{\cdot}1927 \beta_2^2) A_{23} = 0 \qquad (42a)$$

$$\frac{\partial J}{\partial A_{23}} = 0 \rightarrow (-1{\cdot}1927 \beta_2^2) A_{22} +$$
$$+ (197{\cdot}39 - 3{\cdot}9852 \beta_2^2) A_{23} = 0 \qquad (42b)$$

By setting the determinant of the coefficients equal to zero, there results a polynomial in β_2^2, the smallest root of which

$$\beta_2^2 = 20{\cdot}929 \qquad (43)$$

provides the second eigenvalue. Next, the constants A_{21}, A_{22} and A_{23} are found by utilizing either of equations (42) in conjunction with (41a) plus an additional condition. In this instance, as a matter of variety, we will impose the condition that the eigenfunction be normalized, i.e. $I_2 = 1$. There is thus sufficient information

to determine all the constants, and the final expression for the eigenfunction R_2 becomes:

$$R_2 = 0{\cdot}067685 - 0{\cdot}92477 \cos \pi X \cos \pi Y - \\ - 0{\cdot}20252 [\cos \pi X \cos 2\pi Y + \\ + \cos 2\pi X \cos \pi Y] \quad (44)$$

The last bit of information needed to compute temperature distribution results from equation (35) is the constant C_2. Imposing the condition that $T = T_0$ at the entrance section ($Z = 0$), equation (35) becomes

$$\sum_{n=1}^{\infty} C_n R_n = -\phi \quad (45a)$$

Then, multiplying through by $(w/\bar{w})R_m$ and integrating over X and Y from 0 to 1, it follows by use of the orthogonality condition (38a) that

$$C_n = -\frac{\int_0^1\int_0^1 (w/\bar{w})R_n\phi \, dX \, dY}{\int_0^1\int_0^1 (w/\bar{w})R_n^2 \, dX \, dY} \quad (45b)$$

Carrying out the integration for R_2, it is found that

$$C_2 = -0{\cdot}2467 \quad (46)$$

This completes the computation for the second eigenfunction. To check the level of accuracy of the results, the variational procedure might be reapplied to an expression for R_2 which contains additional terms. But, we have decided instead to redo the problem using a completely different approximation procedure. The method is a modification of an idea presented by Millsaps and Pohlhausen [13] and its application to the current problem is discussed briefly in the Appendix. The results of this alternate computation are in very good agreement with those of the variational method.

With the second eigenvalue at our disposal, we can now turn to a discussion of the heat transfer results. The temperature distribution corresponding to the prescribed heat flux is given by equation (35), where ϕ represents the fully developed solution as written in equation (34), while C_2, R_2 and β_2^2 are given by equations (46), (44) and (43), respectively. Since we have only one term of the series ($C_1 = 0$), attention must be directed to that portion of the duct near the fully developed region. When the heat flux is prescribed, the information of greatest interest is the resulting wall temperature. In this instance, where the heat flux is everywhere uniform, the wall temperature will vary around the periphery in any cross-section, as well as along the length. Because of the symmetry of the problem, consideration need only be given to a typical part of the wall: $X = 1$, $0 \leqslant Y \leqslant 1$. The wall-temperature result can be put in a convenient form by first introducing the bulk temperature T_b:

$$\frac{T_b - T_0}{Q/8k} = \frac{2Z}{Re_a Pr} \quad (47)$$

and then, it may be observed that under fully developed conditions

$$\frac{(T - T_b)_{fd}}{Q/8k} = \phi \quad (48)$$

With these, equation (35) can be rephrased as:

$$\frac{T - T_b}{(T - T_b)_{fd}} = 1 + \frac{\sum_{n=1}^{\infty} C_n R_n \exp\left(-\frac{\beta_n^2}{Re_a Pr} Z\right)}{\phi} \quad (49)$$

Finally, at the wall ($X = 1$, $0 \leqslant Y \leqslant 1$), there is obtained

$$\left.\begin{aligned} \frac{T_w - T_b}{(T_w - T_b)_{fd}} = \\ 1 + C_2 \left[\frac{R_2}{\phi}\right]_{X=1} \exp\left(-\frac{\beta_2^2}{Re_a Pr} Z\right), \\ 0 \leqslant Y \leqslant 1 \end{aligned}\right\} \quad (50)$$

where the series has been truncated after $n = 2$. The group $C_2(R_2/\phi)_{X=1}$ as evaluated from the variational method has been plotted as a solid line on Fig. 2. In the region near the mid-wall ($Y = 0$), the group has negative values; while near the corner, the group has positive values. Using this information in conjunction with equation (50), it is seen that for locations near the corner, the wall-to-bulk temperature difference is greater in some part of the entrance-region than it is in the fully developed region.

Vol. 1 1960

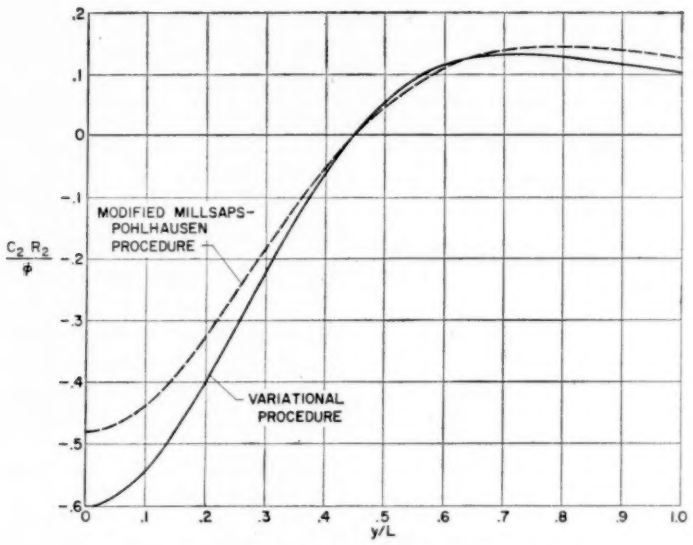

FIG. 2. Shape of temperature distribution along wall.

Of course, without additional terms in the series, it is not possible to know the extent of the entrance region where $(T_w - T_b) > (T_w - T_b)_{fd}$. This finding is somewhat surprising in view of previous experience with one-dimensional geometries such as the circular-tube and parallel-plate channel. In those configurations, where peripheral variations are absent, $T_w - T_b$ in the entrance-region is always less than the fully developed temperature difference. In the present instance, where there are peripheral variations, it is the feeling of the writers that $T_w - T_b$ is not the governing driving force for heat transfer at local positions around the periphery. Hence, there would be no reason to expect that the longitudinal variation of $T_w - T_b$ should follow the same trend here as was found in the simpler geometries. The fact that the longitudinal temperature variations are different in different parts of the cross-section suggests that there is little utility in computing average Nusselt numbers.

The findings derived from the variational method are closely confirmed by the alternate computation of the Appendix, as may be seen from the dashed line of Fig. 2. This good agreement increases our confidence in the results, but ultimate confirmation awaits some more exact solution, an approach to which is currently not apparent to the writers.

CONCLUDING REMARKS

The examples considered here are meant to illustrate the method and by no means exhaust the problems to which the variational technique can be applied.

Although the illustrations were concerned with the uniform heat flux case, solutions for uniform wall temperature are obtained with equal facility. In the latter case, the functions R_{ni} which make up the eigenfunction expression (8) would be selected to have zero values at the wall, rather than zero derivatives as in the former. It is also worth noting that the first eigenvalue for the uniform wall temperature situation will not be zero, nor will R_1 be a constant. Aside from these matters, the method is applied exactly as has been illustrated.

In principle, the variational procedure could be applied to problems in turbulent heat transfer. However, no work has thus far been done along these lines.

APPENDIX

Alternate Eigenvalue Calculation

According to the idea of Millsaps and Pohlhausen [13], the eigenfunctions for a laminar

convective, heat transfer problem are expanded in terms of the eigenfunctions of the slug-flow problem. For the square duct, such an expansion for R_2 which is truncated after three terms is

$$R_2 = D_1 \cos \pi X \cos \pi Y + \\ + D_2(\cos \pi X \cos 2\pi Y + \cos 2\pi X \cos \pi Y) + \\ + D_3(\cos 2\pi X \cos 2\pi Y) \quad (51)$$

where D_1, D_2 and D_3 remain to be determined. Introducing this expression into the governing equation (36a) gives:

$$2\pi^2 D_1 \cos \pi X \cos \pi Y + \\ + 5\pi^2 D_2(\cos \pi X \cos 2\pi Y + \\ + \cos 2\pi X \cos \pi Y) + \\ + 8\pi^2 D_3(\cos 2\pi X \cos 2\pi Y) = \beta_2^2(w/\bar{w})R_2 \quad (52)$$

Then, equation (52) is multiplied through by $\cos \pi X \cos \pi Y$ and integrated over X and Y from 0 to 1. Next, equation (52) is multiplied by $(\cos \pi X \cos 2\pi Y + \cos 2\pi X \cos \pi Y)$ and integrated over the same range. Finally, this same procedure is carried through with $\cos 2\pi X \cos 2\pi Y$. The result of these operations is three linear, homogeneous, algebraic equations for the D_1, D_2 and D_3, the coefficients of which contain β_2^2. To obtain a nontrivial solution, the determinant of the coefficients is equated to zero, and this gives:

$$\beta_2^2 = 20{\cdot}222 \quad (53)$$

which is rather good agreement with equation (43) from the variational procedure. The D-values are then found by returning to the homogeneous algebraic equations, from which two of the three D's can be determined in terms of the third one. The third D value may be left unspecified or else arbitrarily assigned. This will have no effect on the final result for the desired quantity C_nR_n (see equation (35)), since a change in the level of R_n will be automatically compensated by a corresponding change in C_n. Then, turning to the computation of C_2, the R_2 expression (with D-values now known) is introduced into equation (45b) and the integration carried out. With this, the final result for the C_2R_2 product is

$$C_2R_2 = 0{\cdot}2140 \cos \pi X \cos \pi Y + \\ + 0{\cdot}01740 \cos 2\pi X \cos 2\pi Y + \\ + 0{\cdot}04698(\cos \pi X \cos 2\pi Y + \\ + \cos 2\pi X \cos \pi Y) \quad (54)$$

Since the form of (54) is somewhat different from that of the variational eigenfunction, comparisons are best made by evaluating the expressions at specific X- and Y-values. Fig. 2 shows a comparison made along the wall, $X = 1$, $0 \leqslant Y \leqslant 1$, with quite good agreement. A similar comparison has been made along the center-line in the fluid, $X = 0$, $0 \leqslant Y \leqslant 1$, with about the same level of agreement.

ACKNOWLEDGEMENT

The writers gratefully acknowledge the valuable discussions on variational methods with Dr. S. H. MASLEN of the NASA Lewis Research Center.

REFERENCES

1. E. M. SPARROW and R. SIEGEL, *J. Heat Transfer, Trans. Amer. Soc. Mech. Engrs.* C **81**, 157 (1959).
2. M. JAKOB, *Heat Transfer* Vol. 1, pp. 451–461. John Wiley, New York (1949).
3. V. J. BERRY, *Appl. Sci. Res., Hague* A **4**, 61 (1953).
4. C. A. SLEICHER, JR. and M. TRIBUS, *Trans. Amer. Soc. Mech. Engrs.* **79**, 789 (1957).
5. E. M. SPARROW, T. M. HALLMAN and R. SIEGEL, *Appl. Sci. Res., Hague* A **7**, 37 (1957).
6. R. SIEGEL, E. M. SPARROW and T. M. HALLMAN, *Appl. Sci. Res., Hague* A **7**, 386 (1958).
7. C. S. YIH and J. E. CERMAK, *Laminar Heat Convection in Pipes and Ducts*. Report No. 5, Civil Engineering Department, Colorado Agricultural and Mechanical College (1951).
8. J. R. SELLARS, M. TRIBUS and J. S. KLEIN, *Trans. Amer. Soc. Mech. Engrs.* **78**, 441 (1956).
9. L. S. DZUNG, Heat transfer in a round duct with sinusoidal heat flux distribution. *Proceedings of the Second International Conference on the Peaceful Uses of Atomic Energy, Geneva*, 1958, paper P253. United Nations, New York (1958).
10. R. D. CESS, *J. Aero. Space Sci.* **26**, 723 (1958).
11. F. B. HILDEBRAND, *Methods of Applied Mathematics* Chapter 2. Prentice-Hall, New York (1952).
12. J. D. TAMARKIN and W. FELLER, *Partial Differential Equations* p. 267. Notes prepared for Brown University Summer Session for Advanced Instruction and Research in Mechanics, Brown University Press (1941).
13. K. MILLSAPS and K. POHLHAUSEN, Heat transfer to Hagen–Poiseuille flows. *Proceedings, Conference on Differential Equations, University of Maryland* (1955).

Vol. 1 1960

Int. J. Heat Mass Transfer. Vol. 1, pp. 173–191. Pergamon Press 1960. Printed in Great Britain.

ANALYSIS OF THE FLOW AND ENERGY SEPARATION IN A TURBULENT VORTEX

R. G. DEISSLER and M. PERLMUTTER
Lewis Research Center, National Aeronautics and Space Administration,
Cleveland, Ohio

(*Received* 16 *June* 1959)

Abstract—An analysis is made of the velocity, temperature and pressure distributions in a turbulent vortex with radial and axial flow. For making the calculations the vortex is divided into a core and an annular region, each with a different uniform axial mass velocity, although the equations obtained are applicable to an arbitrary axial mass velocity distribution. Tangential velocity, temperature and pressure distributions, as well as curves for overall energy or temperature separation, are presented and compared with experiment.

Using the analytical results, the causes of the energy separation are studied. It is concluded that the most important factor affecting the total temperature of a fluid element in a compressible vortex is the turbulent shear work done on or by the element.

Résumé—Une analyse est faite des distributions de vitesses, de températures et de pressions dans un tourbillon turbulent à écoulement radial et axial. Pour faire les calculs, le tourbillon a été divisé en deux régions: noyau et région annulaire, chaque région possédant une vitesse axiale uniforme différente, bien que les équations obtenues soient applicables à une distribution arbitraire des vitesses axiales. Les distributions de vitesses tangentielles, de températures et de pressions, ainsi que des courbes pour la séparation d'énergie et de température de l'ensemble, sont présentées et comparées à l'expérience.

Les causes de la séparation d'énergie sont étudiées à partir des résultats analytiques. En conclusion, le facteur le plus important affectant la température totale d'un élément de fluide dans un tourbillon compressible est le travail de cisaillement turbulent effectué sur, ou par, l'élément.

Zusammenfassung—Die Verteilungen der Geschwindigkeit, der Temperatur und des Drucks in einem turbulenten Wirbel wurden für radialen und axialen Strom untersucht. Hierzu wurde der Wirbel in einen Kern und einer Ringzone eingeteilt, wobei für jede eine verschiedene, aber einheitliche axiale Massengeschwindigkeit angenommen wurde, obwohl die erhaltenen Gleichungen auch für eine beliebige Verteilung der axialen Massengeschwindigkeit gelten. Die Verteilungen der Tangentialgeschwindigkeit, der Temperatur und des Druckes wurden ebenso wie die Kurven für die Trennung der Gesamtenergie oder der Temperatur angegeben und mit dem Experiment verglichen.

Unter Benutzung dieser Rechenergebnisse wurden die Ursachen für die Energietrennung untersucht. Es wird geschlossen, daß der wichtigste Faktor, der die Gesamttemperatur eines Flüssigkeitselementes in einem kompressiblen Wirbel beeinflußt, die turbulente Scherarbeit ist, die an einem oder durch ein Element geleistet wird.

Abstract—Основной задачей настоящей работы является исследование распределения скорости, температуры и давления в турбулентном вихре. В основе анализа положено схематическое представление о разделении вихря на ядро и наружную область. Каждая область имеет свою собственную постоянную скорость перемещения массы вдоль оси, хотя полученные уравнения можно применить для случая произвольного распределения скорости и движения массы по осям. Получены графики распределения температуры, давления, потенциальной скорости, а так же поля температуры и энергии, которые сопоставлены с экспериментальными данными. На основе аналитического исследования авторы пришли к заключению, что наиболее важным фактором, влияющим на полную локальную температуру газо-жидкостного сжимаемого вихря, является работа турбулентного перемещения.

NOMENCLATURE

c_p, specific heat;
$\frac{D}{D\theta}$, substantial derivative; $u\frac{d}{dr}$ as used here;
K, parameter $\left[W_h\left(\frac{r_0}{r_i}\right)^2 - 1\right] \Big/ W_c$;
k, thermal conductivity;
M_0 Mach number based on tangential velocity at outer radius;
P, stagnation or total pressure;
p, static pressure;
Re_i, Reynolds number, $-u_i r_i \rho_i / \rho\varepsilon$;
Re_0 Reynolds number based on outer radius; $Re_i\, W/W_c$;
r', nondimensional distance along radial co-ordinate, r/r_i;
T, t, total and static temperatures;
T', t', nondimensional total and static temperature, $T/(v_i^2/2c_p)$, $t/v_i^2/2c_p$;
T_c, mean total temperature of fluid leaving core;
T_e, mean total temperature of fluid entering vortex tube;
T_h, mean total temperature of fluid leaving annulus;
u, v, w, radial, angular and axial components of velocity;
W, total mass flow entering system;
W_c, mass flow leaving core;
W_h, mass flow leaving annulus;
v', nondimensional angular velocity, v/v_i;
z, distance along axial co-ordinate;
γ, ratio of specific heats;
ε, eddy diffusivity;
θ, time;
θ', dimensionless time; $-(u_i/r_i)\theta$;
μ, viscosity;
ρ, density;
τ, turbulent shear stress, $\rho\varepsilon(dv/dr - v/r)$;
τ', dimensionless turbulent shear stress $\frac{1}{Re_i}\left(\frac{dv'}{dr'} - \frac{v'}{r'}\right)$;
ϕ, turbulent dissipation $= \rho\varepsilon(dv/dr - v/r)^2$;
ϕ', dimensionless turbulent dissipation; $\frac{2}{Re_i}\left(\frac{dv'}{dr'} - \frac{v'}{r'}\right)^2$.

Subscripts

i, pertaining to core or reference radius;
0, pertaining to outer radius of vortex.

INTRODUCTION

THE problem considered here is that of the velocity and temperature distributions in a turbulent compressible vortex with radial and axial flow. That problem occurs, for instance, in connection with the Ranque–Hilsch vortex tube [1]. In that apparatus gas enters a tube tangentially through nozzles so as to form a vortex within the tube. Cold gas can then be withdrawn axially from the region near the center of the tube and hot gas from the annular region at larger radii. A total temperature or energy separation thus occurs within the vortex. The vortex tube should be useful for obtaining quantities of either hot or cold air. The feature of no moving parts might make it especially attractive for applications where extreme temperatures are desired. For instance, a vortex tube might conceivably be used to obtain higher propellant temperatures in a nuclear rocket than could be obtained by the nuclear reactor alone, which is limited in temperature by the reactor materials. The walls of the vortex tube could be cooled to prevent melting, and the cold stream from the vortex could be reheated in the reactor.

A great deal of work, both experimental and analytical, has been done in connection with the phenomenon described above. A summary of the work done between 1931 and 1953 is given in [2]. Some additional investigations since that time are given in [3, 7, 12]. Although many of the important factors in the phenomenon have been considered in one or another of the previous papers, it appears that all of the analyses neglected at least some of the important factors. Also, a more thorough discussion of the causes of the energy separation would be desirable. The present writers in a preliminary study [5], of which the present paper is a refinement and extension, have attempted to include the pertinent terms in the compressible laminar and turbulent momentum and energy equations. Only the turbulent case is considered herein, inasmuch as it was shown in [5] that the energy separation in actual vortex tubes cannot be accounted for by considering a laminar vortex.

Vol. 1 1960

(Energy separation can also occur in a laminar vortex but the radial flow must be extremely small.) The effect of energy diffusion due to the expansion and contraction of the turbulent eddies as they move radially in a pressure gradient is included in the equations.

The model considered (Fig. 1) is an axially symmetric vortex in which the tangential velocity and temperature are independent of axial position. The tangential and radial velocities, as well as the temperature, are specified at a reference radius. In addition, the axial mass

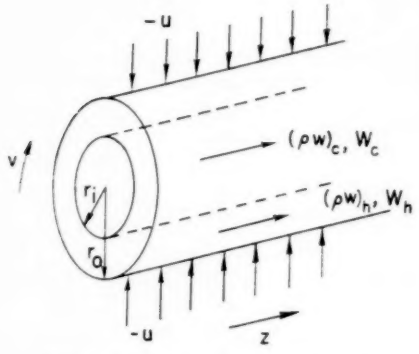

FIG. 1. Vortex model used in analysis.

velocity is specified as a function of radius and axial position. As will be shown, only a linear variation of axial mass velocity with axial position is consistent with the assumption of a tangential velocity independent of axial position, but the variation of axial velocity with radius can be arbitrary. For the present calculations a uniform axial mass velocity $(\rho w)_c$ in a region near the center and a different uniform axial velocity $(\rho w)_h$ in the remaining annular region were assumed. The analysis predicts the tangential velocity and temperature as functions of radius. For calculating the temperature distributions it was assumed, in order to make the equations tractable, that squares of axial and radial velocities are small compared with squares of the tangential velocities.

VELOCITY DISTRIBUTIONS

In the present model the flow is taken to be axially symmetric and steady state with no body forces. For that case the compressible Navier–Stokes equation for the tangential component of the velocity [8], reduces to

$$\rho u \frac{\partial v}{\partial r} + \rho w \frac{\partial v}{\partial z} + \frac{\rho u v}{r} = \frac{\partial}{\partial z}\left(\mu \frac{\partial v}{\partial z}\right) + \frac{\partial}{\partial r}\left\{\mu\left(\frac{\partial v}{\partial r} - \frac{v}{r}\right)\right\} + \frac{2\mu}{r}\left(\frac{\partial v}{\partial r} - \frac{v}{r}\right) \quad (1)$$

For turbulent flow the increased shear stress due to the turbulence can be accounted for by replacing μ by $\mu + \rho\varepsilon$ in the momentum equation. The quantity $\rho\varepsilon$ is the eddy viscosity and depends on the turbulent mixing at a point. Except near boundaries, or at low Reynolds numbers, μ is small compared to $\rho\varepsilon$ and can be neglected. Although $\rho\varepsilon$ is in general a variable, it appears reasonable to assume that it can be considered constant for a vortex with radial flow. This assumption is in agreement with the experiments in [6] for incompressible flow. Because of lack of information on compressible vortex flow, and because of the considerable simplification obtained, we will assume that $\rho\varepsilon$ can be considered constant also for compressible flow and then attempt to justify the assumption by comparison of the results with experiment.

Inasmuch as our model assumes that v is independent of z, equation (1) becomes, for turbulent flow:

$$\rho u \frac{dv}{dr} + \frac{\rho u v}{r} = \rho\varepsilon\left(\frac{d^2v}{dr^2} + \frac{1}{r}\frac{dv}{dr} - \frac{v}{r^2}\right) \quad (2)$$

Essentially the same result could have been obtained by dividing the instantaneous velocities and densities in equation (1) into mean and fluctuating components, taking time averages, and setting the Reynolds stress

$$\overline{u'v'} = -\varepsilon(dv/dr - v/r)$$

by analogy with the laminar shear stress. Note from equation (2) that the assumption that v is independent of z implies that ρu is also independent of z. The general solution of equation (2) is:

$$v = \frac{c_1}{r}\int r \exp\left(\int \frac{\rho u}{\rho\varepsilon}\, dr\right) dr + \frac{c_2}{r} \quad (3)$$

Using the boundary condition that the velocities at the axis of the vortex cannot be infinite, equation (3) can be written in dimensionless form as

$$v' = \frac{\int_0^{r'} r' \exp\left(\int_0^{r'} \frac{\rho u r_i}{\rho \varepsilon}\, dr'\right) dr'}{r' \int_0^1 r' \exp\left(\int_0^{r'} \frac{\rho u r_i}{\rho \varepsilon}\, dr'\right) dr'} \tag{4}$$

where the subscript i refers to values at a reference radius and the primes indicate that the quantities have been divided by their values at r_i.

In order to relate the radial flow to the axial flow, we use the continuity relation

$$\frac{\partial (r\rho u)}{\partial r} + \frac{\partial (r\rho w)}{\partial z} = 0 \tag{5}$$

Integrating equation (5) between the axis and the radius r results in

$$r\rho u = -\int_0^r \frac{\partial(\rho w)}{\partial z}\, r\, dr \tag{6}$$

Inasmuch as ρu is a function only of r, equation (6) shows that $\partial(\rho w)/\partial z$ is a function only of r. Therefore

$$\rho w = [\rho w(r)]_0 + f(r)z \tag{7}$$

where the subscript zero refers to values at $z = 0$.

In order to make numerical calculations it is necessary to assume a variation of $\partial(\rho w)/\partial z$ or of ρw with r. The vortex is divided into two regions, a core with radius r_i, and an annular region with inner and outer radii r_i and r_0 (Fig. 1). In each of these regions ρw, and thus $\partial(\rho w)/\partial z$ (equation (7)), is assumed independent of r, but there can be a step change in ρw at the interface between the two regions. Note that it is not necessary for the axial flow to be in the positive direction in both regions.

Consider first the core region. Dividing equation (6) by the same equation evaluated at r_i, and integrating, show that

$$\rho u/\rho_i u_i = r/r_i \tag{8}$$

Equation (4) then becomes

$$v' = \frac{1}{r'}\left(\frac{1 - \exp(-Re_i r'^2/2)}{1 - \exp(-Re_i/2)}\right) \tag{9}$$

where

$$Re_i = -\frac{\rho_i u_i r_i}{\rho \varepsilon}$$

The negative sign is included in the definition of Reynolds number because u_i is negative in the cases of interest here. Equation (9) was obtained by Einstein and Li [6]. For very large radial flows, equation (9) reduces to $v' = 1/r'$ (inviscid flow) except close to the center, whereas for small radial flows, $v' = r'$ (wheel flow).

For calculating velocities in the annulus, with ρw independent of r, one can break the integral in equation (6) into two parts, one with limits 0 and r_i, the other with limits r_i and r. Dividing the equation by $r_i \rho_i u_i$, integrating and making use of equation (7), result in

$$\frac{r\rho u}{r_i \rho_i u_i} = 1 + K(r'^2 - 1) \tag{10}$$

where

$$K = \frac{W_h/W_c}{(r_0/r_i)^2 - 1} \tag{11}$$

and W_h and W_c are the total axial flow out of the annulus and the core, respectively. Breaking the integrals in the numerator of equation (4) into two parts, substituting equations (8) and (10), and carrying out the integrations, result in the following equation for v' for the annulus.

$$v' = \frac{Re_i \exp(Re_i K/2)}{\exp(Re_i/2) - 1}\,\frac{1}{r'}\int_1^{r'} r'^{\,Re_i (K-1)+1} \times \times \exp(-Re_i\, Kr'^2/2)\, dr' + \frac{1}{r'} \tag{12}$$

Equations (9) and (12) automatically satisfy the condition that dv'/dr' is continuous at $r' = 1$. Equation (12) can be integrated numerically.

Typical predicted tangential velocity distributions for several values of turbulent Reynolds number and of axial mass-flow ratio are presented in Fig. 2. In these curves Re_0 rather than Re_i is used as a parameter, where

$$Re_0 \equiv \rho_0 u_0 r_0/\rho\varepsilon = Re_i\, W/W_c$$

Vol. 1 1960

W is the total flow out of both the core region and the annulus. (A possible method for predicting the turbulent Reynolds number will be discussed in the next section.) These curves were calculated for a radius ratio r_0/r_i of 2·2. Other radius ratios give similar results, but the peaks of the curves fall closer to the center of the vortex

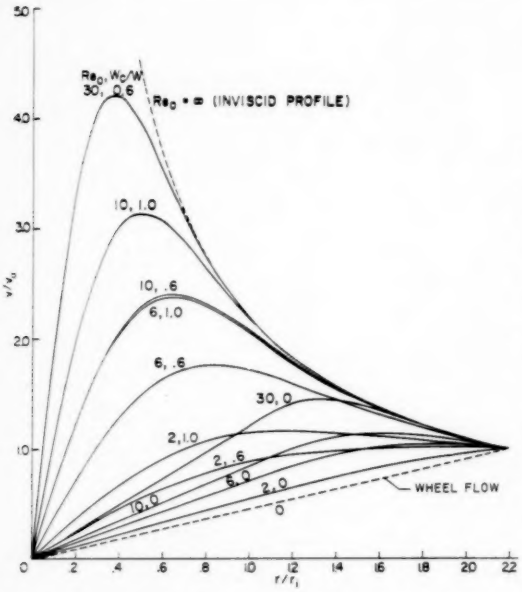

FIG. 2. Tangential velocity distributions in vortex. $r_0/r_i = 2{\cdot}2$.

for higher radius ratios. The radial flow in these figures, as well as in all of the subsequent figures, is toward the center of the vortex. It should be mentioned that these curves apply to laminar flow if $\rho\varepsilon$ in the Reynolds number is replaced by μ.

The curves for large values of W_c/W and small Reynolds number behave similarly to those for large values of Reynolds number and small W_c/W. The limiting curve for a radial flow Reynolds number of zero corresponds to wheel flow, whereas the curve for $Re_0 = \infty$ corresponds to inviscid vortex flow. Except at the lower Reynolds numbers the curves tend to approach the inviscid flow line ($v/v_0 = r_0/r$) in the outer region, whereas they approach wheel flow near the center. That is, it appears that the flow in the outer region is governed by inertia effects, whereas near the center the viscous effects become more important. This can be seen more clearly if we write the momentum equation (equation (2)) in the following form:

$$\frac{\rho}{\rho_i}\frac{Dv'}{D\theta'} = \frac{\rho u}{\rho_i u_i}\frac{v'}{r'} + \left(\frac{d\tau'}{dr'} + \frac{2\tau'}{r'}\right) \qquad (13)$$

where $\theta' \equiv -u_i\theta/r_i$ is a dimensionless time,

$$\tau' \equiv (dv'/dr' - v'/r')/Re_i \qquad (14)$$

is a dimensionless shear stress, and Re_i is the radial flow Reynolds number evaluated at some reference radius. The terms on the right side of this equation give the contributions which go to increase or decrease the tangential velocity of a particle at a given radius, as it moves toward the center of the vortex. The first term on the right side represents an inertia force per unit volume and tends to accelerate the particle in order to maintain constant angular momentum. The second term represents the net viscous shear force acting on the particle and tends to slow it down. These terms, together with the term on the left side of the equation giving the net rate of change of velocity of the particle, are plotted in Fig. 3 for the case where the axial velocity is uniform throughout the vortex. This case is shown for illustrative purposes; other axial velocity distributions should give qualitatively similar results. It is seen that in the outer regions (or for high Reynolds numbers) the net viscous force tending to slow the particle down is negligible compared with the inertia effect, so that constant angular momentum is preserved in that region. (Note that the curve for the inertia term also represents the tangential velocity profile in this particular case.) The fact that the net viscous shear force on the element is negligible means only that the tangential shearing forces on the sides of the element cancel, although they may be individually appreciable. In the region closer to the center (or for lower Reynolds numbers) the inertia and viscous forces become of the same order of magnitude, and at the center the ratio of viscous to inertia terms approaches 2. Thus the fluid particle decelerates in that region. Inasmuch as the radial velocity goes to zero at the center,

one might have expected the ratio of viscous to inertia terms to approach infinity rather than 2 at that point. However, it should be pointed out that the viscous stress exists only because of the inertia effect; for wheel flow there would be no viscous stress. It is the deviation from wheel flow produced by the inertia effect which gives rise to the viscous shear stress.

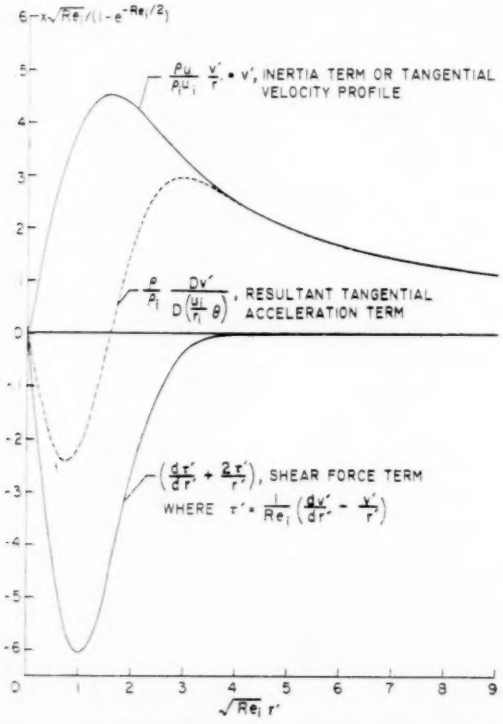

FIG. 3. Terms in momentum equation (equation (13)) contributing to local rate of change of velocity of fluid element with respect to time. Uniform axial mass velocity.

In order to determine whether the analytical method gives velocity distributions in reasonable agreement with experiment, the data of Hartnett and Eckert [7] were used. Those investigators measured velocity and temperature distributions at various axial positions in a vortex tube. Most of the axial flow occurred in the outer regions of the vortex, inasmuch as there was no opening at the vortex center. Although the axial mass velocity was not uniform in the outer region, it was assumed for purposes of comparison with the analysis, that the vortex could be divided into an outer region with uniform axial mass velocity, and an inner core, where the axial velocity is zero. It would have been possible to work out the analysis using the experimental axial velocity distributions, but the above simpler procedure was adopted. The data closest to the inlet nozzle are compared with analytical results for $W_c/W = 0$ in Fig. 4. For calculating the analytical curves, it was estimated from the data that

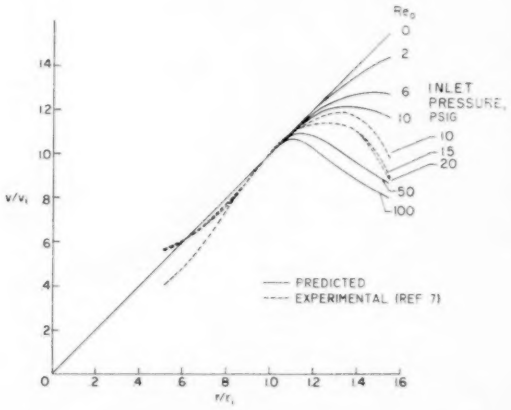

FIG. 4. Comparison of analytical tangential velocity profiles with experiments in [7].
$W_c/W = 0$, $r_0/r_i = 1{\cdot}54$.

the radius ratio for the outer and inner regions is about 1·54. This value gives approximately no net axial flow in the core for the experimental data. The shapes of the analytical and experimental curves agree reasonably well, indicating that the turbulent radial flow Reynolds numbers Re_0 lie between 10 and 50. These values are probably too high, however, because the effect of viscosity tends to make the velocities low near the tube wall. Viscous boundary layer effects are, of course, neglected in the analysis.

TEMPERATURE AND PRESSURE DISTRIBUTIONS

The steady-state energy equation for the compressible, axially symmetric flow of a perfect gas is [8]

Vol. 1 1960

$$\left.\begin{aligned}\rho c_p\left(u\frac{\partial t}{\partial r}+w\frac{\partial t}{\partial z}\right)-u\frac{\partial p}{\partial r}-w\frac{\partial p}{\partial z}=\\ =\frac{1}{r}\frac{\partial}{\partial r}\left(rk\frac{\partial t}{\partial r}\right)+\frac{\partial}{\partial z}\left(k\frac{\partial t}{\partial z}\right)+\\ +\mu\left[2\left\{\left(\frac{\partial u}{\partial r}\right)^2+\left(\frac{u}{r}\right)^2+\left(\frac{\partial w}{\partial z}\right)^2\right\}+\right.\\ \left.+\left(\frac{\partial u}{\partial z}+\frac{\partial w}{\partial r}\right)^2+\left(\frac{\partial v}{\partial r}-\frac{v}{r}\right)^2\right]-\\ -\frac{2\mu}{3}\left(\frac{\partial u}{\partial r}+\frac{u}{r}+\frac{\partial w}{\partial z}\right)^2\end{aligned}\right\}\quad(15)$$

Assuming that t and v (and consequently u) are independent of z, neglecting squares and products of small quantities, where u and w are considered small compared to v, and combining equation (15) with the three momentum equations so as to eliminate the pressure gradients, result in

$$\left.\begin{aligned}c_p\rho ur\frac{\partial t}{\partial r}+r\rho u\frac{\partial (v^2/2)}{\partial r}-k\frac{\partial\,(r\;\partial t/\partial r)}{\partial r}\\ =\mu\frac{\partial}{\partial r}\left\{rv\left(\frac{\partial v}{\partial r}-\frac{v}{r}\right)\right\}\end{aligned}\right\}\quad(16)$$

In laminar flow with small radial velocities, or large viscosity, equation (16) shows that $t = \text{constant}$, that is, the static temperature is uniform because of conduction. For large radial flow or small viscosity $t + v^2/2\,c_p = \text{constant}$, or the total temperature is uniform.

The energy equation (16) can be adapted to turbulent flow by replacing μ and k by $\rho\varepsilon$ and $\rho c_p \varepsilon_h$, respectively. The quantities ε and ε_h are the eddy diffusivities for momentum and heat transfer. Inasmuch as the assumption $\varepsilon = \varepsilon_h$ has given good results for flow through tubes, that assumption will be retained here in the absence of other experimental information. Adding a term to account for the effect of radial pressure gradient on the turbulent heat transfer, which will be discussed in the next paragraph, equation (16) becomes

$$\left.\begin{aligned}c_p\rho ur\frac{dt}{dr}+\frac{r\rho u}{2}\frac{dv^2}{dr}=\\ =\frac{d}{dr}\left[r\left\{\rho c_p\varepsilon\left(\frac{dt}{dr}-\frac{1}{\rho c_p}\frac{dp}{dr}\right)\right\}\right]+\\ +\frac{d}{dr}\left\{\rho\varepsilon rv\left(\frac{dv}{dr}-\frac{v}{r}\right)\right\}\end{aligned}\right\}\quad(17)$$

As in the case of the equation of turbulent momentum, equation (17) could have been obtained by breaking the instantaneous temperatures, velocities, and densities into mean and fluctuating components and setting

$$\overline{u't'} = -\varepsilon(dt/dr - (1/\rho c_p)\,dp/dr)$$

and $$\overline{u'v'} = -\varepsilon(dv/dr - v/r).$$

The term $-(1/\rho c_p)\,dp/dr$ is added to dt/dr in equation (17) inasmuch as the turbulent heat transfer appears to be a function of pressure gradient as well as of temperature gradient. That assumption has been made by several authors [4, 7, 9]. When the turbulent particles move radially to regions of different pressure they expand or contract so that they arrive at the point of mixing at a temperature different than they would have had in a uniform pressure field. It was found in [10] that turbulent particles appear to move adiabatically except at low Peclet or Reynolds numbers, where the effect of conduction to a particle may become appreciable. Assuming the isentropic expansion or contraction of eddies, one would expect that for the case of no net heat transfer, the temperature distribution should be isentropic rather than isothermal.* That is, the relation between temperature and pressure should be given by

$$t = \text{const.}\ p^{\gamma-1/\gamma},\ \text{or}\ \frac{dt}{dr}=\frac{1}{\rho c_p}\frac{dp}{dr}\quad(18)$$

which is identical to equation (17) for the case of no radial heat transfer. The addition of the term $(1/\rho c_p)\,dt/dr$ to equation (17) therefore appears to be justified. The term can also be obtained by means of a modified mixing-length theory which is given in the Appendix.

The above assumption concerning the expansion and contraction of eddies also appears to receive strong support from meteorological observations. An isentropic relation between temperature and pressure as altitude increases

* Although irreversible effects are operative in the fluid as a whole, it appears that the expansion or contraction of an individual eddy might be considered isentropic, inasmuch as the normal viscous stress is usually negligible in the absence of shock waves. The assumption is supported by experiment, especially by meteorological observations.

has been found for highly turbulent atmospheres, whereas for quiescent conditions the atmosphere is isothermal [11].

For small radial and axial velocities the momentum equation for the radial direction reduces approximately to

$$\frac{dp}{dr} = \frac{\rho v^2}{r} \tag{19}$$

Substituting equation (19) into (17) one finds that for large radial flows or small turbulent diffusivities the total temperature is constant as in the case of laminar flow. On the other hand, for small radial flows or large turbulent diffusivities $t - t_i = (v_i^2/2c_p r_i^2)(r^2 - r_i^2)$, in contrast to the laminar case, where the static temperature was uniform. The static temperature difference in the turbulent case is caused by the expansion and contraction of the eddies moving radially as discussed above. As in the case of the velocity distributions $\rho\varepsilon$ is considered constant.

If we divide the vortex into an annular and a core region, each with a uniform mass velocity as before, we obtain, for the core

$$\left.\begin{aligned}
&\frac{\{1 - \exp(-Re_i/2)\}^2}{2Re_i}\, r' \frac{dt'}{dr'} = \\
&= \frac{3}{Re_i r'^2}\{\exp(-Re_i r'^2/2) - 1\}^2 + \\
&+ \exp(-Re_i r'^2/2) + \\
&+ \exp(-Re_i r'^2/2)\left[4\ln\{\sqrt{(Re_i)}\, r'\} - \right. \\
&\left. - Ei\left(\frac{Re_i r'^2}{2}\right) - Ei\left(-\frac{Re_i r'^2}{2}\right) - 1{\cdot}2319\right]
\end{aligned}\right\} \tag{20}$$

where it was assumed that dt'/dr' cannot be infinite at $r' = 0$. For the annular region

$$\left.\begin{aligned}
&\exp(Re_i K r'^2/2)\, r'^{1 - Re_i(K-1)} \frac{dt'}{dr'} = \\
&= \left(\frac{dt'}{dr'}\right)_{r'=1} \exp(Re_i K/2) + \\
&+ \int_1^{r'} \exp(Re_i K r'^2/2)\, r'^{-Re_i(K-1)} \\
&\left[-r' \frac{d^2 v'^2}{dr'^2} + \frac{dv'^2}{dr'}\right. \\
&\left.\left\{3 - Re_i r'\left(\frac{1}{r'} - \frac{K}{r'} + Kr'\right)\right\}\right] dr'
\end{aligned}\right\} \tag{21}$$

where $(dt'/dr')_{r'=1}$ is obtained from the solution for the core. Equation (21) was integrated numerically. The derivatives of v' are obtained from the solutions for the velocity equation. The quantity t' can then be obtained by numerical integration of the equation

$$t' - t_i' = \int_1^{r'} \left(\frac{dt'}{dr'}\right) dr' \tag{22}$$

In equation (20) we can see that

$$t'\{1 - \exp(-Re_i/2)\}^2/Re_i$$

is a function only of $\sqrt{(Re_i)}\, r$, so that the equation can be integrated once for all Reynolds numbers. The dimensionless total temperature difference can be obtained from the static temperature by the equation

$$T' - T_i' = t' - t_i' - 1 + v'^2.$$

Typical total and static temperature distributions are plotted in Figs. 5 and 6. The total temperature distributions are probably of more direct interest in connection with energy separation, inasmuch as the fluid will eventually be brought to rest outside the vortex; the static temperature distributions are included for comparison and also indicate the direction of heat flow by conduction. The limiting curves for zero Reynolds number

$$\{(T - T_0)/(v_0^2/2c_p) = 2(r/r_0)^2 - 1\}$$

and for infinite Reynolds number

$$\{(T - T_0)/(v_0^2/2c_p) = 0\}$$

are shown dashed.

The total temperature curves indicate considerable energy or temperature separation, the temperatures first rising (for large W_c/W) and then dropping as the center is approached. (For the curves where the total temperatures continuously fall as the center is approached, an overall energy balance on the vortex tube, to be discussed in the next section, indicates that the region of increasing temperatures lies between the vortex analyzed here and the tube wall.) As in the case of the velocity distributions the curves for low Re_0 and high W_c/W are somewhat similar to those for high Re_0 and low W_c/W. This is apparently due to the fact that

Vol. 1 1960

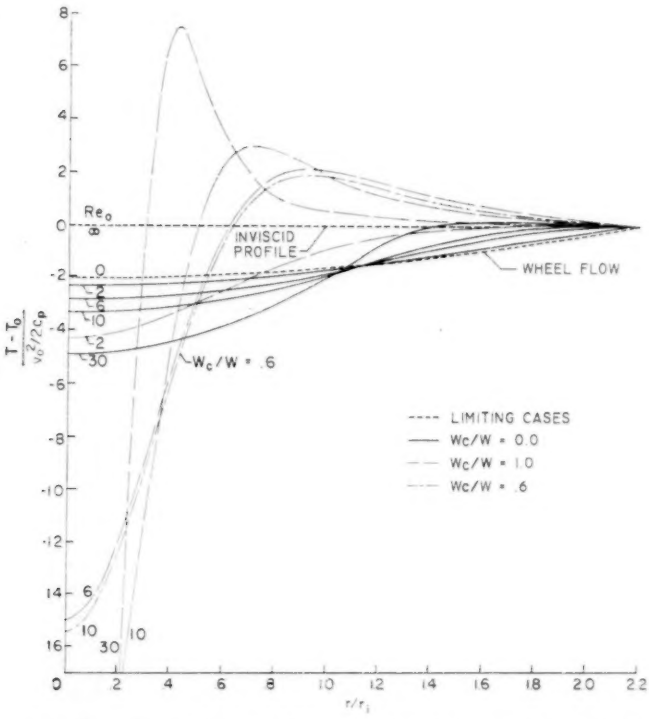

FIG. 5. Total temperature distributions in turbulent vortex. $r_0/r_i = 2{\cdot}2$.

the flow out of the core region, which seems to control the shape of the curves, tends to be the same in both cases. The static temperature curves indicate that in all cases the heat conduction due to temperature gradients is toward the center of the vortex. Thus the cooling at the center cannot be caused by conduction due to temperature gradients; it may be caused by the expansion and contraction of the turbulent eddies or by viscous shear. The causes of the energy separation will be considered in detail in a later section.

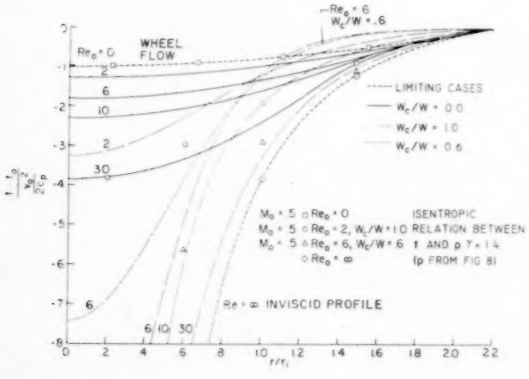
Re₀ = 6
Wc/W = .6
WHEEL FLOW
Re₀ = 0
LIMITING CASES
Wc/W = 0.0
Wc/W = 1.0
Wc/W = 0.6
M₀ = .5 □ Re₀ = 0
M₀ = .5 ○ Re₀ = 2, Wc/W = 1.0
M₀ = .5 △ Re₀ = 6, Wc/W = 0.6
○ Re₀ = ∞
ISENTROPIC RELATION BETWEEN p AND ρ, γ = 1.4 (p FROM FIG 8)
Re = ∞ INVISCID PROFILE
r/r_i

FIG. 6. Static temperature distributions in turbulent vortex. $r_0/r_i = 2{\cdot}2$.

For purposes of comparison with the predicted static temperature distributions in a vortex, temperatures obtained for an isentropic relation between static temperature and pressure (pressures from Fig. 8) are plotted as points in Fig. 6. For small radial flows the temperatures are in approximate isentropic equilibrium with the pressures because of expansion and contraction of eddies. For larger radial flows the deviation of the vortex temperatures from the equilibrium temperatures increases. For very high radial-flow Reynolds numbers the distributions are again isentropic. However, there is no total temperature separation in that case. The same result is obtained for laminar flow.

To check the temperature results against experiment we again use the experimental data of [7]. The same assumptions as were used in comparing the velocity results are used here. The comparison is shown in Fig. 7. The shapes of the analytical and experimental curves agree reasonably well, indicating lower turbulent Reynolds

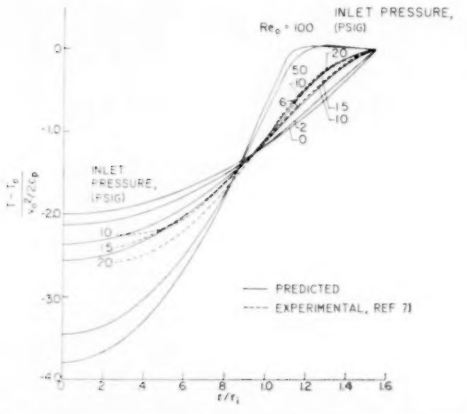

FIG. 7. Comparison of analytical total temperature profiles with experiments in [7]. $W_c/W = 0$, $r_0/r_i = 1{\cdot}54$.

numbers than were indicated for the velocity profiles. As was mentioned in connection with the velocity profiles, the indicated turbulent Reynolds numbers there might be too high because of boundary layer effects near the tube wall.

Turbulent Reynolds number

Thus far the turbulent Reynolds number Re_0 has been considered as a free parameter in the analysis, and no attempt has been made to predict its value. The unknown quantity in that parameter is, of course, the eddy diffusivity or eddy viscosity. It is of interest to attempt to predict the eddy diffusivity by using von Kármán's similarity hypothesis, which has been successful for flow through tubes. The expression will first be modified for circular flow as follows: For purposes of analysis it is assumed that the turbulence at a point is dependent only on the shearing deformation at the point and in the vicinity of the point; that is, it is a function of the deformation and its derivatives. If we exclude derivatives higher than the first, then $\varepsilon = f\{(dv/dr - v/r), d/dr(dv/dr - v/r)\}$. Application of dimensional analysis then gives

$$\varepsilon = \frac{-\kappa^2 (dv/dr - v/r)^3}{[d/dr\ (dv/dr - v/r)]^2} \tag{23}$$

The derivation for equation (23) can also be used to obtain the usual Kármán expression for the case of rectilinear flow. For the outer portion of the vortex, except at the lowest Reynolds numbers, the tangential velocity is given approximately by $v = v_0 r_0/r$. The expression for ε at the outer edge of the vortex then becomes

$$\epsilon = \kappa^2 v_0 r_0/2, \text{ or}$$

$$Re_0 = -\frac{2}{\kappa^2}\frac{u_0}{v_0} \tag{24}$$

In the present analysis it is assumed that Re_0 is uniform ($\rho\varepsilon$ = constant), so that equation (24) is applied throughout the vortex. For flow through a tube or channel, κ has been found to lie between 0·3 and 0·4. If we take $\kappa = 0{\cdot}3$, then for the experiments in [7], the following values of Re_0 are calculated from equation (24): For inlet pressure $p = 10$ lb/in² gauge, $Re_0 = 6{\cdot}9$, for $p = 15$, $Re_0 = 6{\cdot}7$. and for $p = 20$, $Re_0 = 7{\cdot}1$. Comparison of these values with those indicated by the experimental and analytical temperature distributions in Fig. 7 indicates reasonable agreement. However, more work should be done to prove or disprove the general validity of equations (23) or (24). It appears that in some cases the turbulence in the vortex might be influenced by the presence of the tangential nozzles in the wall.

Pressure distributions

In order to obtain an idea of the pumping power required to force the fluid through the vortex, the pressure distribution in the vortex is required. Both the static and total pressures will be calculated, inasmuch as part of the rotational kinetic energy leaving the vortex can probably be recovered. To calculate the static pressure distributions we use equation (19) and the perfect gas law to obtain

Vol. 1 1960

$$\frac{p}{p_0} = \exp\left[\frac{2\gamma}{\gamma - 1} \times \right.$$
$$\left. \times \int_{r_0}^{r'} \frac{(v/v_0)^2\, dr'}{r'\,\{(t - t_0)/(v_0^2/2c_p) + 2/(\gamma - 1)M_0^2\}}\right] \quad (25)$$

Thus in order to plot the pressure distributions the parameters M_0 and γ, in addition to those required for the velocity and temperature distributions, must be used. Total pressure distributions can be obtained from the static pressure distributions by the relation

$$\frac{P}{P_0} = \frac{p}{p_0} \times$$
$$\times \left[\frac{1 + \{(v/v_0)^2/[(t - t_0)/(v_0^2/2c_p) + 2/\{(\gamma - 1)M_0^2\}]\}}{1 + \{(\gamma - 1)/2\}\, M_0^2}\right]^{\gamma/(\gamma-1)} \quad (26)$$

Note that for these equations to apply the quantity $t - t_0/(v_0^2/2c_p) + 2/(\gamma - 1)M_0^2$ must be greater than zero, inasmuch as the pressure (and temperature) will go to zero as that quantity approaches zero.

Static and total pressure distributions for some typical cases are plotted in Figs. 8 and 9. For $Re_0 = \infty$ the total pressure is uniform, inasmuch as the flow is inviscid for that case, although the static pressure drops sharply as the center is approached. However, for realistic Reynolds numbers the differences between the static and total pressure curves are not nearly as great.

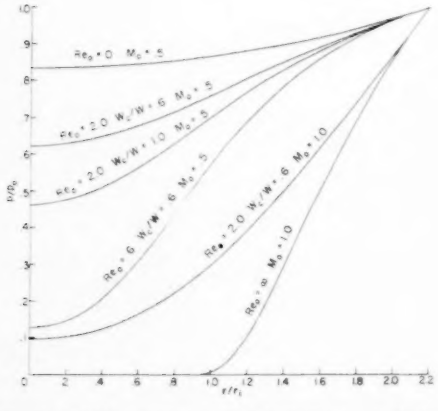

FIG. 8. Static pressure distributions in turbulent vortex. $r_0/r_i = 2{\cdot}2$, $\gamma = 1{\cdot}4$.

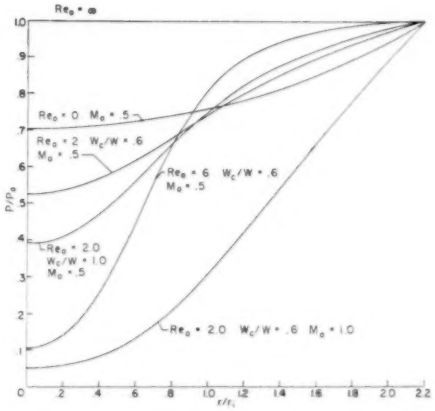

FIG. 9. Total pressure distributions in turbulent vortex. $r_0/r_i = 2{\cdot}2$, $\gamma = 1{\cdot}4$.

The curves for $Re_0 = 2$ and $M_0 = 1{\cdot}0$ correspond approximately to Hilsch's vortex tube data for inlet to outlet pressure ratios of 6 and 10 (Fig. 10). (Hilsch's data will be discussed in the next section.) It is difficult to compare the pressures in the vortex with those measured by Hilsch outside the vortex because of uncertainty in the losses between the vortex and the environment. However, the pressure distribution curves in Fig. 8 and 9 indicate both static and total pressure ratios between the outer radius and some average radius in the core of the same order of magnitude as the pressure ratios obtained by Hilsch. (Inlet pressure in atmospheres on Fig. 10 is equivalent to pressure ratio between inlet and outlet.)

Ranque–Hilsch tube

In comparing the analytical results with experimental results obtained in actual vortex tubes, one cannot consider the containing tube to be coincident with the outer radius of the vortex which has been analyzed. The velocity at the tube wall is zero, whereas that at the outer radius of the vortex is finite. Also, the heat conducted through the tube wall can be neglected, whereas that conducted across the outer radius of the vortex is not negligible. In addition, the presence of tangential nozzles in the wall for the entering fluid will tend to destroy the axial symmetry of the flow near the wall. It is therefore assumed that there is a region of fluid

between the outer radius of the vortex and the tube in which there is no axial flow. The flow in this region will be complicated and no attempt will be made to analyze it in detail. However, the difference between the total temperature of the fluid entering the tube through the tangential nozzles and the temperature at the outer radius can be obtained from an overall energy balance on the system as

$$T_e - T_0 = (W_c/W)(T_c - T_0) + \\ + (1 - W_c/W)(T_h - T_0)$$

where the specific heat is assumed uniform and the tube is adiabatic. The temperature T_e in general differs from the total temperature at the outer radius of the vortex. The temperatures T_c and T_h are the integrated mixed mean temperatures of the fluid leaving the system axially from the core and from the annulus of the vortex and are obtained from the total temperature distributions and the following equations:

$$T_c - T_0 = 2\int_0^1 (T - T_0)r'dr' \qquad (27)$$

and

$$T_h - T_0 = \frac{2\int_1^{r_0/r_i} (T - T_0)r'dr'}{(r_0/r_i)^2 - 1} \qquad (28)$$

Predicted values of $(T_h - T_e)/(v_0^2/2c_p)$ and $(T_c - T_e)/(v_0^2/2c_p)$ are plotted in Fig. 10 as functions of the ratio of axial mass flow through the core to total mass flow and turbulent Reynolds number for a radius ratio of 2·2. The upper and lower sets of curves are related by the overall energy balance

$$\frac{W_c}{W}(T_c - T_e) + \left(1 - \frac{W_c}{W}\right)(T_h - T_e) = 0 \qquad (29)$$

The limiting curves for $Re_0 = 0$ are given by

$$(T_h - T_e)/(v_0^2/2c_p) = W_c/W$$

and

$$(T_c - T_e)/(v_0^2/2c_p) = (W_c/W) - 1$$

For $Re_0 = \infty$ and $W_c/W > 0$,

$$T_h - T_e = T_c - T_e = 0$$

The curves indicate that the total temperature separation between the two streams emerging from the vortex increases as the turbulent radial flow Reynolds number Re_0 increases, but that the value of W_c/W for maximum temperature depression approaches zero for large Re_0.* For very large values of Re_0 no total temperature separation will occur between the hot and cold streams except for values of W_c/W essentially equal to zero. This result indicates why turbulent rather than laminar flow is necessary to explain the energy separation in actual vortex tubes. (The curves for turbulent flow are qualitatively similar to those for laminar flow when $\rho\varepsilon$ in the Reynolds number is replaced by μ.) The laminar Reynolds numbers in vortex tubes are several orders of magnitude higher than the values of Re_0 shown in Fig. 10. Thus if the vortex is laminar, the effective Reynolds number will be so high that essentially no energy separation can take place.

For a given Reynolds number the curves indicate that the energy separation could be increased by increasing the tangential velocity v_0 or by decreasing c_p. The optimum value of Re_0 for favorable energy separation for a range of values of W_c/W appears to be about 6. Comparison with the velocity distribution curves in Fig. 2 indicates that the velocity gradients and viscous shear are reasonably large throughout the vortex for a Reynolds number of 6. As will be seen later, the energy separation is related to the viscous shear. The viscous shear is also large for much larger Reynolds numbers, but for those Reynolds numbers the fluid does not remain in the vortex long enough for appreciable energy separation to take place (except very close to the center).

Note that in general low total temperatures in the cold stream are obtained at low values of W_c/W, whereas high temperatures in the hot stream are more readily obtained at large values of W_c/W.

Experimental data obtained by Hilsch [1] are plotted in Fig. 10 as dashed lines. His apparatus consisted of a tube with a nozzle

* The difference between the appearance of these curves and corresponding curves in [5] is due to the fact that the Reynolds number in [5] was based on the inside rather than on the outside radius.

Vol. 1 1960

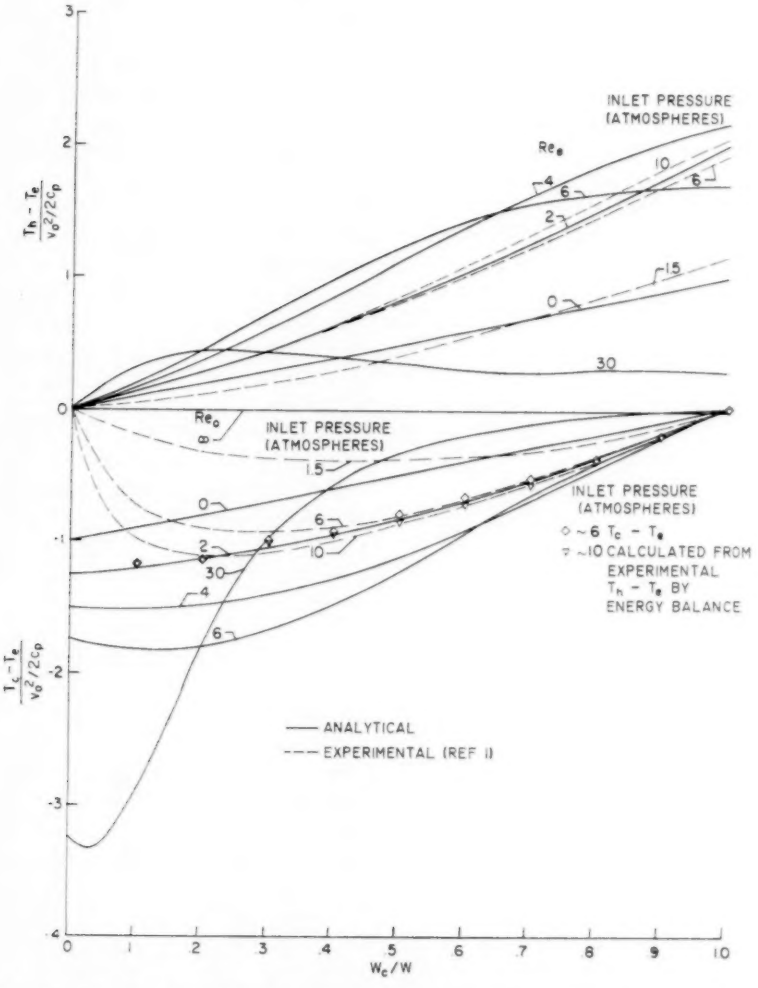

FIG. 10. Predicted overall energy separation for turbulent vortex tube and comparison with experiments in [1]. $r_0/r_i = 2{\cdot}2$.

through which air could enter tangentially so as to form a vortex within the tube. Hot air could then be withdrawn through an annular valve at one end of the tube and cold air through an orifice at the other end. The entrance nozzle was near the end of the tube where the orifice was located. In comparing the analytical and experimental results it was assumed that the air entered the tube at Mach 1, inasmuch as the mass flow was independent of the exit valve setting for a given inlet pressure. The experimental curves for various inlet pressures shown in Fig. 10 should therefore correspond to our curves for various $Re_0 \equiv \rho_0 u_0 r_0/\rho\varepsilon$ if it is assumed that $\rho\varepsilon$ is a function only of entering conditions and is thus independent of W_c/W. The radius ratio in the analysis was taken as 2·2, corresponding to the ratio of the tube to orifice radius in the experiment.

Good agreement is indicated between the analytical curve for $Re_0 = 2$ and the experimental curves for inlet pressures of 6 and 10 atm

except at the lower values of W_c/W. However, if we calculate the cold-stream temperatures from the experimental hot-stream temperatures and the energy balance equation (equation (29)), the results agree closely with the analytical curve for all values of W_c/W. Thus, the experimental cold-stream temperatures are probably too high because of thermal conduction radially along the tube end wall or from the atmosphere to the stream. This possibility was mentioned by Hilsch. The fact that the curve for an inlet pressure of 1·5 atm (low flow rate) lies above the curve for $Re_0 = 0$ can probably also be explained by external conduction.

In order to study the effect of radius ratio, curves for total temperature separation at various radius ratios are plotted in Fig. 11 for a

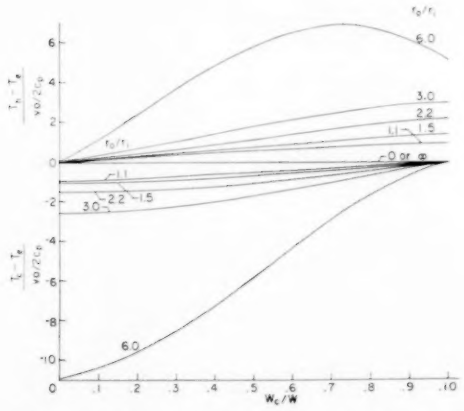

FIG. 11. Effect of radius ratio on overall energy separation for turbulent vortex tube. $Re_0 = 4{\cdot}0$.

Reynolds number of 4. A considerable increase in temperature separation is indicated as the radius ratio increases from 1·1 to 6. This is apparently due to the fact that the total temperature drops as the vortex center is approached (Fig. 5). A narrow cold stream will therefore have a lower average total temperature than a wider one.

CAUSES OF THE TOTAL TEMPERATURE SEPARATION

Although a considerable amount of discussion exists in the literature concerning the causes of the temperature separation in the vortex tube, no general agreement seems to have been reached. In the present section the causes of the separation are studied by examining the magnitudes of the various terms in the energy equation.

In order to determine whether compressibility in a fluid is necessary for temperature separation to occur, the incompressible case will first be considered. For this case it is convenient to consider static, rather than total temperatures, inasmuch as the total or stagnation temperature depends on the process by which the fluid is brought to rest. If the fluid is brought to rest isentropically, the total and static temperatures will be equal. In other cases the total temperature will be higher because of friction.

For an incompressible fluid the static temperature change of a fluid element depends only on the heat added to the element by conduction and by dissipation. The energy equation thus can be written as

$$\rho c_v \frac{Dt}{D\theta} = \rho c_v \varepsilon \frac{1}{r} \frac{d}{dr}\left(r \frac{dt}{dr}\right) + \phi \qquad (30)$$

where the first term is the rate of change of internal energy per unit volume of the element, the second term is the rate at which heat is being transferred into the element by turbulent conduction, and the last term is the dissipation. If it is assumed that the rate of production of turbulent energy at a point equals the rate of turbulent dissipation, the expression for ϕ can be written as $\phi = \rho\varepsilon(dv/dr - v/r)^2$. In dimensionless form the energy equation becomes

$$\frac{Dt'}{D\theta'} = \frac{1}{Re_i r'} \frac{d}{dr'}\left(r' \frac{dt'}{dr'}\right) + \frac{2}{Re_i}\left(\frac{dv'}{dr'} - \frac{v'}{r'}\right)^2 \qquad (31)$$

The terms in the incompressible energy equation are plotted in Fig. 12 for the case of uniform axial flow. As a fluid element moves toward the center the dissipation term tends to increase the temperature of the particle, as would be expected. Because of the higher temperatures near the center, the center portion then tends to lose heat by conduction and the outer regions gain heat. However, the net result (shown dashed) is that the particle continuously increases in static temperature as it spirals inward toward the center.

Vol. 1 1960

The total temperature at any radius will never be lower than the static temperature, as discussed earlier. Therefore for an incompressible fluid there appears to be no possibility of obtaining an energy separation in which the total temperature at the center of the vortex is lower than the entering temperature.

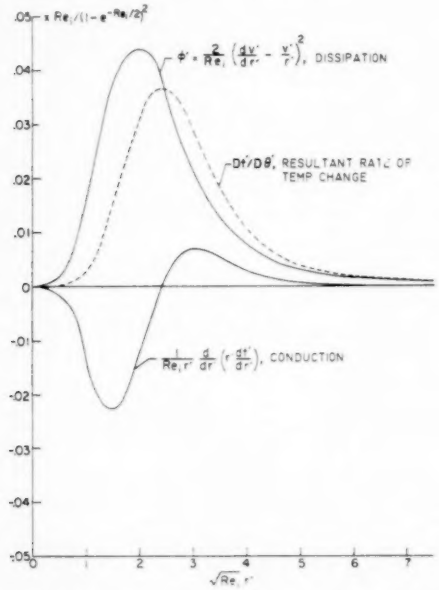

FIG. 12. Terms in incompressible energy equation (equation (31)) contributing to rate of change of temperature of fluid element with respect to time. Uniform axial mass velocity.

Thus the first requirement for energy separation to take place in a vortex is that the fluid be compressible. It should be remembered, however, that the expansion of a compressible fluid does not always produce a cooling of the fluid. As is well known, the expansion of a perfect gas flowing through an adiabatic tube or nozzle does not result in a total temperature drop. In order for cooling to take place, it is necessary that the fluid do work while it expands, as in a turbine, or that heat be transferred out of the fluid. Similarly, for the total temperature increase, work would have to be done on the fluid, or heat transferred into it. In order to see how these observations apply to the vortex, we rewrite the energy equation for a perfect gas (equation 17)):

$$\rho c_p \frac{D}{D\theta}\left(t + \frac{v^2}{2c_p}\right) = \frac{1}{r}\frac{d}{dr}\left(r\rho c_p \varepsilon \frac{dt}{dr}\right) - \frac{1}{r}\frac{d}{dr}\left(\frac{r\rho\varepsilon}{\rho}\frac{dp}{dr}\right) + \frac{1}{r}\frac{d}{dr}(rv\tau) \quad (32)$$

The left side of this equation can be written as $\rho c_p\, DT/D\theta$. Equation (32) shows that the rate of change of total temperature of a fluid element as it spirals toward the center depends on the following contributions:

$\frac{1}{r}\frac{d}{dr}\left(r\rho c_p \varepsilon \frac{dt}{dr}\right)$, turbulent heat transfer into fluid element by temperature gradients;

$-\frac{1}{r}\frac{d}{dr}\left(\frac{r\rho\varepsilon}{\rho}\frac{dp}{dr}\right)$, turbulent heat transfer into fluid element by pressure gradients (by expansion and contraction of eddies);

$\frac{1}{r}\frac{d}{dr}(rv\tau)$, turbulent shear work done on element.

Equation (32) can be written in dimensionless form as

$$\frac{\rho}{\rho_i}\frac{DT'}{D\theta'} = \frac{1}{Re_i r'}\frac{d}{dr'}\left(r'\frac{dt'}{dr'}\right) - \frac{2}{Re_i r'}\frac{dv'^2}{dr'} + \frac{2}{Re_i r'}\frac{d}{dr'}\left\{r'v'\left(\frac{dv'}{dr'} - \frac{v'}{r'}\right)\right\} \quad (33)$$

where equation (19) was used for $(1/\rho)dp/dr$, and the turbulent shear stress τ was set equal to $\rho\varepsilon(dv/dr - v/r)$.

In order to illustrate the magnitudes of the contributions to the rate of change of total temperature of a particle we again consider the case of uniform axial flow. Other axial flow distributions should give qualitatively similar results. The various contributions are plotted in Fig. 13. Although the terms for turbulent conduction due to temperature gradients and to pressure gradients are individually very large, especially near the vortex center, they tend to cancel. That is, the conduction of heat into the core region by temperature gradients is about equal to the heat conducted out by pressure gradients, or by expansion and contraction of eddies. Thus the shear work term produces most

of the energy separation. This is indicated by the fact that the curve for the sum of the contributions to the total temperature change (shown dashed) follows fairly closely the contribution due to shear work. Although the net conduction effect on $dT/d\theta$ is reasonably small, it is negligible

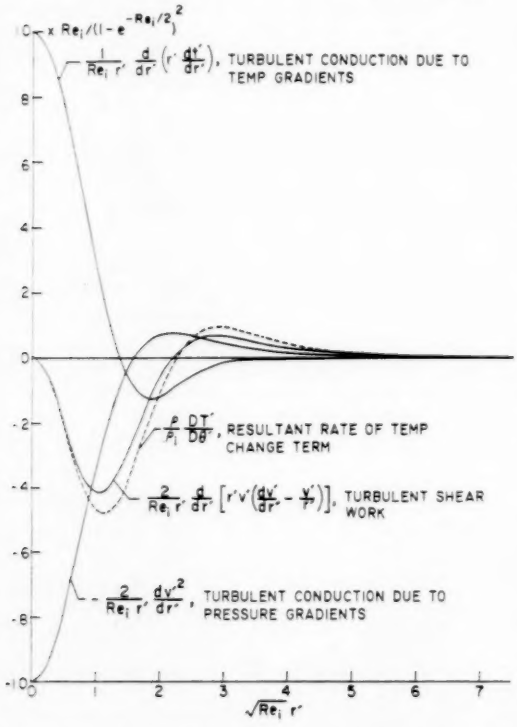
$\frac{1}{Re_i\, r'} \frac{d}{dr'}\left(r' \frac{dt'}{dr'}\right)$, TURBULENT CONDUCTION DUE TO TEMP GRADIENTS
$\frac{\rho}{\rho_i} \frac{DT'}{D\theta'}$, RESULTANT RATE OF TEMP CHANGE TERM
$\frac{2}{Re_i\, r'} \frac{d}{dr'}\left[r'v'\left(\frac{dv'}{dr'} - \frac{v'}{r'}\right)\right]$, TURBULENT SHEAR WORK
$-\frac{2}{Re_i\, r'} \frac{dv'^2}{dr'^2}$, TURBULENT CONDUCTION DUE TO PRESSURE GRADIENTS
$\sqrt{Re_i}\, r'$

FIG. 13. Terms in compressible energy equation (equation (33)) contributing to rate of change of total temperature of fluid element with time. Uniform axial mass velocity.

only for very small radii or radial flow Reynolds numbers. More will be said about this limiting case later. At very large radii the shear work done on a fluid element is essentially zero because of the small tangential velocities and velocity gradients in that region. At slightly smaller radii the shear work becomes positive and the total temperature of a fluid element increases with time. At still smaller radii the shear becomes negative and the total temperature of an element decreases with time. Comparison of these curves with the tangential velocity profile curve in Fig. 3 indicates that the region of positive shear work or of increasing total temperature corresponds to the region in which the velocity profile is still essentially inviscid ($v \propto r^{-1}$). Then as the fluid element moves to smaller radii the viscous or turbulence effects cause the velocity profile to depart from the $1/r$ variation. In that region the shear work done on the element becomes negative due to the slowing-down tendency of the turbulent viscosity, and the total temperature drops. Thus the energy separation is dependent on the tangential velocity profile. The overall result is that the fluid in the core region does shear work on the fluid in the outer region as it expands while traveling toward the center. Thus energy is transferred from the core region to the annular region with a resultant total temperature separation. A smaller additional energy transfer is effected by the expansion and contraction of eddies in a radial pressure gradient.

Inasmuch as the shear work term in the compressible energy equation gives the most important contribution to the change in total temperature of a fluid element as it moves radially, it is instructive to determine the contributions of various other physical processes to that term. This can be done by multiplying the momentum equation (2) by v and combining with the other momentum equation (19) to give

$$\frac{1}{r}\frac{d}{dr}(rv\tau) = \rho\varepsilon\left(\frac{dv}{dr} - \frac{v}{r}\right)^2 + \rho u\left[\frac{d(v^2/2)}{dr} + \frac{1}{\rho}\frac{dp}{dr}\right] \qquad (34)$$

That is, the shear work is distributed between a dissipation term, a kinetic energy term and a potential or pressure energy term. In the region where the shear work term and $DT/d\theta$ are positive, the velocity distribution is approximately that for inviscid flow ($v \propto r^{-1}$). Thus the kinetic and potential energy terms nearly cancel (substitute equation (19) for dp/dr), so that the important contribution to the shear work in that region is the dissipation. The increase in total temperature with time of a fluid element in the annular region is therefore due principally to viscous (or turbulent) dissipation. The dissipation can be important in a region where the

Vol. 1 1960

velocity profile is approximately that for inviscid flow because the shear stresses on the sides of a fluid element, although individually large, nearly cancel. Thus the shear stress can have a negligible effect on the velocity profile and still produce significant dissipation.

In the region near the center, where the shear work and $DT/d\theta$ are negative, wheel flow is approached, and the dissipation becomes less important. The important contributions to the negative shear work, and thus to the drop in total temperature of a fluid element in that region are then the kinetic and the potential or pressure energy terms, both of which are negative. For wheel flow the two terms are equal.

For the special case of no radial flow ($Re_0 = 0$) Fig. 13 apparently yields no pertinent information; for that case $DT/d\theta$ for a fluid particle is zero. Nevertheless the total temperature at the center of such a vortex is lower than that in the outer region (Fig. 5). In that case we can consider the total temperature separation to take place somewhat as follows: For purposes of discussion we first neglect conduction due to expansion and contraction of eddies. The static temperature will then tend to be uniform, inasmuch as conduction due to temperature gradients will iron out any temperature differences (no external heat transfer). Also, for no radial flow the fluid rotates as a solid body ($v \propto r$). Thus since the static temperature is uniform, the total temperature will be lower near the center because of the lower velocities there. If turbulence occurs in the vortex, the total temperature near the center will be lowered still more because of heat conducted toward the outer regions by expansion and contraction of eddies in a pressure gradient.

If the radial flow is not zero but very small, the above picture will still apply, inasmuch as the very small radial flow should not alter the velocity and temperature distributions appreciably. In this case we could, of course, also consider the cooling of a fluid element as being due to the shear work as discussed earlier in connection with Fig. 13. The two ways of looking at the energy separation are closely related, inasmuch as the shear work can be divided into a kinetic energy term and a pressure gradient term (equation (34)) the dissipation term drops out for wheel flow). The pressure gradient in turn is related to the temperature gradient by equation (18). Thus the drop in total temperature of a fluid element as it moves slowly toward the center can be thought of as being due either to the shear work done by the particle or to the lower velocities and static temperatures of the fluid near the center. The static temperatures are lower near the center because of the heat transferred to larger radii by pressure gradients.

It should be noticed that, although a long tube extending considerably beyond the location of the tangential nozzles for the entering fluid is usually used in investigations of energy separation, the present model makes no mention of such a tube. The energy separation is assumed to take place entirely within the vortex where the tangential nozzles are located. This is in agreement with the experiments in [7], where the greatest energy separation was found to take place in the tube cross-section near the tangential nozzles. In addition, some recent experiments by Savino and Ragsdale [13] indicate that considerable energy separation can take place in a vortex contained between two flat disks without an attached tube. The flow emerged from an opening at the center with a diameter on the order of the plate spacing. Most of the energy separation took place near the opening.

The energy separation in vortex tubes is sometimes attributed to unsteady effects (other than the turbulence effects considered here). Although such effects might augment the energy separation under certain conditions, the present analysis indicates that considerable separation can be accounted for by considering only steady-state effects.

CONCLUSIONS

The analysis indicated that the dimensionless tangential velocity and temperature distributions are functions of the following parameters: The ratio of axial flow out of the core of the vortex to the total mass flow, the ratio of the core radius to the radius of the vortex, and a turbulent radial-flow Reynolds number which contains the eddy viscosity rather than the molecular viscosity. For the pressure distributions it was necessary in addition to specify the Mach number at a given radius and the ratio of the heat capacities.

The importance of turbulence for energy separation was found to be twofold: First, it causes the effective Reynolds number to remain low (where energy separation can take place), even when the laminar Reynolds number is high. This is because the turbulent viscosity may be several orders of magnitude higher than the molecular viscosity. (However, it would not pay to increase the turbulence level indefinitely, inasmuch as an optimum turbulent Reynolds number was obtained.) Secondly, there is an additional energy separation in the turbulent case due to the expansion and contraction of the eddies as they move radially in a pressure gradient. The predicted curves for velocity and temperature distributions, as well as for overall energy separation, closely resembled experimental curves, so that it appears that the model analyzed displays most of the features of actual vortex tubes.

In analyzing the causes of the energy separation it was determined first that the fluid must be compressible, since the total temperature of a particle in an incompressible vortex can only increase, owing to the dissipation. By considering the magnitudes of the terms in the compressible energy equation, it was found that the terms for turbulent conduction due to temperature gradients and to pressure gradients, although individually large, tended to cancel. Thus most of the total temperature change of a fluid element as it spiraled toward the center was due to the shear work done on the element (positive in the outer region, negative in the core). Therefore the energy separation depends on the tangential velocity profile, in particular, on the deviation of the profile near the center from that for inviscid flow. The overall effect is that the fluid in the core region does shear work on the fluid in the outer region with a resultant total temperature separation. The shear work term was further divided into a dissipation term, a kinetic energy term and a potential or pressure energy term. In the region of high total temperatures the dissipation term was found to produce most of the heating of a fluid element. The decrease of total temperature of an element as it moves in the core region was due principally to the kinetic and pressure energy terms, both of which are negative in that region.

APPENDIX

Derivation of Pressure Gradient Conduction Term by Modified Mixing-length Theory

Although the mixing-length theory may be an oversimplification of the actual turbulent transfer in a vortex, it provides a convenient way of arriving at the pressure gradient conduction term in equation (17). In the following analysis, eddies are assumed to move transversely in the vortex between cylindrical surfaces (1) and (2) which are separated by the small distance l, the average mixing length at a particular radius.

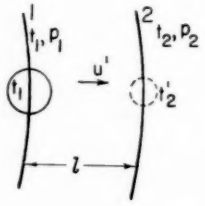

Eddies also move axially and tangentially, but these should not affect the radial heat transfer. The eddies originate from an instability at either surface (1) or (2) and travel to the other surface where they mix with the fluid. Consider an eddy of fluid which originates at the inner surface (1), where it has the time average temperature and pressure of the fluid at surface (1). As discussed in the body of the text the eddy is assumed to be compressed isentropically as it moves to the region of higher pressure at (2). As the eddy arrives at surface (2), conservation of mass requires that an equal mass of fluid must leave. The net heat transported to surface (2) is then equal to the mass of the eddy multiplied by $c_p(t_2' - t_2)$, where t_2' is the temperature of the eddy as it arrives at surface (2) and t_2 is the temperature of the surrounding fluid. The turbulent heat transfer per unit area per unit time from surface (1) to surface (2) is then given by

$$q_t = c_p \rho f u'(t_2' - t_2) \qquad \text{(A1)}$$

where f is the fraction of surface (2) on which eddies are arriving, and u' is the average velocity of the eddies. Equation (A1) can be written as

$$q_t = -c_p \rho f u' l \left(\frac{\Delta t_f}{l} - \frac{\Delta t_e}{l} \right) \qquad \text{(A2)}$$

Vol. 1 1960

where Δt_f is the change in average fluid temperature between (1) and (2) and Δt_e is the corresponding change in eddy temperature. In differential form equation (A2) becomes

$$q_t = - c_p \rho f u' l \left(\frac{dt}{dr} - \frac{dt_e}{dr} \right)$$

For an isentropic compression equation (18) can be substituted to give

$$q_t = - c_p \rho \varepsilon \left(\frac{dt}{dr} - \frac{1}{\rho c_p} \frac{dp}{dr} \right) \qquad \text{(A3)}$$

where the eddy diffusivity ε was substituted for $fu'l$. This expression for turbulent heat transfer is the same as the expression for turbulent heat transfer in equation (17).

REFERENCES

1. R. Hilsch, *Rev. Sci. Instrum.* **18**, (1947).
2. R. Westley, *A Bibliography and Survey of the Vortex Tube*. The College of Aeronautics, Cranfield (1954).
3. C. D. Pengelley, *Flow in a Viscous Vortex*. Report 494C-1, TN 56-126, Southwest Research Institute (1956).
4. J. J. Van Deemter, *Appl. Sci. Res.* A **3**, 3 (1952).
5. R. G. Deissler and M. Perlmutter, *An Analysis of the Energy Separation in Laminar and Turbulent Compressible Vortex Flows*. Heat Transfer and Fluid Mechanics Institute, Stanford University Press (1958).
6. H. A. Einstein and H. Li, *Steady Vortex Flow in a Real Fluid*. Heat Transfer and Fluid Mechanics Institute, Stanford University Press (1951).
7. J. P. Hartnett and E. R. G. Eckert, *Experimental Study of the Velocity and Temperature Distribution in a High Velocity Vortex Type Flow*. Heat Transfer and Fluid Mechanics Institute, Stanford University Press (1956).
8. S. Pai, *Viscous Flow Theory*, pp. 37, 43. Van Nostrand, New York (1956).
9. R. Kassner and E. Knoernschild, *Friction Laws and Energy Transfer in Circular Flow*. TR No. F-TR2198-ND, WADC (1948).
10. R. G. Deissler, *Analysis of Fully Developed Turbulent Heat Transfer at Low Peclet Numbers in Smooth Tubes with Applications to Liquid Metals*. NACA RM E52F05 (1952).
11. *Meteorology and Atomic Energy* p. 27. Supt. Docs., U.S. GPO, Wash., D.C. (1955).
12. J. E. Lay, *Trans. Amer. Soc. Mech. Engrs.* 202 (1959).
13. J. M. Savino and R. T. Ragsdale, *Some Temperature and Pressure Measurements in Confined Vortex Fields*. ASME Preprint No. 60-SA-4 (1960).

Int. J. Heat Mass Transfer. Vol. 1, pp. 192–207. Pergamon Press 1960. Printed in Great Britain.

A STANDARD FORMULATION OF THE STEADY CONVECTIVE MASS TRANSFER PROBLEM

D. B. SPALDING†

Imperial College of Science and Technology, London S.W.7

(*Received* 24 *October* 1959)

Abstract—It is shown that, provided that certain relations exist between the transport properties, every mass transfer problem, including those with simultaneous heat transfer and chemical reaction, can be expressed by relations of the "Ohm's Law" type: $\dot{m}'' = g \, . \, B$, where $\dot{m}''$ is the required mass transfer rate through the surface, g is a surface conductance dependent on aerodynamic factors, and B is a dimensionless driving-force dependent on the thermodynamic properties of the main stream, of the fluid in contact with the phase boundary, and of the transferred substance.

The standard formulation is derived from the differential equations of conservation and flux and by reference to a wall-flux boundary condition. Thereafter examples are given of methods of calculating g, followed by examples of expressions for B valid for particular cases.

Résumé—A condition que certaines relations existent entre les propriétés de transport, on montre que tout problème de transport de masse, même s'il comprend à la fois transfert de chaleur et réaction chimique, peut être exprimé par des relations du type de la loi d'Ohm: $\dot{m}'' = g \, . \, B$ où $\dot{m}''$ est la densité de flux de masse transportée à travers la surface, g est la conductance de surface qui dépend des facteurs aérodynamiques et B est la force agissante, sous forme adimensionnelle, qui dépend des propriétés thermodynamiques de l'écoulement principal, du fluide en contact avec la surface de séparation, et de la substance transportée.

La formulation générale est obtenue à partir des équations aux dérivées partielles de conservation et de transport, rapportées aux conditions aux limites du transports à la paroi.

Des exemples sont donnés ensuite pour les méthodes permettant le calcul de g, et sont suivis par différentes expressions de B valables dans des cas particuliers.

Zusammenfassung—Es wird gezeigt, dass jedes Problem der Stoffübertragung einschliesslich derer mit gleichzeitiger Wärmeübertragung und chemischer Reaktion in Form eines Ohm'schen Gesetzes $\dot{m}'' = g \, . \, B$ ausgedrückt werden kann, sofern gewisse Beziehungen zwischen den Transportgrössen bestehen. Es bedeutet $\dot{m}''$ die gesuchte Mengenstromdichte an der Oberfläche, g eine Oberflächenleitfähigkeit, abhängig von aerodynamischen Faktoren und B eine dimensionslose treibende Kraft, die von den thermodynamischen Eigenschaften des Hauptstroms, der Flüssigkeit im Kontakt mit der Phasengrenzfläche und des übertragenen Stoffes abhängt. Aus den Differentialgleichungen der Erhaltung und der Strömung unter Bezugnahme auf eine Grenzbedingung der Wandströmung wurde eine einheitliche Formulierung abgeleitet. Beispiele für die Methoden zur Berechnung von g werden mitgeteilt und schliesslich werden die Ausdrücke von B für besondere Fälle angegeben.

Abstract—Показано, что при условии существования определенных соотношений между характеристиками переноса каждая задача переноса, включая также задачи с одновременно происходящими химической реакцией и переносом тепла, может быть выражена при помощи соотношений, подобных закону Ома: $\dot{m}'' = g.B$, где $\dot{m}''$–требуемая скорость переноса массы через поверхность, g–поверхностная проводимость, зависящая от аэродинамических факторов, B–безразмерная движущая сила, зависящая от термодинамических свойств основного потока, жидкости, соприкасающейся с поверхностью раздела фаз, а также переносимой субстанции.

Общая постановка задачи получена из анализа дифференциальных уравнений сохранения и потока с учётом условий на границе сменнога иомока Приводятся методы вычисления g, сопровождаемые примерами выражений для B, справедливых для частных случаев.

† Professor of Heat Transfer.

Vol. 1 1960

NOTATION

b, dimensionless transferred property, equation (28);
B, dimensionless driving force for mass transfer ($\equiv b_G - b_S$), equation (33);
c, specific heat of fluid mixture at constant pressure (B.t.u./lb °F);†
D, diffusion coefficient (ft²/hr);
f, mass fraction in fluid mixture of one component in a two-stream flow, regardless of state of chemical aggregation (dimensionless);
F, function of B and μ/γ appearing in equation (36);
g, surface conductance for mass transfer, equations (34) and (34a), (lb/ft²hr);
g^*, value of g when $B = 0$, equation (45), (lb/ft²hr);
$\mathbf{G}$, vectorial total mass flux at any point in fluid (lb/ft²hr);
G, "mass velocity" at reference point in stream (lb/ft²hr);
h, specific enthalpy of mixture ($\equiv \Sigma_j m_j h_j$), (B.t.u./lb);
h_j, partial enthalpy of substance j (B.t.u./lb);
h_{LS}, "latent heat" of phase change of transferred substance (B.t.u./lb);
H, heat of reaction of "fuel" at constant-pressure (B.t.u./lb);
k, thermal conductivity of mixture (B.t.u./ft hr °F);
K, function of B and μ/γ appearing in equation (36), equal to ordinate of Fig. 2;
l, typical dimension of body (ft);
m_j, mass of j in unit mass of mixture (dimensionless);
$\dot{m}''$, total mass flux across phase boundary into considered phase (lb/ft²hr);
$\dot{m}''_{j,S}$, mass flux of substance j across control surface S into considered phase (lb/ft²hr);
$\dot{m}''_{a}$, mass flux of chemical element a into considered phase (lb/ft²hr);
$\dot{m}'''_{j}$, volumetric rate of generation of substance j by homogeneous chemical reaction (lb/ft³hr);
n_a, mass of chemical element a in unit mass of mixture (dimensionless);
$n_{a,j}$, mass of chemical element a in unit mass of substance j (dimensionless);
P, conserved property, equation (26);
P_1, conserved property, equation (16);
P_2, conserved property, equation (20);
P_3, conserved property, equation (21);
$\dot{q}''_L$, heat flux away from considered phase across the L control surface, Fig. 3 (B.t.u./ft²hr);
$\dot{q}''_S$ heat flux away from considered phase across the S control surface, Figs. 1 and 3, (B.t.u./ft²hr);
Q, heat flux across S per unit mass transfer, equation (54), (B.t.u./lb);
r, mass of "oxidant" combining with unit mass of "fuel" in simple chemical reaction (dimensionless);
R, distance of location on surface from axis of symmetry, equation (36) (ft);
t, temperature (°F);
x, distance along surface in stream-wise direction (ft);
y, distance normal to surface (ft);
α, surface heat transfer coefficient (B.t.u./ft²hr °F);
γ, "exchange coefficient", $= D\rho$ (lb/ft hr);
Γ, "thermal exchange coefficient" $\equiv k/c$ (lb/ft hr);
μ, dynamic viscosity (lb/ft hr).

Subscripts

a, chemical element;
i, inert chemical compound;
j, chemical compound;
fu, reactant in a simple reaction, e.g. fuel;
ox, reactant in a simple reaction, e.g. oxidant;
prod, product in a simple reaction, e.g. product;
steel, steel;
cool, coolant gas in transpiration-cooling;
Fe, iron;
C, carbon;

† The abbreviation for the pound mass is lb, and for the pound force Lb throughout the paper.

G, state of fluid mixture in main stream;
S, state of fluid mixture at S control surface;
T, state of transferred substance, see Section 2.2;
L, state of fluid mixture at L control surface;
O, state of transpiration coolant in supply reservoir;
0, reference state;
e, main stream at outer "edge" of boundary layer.

1. INTRODUCTION

1.1. *Purpose of the paper*

THERE are many methods available for the calculation of mass transfer rates in particular circumstances. The notation, generality, and the physical and mathematical exactness of the methods currently differ according to the industry in which the problem has arisen. Thus, to name just two examples, chemical engineers calculating absorption rates use molal concentrations, the "stagnant-film" idealization, and an empirical equation for the surface conductance; while aeronautical engineers concerned with transpiration cooling use mass concentrations and exact or approximate theoretical solutions of the laminar boundary-layer equations.

It is the aim of the present paper to outline a formulation of the mass transfer problem which is sufficiently flexible and general to accommodate all mass transfer processes and sufficiently simple in use to be accessible to design engineers.

1.2. *Outline of the proposed method*

The Ohm's law of mass transfer. The aim of convective mass transfer theory is to calculate the rate of transfer of material across a stream boundary. We give this quantity the symbol $\dot{m}''$, with units: lb/ft²hr.

The laws governing mass transfer processes permit the mass transfer rate to be related to the stream and boundary properties by an equation of the Ohm's law form, namely:

$$\dot{m}'' = g \, . \, B \tag{34}$$

where B is a dimensionless driving force, dependent for its value on the composition and temperature of the main stream, of the fluid in contact with the surface, and of the transferred substance;
g is a surface conductance (units = lb/ft²hr) expressing the influence of fluid-mechanical factors: stream velocity, surface shape, etc.

Methods of calculating the conductance g are discussed in Section 2.5 below. The whole of Section 3 is devoted to the evaluation of the driving-force B in particular circumstances.

Range of applicability of the method. The method is valid for both gases and liquids in laminar or turbulent steady flow. Chemical reaction may occur. In the latter case, however, the permissible transport-property variations are restricted. These restrictions are discussed in Section 2.3.

1.3. *Relation to earlier work*

Origins. The present method arose out of studies of the work of Hatta [1] on liquid-phase reactions, as presented in the book by Sherwood [2], and of the work of Nusselt [3] and Burke and Schumann [4] on the combustion of carbon. The emphasis on concordance with boundary-layer theory was stimulated by the work of Eckert and Lieblein [5] but, by a fruitful accident, mass concentrations were used rather than molal ones.

The first presentations of the general method, using the differential equations of atomic and energy conservation [6] and with derivation of corresponding approximate solutions of the laminar boundary-layer equations [7] were made in connexion with studies of the combustion of liquid fuels. The first exact solutions of the boundary-layer equations in the present terms were published by Emmons [8]. The formulation was later somewhat elaborated [9, 10] particularly in the direction of the use of constructions on enthalpy–composition diagrams for the solution of simultaneous-transfer problems [11, 12, 13]; the latter are not discussed here.

The present paper represents a development of the above work, being improved as regards rigour of derivation, note having been taken of the criticisms of Merk [14]. A more careful

Vol. 1 1960

definition of the concept of the "transferred substance" has permitted extension of the method to processes, common in chemical-engineering equipment, in which substances are transferred through the phase boundary in both directions simultaneously.

Parallel work. The ideas and techniques which will be presented have also been independently invented and exploited by many other authors. It is only possible to mention the main contributors here.

An important stream of related work is that started by Busemann [15] and continued by Bosnjakovic [16–20]. The latter author has made particularly extensive use of graphical methods for transfer calculations, and has made a thorough study of the simultaneous processes of mass transfer, heat transfer and chemical reaction which occur in the gas producer.

The simplifications which can be made to the differential equations when equality exists between the diffusivities of matter and heat have long been exploited in the theory of gaseous flames. Particular mention must be made of the early contributions in this regard by the Russian workers, Zeldovich and Frank-Kamenetsky [21] and Schwab [22]. These authors studied the system designated "simple chemical reaction" below (simplifying assumptions (iii), (iv), (v), (vii), (viii) and (ix)), but did not consider mass transfer across a phase boundary.

Since World War II, numerous theoretical studies have been made of the combustion of liquid-fuel droplets in oxidizing atmospheres; workers who use methods similar to the author's include Varshavskii [23], Goldsmith and Penner [24], and Agafanova *et al.* [25]. A generalization has been made by Coffin and Brokaw [26].

Still more recently, interest in simultaneous mass transfer and chemical reaction has been awakened among aerodynamicists concerned with the cooling of the surfaces of high-speed missiles. The most extensive theoretical study of this subject is that of Lees [27]. Related publications are those of Sutton [28], Hartnett and Eckert [29], Bromberg and Lipkis [30], and others too numerous to mention.

Remarks on notation. The notation used by the above authors naturally exhibits wide deviations from that used here, and cannot be reviewed in detail. However, the following remarks may be of assistance.

In the chemical-engineering literature (see, for example, Sherwood and Pigford [31]), the symbol k_G for gas-side surface conductance is equivalent to g, used here, divided by (absolute pressure times local mixture molecular weight). The symbols k_L and k_c are equivalent to g divided by local mixture density. Many of the symbols for surface conductance used by other authors have the latter significance.

Our surface conductance g is equal to the surface heat transfer coefficient α divided by the constant-pressure specific heat of the mixture c, if enthalpy transfer is in question. Therefore $g\,l/(k/c)$ has the significance of a Nusselt number, where l is a reference dimension of the body and k is the mixture thermal conductivity. The writer finds it preferable to introduce the symbol Γ for k/c, and the symbol γ for $D\rho$ where D is the diffusion coefficient and ρ the local density.

The driving force B, was referred to as the "transfer number" in the writer's previous work. The symbol B' used by Lees [27] has the same significance.

In the present work the mass fraction, m_j, will be used as the measure of concentration, regardless of the phase of the mixture. Thus, in the present notation, m_j signifies the mass of chemical compound j to be found in unit mass of local mixture.

1.4. *Guide to the remainder of the paper*

Sections 2.1, 2.2, 2.3 and 2.4 contain, in condensed form, the analysis leading from the laws of physics to the standard differential equation and boundary condition of mass transfer; the various sets of essential simplifying assumptions appear in Section 2.3. *All these sections can be skipped by readers interested only in the use of the method.*

Section 2.5 explains how the surface conductance g can be calculated in a variety of practical cases; the formulae are stated but not derived. Section 2.6 then summarizes the calculation procedure which is recommended for predicting mass transfer rates.

Section 3 shows, by way of a series of examples, the manner in which the driving force

B can be calculated. The examples are chosen so as to cover processes arising in chemical, aeronautical and mechanical engineering.

2. SIMPLIFICATION, STANDARD FORMULATION, AND SOLUTION OF THE DIFFERENTIAL EQUATIONS

2.1. *Differential equations of conservation and flux*

The experimental laws governing the distribution of (time—mean) concentration and enthalpy in a non-uniform steady fluid stream can be represented by differential equations. The laws comprise the conservation of matter, the First Law of Thermodynamics, the Fick Diffusion Law, and the Fourier Law of Heat Conduction.

"Coupling" of the fluxes is disregarded, i.e. it is supposed that no diffusion of mixture-component j occurs in the absence of a gradient in the mass fraction of j, m_j, and that no heat transfer occurs in the absence of a temperature gradient. The barycentric co-ordinate system is used; this means that the diffusion flux of mixture-component j is defined as equal to the total mass flux vector of j at the point in question minus the convective mass flux vector of j; the latter quantity is defined as $m_j\mathbf{G}$, where m_j is the local mass fraction of j, while $\mathbf{G}$ is the net mass flux vector, i.e. the sum of the total mass flux vectors of all the components of the mixture.

The equations are written in vector form for the sake of compactness;† they are:

for a chemically inert substance, i

$$\mathbf{G}.\nabla(m_i) - \nabla\{\gamma_i(\nabla m_i)\} = 0 \qquad (1)$$

for a substance j, which *may* enter into a chemical reaction

$$\mathbf{G}.(\nabla m_j) - \nabla\{\gamma_j(\nabla m_j)\} = \dot{m}'''_j \qquad (2)$$

where $\dot{m}'''_j$ is the rate of generation of substance j by chemical reaction (units, lb/ft^{3}hr)

For a chemical element a:

$$\mathbf{G}.(\nabla n_a) - \nabla\{\sum_j \gamma_j n_{a,j}(\nabla m_j)\} = 0 \qquad (3)$$

where $n_{a,j}$ is the mass of chemical element a contained in unit mass of chemical compound j;

n_a is the mass of chemical element a contained in unit mass of local mixture.

For the enthalpies, when shear work,‡ kinetic energy, gravitational potential energy and electrical and magnetic effects can be neglected:

$$\mathbf{G}.(\nabla h) - \nabla\{\sum_j \gamma_j h_j(\nabla m_j)\} - \nabla\{\Gamma c(\nabla t)\} = 0 \qquad (4)$$

where h_j is the partial enthalpy of component j in the local mixture (B.t.u./lb);

h is the specific enthalpy of the mixture ($\equiv \sum_j h_j m_j$).

In equation (4), the first term represents the convective enthalpy flux, the second term represents the enthalpy flux associated with diffusion, while the third represents the heat flux (since $\Gamma c \equiv k$, the thermal conductivity. The reason for preferring the use of Γ should become apparent later when the simplified forms of the equation are dealt with).

2.2. *The wall-flux boundary condition*

Consider an element, illustrated in Fig. 1, of a surface separating the fluid under consideration from a neighbouring phase; this surface can be termed variously "phase boundary", "interface"

† Some readers may like to be reminded that, in Cartesian form, equation (1), for example, would read:

$$\rho u\frac{\partial m_i}{\partial x} + \rho v\frac{\partial m_i}{\partial y} + \rho w\frac{\partial m_i}{\partial z} - \frac{\partial}{\partial x}\left(\gamma_i\frac{\partial m_i}{\partial x}\right) -$$

$$-\frac{\partial}{\partial y}\left(\gamma_i\frac{\partial m_i}{\partial y}\right) - \frac{\partial}{\partial x}\left(\gamma_i\frac{\partial m_i}{\partial z}\right) = 0$$

where x, y and z are the Cartesian co-ordinate directions;
u, v and w are the local fluid velocities in these directions, defined so that, if ρ is the local fluid density, then
ρu, ρv and ρw are the components of the total mass flux vector $\mathbf{G}$.

The other equations can be similarly translated; although the presence of the summations, $\sum_j$, renders them rather unwieldy.

‡ At high velocities, the enthalpy h in the first term must be replaced by the *stagnation* enthalpy of the mixture, and a further term must be added expressing the shear work per unit volume. Details are given in the Appendix.

Vol. 1 1960

or "wall". The surface is pervious to material; we shall relate the magnitude of the mass flux through it, $\dot{m}''$, to the gradients in stream properties measured at the control surface S which is in the fluid immediately adjacent to the interface. To do this we must consider two states: the S-state and the T-state.

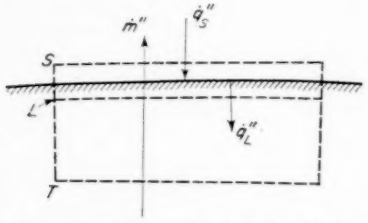

FIG. 1. Control volume used in deriving the boundary conditions, equations (9), (10) and (11).

The S-state is the state (time–mean composition, temperature, etc.) of the fluid mixture at the control surface S. The quantities $m_{j,S}$, t_S, $h_{j,S}$, etc., can in principle be measured by the usual sampling and analysis instruments.

The T-state, i.e. the state of the *transferred substance*, may be regarded as a fictitious mixture state: it does not exist at any particular point, but is defined as follows. Its *composition* is sufficiently defined in terms of the mass fractions $m_{i,T}$, $n_{\alpha,T}$, etc., via the equations involving mass fluxes:

$$m_{i,T} \equiv \dot{m}''_i/\dot{m}'' \tag{5}$$

where $\dot{m}''_i$ is the total (i.e. convective plus diffusive) mass flux of the inert substance i into the fluid phase; and

$$n_{\alpha,T} \equiv \dot{m}''_\alpha/\dot{m}'' \tag{6}$$

where $\dot{m}''_\alpha$ is the total mass flux of the chemical element α into the fluid phase, irrespective of the chemical compounds in which α happens to find itself.

The state of chemical aggregation of the transferred substance is not completely specified by these definitions; it is not required. The quantity $\dot{m}''_\alpha$ is conveniently evaluated in terms of the total mass fluxes of the various substances, $\dot{m}''_{j,S}$, through the control surface S, by way of equation:

$$\dot{m}''_\alpha = \sum_j n_{\alpha,j}\, \dot{m}''_{j,S} \tag{7}$$

In contrast to the practice for $\dot{m}''_i$ and $\dot{m}''_\alpha$, a suffix (here S) has to be appended to $\dot{m}''_j$ because, in general, j may take part in a chemical reaction; thus an evaluation of $\dot{m}''_j$ at the control surface L of Fig. 3 would, in general, yield a different value from an evaluation at S. But of course

$$\sum_j n_{\alpha,j}\, \dot{m}''_{j,S}$$

must be equal to

$$\sum_j n_{\alpha,j}\, \dot{m}''_{j,L}$$

because chemical elements are neither created nor destroyed. Evaluation at the S control surface is preferable for present purposes because this surface lies in the fluid under consideration.

The *enthalpy of the transferred substance*, h_T, is defined for similar reasons by the equation:

$$h_T\, \dot{m}'' \equiv \sum_j h_{j,S}\, \dot{m}''_{j,S} - \dot{q}''_S \tag{8}$$

where $\dot{q}''_S$ is the heat flux caused by the temperature gradient across the control surface S, directed outward from the fluid under consideration.

The T-state may thus be interpreted as that which must prevail at the lower surface of the fictitious control volume of Fig. 1 if the conservation laws are to hold and if there is no diffusion or heat transfer across this surface.

Application of the conservation and flux laws underlying equations (1), (3) and (4) to the control volume of Fig. 1 now yields the following boundary conditions:

For the chemically inert substance i:

$$\dot{m}'' = \frac{\{\gamma_i\ (\partial m_i/\partial y)\}_S}{m_{i,S} - m_{i,T}} \tag{9}$$

where y is the distance normal to the wall.

For the chemical element α:

$$\dot{m}'' = \frac{\sum_j \{\gamma_j n_{\alpha,j}\ (\partial m_j/\partial y)\}_S}{n_{\alpha,S} - n_{\alpha,T}} \tag{10}$$

For the enthalpy:

$$\dot{m}'' = \frac{\sum_j \{\gamma_j h_j\ (\partial m_j/\partial y)\}_S + \{\Gamma c\ (\partial t/\partial y)\}_S}{h_S - h_T} \tag{11}$$

No such boundary condition is available in general for the chemical substance j since the

state of chemical aggregation of the transferred substance is not specified (j may react *at* the phase boundary).

2.3. *Simplifications necessary if reaction-kinetic considerations are to be avoided*

Because of the term appearing on the right-hand side of equation (2), evaluation of which involves knowledge of the reaction kinetics of the fluid phase, solution of the equations (3) and (4), with boundary conditions (10) and (11), is not possible unless simplifying assumptions are made. The validity of these assumptions will not be examined here, but it should be remarked that those relating to the transport coefficients are close to reality for all fully turbulent fluids and for gases containing components of roughly uniform molecular weight. The simplifying assumptions represent *alternatives*.

Simplifying assumption (i). When, at any particular point in the stream, all the γ_j's of substances containing element a are equal to ach other, equations (3) and (10) reduce to:

$$\mathbf{G}.\,(\nabla n_a) - \nabla\{\gamma_a(\nabla n_a)\} = 0 \qquad (12)$$

and

$$\dot{m}'' = \frac{\{\gamma_a\,(\partial n_a/\partial y)\}_S}{n_{a,S} - n_{a,T}} \qquad (13)$$

where γ_a is the common value of the set of γ_j's.

Simplifying assumption (ii). When, at any particular point in the stream, all the γ_j's are equal to each other *and* to the quantity Γ, equations (4) and (11) reduce to:

$$\mathbf{G}.\,(\nabla h) - \nabla\{\Gamma(\nabla h)\} = 0 \qquad (14)$$

and

$$\dot{m}'' = \frac{\{\Gamma\,(\partial h/\partial y)\}_S}{h_S - h_T} \qquad (15)$$

Simplifying assumption (iii). Suppose that two substances, designated "fuel" and "oxidant" for concreteness, take part in a simple chemical reaction to produce a third substance (product) without intermediate transformations; suppose further that the quantities γ_{fu} and γ_{ox} are equal to each other at every point in the stream then, if we define a quantity P_1, through:

$$P_1 = m_{\mathrm{fu}} - m_{\mathrm{ox}}/r \qquad (16)$$

where r is the mass ratio of oxidant to fuel in the stoichiometric equation, then the recognition that, for this reaction, we can put:

$$\dot{m}'''_{\mathrm{fu}} = \dot{m}'''_{\mathrm{ox}}/r \qquad (17)$$

permits us to deduce from equation (2) that:

$$\mathbf{G}.\,(\nabla P_1) - \nabla\{\gamma_1(\nabla P_1)\} = 0 \qquad (18)$$

The quantity $P_{1,T}$ can be evaluated, since it does not entail knowledge of the state of chemical aggregation of the transferred substance. Consideration of the control volume of Fig. 1 now yields the boundary condition:

$$\dot{m}'' = \frac{\{\gamma_1(\partial P_1/\partial y)\}_S}{P_{1,S} - P_{1,T}} \qquad (19)$$

γ_1 is of course the common γ of the substances designated "fuel" and "oxidant". Obviously, despite the use of the latter terms, the analysis is in no way restricted to combustion reactions.

As alternatives to the assumptions leading to (18) and (19), two further cases may be considered, namely:

(iv) If the γ's of fuel and product are equal to each other at every point in the stream, having the common value γ_2; and if a quantity P_2 is defined by:

$$P_2 \equiv m_{\mathrm{fu}} + m_{\mathrm{prod}}/(1 + r) \qquad (20)$$

then equations (18) and (19) hold with the subscript (2) in place of subscript (1).

(v) If the γ's of oxidant and product are equal (to γ_3) at each point, and P_3 is defined by:

$$P_3 = m_{\mathrm{ox}}/r + m_{\mathrm{prod}}/(1 + r) \qquad (21)$$

then the equations (18) and (19) hold with the subscript (3) in place of subscript (1).

Simplifying assumption (vi). When chemical reaction is absent, the fluid mixture is ideal, and the specific heat of the fluid is uniform, equations (4) and (11) again reduce to (14) and (15). The enthalpy h can in this case be expressed in terms of temperature, at any rate within the phase under consideration, via:

$$h \equiv c(t - t_0) \qquad (22)$$

where t_0 is an arbitrary reference temperature. No restriction on the γ's need be imposed.

Simplifying assumption (vii). When a single

Vol. 1 1960

simple chemical reaction takes place, of the type described under (iii), if the fluid mixture is otherwise ideal with uniform specific heat, and if further the γ of fuel is equal to Γ at every point in the mixture, equations (4) and (11) again reduce to equations (14) and (15). This time the fluid-phase enthalpy can be expressed as:

$$h \equiv m_{\text{fu}} H + c(t - t_0) \tag{23}$$

where H is the heat of reaction per unit mass of fuel.

Alternative simplifications are clearly possible, as follows:

(viii) If, instead of $\gamma_{\text{fu}} = \Gamma$, we have $\gamma_{\text{ox}} = \Gamma$ at every point, equations (14) and (15) now hold with:

$$h \equiv m_{\text{ox}} H/r + c(t - t_0) \tag{24}$$

(ix) If, alternatively, $\gamma_{\text{prod}} = \Gamma$, equations (14) and (15) hold with the fluid-phase enthalpy defined through:

$$h \equiv -m_{\text{prod}} H/(1 + r) + c(t - t_0) \tag{25}$$

Further simplifying assumptions. The above nine cases do not exhaust the possibilities. Other simplifications involving a different mixture of restrictions on the transport properties and restrictions on the thermodynamic properties can be easily envisaged; they may be convenient in the analysis of particular cases.

Generalization. Comparison of the pairs of equations (1) and (9), (12) and (13), (14) and (15), (18) and (19), shows that they have a common form which we may write as:

$$\mathbf{G}.(\nabla P) - \nabla\{\gamma(\nabla P)\} = 0 \tag{26}$$

and

$$\dot{m}'' = \frac{\{\gamma(\partial P/\partial y)\}_S}{P_S - P_T} \tag{27}$$

where $P \equiv m_i, n_a, h, P_1, P_2, P_3$, or any other conserved property,† and γ may be replaced by Γ if enthalpy is in question.

† Fluid properties obeying equation (26) might be called "conserved properties of the second class" to distinguish them from "conserved properties of the first class" which are conserved in adiabatic steady-flow mixing processes.

2.4. *Re-arrangement for the case of uniform* S- *and* T-*states*

All the solutions of the equation (26) which are known to the author (except those for $\dot{m}'' = 0$) relate to cases in which the state of the fluid in contact with the surface *and* the state of the transferred substance are uniform over the boundaries of the field of integration through which mass transfer occurs. This means that P_S and P_T are constants in the integration procedure.

In such cases it is convenient to reduce all mass transfer problems to a common form by introducing the new variable b, defined as:

$$b \equiv \frac{P - P_S}{P_S - P_T} \tag{28}$$

Equations (26) and (27) then reduce to:

$$\mathbf{G}.(\nabla b) - \nabla\{\gamma(\nabla b)\} = 0 \tag{29}$$

$$\dot{m}'' = \left(\gamma \frac{\partial b}{\partial y}\right)_S \tag{30}$$

Nature of the mathematical problem. We now see that, whatever the nature of the conserved property which is under consideration, the task of predicting mass transfer rates reduces to the solution of equation (29) with, as boundary conditions at the wall, equation (30) and:

$$b_S = 0 \tag{31}$$

Since $\mathbf{G}$ and γ appear in (29), solution of this equation requires prior (or sometimes simultaneous) solution of the momentum and continuity equations for the fluid stream, and also a proper accounting for the dependence of γ on the fluid state, i.e. on b.

Behaviour of the solution. Without treating any particular configuration of surface and stream, it is possible to conclude, from dimensional analysis and other general considerations, that the solution to any forced-convection mass transfer problem with uniform S- and T-states can be cast in the form:

$$\frac{\dot{m}''}{G} = f\left\{B, \frac{Gl}{\mu_0}, \frac{\mu_0}{\gamma_0}\right\} \tag{32}$$

where G is the mass velocity in the main stream, say at entry;

l is an apparatus dimension;
μ_0 is the fluid viscosity measured at some reference state;
γ_0 is the corresponding value of the exchange coefficient of the relevant P;
$B \equiv b_G$, the value of b in the main stream.

The latter definition leads to the important relation:

$$B \equiv \frac{P_G - P_S}{P_S - P_T} \tag{33}$$

Further thought about the solution reveals that it may be convenient to introduce a quantity g (units, lb/ft²hr) via the definition:

$$\dot{m}'' \equiv gB \tag{34}$$

and to express the solution to equation (29) in the form:

$$\frac{g}{G} = f\left\{B, \frac{Gl}{\mu_0}, \frac{\mu_0}{\gamma_0}\right\} \tag{35}$$

The quantity on the left-hand side of (35) is akin to the *Stanton* number; Gl/μ_0 is a Reynolds number; and μ_0/γ_0 is a Prandtl or Schmidt number according to the nature of the conserved property appearing in B. Alternatively, the group, gl/γ_0 a sort of Nusselt number, may appear on the left-hand side.

By comparing equations (30) and (34), we see that g is obtained from the solution of equation (29) via:

$$g = \left\{\gamma \frac{\partial b}{\partial y}\right\}_s \Big/ B \tag{34a}$$

2.5. *Some solutions or calculation procedures for* g

Solution for the flat plate in laminar flow. As an example, Fig. 2 presents a plot, based on the exact boundary-layer solutions of Mickley *et al.* [32], of $(gx/\gamma)/\sqrt{(G_e x/\mu)}$ vs. B for the flat plate in a laminar stream. The transport properties μ and γ are supposed uniform; x is the distance from the leading edge at which g prevails, and G_e is the uniform mass velocity of the stream. Each curve is valid for a particular μ/γ (Prandtl or Schmidt number).

Exact solutions are not available for very high or very low values of μ/γ. However, for high

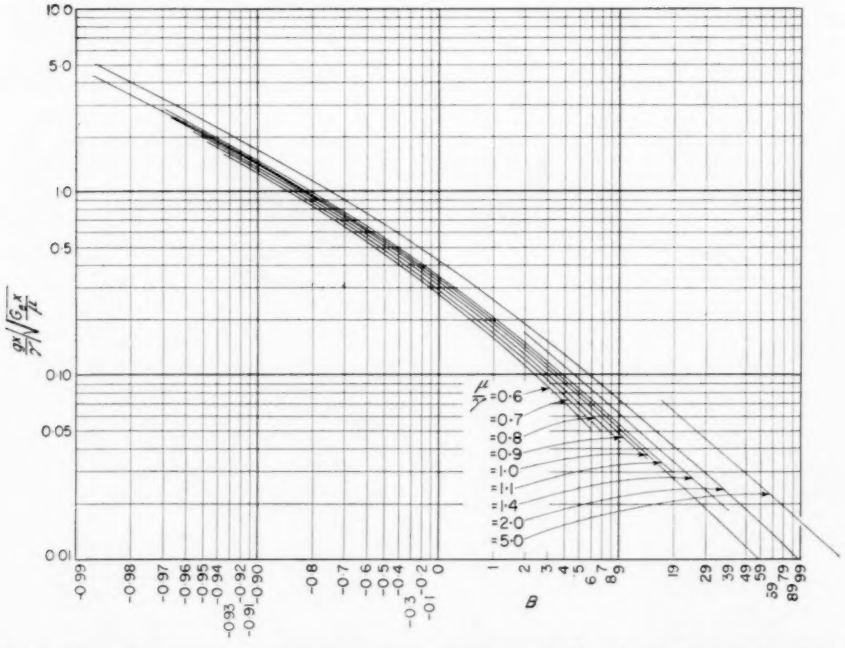

FIG. 2. Exact solutions of the boundary-layer equations for the flat plate in laminar flow [32].

values with B lying between $-0{\cdot}5$ and $+1{\cdot}0$, the asymptotic solution of Merk [33] can be used for the ordinate of Fig. 2: it is

$$0{\cdot}3387\,(\mu/\gamma)^{1/3}/(1 + 0{\cdot}566\,B).$$

Other solutions for laminar boundary-layer flows. Surprisingly, only a handful of exact solutions of the laminar boundary-layer equations are available for other cases than the flat plate. Spalding and Smith [41] have recommended that mass transfer through two-dimensional or axi-symmetrical laminar boundary layers in general should be calculated from an approximate quadrature formula which, in the present terms, runs:

$$g = K(\gamma/\mu^{1/2})\left(R^2 G_e^F / \int_0^x R^2 G_e^{F-1}\,dx\right)^{1/2} \quad (36)$$

where x is the stream-wise distance from the location at which mass transfer begins;

R is the distance of the section in question from the axis of symmetry (N.B. the R's disappear for a two-dimensional flow);

G_e is the mass velocity at the outer "edge" of the boundary layer at location x;

g is the surface conductance, defined by (34), valid for location x;

K is a function of B and μ/γ (in fact it is equal to the ordinate of Fig. 2);

F is a function of B and μ/γ.

Interpolating in exact solutions tabulated by Livingood and Donoughe [35], Spalding and Smith have deduced some values of K and F valid for $\mu/\gamma = 0{\cdot}7$; these values are contained in Table 1. At other values of μ/γ, K may be obtained from Fig. 2; F tends to 3·8 for all B at high μ/γ.

Table 1

B	0	0·5	1·0	2·0	3·0	4·0	5·0
K	0·292	0·213	0·169	0·120	0·0930	0·0770	0·0670
F	2·68	3·07	3·43	3·73	4·04	4·36	4·43

There is a great need for extended tables of K and F, covering both positive and negative B values and a wide range of μ/γ. Thereafter the influence of variable μ and γ needs to be thoroughly investigated; only a few isolated studies of this effect have been made so far. Efforts to fill these gaps are being made in the writer's laboratory.

Calculation method for mass transfer through turbulent boundary layers. Still fewer studies have been made of mass transfer through turbulent boundary layers. A quadrature formula which is simple, and probably fairly reliable, can be derived by extending the method of Ambrok [36] to mass transfer; one obtains for $\mu/\gamma = 0{\cdot}7$

$$\frac{g}{G_e} = 0{\cdot}0365\left[\frac{\ln(1+B)}{B}\right]\left[\frac{\mu R^{5/4}}{\int_0^x R^{5/4} G_e\,dx}\right]^{1/5} \quad (37)$$

Once again there is a great need for experimental and theoretical research in this field; important contributions are being made by Mickley and co-workers [32, 37], and by Rubesin and co-workers [38, 39].

Other methods. Of course the value of g need not be obtained by theoretical analysis at all: it may be obtained from experiment. The book of Sherwood and Pigford [31] contains many such experimentally derived values, most of them obtained with B values close to zero, and with almost uniform transport properties (but see "remarks on notation" above). The value of g may also be obtained by way of the Reynolds analogy; it is equal to the shear stress divided by the stream velocity. This value is of course usually only approximate, as is well known.

2.6. *General procedure for calculating mass transfer rates*

The practical importance of the way in which the mass transfer problem has been formulated above will now be summarized:

(a) The influences of the shape of mass transfer surface, the fluid velocity, the transport properties, etc., may be determined by aerodynamic analysis; this results in graphs or formulae of the type just presented. These graphs or formulae are independent of the

nature of the transfer process, i.e. they hold whether the process comprises vaporization, combustion, transpiration-cooling, distillation or any other process.

(b) The influences of the particular process are expressed through the value of the driving force B, defined by equation (33). B depends only on conditions in the G- (main stream), S- and T-states, and not on the aerodynamics. Examples of the evaluation of B are given below.

(c) With B obtained from the thermodynamic analysis of (b) and g obtained from the aerodynamic analysis of (a), the required mass transfer rate is obtained from equation (34).

(d) Separation of the aerodynamic and thermodynamic aspects is unfortunately not quite complete, a connexion is effected when the variation of the transport properties μ and γ with temperature, etc., is appreciable. This difficulty can be partially overcome by judicious use of "average" values of the transport properties.

3. SOME DRIVING-FORCE EXPRESSIONS

In this section we show how the analysis of Sections 2.1, 2.2 and 2.3 can be used to enable the numerical value of the driving force B to be determined in various particular cases. The list of driving-force expressions is not exhaustive, but should suffice as an illustration of the method. For concreteness, the "simple reaction" is discussed in terms of combustion; the analysis is of course equally applicable to a liquid-phase reaction, such as that between ammonia and sulphuric acid solutions.

In the interests of brevity, the practical implications of the driving-force expressions are not discussed.

3.1. *Transfer of an inert chemical substance*

No simplifying assumptions are needed to convert equations (1) and (9) to the standard form of (29) and (30). We can therefore write the driving-force expression for this case, without restriction, as:

$$B = \frac{m_{i,G} - m_{i,S}}{m_{i,S} - m_{i,T}} \tag{38}$$

In this general form the driving force may be used when many substances are transferred simultaneously, as in rectification of a multi-component mixture, and irrespective of whether some of the other (non-i) components are reacting chemically. Often $m_{i,T}$ must be determined by simultaneous consideration of transfer on the liquid and gas sides of the phase boundary.

Special cases. When i is the *only* mixture component transferred (e.g. $i \equiv H_2O$ when steam condenses from a steam–air mixture), we have:

$$m_{i,T} = 1 \tag{39}$$

then

$$B = \frac{m_{i,G} - m_{i,S}}{m_{i,S} - 1} \tag{40}$$

This expression is also valid in many drying, absorption and stripping problems. Clearly, since $m_i \leqslant 1$, B and $\dot{m}''$ are positive when $m_{i,G} \leqslant m_{i,S}$.

When i is not transferred at all, for example $i \equiv$ air in a drying process, we have:

$$B = \frac{m_{i,G} - m_{i,S}}{m_{i,S}} \tag{41}$$

3.2. *Transfer of a chemical element; simplifying assumption* (i)

For this case we have, as the driving-force expression:

$$B = \frac{n_{a,G} - n_{a,S}}{n_{a,S} - n_{a,T}} \tag{42}$$

This expression is useful when several chemical reactions take place, as for example in the gas producer. If it is further permissible to assume $\gamma_\alpha = \gamma_\beta$, any linear combination of n_α and n_β can be used as the conserved property. This fact can be used to derive B-expressions which are easy to evaluate (see [10] for a gas-producer example).

If, further, all γ_a's are equal and only two streams of substance enter the mixing field (e.g. main stream and transferred substance) it is meaningful to define a quantity f as mass of material from one of the streams per unit mass of mixture, irrespective of the state of chemical aggregation. Since f is a linear combination of the n_a's, we can write the driving force as:

$$B = \frac{f_G - f_S}{f_S - f_T} \tag{43}$$

Vol. 1 1960

This step is one of the foundations of the graphical method of determining B using enthalpy–composition diagrams (see [11, 12, 13, 34] for examples). The first use of such diagrams for transfer calculations was made by Busemann [15] in a pioneer work that has been undeservedly neglected; an important series of contributions to their development has been made by Bosnjakovic [17–20].

3.3. *Enthalpy transfer; simplifying assumption* (ii)

For this case the relevant driving-force expression is:

$$B = \frac{h_G - h_S}{h_S - h_T} \tag{44}$$

This expression is the second foundation of the graphical method just referred to; it also is particularly useful when complex chemical reactions occur.

Special case. When the wall is impervious to mass transfer it is easy to show, by introducing (44) and letting B tend to zero, that equation (34) degenerates to:

$$\dot{q}''_L = g^* (h_G - h_S) \tag{45}$$

where $\dot{q}''_L$ is the heat flux away from the phase boundary (Fig. 2);

g^* is the value of g valid for $B = 0$.

This expression is useful when calculating heat transfer rates from dissociated gas mixtures, as has recently become widely recognized (see, for example [40]).

3.4. *Mass transfer with a simple chemical reaction*

Simplifying assumption (iii). Inspection of equation (16) shows that this time we have:

$$B = \frac{(m_{fu} - m_{ox}/r)_G - (m_{fu} - m_{ox}/r)_S}{(m_{fu} - m_{ox}/r)_S - (m_{fu} - m_{ox}/r)_T} \tag{46}$$

Special cases. (a) We consider the case in which one of the reactants, say fuel, is the only transferred substance. In this case it is usual for the main-stream value of the concentration of unburned fuel to be zero. Thus:

$$\left.\begin{aligned} m_{fu,T} &= 1 \\ m_{ox,T} &= 0 \\ m_{fu,G} &= 0 \end{aligned}\right\} \tag{47}$$

Inserting (47) in (46), we obtain:

$$B = \frac{-m_{ox,G}/r - (m_{fu} - m_{ox}/r)_S}{(m_{fu} - m_{ox}/r)_S - 1} \tag{48}$$

(b) If the surface fuel concentration is zero ($m_{fu,S} = 0$), equation (48) reduces to:

$$B = \frac{m_{ox,G}/r - m_{ox,S}/r}{1 + m_{ox,S}/r} \tag{49}$$

This expression is relevant to the combustion of a non-volatile fuel. If, further, the chemical reactivity of the fuel surface is such that $m_{ox,S}$ also equals zero, the driving-force expression of (49) takes up its maximum possible value, namely:

$$B = \frac{m_{ox,G}}{r} \tag{50}$$

Equation (49) is also relevant to the burning of gaseous fuels (transpiration-coolants) which are expelled at such low rates that chemical reaction takes place within the porous walls. (Of course the cooling effect of such a procedure would not be large!)

(c) If the surface oxygen concentration is zero, equation (48) reduces to:

$$B = \frac{m_{ox,G}/r + m_{fu,S}}{1 - m_{fu,S}} \tag{51}$$

This expression usually applies to volatile liquid fuels, and to gaseous fuels injected through the wall at a high rate. However, the expression is seldom useful for determining B; for the quantity $m_{fu,S}$ is not as a rule among the data of the problem.

(d) A special case of equation (46) arises in the combustion of steel. This may be regarded as a non-volatile fuel which also happens to have a mainly non-volatile oxide. The latter fact leads to an interesting expression for $P_{1,T}$; it is:

$$(m_{fu} - m_{ox}/r)_T = 1/\{n_{C,steel}(1 + r_{Fe})\} - r_{Fe} \tag{52}$$

where $n_{C,steel}$ is the mass of carbon per unit mass of steel;

r_{Fe} is the mass of oxidant (usually oxygen) combining with unit mass of iron.

The resulting driving-force expression is:

$$B = \frac{m_{ox,G} - m_{ox,S}}{(n_{Fe}\, r_{Fe} + n_{C,steel}\, r_C)\,(n_{C,steel}(1 + r_{Fe}) - r_{Fe}) + m_{ox,S}} \quad (53)$$

where r_C is the mass of oxidant combining with unit mass of carbon.

The expression on the right-hand side of equation (53) is usually negative and close to the minimum possible value of any B, namely -1 (because $m_{ox,S} \simeq 0$ and $n_{C,steel}$ is small). It is useful in analyses of the oxygen-cutting process of workshop practice. The process sometimes also occurs inadvertently in rocket motors!

3.5. *Mass transfer with a simple chemical reaction*

Simplifying assumptions (iv) *and* (v). Driving-force expressions may also be derived in terms of the conserved properties P_1 and P_2. They are useful if it is desired to *calculate* the product concentration at the surface, the mass transfer rate being given.

3.6. *Heat transfer without chemical reaction*

Simplifying assumption (vi). The driving force expression for this case is obtained most simply if the reference temperature for the fluid-phase enthalpy in equation (22) is taken as t_S. Equation (8) is simplified thereby, and because of the absence of chemical reaction, to:

$$h_T = -\dot{q}''_S/\dot{m}'' = -Q, \text{ say} \quad (54)$$

There results:

$$B = \frac{c(t_G - t_S)}{Q} \quad (55)$$

Special cases. (a) Equation (55) is useful in many vaporization, drying and condensation problems. It holds even when the specific heats are not uniform, provided that only small concentrations differences occur or that $\gamma = \Gamma$; then c is the specific heat of the mixture of mainstream composition. In *adiabatic vaporization*, $Q = h_{LS}$ where h_{LS} is the latent heat of vaporization of the liquid. So equation (55) reduces to:

$$B = \frac{c(t_G - t_S)}{h_{LS}} \quad (56)$$

(b) In transpiration-cooling by an inert gas, the quantity Q is given by:

$$Q = c_{cool}\,(t_S - t_0) \quad (57)$$

where c_{cool} is the constant pressure specific heat of the coolant;

t_0 is the coolant temperature in the reservoir from which it is supplied.

For this case, the driving-force expression becomes

$$B = \frac{c(t_G - t_S)}{c_{cool}\,(t_S - t_0)} \quad (58)$$

This shows that, with t_G, t_S and t_0 fixed, B is smaller (and, with it, the necessary coolant flow rate) the larger is the specific heat of the coolant.

3.7. *Thermal analysis of mass transfer with a simple chemical reaction*

Simplifying assumptions (vii) (viii) *and* (ix). Restricting consideration to the case in which the only transferred substance is one of the reactants, say fuel, and noting by reference to Fig. 3 that

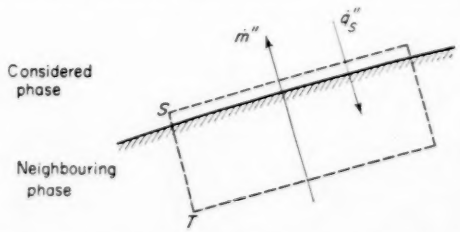

FIG. 3. Control volumes useful in deriving expressions for h_T when only one substance is transferred.

the definition (8) of the enthalpy of the T-state also implies:

$$h_T\,\dot{m}'' = \sum_j h_{j,L}\,\dot{m}''_{j,L} - \dot{q}''_L \quad (59)$$

we deduce:

$$h_T = h_{fu,L} - \dot{q}''_L/\dot{m}'' \quad (60)$$

This assumes that only fuel is present on the L-side of the phase boundary.

The driving-force expression resulting from the substitution of (24) and (60) in (33) is:

$$B = \frac{(m_{ox,G} - m_{ox,S})\,H/r + c(t_G - t_S)}{h_{LS} + \dot{q}''_L/\dot{m}''} \quad (61)$$

Vol. 1 1960

where h_{LS} is the enthalpy increase of the fuel in changing from the L- phase to the S- phase at constant temperature $t_L\ (= t_S)$.

Equation (61) is appropriate to simplifying assumption (viii).

If simplifying assumption (vii) holds, so that the enthalpy expressed by equation (23) is a conserved property, the driving force expression is found in a similar fashion to be:

$$B = \frac{(m_{\mathrm{fu},G} - m_{\mathrm{fu},S})\,H + c(t_G - t_S)}{m_{\mathrm{fu},S}\,H + h_{LS} + \dot{q}''_L/\dot{m}''} \tag{62}$$

A similar expression in terms of m_{prod} can be derived if simplifying assumption (ix) holds.

Special cases. (a) If the surface oxygen content is zero, as is usual for volatile liquid fuels and for burning transpiration-coolants (e.g. hydrogen gas) at high blowing rates, equation (61) reduces to:

$$B = \frac{m_{\mathrm{ox},G}\,H/r + c(t_G - t_S)}{h_{LS} + \dot{q}''_L/\dot{m}''} \tag{63}$$

This expression is often easy to evaluate.

In the case of transpiration-coolants, when radiant heat transfer is absent, we have:

$$\left.\begin{aligned} h_{LS} &= 0 \\ \dot{q}''_L/\dot{m}'' &= c_{\mathrm{cool}}\,(t_S - t_0) \end{aligned}\right\} \tag{64}$$

then

$$B = \frac{m_{\mathrm{ox},G}\,H/r + c(t_G - t_S)}{c_{\mathrm{cool}}\,(t_S - t_0)} \tag{65}$$

This should be contrasted with equation (58).

(b) If the surface fuel concentration is zero, as occurs with non-volatile fuels or (sometimes) with combustible transpiration-coolants injected at low rates, and if we can also assume that there is no free fuel in the main stream, equation (62) reduces to:

$$B = \frac{c(t_G - t_S)}{h_{LS} + \dot{q}''_L/\dot{m}''} \tag{66}$$

This expression is sometimes useful for calculating the surface temperature when the driving force B has been previously specified.

(c) If a radiant heat flux is present at the surface, this should clearly be added to $\dot{q}''_L$ with appropriate sign.

3.8. *Other forms of driving force*

Many other expressions can be derived for the driving force for mass transfer in terms of mixture properties in the G-, S- and T-states. In a particular flow, many of them are valid simultaneously. Where there is a choice, that form of B is to be preferred which is most easily evaluated by reference to known quantities; for example, in determining the mass flow-rate of transpiration-coolant which is necessary to maintain a given surface temperature, the B-expression of (65) is usually preferable to that of (51), since $m_{\mathrm{fu},S}$ is not known.

4. MORE COMPLEX PROBLEMS

The analysis presented in Sections 2 and 3 suffices for the calculation of the mass transfer rate, $\dot{m}''$, if sufficient data are available concerning the properties of the G-, S- and T-states. However, the data concerning the latter two states are often only given indirectly. Here we merely list the considerations which must be invoked when these more complex situations are encountered.

(a) *Thermodynamic equilibrium at the surface*

In many cases, e.g. vaporization, it is permissible to assume that the S-state mixture is in equilibrium with the adjacent phase (L-state). This assumption provides a link between the surface temperature $t_S\ (= t_L)$ and some of the S-state compositions, e.g. $m_{\mathrm{H_2O},S}$, in a water-vaporization problem. The problem can then be solved by simultaneous use of a B-expression based on mass conservation and the B-expression based on the first law of thermodynamics. Enthalpy-composition diagrams are helpful in the solution [11].

(b) *Simultaneous consideration of two phases*

Often the data are given in terms of conductances on both sides of a phase boundary; these may involve both mass and heat transfer conductances. Then, using the equality for the two phases of the mass transfer rate and of the T-state (unless surface radiation is present), simultaneous solution of the Ohm's law relation for the two phases permits the determination of $\dot{m}''$.

(c) *Reaction-kinetic considerations*

Sometimes chemical reaction rates are insufficiently rapid for thermodynamic equilibrium to prevail. In the case of heterogeneous reactions, a reaction-kinetic relation between $\dot{m}''$ and the S-state must be invoked; this sometimes results in a non-uniform S-state, necessitating a return to equations (26) and (27) instead of (29) and (30). In the case of homogeneous reactions at least one equation of the type of equation (2) must be solved.

5. CONCLUSIONS

(a) A standard formulation for the steady convective mass transfer problem has been presented which is capable of accommodating the problems arising in chemical engineering, aeronautical engineering, air-conditioning practice, etc.

(b) The centre-piece of this formulation is the Ohm's law relation, equation (34).

(c) The formulation achieves a separation between aerodynamic factors, incorporated in the conductance g, and thermodynamic factors, incorporated in the driving force B. The separation is only rendered incomplete by non-uniformity of transport properties in the boundary layer.

(d) The formulation is valid when chemical reaction occurs provided that certain restrictions are placed on the relations between the transport properties.

(e) There is still a great need for standard solutions of the boundary layer equations in the presence of mass transfer.

REFERENCES

1. S. HATTA, *Tech. Rep. Tohoku Imp. Univ.* **8**, 1 (1928–1929); **10**, 119 (1932).
2. T. K. SHERWOOD, *Absorption and Extraction* (1st Ed.). McGraw-Hill, New York (1937).
3. W. NUSSELT, *Z. ver. dtsch. Ing.* **60**, 102 (1916).
4. S. P. BURKE and T. E. W. SCHUMANN, *Proceedings of the Third International Conference on Bituminous Coal* Vol. 2, p. 485 (1931).
5. E. R. G. ECKERT and V. LIEBLEIN, *Forsch. Ing. Wes.* **16**, 33 (1949).
6. D. B. SPALDING, *Fourth Symposium on Combustion* p. 847. Williams and Wilkins, Baltimore (1953).
7. D. B. SPALDING, *Proc. Roy. Soc.* A. **221**, 78 and 100 (1954).
8. H. W. EMMONS, *Z. angew. Math. Mech.* **36**, 60 (1956).
9. D. B. SPALDING, *Proc. Inst. Mech. Engrs.* **168**, 545 (1954).
10. D. B. SPALDING, *Some Fundamentals of Combustion.* Butterworths, London (1955).
12. D. B. SPALDING, Part I. *Chem. Engng. Sci.* **11**, 183–193 (1959); Part II. *Chem. Engng. Sci.* **11**, 225–241 (1959).
11. D. B. SPALDING, *Proc. Inst. Mech. Engrs.* **172**, No. 28 (1958).
13. D. B. SPALDING and R. D. TYLER, in *Conference on Thermodynamic and Transport Properties of Fluids* Session 4, Paper 1. Institute of Mechanical Engineers, London (1957).
14. H. J. MERK, *Appl. Sci. Res.* A. **8**, 73 (1959).
15. A. BUSEMANN, *Der Wärme- und Stoffaustausch.* Julius Springer, Berlin (1933).
16. F. BOSNJAKOVIC, *Technische Thermodynamik.* Steinkopf, Dresden (1937).
17. F. BOSNJAKOVIC, *Wärmediagramme für Vergasung, Verbrennung und Russbildung.* Julius Springer, Berlin (1956).
18. F. BOSNJAKOVIC, *Chem.- Ing.- Techn.* **29**, 187 (1957).
19. F. BOSNJAKOVIC, *Kältetechnik* **9**, 266; **10**, 309 (1957).
20. F. BOSNJAKOVIC, *Kyltekn. Tidskr.* No. 3, 142 (1957).
21. Y. B. ZELDOVICH, and D. A. FRANK-KAMENETSKY, *J. Phys. Chem., Moscow* **12**, 100 (1938).
22. V. A. SHWAB, *Relation between the Temperature and Velocity Fields of the Flame of a Gas Burner.* Gos. Energ. izd., Moscow and Leningrad (1948); cited by Y. B. ZELDOVICH, *Zh. tekh. fiz.* **19**, 1199 (1949); translated as NACA TM 1296 (1951).
23. G. A. VARSHAVSKII (1945), Burning of liquid fuel drop (diffusion theory), cited by AGAFANOVA *et. al.* [25].
24. M. GOLDSMITH and S. S. PENNER, *J. Amer. Rocket Soc.* **24**, 245 (1954).
25. F. A. AGAFANOVA, M. A. GUREVICH and I. I. PALEEV, *Sov. Phys. Tech. Phys.* **2**, 1689 (1958).
26. K. P. COFFIN and R. S. BROKAW, *A General System for Calculating Burning Rates of Particles and Drops and Comparison of Calculated Rates for Carbon, Boron, Magnesium and Iso-octane.* NACA TN 3929 (1957).
27. L. LEES, Convective heat transfer with mass addition and chemical reactions, in *Combustion and Propulsion* p. 451. Third AGARD Colloquim, Pergamon Press, London (1958).
28. G. W. SUTTON, *Seventh Symposium on Combustion* p. 539. Butterworths, London (1959).
29. J. P. HARTNETT and E. R. G. ECKERT, *Mass Transfer Cooling with Combustion in a Laminar Boundary Layer.* Heat Transfer and Fluid Mechanics Institute, Stanford University Press, California (1958).
30. R. BROMBERG and R. P. LIPKIS, *Jet Propulsion* **28**, 659 and 668 (1958).
31. T. K. SHERWOOD and R. L. PIGFORD, *Absorption and Extraction* (2nd Ed.). McGraw-Hill, New York (1952).
32. H. S. MICKLEY, R. C. ROSS, A. L. SQUYERS and W. E. STEWART, *Heat, Mass and Momentum Transfer for Flow over a Flat Plate with Blowing or Suction.* NACA TN 3208 (1954).

Vol. 1 1960

33. H. J. MERK, *Appl. Sci. Res.* A **8**, 237 (1959).
34. D. B. SPALDING, *J. Amer. Rocket Soc.* **29**, 666 (1959).
35. J. N. B. LIVINGOOD and P. L. DONOUGHE, *Summary of Laminar Boundary Layer Solutions for Wedge-type Flow over Convection and Transpiration-cooled Surfaces*. NACA TN 3588 (1955).
36. G. S. AMBROK, *Sov. Phys. Tech. Phys.* **2**, 1979 (1957).
37. H. S. MICKLEY and R. S. DAVIS, *Momentum Transfer for Flow over a Flat Plate with Blowing*. NACA TN 4017 (1957).
38. M. W. RUBESIN, *An Analytical Estimation of the Effect of Transpiration Cooling on the Heat-transfer and Skin-friction Characteristics of a Compressible Turbulent Boundary Layer*. NACA TN 3341 (1954).
39. M. W. RUBESIN and C. C. PAPPAS, *An Analysis of the Turbulent Boundary-layer Characteristics on a Flat Plate with Distributed Light-gas Injection*. NACA TN 4149 (1958).
40. J. A. FAY and F. R. RIDDELL, *J. Aero. Space Sci.* **25**, 73 (1958).
41. D. B. SPALDING and A. G. SMITH, *Brennst.-Wärmekr.* **10**, 271 (1958).

APPENDIX

The Energy Equation Including Kinetic Energy and Shear Work

A more complete form of equation (4) is

$$\mathbf{G}.(\nabla h^0) - \nabla\{\Sigma_j \gamma_j h_j (\nabla m_j)\} - \nabla.\{\Gamma c (\nabla t)\} - \\ - \nabla\left\{\frac{\mu}{g_0 J}\left[\nabla(V^2/2) - \frac{V^2}{R_S}\cdot\frac{\mathbf{R}_S}{R_S}\right]\right\} = 0 \quad \text{(A.1)}$$

where

h^0 = stagnation enthalpy of fluid mixture
$= h + V^2/2g_0J$ (B.t.u./lb);

V = velocity of fluid mixture defined as G/ρ (ft/hr);

μ = viscosity of fluid mixture (lb/ft hr);

g_0 = constant in Newton's Second Law of motion,
$= 4{\cdot}1 \times 10^8$ (lb ft/Lb hr^2);

J = mechanical equivalent of heat
$= 778$ (ft Lb/B.t.u.);

$\mathbf{R}_S$ = vectorial radius of curvature of local stream line;

R_S = scalar magnitude of $\mathbf{R}_S$ (ft).

Equation (A.1) simplifies in the same manner as equation (4) provided that $\gamma_j = \Gamma$ for all j and further that (a) we also have $\Gamma = \mu$ (Prandtl number $= 1$), and that (b) the radius of curvature of the steamlines R_S is large. The resulting simplified equation is:

$$\mathbf{G}.(\nabla h^0) - \nabla\{\Gamma(\nabla h^0)\} = 0 \quad \text{(A.2)}$$

This equation has the standard form. It differs from equation (14) only in that h^0 replaces h.

The wall-flux boundary conditions for equations (A.1) and (A.2) are identical with those for equations (4) and (14); for the fluid kinetic energy is negligible at the wall, so that h and h^0 are identical. It follows that the stagnation enthalpy h^0 is a "conserved property of the second class"; it may therefore be used for the derivation of a driving-force expression.

The simplification of the energy equation which results when $Pr = 1$ is of course well known, being usually attributed to Crocco. The present proof appears to be rather simpler and more general than those usually given.

Int. J. Heat Mass Transfer. Vol. 1, pp. 208–218. Pergamon Press 1960. Printed in Great Britain.

THE STEADY AND TRANSIENT FREE CONVECTION BOUNDARY LAYER ON A UNIFORMLY HEATED VERTICAL PLATE

R. J. GOLDSTEIN* and E. R. G. ECKERT†
Heat Transfer Laboratory, University of Minnesota, Minneapolis

(*Received* 3 *July* 1959)

Abstract—A Zehnder–Mach interferometer was used to study the free convection thermal boundary layer about a uniformly heated vertical plate and to derive the heat transfer coefficients connected with this situation. The experiments were performed when the plate was immersed in water and the steady state boundary layer, as well as its transient development from an initial state at rest and with uniform temperature to steady state condition, was investigated when a step function in the power input to the plate was applied. Results for the steady state runs agree very well with the results of an analysis by Sparrow and Gregg. The transient runs indicate that the temperature field in the fluid develops initially in the same way as for heat conduction into a semi-infinite solid. After a short transition period, the steady state condition is reached. The boundary layer grows with time in such a way that it increases at first with increasing time, reaches a maximum, and decreases again until it settles to its steady state value. The wall temperature and the local heat transfer coefficient can be predicted for the whole period from start to steady state by the solution for one-dimensional unsteady conduction or for the steady state boundary layer.

Résumé—Un interféromètre de Zehnder–Mach a été utilisé pour étudier la couche limite thermique de convection libre sur une plaque verticale uniformément chauffé et pour déterminer les coefficients de transmission de chaleur relatifs à cette disposition. Dans ces expériences, la plaque était immergée dans l'eau et la couche limite en régime permanent, ainsi que son développement transitoire à partir d'un état de repos initial et d'une température constante, a été étudiée quand on applique à la plaque une augmentation échelon de la puissance de chauffage.

Les résultats pour le régime permanent concordent très bien avec ceux d'une étude de Sparrow et Gregg. En régime transitoire, le champ de température évolue de la même façon que la conduction dans un solide semi-infini. Après une courte période de transition la condition du régime permanent est atteinte. La couche limite évolue avec le temps de façon à s'épaissir dans les premiers instants, elle atteint ensuite un maximum, puis décroit jusqu'à sa valeur du régime permanent. La température de paroi et le coefficient local de transfert de chaleur peuvent être calculés, pour la période allant du départ de l'expérience jusqu'au régime permanent, en utilisant la solution de la conduction non permenente unidimensionnelle ou de la couche limite permanente.

Zusammenfassung—Mit Hilfe eines Zehnder–Mach-Interferometers wurde die thermische Grenzschicht bei freier Konvektion an einer gleichförmig geheizten senkrechten Platte untersucht und daraus die Wärmeübergangskoeffizienten abgeleitet. Die Platte war bei den Versuchen in Wasser getaucht. Die stationäre Grenzschicht und ihre Entwicklung aus einem Anfangszustand in Ruhe mit gleichförmiger Temperatur zum stationären Zustand wurden bei schrittweiser Änderung der Heizleistung der Platte untersucht. Die Ergebnisse der stationären Versuche stimmen gut mit den Rechenergebnissen von Sparrow und Gregg überein. Die nichtstationären Versuche zeigen, daß sich das Temperaturfeld in der Flüssigkeit anfänglich wie bei der Wärmeleitung in einen halb-unendlichen Körper entwickelt. Nach einer kurzen Übergangsperiode wird der stationäre Zustand erreicht. Die Grenzschichtdicke steigt anfänglich mit der Zeit an und fällt nach Erreichen eines Maximums auf ihren stationären Wert ab. Die Wandtemperatur und die örtlichen Wärmeübergangskoeffizienten können für die ganze Periode vom Start bis zum stationären Zustand durch die Lösungen für die eindimensionale nicht-stationäre Wärmeleitung oder für die stationäre Grenzschicht vorausgesagt werden.

* Assistant Professor, Brown University. † Professor, University of Minnesota.

Vol. 1 1960

Abstact—Для изучения теплового пограничного слоя на равномерно нагретой вертикальной плите в условиях свободной конвекции и для получения соответствующих коэффициентов переноса тепла использовался интерферометр Маха-Цендера. Были проведены опыты с погружённой в воду плитой и исследован пограничный слой как установившийся, так и в переходном режиме от начального состояния покоя и одинаковой температуры к стационарному состоянию при ступенчатом подводе энергии к плите. Результаты для установившихся потоков хорошо согласуются с результатами анализа Грегга и Спэрроу. Неустановившиеся потоки означают, что температурное поле в жидкости (газе) развивается так же, как и в теплопроводящем полуограниченном твердом теле. После короткого переходного периода достигается установившееся состояние. Пограничный слой изменяется со временем следующим образом: сперва он растёт, достигает максимума и уменьшается до тех пор пока не достигает величины, отвечающей установившемуся состоянию. Температура стенки и локальный коэффициент теплообмена могут быть получены для всего периода, от начала до установившегося состояния, с помощью решения для одномерной нестационарной теплопроводности или для установившегося пограничного слоя.

NOMENCLATURE

g = gravitational acceleration;
h = local heat transfer coefficient;
k = heat conductivity;
q = heat flow through plate surface per unit time and area;
x = distance from lower plate end;
y = distance from plate surface;
a = thermal diffusivity;
β = thermal expansion coefficient;
ϑ = difference between temperature in boundary layer and in bulk of fluid;
ϑ_w = difference between plate surface temperature and fluid bulk temperature;
τ = time;
ν = kinematic viscosity;
$Gr = \dfrac{g\beta\vartheta_w x^3}{\nu^2}$ Grashof number;
$Nu = \dfrac{h\,x}{k}$ Nusselt number;
$Pr = \dfrac{\nu}{a}$ Prandtl number.

INTRODUCTION

STUDIES of convective heat transfer were, in the past, restricted almost exclusively to steady state conditions. This was justified because the heat capacity of boundary layers is generally so small that steady state relations describe heat transfer coefficients with sufficient accuracy even in situations where the temperatures at the surface and outside the boundary layer vary with time. Such a situation is commonly referred to as "quasi steady". Only recent developments in engineering have led to conditions under which temperatures vary so rapidly that convective heat transfer coefficients become significantly different from the steady values. As a consequence, analytical studies of unsteady boundary layers have been published in various magazines. Experimental information on unsteady boundary layers, however, is still very restricted.

Unsteady free convection boundary layers are of special interest since they are generally thicker and have, therefore, a larger heat capacity than boundary layers in forced flow. As a consequence, heat transfer coefficients differ from the steady state values already at relatively small rates of temperature variations with time. Such unsteady free convection boundary layers arise, for instance, in nuclear reactors when the pumps for the cooling system fail or with power fluctuations in reactors cooled by free convection.

The earliest analysis of a free convection unsteady boundary layer on a flat plate, infinite in extent, has been performed by Illingworth [1]. The temperature field in the boundary layer was found to be identical with the temperature field for unsteady one-dimensional heat conduction into a semi-infinite body. Sugawara and Michiyoshi [2] included in their analysis conditions near the leading edge of the plate. Their calculation mainly covers the very early stages of the boundary layer growth. Siegel [3] investigated analytically the boundary layer growth up to the time when steady state is obtained for the condition that the surface temperature or the surface heat flux changes in a step-wise fashion from

zero to a finite value. His results are of special interest in the present study and will be discussed in more detail later on.

Ostroumov [4] and Gillam *et al.* [5] performed experimental studies of transient free convection existing on a horizontal wire. The measurements were essentially restricted to a determination of the wire temperature and of the heat flux to the surrounding fluid as a function of time. Klei [6] performed similar experiments on a 0·0005 in. thick and 1 in. high platinum foil which was suddenly heated by an electric current. McLean *et al.* [7] made a study on a horizontal nichrome foil in a water tank, using a Zehnder–Mach interferometer. In this last study interest was restricted to the early stages of the boundary layer development.

The present paper describes an experimental investigation of an unsteady free convection boundary layer on a vertical flat plate under the condition that the heat flux at the surface is locally constant and changes in a step-wise fashion with time. Complete information on the temperature field in the boundary layer as a function of time has been obtained by use of a Zehnder–Mach interferometer and the study includes the whole range from the beginning of the boundary layer development to the steady state condition. The experiments were originally carried out in air. It was found, however, that the above boundary conditions could be obtained in a much cleaner way by a study in water, and the results reported in this paper will be restricted to this fluid. The fact that the change in optical refraction coefficient of water with temperature is much larger than that of air made it necessary to carry out the experiments with very small temperature differences. This, however, turned out to be an advantage, because the results of these experiments can well be compared with analytical results which have all been obtained for a fluid of constant properties. The study of free convection in water makes it also possible to investigate heat transfer to a fluid with internal heat sources. The internal heat generation can easily be obtained when the water is made slightly conducting and when an electric current is directed through it. A brief study of this kind was reported by Goldstein [8].

EXPERIMENTAL EQUIPMENT AND INSTRUMENTATION

The main requirement for the heated vertical plate is that it has a heat capacity which is as small as possible so that it can follow time-wise variations of temperature readily. For this purpose a 0·001 in. thick foil of 302 stainless steel was used. The foil was stretched tightly between two horizontal straight edges by six screws on each end of the foil. This can be recognized in Fig. 1. Two horizontal straight edges *a* are fastened to an aluminum plate *b* and this plate in turn is connected through the rods *c* and a bridge *d* shown in the figure with the frame of the interferometer. The vertical part of the foil *e* between the two edges which represents the heated vertical plate has a dimension of 4·01 in. in horizontal and 6·503 in. in vertical direction.

The foil was heated by passing an electric current through it. For this purpose, two strips *f* of copper, 0·005 in. thick, were soldered to the upper and lower end of the foil. The strip at the lower end was moved as closely as possible to the location of the straight edge so that the heated part of the foil started very close to the point where it bent into the vertical direction. The copper strips in turn were connected by heavy conducting cables to three storage batteries connected in parallel. A bank of resistors in series with the foil allowed adjustments in the internal heat generation in the foil. A precision shunt and a calibrated millivoltmeter (Weston Model 1) measured the current and a similar millivoltmeter measured the potential drop in the foil. A hand-operated switch turned the current on and off. The uniformity of the heated foil was checked by a super-micrometer and by weighing small pieces cut out of the sheet. No variations greater than 1 per cent in local thickness and weight were found. The electric resistance of the sheet was 0·0431 Ω. The uniformity of the foil guaranteed a locally uniform heat generation by the electric current.

The heated vertical plate was put into a prismatic water tank as shown in Fig. 2. The tank *a* had the dimensions 12 × 14½ in. in a horizontal plane and a height of 24 in. The most important elements of the tank were the two windows which were required in order to pass the light

Vol. 1 1960

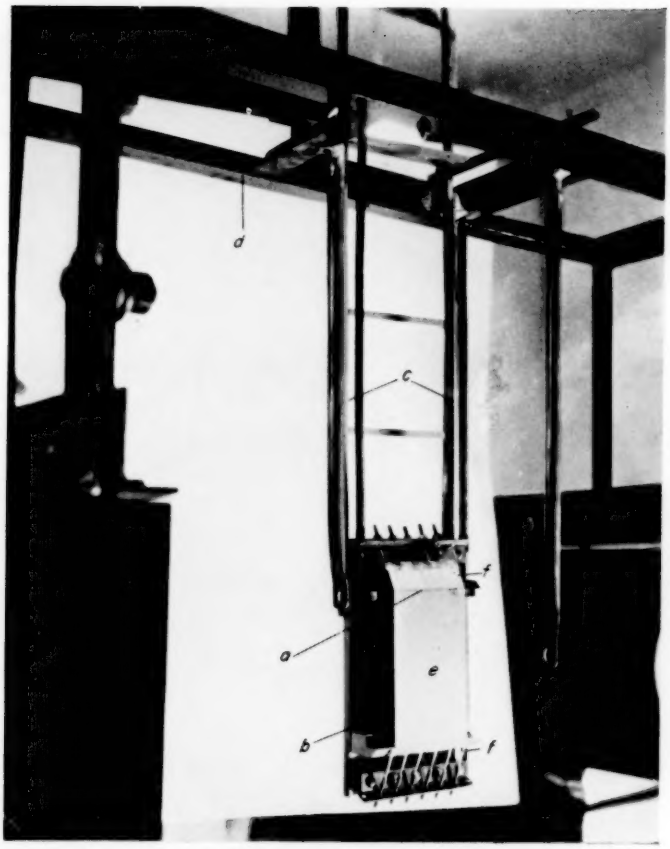

FIG. 1. Heated sheet and holder: *a*, horizontal straight edges; *b*, aluminum plate; *c*, connecting rods; *d*, bridge construction; *e*, heated foil; *f*, copper strips.

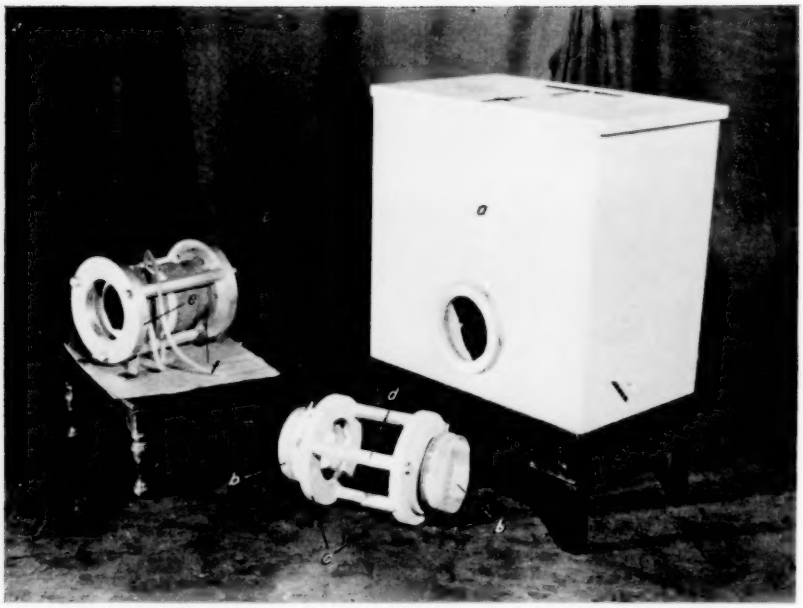

FIG. 2. Water tank, compensating tank, and window support frame for main tank: *a*, main water tank; *b*, glass windows; *c*, aluminum rings; *d*, aluminum rods; *e*, compensating tank; *f*, rubber inner tube.

Vol. 1 1960

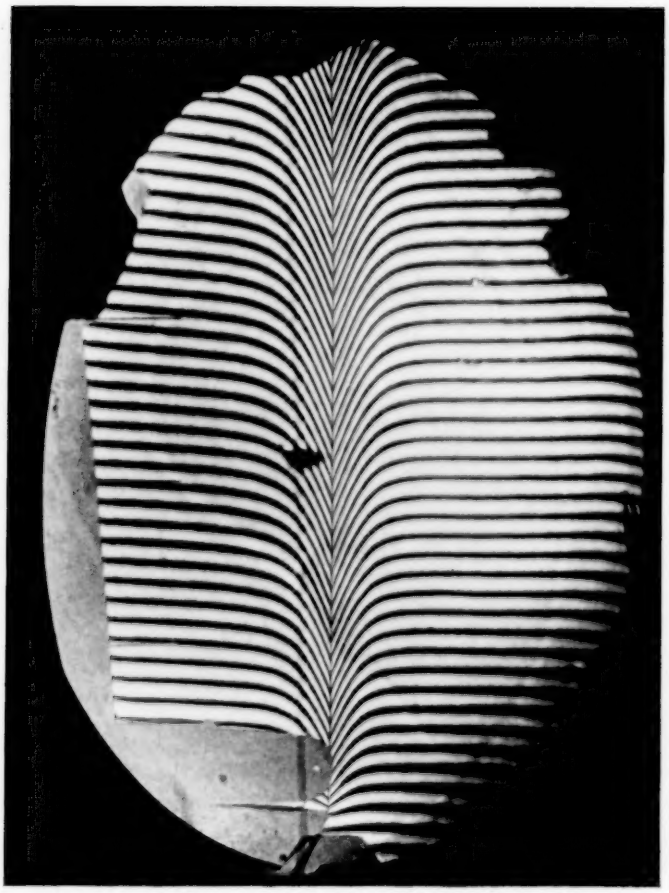

FIG. 3. Interferogram of heated foil with boundary layers.

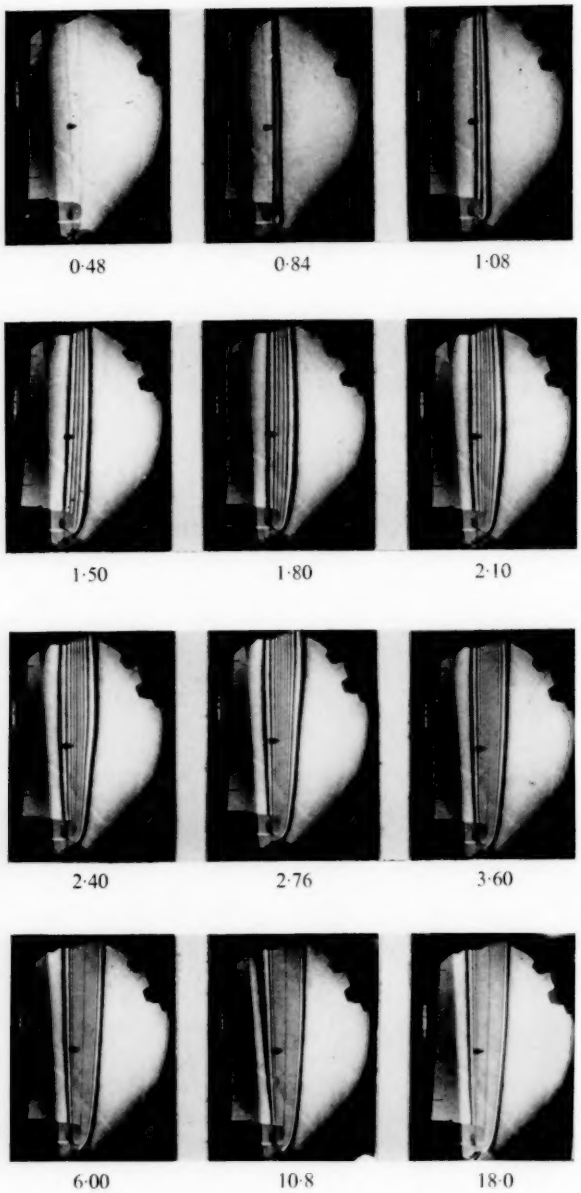

FIG. 8. Interferograms of the unsteady free convection boundary layer. The numbers under the photos give the time from the start of the heat pulse in seconds.

Vol. 1 1960

beam of a Zehnder–Mach interferometer past the heated plate. The two windows *b* were made of plate glass, 1 in. thick and 6 in. in diameter, and polished so that each surface was flat to one-fourth wavelength. Each plate was checked individually for the absence of schlieren by placing it into the light beam of the interferometer. The two windows were held 8 in. apart in a special frame which can be recognized in Fig. 2 arranged in front of the tank. The glass plates were fastened between two aluminum rings *c* and these in turn were held in the proper distance by three hexagonal aluminum rods *d* with screws at both ends. This frame was attached by the three vertical rods *g*, which can be seen in Fig. 1, to the interferometer frame. The space between the aluminum disks which held the windows and the walls of the tank was sealed off by two pieces cut from a rubber inner tube. The design of the window frame was made in this way to enable the experimenter to adjust the two windows so that they are parallel to each other and normal to the light beam direction and also to connect them rigidly with the interferometer.

The tank was filled with distilled water and this filling was replaced several times during the experiments. A platinum resistance thermometer and a Mueller bridge were used to determine the bulk water temperature in the tank. This thermometer was calibrated with a second resistance thermometer whose calibration had been obtained from the National Bureau of Standards.

The presence of the two glass windows and of the water in one of the light beams of the interferometer increases the optical path length of this beam. A compensating tank *e* was therefore arranged in the second light beam. This tank was similar in design to the window frame in the main tank. It is shown on the left-hand side in Fig. 2. A piece of rubber inner tube *f* connected the aluminum rings which held the glass windows. The interior of the tube was filled with distilled water. The windows themselves were of the same optical quality as the ones in the main tank.

A Zehnder–Mach interferometer was the main tool in these experiments. This instrument was constructed at the Heat Transfer Laboratory. It is very similar in design to one which had been built by Eckert *et al.* [9]. The basic system of the interferometer consists of four properly coated plates of optical glass with 6 in. diameter spaced at the corners of a rectangle with 55 and 27·5 in. side lengths. The opening of the interferometer in which the test equipment can be arranged is 40 in. in light beam direction. A detailed description of the interferometer and its operation is contained in [9] and will not be repeated here. The main difference in the instrument used in the present tests and the one described in the reference lies in the fact that in the Heat Transfer Laboratory Interferometer the optical path in one of the two beams can be changed by a lateral movement of one mirror. Fig. 3 shows an interferogram as it is obtained in the interferometer. This specific photo is from the initial series in which the experiments were carried out in air. Corresponding photos were obtained in the water runs; they are, however, less suitable for reproduction. It can be observed that the interferometer was, in the experiments, adjusted in such a way that horizontal fringes appear in the interferogram when the light beam travels through a field of locally uniform density. In the heated boundary layer, the fringes are bent in a downward direction. The image of the heated vertical foil can also be recognized. For the tests in water, the difference between the temperature of the heated foil and the bulk temperature of the fluid outside the boundary layer was kept to values below 3°F since considerably larger temperature differences caused the interference fringes to bend excessively and in this way to become indistinguishable. The small temperature difference made it necessary to keep the fluid bulk temperature very uniform and constant during the duration of an experiment. For this reason, the water tank was well insulated and the bulk temperature of the water was kept to a value close to room temperature. A maximum rate of change of the water temperature of 0·0005°C/min was allowed during the experiments. This results in a fringe shift of 0·1 fringe in 5 min. For the transient runs, a movie camera was mounted with its electric drive mechanism on the interferometer frame. An electric clock timer was arranged so that it appeared on the film simultaneously with the interferogram.

o

The evaluation procedure of the interference photos is described in detail in [8]. Two main errors have to be considered if a temperature field is determined by evaluation of an interferogram. A refraction error will arise as a consequence of the fact that the rays in the light beam are slightly bent from their original direction when the beam travels parallel to the plate surface through the boundary layer, because a transverse temperature gradient exists in the boundary layer. This error was calculated following the procedure described in [10] and was found to be less than $\frac{1}{2}$ per cent during all steady state runs. During the very early part of the transient runs when the boundary layer is very thin, the error can be considerably larger. This, however, is not the main time of interest. A second error is caused by the fact that the temperature field does not end abruptly in the two planes containing the two vertical ends of the plate and normal to it, but extends somewhat beyond the plate length.

For a thin plate within which uniform heat generation is taking place, there should be no first-order error in the average temperature gradient in the fluid at the plate surface due to end-effects. This follows from the effective integration of the temperature field by the light beam and from the fact that, with the present symmetry, all the heat must leave the plane of the plate. The validity of this reasoning is confirmed by the good agreement between the measured heat flux and the electrical power input. A calculation [8] similar to that of Eckert and Soehngen [11], indicated a small (approximately 1 per cent) positive error in the plate temperature due to end-effects. This holds for a plate whose temperature is uniform. With the actual system, the temperature at the edges tends to fall off slightly, compensating this error, and it was assumed that the results could be used directly. Confirmation of this comes from the good agreement with available analytical solutions.

The properties of water which are required for an evaluation of the interferograms and of the dimensionless parameters in which the test results are presented, have been taken from the literature. Values of the index of refraction for water are contained in a paper by Tilton and Taylor [12]. They were also checked in the following way: The water in the main tank was heated to various temperature levels and the shifts of the zero interference fringe corresponding to the step-wise temperature increases were recorded. The change of the index of refraction with temperature could then be readily calculated from the fringe shifts. Only this value is needed for the evaluation of the interferograms. The measured values agreed within ± 2 per cent with those taken from the literature.

In any temperature boundary layer, the problem arises at what reference temperature the properties should be inserted into the dimensionless parameters which describe the process. In the present experiments this question is relatively insignificant because of the small temperature differences existing within the boundary layer. A film temperature half-way between the wall and the fluid bulk temperature was used as reference temperature.

PRESENTATION AND DISCUSSION OF RESULTS

Two groups of experiments were performed. In the first one, the boundary layer characteristics and heat transfer were investigated for steady state condition. The second group dealt with the transient development of the free convection boundary layer.

Vol. 1 1960

Steady state studies

Figs. 4 to 7 present the results of the experiments for steady state. In Fig. 4, the heat flow q from the surface of the heated plate into the water per unit area and time is plotted over the distance x from the leading edge measured in

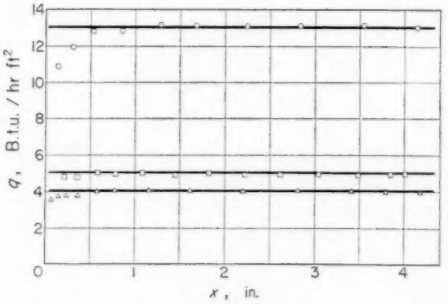

FIG. 4. Heat flow q from surface of heated plate by steady free convection as obtained from electric measurements and from interferogram.

vertical direction along the plate surface. Three runs are evaluated which differ by the amount of current passed through the plate. The horizontal lines indicate the electric power converted into heat per unit surface area. These values were obtained from the readings of the amperemeter and the voltmeter. The points in Fig. 4 have been obtained from the evaluation of the interferograms. The temperature gradient at the plate surface determined from the shift of the interference fringes was multiplied with the heat conductivity of water at the plate surface temperature. The agreement between heat generation in the plate and the heat flux through the plate surface is excellent except for a small region near the leading edge. Apart from this region the condition of a locally constant heat flux is therefore satisfactorily fulfilled.

Fig. 5 presents the temperature ϑ_w of the plate surface as measured above the bulk temperature of the water, again plotted over the distance x.

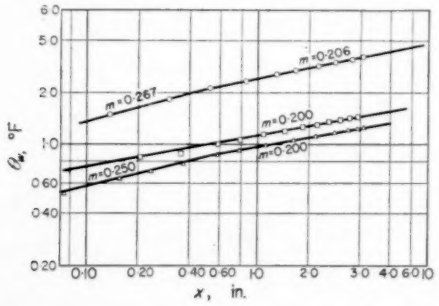

FIG. 5. Temperature variation along the height x of the heated plate for steady free convection. Three experiments with the heat fluxes indicated in Fig. 4 are presented in this and the following figure; ϑ_w = temperature difference between wall surface and fluid bulk; m = exponent expressing the temperature variation.

The temperature of the plate surface was again determined from the interferograms. In this connection it proved advantageous that two symmetrical boundary layers on both sides of the foil representing the plate could be observed. The temperature profiles obtained from the fringe shifts on both sides of the plate were extrapolated to the plate center line. The temperature indicated by the profile at a distance from the center line equal to half the plate thickness was then interpreted as the plate surface temperature. It may be observed in the figure that this plate temperature increases proportional to a power $m = 0{\cdot}200$ to $0{\cdot}206$ of the distance x when the region near the plate leading edge is excluded. This is in excellent agreement with the analysis by Sparrow and Gregg [13] which predicts that the surface temperature of a vertical plate in steady free convection flow increases proportionally to the one-fifth power of the distance x when a locally constant heat flux at the plate surface is prescribed. For the region near the leading edge, a constant heat flux would lead to very steep temperature gradients. Heat conduction in the plate along the direction x will tend to reduce these temperature differences and to decrease the temperatures as compared with those for constant heat flux. This conclusion agrees with the results presented in Fig. 5.

Fig. 6 presents the local Nusselt number Nu plotted over the parameter Grashof times Prandtl. The points are again the results obtained from the interferograms, the full line presents the results of the analysis [13]. The product $GrPr$ has been selected because the Nusselt number is almost a function of $GrPr$ only

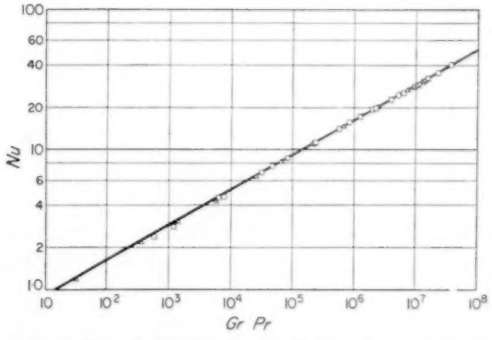

FIG. 6. Nusselt number for steady free convection as a function of the product Grashof times Prandtl number.

	q (B.t.u./hr ft²)	t_∞ (°F)
○	130·2	72·64
□	50·8	73·51
△	40·8	72·64

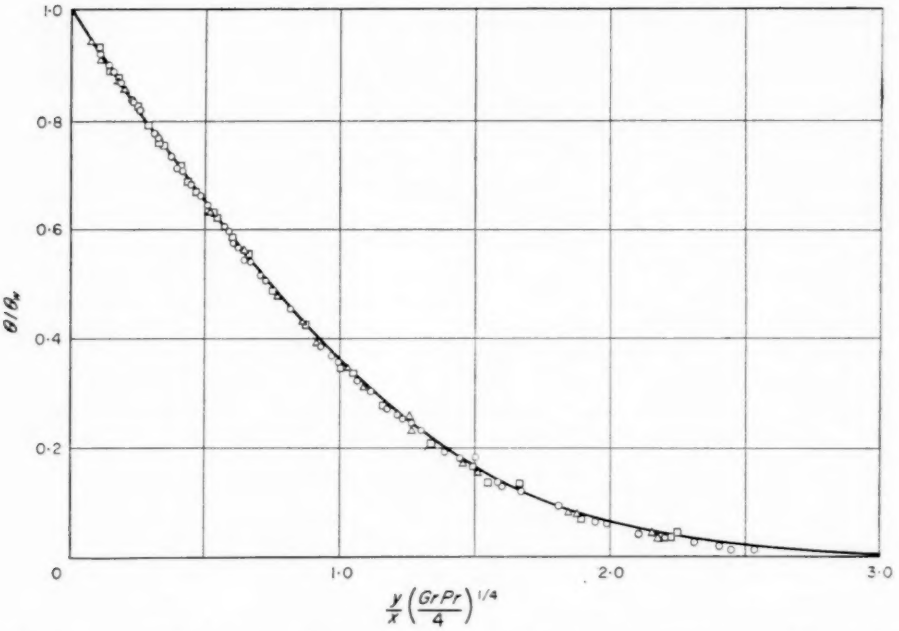

FIG. 7. Temperature profile in the steady free convection boundary layer. ϑ = temperature difference between a location at distance y from the plate and the fluid bulk. ϑ_w = temperature difference between the plate and the fluid bulk. x = distance from the lower end of the foil.

	q (B.t.u./hr ft²)	t_∞ (°F)
○	130·2	72·64
□	50·8	73·51
△	40·8	72·64

according to analysis. In this way small changes of the bulk temperature of the water which occurred between the individual tests are suppressed in the figure. It may be observed in Fig. 6 that the agreement between measured and analytical results is excellent. Using the experimental points for the distance x, for which the heat flow is locally constant, an average value of 0·513 with a standard deviation of $\frac{1}{2}$ per cent is obtained for the parameter $Nu/(GrPr)^{1/4}$. This compares with the value 0·5146 resulting from the analysis.

Fig. 7 shows the temperature profile within the boundary layer in a dimensionless presentation. The ratio of the local temperature ϑ within the boundary layer to the plate surface temperature ϑ_w, both measured above the fluid bulk temperature, is plotted over a dimensionless wall distance parameter as it has evolved from the analysis. The experimental points can be compared with the full line which represents the results of the analysis by Sparrow and Gregg for a Prandtl number 6·4.* It may be observed that the agreement between the calculated and measured temperature profiles is excellent.

Transient studies

Fig. 8 shows a series of interferograms obtained in the transient studies. These photos were taken

* The results for $Pr = 6{\cdot}4$ are not contained in [13]. They were calculated for us by the authors, which is gratefully acknowledged.

Vol. 1 1960

when the heated plate was surrounded by air. The adjustment of the interferometer was such that no interference lines could be observed in a field of constant temperature. The interference fringes within the heated boundary layer are then practically lines of constant temperature. The figures below the individual photos give the time from the start of the experiment. Similar photos have been obtained from the tests with water as the fluid surrounding the plate. These photos, however, are less suitable for reproduction.

Fig. 8 indicates that the thermal boundary layer grows at first with locally uniform thickness. In other words, the boundary layer thickness is originally independent of the location x. Later on the influence of the lower plate edge makes itself felt by the fact that the boundary layer stays thinner in the region near this edge. The position on the sheet up to which the boundary layer is a function of x moves gradually upward with increasing time.

These conclusions, obtained from an observation of the interferograms, are substantiated by the evaluations which are presented in the Figs. 9 through 12. Fig. 9 presents the heat flux q per unit surface area in unit time as a function of the time measured from the moment where the electric current is turned on. Two runs with different heating rates and four positions along the heated plate have been evaluated. The points are again obtained from the interferograms and the full line from the electric measurements. It may be observed from the figure that, a few seconds after the initiation of the heat generation, the heat flux from the surface of the plate is independent of time as well as of location.

Fig. 10 presents the surface temperature ϑ_w of the heated plate as a function of time for four locations x along the plate and for two different heating rates. The figure indicates clearly that for a considerable period the wall temperature is independent of location. After a short transition time it becomes independent of time, but is now dependent on the distance x. For the second period, therefore, steady state has been reached. The transition from the first to the second period is rather short and occurs at increasing times for increasing distance x.

Illingworth [1] has shown that the unsteady free convection temperature boundary layer in front of an infinite plate is described by the equation which represents unsteady one-dimensional heat conduction into a semi-infinite body. He considered a step in the wall temperature. For a step in the heat flux, the following equation describes, according to [14],

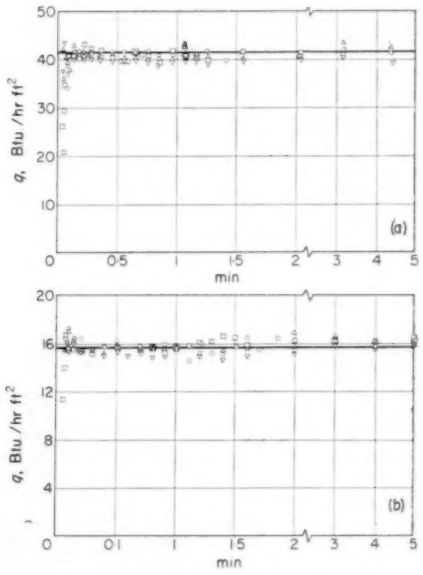

FIG. 9. Heat flux at the surface of the plate as a function of the time from the start of the heat pulse for two different heat fluxes.
$\triangledown x = 0{\cdot}32$ in. $\triangle$ 1·03 in. $\bigcirc$ 2·10 in. $\square$ 3·80 in.

the temperature field for unsteady heat conduction in a semi-infinite wall

$$\vartheta = q\frac{\sqrt{(a\tau)}}{k}\left\{\frac{2}{\sqrt{\pi}}\exp\left(\frac{-y^2}{4a\tau}\right) - \right.$$

$$\left. - \frac{y}{\sqrt{(a\tau)}}\operatorname{erfc}\frac{y}{2\sqrt{(a\tau)}}\right\} \quad (1)$$

The wall temperature is given by the relation

$$\vartheta_w = q\frac{2}{k}\sqrt{\left(\frac{a\tau}{\pi}\right)} \quad (2)$$

and the heat transfer coefficient by the equation

$$h = \frac{k}{2}\sqrt{\left(\frac{\pi}{a\tau}\right)} \quad (3)$$

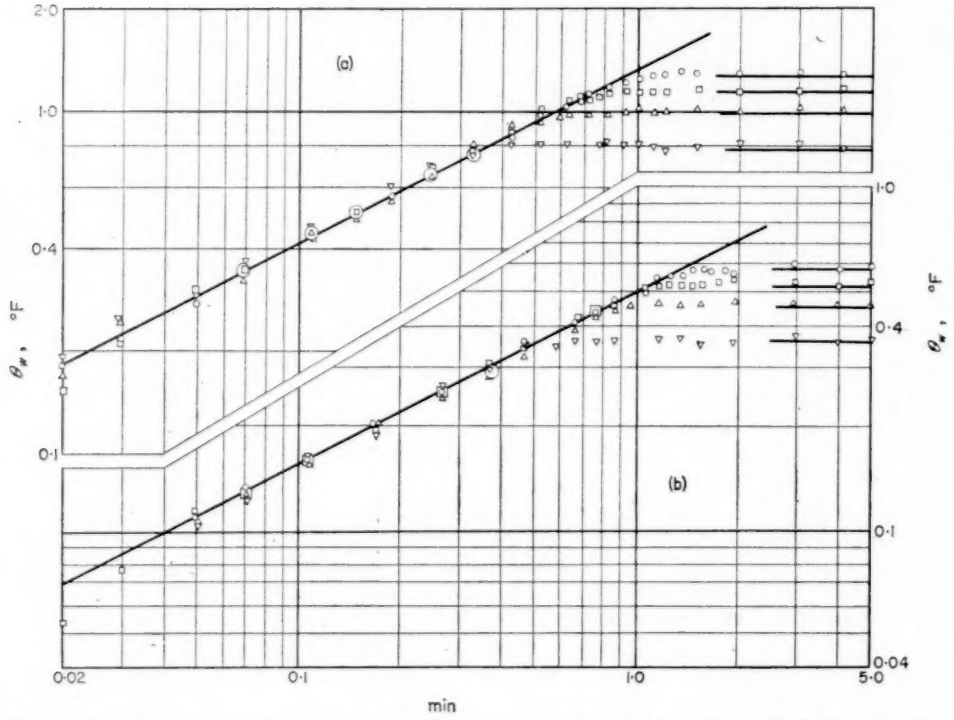

FIG. 10. Temperature increase of the heated plate as a function of time from the start of the heat pulse. ϑ_w temperature difference between the plate surface and the fluid bulk. The notation (a) and (b) in this and the following figures corresponds to the one in Fig. 9.
$\triangledown x = 0{\cdot}32$ in. $\triangle$ 1·03 in. $\square$ 2·10 in. $\bigcirc$ 3·80 in.

The relation expressed by equation (2) is inserted in Fig. 10 as the heavy inclined line. It can be observed that the measured points agree closely with this analytical solution, indicating that, in the initial stages, an unsteady free convection boundary layer grows on a finite plate in the same way as on one which is infinite in extent. The solution obtained by Sparrow and Gregg [13] for a steady state free convection boundary layer on a vertical plate with constant heat flux through its surface can be expressed in the following form for ($Pr \approx 6{\cdot}4$):

$$Nu = 0{\cdot}726 \left(\frac{GrPr}{4}\right)^{1/4} \tag{4}$$

The plate surface temperature as obtained from this equation and from the condition that the heat flow is independent of location is

$$\vartheta_w = x^{1/5} \left(\frac{q\sqrt{(2)}}{0{\cdot}726k}\right)^{4/5} \left(\frac{va}{g\beta}\right)^{1/5} \tag{5}$$

The values of the wall temperature calculated from this equation for the condition existing in the experiments are indicated by the horizontal lines in Fig. 10. The agreement with the experimental points is very good.

Fig. 11 shows the heat transfer coefficient as a function of time. The inclined line gives the heat conduction solution (equation (3)) and the short horizontal lines represent the heat transfer coefficients obtained from equation (4). From the Figs. 10 and 11, the following rule for a calculation of the wall temperature and of the local heat transfer coefficients in an unsteady free convection boundary layer on a vertical plate can be derived. One calculates both parameters for the initial conduction phase as

Vol. 1 1960

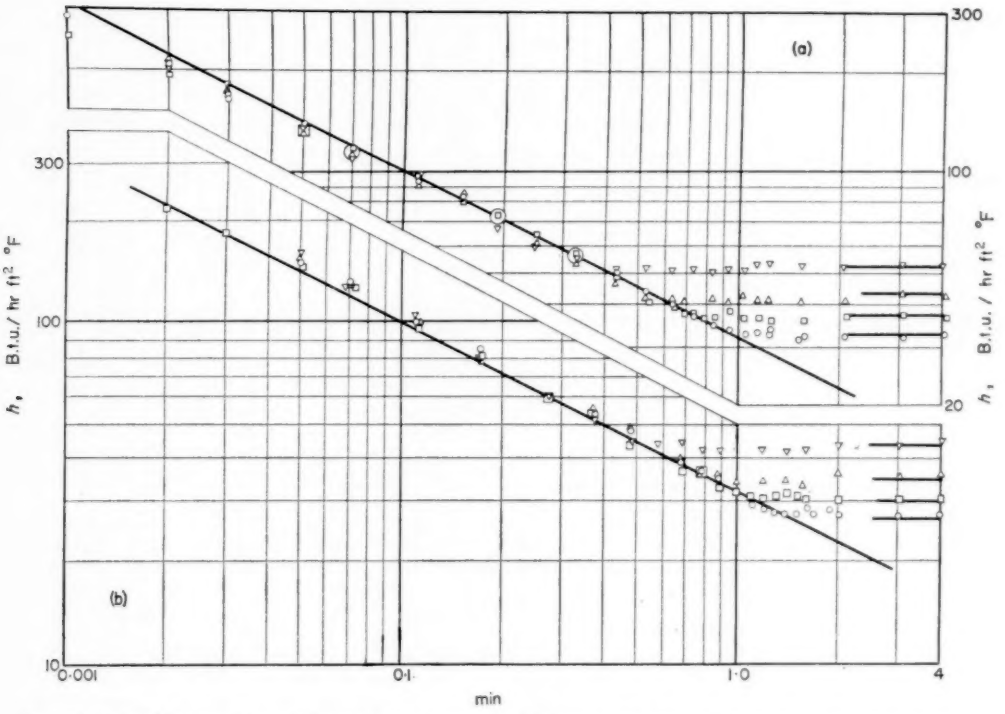

FIG. 11. Local heat transfer coefficient h at the plate surface as a function of time from the start of the heat pulse.
▽ $x = 0{\cdot}32$ in. △ 1·03 in. □ 2·10 in. ○ 3·80 in.

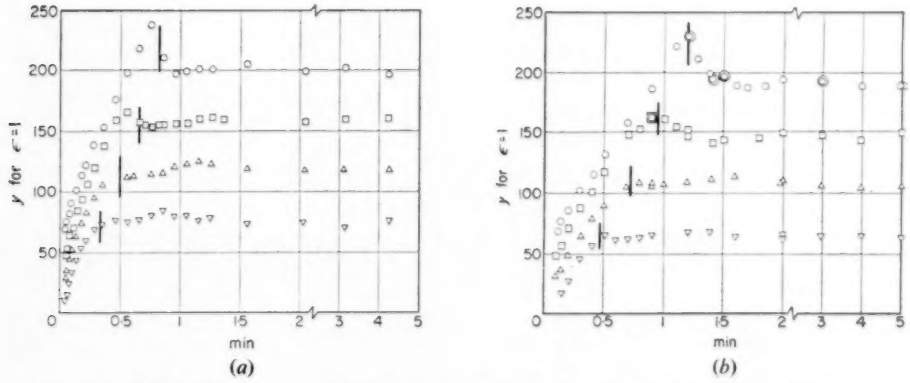

FIG. 12. Wall distance y, at which the temperature increase caused one fringe shift in the interferogram, as a function of time from the start of the heat pulse.
▽ $x = 0{\cdot}32$ in. △ 1·03 in. □ 2·10 in. ○ 3·80 in.

well as for steady state condition. The smaller one of the two temperatures describes the actual wall temperature satisfactorily and the larger one of the two heat transfer coefficients gives the local heat transfer coefficient with good accuracy.

Siegel [3] performed an analysis of the unsteady free convection boundary layer on a vertical plate. He used for this purpose the integrated momentum and energy boundary layer equations together with plausible assumptions on the shape of the velocity and temperature profiles. On the basis of his analysis, he predicted that the boundary layer grows initially in thickness with increasing time; that it reaches a maximum, and decreases again before it settles to its steady state value. Correspondingly, the heat transfer coefficient is predicted to decrease initially, to pass through a minimum and then to increase again to its steady state value. The heat transfer coefficients, as presented in Fig. 11, appear to indicate such a minimum. It is, however, very slight and possibly within the accuracy of the measurements. In order to compare the predicted growth of the boundary layer thickness with the measured one, the following procedure was used: the distance from the plate at which the temperature has increased by such an amount that it caused one fringe shift was measured in the interferograms and is plotted in Fig. 12, again for two heating rates and for four positions x. Siegel's prediction that the boundary layer development with time goes through a maximum is, according to this figure, well verified. The vertical lines in Fig. 12 indicate the time for which, according to the analysis, the pure conduction period ends. These times again agree remarkably well with the times at which the maximum of the boundary layer thickness occurs. The fact that this maximum is not accompanied by an equally pronounced minimum in the heat transfer coefficient must obviously indicate that the shape of the temperature profile changes during the transition period from pure conduction to steady state.

REFERENCES

1. C. R. Illingworth, *Proc. Camb. Phil. Soc.* **46**, 603 (1950).
2. S. Sugawara and I. Michiyoshi, *Proc. 1st. Japan Nat. Congr. Appl. Mech.* p. 501. (1951).
3. R. Siegel, *Trans. Amer. Soc. Mech. Engrs.* **80**, 347 (1958).
4. G. Ostroumov, *Sov. Phys. Tech. Phys.* **26**, 2720 (1956).
5. D. G. Gillam, L. Romben, H. Nissen and O. Lamm, *Acta Chem. Scand.* **9**, 641 (1955).
6. H. Klei, *Transient Free Convection from a Vertical Flat Plate*. B.A. Thesis in Chemical Engineering, Massachusetts Institute of Technology (1957).
7. E. A. McLean, V. E. Scherrer, C. A. Nanney and C. E. Faneuff, *Rev. Sci. Instrum.* **29**, 225 (1958).
8. R. J. Goldstein, *Interferometric Study of the Steady State and Transient Free Convection Thermal Boundary Layers in Air and in Water about a Uniformly Heated Vertical Flat Plate*. Ph.D. Thesis in Mechanical Engineering, University of Minnesota (1959).
9. E. Eckert, R. Drake and E. Soehngen, *Manufacture of a Zehnder–Mach Interferometer*. USAF, Air Material Command, Dayton, Ohio, Technical Report 5721 (1948).
10. E. Eckert and E. Soehngen, *Trans. Amer. Soc. Mech. Engrs.* **74**, 343 (1952).
11. E. Eckert and E. Soehngen, *Studies on Heat Transfer in Laminar Free Convection with the Zehnder–Mach Interferometer*. USAF, Air Material Command, Dayton, Ohio, Technical Report 5747 (1948).
12. L. Tilton and J. Taylor, *J. Res. Nat. Bur. Stand.* **20**, 419 (1938).
13. E. Sparrow and J. Gregg, *Trans. Amer. Soc. Mech. Engrs.* **78**, 435 (1956).
14. H. S. Carslaw and J. C. Jaeger, *Conduction of Heat in Solids*. Oxford University Press, London (1947).

Vol. 1 1960

Int. J. Heat Mass Transfer. Vol. 1, pp. 219–235. Pergamon Press 1960. Printed in Great Britain.

ON THE CORRELATION OF NUCLEATE BOILING HEAT TRANSFER

K. NISHIKAWA* and K. YAMAGATA†

Department of Mechanical Engineering, Kyushu University, Hakozaki, Fukuoka-shi, Japan

(*Received* 22 *September* 1959; *revised* 8 *December* 1959)

Abstract—A generalized equation to describe nucleate boiling is derived. The expression which correlates all fluid independently of pressure and heating surface–fluid combination is as follows:

$$Y = 8{\cdot}0\,(f_\zeta^{1/2} f_p X)^{2/3}$$

where

$$X = \left(\frac{1}{M^2 P}\,\frac{c_p \gamma'^2}{\lambda \sigma r \gamma''}\right)^{1/2} R^{3/2} q$$

$$Y = \frac{\alpha R}{\lambda}$$

and

c_p = specific heat of liquid;
γ' and γ'' = specific weight of liquid and vapour;
λ = thermal conductivity of liquid;
σ = surface tension of liquid;
R = the representative length of heating surface;
q = heat flux;
α = coefficient of heat transfer;
$M = 900\ \mathrm{m}^{-1}$, $P = 1{\cdot}699$ kcal/hr.
f_ζ = foamability, and f_p = pressure factor.

Furthermore, it is indicated that this correlating equation is applicable to forced-convection saturated or surface boiling. The proposed correlating equation has been theoretically sought by analysing the elementary processes of phenomena, but it is not based on dimensional analysis. In order to reach the final solution of the problem, it is necessary to analyse the elementary processes of boiling phenomena and elucidate the relations underlying the problem.

Résumé—Une équation générale représentant le phénomène d'ébullition a été obtenue. Cette expression, valable pour tout fluide indépendamment de la pression et de la disposition de la surface chauffante est la suivante:

$$Y = 8{,}0(f_\zeta^{1/2} f_p X)^{2/3}$$

ou

$$X = \left(\frac{1}{M^2 P}\,\frac{c_p \gamma'^2}{\lambda \sigma r \gamma''}\right)^{1/2} R^{3/2} q$$

$$Y = \frac{\alpha R}{\lambda}$$

et

c_p = chaleur spécifique du liquide,
γ' et γ'' = poids spécifique du liquide et de la vapeur,
λ = conductibilité thermique du liquide,
σ = tension superficielle du liquide,

* Assistant Professor of Mechanical Engineering, Faculty of Engineering, Kyushu University, Fukuoka, Japan.
† Professor of Mechanical Engineering, Faculty of Engineering, Kyushu University.

R = longueur caractéristique de la surface chauffante,
q = flux de chaleur,
a = coefficient de transmission de chaleur,
M = 900 m^{-1}, P = 1,699 kcal/h
f_ζ = pouvoir moussant, et f_p = facteur de pression.

De plus, il est indiqué que cette équation de corrélation est applicable à l'ébullition saturée ou de surface avec convection forcée. L'équation proposée a été obtenue théoriquement en analysant les processus élémentaires du phénomène, mais elle n'est pas fondée sur l'analyse dimensionnelle. Pour atteindre la solution finale du problème, il est nécessaire d'analyser les processus élémentaires du phénomène d'ébullition et d'expliquer les relations en approfondissant le problème.

Zusammenfassung—Zur Beschreibung des Filmsiedens wird eine verallgemeinerte Gleichung abgeleitet. Dieser Ausdruck, der für alle Flüssigkeiten, aber unabhängig vom Druck und unabhängig von der Kombination Heizfläche-Flüssigkeit, gilt, lautet:

$$Y = 8{,}0(f_\zeta^{1/2} f_p X)^{2/3}$$

Darin ist

$$X = \left(\frac{1}{M^2 P}\,\frac{c_p \gamma'^2}{\lambda \sigma r \gamma''}\right)^{1/2} R^{3/2}\, q$$

$$Y = \frac{aR}{\lambda}$$

und

c_p = spezifische Wärmekapazität der Flüssigkeit
γ' und γ'' = Gewicht von Flüssigkeit und Dampf
λ = Wärmeleitfähigkeit der Flüssigkeit
σ = Oberflächenspannung der Flüssigkeit
R = Kennzeichnende Länge der Heizfläche
q = Wärmestromdichte
a = Wärmeübergangskoeffizient
M = 900 m^{-1}, P = 1,699 kcal/h
f_ζ = Schaumfähigkeit, und f_p = Druckfaktor

Diese Beziehung ist auch auf die erzwungene Konvektion in gesättigter oder unterkühlter Flüssigkeit (örtliches Sieden) anwendbar. Sie wurde durch eine theoretische Untersuchung der Elementarvorgänge gefunden und beruht nicht auf einer Dimensionsanalyse. Um die endgültige Lösung des Problems zu erhalten, muss man die Beziehungen aufklären, die den Elementarprozessen des Siedevorgangs zu Grunde liegen.

Abstract—Выведено обобщенное уравнение, описывающее пузырчатое кипение. Выражение, устанавливающее корреляционную связь для всей жидкости независимо от давления и комбинации «нагревающая поверхность–жидкость», имеет следующий вид:

$$Y = 8{,}0\,(f_\zeta^{1/2} f_p X)^{2/3}$$

где

$$X = \left(\frac{1}{M^2 P}\,\frac{c_p \gamma'^2}{\lambda \sigma r \gamma''}\right)^{1/2} R^{3/2}\, q$$

$$Y = \frac{aR}{\lambda}$$

и

c_p = удельная теплоёмкость жидкости,
γ' и γ'' = удельный вес жидкости и пара соответственно,
λ = теплопроводность жидкости,
σ = поверхностное натяжение жидкости,
R = определяющая длина нагревающей поверхности,
q = тепловой поток,
a = коэффициент теплопереноса,

Vol. 1 1960

M = 900 м$^{-1}$, P = 1,699 ккал/час,
f_ζ = способность к образованию пузырей, и f_p = коэффициент давления.

Кроме того, указывается, что корреляционное уравнение может быть применено к насыщенному кипению при вынужденной конвекции или плёночному кипению. Предлагаемое корреляционное уравнение было выведено теоретически путём анализа элементарных процессов рассматриваемых явлений, а не путём анализа размерностей. Для того чтобы получить окончательное решение задачи, необходимо проанализировать элементарные процессы, из которых складывается кипение, и объяснить лежащие в основе задачи соотношения.

NOMENCLATURE

A, area of heating surface (m^2);
D, diameter of tube (m);
H, liquid level (m);
H_e, effective stirring length of bubbles in saturated boiling (m);
H_{es}, effective stirring length of bubbles in surface boiling (m);
R, representative dimension of heating surface (m);
U, rising velocity of a bubble at the optional point (m/hr);
U_m, average rising velocity of a bubble (m/hr);
V, volume of a rising bubble at the optional point (m^3);
V_0, volume of a bubble just leaving the heating surface (m^3);
W, total convective driving force for heat transfer (m);
W_t, average convective driving force due to the change of density (m);
W_b, average convective driving force due to the stirring of bubbles (m);
c_p, specific heat of liquid (kcal/kg°C);
d_0, diameter of a bubble just leaving the heating surface (m);
d_u, diameter of a bubble just leaving the free liquid surface (m);
f, frequency of bubble formation (sec^{-1});
f_p, pressure factor;
f_ζ, foamability;
g, acceleration due to gravity (m/sec^2);
h, rising height of a bubble (m);
n, number of vapour columns;
p, any pressure (kg/cm^2);
p_s, atmospheric pressure (kg/cm^2);
q, heat flux of heating surface (kcal/m^2 hr);
q_c, convective heat flux (kcal/m^2 hr);
q_b, saturated boiling heat flux (kcal/m^2 hr);
r, latent heat of evaporation (kcal/kg);
v, velocity of fluid (m/sec);
α, coefficient of heat transfer (kcal/m^2 hr °C);
α_c, coefficient of convective heat transfer (kcal/m^2 hr °C);
α_b, coefficient of boiling heat transfer (kcal/m^2 hr °C);
β, coefficient of cubic expansion (°C^{-1});
γ', specific weight of liquid (kg/m^3);
γ'', specific weight of vapour (kg/m^3);
δ, thickness of temperature boundary layer (mm);
ζ, coefficient of foaming capacity of the combination of the surface and liquid in question (kcal/m hr °C^3);
ζ_s, coefficient of foaming capacity of pure liquid on the fresh and smooth surface (kcal/m hr °C^3);
η, viscosity of liquid (kg hr/m^2);
θ_L, temperature of liquid (°C);
θ_p, temperature of heating surface (°C);
θ_s, saturation temperature of liquid (°C);
$\Delta\theta$, temperature difference between heating surface and liquid (°C);
$\Delta\theta_s$, surface temperature minus saturation temperature (°C);
λ, thermal conductivity of liquid (kcal/m hr °C);
ν, kinematic viscosity of liquid (m^2/hr);
σ, surface tension of liquid (kg/m);
τ, period of bubble formation (sec);
χ, (diameter of a bubble just leaving the heating surface) (frequency of bubble formation) (m/hr);
Gr, Grashof number;
Gr^*, equivalent Grashof number;
Nu, Nusselt number;
Pr, Prandtl number;
Re, Reynolds number;
$\bar{Re}_b$, bubble Reynolds number.

1. INTRODUCTION

THE study of heat transfer in a boiling liquid is one of the most neglected in the field of heat engineering. An effort to unify heat transfer in nucleate boiling of various kinds of liquids that have different physical properties into one correlating equation is being made by a few research workers, but the equation concerned with the irreproducibility of phenomenon has yet to be perfected. The difficulties in the investigation of boiling can be attributed to the fact that boiling is not only a complex process involving fluid motion, heat transfer, surface phenomenon and phase change, but that it is also irreproducible.

Even if a liquid is always boiled in one and the same vessel under the same conditions of heating, sometimes a few bubbles are generated and rise expanding rapidly and, at other times, a great number of small bubbles rise quietly, thus causing much difference in the phases of heat transfer in each individual case. Before studying the origin of this irreproducibility of boiling, it is necessary first to analyse the composite phenomena of boiling into elementary processes. It is only after this analysis that the problem of irreproducibility as well as the nature of boiling phenomenon will be clarified.

It is a fact of course that the problem of heat transfer holds the key to the consideration of boiling phenomena from the standpoint of engineering. However, to rely on that viewpoint is to develop as a whole the relations between the coefficient of heat transfer and various other quantities by means of dimensional analysis rather than by treating the various elementary processes analytically. For instance, McAdams [15] collected the existing data in his book. This synthetic treatment seems to be a direct method, but the problem of irreproducibility cannot be solved extensively by it. Moreover, in the application of dimensional analysis, there will arise questions of what dimensionless quantities to select. It is because of this ambiguity that empirical equations hitherto proposed are different from one another in the introduction of dimensionless quantities.

In order to eliminate such disadvantages, a law which is valid for individual elementary process should be confirmed and then unified. The reason why Jakob's studies [11] are held in high esteem even now is that his study was the only one that took a correct course, though it still leaves much to be clarified. Rising current interest in research into the bubble dynamics of boiling may be due to the fact that the pursuit of the elementary processes involving generation, growth and collapse of bubbles is the key to the clarification of boiling phenomena. As there is a limit to the complete theoretical explanation of every elementary process, it is necessary to study each one experimentally.

In this paper we consider the derivation of the correlating equation of nucleate boiling heat transfer based on the above-mentioned viewpoint and its application to the forced-convection saturated or surface boiling.

2. DERIVATION OF CORRELATING EQUATION

Consider the case of pool boiling of a saturated liquid. Two kinds of driving force for convection at nucleate boiling, are conceivable. The first driving force of convection is the buoyancy due to the change of density accompanying heating, similar to the case of purely free convection. The buoyancy that acts upon the unit weight is plainly expressed as follows:

$$\beta\,(\theta - \theta_L)$$

and average convective driving force W_t against the whole liquid will be expressed as follows in the form:

$$W_t = \int_0^\delta \beta(\theta - \theta_L)\,dy \qquad (1)$$

where

β = coefficient of cubic expansion of liquid;
y = vertical distance from heating surface;
δ = average thickness of the boundary layer of the liquid along the heating surface;
θ = temperature of the liquid at the point $y(<\delta)$;
θ_L = temperature of the liquid at the point $y(>\delta)$.

The second driving force of convection is the liquid stirring force of rising bubbles and can be considered as follows. Let:

V = volume of one rising bubble at the optional point y;

Vol. 1 1960

U = rising velocity of the bubble at the optional point y;
τ = period of bubble formation;
A = heating surface area;
n = number of vapour columns.

The average volume of the vapour–liquid mixture containing one bubble at an optional height is $(A/n)U\tau$. Therefore, the convective force due to the change in bulk density acting on a unit weight of liquid may be expressed as follows, assuming that the weight of vapour be neglected compared with that of liquid:

$$nV/AU\tau$$

Accordingly the convective driving force W_b due to the stirring of bubbles for the entire liquid may be expressed as follows:

$$W_b = \int_0^{H_e} \frac{n}{A\tau} \frac{V}{U} F(y)\, dy \qquad (2)$$

Here H_e is the "effective stirring length of bubbles". The effective stirring length of bubbles is the distance from the heating surface where the liquid stirring effect of bubbles disappears, for it is considered that when the bubbles rise from the heating surface, the nearer they are to the heating surface, the greater their stirring effect upon the boundary layer near the heating surface gets, and the greater the distance of bubbles from the heating surface is, the weaker their effect becomes. $F(y)$ represents the discrepancies of the liquid stirring effect due to the rising position of bubbles and its limiting value should be as follows:

$$F(0) = 1,\ F(H_e) = 0 \qquad (3)$$

Since these two convective driving forces operate at the same time, the total convective driving force W may be expressed as follows:

$$W = W_t + W_b \qquad (4)$$

A coefficient of no dimension will be defined as follows in order to express equations (1) and (2) in a simple way:

$$c_t = \int_0^1 \frac{\theta - \theta_L}{\theta_p - \theta_L}\, d\eta \quad , \quad \eta = \frac{y}{\delta} \qquad (5)$$

$$c_b = \frac{1}{6} \int_0^{H_e} \frac{V(y)}{V_0} \frac{U_m}{U(y)} F(y) \frac{dy}{H_e} \qquad (6)$$

If the above coefficients are used, equation (4) will be as follows:

$$W = c_t \beta(\theta_p - \theta_L)\, \delta + c_b \frac{nd_0^2}{R^2} \frac{\chi}{U_m} H_e \qquad (7)$$

where
θ_p = average temperature of heating surface;
V_0 = volume of a bubble just leaving the heating surface;
U_m = average rising velocity of a bubble;
d_0 = diameter of a bubble just leaving the heating surface (transformed to a sphere);
R = representative dimension of heating surface (radius in case of horizontal circular plate);
$\chi = d_0/\tau$.

Since the following Grashof number

$$Gr = \frac{R^3 g \beta(\theta_p - \theta_L)}{\nu^2} = \frac{R^3 g}{\nu^2} \frac{W_t}{c_t \delta} \qquad (8)$$

is used to express the driving force of a free convection W_t, the equivalent Grashof number may be introduced in this case, too:

$$Gr^* = \frac{R^3 g}{\nu^2} \frac{W}{c_t \delta} =$$

$$= Gr + \left(\frac{c_b}{c_t}\right) \left(\frac{nd_0^2}{R^2}\right) \left(\frac{\chi}{U_m}\right) \left(\frac{H_e}{\delta}\right) \left(\frac{gR^3}{\nu^2}\right) \qquad (9)$$

where
Gr = Grashof number;
g = acceleration due to gravity;
ν = kinematic viscosity of liquid.

However, it was recognized by writers [8] that the key factor that controls the transfer in nucleate boiling is the stirring effect of bubbles, and that W_t can be neglected, compared with W_b while estimating their order. In view of the difficulty of obtaining directly the equation for heat transfer in nucleate boiling, it is conceivable that, with the rule of heat transfer in the case of free convection indicated by the following expression, an equation which uses Gr^* instead of Gr is applicable in the case of nucleate boiling.

$$Nu = K\,(Gr.Pr)^m \qquad (10)$$

where

Nu = Nusselt number;
Pr = Prandtl number;
K and m = constants.

On the other hand, according to the writers' experiment [26], there exists the following relation between the coefficient of heat transfer α and δ as shown in Fig. 1:

$$\alpha^s \propto \delta^{-1}$$

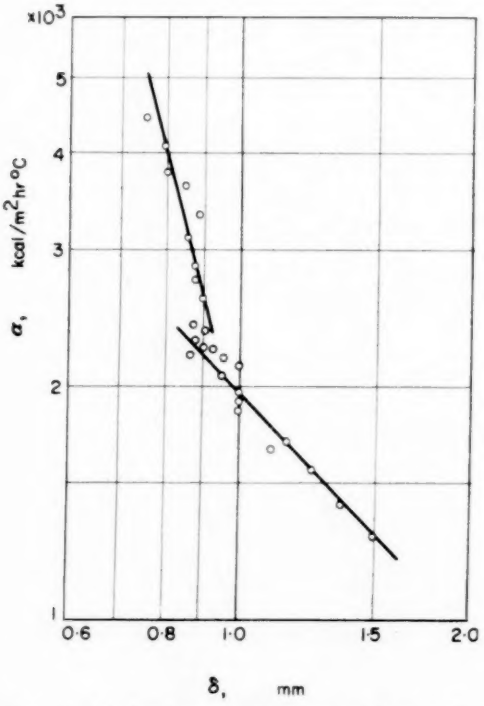

FIG. 1. Relation between the heat transfer coefficient, α, and thickness of the temperature boundary-layer, δ. [26].

Accordingly,

$$Nu^s \frac{\delta}{R} = B \tag{11}$$

is established, in which both s and B are constants. Therefore, neglecting Gr and substituting equations (9) and (11) into equation (10), the following formula will be obtained:

$$Nu = K^* \left(n\,Pr \frac{gH_e d_0^2}{\nu} \frac{\chi}{U_m} \right)^{m/(1-sm)} \tag{12}$$

where

$$K^* = (K)^{1/(1-sm)} \left(\frac{c_b}{c_l B} \right)^{m/(1-sm)} \tag{13}$$

Now, if the heat flux q is presumed to be carried away by bubbles, the number of vapour columns n is expressed by the following equation:

$$n = \frac{6}{r\gamma''} \frac{R^2 q}{d_u^3 f} \tag{14}$$

where

γ'' = specific weight of vapour;
r = latent heat of evaporation;
d_u = diameter of a bubble just leaving the free liquid surface (transformed into a sphere);
f = frequency of bubble formation.

However, the writers have verified by their experiment on water [17] that there exists the following relation between d_u and d_0:

$$\left(\frac{d_u}{d_0} \right)^3 = M n^{-1/2} R \tag{15}$$

The numerical value of M in equation (15) is 900 m^{-1}, for boiling water under atmospheric pressure (see Appendix). Here, M is assumed to be a constant that has nothing to do with the physical properties of liquid, because it has been ascertained experimentally, as will be shown later, that M is a function only of the pressure. Substituting equation (15) into equation (14) and eliminating d_u, one can obtain the following expression:

$$n = \left(\frac{6}{r\gamma''} \frac{Rq}{Md_0^3 f} \right)^2 \tag{16}$$

Then U_m in the domain of heat transfer in nucleate boiling may be expressed experimentally by the following formula according to the study of Peebles and Garber [21].

$$U_m = b \left(\frac{\sigma g^2}{\gamma'} \right)^{1/4} \tag{17}$$

where

σ = surface tension of liquid;
γ' = specific weight of liquid;
b = constant which has nothing to do with the physical properties of liquid.

Vol. 1 1960

Now if distilled water is taken up as the standard when it boils under atmospheric pressure on a fresh and smooth plane and its value is expressed by the suffix s, the bubbles of any optional kind of liquid are considered to require ϕ times as much energy as those of distilled water when they leave the heating surface; in which case the formula will be as follows from Jakob's study [12]:

$$\phi = \left(\frac{d_0}{d_{0s}}\right)^3 \left(\frac{\gamma''}{\gamma_s''}\right) \left(\frac{r}{r_s}\right) \tag{18}$$

On the other hand, supposing that the frequency of bubble formation varies in accordance with the following expression:

$$f = f_s/\phi \tag{19}$$

the formula $\chi = 400$ m/hr = (constant) from the writers' experiment [26] will bring forth the following expression:

$$\chi = d_0 f = \frac{d_0}{d_{0s}} \frac{d_{0s} f_s}{\phi} = 400 \left(\frac{d_{0s}}{d_0}\right)^2 \frac{\gamma_s''}{\gamma''} \frac{r_s}{r}$$

Therefore $$\chi = P/(d_0^2 \gamma'' r) \tag{20}$$

where

$$P \equiv 400\, d_{0s}^2\, \gamma_s''\, r_s \tag{21}$$

According to the result of an experiment conducted by the writers [25] when air is injected into the liquid through one outlet, there is a distance from the heating surface at which the liquid stirring effect of the air bubble disappears when the air injecting outlet rises from the heating surface, and this distance varies according to the property of liquid. This distance is called "the effective stirring length of bubbles", and there also exists a similar length for nucleate boiling. The writers investigated the effect of the liquid level H on boiling heat transfer for some kinds of liquid, and found that the value of the coefficient of heat transfer for a certain liquid level remains constant, irrespective of the liquid level and begins to change below this level. Fig. 2 shows several examples. The liquid level where α begins to change is independent of heat flux for the specified liquid. Therefore, the writers have called the distance from the heating surface, which is equal to the liquid level where α begins to change, the effective stirring length of

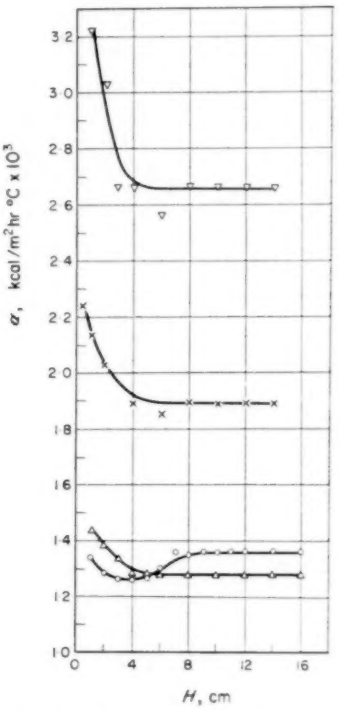

FIG. 2. Relation between the liquid level and the coefficient of boiling heat transfer.

	R (m)	$q \times 10^4$ (kcal/m²hr)	Liquid
▽	3·5	2·50	Distilled water
×	5·0	1·75	Distilled water
△	7·0	1·25	Distilled water
○	5·0	1·75	30% sugar water

bubbles. The following relation holds between the effective stirring length of bubbles H_e and bubble Reynolds number $\bar{R}e_b$, as seen in Fig. 3:

$$\frac{H_e}{R} = T^* (\bar{R}e_b)^{-1} \equiv T^* \left(\frac{d_0 U_m}{\nu}\right)^{-1} \tag{22}$$

and d_0 is expressed by the following equation from Fritz's study [6]:

$$d_0 = a \sqrt{\left(\frac{\sigma}{\gamma'}\right)} \tag{23}$$

where T^* and a are proportional constants.

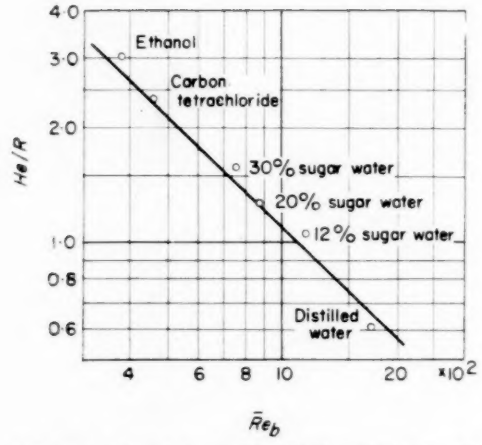

FIG. 3. Relation between the effective stirring length of bubbles, H_e, and bubble Reynolds number, $\bar{R}e_b$. [16].

According to the above formula, H_e decreases with increase in diameter of the bubble. This fact is hard to understand if only one bubble is considered. It should be kept in mind, however, that H_e is determined by the stirring effect of the total bubble which is the product of the average liquid stirring force for one vapour column and the number of vapour columns.

Finally, substituting equations (16), (17), (20), (22) and (23) into equation (12), the following equation is obtained:

$$Y = K^*\phi^* X^{2k} \tag{24}$$

where

$$Y \equiv \alpha R/\lambda; \tag{25}$$

$$\phi^* \equiv \frac{6^{2k} T^{*k}}{(ab^2)^k}; \tag{26}$$

$$X \equiv \left[\frac{1}{M^2 P} \frac{c_p \gamma'^2}{\lambda \sigma r \gamma''}\right]^{1/2} R^{3/2} q; \tag{27}$$

$$k = m/(1 - sm); \tag{28}$$

M = 900 m^{-1} (the value of a clean and smooth surface under the atmospheric pressure);

P = 400 $d_{0s}^2 \gamma_s'' r_s$ = 1·699 kcal/hr;

c_p = specific heat of liquid at constant pressure;

λ = thermal conductivity of liquid.

As for R, the radius was taken to a horizontal circular plate, height to a vertical plate and diameter to a horizontal cylinder.

An attempt will be made to calculate the constant term by putting a suffix l in laminar flow and another suffix t in turbulent flow

$$K_l = 0{\cdot}56, \qquad K_t = 0{\cdot}13;$$

$$K_l^* = 0{\cdot}211, \qquad K_t^* = 0{\cdot}201;$$

$$m = \tfrac{1}{4}, s = 1, \quad m = \tfrac{1}{3}, s = \tfrac{1}{4};$$

Therefore $k = \tfrac{1}{3}$, $k = \tfrac{4}{11}$.

And as $T^* = 1100$, $a = 1{\cdot}034$ and $b = 1{\cdot}18$, it will follow that

$$\phi_l^* = 30{\cdot}1, \qquad \phi_t^* = 41{\cdot}1;$$

Accordingly, the resulting formula will be

$$Y = 6{\cdot}35\ X^{2/3} \text{ (laminar)} \tag{29}$$

$$Y = 8{\cdot}26\ X^{8/11} \text{ (turbulent)} \tag{30}$$

and the experimental points will be contained almost between these two lines as seen in Fig. 5. As to the average for experimental points,

$$Y = 8{\cdot}0\ X^{2/3} \tag{31}$$

will be better. Since the numerical values determined by experiments at atmospheric pressure are used in deriving these formulae, equation (31) is the correlating equation of nucleate boiling heat transfer in the fresh and smooth surface under atmospheric pressure.

3. EFFECT OF PRESSURE

If the results of experiments which are either above or below the atmospheric pressure are correlated by the above-mentioned method, the experimental points will slip up in parallel with the straight lines of the formulae of equation (31) or (29) making the pressure a parameter (see, for example, Fig. 4). In order to unify these experimental points into one line, a definition will be made here for the pressure factor f_p as follows:

$$f_p = p/p_s \tag{32}$$

where

p = pressure in question;

p_s = atmospheric pressure.

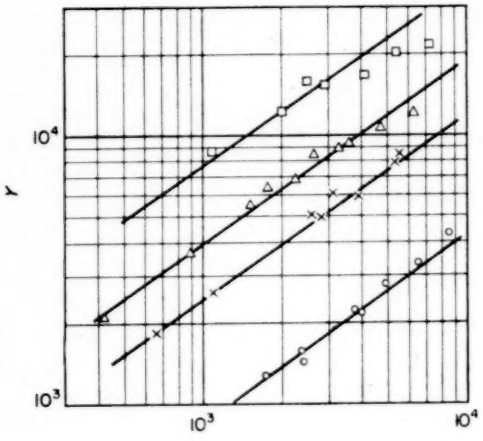

FIG. 4. Correlation of heat transfer in nucleate boiling for $X \sim Y$ at various pressures (data of Cichelli and Bonilla [3]).

Ethanol: ○, 1·03 atm; ×, 3·87 atm; △, 8·09 atm □, 18·63 atm.

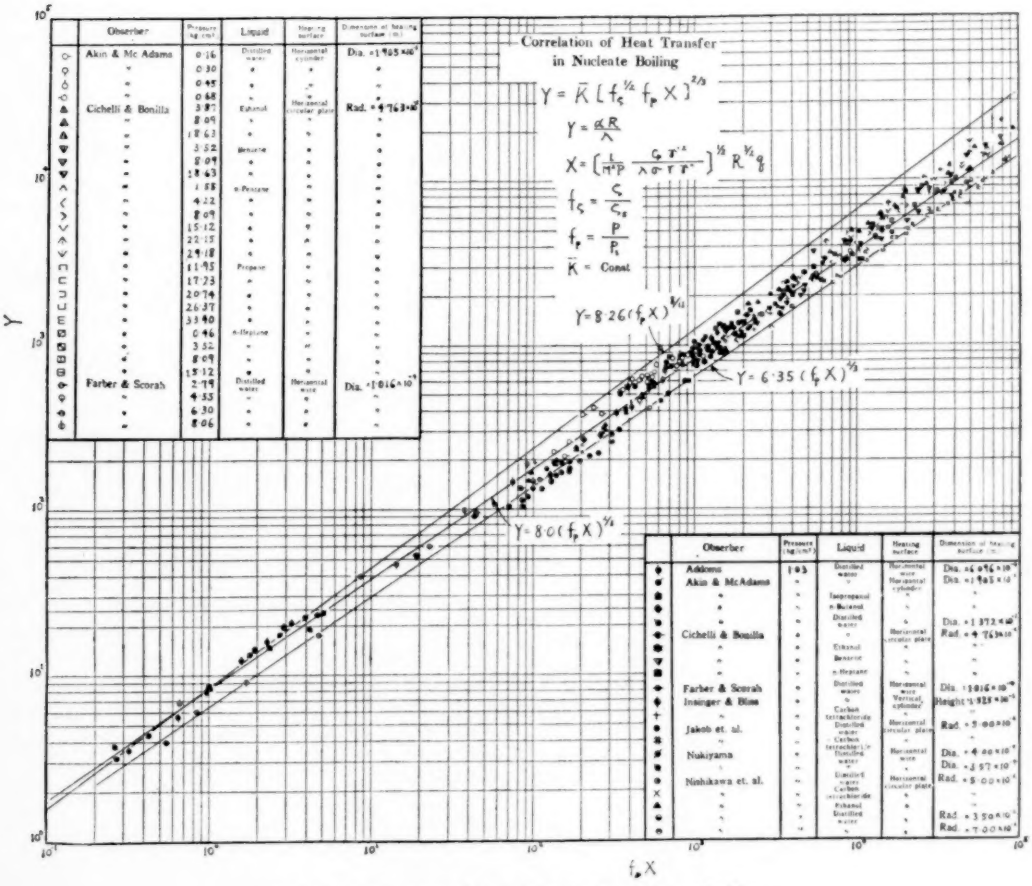
Correlation of Heat Transfer in Nucleate Boiling
$Y = \bar{K}\,[f_\varsigma^{1/2} f_p X]^{2/3}$
$Y = \frac{\alpha R}{\lambda}$
$X = \left[\frac{1}{H^2 P}\,\frac{C_p T^{1.5}}{\lambda \sigma^{1/2} \gamma^{1/2}}\right]^{1/2} R^{1/2} q$
$f_\varsigma = \frac{\varsigma}{\varsigma_s}$
$f_p = \frac{P}{P_s}$
$\bar{K}$ = Const
$Y = 8{\cdot}26 (f_p X)^{1/4}$
$Y = 6{\cdot}35 (f_p X)^{1/3}$
$Y = 8{\cdot}0 (f_p X)^{1/4}$
Y
$f_p X$

FIG. 5. Correlation of heat transfer in nucleate boiling.

The formula (31) may be rewritten as follows, using this pressure factor:

$$Y = 8{\cdot}0\,(f_p X)^{2\cdot3} \tag{33}$$

If the data of the writers [26], Jakob [11], Cichelli and Bonilla [3], Addoms [1], Insinger and Bliss [10], Akin and McAdams [2], Nukiyama [20] and Farber and Scorah [5] are plotted out by adopting Y as ordinate and $f_p X$ as abscissa, Fig. 5 is obtained and the experimental points will be unified with 20 per cent on the whole.

Since the variation of the physical properties of the liquid with pressure is taken into account in the terms X and Y of equation (33), it is considered that the pressure factor f_p is the correction factor of M in equation (15). Eliminating d_{ti} from equations (14) and (15), an expression will be formed as follows:

$$M = \frac{1}{\sqrt{(n)}}\left(\frac{6}{r\gamma''}\,\frac{Rq}{d_0^3 f}\right) \tag{34}$$

On the other hand, the following expression must hold, assuming that f_p is the correction factor of M only,

$$M\,p = M_s p_s \tag{35}$$

Here, the suffix s refers to the values at atmospheric pressure. In other words, the factor concerning the rate of growth of bubble M is inversely proportional to pressure p. As the writers [18] measured not only a and q but also n, d_0 and f in the experiment of nucleate boiling of water under reduced pressures, one can calculate M from equation (34). Plotting the relation between p and M determined by equation (34), Fig. 6 is obtained and it is ascertained that the relation (35) holds. The right-hand side of equation (34) contains the physical properties of liquid and the constants which must be determined by a boiling experiment and vary according to the kind of liquid. Therefore, it can be said that the pressure factor f_p is the correction factor which modifies only the factor concerning the rate of growth of the bubble with pressure, and the assumption in the preceding paragraph in which M is only a function of the pressure, independent of properties of liquid, could be indirectly proved.

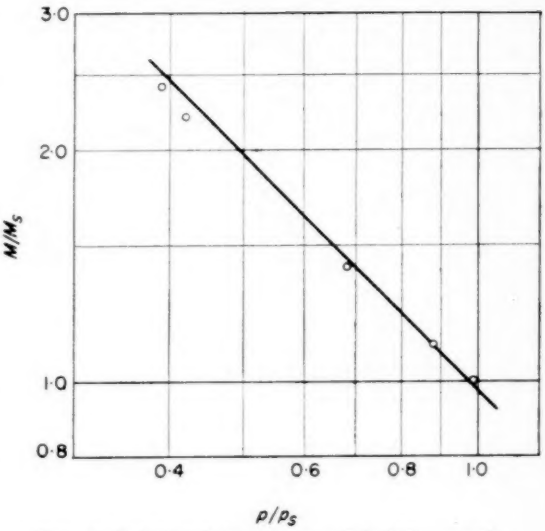

FIG. 6. Relation between rate of bubble growth, M, and pressure, p. [18].

4. EFFECT OF CONDITION OF HEATING SURFACE

Since formula (33) is based on a fresh and smooth surface as mentioned before, consideration should be given to various other kinds of surface conditions, e.g. surfaces that are contaminated, roughened or air-adsorbed, in regard to the foaming capacity of the surface as has been pointed out. The writers previously carried out an experiment [9] on nucleate boiling by using water containing salt and obtained a result as follows. When the heat flux q increases $q_1 \rightarrow q_2 \rightarrow q_3$ and decreases as $q_3 \rightarrow q_2 \rightarrow q_1$ and if these cycles are repeated, the degree of contamination on the surface is considered to be definite during one cycle. If the result of the experiment is expressed by the curve $a \sim \Delta\theta$ ($\Delta\theta$ = the temperature difference between heating surface and liquid), it will resemble Fig. 7, i.e. it will produce $a \propto \Delta\theta^2$ which will go on changing its position every time the cycle is repeated, maintaining the preceding relation. Accordingly, ζ which is defined in equation (36) expresses the foaming capacity of the specified liquid:

$$\zeta \equiv aR/\Delta\theta^2 = (aR)^3/(qR)^2 \tag{36}$$

When the physical properties are different, it is necessary to have a separate term which indicates nothing but the foaming capacity, for ζ is

Vol. 1 1960

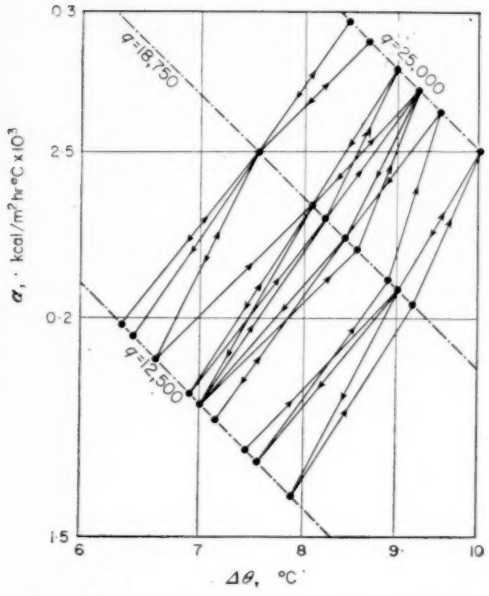

FIG. 7. Change of the relation $\alpha \sim \Delta\theta$ due to the repetition of cyclic heating [9].

included in the effect of physical properties. Therefore, if f_ζ (see equation (37)) is defined as foamability, it may be looked upon as the factor that indicates only the foaming capacity in a form from which the effect of physical property has been eliminated:

$$f_\zeta = \zeta/\zeta_s \tag{37}$$

where ζ_s is the coefficient of foaming capacity of pure liquid on the fresh and smooth surface while ζ represents the coefficient of foaming capacity of a combination of the surface and the liquid in question. The formula of heat transfer in nucleate boiling, in which the condition of the heating surface is considered, may be obtained by rewriting the formula (33) as follows using f_ζ:

$$Y = 8{\cdot}0\,(f_\zeta^{1/2} f_p X)^{2/3} \tag{38}$$

That is to say, formula (38) is an expression that includes all the cases of heat transfer in nucleate boiling. The foamability is something that resembles to emissivity in heat radiation, which is decided by a combination of the condition of the heating surface and of the liquid.

Generally, when the heating surface is contaminated, foaming capacity either increases or decreases. But, it is sufficient to regard $f_\zeta = 1$ in an ordinary contaminated or roughened surface, but not in a very contaminated or artificially grooved surface. Though it is necessary to determine f_ζ experimentally in order to know the accurate value of the coefficient of heat transfer, in many cases it is sufficient to take $f_\zeta = 1$ in design practice.

5. APPLICATION TO FORCED CONVECTION BOILING HEAT TRANSFER

5.1. *Saturated boiling*

In a case where the saturated liquid flows in a tube, the value of the coefficient of heat transfer becomes somewhat larger than that of pool boiling heat transfer, for which Rohsenow

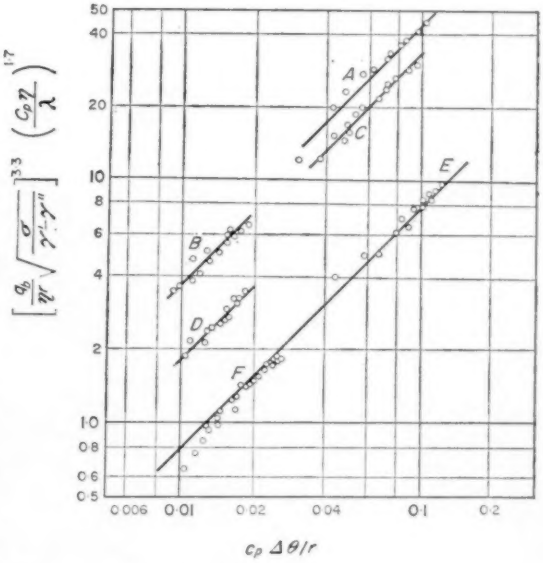

FIG. 8. Correlation of boiling heat transfer inside tubes by Rohsenow's method [22].

		C_{sf}
A	*iso*Propyl alcohol	0·00225
B	50% potassium carbonate	0·00275
C	n-Butyl alcohol	0·00305
D	35% potassium cabonate	0·0054
E	Carbon tetrachloride	0·013
F	Water	0·013

[24] has suggested a correlating method such as follows, that is, the total heat flux q at forced-convection boiling consists of boiling heat flux q_b and convective heat flux q_c:

$$q = q_b + q_c \tag{39}$$

q_c will be calculated by the conventional Dittus–Boelter equation, modified by using a coefficient of 0·019 instead of 0·023.

$$q_c = \alpha_c \Delta\theta \tag{40}$$

$$Nu_c = 0{\cdot}019\ Re^{0{\cdot}8}\ Pr^{1/3} \tag{41}$$

where

α_c = coefficient of convective heat transfer;
Nu_c = Nusselt number $\equiv \alpha_c D/\lambda$;
D = diameter of tube;
Re = Reynolds number $\equiv vD/\nu$;
v = velocity of fluid;
Pr = Prandtl number.

As for q_b, Rohsenow uses a correlating equation of his own, i.e.

$$\frac{c_p \Delta\theta}{r} = C_{sf}\left\{\frac{q_b}{\eta r}\sqrt{\left(\frac{\sigma}{\gamma' - \gamma''}\right)}\right\}^{0{\cdot}33}(Pr)^{1{\cdot}7} \tag{42}$$

where

η = viscosity of liquid;
C_{sf} = surface coefficient determined by the combination of liquid and heating surface (function of contact angle).

The experimental values of each liquid or each experimental condition can be expressed by a group of paralleles if correlated by Rohsenow's formula, as shown in Fig. 8, but it causes a serious difference to the value of surface coefficient C_{sf}. Accordingly, the writers followed up q_b by applying their correlating equation (31) to the results of an experiment conducted by Piret and Isbin [22]. The latter took several liquids of different physical properties, and caused them to flow through a vertical copper tube, 25·4 mm in diameter and 1·46 m in length, boiling under atmospheric pressure. We obtained an excellently unified result which is indicated in Fig. 9. The reason why data of 30 per cent and 50 per cent potassium carbonate are omitted in Fig. 9 is that these data are considered for the contaminated surface. As a result, it may be said that Rohsenow's conception on the forced-convection boiling heat transfer is approximately correct

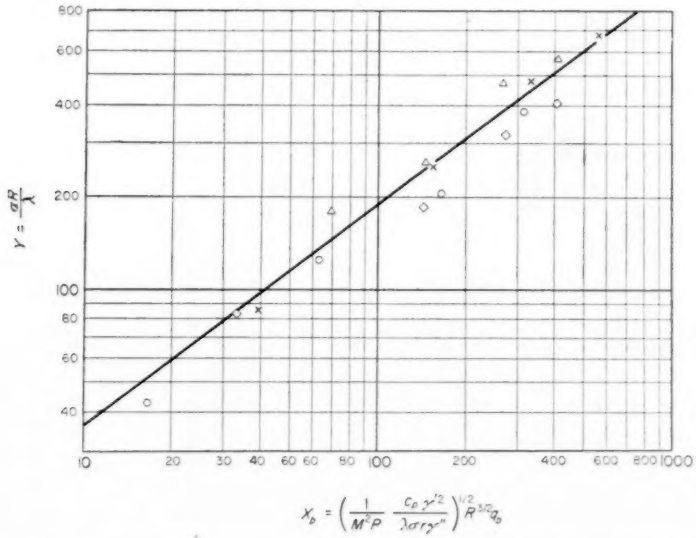

FIG. 9. Correlation of boiling heat transfer inside tubes by writers' method.
○, water; ×, *iso*propyl alcohol; △, *n*-butanol; ◇, carbon tetrachloride.

where he believes the total flux in the forced-convection boiling to be the sum of convective heat flux and boiling heat flux; however, in Rohsenow's coefficient of surface factors are included conditions other than that of interface between solid and liquid.

If the line of thought shown in formula (39) is applied, the liquid boiling inside the tubes will be satisfactorily correlated by using the writers' correlating equation, but it can be applied only to cases in which vapour and liquid are quite evenly mixed. In those cases where vapour is formed into a piston by the excess of vapour, such a way of thinking is invalid. It will be necessary to make further studies on the flowing aspect of vapour–liquid mixtures in these instances.

5.2. *Surface boiling*

Rohsenow holds that the correlating equation he has proposed for saturated boiling is also applicable to surface boiling, but the writers are not satisfied with it for the following reasons:

(1) In the process of deriving this empirical formula, it is assumed $n \propto q_b$ but according to experiments carried out by the writers, it turned out that $n \propto q_b^2$.

(2) Though Rohsenow and Clark state that the contamination of the heating surface causes a change in the exponent of Pr, the writers believe that the effect of the condition of the heating surface ought to be included in the surface coefficient C_{sf} but not in the exponent of Pr.

(3) According to the former, the value of C_{sf} is different for surface boiling and for saturated boiling respectively, even if the combination of the liquid and the heating surface is the same, but the writers presume that C_{sf} ought to assume the same value for surface boiling as for saturated boiling.

The writers tentatively co-ordinated the experimental results on heat transfer in surface boiling based on the correlating equation which they had proposed for pool boiling, though it seems to be a questionable treating of the mechanism of surface boiling to apply a correlating equation which uses the concept of the effective stirring length of bubbles.

First, assuming equations (39), (40) and (41) valid, q_b was evaluated. Next, $q - \Delta\theta$ diagrams are often used in treating the data of surface boiling. When such a correlation is used, several parallel lines are formed having the subcooling degree of the liquid as a changing parameter. If $q - \Delta\theta_s$ diagrams are used, these parallel lines can be represented by a single curve, where $\Delta\theta_s$ is surface temperature θ_p minus saturation temperature θ_s. From these results as well as from the experimental results on the formation and collapse of bubbles in surface boiling, the driving force in the surface boiling heat transfer is considered as $\Delta\theta_s$. The writers used heat flux as a measure of the driving force of heat transfer in place of temperature difference. Thus the writers tentatively used $q_{bs} \equiv q_b(\Delta\theta_s/\Delta\theta)$ as the heat flux in X of equation (27). A satisfactory correlation could not be obtained by this treatment alone, though this is to be expected. Accordingly, the writers accounted for the correction of the effective stirring length of bubbles.

In the writers' correlating equation corresponding to the saturated boiling, the effect of the effective stirring length of bubbles is included in the form of $(T^*)^{1/3}$ in the ϕ^* term of equation (24). T^* is the constant connecting the effective stirring length of bubbles to the bubble Reynolds number, and it satisfies equation (22). The writers considered that the value of the effective stirring length of bubbles in surface boiling differs from that in saturated boiling, even in the same liquid, and modified equation (22) as follows:

$$\frac{H_{es}}{R} = \bar{T}\, T^* (\bar{R}e_b)^{-1} \tag{43}$$

Therefore

$$\bar{T} = H_{es}/H_e \tag{44}$$

where H_{es} is the effective stirring length of bubbles in surface boiling. Though ϕ^* in equation (24) should be modified by this correction factor $\bar{T}$, the writers corrected X for the sake of convenience.

Now, according to the experiments of Gunther [7] and Rohsenow and Clark [23], the maximum diameter of generated bubbles is 3 mm at most and about 1 mm in the mean diameter. On the other hand, since the effective stirring length of bubbles determined on saturated water under

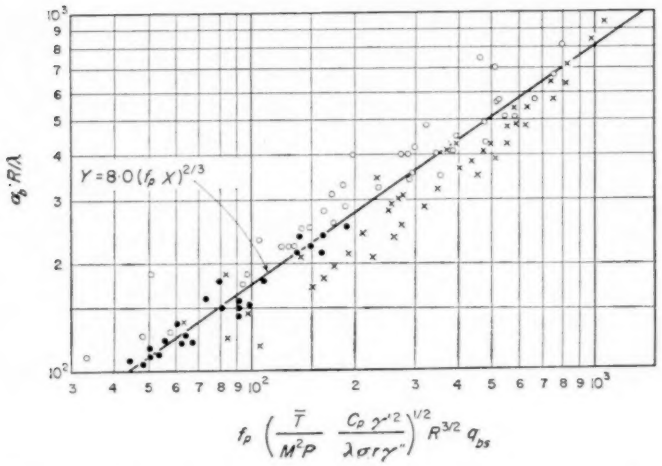

FIG. 10. Correlation of surface boiling heat transfer by the writers' method.

	Authors	p (atm)	v (m/sec)	$\Delta\theta_s$ (°C)	D and R (m)
○	Kreith–Summerfield	1–15	1·5–4	50–150	$1{\cdot}49 \times 10^{-2}$ (*D*)
×	Rohsenow–Clark	140	3–9	60–150	$4{\cdot}59 \times 10^{-3}$ (*D*)
●	Nishikawa–Urakawa	1	0	0–7	0·05 (*R*)

atmospheric pressure by the writers [16] is 30 mm. A satisfactory result has been obtained for saturated boiling inside tubes, in which case the effective stirring length of bubbles determined in the horizontal heating surface is used. Presuming the effective stirring length of bubbles in surface boiling is of the same order of magnitude as the diameter of bubbles, it may be reasonable to assume that $\bar{T} = d_0/H_e = 3/30 = 1/10$ for water.

The experimental data of Kreith and Summerfield [13] and of Rohsenow and Clark [4] were treated in this way, and the results are shown in Fig. 10. As seen in the figure, the experimental points are not only favourably arranged in a straight line, but are strongly suggestive of the fact that both surface boiling and saturated boiling can be represented by a single straight line. The same experimental data were treated by the formula of Rohsenow and the results are shown in Fig. 11.

The value of $\bar{T}$ may depend upon the degree of subcooling, the flowing condition and the heat flux. The writers [19] carried out the experiment on free convection surface boiling in order to clarify the effect of the degree of subcooling. They found that the relation shown in Fig. 12 holds between the rising height of bubble h, i.e. the height to which bubbles could rise without disappearance, and the degree of subcooling $(\theta_s - \theta_L)$. Since Fig. 12 was obtained from an experiment for a narrow range of heat flux, the data should be correlated by taking the heat flux as the changing parameter in the case of a large range of heat flux. In surface boiling, a bubble that has been generated on the heating surface condenses on its way up. The stirring effect of bubbles therefore gets smaller and smaller for two reasons, i.e. that the bubble goes up from the heating surface and that the size of bubble becomes smaller. Consequently, the writers assume that the effective stirring length

Vol. 1 1960

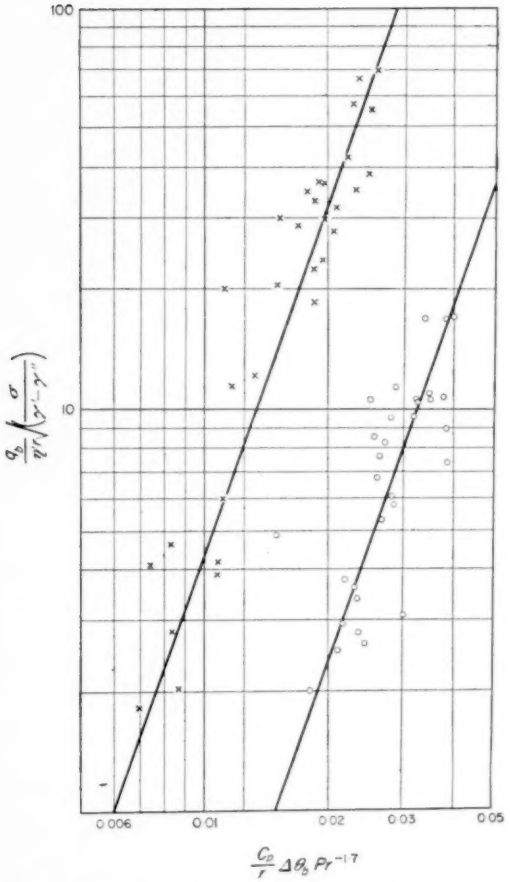

FIG. 11. Correlation of surface boiling heat transfer by Rohsenow's method.

○, Kreith–Summerfield; ×, Rohsenow–Clark.

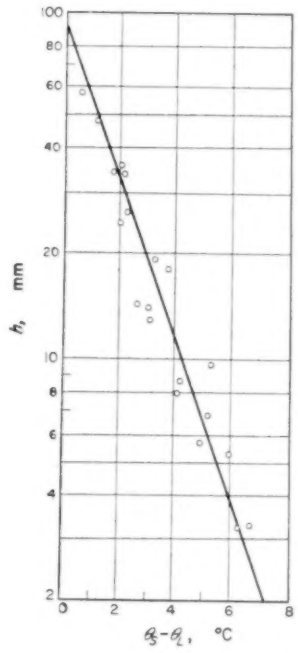

FIG. 12. Relation between rising height of bubble, h, and subcooling degree of liquid, $\theta_s - \theta_L$. (q = 15,000–26,000 kcal/m² hr).

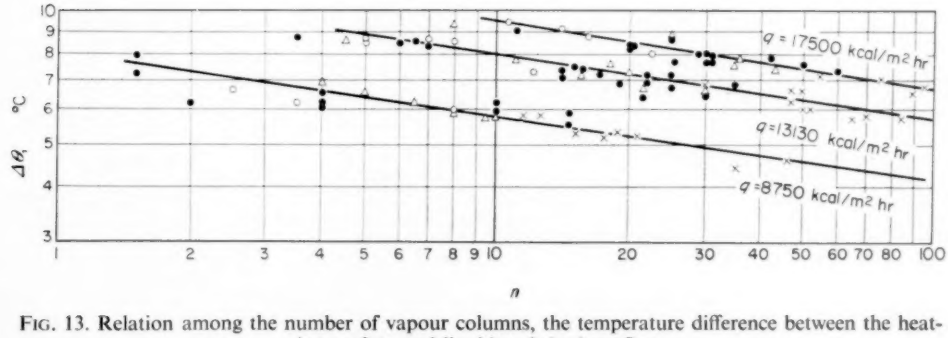

FIG. 13. Relation among the number of vapour columns, the temperature difference between the heating surface and liquid and the heat flux.

○, distilled water; ●, saponin solution; △, sodium oleate solution (3 p.p.m.); ×, sodium oleate solution (15 p.p.m.).

of bubbles is equal to the height of the circular cylinder that has the same volume of cone with one vapour column replaced. The result based on the above-mentioned assumption is plotted in Fig. 10.

The above-mentioned correlating method is only an example of the application of the writers' correlating equation. The behaviour of bubble generation in surface boiling differs from the case of saturated boiling. Therefore it is necessary to clarify the mechanism of heat transfer in surface boiling in order to obtain the correct correlation of surface boiling heat transfer.

6. CONCLUSION

The writers have logically derived a correlating equation of heat transfer in nucleate boiling for various kinds of liquids whose physical properties are different and indicated that this correlating equation is applicable to forced-convection saturated boiling or surface boiling. The writers' correlating equation has been obtained theoretically by analysing the elementary processes of the phenomena and is not based on a dimensional analysis. It is, therefore, considered that a good correlation between the proposed equation and the data of heat transfer shows the adequacy of the results of bubble dynamics obtained by the writers, and it is necessary to analyse the elementary processes of boiling phenomena and elucidate the relations underlying them in order to reach a final solution to the problem.

APPENDIX

The value of M in equation (15) for boiling water under atmospheric pressure is determined as shown below. Equation (14) can be rewritten as follows:

$$qR^2 = \left(\frac{r\gamma''}{6}\right) n d_u^3 f = \left(\frac{r\gamma''}{6}\right) n d_0^3 f \left(\frac{d_u}{d_0}\right)^3 \quad \text{(A1)}$$

As seen from Fig. 13, the following relation holds for boiling water under atmospheric pressure:

$$\Delta\theta = c_q\, n^{-1/6}\, (qR)^{2/3} \quad \text{(A2)}$$

where $\Delta\theta = \theta_p - \theta_L$ and c_q is the constant which varies according to the type of liquid.

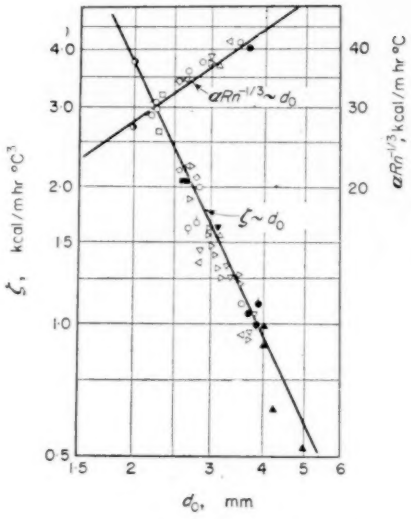

FIG. 14. Relation between bubble diameter just leaving the heating surface and foamability.

○, roughened surface with concentric grooves (average depth of groove, 0·1701 mm);
△, roughened surface with concentric grooves (average depth of groove, 0·0846 mm);
×, roughened surface with concentric grooves (average depth of groove, 0·0425 mm);
◎, roughened surface with concentric grooves (average depth of groove, 0·0090 mm);
◇, roughened surface with concentric grooves (average depth of groove, 0·0750 mm);
□, roughened surface with concentric grooves (average depth of groove, 0·1299 mm);
▽, roughened surface with concentric grooves (average depth of groove, 0·0192 mm);
▷, roughened surface with concentric grooves (average depth of groove, 0·0578 mm);
■, roughened surface with concentric grooves (average depth of groove, 0·0048 mm);
▼, roughened surface with crosswise grooves (average depth of groove, 0·0375 mm);
○, Nekal X water solution (Jakob);
▲, sugar water (Urakawa);
●, smooth surface $R = 5$ cm;
●, smooth surface $R = 7$ cm;
●, smooth surface $R = 3{\cdot}5$ cm;
○–, water solution of saponin;
○, sodium oelate solution (3 p.p.m);
–○, sodium oleate solution (15 p.p.m.).

Equation (A2) can be rewritten as follows:

$$\alpha\ R = \left(\frac{1}{c_q}\right) n^{1/6}\, (qR)^{1/3} \quad \text{(A3)}$$

Vol. 1 1960

On the other hand, equation (12) in laminar flow will be rewritten as follows by combining the physical constants and the variables which are considered not to change for a specified liquid:

$$\alpha R = c_K n^{1/3} (d_0^3 f)^{1/3} = c_K \chi^{1/3} n^{-1/3} d_0^{2/3} \quad \text{(A4)}$$

where

$$c_K \equiv \lambda K^* \left(Pr \frac{g H_e}{\nu^2} \frac{1}{U_m} \right)^{1/3}$$

Eliminating α from equations (A3) and (A4), the following expression can be obtained:

$$n = \left(\frac{1}{c_q c_K} \right)^6 (d_0^3 f)^2 (qR^2) \quad \text{(A5)}$$

Eliminating q from equations (A1) and (A2), the following equation can be obtained finally:

$$\left(\frac{d_u}{d_0} \right)^3 = M n^{-1/2} R \quad \text{(A6)}$$

where

$$M = \left(\frac{6}{r\gamma''} \right) (c_K c_q)^3 n^{-1/2} R$$

Since $c_q = 0{\cdot}149$ mhr$^{2/3}$°C/(kcal)$^{2/3}$, $r = 538{\cdot}8$, kcal/kg, $\gamma'' = 0{\cdot}598$, kg/m^3, $\chi = 400$ m/hr and $c_K \chi^{1/3} = 1800$ kcal/m$^{5/3}$hr°C (from Fig. 14) for the boiling water under the atmospheric pressure, the numerical value of M in this case is $M \fallingdotseq 900$ m^{-1}.

REFERENCES

1. J. N. Addoms, *Heat Transfer at High Rates to Water Boiling Outside Cylinders*. D.Sc. Thesis, Department of Chemical Engineering, MIT (1948).
2. G. A. Akin and W. H. McAdams, *Trans. Amer. Inst. Chem. Engrs.* **45**, 137 (1937).
3. M. T. Cichelli and C. F. Bonilla, *Trans. Amer. Inst. Chem. Engrs.* **41**, 755 (1945).
4. J. A. Clark and W. M. Rohsenow, *Trans. Amer. Soc. Mech. Engrs.* **76**, 553 (1954).
5. E. A. Farber and R. L. Scorah, *Trans. Amer. Soc. Mech. Engrs.* **70**, 369 (1948).
6. W. Fritz, *Phys. Z.* **36**, 379 (1935).
7. F. C. Gunther, *Trans. Amer. Soc. Mech. Engrs.* **73**, 115 (1951).
8. F. Hirano and K. Nishikawa, *Trans. Soc. Mech. Engrs. (Japan)* **18**, No. 72, 23 (1952).
9. F. Hirano and K. Nishikawa, *Trans. Soc. Mech. Engrs., (Japan)* **19**, No. 88, 33 (1953).
10. T. H. Insinger and H. Bliss, *Trans. Amer. Inst. Chem. Engrs.* **36**, 491 (1940).
11. M. Jakob, *Heat Transfer* Vol. 1, pp. 614–657. Wiley, New York (1949).
12. M. Jakob, *Proceedings of the Fifth International Congress on Applied Mechanics* pp. 561–564 (1938).
13. F. Kreith and M. Summerfield, *Trans. Amer. Soc. Mech. Engrs.* **71**, 805 (1949).
14. F. Kreith and A. S. Foust, *Remarks on the Mechanism and Stability of Surface Boiling Heat Transfer*. ASME, Paper No. 54–A–146, 1–10 (1954).
15. W. H. McAdams, *Heat Transmission*, pp. 368–409. McGraw Hill, New York (1954).
16. K. Nishikawa, *Mem. Fac. Engng., Kyushu University* **16**, No. 1, 1 (1956).
17. K. Nishikawa, *Mem. Fac. Engng., Kyushu University* **17**, No. 2, 85 (1958).
18. K. Nishikawa and K. Urakawa, *Trans. Soc. Mech. Engrs. (Japan)* **23**, No. 136, 935 (1958).
19. K. Nishikawa and K. Urakawa, *Tech. Rep. Kyushu University* **32**, No. 2, 98 (1959).
20. S. Nukiyama, *J. Soc. Mech. Engrs. (Japan)* **37**, No. 206, 367 (1934).
21. F. N. Peebles and H. T. Garber, *Chem. Engng. Progr.* **49**, No. 2, 88 (1953).
22. E. L. Piret and H. S. Isbin, *Chem. Engng. Progr.* **50**, No. 6, 305–311 (1954).
23. W. M. Rohsenow and J. A. Clark, *Trans. Amer. Soc. Mech. Engrs.* **73**, 609 (1951).
24. W. M. Rohsenow, *Heat Transfer with Evaporation, Lectures at Symposium on Heat Transfer* pp. 101–149. University of Michigan (1953).
25. K. Yamagata, F. Hirano and K. Nishikawa, *Trans. Soc. Mech. Engrs. (Japan)* **19**, No. 84, 4 (1953).
26. K. Yamagata, F. Hirano, K. Nishikawa and H. Matsuoka, *Mem. Fac. Engng., Kyushu University* **15**, No. 1, 97 (1955).

Int. J. Heat Mass Transfer. Vol. 1, pp. 236–241. Pergamon Press 1960. Printed in Great Britain

A COOLING PROBLEM OF PEBBLE-BED NUCLEAR REACTORS

L. S. DZUNG

Brown, Boveri & Co., Baden, Switzerland

(*Received* 15 *June* 1959; *revised* 19 *February* 1960)

Abstract—The fundamental equations for the steady-state flow of a gas through a porous medium with prescribed heat source are derived. Application of these equations enable the pressure drop and the flow distribution of a gaseous coolant through a pebble-bed type nuclear reactor to be calculated. One exact solution is given. The maximum gas temperature is found to be very much higher than the mixed mean value.

Résumé—Les équations fondamentales de l'écoulement permanent d'un gaz dans un milieux poreux ont été établies en présence d'une source de chaleur. L'application de ces équations conduit au calcul de la perte de charge et de la distribution de l'écoulement d'un fluide refroidisseur gazeux dans un réacteur du type à lit granuleux. Une solution exacte est obtenue. La température maximum du gaz est trouvée bien supérieure à celle donnée par la valeur moyenne du mélange.

Zusammenfassung—Für die stationäre Strömung eines Gases durch ein poröses Medium mit vorgegebener Wärmequelle werden die Grundgleichungen abgeleitet. Diese Gleichungen gestatten die Berechnung des Druckabfalls und der Strömungsverteilung eines Kühlgases beim Durchtritt durch einen Kernreaktor vom pebble-bed-Typ. Eine exakte Lösung wird mitgeteilt. Man findet, dass die höchste Gastemperatur sehr viel höher als der Mittelwert ist.

Abstract—Выведены основные уравнения переноса газа через пористую среду для стационарного режима с заданным тепловым источником. Применение этих уравнений позволяет вычислить перепад давлений и распределение скорости потока газа в среде крупнозернистого ядерного топлива реактора. Получено точное решение поставленной задачи. Найдено, что максимальная температура газа значительно превышает среднюю температуру смеси.

Vol. 1 1960

NOTATION

Any coherent set of units may be used.

a, b, defined in equation (6);
f defined in equation (18);
F, F', defined in equations (4), (5);
h, specific enthalpy;
k, isentropic exponent;
L, reactor core length;
p, pressure;
Q, heat generation per unit time and volume;
r, radial co-ordinate;
R, reactor core radius;
s, root of equation (12);
T, temperature;
v, specific volume;
w, $= r/R$;
z, axial co-ordinate.
Z, defined in equation (27)

Greek symbols

β, defined in equation (18);
θ, defined in equation (15);
κ, defined in equation (21);
λ $= k/(k-1)$;
μ, defined in equation (15);
ξ $= \pi z/L$;
ρ, density;
σ, defined in equation (13);
τ, defined in equation (16);
ψ $= \pi R/L$.

Subscripts

i, tensor index;
r, radial component;
z, axial component;
0, inlet condition.

INTRODUCTION

THE problem of flow distribution in gas-cooled nuclear reactor cylindrical channels has been treated in a previous paper [1]. It was shown that if the cooling channels are of the same size the non-uniformity of heat generation in the reactor core distorts the coolant flow in a very unfavourable way, such that hot spots are cooled by a smaller quantity of gas. In order to achieve a more uniform temperature distribution in such reactors, it is therefore necessary to vary the size of the cooling channels or to use suitable throttling devices at certain channels.

In case of the so-called pebble-bed reactors, the coolant flows through the rather irregular space between the pebbles. There are no straight guiding channels for the flow. Since cross-flow is possible in this case, the effect of non-uniform heating will be accentuated and the flow phenomenon is very much more complex than in the case of straight channels.

In this paper the fundamental equations of such a gas flow through a porous mass with non-uniform heat generation will be formulated. One exact solution of these equations for a typical case can be given. In general, however, only numerical solutions using digital computers would be feasible.

THE FUNDAMENTAL EQUATIONS

Consider the steady-state flow of a gas through a pebble-bed reactor. Since the flow space between the pebbles is irregular, it would be impossible to treat the flow field in detail. We shall therefore take the whole pebble-bed as an isotropic porous medium and consider only the mean velocity of gas flow through a unit section perpendicular to the average mass flow. Let u_i be this mean velocity vector.* Then the continuity equation may be written as

$$\operatorname{div}(\rho u_i) = 0$$

$\rho = 1/v$ being the density of the flowing gas. The energy equation, neglecting heat conduction through the mass, is:

$$\rho u_i \,.\, \operatorname{grad} h = Q$$

where h is the enthalpy per unit mass of the gas and Q is the density of heat generation. Introducing the Nabla operator, the above equations may be written as

$$\nabla_i u_i = \rho u_i \nabla_i v \tag{1}$$

$$\rho u_i \nabla_i h = Q \tag{2}$$

The equation of motion for the flow in a porous medium can be written in the following form in the case of laminar flow [3]:

$$\nabla_i p + a u_i = 0 \tag{3}$$

Namely, the pressure gradient is proportional and parallel to the velocity vector, a being the Darcy coefficient, which is proportional to the viscosity of the gas. For turbulent flow in one-dimensional case, the pressure head drop is related to the velocity head by: [3]†

$$(dp/dx) + F' \rho u^2 = 0 \tag{4}$$

where F' depends on the Reynolds number of flow. A generalization of this expression to a three-dimensional case can be accomplished by assuming that, on account of isotropy, the pressure gradient is in the same direction as the mean flow and that its magnitude depends only on the magnitude of the mass flux density; thus

$$\nabla_i p + F(\rho|u|)u_i = 0 \tag{5}$$

where $F(=F'\rho|u|)$ actually is a function of the Reynolds number, but the dependence on viscosity and on porous structure is ignored in the present study. F may be taken as

$$F = a + b\rho|u| \tag{6}$$

where a and b depend only upon the viscosity of the gas and the structure of the porous mass, The one-dimensional case of (5) reduces to a well-known form [3] of equation (4). Equation (3) is included in (5) if $b = 0$ or at small mass flux.

* No distinction is made between a vector and its components nor between its covariant and contravariant components in case of non-Cartesian co-ordinates [2]. There should be no danger of confusion. The summation convention of tensor notation is understood where it applies.

† For high Mach numbers, a term proportional to $\rho u(du/dx)$ must be included. This term may be neglected in the present application.

One more equation is needed to complete the description of the flow. The coolant will be taken as a polytropic gas (i.e. ideal gas with constant specific heats) or more generally a polytropic vapour [4]. Then the specific enthalpy is given by:

$$h = \lambda pv + \text{const.} \qquad \lambda \equiv k/(k-1) \tag{7}$$

where k is the isentropic exponent.

Equations (1), (2), (5) and (7) are now completely sufficient for the problem. If the boundary conditions and the heat source Q are given, the unknown quantities u_i, p, v, h can be solved. It is evident that an exact solution is impossible in the majority of cases.

In the application to pebble-bed reactors, it can be assumed that the pressure drop through the reactor is only about a few per cent of the absolute pressure [1]. In equation (7) the effect of pressure change on enthalpy can then be neglected and the flow can be considered as practically isobaric with respect to density and temperature changes. Equation (7) can be written as

$$\nabla_i h = \lambda \bar{p} \nabla_i v$$

where $\bar{p}$ is the mean pressure. Substitution into equation (2) results in

$$\rho u_i \nabla_i v = u_i \nabla_i (\log v) = Q/\lambda \bar{p} \tag{8}$$

and, using equation (1),

$$\nabla_i u_i = Q/\lambda \bar{p} \tag{9}$$

We thus obtain the interesting result that the velocity field corresponds to that of an incompressible flow having a mass-source distribution proportional to the actual heat source.

THE CYLINDRICAL REACTOR PROBLEM

We shall now apply the above set of equations to a cylindrical reactor core with radius R and length L, Fig. 1. The cooling gas enters from one end at the cylindrical co-ordinate $z = 0$ and leaves the other end at $z = L$. The heat source density is assumed to be axisymmetrical and is given by [1]:

$$Q(r, z) = \bar{Q} \cdot \frac{\pi}{2} \cdot \frac{s}{2J_1(s)} J_0(ws) \sin \xi \tag{10}$$

where

$$w \equiv r/R, \qquad \xi \equiv \pi z/L \tag{11}$$

and $\bar{Q}$ is the average density of heat source in the entire reactor core. s is the smallest root of the equation

$$J_0(s) = \sigma s J_1(s) \tag{12}$$

and

$$\sigma R \equiv \left[\frac{Q}{-dQ/dr}\right]_{r=R}$$

is the so-called extrapolation length, which depends on the effectiveness of the reflector on the cylindrical surface.

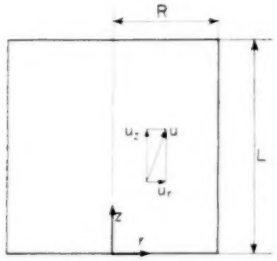

FIG. 1. Cylinder co-ordinates of the reactor core. Gas flows vertically upward.

Using (10), equation (9) in cylindrical co-ordinates becomes

$$\psi \frac{\partial \mu_z}{\partial \xi} + \frac{1}{w} \cdot \frac{\partial (w\mu_r)}{\partial w} = \psi\theta \cdot \frac{s}{4J_1(s)} \cdot J_0(ws) \sin \xi \tag{14}$$

where

$$\left.\begin{aligned} &\mu_z \equiv u_z/\bar{u}_0, \mu_r \equiv u_r/\bar{u}_0, \psi \equiv \pi R/L \\ &\theta \equiv (\overline{\Delta T})/T_0 = (\pi R^2 L \bar{Q})/(\pi R^2 \bar{u}_0 \lambda \bar{p}) \end{aligned}\right\} \tag{15}$$

u_z, u_r are the axial and radial components of the velocity vector, $\bar{u}_0$ being the mean velocity at entry. θ is the ratio of the mixed mean temperature rise ($\overline{\Delta T}$) to the absolute temperature* T_0 of the gas at entry.

Now define

$$\tau \equiv v/v_0 \tag{16}$$

* This is correct only for polytropic gas. For polytropic vapour, the modification is obvious.

Vol. 1 1960

where v_0 is the specific volume at entry. Since the pressure has been assumed constant, τ is also the ratio of absolute temperatures. Substitution of (10) into equation (8) gives

$$\psi\mu_z \cdot \frac{\partial \log \tau}{\partial \xi} + \mu_r \cdot \frac{\partial \log \tau}{\partial w} = \\ = \psi\theta \cdot \frac{s}{4J_1(s)} \cdot J_0(sw) \sin \xi \qquad (17)$$

Finally, writing

$$\left.\begin{aligned} &\beta \equiv \pi(p_0 - p)/(\Delta p)_0, (\Delta p)_0 \equiv F(\rho_0 \bar{u}_0)\bar{u}_0 L \\ &f \equiv F(\rho|u|)/F(\rho_0 \bar{u}_0) \end{aligned}\right\} \qquad (18)$$

equation (4) can be separated into its components:

$$\frac{\partial \beta}{\partial \xi} = f\left(\frac{|\mu|}{\tau}\right) \cdot \mu_z, \quad \frac{\partial \beta}{\partial w} = \psi f \left(\frac{|\mu|}{\tau}\right) \mu_r \qquad (19)$$

The normalization denominator $(\Delta p)_0$ is evidently the pressure drop which would result if there were no heat generation and the gas conditions at entry could remain unchanged during the through flow.

The four equations (14), (17), (19) now form a simultaneous set for the four unknown quantities $\mu_z, \mu_r, \tau, \beta$. The boundary conditions are

$$\left.\begin{aligned} &\left.\begin{aligned} &\mu_r = 0, \beta = 0 \\ &\bar{\mu}_z \equiv \int_0^1 2\mu_z w \, dw = 1 \end{aligned}\right\} \text{for } \xi = 0 \\ &\mu_r = \frac{\partial \beta}{\partial w} = 0 \text{ for } \xi = \pi, \\ &\qquad \text{or } w = 0 \text{ and } w = 1 \end{aligned}\right\} \qquad (20)$$

If equation (6) is used, the function f can be written as

$$f = \frac{1 + \kappa|\mu|/\tau}{1 + \kappa}, \quad \kappa \equiv \frac{b\rho_0 \bar{u}_0}{a} \qquad (21)$$

κ is a measure of the degree of turbulence and depends upon the Reynolds number at entry.

LAMINAR FLOW

One exact solution is possible for a special form of f, namely if in equation (5) F is constant or in (21) $f = 1$, which is the case if the flow is everywhere laminar and if the change of viscosity with temperature is negligible. Then equation (3) applies and equations (19) become

$$\frac{\partial \beta}{\partial \xi} = \mu_z, \quad \frac{\partial \beta}{\partial w} = \psi\mu_r \qquad (22)$$

Taking the divergence of equation (3) or of equations (22) and substituting equation (9) or equation (14), one obtains a Poisson's equation:

$$\nabla_i \nabla_i p + \frac{a}{\lambda \bar{p}} \cdot Q = 0 \qquad (23)$$

for the general case and

$$\psi^2 \frac{\partial^2 \beta}{\partial \xi^2} + \frac{1}{w} \cdot \frac{\partial}{\partial w}\left(w \frac{\partial \beta}{\partial w}\right) \\ = \theta \cdot \frac{\psi^2 s}{4J_1(s)} \cdot J_0(sw) \sin \xi \qquad (24)$$

for the special case of equation (10).

Equation (24) with the boundary conditions (20) can be readily solved analytically by classical means. The result is

$$\left.\begin{aligned} \beta(w, \xi) &= \left(1 + \frac{\theta}{2}\right)\xi - \\ &- \frac{\theta}{4} \cdot \frac{\psi^2 s^2}{\psi^2 + s^2}\left[\frac{J_0(ws)}{sJ_1(s)} + \frac{I_0(\psi w)}{\psi I_1(\psi)}\right] \sin \xi \\ \mu_z(w, \xi) &= \frac{\partial \beta}{\partial \xi} = 1 + \frac{\theta}{2} - \\ &- \frac{\theta}{4} \cdot \frac{\psi^2 s^2}{\psi^2 + s^2}\left[\frac{J_0(ws)}{sJ_1(s)} + \frac{I_0(w\psi)}{\psi I_1(\psi)}\right] \cos \xi \\ \mu_r(w, \xi) &= \frac{1}{\psi} \cdot \frac{\partial \beta}{\partial w} = \\ &= \frac{\theta}{4} \cdot \frac{\psi s^2}{\psi^2 + s^2}\left[\frac{J_1(ws)}{J_1(s)} - \frac{I_1(w\psi)}{I_1(\psi)}\right] \sin \xi \end{aligned}\right\} \qquad (25)$$

J and I are the two Bessel's functions. The correctness of (25) can be easily verified by substituting into equations (20) and (24).

Fig. 2 shows the velocity components μ_z and μ_r for $\sigma = 0$, $(s = 2{\cdot}405)$ and $\psi = \pi/2 (L = R2)$. It may be noted that the velocity field is practically axial if θ is not very much greater than unity.

To determine the temperature field, it will be necessary to solve equation (17) together with (25). The boundary condition is

$$\tau = 1 \text{ for } \xi = 0 \qquad (26)$$

This is a differential equation of first order and

can be solved numerically or graphically using the well-known isocline method. Owing to the complexity of equation (25) an analytical solution is difficult.

If only the maximum temperature $\tau_m = T_m/T_0$ is needed, then this can be determined analytically. It can be seen that the maximum temperature must occur on the stream line through the cylindrical axis. For this stream line, we have

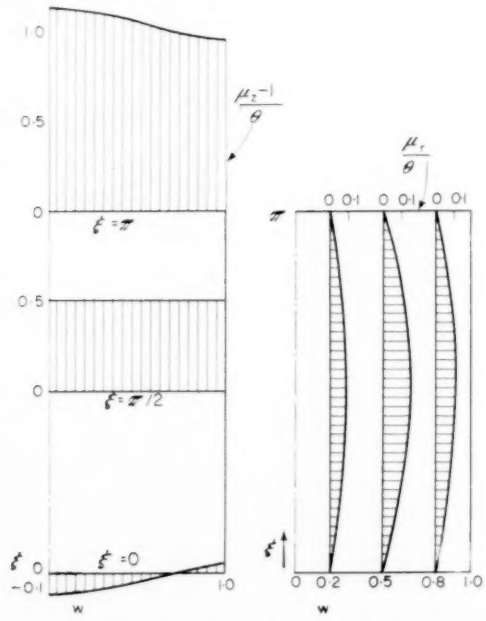

FIG. 2. Coolant velocity field within the reactor core. The plotted values are the axial and radial components of the additional velocity above the adiabatic incompressible values. The additional velocity is proportional to the average heat generation.

evidently $\mu_r = 0$ always due to symmetry. Then equation (17) becomes:

$$\mu_z(0, \xi)\frac{d\log\tau}{d\xi} = \frac{\theta}{4}\cdot\frac{s}{J_1(s)}\cdot\sin\xi$$

and substituting μ_z from (25):

$$d\log\tau = \frac{(\theta/4)\,[s/J_1(s)]\sin\xi\,d\xi}{(1+\theta/2) - (\theta/4)\,Z(\psi, s)\cos\xi}$$

$$Z(\psi, s) \equiv \frac{\psi^2 s^2}{(\psi^2+s^2)}\left[\frac{1}{sJ_1(s)} + \frac{1}{\psi I_1(\psi)}\right] \quad (27)$$

This is readily integrated. The maximum temperature is at the exit point $\xi = \pi$ and its value is

$$\tau_m = \left\{\frac{(1+\theta/2) + (\theta/4)\,Z(\psi, s)}{(1+\theta/2) - (\theta/4)\,Z(\psi, s)}\right\}^n$$

$$n \equiv \frac{1 + s^2/\psi^2}{1 + sJ_1(s)/\psi I_1(\psi)} \quad (28)$$

For the data above ($s = 2{\cdot}405$, $\psi = \pi/2$), the evaluation of (28) results in

$$\left.\begin{aligned}\tau_m &= 5{\cdot}15, \text{ for } \theta = 1\\ \tau_m &= 14{\cdot}7, \text{ for } \theta = 2\end{aligned}\right\} \quad (29)$$

These values are very much higher than the mixed mean temperature, which is, by definition, given by

$$\bar{\tau} = 1 + \theta \quad (30)$$

The maximum temperature rise can therefore be many times the average temperature rise.

TURBULENT FLOW

The assumption of laminar flow is perhaps non-realistic for the application to pebble-bed reactors. If turbulence is assumed, then the general expression (21) must be used in equation (19), and only numerical solution using digital computer would be feasible. However, some qualitative effects of turbulence may be inferred from the basic equations. Since according to Fig. 2 the magnitude $|\mu|$ of the velocity does not vary very much at sections perpendicular to the axis, the mass flux density in one section will be principally determined by the temperature, i.e. τ in equation (21). Near the axis the heat rate and hence the temperature is high. The frictional force f is smaller according to (21). Equations (19) then show that the velocity there will be higher than in the laminar case. This would mean that the central part gets more cooling gas and the temperature is therefore less acute than in the laminar case. Hence turbulence favours the temperature distribution.

CONCLUSION

It is seen from the calculation that although

Vol. 1 1960

the velocity field depends mainly upon the average heating rate of the cooling gas and is rather uniform throughout a cross-section of the flow, the temperature field may be quite non-uniform for laminar flow. The maximum value of the temperature rise may be many times the average value. Turbulence in the flow may flatten the temperature peak, but the exact value cannot be determined without a more thorough solution of the given equations.

REFERENCES

1. L. S. DZUNG, *Brown Boveri Rev.* **45**, 14 (1958).
2. L. S. DZUNG, *Brown Boveri Rev.* **40**, 321 (1953).
3. P. C. CARMAN, *Flow of Gases through Porous Media.* Butterworths, London (1956).
4. L. S. DZUNG, *Z. angew. Math. Phys.* **6**, 207 (1955).

ol.
960

Int. J. Heat Mass Transfer. Vol. 1, pp. 242–254. Pergamon Press 1960. Printed in Great Britain.

THE THERMAL CONDUCTIVITY OF HEAVY WATER BETWEEN 75° AND 260°C AT PRESSURES UP TO 300 ATM

H. ZIEBLAND and J. T. A. BURTON

Explosives Research and Development Establishment,
Waltham Abbey, Essex

(*Received* 28 *September* 1959)

Abstract—The thermal conductivity of heavy water having an isotopic purity of 99·85 per cent was measured with a vertical coaxial cylinder apparatus at pressures between 24 and 294 atm in the temperature range 75° to 260°C. The pressure range of the experiments included the critical pressure (218 atm).

Identical with the trend exhibited by water, the thermal conductivity of heavy water was found to increase with rising temperature to a shallow maximum near 110°C and to fall with a further rise in temperature. The influence of pressure on thermal conductivity was small, and at 75°C amounted to an increase of 0·77 per cent for a pressure rise from 1 to 100 atm. This is similar to the values reported for natural water by previous investigators [9, 11].

In comparison with natural water, the thermal conductivity of heavy water, in the range investigated, was always lower. According to these tests the ratio k_{H_2O}/k_{D_2O} increased almost linearly from 1·045 at 75°C to a value of 1·134 at 260°C.

No measurements of the thermal conductivity of heavy water have previously been reported at temperatures above 82°C. Below this temperature the present data are in good agreement with earlier work.

Résumé—La conductivité thermique de l'eau lourde ayant une pureté isotopique de 99,85 pour cent a été mesurée avec un appareillage à cylindres coaxiaux verticaux à des pressions variant de 24 à 294 atmosphères et à des températures variant de 75° à 260°C; le domaine des pressions utilisé dans l'expérience comprenanit la pression critique (218 atm).

Suivant la tendance montrée par l'eau, la conductivité thermique de l'eau lourde augmentait avec la température, jusqu'à un maximum aplati à 110°C environ et décroissait quand la température augmentait encore. L'influence de la pression sur la conductivité thermique était faible et, à 75°C, correspondait à une augmentation de 0,77 pour cent pour une augmentation de pression de 1 à 100 atm. Ces résultats sont analogues à ceux trouvés pour l'eau naturelle par les auteurs précédents [9, 11].

Comparée à celle de l'eau naturelle, la conductivité thermique de l'eau lourde était toujours inférieure, dans le domaine étudié. D'après ces expériences, le rapport k_{H_2O}/k_{D_2O} augmentait presque linéairement de 1,045 à 75°C à 1,134 à 260°C.

Jusqu'à présent, il n'existait pas de résultats connus de mesures de conductibilité thermique de l'eau lourde à des températures dépassant 82°C. Au-dessous de cette température, les résultats présents sont en bon accord avec les études précédentes.

Zusammenfassung—Die Wärmeleitfähigkeit von schwerem Wasser mit einer Isotopenreinheit von 99,85 Prozent wurde in einer Apparatur mit senkrechten koaxialen Zylindern bei Drücken von 24 bis 294 atm und Temperaturen von 75° bis 260 °C gemessen (kritischer Druck 218 atm).

Ähnlich wie bei leichtem Wasser hat auch die Wärmeleitfähigkeit von schwerem Wasser ein flaches Maximum bei 110 °C. Der Druckeinfluss ist gering; bei 75 °C erhöht sich die Wärmeleitfähigkeit um 0,77 Prozent bei Druckerhöhung von 0 auf 100 atm. Für leichtes Wasser wurde ähnliches beobachtet [9, 11].

Im Versuchsbereich war die Wärmeleitfähigkeit von schwerem Wasser geringer als die von leichtem Wasser. Das Verhältnis k_{H_2O}/k_{D_2O} steigt linear von 1,045 bei 75 °C zu 1,134 bei 260 °C an.

Für den Bereich oberhalb 82 °C wurden bisher keine Ergebnisse mitgeteilt. Unterhalb dieser Temperatur stimmen die Werte dieser Arbeit gut mit früher veröffentlichten überein.

Vol.
1
1960

Abstract—«Исследование теплопроводности тяжелой воды в интервале температур от 75° до 260°C и давления до 300 ат.»

Коэффициент теплопроводности тяжелой воды с изотопной чистотой 99,85% определяется обычным методом в диапозоне температуры от 75° до 260°C и давлений от 24 до 294 ат, включая и критическое давление (218 ат).

Было установлено, что с повышением температуры коэффициент теплопроводности тяжелой воды увеличивается, при температуре 110°C достигает максимума, а затем уменьшается. Повышение давления мало влияет на величину коэффициента теплопроводности, например, при увеличении давления от 1 до 100 ат. при 75°C изменение теплопроводности составляет 0,77%. Аналогичные данные были получены другими исследователями [9,11] для обычной воды.

Коэффициент теплопроводности тяжелой воды k_{D_2O} при исследованных режимных параметрах меньше коэффициента теплопроводности обычной воды k_{H_2O}. Ожижение $\frac{k_{H_2O}}{k_{D_2O}}$ является линейной функцией температуры, при 75°C это ожижение равно 1,045, а при 260°C — 1,134. Экспериментальные данные по коэффициенту теплопроводности тяжелой воды при температурах выше 82°C впервые приведены в этой статье, при температурах ниже 82°C данные авторов совпадают с ранее опубликованными.

LIST OF SYMBOLS AND DIMENSIONS

k = thermal conductivity (cal cm^{-1} $°C^{-1}$ sec^{-1});
k_0 = thermal conductivity at zero pressure (cal cm^{-1} $°C^{-1}$ sec^{-1});
L = length of emitting cylinder (cm);
P = absolute pressure (atm);*
Q = heat flow (cal sec^{-1});†
r_1, r_2 = radii of emitting and receiving cylinders, respectively (cm);
t_1, t_2 = surface temperatures of emitting and receiving cylinders, respectively (°C);
T = absolute temperature (°K);
α = pressure coefficient of thermal conductivity (atm^{-1}).

1. INTRODUCTION

THE thermal conductivity of heavy water in its liquid phase at 1 atm pressure has been studied by three investigators.

Bonilla and Wang [1] measured the thermal conductivity of 93 per cent pure heavy water relative to natural water in a two-gap horizontal plate apparatus between 15° and 60°C. According to these authors' observations the ratio of the respective conductivities k_{H_2O}/k_{D_2O} varied linearly with temperature, rising from 1·016 at 10°C to 1·033 at 60°C.

Meyer and Eigen [2] investigated a sample of heavy water of 95 per cent purity using a modification of the flat plate apparatus characterized by an unusually wide gap (5 cm) and a small cross-section (3 cm^2).

The most extensive measurements are due to Challoner and Powell [3] who studied the thermal conductivity of 99·95 per cent pure heavy water in a guarded hot-plate apparatus over the range from 2° to 82°C.

Despite the good numerical agreement between the results of the various authors—the deviation of individual data from a mean curve was rarely more than 1 per cent—some characteristic trends and differences became apparent during a recent survey of these three investigations, on the basis of which new values were proposed for the thermal conductivity of heavy water in the temperature interval from 10° to 80°C [11].

Heavy water is used in atomic power plants as a reactor coolant and moderator, and it was chiefly because of the former application that more data on its thermal conductivity were required covering a wide range of temperature and pressure.

2. DESCRIPTION OF METHOD

The vertical co-axial cylinder method with guard rings, which had been successfully employed in two previous investigations on the thermal conductivity of liquefied gases [4, 5], was also chosen for the determination of the thermal conductivity of heavy water. In this method, heat is generated in an inner emitting cylinder, and conducted radially through the narrow fluid-filled annulus to a co-axial receiving cylinder. From the measured surface

* 1 atm = 660 mm Hg.
† 1 cal = 4·184 J.

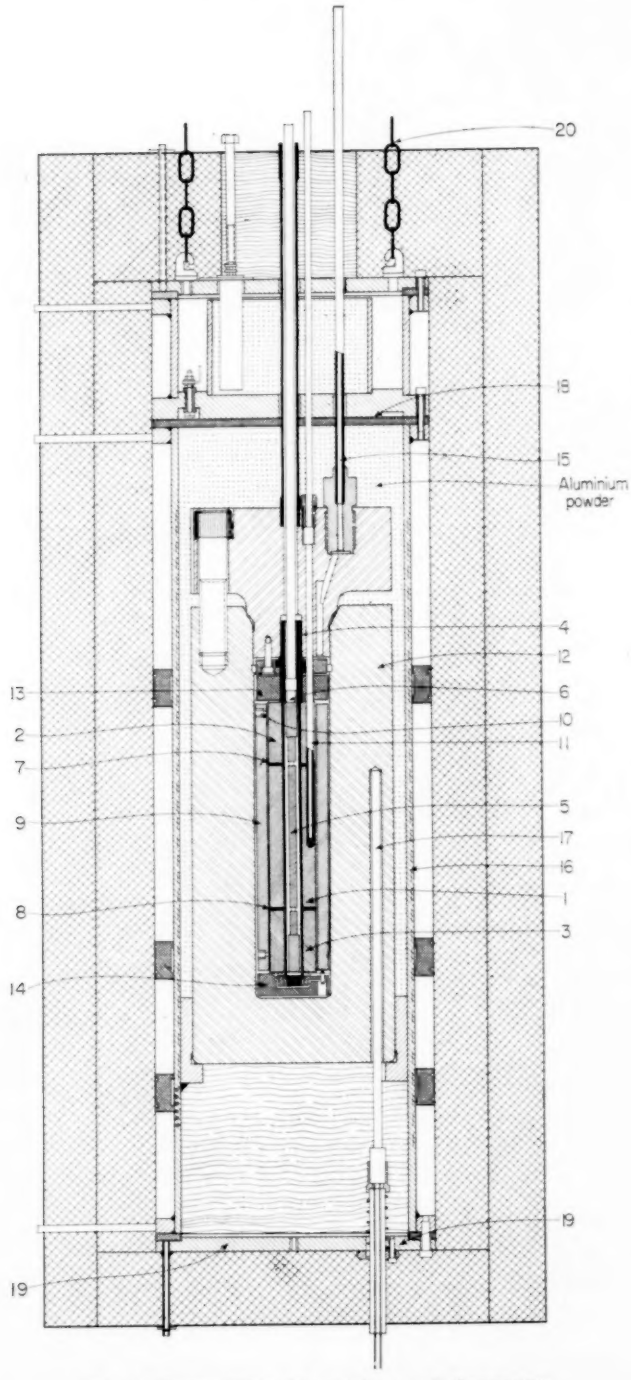

FIG. 1. Cross-section of autoclave and thermostat.

Vol.
1
1960

temperature of the emitting and receiving cylinders, the amount of heat conducted radially through the annulus, and the dimensions of the apparatus, the thermal conductivity can be evaluated from the following equation:

$$k = Q \ln (r_2/r_1)/2\pi L(t_2 - t_1).$$

3. EXPERIMENTAL

3.1 *The conductivity cell*

An annotated cross-section of the conductivity cell, the retaining autoclave and the thermostat is shown in Fig. 1.

The inner emitting cylinder (1) and two heat guards (2) and (3) of the same diameter were mounted on a stainless steel sheath (4). The emitting cylinder and each heat guard were heated by independently controlled electric heaters (5), consisting of uniform windings of constantan wire on a glass former (6). Each heat guard was separated from the emitting cylinder by mica washers (7) and (8) of 0·1 cm thickness. Current for the heaters was drawn from a large nickel–iron battery. An outer receiving cylinder (9) was arranged coaxially about the emitting cylinder to form an annulus of nominally 0·02 cm width. Accurate coaxial alignment was achieved by three uniformly spaced mica leaves of equal thickness, inserted into each end of the annulus and held in place by grub screws (10).

Holes were drilled through the emitting and receiving cylinders, and into these holes, close fitting thin walled stainless steel sheaths (11) were inserted, to protect the thermocouples placed in them from the effects of pressure and the chemical action of the substance investigated.

The cylinders were made of Hidural 5, a high conductivity copper alloy, supplied by Langley Alloys, Ltd., Slough. The conductivity cell was placed within a monel autoclave (12) designed for pressures up to 300 atm at 400°C. To reduce convection in the experimental fluid in the autoclave, the free spaces above and below the emitting and receiving cylinders were filled as far as possible with suitably shaped pieces of fired pyrophillite (wonderstone) (13) and (14). The autoclave was filled by means of the inlet connexion (15) in the lid.

3.2. *The thermostat*

The assembled autoclave was placed in a heavy gauge steel tube (16) which carried on its external surface an electric heater. To ensure good thermal contact, whilst at the same time providing for the differential thermal expansion, the inter-space between the heat tube and the autoclave was filled with aluminium powder. The temperature of the conductivity cell was maintained by a Sunvic Resistance Thermometer Controller, Type RT 2, which controlled the current in the thermostat heater. The temperature-sensing element, a platinum resistance thermometer (17), was placed in a hole drilled in the body of the autoclave.

In addition, manually controlled electric heaters (18) and (19) were fitted to the top and bottom of the heater tube to compensate for end losses. All thermostat heaters were fed from the electric mains via a common voltage stabilizer and individual variable transformers. Chromel–alumel thermocouples were attached to various parts of the thermostat, so that axial temperatures could be checked and the heater controls adjusted accordingly (see Fig. 2).

The complete assembly of autoclave and thermostat was suspended on four chains (20) and was thermally insulated. The temperature stability with this arrangement was very good. Variations from a chosen value over a period of several hours were less than 0·01°C, and in some cases this stability was maintained for several days.

3.3. *The pressure transmitter and expansion vessel* (*Fig.* 2)

Part of the investigation was conducted at elevated pressures not only because of the increasing saturation pressure with increasing temperature, but also because it was intended to study in general the effect of pressure on the thermal conductivity in the temperature region above 100°C. In view of the wide range of experimental conditions (pressure, temperature), some expansion of the test fluid, filled initially at ambient conditions into the autoclave, will take place. To allow for these changes in volume, and at the same time separate the heavy water from the pressurizing fluid, an expansion and pressure transmitting vessel *PT* was arranged between the autoclave containing the conductivity cell and

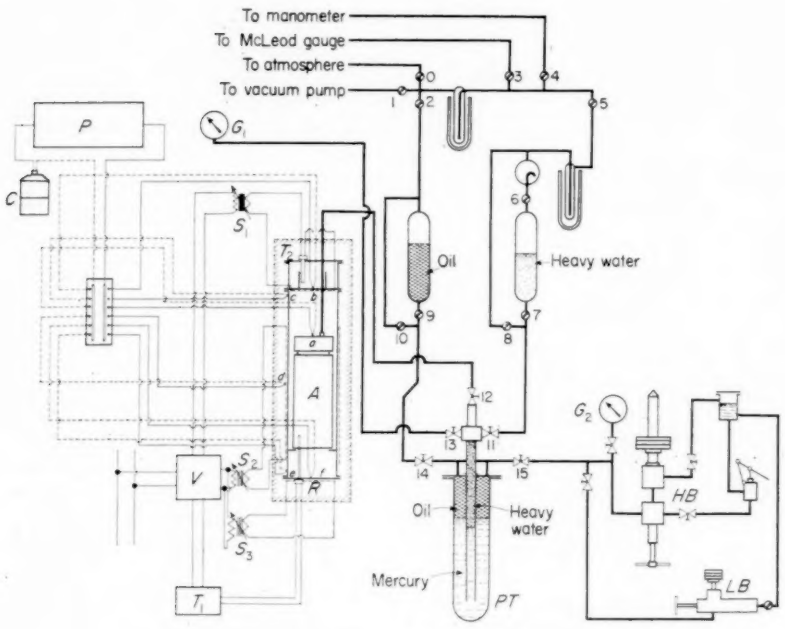

FIG. 2. Schematic lay-out of experimental apparatus.

A	Conductivity cell.	R	Resistance thermometer
P	Potentiometer	S_1, S_2, S_3	Variable transformer
C	Cold junction	G_1, G_2	Pressure gauges
a—f	Thermocouples	HB	High pressure balance
V	Voltage stabilizer	LB	Low pressure blance
T_1, T_2	Thermostat controller	PT	Pressure transmitter.

the high pressure and low pressure balances *HB* and *LB*.

The lower half of this vessel was filled with mercury as a separating fluid between the oil from the pressure balance and the heavy water that rested in the immersion tube above the mercury. The volume of the immersion tube was sufficiently large to allow for the expansion of the quantity of liquid contained in the autoclave. The pressure of the test fluid in the autoclave was kept constant at a desired value by occasionally operating the oil presses of the high or the low pressure balances *HB* or *LB*, respectively.

3.4. *Temperature measurement and calibration of thermocouples*

All temperatures were measured with copper–constantan thermocouples, and an ice bath was used to provide a reference temperature. The e.m.f.s generated by the couples were measured with a Diesselhorst potentiometer having a least count of 0·1 μV. With these thermocouples a temperature variation of 0·0025°C could be detected.

The thermocouples were made of multi-stranded wires to minimize the effects of inhomogeneities on thermal e.m.f.s; twelve wires, 44 s.w.g. formed the constantan member, and four wires, 40 s.w.g. the copper member. The junctions were silver-soldered into small copper cylinders which, in turn, were hard-soldered to the ends of thin-walled stainless steel tubes. Electrical insulation inside the stainless steel tube was provided by twin-bore alumina tubing. The cold junctions were made in an identical way, with the exception that the wires were supported by twin-bore silica tubes and the soldered junctions at the ends were electrically insulated by a thermo-setting resin. The upper

ends of the hot junctions contained in the stainless steel tubes were also sealed by a thermosetting resin after they had been dried by heating to about 300°C. This construction eliminated slow oxidation of the thermocouples and the ensuing effects on the thermal e.m.f.s.

The two thermocouples for measuring the important temperature difference across the fluid-filled annulus were located in the middle of the emitting and receiving cylinders, respectively. For the control of the heat guards, a thermocouple was placed in each guard cylinder about 3 mm from the separating mica washer. By means of steel springs, which pressed the thermal junctions against the closed end of the retaining sheaths, good thermal contact was ensured.

The calibration was performed by replacing the autoclave shown in Fig. 1 by a block of copper of the same dimensions. A central hole was drilled in the block to accommodate a NPL-calibrated platinum resistance thermometer, and the thermocouples were placed in holes drilled on a pitch circle round it. The temperature was then controlled by the same thermostat that was used when making conductivity measurements. An ice bath provided the reference temperature. Over the temperature range from 20° to 385°C the e.m.f.–temperature relationship could be represented by a cubic equation.

Although multistranded wires were used in the construction of the couples, small differences of the order of 1 μV were observed for the same temperature between individual couples. The thermocouples were therefore frequently intercalibrated *in situ* in the thermal conductivity cell with the emitter heaters switched off, as explained later.

3.5. *The geometric constant, and its dependence on temperature*

The equation for the evaluation of the thermal conductivity given in Section 2 contains the term $\ln (r_2/r_1)/2\pi L$ which is solely dependent on the linear dimensions of the apparatus used. It is usually referred to as the geometric constant of the conductivity cell.

To obtain a high degree of absolute accuracy, precision machining of the emitting and receiving cylinders was essential. The construction of the cell used in this research was carried out by Pitter Gauge and Precision Tool Company, Ltd., Woolwich, who also determined the dimensions contained in the geometric constant.

It was found that the deviations of the diameters of emitting and receiving cylinders from mean values of 3·3062 cm and 3·3493 cm, respectively, were less than 0·0001 cm at any part of their entire length.

The dimensions of the cylinders at the temperature of the experiments were calculated from the known dimensions at 20°C and the coefficient of thermal expansion of Hidural 5 quoted by Langley Alloys, Ltd., Slough [6]. The geometric constant changes only by 5 per cent over the temperature range from 75° to 360°C, so that, even if the data for Hidural 5 were somewhat in error, the effect on the accuracy of the reported data on the thermal conductivity of heavy water would be almost negligible.

Because of the low compressibility of metals, pressure had an insignificant effect on the dimensions of the cylinders.

3.6. *The heater and electrical energy measurement*

The emitting cylinder and the two guard sections were heated by an electrical heating element which consisted of three separate, closely wound sections of 30 s.w.g. glass-covered, oxidized constantan wire.

Various configurations of this kind of heater were constructed and tried; the one described below was found to be the most satisfactory for use at elevated temperatures.

It consisted of a central, 2 ft long, thin-walled, stainless steel tube of 0·25 cm external diameter as structural support, on the surface of which, alternately, glass tubes and glass rods of 0·2 cm diameter and a total length equal to that of the heater were fastened. Over this assembly the three heater sections were wound and hard-soldered to 22 s.w.g. pure silver leads, which were brought down to the requisite position inside the glass tubes. In addition to the current-carrying leads, a pair of potential leads was connected to the centre section of the heater. Several layers of glass tape wound over all sections provided additional protection against mechanical and electrical hazards, and also ensured a close fit in the heater sheath.

This construction offered a number of advantages over previous designs, the principal one being a considerable reduction, if not elimination, of axial heat exchange between individual heater sections. The heat dissipated in the emitting cylinder was evaluated from measurements of the current flowing through the appropriate heater section and the potential difference across it. The current was determined by measuring the potential difference across a standard resistance of 0·01 Ω; the potential difference across the heater was obtained with the aid of a potential divider having a ratio of 10^4:1. All measurements of potential differences were made with a Diesselhorst-pattern potentiometer, made by H. Tinsley and Co., Ltd., London.

Because of the small currents employed, and the high electrical conductance of the leads, no corrections were required for the small quantity of Joule's heat generated in those portions of the leads which were situated in the centre section of the heater.

A further error could arise through conduction of heat along the 22 s.w.g. silver leads which carried the current to the main heater. The guard ring heaters, however, were always carefully adjusted so that the axial temperature difference between the centre of the emitter and the guard rings was only about 0·045°C. Because of the close contact between the heater and the metallic heater sheath (4), which in turn fitted with a press fit into the emitter cylinder assembly, a similar small axial temperature variation can be assumed for the heater itself. As, furthermore, the leads to the main heater section are exposed over a length of about 5 cm to near isothermal conditions it was considered unlikely that heat conduction along those leads was of any significance.

3.7. *The filling and emptying of autoclave and pressure transmitter*

Just above the pressure transmitter *PT* in Fig. 2, a glass apparatus is shown, the main purpose of which was to ensure gas-free filling of heavy water into the autoclave and the relevant section of the pressure transmitter, and, in view of the high cost of heavy water, also to facilitate its complete recovery from all parts of the experimental apparatus after the tests.

It can be seen from Fig. 2 that the pressure transmitter consists in effect of three chambers, occupied by mercury, oil and heavy water, respectively. To fill this vessel, valve (12) was temporarily removed and mercury admitted through the open connexion up to half the height of the immersion tube. Valve (12) was then replaced, and the oil and heavy water chambers simultaneously evacuated via valves (10) and (8), respectively. A vacuum better than 0·1 mm Hg was attained. The oil chamber was then filled with previously outgassed vacuum oil through valves (9) and (14), valve (15) being kept closed during that operation. After closing of valve (14), the heavy water chambers of the pressure transmitter and the autoclave were evacuated through valves (11) and (12), and previously outgassed heavy water was admitted by opening valve (7). Valve (11) was then closed. On opening valve (15) the pressure of the test fluid in the autoclave could then be adjusted to any desired value by manipulation of the dead-load balance.

The heavy water contained in the pressure transmitter was recovered by opening valve (11), closing valves (12) and (14), and forcing oil from the dead-load balance into the oil chamber of the pressure transmitter until mercury appeared at valve (7). Valve (7) was then closed, and the mercury level was lowered by returning the oil to the dead-load balance or to the oil reservoir, and opening valve (12). The small amount of heavy water (about 50 ml) remaining in the conductivity cell and the inlet pipe was recovered by distillation at reduced pressure through valves (11), (12) and (18) and freezing out in two cold traps.

3.8. *Corrections to thermal conductivity measurements*

3.8.1. *Temperature drop in walls.* Owing to the location of the thermocouples somewhat below the surfaces of the emitting and receiving cylinders, the measured temperature differences between them included the temperature drop through the metal layers between the thermocouples and the surfaces of the cylinders.

On the basis of some thermal conductivity data quoted by Langley Alloys, Ltd. (who state that the measurements were made by Bristol Aeroplane Company, Ltd.), for Hidural 5 [7], the

Vol. 1 1960

correction for this effect was found to amount to about 9 per cent of the measured total temperature difference.

Thus to a small extent the accuracy of the reported values of the thermal conductivity of heavy water depends on the reliability of the data available for the thermal conductivity of Hidural 5.

3.8.2. *Intercalibration of thermocouples.* In order to determine the temperature difference across the annulus as accurately as possible, it was first necessary to compare carefully the e.m.f.s generated by the emitter and receiver thermocouples under isothermal conditions. This was achieved by operating the thermostat with the emitter and guard ring heaters switched off. It was found that over the temperature range from 75° to 360°C the receiver thermocouple always read 0·3 μV, i.e. about 0·006°C, lower than the emitter thermocouple. The appropriate correction was made to the measured temperatures before evaluating the temperature difference across the annulus, which was between 0·5° and 1°C.

Owing to small axial temperature gradients in the autoclave, the guard ring thermocouples could not be compared *in situ* with the same accuracy as the emitter and receiver thermocouples, since the former are located about 12 cm apart. However, it is considered that the total errors in calibration of the guard ring thermocouples and in the matching of the temperatures of the emitter and guard rings did not exceed 2 μV in any of the experiments. This corresponds to an error of less than 0·4 per cent in the reported values of thermal conductivity.

3.8.3. *Effect of radiation and correction.* When making measurements of thermal conductivity, it is essential that heat transfer by radiation and by convection should either be negligible, or should be accurately determined. It will be shown that convection had no effect, and that radiation had only a negligible effect, on the thermal conductivity data reported here.

Radiation. If the least favourable of the experiments are considered, viz. those at the highest temperature and for the largest temperature differences, and if one assumes an extreme case, viz. that the surface of the emitting and receiving cylinders are black bodies and that heavy water is perfectly transparent to black body radiation at this temperature (both assumptions being unnecessarily conservative), it can be shown by Stefan's law that the heat transferred by radiation must be less than 1·4 per cent of that transferred by thermal conduction. In view of the fact that conditions are much more favourable in reality, heat transfer by radiation will be considerably smaller than the above figure. No corrections were applied therefore for this effect in these tests.

Convection. It has been shown that thermal conductivity measurements are unaffected by convection, provided the product of the Grashof and Prandtl numbers proper to the experimental conditions is less than a certain value known as Rayleigh's criterion, which for vertical cylinders has a value of about 1,000. In the present experiments the product of the Grashof and Prandtl numbers was always considerably less than that value.

3.8.4. *Axial heat losses and gains.* As already stated in Section 3.6 the guard ring heaters were always adjusted with great care so that the temperature difference between the centre of the emitter and the guard rings amounted to not more than the reproducible limit of accuracy established by the calibration of the guard ring thermocouples which amounted to ± 2 μV, or expressed in terms of a temperature difference, to $\pm 0{\cdot}045$°C.

Using a computed value of overall conductance between the emitting cylinder and the guard rings, a temperature difference of the above magnitude would cause an error in the thermal conductivity of less than $\pm 0{\cdot}4$ per cent.

Apart from the axial energy exchange between the guard rings and the emitting cylinder due to imperfect matching of their temperatures, there is another possible source of error, viz. an error in the measurement of temperature caused by the axial conduction of heat along the thermocouple leads to, or from the thermal junction. This influence was studied experimentally in some earlier work by the present writers [4]. It was found that deliberate heating of the thin-walled stainless steel tube retaining the thermocouple leads at a point where it emerged from the thermal insulation surrounding the apparatus, had no significant effect on the e.m.f. observed

for that particular thermocouple. This test was applied to the thermocouple with the shortest depth of immersion in a zone of near-uniform temperature, viz. the top guard ring thermocouple. Temperatures of more than 300°C above the temperature of the thermal junction were applied before a measurable change of the e.m.f. was noticed. This observation is perhaps not so surprising when one considers that the vertical distance between the thermal junction and the heated area was about 45 cm and that the thermocouple leads traversed a near-isothermal zone of about 23 cm.

As the geometry and general arrangement of the apparatus used in this research resembles closely the one used in the above-mentioned tests, it was concluded that the same conditions would apply to the present case.

3.9. *Purity of heavy water*

The heavy water used in this research was supplied by A.E.R.E., Harwell, and was stated to have an isotopic purity of 99·85 per cent. Before filling the apparatus, dissolved gases were removed from the heavy water by boiling at reduced pressure.

4. EXPERIMENTAL RESULTS

Thirty-seven determinations were made of the conductivity of heavy water, covering the temperature range from 75° to 260°C at pressures up to 300 atm. Each determination is the mean of up to six complete sets of measurements taken over a period of about 1 hr, the standard deviation of these measurements being of the order of one-third of 1 per cent of the average thermal conductivity. The experimental data are given in Table 1. A smoothed plot of isobars is given in Fig. 3, and smoothed data can be found in Table 4. The numbers in the first column of Table 1 refer to the chronological order in which these experiments were carried out. In the first group of tests (nos. 1 to 29 incl.) experiments were carried out to a maximum temperature of about 260°C, followed by a check on the calibration of all thermocouples used in the conductivity cell. The next group of tests (nos. 30 to 37) was designed to fill some of the rather wide gaps in the preceding series, and at the same time provide a check on the reproducibility of the results of the first group. There is always the possibility that prolonged exposure of the conductivity cell to high pressures and temperatures has led to changes in the geometry of the system and thus affected the geometrical constant of the cell. The plot of experimental points in Fig. 3 shows no difference in trend between the two groups of tests and it can be concluded that no changes affecting the accuracy of these determinations have taken place during these tests.

When the experiments were extended to higher temperatures a progressively increasing deviation

Vol. 1 1960

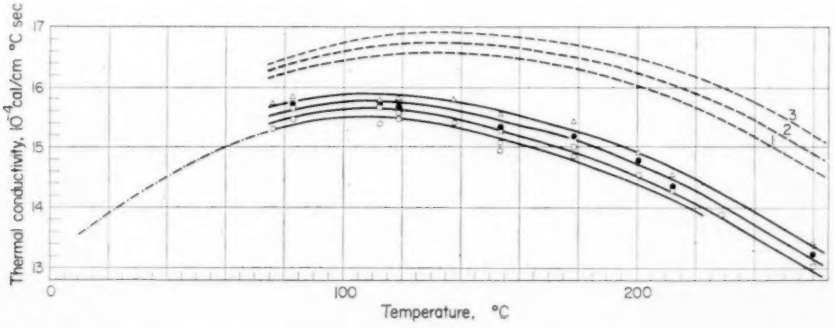

FIG. 3. The thermal conductivity of heavy water. Experimental data and smoothed isobars with the corresponding isobars for light water according to Timrot and Vargaftik [9];

— — Light water, Timrot and Vargaftik[9]; 3. 300 kg/cm²
——— Heavy water, this research; 2. 200 kg/cm²
— · — Heavy water, proposed average of previous investigations[10]. 1. 100 kg/cm²

△ 294 atm ⊗ 195 atm □ 97 atm ○ 24 atm.

Table 1. *Thermal conductivity of heavy water: experimental data*

No.	Temperature (°C)	Pressure (atm)	Thermal conductivity (10^{-4} cal cm^{-1} sec^{-1} $°C^{-1}$)	Number of determinations	Standard deviation 10^{-4} cal cm^{-1} sec^{-1} $°C^{-1}$
33	75·7	294	15·73	5	0·031
32	75·8	24	15·31	7	0·036
12	82·5	97	15·65	6	0·056
11	82·5	195	15·74	5	0·045
10	82·5	294	15·84	6	0·054
9	82·6	24	15·48	6	0·049
8	112·1	97	15·66	5	0·024
5	112·2	24	15·42	5	0·040
7	112·2	195	15·69	6	0·029
6	112·2	294	15·79	7	0·063
4	118·4	97	15·58	7	0·038
3	118·4	195	15·68	5	0·025
2	118·4	294	15·83	6	0·057
1	118·5	24	15·48	9	0·072
30	137·4	24	15·42	6	0·086
31	137·4	294	15·81	6	0·092
16	153·2	97	15·27	4	0·089
18	153·3	24	15·09	4	0·072
13	153·3	24	14·95	7	0·055
15	153·3	195	15·35	6	0·070
14	153·3	294	15·39	6	0·053
17	153·3	294	15·55	4	0·048
22	178·0	97	15·01	5	0·044
23	178·0	97	15·15	5	0·021
21	178·0	195	15·14	7	0·054
19	178·1	24	14·85	6	0·061
20	178·1	294	15·43	6	0·141
37	200·6	195	14·79	5	0·022
35	200·7	97	14·55	6	0·044
36	200·7	294	14·92	4	0·042
24	212·0	97	14·28	8	0·047
25	212·0	195	14·36	5	0·025
26	212·0	294	14·55	6	0·045
34	228·6	97	13·89	6	0·077
29	259·6	195	13·23	5	0·040
28	259·6	294	13·42	6	0·032
27	259·8	97	13·04	5	0·034

from previously established trends, mainly the dependence of k_{H_2O}/k_{D_2O} on temperature, was noticed. The experimental work was unfortunately terminated by the occurrence of a leak in the lid of the autoclave whilst operating the apparatus at 300 atm and 370°C. The opportunity was taken to inspect the conductivity cell and redetermine its vital dimensions. It was found that the dimensions of the receiver (part (9) in Fig. 1) were virtually unchanged, whereas the average diameter of the emitter and the guard rings (parts (1), (2) and (3), respectively) had increased from their original value of 3·3062 cm to 3·3129 cm. The investigation into the causes of this unexpected phenomenon revealed that the material used for the construction of the receiver had been annealed prior to the final machining operations, whilst the material for the emitter had been used as received from the manufacturers of the alloy.

The material used for the construction of the conductivity cell was a precipitation hardening alloy and according to the manufacturers the dimensional changes observed are associated with

the precipitation of the alloying constituents. The material for the receiver which had been annealed and slowly cooled to ambient temperature was therefore in a more stable condition.

From the reproducibility of these experiments, demonstrated by the results of test (30) to (37), it can be concluded that no irreversible change of the dimensions of the emitter assembly took place below an operating temperature of 260°C. Above this temperature, the linear dimensions of the emitter continually and irreversibly increased. It was thus impossible to apply the appropriate corrections to the individual results obtained during this phase and they were consequently omitted from this paper. The only result which appeared worthwhile studying was the point obtained immediately before the leak in the apparatus terminated the experimental work. Re-evaluating this result with the cell dimensions obtained after the inspection gave a value of the thermal conductivity which seems to suggest that the ratio of the thermal conductivity of light water to that of heavy water continues to rise with increasing temperature.

5. DISCUSSION

A comparison of the results of this research with those by other authors was confined to the lower end of the temperature range of this work (75°C) which slightly overlapped the range of Challoner and Powell's [3] investigation. The data of the latter authors, together with those by Bonilla and Wang [1], and Meyer and Eigen [2] were reviewed in a recent publication by one of the writers [10] and new mean values between 10° and 80°C for the thermal conductivity of heavy water were proposed. Table 2 contains the individual values and the proposed best average value for the thermal conductivity of heavy water at 75°C and 1 atm. Given in parentheses are the individual deviations from the new mean value. As can be seen the agreement is excellent which is the more noteworthy as different experimental methods were used by the various authors.

Table 2. Thermal conductivity of heavy water at 75°C *and* 1 atm (10^{-4} cal cm^{-1} sec^{-1} $°C^{-1}$).
(Deviation from proposed average value in parentheses below.)

Challoner and Powell [3]	Bonilla and Wang [1]	This research	Proposed average value
15·21 (−0·39%)	15·32 (+0·33%)	15·27 ±0·00%	15·27

The general trend in the variation of the thermal conductivity of heavy water with temperature, as exhibited in Fig. 3, is analogous to that of light water. There is a rise of thermal conductivity with temperature up to a shallow maximum which occurs at a somewhat lower temperature than for light water, viz. at about 110°C, followed by a gradual fall towards higher temperatures.

The influence of pressure on the thermal conductivity of heavy water was studied over the entire temperature range of these experiments. Analysis of the experimental data showed that over the comparatively narrow range investigated, the effect of pressure on the thermal conductivity can be adequately expressed by a linear equation

$$k = k_0 + (\partial k/\partial P)_T . P \qquad (2)$$

The choice of the fictitious quantity k_0 appeared to be justified as it was immediately obtainable by direct extrapolation of the experimental pressure—thermal conductivity isotherms to zero pressure without further recourse to other physical properties not studied in this investigation. Modifying this equation leads to

$$k = k_0 + k_0 . (1/k_0) . (\partial k/\partial P)_T . P = \\ = k_0(1 + \alpha P) \qquad (2a)$$

where $\alpha = (1/k_0)(\partial k/\partial P)_T$, is the pressure coefficient of the thermal conductivity.

The constants required in equation (2a) were found from a least square analysis of the unsmoothed isothermal experimental results. The resultant pressure coefficients were plotted in Fig. 4 where they are compared with the corresponding values on light water obtained from an analysis of the smoothed data of the thermal conductivity of light water by Timrot and Vargaftik [9]. These observers conducted their experiments over ranges of pressure and temperature similar to those on this investigation. Identical trends and similar numerical values were found for the pressure coefficients of the thermal conductivity

Vol. 1 1960

of light and heavy water. The results of this research on the latter substance were correlated by the empirical relation

$$\alpha = 1{\cdot}81 \times 10^{-3}\, T \exp\left(4{\cdot}264 \times 10^{-9}\, T^3\right) \quad (3)$$

In view of the scatter of the α-values derived from these experiments, it does not seem justified to attach any physical significance to the small difference in the pressure coefficients for light and heavy water. This opinion is supported by the results of a recent study by Lawson *et al.* on the thermal conductivity of light water at pressures up to 8000 kg/cm² and temperatures from 30° to 130°C [11]. The analysis of the data of these authors within the pressure range of linear dependence between pressure and thermal conductivity, yielded α-values which are distinctly lower than those derived from Timrot's and Vargaftik's measurements, and even fall below those for heavy water.

In view of this discrepancy it was not possible to decide with certainty whether the pressure coefficients of light and heavy are different.

Values of the pressure coefficient α for heavy water were computed from equation (3) and were compiled in Table 3. With the aid of these values the thermal conductivity of heavy water was calculated up to 500 atm and 260°C. These data can be found in Table 4.

In a previous paper [10] the usefulness of the ratio of the thermal conductivity of light water

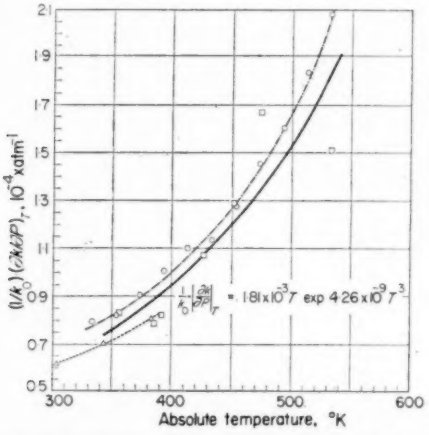

FIG. 4. Experimental values of the pressure coefficient of the thermal conductivity of light and heavy water:
····△···· H_2O, Lawson *et al.*[11];
—·—○—·— H_2O, Timrot and Vargaftik[9];
—⊡— D_2O, this research.

Table 3. The pressure coefficient of the thermal conductivity of heavy water.

$$\left[\alpha = 1/k_0 \times \left(\frac{\partial k}{\partial P}\right)_T\right].$$

t (°C)	$\alpha \times 10^4$ (atm^{-1})	t (°C)	$\alpha \times 10^4$ (atm^{-1})
80	0·77	180	1·22
100	0·84	200	1·35
120	0·92	220	1·49
140	1·01	240	1·65
160	1·11	260	1·84

Table 4. Thermal conductivity of heavy water (10^{-4} cal cm^{-1} °C^{-1} sec^{-1})*

(Smoothed data)

Pressure (atm)	Temperature (°C)									
	80	100	120	140	160	180	200	220	240	260
100	15·52	15·66	15·60	15·43	15·20	14·91	14·53	14·09	13·53	12·91
200	15·64	15·79	15·74	15·59	15·36	15·09	14·73	14·29	13·75	13·15
300	15·76	15·93	15·89	15·74	15·53	15·27	14·92	14·50	13·97	13·38
400	15·87	16·06	16·03	15·90	15·70	15·45	15·11	14·71	14·19	13·61
500	15·99	16·20	16·17	16·05	15·86	15·63	15·31	14·91	14·41	13·85

* To convert cal cm^{-1} °C^{-1} sec^{-1} into W cm^{-1} °C^{-1} multiply by 0·2389.

Table 5. The ratio $k_{H_2O}k/_{D_2O}$. Values for k_{H_2O} derived from Timrot's and Vargaftik's paper [9], those for k_{D_2O} from Table 4

Pressure (atm)	Temperature (°C)									
	80	100	120	140	160	180	200	220	240	260
100	1·0453	1·0522	1·0611	1·0727	1·0839	1·0936	1·1047	1·1121	1·1230	1·1315
200	1·0463	1·0520	1·0621	1·0727	1·0830	1·0917	1·1015	1·1116	1·1253	1·1325
300	1·0450	1·0518	1·0631	1·0728	1·0839	1·0915	1·1040	1·1149	1·1275	1·1356
400	1·0482	1·0516	1·0640	1·0746	1·0848	1·0950	1·1064	1·1162	1·1297	1·1386
Mean value	1·0462	1·0519	1·0626	1·0732	1·0839	1·0929	1·1041	1·1137	1·1264	1·1345
Standard deviation	0·0012	0·0002	0·0011	0·0008	0·0006	0·0014	0·0018	0·0019	0·0025	0·0028

to that of heavy water, k_{H_2O}/k_{D_2O}, as a quantity for checking the internal consistency of experimental results was demonstrated. This quantity was computed using the smoothed experimental results contained in Table 4 for heavy water and Timrot's and Vargaftik's smoothed values of the thermal conductivity of light water. These k_{H_2O}/k_{D_2O}-values were compiled in Table 5 and two facts worth mentioning can be observed, viz.:

(a) the ratio k_{H_2O}/k_{D_2O} appears to be independent of pressure within the ranges of pressure and temperature covered in this investigation.

(b) between 100° and 260°C all values can be satisfactorily correlated by the following linear expression

$$k_{H_2O}/k_{D_2O} = 5{\cdot}3 \times 10^{-4} \times t + 1{\cdot}00 \quad (4)$$

where t is the temperature in degrees Centigrade. At the lower end of the temperature range of this work, i.e. between 80° and 100°C, the experimental k_{H_2O}/k_{D_2O}-values begin to deviate slightly from the linear equation (4), but are in good agreement with the corresponding values derived from the analysis of the results of earlier workers [10].

Preparations are in hand to extend the range of this work to the critical temperature of heavy water with an improved apparatus. The opportunity may then be taken to redetermine the conductivity of light water between 260° and 400°C, which so far has been investigated only once, viz. by Timrot and Vargaftik [9] in 1940. The remarkable consistency of certain properties of heavy and light water, derived from this work and from Timrot and Vargaftik's experiments, appears to lend support for the validity of the latter authors' data on light water within the ranges of temperature and pressure covered in this research.

ACKNOWLEDGEMENTS

The work described in this report was jointly sponsored by the Atomic Energy Research Establishment, Harwell, and Atomic Energy of Canada, Ltd., Chalk River, Ontario, whose permission to publish these data is gratefully acknowledged.

REFERENCES

1. C. F. Bonilla and G. J. Wang, Progress Report, Dec. 1950–Feb. 1951, Atomic Energy Division, Columbia University and E. I. DuPont de Nemours and Co., D.P. 12 (1951).
2. F. Meyer and M. Eigen, *Z. Naturf.* **8a**, 500 (1953).
3. A. R. Challoner and R. W. Powell, *Proc. Roy. Soc.* A **238**, 90 (1956).
4. H. Ziebland and J. T. A. Burton, *Brit. J. Appl. Phys.* **6**, 416 (1955).
5. H. Ziebland and J. T. A. Burton, *Brit. J. Appl. Phys.* **9**, 52 (1958).
6. Langley Alloys Limited. Private communication (1953).
7. Langley Alloys Limited. Private communication (1953).
8. R. W. Powell, *Phil. Mag.* (Supplement) **7**, 276 (1958).
9. D. L. Timrot and N. B. Vargaftik, *Zh. tech. Fiz. Moskva* **10**, 1063 (1940).
10. H. Ziebland, *Allg. Wärme-Techn.* **9**, 37 (1959).
11. A. W. Lawson, R. Lowell and A. L. Jain, *J. Chem. Phys.* **30**, 643 (1959).

Int. J. Heat Mass Transfer. Vol. 1, pp. 255–268. Pergamon Press 1960. Printed in Great Britain.

HEAT TRANSFER BIBLIOGRAPHY

E. R. G. ECKERT, J. P. HARTNETT and E. M. SPARROW
Department Mechanical Engineering, Institute of Technology,
University of Minnesota, Minneapolis 14, Minnesota, U.S.A.

(*Received* 17 *March* 1960)

APPLICATIONS

ROGER A. ANDERSON and WILLIAM A. BROOKS, Effectiveness of radiation as a structural cooling technique for hypersonic vehicles. *J. Aero. Space Sci.* **27**, No. 1, 41 (1960).

PAUL D. ARTHUR and JAMES C. WILLIAMS, Maximum turbulent boundary layer heating rates on a hemispherical nose. *J. Amer. Rocket Soc.* **30**, No. 2, 207 (1960).

ING H. D. BAEHR, Grundprobleme der Wärmeübertragung in Kernreaktoren. *Allg. Wärmetechn.* **9**, No. 6, 116 (1959).

J. F. BARNES, *The Calculation of Gas Flow Passage Sizes in Heat Exchangers and Nuclear Reactors When the Heat Transfer Requirements and the Gas Inlet and Outlet Temperatures are Specified.* National Gas Turbine Establishment. (Gt. Brit.) N–77922 (1959).

T. H. BENZINGER, On physical heat regulation and the sense of temperature in Man. *Proc. Nat. Acad. Sci.* **45**, No. 4, 645 (1959).

DEAN R. CHAPMAN, *An Approximate Analytical Method for Studying Entry into Planetary Atmospheres.* NASA TR R–11 (1959).

J. B. CLADIS, *Stimulation of Thermal Environment in Space.* ASME Aviation Conf. Pap. 59–AV–26 (1959).

G. I. DARCHIYA, Heat-transfer calculation for heating panels (Raschet Teplootdachi Otopitel'nykh Paneley). *Vopr. Otopleniya i Ventilayatsii*, V sb., Nr. 3, **5**, Moscow (1956).

ALFRED J. EGGERS, THOMAS J. WONG and ROBERT E. SLYE, Some general considerations of the heating of satellites. *J. Heat Transfer* **81**, No. 3, 308 (1959).

RUDOLF ERNST, Wärmeübergang und Wärmeaustauschern im Moving Bed. *Chem.-Ing.-Tech.* Heft 1, No. 32, 17 (1960).

JACK B. ESGAR, ROBERT O. HICKEL and FRANCIS S. STEPKA, *Preliminary Survey of Possible Cooling Methods for Hypersonic Aircraft.* NACA RM E57L19 (1958).

CARL GAZLEY, The penetration of planetary atmospheres. *J. Heat Transfer* **81**, No. 4, 315 (1959).

H. HAUSEN, *Wissenschaftliche Fragen auf dem Gebiete der Heizungstechnik.* Aus dem Jahrbuch der Technischen Hochschule Hannover (1955–1958).

H. HAUSENBLAS, The mean temperature difference in hairpin heat exchangers (in German). *Brennstoff-Warme-Kraft.* **11**, No. 3, 114 (1959).

J. C. HEAP, *Thermodynamics of Unsteady Flow Processes Involving Transfer of Heat for Vented Containment Systems.* USAEC ANL–5987 (1959).

WICKLIFFE B. HENDRY, *A Systematic Approach to the Design of Compact Heat Exchangers.* ASME Paper No. 59–A–193 (1959).

H. HOPPE, Berechnung der Wärmeübertragung in Regeneratoren bei Kreuzstrombetrieb. *Forschung.* Bd. 20, 150 (1954).

A. HUBER, Parallel flow recuperation with temperature-dependent overall heat transfer coefficient (in German). *Öst. Ing.-Arch.* **12**, 41 (1958).

W. M. KAYS and T. R. LOESCHNER, *The Heat Transfer and Flow Friction Characteristics of an Elliptical Pin-Fin Heat Exchanger Surface.* Dept. of Mech. Eng., Stanford Univ. TR No. 44 (1959).

DOUGLAS L. KERR, Radiator areas of thermopile generators in space. *Aero. Space Eng.* **18** (1959).

WILLIAM H. KINARD, *The Behavior of Beryllium and Beryllium Copper in a* 4000°*F Supersonic*

Air Jet at a Mach Number of 2. NACA RM L57G31 (1957).

G. K. KULLBERG and H. B. KENDALL, Improve heat transfer coefficients with silicone resin coatings. *Chem. Eng. Prog.* **56**, No. 1, 82 (1960).

E. H. MANSFIELD, *The Influence of Aerodynamic Heating on the Flexural Rigidity of a Thin Wing*. Aeronautical Research Council (Gt. Brit.) N–59686X (1959).

M. F. NAGIYEV and P. V. KARAMZIN, An experimental research on heat transfer processes in a tube-in-tube type of exchanger (in Azerb). *Izv. Akad. Nauk Azerb SSR* No. 2, 23–35 (1957). *Ref. Zh. Mekh.* No. 1, Rev. 776 (1958).

L. W. PHIPPS, Semi-automatic control system for producing constant cooling rates. *J. Sci. Instrum.* **36**, No. 11, 449 (1959).

BERNARD RASHIS, *Preliminary Indications of the Cooling Achieved by Ejecting Water Upstream from the Stagnation Point of Hemispherical, 80° Conical and Flat-Faced Nose Shapes at a Stagnation Temperature of* 4000°*F*. NACA RM L57I03 (1957).

D. H. ROBEY, Cold re-entry of space vehicles at meteor speeds. *Astro. Acta.* **5**, No. 3–4, 224 (1959).

CHARLES RUMSEY, ROBERT PILAND and RUSSELL HOPKO, *Aerodynamic-Heating Data Obtained from Free-Flight Tests Between Mach Numbers of* 1 *and* 5. NASA TN D–216 (1960).

D. A. SPENCE, *Two Heat Diffusion Problems With Shock Tube Applications*. Royal Aircraft Est. (Gt. Brit.) N–78487 (1959).

FRANCIS S. STEPKA and REEVES P. COCHRAN, *Experimental and Analytical Investigation of Heat Transfer Characteristics of a Return-Flow Air-Cooled Turbine Rotor Blade*. NASA TN D–202 (1959).

W. A. SUTHERLAND, *Reactor Heat Transfer—A Preliminary Design Procedure*. ASME Semiann. Meet, St. Louis, Mo., Paper 59–SA–16 (1959).

J. W. TATOM, Transient and steady-state behavior of an idealized solar powered heat exchanger. *J. Amer. Rocket Soc.* **30**, No. 1, 116 (1960).

F. M. TEETZEL, J. A. WILLIAMSON, A. E. ABBOT and R. L. MADDOX, Screw equipment temperature problems. *Chem. Eng. Prog.* **55**, No. 12, 39 (1959).

R. G. THOMSON, *Effects of Cross-Sectional Shape, Solidity and Distribution of Heat-Transfer Coefficient on Torsional Stiffness of Wings Subjected to Aerodynamic Heating*. NASA Memo. 1–30–59L (1959).

G. A. TIRSKIY and V. A. TRENOGIN, The determination of the temperature field of a gas turbine cooling vane (Opredeleniye Temperaturnogo Polya Okhlazhdayemoy Lopatki Gazovoy Turbiny). *Izv. Akad. Nauk SSSR, Otd. Tekh. Nauk, Energet. Avtomat.* Nr. 2, 45 (1959).

OTTO F. TROUT, *Exploratory Investigation of Several Coated and Uncoated Metal, Refractory and Graphite Models in a* 3800°*F Stagnation Air Jet*. NASA TN D–190 (1960).

V. A. TSIKUNOV, On a method of determining the coefficient of turbulent heat transfer in the surface layer of the sea (Ob odnom Metode Opredeleniya Koeffitsiyenta Turbulentnoy Teploprovodnosti v verkhnem sloye morya). *Tr. Gos. Okeanogr. in-ta.* Nr. 33 (45), 80 (1956).

HANS C. VETTER, Note on the calculation of equilibrium skin temperatures. *J. Aero Space Sci.* **26**, No. 11, 757 (1959).

J. P. WELSH and T. J. WALSH, *Handbook of Methods of Cooling Air Force Ground Electronic Equipment*. ASTIA Doc. 148907 (Equipment). RADC TR58–126 (Electronic) (1959).

V. S. ZARUBIN, On a problem of unsteady heat conductivity (Odna Zadacha Nestatsionarnoy Teploprovodnosti). *Izv. Akad. Nauk SSSR, Otd. Tekh. Nauk, Energet. Avtomat.* Nr. 2, 38 (1959).

BOOKS

H. S. CARSLAW and J. C. JAEGER, *Conduction of Heat in Solids*. Oxford University Press, New York (1959).

D. A. FRANK-KAMENETZKI, *Mass and Heat Transfer in Chemical Kinetics (Stoff- und Wärmeübertragung in der Chemischen Kinetik)*. Springer-Verlag, Berlin (1959).

J. O. HINZE, *Turbulence*. McGraw-Hill, New York (1959).

Jet Propulsion Laboratory. *Astronautics Information-Abstracts with Index*. Vol. 1, Abstracts 1001–1726. Jet Propulsion Laboratory, Calif. Inst. of Tech. (1960).

H. SCHENCK, *Heat Transfer Engineering*. Prentice-Hall, New York (1959).

BOUNDARY LAYERS

G. E. Anderson, C. J. Scott and D. R. Elgin, *Mass Transfer Cooling Experiments on a Hemisphere at $M = 5$*. Rosemount Aeronautical Lab., Inst. of Tech., Univ. of Minn. Res. Rep. No. 166 (1959).

Ivan E. Beckwith and James J. Gallagher, *Local Heat Transfer and Recovery Temperatures on a Yawed Cylinder at a Mach Number of 4·15 and High Reynolds Numbers*. NASA Memo. 2–27–59p (1959).

M. H. Bloom and M. H. Steiger, Some compressibility and heat transfer characteristics of the wall jet. *Proc. Third U.S. Nat. Congr. Appl. Mech.* (1958); Amer. Soc. Mech. Engrs., p. 717 (1958).

Willis H. Braun, *Turbulent Boundary Layer on a Yawed Cone in a Supersonic Stream*. NASA TN 4208 (1959).

William B. Bush, Compressible flat-plate boundary-layer flow with an applied magnetic field. *J. Aero Space Sci.* **27**, No. 1, 49 (1960).

Gordon L. Cann and Adriano C. Ducati, *Research on High Intensity Ionic Jets*. Plasmadyne Corporation, Santa Ana, Calif. AFOSR TN 59–167 (1959).

Hsien K. Cheng, Similitude of hypersonic real-gas flows over slender bodies with blunted noses. *J. Aero Space Sci.* **26**, 575 (1959).

A. J. Chones, *Heat-Transfer and Pressure Measurements on Flat-Faced Fared-Tail Circular Cylinders and Normal Disks*. U.S Naval Ordnance Laboratory. NAVORD Rep. 6669 (1959).

Paul M. Chung, *A Simplified Study on the Nonequilibrium Couette and Boundary-Layer Flows with Air Injections*. NASA TN D–306 (1960).

Raul J. Conti, *Heat-Transfer Measurements at a Mach Number of 2 in the Turbulent Boundary Layer on a Flat-Plate Having a Step-Wise Temperature Distribution*. NASA TN D–159, Nov. (1959).

M. Cooper and P. C. Stainback, *Influence of Large Positive Dihedral on Heat Transfer to Leading Edges of Highly Swept Wings at Very High Mach Numbers*. NASA Memo. 3–7–59L, 18p, Apr. (1959).

R. N. Cox, General characteristics of hypersonic flow fields. *J. Roy. Aero. Soc.* **63**, 503 (1959).

Bernard E. Cunningham and Samuel Kraus, *Experimental Investigation of the Effect of Yaw on Rates of Heat Transfer to Transverse Circular Cylinders in a 6500-Foot-Per-Second Hypersonic Air Stream*. NACA RM A58E19 (1958).

N. Curle, Steady compressible laminar boundary-layer, with arbitary pressure gradient and uniform wall temperature. *Roy. Soc.—Proc.* **249**, No. 1257, 206 (1959).

D. R. Davies and D. E. Bourne, Heat and mass transfer in a turbulent boundary layer (in English). *Ninth Congrès Int. Méc. Appl. Univ. Bruxelles*. **4**, p. 50 (1957).

Robert G. Deissler and Albert L. Loeffler, *Analysis of Turbulent Flow and Heat Transfer on a Flat Plate at High Mach Numbers with Variable Fluid Properties*. NASA TR R–17 (1959).

Jean-Francois Dorand, *Explorations de la Couche Limite, en Turbulence Naturelle et en Turbulence Provoquee, dans le cas d'un Ecoulement Supersonique le Long D'une Plaque Plane*. Publications Scientifiques et Technique du Ministere de L'air, Centre National de la Recherche Scientifique, Laboratoire d'Aerothermique Publication No. 123 (1959).

S. K. Friedlander and Mitchell Litt, Rapid chemical reaction in a laminar boundary layer. *Appl. Sci. Res.* A **8**, No. 6, 403 (1959).

R. E. Geiger, On the frozen flow of a dissociated gas. *J. Aero Space Sci.* **26**, No. 12, 834 (1959).

Glen Goodwin, Marcus O. Creager and Ernest L. Winkler, *Investigation of Local Heat-Transfer and Pressure Drag Characteristics of a Yawed Circular Cylinder at Supersonic Speeds*. NACA RM A55H31 (1956).

R. V. Hess, *Some Basic Aspects of Magnetohydrodynamic Boundary-Layer Flows*. NASA Memo. 4–9–59L (1959).

Robert Goulard, *Liepmann's Heat Transfer Method in Aerothermochemistry*. Purdue Research Foundation, Research Project No. 1717. Rep. No. A–59–5 (1959).

Harvey P. Greenspan, *On the Flow of a Viscuous Electrically Conducting Fluid*. AVCO Everett Research Laboratory. AFOSR TN 59–1221. Res. Rep. No. 73 (1959).

J. F. Gross, J. P. Hartnett, D. J. Masson and

CARL J. GAZLEY, *A Review of Binary Boundary Layer Characteristics*. Engineering Division, The Rand Corporation. P–1729 (1959).

A. A. HAYDAY, *Mass Transfer Cooling in a Steady Laminar Boundary Layer Near the Stagnation Point*. Heat Trans. and Fluid Mech. Inst. p. 156 (1959).

M. R. HEAD, *Approximate Calculations of the Laminar Boundary-Layer with Suction, With Particular Reference to the Suction Requirements for Boundary-Layer Stability on Aerofoils of Different Thickness/Chord Ratios*. Aeronautical Research Council (Gt. Brit.) N–57724X (1959).

M. R. HEAD, *An Approximate Method of Calculating the Laminar Boundary-Layer in Two-Dimensional Incompressible Flow*. Aeronautical Research Council (Gt. Brit.) N–58536X (1959).

J. A. HILL, Integral methods for laminar forced convection calculations—an evaluation of two approaches (in English). *Ninth Congrés Int. Mèc. Appl. Univ. Bruxelles.* **4**, 108 (1957).

H. HOSHIZAKI, The effect of shock-generated vorticity, surface slip and temperature jump on stagnation-point heat-transfer rates. *J. Aero. Space Sci.* **27**, No. 2, 135 (1960).

C. P. HOWARD, *The Effect of Pressure Gradient on the Average Convective Heat Transfer Coefficient for a Two-Dimensional Laminar Compressible Boundary Layer on a Flat Plate*. Dept. of Mech. Engr., Stanford University. TR No. 46 (1959).

D. S. JOHNSON, Velocity, temperature and heat-transfer measurements in a turbulent boundary layer downstream of a stepwise discontinuity in wall temperature. *J. Appl. Mech.* **24**, No. 1, 2 (1957).

JEROME D. JULIUS, *Measurements of Pressure and Local Heat Transfer on a* 20° *Cone at Angles of Attack up to* 20° *for a Mach Number of* 4·95. NASA TN D–179, Dec. (1959).

R. F. KRAMER and H. M. LIEBERSTEIN, Numerical solution of boundary-layer equations without similarity assumptions. *J. Aero. Space Sci.* **26**, No. 8, 508 (1959).

L. I. KUDRYSHEV and B. M. TEVEROVSKIY, On some new forms of generalized integral relationships for the hydrodynamic and thermal boundary-layer. (O Nekotorykh Novykh-formakh Obobshchennykh Integral' nykh soot-nosheniy dlya gidrodinamicheskogo i Teplovo-go Pogranichnogo Sloya). *Tr. Kuybyshevsk. Aviats. in-ta.* Nr. 3, 3 (1957).

H. A. LAUWERIER, A diffusion problem with chemical reaction. *Appl. Sci. Res.* A **8**, No. 5, 366 (1959).

DOROTHY B. LEE and ANDREW G. SWANSON, *Heat Transfer Measured on a Flat-Face Cylinder-Flare Configuration in Free Flight at Mach Numbers from* 1·6 *to* 2·7. NACA RM L58A06 (1958).

CHING-SHI LIU and ALI BULENT CAMBEL, Magnetogas dynamic flow regimes. *J. Amer. Rocket Soc.* **29**, 871 (1959).

K. W. MANGLER, Some special aspects of hypersonic flow fields. *J. Roy. Aero. Soc.* **63**, 508 (1959).

THOMAS J. MARKLEY, *Heat Transfer and Pressure Measurement on a* 5*-inch Hemispherical Concave Nose at a Mach Number of* 2·0. NACA RM L58C14a (1958).

A. MCD. MERCER, The growth of the thermal boundary layer in laminar flow between parallel flat plates. *Appl. Sci. Res., Hague* A **8**, No. 5, 357 (1959).

R. J. MONAGHAN, Problems of hypersonic aerodynamics—a survey. *J. Roy. Aero. Soc.* **63**, 489 (1959).

H. T. NAGAMATSU, J. B. WORKMAN and R. E. SHEER, *Hypersonic Nozzle Expansion with Air Atom Recombination Present*. Research Laboratory, G.E., Report No. 60–RL–2332C (1960).

YOSHINARI NAKAGAWA, Heat Transport by convection in presence of an impressed magnetic field. *Phys. Fluids* **3**, No. 1, 8 (1960).

RICHARD J. NICKERSON, *The Effect of the Free-Stream Oscillations on the Laminar Layers on a Flat Plate*. U.S. Air Force, WADC TR 57–481 (1958).

E. OFFENHARTZ and H. WEISBLATT, *Experimental Determination of the Turbulent Heat Transfer Rate Distribution Along a Slender Blunt Nosed Body from Shock Tube Tests*. AVCO, Research and Advanced Development Div. RADTR–9–59–18 (1959).

GEORGE M. PALMER and FRANK L. PARIS, *An Experimental Study of the Operating Characteristic and Electrode Heat Transfer of a*

Direct Current Electric Arc in a Pressurized Argon Environment. Purdue Research Foundation, Research Project No. 1717, Rep. No. A–59–10 (1959).

GEORGE M. PALMER, *A Study of the Overall Problems of the True-Temperature, Hypersonic Wind Tunnel Having Semi-Continuous Operation and the Preferred Methods of Solution*. Purdue Research Foundation, Research Project No. 1717, Rep. No. A–59–14 (1959).

HAROLD S. PERGAMENT and MELVIN EPSTEIN, Approximate method for determining laminar heat transfer rates. *J. Amer. Rocket Soc.* **30**, No. 2, 206, Feb. (1960).

O. E. POTTER, Chemical reaction in the laminar boundary-layer—instantaneous reaction. *Trans. Instn. Chem. Engrs.* **36**, No. 6, 415 (1958).

LEONARD RABB and JOHN H. DISHER, *Boundary-Layer Transition at High Reynolds Numbers as Obtained in Flight of a* 20° *Cone-Cylinder with Wall to Local Stream Temperature Ratios Near* 1·0. NACA RM E55115, Nov. (1955).

BERNARD RASHIS and ALECK C. BOND, *Free-Flight Skin-Temperature and Surface-Pressure Measurements on a Highly Polished Nose Having a* 100° *Total Angle Cone and a* 10° *Half-Angle Conical Flare Section Up to a Mach Number of* 4·08. NACA RM 157G30 (1957).

JOHN O. RELLER and FRANK M. HAMAKER, *Temperature Recovery Factors on a Slender* 12° *Cone-Cylinder at Mach Numbers from* 3·0 *to* 6·3 *and Angles of Attack Up to* 45°. NACA RM A55G20 (1955).

DANIEL E. ROSHER, *On the Effects of Diffusion and Chemical Reaction in Convective Heat Transfer*. AERO CHEM Research Laboratories, Inc. TM–13 (1959).

CHARLES B. RUMSEY and DOROTHY B. LEE, *Measurements of Aerodynamic Heat Transfer and Boundary-Layer Transition on a* 10° *Cone in Free Flight at Supersonic Mach Numbers Up to* 5·9. NACA RM L56B07 (1956).

CHARLES B. RUMSEY and DOROTHY B. LEE, *Measurements of Aerodynamic Heat Transfer on a* 15° *Cone-Cylinder-Flare Configuration in Free Flight at Mach Numbers Up to* 4·7. NACA RM 157J10 (1958).

R. W. RUTOWSKI, *Stagnation Point Heat Transfer in a Partially Ionized Gas*. Heat Trans. and Fluid Mech. Inst. p. 110 (1959).

C. E. SHEPARD and D. R. BOLDMAN, *Preliminary Development of Electrodes for Electric-Arc Wind Tunnel*. NASA Memo. 4–14–59E (1959).

V. P. SHESTOPALOV, The laminar flow past a plate in the nonlinear theory of the boundary-layer of a viscous, compressible fluid with an arbitrary temperature distribution along the surface (Laminarnoye Obtekaniye Plastinki v Nelineynoy Teorii Pogranichnogo Sloya Vyazkoy Szhimayemoy Zhidkosti pri Proizvol' nom Raspredelenii Temperatury vdol' Poverkhnosti). *Uch. zap. Khar'kovsk. gos ped. in-ta.* **18**, 121 (1956).

C. J. SCOTT, *Integral Laminar Boundary Layer Solutions Using the Crocco Variables*. University of Minnesota, Engineering Memorandum No. 86, AFOSR TN 59–1304 (1959).

H. H. SOGIN, Laminar transfer from isothermal spanwise strips on a flat plate. *J. Heat Transfer* **81**, No. 4, 53 (1960).

E. M. SPARROW and J. L. GREGG, *Details of Exact Low Prandtl Number Boundary-Layer Solutions for Forced and for Free Convection*. NASA Memo. 2–27–59E (1959).

DRAGUTIN STOJANOVIC, Similar temperature boundary layers. *J. Aero. Space Sci.* **26**, 715 (1959).

B. S. STRATFORD and G. S. BEAVERS, *The Calculation of the Compressible Turbulent Boundary Layer in an Arbitrary Pressure Gradient—a Correlation of Certain Previous Methods*. National Gas Turbine Est. (Gt. Brit.) N–77923 (1959).

WILLIAM J. THIEVON, GERALD A. STERBUTZEL and JOHN L. BEAL, *The Influence of Gas Dissociation of Heat Transfer*. WADC TR 59–450 (1959).

U.S. Naval Ordnance Laboratory. *Investigation of Flat Plate Hypersonic Turbulent Boundary-Layers with Heat Transfer at a Mach Number of* 5·2. NAVORD Rep. 6631 (1959).

R. VAGLIO-LAURIN, *Heat Transfer on Blunt-Nosed Bodies in General Three-Dimensional Hypersonic Flow*. Heat Trans. and Fluid Mech. Inst. p. 95 (1959).

J. WADSWORTH, *The Experimental Examination*

of the Local Heat Transfer on the Surface of a Sphere When Subjected to Forced Convective Cooling. Nat. Res. Counc. Canada, Div. Mech. Engng. Rep. MT–39 (1958).

RICHARD J. WINSNIEWSKI, *Methods of Predicting Laminar Heat Rates on Hypersonic Vehicles*. NASA TN D–201 (1959).

VICTOR ZAKKAY, Heat transfer at a corner. *J. Aero. Space Sci.* **27**, No. 2, 157 (1960).

CHANGE OF PHASE

M. ALTMAN, R. H. NORRIS and F. W. STAUB, *Local and Average Heat-Transfer and Pressure-Drop for Refrigerants Evaporating in Horizontal Tubes*. ASME Paper 59–A–278 (1959).

J. A. R. BENNETT, J. G. COLLIER, H. R. C. PRATT and J. D. THORNTON, *Heat Transfer to Two Phase Gas-Liquid Systems. Part* 1, *Steam-Water in the Liquid-Dispersed Region in an Annulus*. (UK AEA) AERE–R 3159 (1959).

A. G. BONDAR', An experimental investigation of the transfer of heat to a boiling sodium-hydroxide solution circulating freely in a vertical boiler tube of an industrial evaporator (Eksperimental'noye Issledovaniye Teplootdachi Kipyashchin Rastvorom Yedkogo Natra v Vertikal'noy Trube pri Yestestvennoy Tsirkulyatsii.) *Izv. Kiyevsk. Politekhn. in-ta.* **17**, 83 (1956).

I. I. CHERNOBYL'SKIY and YU. M. TANANAYKO, An investigation of the heat transfer to boiling water flowing through narrow annular openings in the presence of moderate heat fluxes (Under conditions approximating those in industrial evaporators) (Issledovaniye Teplootdachi k Kipyashchey vode v Kol'tsevom Prostranstve pri Umerennykh Teplovykh Potokakh). *Izv. Kiyevsk. Politekhn. in-ta.* **17**, 61 (1956).

H. B. CLARK, P. S. STRENGE and J. W. WESTWATER, Active sites for nucleate boiling. *Chem. Engr. Prog. Symposium Series.* **55**, No. 29, 103 (1959).

T. FURMAN and H. HAMPSON, *Experimental Investigation into the Effects of Cross Flow with Condensation of Steam and Steam-Gas Mixtures on a Vertical Tube*. Instn. Mech. Engrs., Prepr. (1958).

H. GLASER, Simplified calculation of the diffusion of water vapor through walls consisting of several layers. Including the effect of water and ice formation. Part II (in German). *Kaltetechnik* **10**, No. 12, 386 (1958).

MELVIN H. GOTTLIEB, Bubble stability in dimethylsilicone solutions. *J. Phys. Chem.* **63**, 1687 (1959).

G. G. HASELDEN and S. A. MALATY, Heat and mass transfer accompanying the absorption of ammonia in water. *Inst. of Chemical Engrs.* **37**, No. 3, 137 (1959).

H. S. ISBIN, H. A. RODRIGUEZ, H. C. LARSON and B. D. PATTIE, Void fractions in two-phase flow. *J. Amer. Inst. Chem. Engrs.* **5**, No. 4, 427 (1959).

H. KLINGENSPOR, Untersuchungen über die Rektifizierwirkung in einer Füllkörpersaule. *Chem.-Ing.-Tech.* **31**, No. 9, 598 (1959).

E. L. KNUTH, Nonstationary phase changes involving a condensed phase and a saturated vapor. *Phys. Fluids* **2**, No. 1, 84 (1959).

V. F. KOVALENKO, An experimental investigation of the vibration effect on heat transfer in the process of boiling (in Russian). *Teploenergetika*. No. 2, 76 (1958).

R. YA KUCHEROV and L. E. RIKENGLAZ, On hydrodynamic boundary conditions for evaporation and condensation. *Soviet Physics—J. of Experimental and Theoretical Physics*. **37**, (10), No. 1, 88 (1960).

D. A. LABOONTZOY, Heat transfer in film condensation of pure vapors on vertical surfaces and horizontal pipes (in Russian). *Teploenergetika*. No. 7, 72 (1957).

V. LAVROVA, Experimental investigation of heat emission by boiling Freon-12 (in Russian). *Kholodil'naya Tekhnika*. No. 3, 55–61 (1957). *Ref. Zh. Mekh.* No. 6, Rev. 6783 (1958).

H. A. LENIGER and J. VELDSTRA, Heat transmission in a thin-layer evaporator. *Chem.-Ing.-Tech.* **31**, 493 (1959).

C. K. LIU, *Heat Transfer Coefficient for a Horizontal Tube of Elliptic Cross-Section in a Condensing Medium*. Army Ballistic Missile Agency. Report DSD–TM–26–59 (1959).

E. L. LUSTENADER, R. RICHTER and F. J. NEUGEBAUER, The use of thin films for increasing evaporation and condensation rates in process equipment. *J. Heat Transfer* **81**, No. 4, 297 (1959).

G. R. MOORE, Vaporization of superheated

Vol. 1 1960

drops in liquid. *J. Amer. Inst. Chem. Engrs.* **5**, No. 4, 458 (1959).

D. E. SEVERSON, A. J. MADDEN and EDGAR L. PIRET, Evaporation rates of liquids to flowing gas streams. *J. Amer. Inst. Chem. Engrs.* **5**, No. 4, 413 (1959).

E. SOKOLOVA, Investigation of heat emission during the condensation of Freon (in Russian). *Skolodil'naya Tekhnika* No. 3, 71–75 (1957). *Ref. Zh. Mekh.* No. 6, Rev. 6781 (1958).

E. M. SPARROW and J. L. GREGG, The effect of vapor drag on rotating condensation. *J. Heat Transfer* **2**, No. 1, 71 (1960).

E. M. SPARROW and J. L. GREGG, Laminar condensation heat transfer on a horizontal cylinder. *J. Heat Transfer* **81**, No. 4, 291 (1959).

L. SZUCS, Analytical examination of changes of state at material and heat transfer at constant liquid temperature (in Hungarian). *Energia es Atomtechnika.* **11**, No. 3, 164 (1958).

M. YU. TANANAYKO, The heat transfer during the boiling of water within the flowing film. (Teplootdacha pri Kipenii vody v stekayushchey plenke). *Izv. Kiyevsk. Politekhn. in-ta.* **17**, 75 (1956).

A. G. TKACHEV, Heat exchange during the melting of ice in freely-moving water. (Teploobmen pri Plavlenii l'da v svobodno Dvizhushcheysya Vode). *Tr. Leningr. in-ta. Kholodil'noy i moloch. prom. sti.* **4**, 48 (1953).

S. J. D. VAN STVALEN, *Warmteoverdracht Aan Kokende Binaire Vloeistofmengsola.* Dissertation. H. Veenman en Zoen N.V., Wageningen (Holland) (1959).

V. I. VOROIN, On the calculation of a laminar boundary layer on rotating bodies in a compressible gas (O raschete Laminarnogo Pogranichnogo Sloya na telakh Vrasheniya v Szhimayemon Gaze). *Voronezhsk. in-ta.* **42**, No. 2, 11 (1956).

A. S. VOS, Superheating and distribution of the temperature in the liquid and vapor of boiling liquids (in Dutch). *Ingenieur* **71**, No. 7, 0. 17–0. 20 (1959).

F. VOTTA and C. A. WALKER, Condensation of vapor in the presence of noncondensing gas. *J. Amer. Inst. Chem. Engrs.* **4**, No. 4, 413 (1958).

CHANNEL FLOW

VEDAT S. ARPACI and JOHN A. CLARK, Dynamic response of heat exchangers having internal heat sources—Part III. *J. Heat Transfer* **81**, No. 4, 253 (1959).

R. B. BIRD, *Zur Theorie des Wärmeübergangs an nicht-Newtonsche Flüssigkeiten bei Laminärer Rohrströmung.* University of Wisconsin. Reprint No. 392, Reprint *Chem.-Ing.-Tech.* **31**, 569 (1959).

R. D. CESS and E. C. SHAFFER, Heat transfer to laminar flow between parallel plates with a prescribed wall heat flux. *Appl. Sci. Res., Hague* A **8**, No. 5, 339 (1959).

S. C. R. DENNIS, A. M. MERCER and G. POOTS, Forced heat convection in laminar flow through rectangular ducts. *Quart. Appl. Math.* **17**, 285 (1959).

L. S. HAN, *Hydrodynamic Entrance Lengths for Incompressible Laminar Flow in Rectangular Ducts.* ASME Paper No. 59–A–82 (1959).

L. S. HAN, Laminar heat transfer in rectangular channels. *ASME Trans.* 81*C* (*J. Heat Transfer*) **2**, 121 May (1959).

H. HAUSEN and L. DÜWEL, Zur Frage nach dem Gleichwertigen Durchmesser Beider Wärmeübertragung in Einseitig Beheizten Spalten. *Kältetechnik.* **11**, Heft 8, 242 (1959).

FRANK KREITH and DAVID MARGOLIS, Heat transfer and friction in turbulent vortex flow. *Appl. Sci. Res., Hague* A **8**, No. 6, 457 (1959).

R. T. LANCET, The effect of surface roughness on the convection heat-transfer coefficient for fully developed turbulent flow in ducts with uniform heat flux. *ASME Trans.* 81*C* (*J. Heat Transfer*) **2**, 168 (1959).

M. F. NAGIYEV and P. V. KARAMZIN, Determination of the coefficient of heat emission of the flow in a tubular space when the hydrodynamic regime is in a transition stage (in Russian). *Izv. AzSSR* No. 5, 35 (1957). *Ref. Zh. Mekh.* No. 6, Rev. 6772 (1958).

S. A. REGIRER, On convective motion of a conducting fluid between parallel vertical plates in a magnetic field. *Soviet Physics—J. of Experimental and Theoretical Physics* **37** (10), No. 1, 149 (1960).

H. L. RITZ, The polyzonal fuel element. *Heaton Works J.* **8**, No. 47, 255 (1958).

N. W. RYAN and M. M. JOHNSON, Transition

from laminar to turbulent flow in pipes. *J. Amer. Inst. Chem. Engrs.* **5**, No. 4, 433 (1959).

J. A. SCANLAN, Effects of normal surface vibration on laminar forced convective heat transfer. *Indust. Engng. Chem.* **50**, No. 10, 1565 (1958).

R. SIEGEL and E. M. SPARROW, Turbulent flow in a circular tube with arbitrary internal heat sources and wall heat transfer. *J. Heat Transfer* **81**, No. 4, 280 (1959).

N. A. SLEZKIN, On the development of the flow of a viscuous heat-conducting gas in a pipe. *J. Appl. Math. Mech.* (PMM) **23**, No. 2, 473 (1959).

JACK M. SPURLOCK, THOMAS W. JACKSON, KENNETH R. PURDY, CALVIN C. OLIVER and HAROLD L. JOHNSON, *The Effect of Resonant Acoustic Vibrations on Heat Transfer to Air Horizontal Tubes.* WADC TN 59–330 (1959).

KARL STEPHAN, Wärmeübergang und Druckabfall bei nicht Ausgebildeter Laminarstromung in Rohren und in Ebenen Spalten. *Chem.-Ing.-Tech.* **31**, No. 12, 773 (1959).

KARL STEPHAN, *Wärmeübergang und Druckabfall Laminarer Strömungen im Einlauf von Rohren und Ebenen Spalten.* Überreicht vom Kältetechn. Institut und Thermodyn. Institut der Technischen Hochschule Karlsruhe (1959).

M. A. STYRIKOVICH and L. E. FAKTOROVICH, Effect of tube length on the magnitude of critical heat flow with forced convection of steam–water mixtures. *Soviet Phys.-Doklady* **3**, No. 3, 518 (1959).

N. V. TSARENKO, An investigation of the heat transfer in a turbulent flow of liquid through a narrow rectangular conduit (Issledovaniye Teplootdach pri Turbulentnom Techenii Zhdokostey v Uzkikh Kanalakh Pryamougol' nogo Secheniya). *Izv. Kiyevsk. Politkhn. in-ta.* **17**, 143 (1956).

L. A. VVEDENSKARA, To the experimental determination of the correction to the hydrodynamic theory of heat exchange for the turbulent flow in pipes (K Eksperimental'nomu Opredeleniyu Popravki k Gidrodinamicheskoy Teorii Teploobmena pri Turbulentnom Dvizhenii v Trubakh). *Sb. Nauch. tr. Kuylshevsk. Industr. in-ta.* Book 1, No. 6, p. 225 (1956).

HELMUT WOLF, Heating and cooling air and carbon dioxide in the thermal entrance region of a circular duct with large gas to wall temperature differences. *J. Heat Transfer* **81**, No. 4, 267 (1959).

V. S. YABLESKIY, Analysis of certain problems of the transport of heated viscous liquids through pipelines (Analiz Nekotorykh Voprosov Perekachki Podogretykh Vyazkikh Zhidkostey po Truboprovodam). *Tr. Mosk. Neft. in-ta.* Nr. 17, 3 (1956).

CONDUCTION

H. R. BAILY, Heat conduction from a cylindrical source with increasing radius. *Quart. Appl. Math.* **17**, 255 (1959).

GEORGE BAKER, JR. and THOMAS A. OLIPHANT, An implicit, numerical method for solving the two-dimensional heat equation. *Quart. Appl. Math.* **17**, No. 4, 361 (1960).

JAMES BECK and H. HURWICZ, Effect of thermocouple cavity on heat sink temperature. *J. Heat Transfer* **82**, No. 1, 27 (1960).

V. A. BERG, On the construction of the temperature field in a snow and ice cover. (O Postroyenii Temperaturnogo Polya v Snego-Ledyanom Pokrove). *Tr. Leningr. Gidrometeorol. in-ta.* Nr. 5–6, 59 (1956).

PAUL L. CHAMBRE, Nonlinear heat transfer problem. *J. Appl. Phys.* **30**, No. 11 (1959).

S. W. CHURCHILL and R. E. BALZHISER, The radial heat flux. *Chem. Engr. Prog. Symposium Series* **55**, No. 29, 127 (1959).

FORBES DEWEY, STEWART I. SCHLESINGER and LAWRENCE SASHKIN. Temperature profiles in a finite solid with moving boundary. *J. Aero. Space Sci.* **27**, No. 1, 59 (1960).

R. E. GIBSON, A heat conduction problem involving a specified moving boundary. *Quart. Appl. Math.* **16**, No. 4, 426. Notes (1959).

E. P. GROSS and S. ZIERING, Heat flow between parallel plates. *Phys. Fluids* **2**, No. 6, 701 (1959).

C. F. HANSEN, R. A. EARLY, F. E. AZOFON and F. C. WITTEBORN, *Theoretical and Experimental Investigation of Heat Conduction in Air, Including Effects of Oxygen Dissociation.* NASA TR NR–27 (1959).

P. R. HILL, *A Method of Computing the Transient Temperature of Thick Walls from Arbitrary Variation of Adiabatic-Wall Temperature and*

Vol. 1 1960

Heat-Transfer Coefficient. NACA Rep. 1372 (1958).

G. HORVAY, Freezing of a growing liquid column. *J. Heat Transfer* **82**, No. 1, 37 (1960).

J. C. JAEGER, The analysis of aquifer test data or thermal conductivity measurements which use a line source. *J. Geophys. Res.* **64**, No. 5, 561 (1959).

J. C. JAEGER, The use of complete temperature–time curves for the determination of thermal conductivity with particular reference to rocks. *Austral. J. Physics* **12**, No. 3, 203 (1959).

S. V. LUTKOVSKIY, On the subject of the establishment of the temperature in a shallow section of the sea during the period immediately preceding its icing over (Kovoprosu o Formirovanii Temperatury Morya na Melkovod'ye v Predledostavnyy period). *Tr. Mor. Gidrofiz. in-ta. AN SSR* 7, 135 (1956).

T. P. NEWCOMB, *Transient Temperatures in Brake Drums and Linings*. Instn. Mech. Engrs. (1958).

R. K. PEFLEY, *Extension of Cooling Fin Theory-Application to Axial Flow Heat Transfer Surfaces with Longitudinal Fins*. Dept. of Mech. Eng., Stanford University. TR No. 47 (1959).

S. P. PUSTOVOIT, Transient thermal convection in a spherical cavity. *Appl. Math. Mech. (Prikl. Math. Mekh.)* **22**, No. 4, 800 (1958).

B. SAELMAR, Integration of some thermal differential equations. *J. Aero. Space Sci.* **26**, No. 11, 754 (1959).

A SELLERIO, A method of false position for the approximate solution of the problem of transmission of heat in the stationary regime (in Italian). *Termotecnica* **12**, No. 7, 306 (1958).

G. STOLZ, Numerical solutions to an inverse problem of heat conduction for simple shapes. *J. Heat Transfer* **82**, No. 1, 20 (1960).

THOMAS E. STONECYPHER, Periodic temperature distribution in a two-layer composite slab. *J. Aero. Space Sci.* **27**, No. 2, 152 (1960).

ROBERT T. SWANN, *Calculated Effective Thermal Conductivities of Honeycomb Sandwich Panels*. NASA TN D–171 (1959).

W. F. G. SWANN, Theory of the A. J. Joffe method for rapid measurement of the thermal conductivity of solids. *J. Franklin Inst.* **267**, No. 5, 363 (1959).

C. J. THORNE, *Temperature Tables, Part I. One-Layer Plate, One-Space Variable, Linear*. NAVORD Rep. 5562. NOTS 1756 (1957).

V. VODICKA, Some problems on heat conduction in Stratiform bodies. *J. Phys. Soc. Japan* **14**, No. 2, 216 (1959).

W. A. WOLFE, Transient response of heated air in an enclosure with heat losses. *Trans. ASME* 81*C* (*J. Heat Transfer*) **1**, 19 (1959).

FLOW WITH SEPARATED REGIONS

W. O. CARLSON, *Heat Transfer in Laminar Separated and Wake Flow Regions*. Heat Trans. and Fluid Mech. Inst. p. 140 (1959).

T. FURMAN and H. HAMPSON, Experimental investigation into the effects of cross flow with condensation of steam and steam–gas mixtures on a vertical tube. *J. Inst. Mech. Engr.* No. 5, 147 (1959).

F. H. GARNER, V. G. JENSON and R. B. KEEY, Flow pattern around spheres and the Reynolds analogy. *Trans. Inst. Chem. Engrs.* **37**, No. 4, 191 (1959).

F. H. GARNER and J. J. LANE, Mass transfer to drops of liquid suspended in a gas stream. Part II—experimental work and results. *Trans. Inst. Chem. Engrs.* **37**, No. 3, 162 (1959).

D. M. KUEHN, *Experimental Investigation of Pressure Rise Required for Incipient Separation of Turbulent Boundary Layers in Two-Dimensional Supersonic Flow*. NASA Memo. 1–21–59A (1959).

HOWARD K. LARSON, Heat transfer in separated flows. *J. Aero. Space Sci.* **26**, No. 11, 731 (1959).

B. H. LOCHTENBERG, Transition in a separated laminar boundary layer. *J. Aero. Space Sci.* **27**, No. 2, 92 (1960).

HELMER V. NIELSEN, *Heat Transfer on an Afterbody Immersed in the Separated Wake of a Hemisphere*. NACA RM A57K07a (1958).

J. F. RICHARDSON and P. AYERS, Heat transfer between particles and a gas in a fluidised bed. *Trans. Inst. Chem. Engrs.* **37**, No. 6, 314 (1959).

R. A. SEBAN, A. EMERY and A. LEVY, Heat transfer to separated and reattached subsonic turbulent flows obtained downstream of a

surface step. *J. Aero. Space Sci.* **26**, No. 12, 809 (1959).

L. E. SCRIVEN and R. L. PIGFORD, Fluid dynamics and diffusion calculations for laminar liquid jets. *J. Amer. Inst. Chem. Engrs.* **5**, No. 3, 397 (1959).

LIQUID METALS

V. M. BORISHANSKII and S. S. KUTATELADZE, Heat transfer and hydraulic resistance during flow of liquid metals in circular tubes. *Soviet Phys.-J. Tech. Phys.* **3**, No. 4, 781 (1958).

S. S. KUTATELADZE, Heat transfer during flow of liquid metals in tubes and on plane plates. *Soviet Phys.-J. Tech. Phys. Nauk SSSR* **28**, No. 4, 848 (1958).

LOW DENSITY

HERBERT L. BOMELBURG, Heat loss from very thin heated wires in rarefied gases. *Phys. Fluias* **2**, No. 6, 717 (1959).

BARRY L. REEVES, *Aerodynamic Heating in the Slip, Intermediate and Free Molecule Flow Regime*. McDonnell Aircraft Corporation Research Dept. Report No. 6859 (1959).

K. TAKAO and T. FUJIMOTO, *Heat Transfer in the Rarefied Gases*. Mem. Fac. Engng., Univ. Nagoya **9**, No. 2, p. 379 (1957).

O. E. TEWFIK and W. H. GIEDT, *Local Heat Transfer, Recovery Factor, Pressure Distribution Around a Circular Cylinder Normal to a Rarefied Supersonic Air Stream*. Heat Trans. and Fluid Mech. Inst. p. 15 (1959).

MEASUREMENT TECHNIQUES

V. P. BABENKO, V. L. BROUDE, V. S. MEDVEDEV and A. F. PRIKHOT'KO, Methods and apparatus for low temperature optical and spectral studies (Metody i Apparatura Nizkotemperaturnykh Opticheskikh i Spektral'nykh Issledovaniy). *Pribory i Teknika Eksperimenta*. Nr. 1, p. 116 (1959).

C. R. BINGHAM, Temperature detectors. *Electronics* **32**, No. 28, 55 (1959).

B. B. BRENDEN, H. W. NEWKIRK and R. D. BIRKHOFF, *Principles of High Temperature Microscopy*. USAEC HW-58303 (1959).

D. A. DAVIS, Two thermocouples suitable for measurement of temperatures up to 2800°C. *J. Sci. Instrum.* **37**, No. 1, 15 (1960).

B. S. DEYCHMAN, Temperature measurement in a high-speed gas flow (Izmereniye Temperatury v Potoke Gaza bol'shikh Skorostey). *Tr. Ufimsk. Aviats. in-ta.* Nr. 2, 23 (1956).

T. C. HARMAN, J. H. CAHN and M. J. LOGAN, Measurement of thermal conductivity by utilization of the Peltier effect. *J. Appl. Phys.* **30**, 1351 (1959).

WILLIAM W. HILL and PAUL E. STANLEY, *Instrumentation Studies for Plasma Jet and Hypersonic Wind Tunnel*. Purdue Research Foundation, Research Project No. 1717, Rep. No. A–59–12 (1959).

C. E. MOELLER, Special thermocouple solves surface–temperature problem. *J. Instrum. Soc. Amer.* **6**, No. 6, 47 (1959).

CHARLES C. MORGAN and JACK C. ANDREWS, "*Morgandyne*" *Heat-Transfer Transducer and Flame-Torch Calibration Technique for Hypervelocity Wind Tunnels*. Arnold Engineering Development Center. USAF AEDC–TR–60–1 (1960).

YU. V. SHARVIN, Anthracite thermometers for various temperature ranges (Ugol'nyye termometry iz Antratsita dlya Razlichnykh Temperaturnykh Intervalov). *Pribory i tekhnika Eksperimenta* Nr. 1, 147 (1959).

C. SHEER, L. H. MEAD, D. L. ROTHACKER and L. H. JOHNSON, *Measurement of Thermal Diffusivity of Various Materials by Means of the High Intensity Electric Arc Technique*. WADC TR 57–226 (PB 131 601; ASTIA AD 142 093) (1957).

RUDOLF STARITZ, Die Elektronische Messung der Stromungsgeschwindigkeit und der Turbulenz. *Ver. Deutsch. Ing. Zeit.* **102**, No. 3S, 94 (1960).

WILLIAM F. VAN TASSELL and EUGENE E. COVERT, Relaxation effects on the interpretation of impact-probe measurements. *J. Aero. Space Sci.* **27**, No. 2, 147 (1960).

K. P. VLASOV, Measuring flame temperature by optical methods. *Teploenergetika* **6**, No. 9, 87 (1959).

NATURAL CONVECTION

V. K. BAYEV, Nonstationary convective flows (Nestatsionarnyye Konvektivnyye Techeniya). *Tr. Tsentr. in-ta Prognozov.* Nr. 43 (70), 3 (1956).

RICHARD P. BABCO, A closed-form solution for

Vol. 1 1960

laminar free convection on a vertical plate with prescribed, nonuniform, wall heat flux. *J. Aero. Space Sci.* **26**, No. 12, 846 (1959).

YE. M. DOBRYSHMAN, A nonstationary problem on convection near a vertical wall (Nestatsionarnaya Zadacha o Konvektsii u Vertikal' noy Stenki). *Tr. Tsentr. in-ta Prognozov.* Nr. 43 (70), 57 (1956).

A. J. EDE, *Natural Convection on Free Vertical Surfaces.* Mech. Engineering Research Lab. Heat 141 (DSIR, Gt. Brit.) (1956).

J. R. FOOTE, An asymptotic method for free convection past a vertical plate (in English). *Z. Angew. Math. Phys.* **9**, No. 1, 64 (1958).

ARTHUR W. GOLDSTEIN, *Stability of a Horizontal Fluid Layer With Unsteady Heating From Below and Time Dependent Body Force.* NASA TR R–4, 15p (1959).

H. HAUSEN, Neue Gleichungen für die Wärmeübertragung bei freier oder erzwungener Strömung. *Allg. Wärmetech.* **9**, Heft 4–5, 75 (1958).

YOSHINARI NAKAGAWA, Heat transport by convection. *Phys. Fluids* **3**, No. 1, 82 (1960).

L. V. NESINA, On the effect of the temperature stratification on the heat exchange in water (O Vliyanii Stratifikatsii Temperatury na Temploobmen v vode). *Tr. Geofiz. Observ.* Nr. 59, 37–39 (1956).

G. A. OSTROUNOV and V. A. TETIUEV, On the question of the theory of free thermal convection in cylindrical cavities. *Soviet Phys.-Tech. Phys.* **3**, No. 6, 1173 (1959).

G. A. OSTROUMOV, The temperature of a horizontal wire heated by alternating current. *Soviet Phys.-Tech. Phys.* **3**, No. 7, 1452 (1959).

D. F. PAVLOV, Formation of a turbulent flow during free convection (in Russian). *Trudi Srednea. In-ta.* No. 91, 67 (1959); *Ref. Zh. Mekh.* No. 5, Rev. 5488 (1958).

W. H. REID and D. L. HARRIS, Streamlines in Benard convection cells. *Phys. Fluids* **2**, No. 6, 716 (1959).

I. G. SEVRUK, Laminar convection over a linear heat source. *Appl. Math. Mech.* (*Prikl. Math. Mekh.*) **22**, No. 4, 807 (1958).

E. E. SOEHNGEN, Interferometric studies on heat transfer (in English). *Ninth Congrès Int. Mèc. Appl. Univ. Bruxelles* **4**, 475 (1957).

K. A. TER-MKRTCHYAN, Investigation of heat exchange processes by the laminar motion of heat carriers in constructions adopted for water heating (in Russian). *Sb. Nauch. Trudi Erevansk. Politekhn. In-ta.* No. 6, 141–149 (1956); *Ref. Zh. Mekh.* No. 1, Rev. 773 (1958).

A. A. TOWNSEND, Temperature fluctuations over a heated horizontal surface. *J. Fluid Mech.* **5**, No. 2, 209 (1959).

PROPERTIES

KENNETH P. COFFIN, Effect of Argon and Helium on the thermal conductivity of the $N_2O_4 \rightleftarrows 2NO_2$ system. *J. Chem. Phys.* **31**, No. 5, 1290 (1959).

NATHANIEL B. COHEN, *Correlation Formulas and Tables of Density and Some Transport Properties of Equilibrium Dissociating Air for Use in Solutions of the Boundary-Layer Equations.* NASA TN D–194 (1960).

JOSEPH KESTIN, WOLFGANG LEIDENFROST and C. Y. LIU, On relative measurements of the viscosity of gases by the oscillating-disk method. *Z. Angew. Math. Phys.* **10**, Fasc. 6, 558 (1959).

D. B. MANN and R. B. STEWART, Thermodynamic properties of Helium at low temperatures and high pressures. *J. Heat Transfer* **81**, No. 4, 323 (1959).

CHARLES A. SCHAEFER and GEORGE THODOS, Thermal conductivity of diatomic gases: liquid and gaseous states. *J. Amer. Inst. Chem. Engrs.* **5**, No. 3, 367 (1959).

ROBERT G. VINES, Measurement of the thermal conductivities of gases at high temperatures. *J. Heat Transfer* **82**, No. 1, 48 (1960).

RADIATION

J. G. BARTAS and W. H. SELLERS, Radiation fin effectiveness. *J. Heat Transfer* **82**, No. 1, 73 (1960).

J. T. BEVANS and R. V. DUNKLE, Radiant interchange within an enclosure. *J. Heat Transfer* **82**, No. 1, 1 (1960).

R. L. CHAMBERS and E. V. SOMERS, Radiation fin efficiency for one-dimensional heat flow in a circular fin. *J. Heat Transfer* **81**, No. 4, 327 (1959).

V. I. DANILOVSKAYA, Temperature field and temperature stresses arising in an elastic half-space due to flow of radiant energy falling

on the boundary of the half-space (Temperaturnoye pole i Temperaturnyye Napryazheniya, Voznikayushchiye v Uprugom Poluprostranstve Vsledstviye Potoka luchistoy Energii, Padayushchey na Granitsu Poluprostranstva). *Izv. Akad. Nauk SSSR, Otd. Tekh. Nauk, Mekh. i Mashinostr.* Nr. 3, 129 (1959).

R. V. DUNKLE, F. EHRENBURG and J. T. GIER, Spectral characteristics of fabrics from 1 to 23 microns. *J. Heat Transfer* **82**, No. 1, 64 (1960).

D. M. FINCH (I), J. M. CHORLTON and H. F. DAVIDSON (II), ISSAC GOODBAR (III), The effect of specular reflection on visibility. (I) physical measurement for the determination of brightness and contrast. (II) field measureements of loss of contrast. (III) new charts for brightness contrast calculations. *Illum. Engng.* **54**, 474 (1959).

P. E. GLASER and H. H. BLAU, A new technique for measuring the spectral emissivity of solids at high temperatures. *ASME* 81*C* (*J. Heat Transfer*) **1**, 92 (1959).

R. GOULARD and MADELEINE GOULARD, *Energy Transfer in the Couette Flow of a Radiant and Chemically Reacting Gas.* Heat Trans. and Fluid Mech. Inst. 126 (1959).

R. GOULARD, *Fluxes and Non Diemensional Parameters in Radiant Gases.* Purdue Research Foundation, Research Project No. 1717, Rep. No. A–59–8 (1959).

GEORG HASS, L. F. DRUMMETER and MILTON SCHACH, Temperature stabilization of highly reflecting spherical satellites. *J. Opt. Soc. Amer.* **49**, 918 (1959).

E. H. HUBBARD, Comparison of different methods of fluidatomizing oil flames and the effect on flame emissivity and radiation of the addition of carbon black to liquid fuels. Comparision of different methods of fluidatomizing oil flames. *J. Inst. Fuel.* 328 (1959).

F. B. HILL and R. H. WILHELM, Radiative and conductive heat transfer in a quiescent gas–solid bed of particles: theory and experiment. *J. Amer. Inst. Chem. Engrs.* **5**, No. 4, 486 (1959).

J. C. KECK, J. C. CAMM, B. KIVEL and T. WENTINK, Radiation from hot air. *Ann. Phys.* **7**, No. 1, 1 (1959).

BENNETH KIVEL, *Radiation From Hot Air and Stagnation Heating.* AVCO Everett Research Laboratory, Res. Rep. 79, AFBMD TR 59–20 (1959).

BERT K. LARKIN and STUART W. CHURCHILL, Heat transfer by radiation through porous insulations. *J. Amer. Inst. Chem. Engrs.* **5**, No. 4, 467 (1959).

SEYMOUR LIEBLEIN, *Analysis of Temperature Distribution and Radiant Heat Transfer Along a Rectangular Fin of Constant Thickness.* NASA TN D–196 (1959).

GUNTER LUCK, Bestrahlung Strahlungsdurchlässiger Körper. *Chem.-Ing.-Tech.* Heft 1, No. 32, 29 (1960).

A. K. OPPENHEIM and J. T. BEVANS, *Geometric Factors for Radiative Heat Transfer Through Absorbing Medium in Cartesian Co-ordinates.* ASME Paper No. 59–A–206 (1959).

W. J. O'SULLIVAN and W. R. WADE, *Theory and Apparatus for Measurement of Emissivity for Radiative Cooling of Hypersonic Aircraft with Data for Inconel and Inconel X.* NACA TN 4121 (1957).

WILLIAM H. ROBBINS, *Analysis of the Transient Radiation Heat Transfer of an Uncooled Rocket Engine Operating Outside Earth's Atmosphere.* NASA TN D–62 (1959).

JOHN STRONG and G. A. VANASSE, Interferometric spectroscopy in the far infrared. *J. Opt. Soc. Amer.* **49**, 844 (1959).

TRANSFER MECHANISMS

DARWIN CLUTTER and A. M. O. SMITH, Analysis of further data on the effect of isolated roughness on boundary-layer transition in supersonic flow. *J. Aero. Space Sci.* **27**, No. 1, 70 (1960).

D. W. DUNN and W. H. REID, *Heat Transfer in Isotropic Turbulence During the Final Period of Decay.* NACA TN 4186 (1958).

J. C. GIBBINGS, On the effect of a narrow band of distributed roughness upon boundary-layer transition. *J. Aero. Space Sci.* **26**, No. 12, 843 (1959).

P. C. JAIN, A theory of homogeneous isotropic turbulence. *Appl. Sci. Res., Hague* A **8**, No. 2–3, 219 (1959).

ROBERT J. MCCARTER and LEROY F. STUTZMAN, Transfer resistance and fluid mechanics. *J. Amer. Inst. Chem. Engrs.* **5**, No. 4, 502 (1959).

R. R. MILLS, A. L. KISTLER, V. O'BRIEN and

Vol. 1 1960

S. CORRSIN, *Turbulence and Temperature Fluctuations Behind a Heated Grid.* NACA TN 4288 (1958).

R. MICHEL, Present knowledge of high speed transition. *Rech. Aeronaut.* No. 71, 29 (1959).

A. S. MONIN, Of diffusion with a finite velocity (in Russian). *Izv. Akad. Nauk SSSR, Ser. Geofiz.* No. 3, 234 (1955); *Ref. Zh. Mekh.* No. 6, Rev. 6805 (1958).

J. ROTTA, Über den Einfluss der Machschen Zahl und des Wärmeübergangs auf das Wandgesetz Turbulenter Strömung. *Z. Flugwissensch.* **7**, 264 (1959).

KENNETH F. STETSON, Boundary-layer transition on blunt bodies with highly cooled boundary-layers. *J. Aero. Space Sci.* **27**, No. 2, 81 (1960).

TRANSPIRATION AND MASS TRANSFER COOLING

ROY E. BARTLE and BERNARD M. LEADON, Experimental evaluation of heat transfer with transpiration cooling in a turbulent boundary-layer at M = 3·2. *J. Aero. Space Sci.* **27**, No. 1, 78 (1960).

J. R. BELL and A. H. NISSAN, Mechanism of drying thick porous bodies during the falling rate period. Part II: A hyroscopic material. *J. Amer. Inst. Chem. Engrs.* **5**, No. 3, 344 (1959).

ALECK C. BOND, BERNARD RASHIS and L. ROSS LEVIN, *Experimental Ablation Cooling.* NACA RM L58E15a (1958).

F. BURGGRAF, J. H. CHIN and L. E. HAYES, *Film-Cooling Data for Multiple Rows of Discrete Louvers, Overall Effectiveness Downstream of One to Twenty Rows of Punched Crescent Louvers.* General Electric Co., Cincinatti, Technical Information Series No. R59FPD804 (1959).

J. H. CHIN, F. BURGGRAF and L. E. HAYES, *Design Data for Multiple-Slot Film Cooling. Part II—Generalized Correlation Downstream of N Slots.* General Electric Co., Cincinatti, Technical Information Series No. R59FPD803 (1959).

PAUL M. CHUNG, *Shielding Stagnation Surfaces of Finite Catalytic Activity by Air Injection in Hypersonic Flight.* NASA TN D–27 (1959).

ALAN Q. ESCHENROEDER, The compressible laminar boundary layer with constant injected mass flux at the surface. *J. Aero. Space Sci.* **26**, No. 11, 762 (1959).

F. H. GARNER and P. KENDRICK (I), F. H. GARNER and J. J. LANE (II). Mass transfer to drops of liquid suspended in a gas stream (I). Experimental work and results (II). *Trans. Inst. Chem. Engrs.* **37**, No. 3, 155 (1959).

S. GEORGIEV, H. HIDLAGO and M. C. ADAMS, *On Ablation for the Recovery of Satellites.* Heat Trans. and Fluid Mech. Inst., Univ. Calif. p. 171 (1959).

S. GEORGIEV, H. HIDALGO and M. C. ADAMS, *On Ablating Heat Shields for Satellite Recovery.* AVCO Everett Research Laboratory, Res. Rep. 65 (AFBMD–TR–59–7) (1959).

T. R. GOODMAN, Aerodynamic ablation of melting bodies. *Proc. Third U.S. Nat. Congr. Appl. Mech.* (1958); *Amer. Soc. Mech. Engrs.* 735 (1958).

LEON GREEN and KENNETH L. NALL, Experiments on porous-wall cooling and flow separation control in a supersonic nozzle. *J. Aero. Space Sci.* **26**, No. 11, 689 (1959).

G. G. HASELDEN and S. A. MALATY, Heat and mass transfer accompanying the absorption of ammonia in water. *Trans. Inst. Chem. Engrs.* **37**, 137 (1959).

HENRY HIDALGO, *A Theory of Ablation of Glassy Materials for Laminar and Turbulent Heating.* AVCO Everett Research Laboratory, Res. Rep. 62 (AFBMD–TN–59–13) (1959).

WILLIAM H. KINARD, *Feasibility of Nose-Cone Cooling by the Upstream Ejection of Solid Coolants at the Stagnation Point.* NACA RM L57K22 (1958).

PAUL A. LIBBY and ROBERT J. CRESCI, *Experimental Investigation of the Downstream Influence of Stagnation Point Mass Transfer.* PIBAL Rep. No. 520, WADC TN 59–210 (1959).

MITCHELL LITT and S. K. FRIEDLANDER, An experimental study of diffusion-controlled reactions in a laminar boundary layer. *J. Amer. Inst. Chem. Engrs.* **5**, No. 4, 483 (1959).

R. I. MACEY, A quasi-steady-state approximation method for diffusion problems. Part I. concentration dependent diffusion coefficients. *Bull. Math. Biophys.* **21**, No. 1, 19 (1959).

H. J. MERK, The microscopic equations for simultaneous heat and mass transfer in

isotropic, continuous and closed systems. *Appl. Sci. Res., Hague* A **8**, No. 1, 73 (1958).

A. H. NISSAN, W. G. KAYE and J. R. BELL, Mechanism of drying thick porous bodies during the falling rate period. Part I—Pseudo-wet-bulb-temperature. *J. Amer. Inst. Chem. Engrs.* **5**, No. 1, 103 (1959).

BERNARD RASHIS, WILLIAM G. WITTE and RUSSELL N. HOPKO, *Qualitative Measurements of the Effective Heats of Ablation of Several Materials in Supersonic Air Jets at Stagnation Temperature up to* 11,000°*F*. NACA RM L58E22 (1958).

L. ROBERTS, *Stagnation-Point Shielding by Melting and Vaporization*. NASA Report No. 10 (1959).

F. R. SEDLUND and C. C. CHANG, Blunt-nosed bodies in a high-temperature gas jet. *Nature, Lond.* **184**, 812 (1959).

S. M. SCALA, *A Study of Hypersonic Ablation*. GE MSVD. Technical Information Series R59SD438 (1959).

S. M. SCALA and N. S. DIACONIS, The stagnation-point ablation of Teflon during hypersonic flight. *J. Aero. Space Sci.* **27**, No. 2, 140 (1960).

S. M. SCALA, Sublimation in a hypersonic environment. *J. Aero. Space Sci.* **27**, No. 1, 1 (1960).

S. M. SCALA, *Vaporization of a Refractory Oxide During Hypersonic Flight*. Heat Trans. and Fluid Mech. Inst., Univ. Calif. p. 181 (1959).

C. J. SCOTT, G. E. ANDERSON and D. R. ELGIN, *Laminar, Transitional and Turbulent Mass Transfer Cooling Experiments at Mach Numbers* 3–5. University of Minnesota, Research Report No. 162. AFOSR TN 59–1305 (1959).

I. T. SHVETS, YE. P. DYBAN and N. M. KONDAK, Investigation of the cooling of turbine wheels by means of air blown through the gaps in the swallow-tail mountings of the blades (Issledovaniye Okhlazhdeniya Diskov Turbin Produvkoy Vozdukha Cherez Montazhnyye Zazory Yelochnykh Khvostovikov Rabochikh Lopatok). *Sb. Tr. In-ta Teploenerg. AN UkrSSR*. Nr. 13, 20 (1956).

G. W. SUTTON, A comparison of several approximate theories of melting ablation. *J. Aero. Space Sci.* **26**, No. 6, 397 (Readers' Forum) (1959).

ROTATING

D. C. BRIGGS, *Heat Transfer in Rotating Turbulent Pipe Flow*. Stanford University TR No. 45 (1959).

D. R. DAVIES, Heat transfer by laminar flow from a rotating disk at large Prandtl numbers. *Quart. J. Mech. Appl. Math.* **12**, No. 1, 14 (1959).

L. A. DORFMAN, Influence of radial temperature gradient on heat transfer from a rotating disk (in Russian). *Izv. Akad. Nauk SSSR. Otd. Tekh. Nauk*. No. 12, 64 (1957).

L. A. DORFMAN, Thermal boundary layer on a rotating disc. *Soviet Phys.-Doklady*. **3**, No. 2, 248 (1958).

F. KREITH, J. H. TAYLOR and J. P. CHONG, Heat and mass transfer from a rotating disk. *ASME* 81*C* (*J. Heat Transfer*) **2**, 95 (1959).

D. W. MOORE, The flow past a rapidly rotating circular cylinder in a uniform stream. *J. Fluid Mech.* **2**, No. 6, 541 (1957).

G. A. TIRSKII, Nonstationary flow with heat transfer in a viscous, incompressible fluid between two revolving discs accompanied by fluid influx. *Soviet Phys.-Doklady*. **3**, No. 2, 237 (1958).

G. A. TIRSKII, On non-stationary heat transmission through a system of discs rotating in a Viscous Liquid (O Nestatsionarnoy Teploperedache Cherez Sistemu Diskov, Vrashchayuschchikhsya v Vyazkoy Zhidkosti). *Izvestiya Akademii nauk SSSR, Otdeleniye Tekhnicheskikh nauk*. p. 106 (1958).

G. VERONIS, Cellular convection with finite amplitude, in a rotating fluid. *J. Fluid Mech.* **5**, No. 3, 401 (1959).

Vol. 1 1960

Int. J. Heat Mass Transfer. Vol. 1, pp. 269–272. Pergamon Press 1961. Printed in Great Britain.

ON THE INVESTIGATION OF HEAT TRANSFER IN THE PRESENCE OF CHEMICAL CONVERSIONS

S. I. ANISIMOV and T. L. PERELMAN

Institute of Energetics of the Academy of Science of B.S.S.R., Podlesnaja 25, Minsk, B.S.S.R.

(*Received* 1 *March* 1960)

Abstract—The simplest boundary problem of unstationary heat-conduction equation, with the source depending on temperature as $\exp(-E^*/T)$ is investigated in this paper.

The uniform convergence of successive approximations is proved for the corresponding integral equation; the solutions have been calculated in the first approximation at various limit cases. It has been also shown here that in the absence of "explosion" the temperature at each point will not exceed at any moment of time the corresponding stationary temperature.

Résumé—Ce travail traite du problème aux limites le plus simple de l'équation de la chaleur en régime non permanent en présence d'une source dépendant de la température comme $\exp(-E^*/T)$.

La convergence uniforme des approximations successives est démontrée pour l'equation intégrale correspondante; les solutions ont été caluculées pour la première approximation dans divers cas limites. On a montré aussi qu'en l'absence d'"explosion" la température en chaque point ne dépasse à aucun moment la température correspondant au régime stationnaire.

Zusammenfassung—Die Arbeit behandelt ein Problem der nichtstationären Wärmeleitung mit einfacher Randbedingung, bei welchem die Wärmequelle von der Temperatur nach der Funktion $\exp(-E^*/T)$ abhängt.

Die gleichmässige Konvergenz für die aufeinanderfolgenden Approximationen wird für die entsprechende Integralgleichung nachgeprüft. Lösungen werden als erste Näherungen für verschiedene Grenzfälle angegeben. Es zeigt sich auch, dass, abgesehen von "Explosionen", die Temperatur an jedem Punkt zu keinem Zeitpunkt die entsprechende stationäre Temperatur überschreitet.

Аннотация—В работе исследуется простейшая краевая задача нестационарного уравнения теплопроводности с источником зависящим от температуры как $\exp(-E^*/T)$.

Доказывается равномерная сходимость последовательных приближений для соответствующего интегрального уравнения; вычислены в первом приближении решения в различных предельных случаях. Показано также, что при отсутствии «взрыва» температура в каждой точке не будет превышать в любой момент времени соответствующую стационарную температуру.

In a number of thermal conductivity problems, e.g. in the case of heat-transfer problem in the capillary–porous media in the presence of chemical conversions† [1], or in the case of heat explosion problem [2, 3], we may meet the heat conduction equation with the heat source depending on the temperature as

$$\exp\left(-\frac{E^*}{T}\right)$$

where $E^* = E/R$ is the activation energy expressed in degrees and T is the absolute temperature.

† As was recommended by Academician Luikov.

Let us consider the boundary problem for the equation

$$\frac{\partial T}{\partial t} = a\nabla^2 T + \frac{K_0}{c_p \rho} \exp\left(-\frac{E^*}{T}\right) \qquad (1)$$

in the range limited by two parallel infinite planes $x = \pm l$

$$T(l, t) = T_c; \frac{\partial T(0, t)}{\partial x} = 0; T(x, 0) = T_0 \qquad (2)$$

Now we introduce dimensionless variables and can take advantage of the similarity criteria known in the heat-transfer theory [1]:

$$\xi = \frac{x}{l};\ Fo \equiv \tau = \frac{at}{l^2};\ Po \equiv \epsilon = \frac{K_0 l^2}{ac_p \rho E^*}$$

$$\theta(\xi, \tau) = \frac{T(x,t)}{E^*};\ \theta_c = \frac{T_c}{E^*};\ \theta_0 = \frac{T_0}{E^*} \qquad (3)$$

where Fo is the ordinary Fourier criterion of homocronism and Po is the modified Pomerantsev criterion.

If we designate the Green function of the heat conduction equation for the range $0 \leqslant \xi \leqslant 1, \tau \geqslant 0$ through $Y(\xi, \xi'; \tau - \tau')$ then for $\theta(\xi, \tau)$ the integral equation takes place:

$$\theta(\xi, \tau) = \psi(\xi, \tau) + \epsilon \int_0^\tau \int_0^1 Y(\xi, \xi'; \tau - \tau') \times \exp\left[-\frac{1}{\theta(\xi', \tau')}\right] d\tau' d\xi' \qquad (4)$$

where

$$\psi(\xi, \tau) = \theta_c - \frac{2}{\pi}(\theta_c - \theta_0) \sum_{n=0}^{\infty} \frac{(-1)^n}{n + \frac{1}{2}} \times \exp\left[-\pi^2 (n + \tfrac{1}{2})^2 \tau\right] \cos(n + \tfrac{1}{2})\pi\xi \qquad (5)$$

and the Green function

$$Y(\xi, \xi'; \tau - \tau') = \tfrac{1}{2}\left\{\vartheta_2\left[\frac{\xi + \xi'}{2}, i\pi(\tau - \tau')\right] + \vartheta_2\left[\frac{\xi - \xi'}{2}, i\pi(\tau - \tau')\right]\right\} \qquad (6)$$

The ϑ-function on the right side of the equation (6) is determined by the equality [4]:

$$\vartheta_2(u, iv) = 2 \sum_{n=0}^{\infty} \exp\left[-\pi(n + \tfrac{1}{2})^2 v\right] \cos(2n+1)\pi u$$

Note that the Green function is symmetric with reference to the variables ξ and ξ' and has nowhere negative values in the range under consideration.

It is possible to solve equation (4) by the method of successive approximation of the form

$$\theta^{(n+1)}(\xi, \tau) = \psi(\xi, \tau) + \epsilon \int_0^\tau \int_0^1 Y(\xi, \xi'; \tau - \tau') \times \exp\left(-\frac{1}{\theta^{(n)}(\xi', \tau')}\right) d\tau' d\xi'$$

$$\theta^{(0)}(\xi, \tau) = \psi(\xi, \tau); \quad (n = 0, 1, \ldots) \qquad (7)$$

If the parameter ϵ is small enough then it is possible to show that the succession of functions converges uniformly to the solution of the equation (4).

For the proof it is necessary to compose the difference

$$\theta^{(n+1)}(\xi, \tau) - \theta^{(n)}(\xi, \tau) = \epsilon \int_0^\tau \int_0^1 Y(\xi, \xi'; \tau - \tau') \left\{\frac{\exp[-1/\theta^{(n)}(\xi', \tau')] - \exp[-1/\theta^{(n-1)}(\xi', \tau')]}{\theta^{(n)}(\xi', \tau') - \theta^{(n-1)}(\xi', \tau')}\right\} \times [\theta^{(n)}(\xi', \tau') - \theta^{(n-1)}(\xi', \tau')] d\tau' d\xi' \qquad (8)$$

It should be noted that,

$\theta^{(n+1)} - \theta^{(n)} \geqslant 0$, since $\theta^{(0)}(\xi, \tau) = \psi(\xi, \tau) \geqslant 0$

and

$$Y(\xi, \xi'; \tau - \tau') \geqslant 0$$

If we designate the maximum of the difference $\theta^{(n+1)} - \theta^{(n)}$ through $M_{n+1} \geqslant 0$ then from the equation (8) it follows that

$$M_{n+1} \leqslant AM_n$$

where

$$A = \max\left\{\epsilon \int_0^\tau \int_0^1 Y \left[\frac{\exp(-1/\theta^{(n)}) - \exp(-1/\theta^{(n-1)})}{\theta^{(n)} - \theta^{(n-1)}}\right] d\tau' d\xi'\right\}$$

It is easy to make sure that $A < 1$, if $\epsilon < e^2/2$. In this case there exists a limit function of sequence (7) which is the solution of the equation (4).

Let us assume the above-mentioned method to get the approximate solutions in some ordinary limit cases. To begin with we shall take the solutions at large values of τ. As a zero approximation it is convenient to admit the stationary temperature distribution which is described by the equation

$$\frac{d^2\theta_{st}(\xi)}{d\xi^2} = -\epsilon \exp\left(-\frac{1}{\theta_{st}(\xi)}\right) \qquad (9)$$

with boundary condition as

$$\theta_{st}(1) = \theta_c;\ \frac{d\theta_{st}(0)}{d\xi} = 0 \qquad (10)$$

Vol. 1 1960

The solution of this equation is of the type:

$$\int_{\theta_c}^{\theta_{st}(\xi)} \frac{\mathrm{d}u}{\sqrt{[\theta_m \exp(-1/\theta_m) - u\exp(-1/u) + \\ + Ei(-1/\theta_m) - Ei(-1/u)]}} = \sqrt{(2\epsilon)}\,(1-\xi) \tag{11}$$

where the parameter θ_m is the maximum value of $\theta_{st}(\xi)$, which can be achieved because of symmetry at $\xi = 0$, and

$$Ei(x) = -\int_{-x}^{\infty} \frac{e^{-t}}{t}\,\mathrm{d}t$$

is the integral exponential function.

The solution (11) agrees with the boundary conditions not at any values of ϵ [2, 3] if ϵ is greater than some ϵ_{cr}, then the establishment of a stationary state is impossible. It means physically that heat supply exceeds heat output and the heat explosion will take place. The critical temperature θ_m^{cr} corresponding to the parameter ϵ_{cr} is being determined from the equation:

$$\left.\begin{aligned} &\frac{\theta_c}{\sqrt{[\theta_m \exp(-1/\theta_m) - \theta_c \exp(-1/\theta_c) + \\ Ei(-1/\theta_m) - Ei(-1/\theta_c)]}} + \\ &+\int_{\theta_c}^{\theta_m} \mathrm{d}u \frac{\theta_m \exp(-1/\theta_m) - u\exp(-1/u) + \\ + 2Ei(-1/\theta_m) - 2Ei(-1/u)}{[\theta_m \exp(-1/\theta_m) - u\exp(-1/u) + \\ + Ei(-1/\theta_m) - Ei(-1/u)]^{3/2}} \\ &= 0 \end{aligned}\right\} \tag{12}$$

[2] gives a physically interesting case of the latter solution when θ_m differs slightly from θ_c.

So, at $\epsilon < \epsilon_{cr}$ and $\tau \gg 4/\pi^2$ the approximation to the stationary state is being described by the relation

$$\theta(\xi, \tau) = \theta_{st}(\xi) + \frac{4}{\pi}\exp\left(-\frac{\pi^2}{4}\tau\right) \cos\frac{\pi}{2}\xi\left[\theta_0 - \frac{\pi}{2}\int_0^1 \theta_{st}(\xi')\cos\frac{\pi}{2}\xi'\mathrm{d}\xi'\right] \tag{13}$$

where $\theta_{st}(\xi)$ is given by the formula (11).

Normally such a case as $\theta \ll 1 (T \ll E^*)$ takes place in chemical kinetics. This allows one to simplify the initial integral equation by the method of "steepest descent"; for large $\tau (> 4/\pi^2)$ we have:

$$\theta(\xi, \tau) = \theta_{st}(\xi) - \frac{4}{\pi}\exp\left(-\frac{\pi^2}{4}\tau\right) \cos\frac{\pi}{2}\xi\left[\theta_c - \theta_0 + 2\sqrt{\left(\frac{2\epsilon}{\pi}\right)}\vartheta_m \exp\left(-\frac{1}{2\theta_m}\right)\right] \tag{14}$$

θ_m has been determined above.

Now we shall consider another extreme case, when τ is small. Here we can take the initial temperature θ_0 as a zero approximation. It is possible to simplify the kernel of the integral equation using the known relation for ϑ-functions [4]:

$$\vartheta_2(u, iv) = \frac{1}{\sqrt{v}}\exp\left(-\frac{\pi u^2}{v}\right)\vartheta_0\left(\frac{u}{iv}, \frac{i}{v}\right)$$

and retaining only the principal terms in the kernel at $\tau \to 0$. All the integrations are being easily carried out and we have:

$$\left.\begin{aligned} \theta(\xi, \tau) = \theta_c + \epsilon\exp(-1/\theta_0)\Bigg\{ &1 - \xi^2 + \\ &+ \sqrt{\left(\frac{\tau}{\pi}\right)}\left[(1-\xi)\exp\left(-\frac{(1-\xi)^2}{4\tau}\right) + \right. \\ &+ (1+\xi)\exp\left(-\frac{(1+\xi)^2}{4\tau}\right) - 2\exp \\ &\left.\left(-\frac{1}{\tau}\right)\right]\Bigg\} + \left\{\theta_0 - \theta_c + \epsilon\exp\left(-\frac{1}{\theta_0}\right)\right. \\ &\left.\left[\frac{(1-\xi)^2}{2} + \tau\right]\right\}\mathrm{erf}\left(\frac{1-\xi}{2\sqrt{\tau}}\right) + \\ &+ \left\{\theta_0 - \theta_c + \epsilon\exp\left(-\frac{1}{\theta_0}\right)\right. \\ &\left.\left[\frac{(1+\xi)^2}{2} + \tau\right]\right\}\mathrm{erf}\left(\frac{1+\xi}{2\sqrt{\tau}}\right) - \\ &- \left\{\theta_0 - \theta_c + \epsilon\exp\left(-\frac{1}{\theta_0}\right)\right. \\ &\left.\left[2 + \tau\right]\right\}\mathrm{erf}\left(\frac{1}{\sqrt{\tau}}\right)\Bigg\} \end{aligned}\right\} \tag{15}$$

Finally, let us consider such a case, when the parameter ϵ is small. One may get the solution in the form of ϵ power series, taking $\psi(\xi, \tau)$ as a zero approximation (see (5)). At $\epsilon \to 0$ the difference $\theta_m - \theta_c \to 0$. If the time is large enough then it is possible to neglect the second term of (5) in comparison with the first one. The same can be done at any point of time, if

$|\theta_c - \theta_0| \ll \theta_c$. In the first approximation we can easily get:

$$\theta(\xi, \tau) = \psi(\xi, \tau) + \epsilon \exp\left(-\frac{1}{\theta_0}\right)\left\{\frac{1-\xi^2}{2} - \right.$$
$$- \frac{2}{\pi^3}\sum_{n=0}^{\infty}\frac{(-1)^n}{(n+1/2)^3}\exp\left[-\pi^2(n+1/2)^2\tau\right]$$
$$\left.\cos(n+1/2)\pi\xi\right\} \qquad (16)$$

We tried on all occasions to write down only the first approximations because of the bulky results. It is difficult to get the higher approximations as it involves difficulty in calculation.

And now we would like to show, that the temperature at any given point for the process as a result of which the stationary distribution will be established ($\epsilon < \epsilon_{cr}$), will not exceed the stationary temperature in the same point. For this the difference will be

$$\Delta(\xi, \tau) = \theta(\xi, \tau) - \theta_{st}(\xi)$$

The latter satisfies the integral equation

$$\Delta(\xi, \tau) = \phi(\xi, \tau) +$$
$$+ \epsilon\int_0^{\tau}\int_0^1 Y(\xi, \xi'; \tau - \tau') \times$$
$$\left\{\exp\left[\frac{-1}{\theta_{st}(\xi') + \Delta(\xi', \tau')}\right] - \right.$$
$$\left. - \exp\left[\frac{-1}{\theta_{st}(\xi')}\right]\right\} d\tau'\, d\xi' \qquad (17)$$

where

$$\phi(\xi, \tau) = 2\sum_{n=0}^{\infty}\left\{\int_0^1 [\theta_0 - \theta_{st}(\xi')] \times \right.$$
$$\left.\cos(n+1/2)\pi\xi'\, d\xi'\right\}\exp\left[-\pi^2(n+1/2)^2\tau\right]$$
$$\times \cos(n+1/2)\pi\xi$$

Applying the method of successive approximations to equation (17) we assume that

$$\Delta^{(0)}(\xi, \tau) = \phi(\xi, \tau)$$

If we take into account that $\phi(\xi, \tau) \leqslant 0$ (at $\theta_c > \theta_0$) and give the reasons analogous to those mentioned above in the proof of the existence of the solution, then it will be possible to find that $\Delta^{(n)}$ is not zero at any finite τ and the difference $\Delta^{(n)} - \Delta^{(n-1)} \to 0$ at $n \to \infty$.

ACKNOWLEDGEMENTS

The writers would like to acknowledge their debt to Academician Luikov for helpful suggestions and critical reading of the manuscript.

REFERENCES

1. A. V. Luikov and Y. A. Mikhailov, *Teoria Perenosa Energii i Veschestva*. Izdanie Akademii Nauk B.S.S.R., Minsk (1960).
2. D. A. Frank-Kamenetskii, *Difuzia i Teploperedacha v Khimicheskoi Kinetike*. Izdanie Akademii Nauk S.S.S.R. (1947).
3. V. N. Condratjev, *Kinetika Khimicheskih Gazovyh Reaktsii*. Izdanie Akademii Nauk S.S.S.R. (1958)
4. F. Mors and G. Feshbah. *Metody teor. fiz.* 1958, **1**, IL.

Vol. 1 1960

Int. J. Heat Mass Transfer. Vol. 1, pp. 273–279. Pergamon Press 1961. Printed in Great Britain.

THE EXPERIMENTAL INVESTIGATION OF HEAT AND MASS TRANSFER IN THE PRESENCE OF CHEMICAL CONVERSIONS

A. V. RALKO
Polytechnical Institute, Kiev

(*Received* 29 *March* 1960)

Abstract—The results of the experimental investigations on heat and mass transfer in the process of kilning the kaolin and the magnesium hydroxide are adduced in this paper. An experimental installation was developed which allows the temperature field of the heated body, its mass loss and the thermophysical characteristics of the body to be determined. The thermal conductivity coefficients and the coefficients of thermal diffusivity, heat capacity and the heat transfer coefficient of the mentioned substances were defined in the temperature range from 200° to 1000°C. It was found that the chemical conversions begin at the surface of the capillary porous body and then spread gradually into the interior of the body. The chemical conversion zone deepens into the body according to the parabolic law.

Résumé—Cet article apporte de nouveaux résultats quant aux recherches expérimentales sur la transport de chaleur et de masse dans le mécanisme de la cuisson du kaolin et de l'hydroxide de magnésium. Une installation a été construite pour mesurer le champ des températures dans le corps chauffé, la perte de masse et les caractéristiques thermiques. Les coefficients de conductibilité thermique, de diffusivité thermique, la capacité calorifique et le coefficient de transmission de chaleur des substances ci-dessus ont été étudiées entre 200 et 1000°C. On a trouvé que les réactions chimiques commencent à la surface du corps poreux et s'étendent graduellement dans l'intérieur du corps. La réaction chimique se développe à l'intérieur du corps suivant une loi parabolique.

Zusammenfassung—Diese Arbeit behandelt den Wärme- und Stofftransport beim Brennen von Kaolin und Magnesiumhydroxyd. In einer Versuchapparatur konnten das Temperaturfeld des geheizten Körpers, sein Massenverlust und seine thermischen Stoffwerte bestimmt werden. Die Wärmeleitfähigkeit, die Temperaturleitfähigkeit, die Wärmekapazität und der Wärmeübergangskoeffizient der genannten Substanzen wurden im Temperaturbereich von 200 bis 1000°C gemessen. Man fand, dass die chemische Reaktion an der Oberfläche des kapillarporösen Körpers begann und sich nach einem Parabelgesetz in das Innere fortpflanzte.

Аннотация—В статье приведены результаты экспериментальных исследований по тепло-и массообмену в процессе обжига каолина и гидроокиси магния. Разработана экспериментальная установка, позволяющая регистрировать температурное поле нагреваемого тела и его массоотдачу, а также определять теплофизические характеристики тела.

Определены коэффициенты теплопроводности и температуропроводности, теплоёмкость, коэффициент теплообмена указанных материалов в интервале температур от 200°C до 1000°C.

Установлено, что химические превращения начинаются на поверхности капиллярнопористого тела, а затем постепенно перемещаются внутрь тела. Зона химических превращений углубляется внутрь тела по закону параболы.

THE present paper deals with the investigation of heat and mass transfer in capillary porous bodies in the presence of chemical conversions. These processes take place more clearly during the kilning of ceramic ware and also of kaolin kilning.

Thermal effects of a different nature become apparent in a certain temperature range when the majority of mineral substances are heated. These phenomena occurring during heating of the mineral substances are described qualitatively by means of the heating–kinetics curves.

An experimental laboratory installation shown in Fig. 1 has been developed to study the kinetics

of the process of the kilning of mineral substances. This installation consists of two electric crucible furnaces of the same type (1 and 2). The cast-iron sleeve-bearings were inserted into the furnace to maintain level temperatures along its height.

A sample of the investigated substance made in the form of a plate or a cylinder was put into one of the furnaces. Three thermocouples were inserted into the sample to measure the temperature drop at various points of it. The temperature drop between the surrounding medium and the surface of the sample was measured by thermocouple (1) (Figs. 1 and 2). Thermocouple (2) shows the difference between the surface temperature and the temperature at the point $x = R/2$ where R is half the plate thickness or the cylinder radius. Thermocouple (3) shows the difference between the surface temperature and the temperature at the centre of the sample (plate or cylinder). The butt ends of the cylindrical sample are covered with the heat-insulating seal made out of burned asbestos thus making it possible to consider the sample as an unlimited cylinder for the purpose of calculation.

An analogous sample suspended on an automatic self-recording balance was kilned in the second furnace (Fig. 1) in order to record the curve of mass-transfer kinetics. The air temperature in the furnaces increased linearly with time (the heating velocity remained constant). This was ensured by the electronic regulator (5) with the command apparatus (see Fig. 1). The resistance boxes (3) and (4) with the galvanic elements served both for zero creep when recording the temperature and for increasing the sensitivity of the self-recording potentiometer.

The specially designed automatic self-recording balance was applied for receiving the weight-drop curve (mass transfer) of the investigated

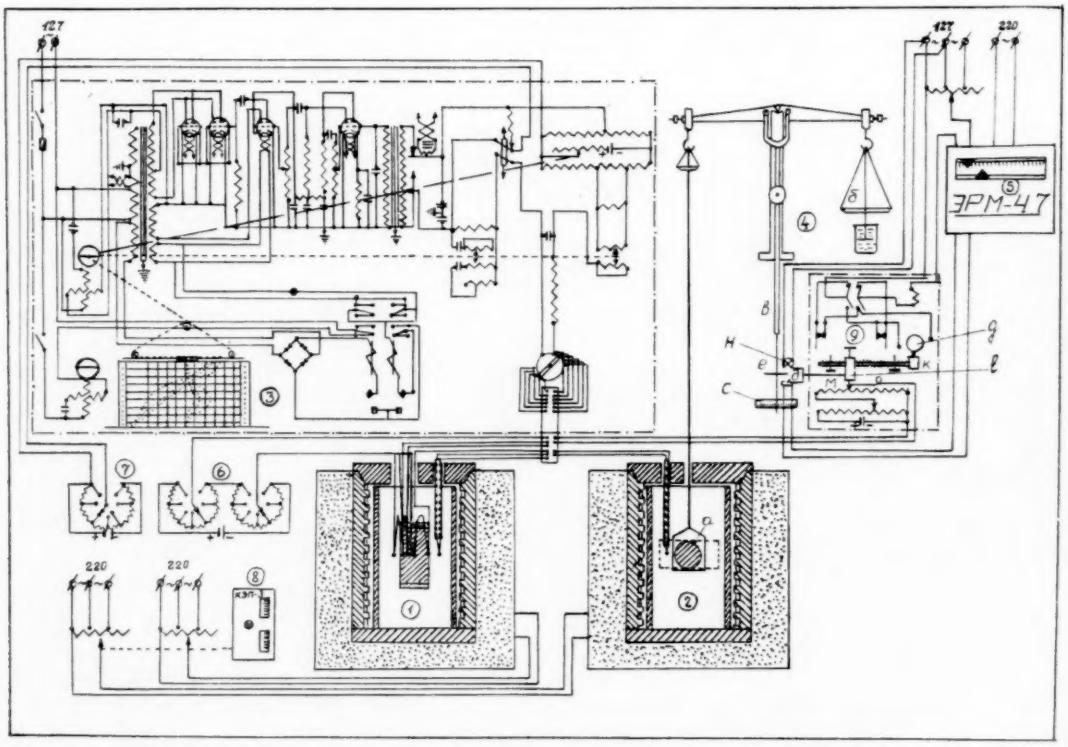

FIG. 1. The scheme of the experimental installation for the record of the curves of the heating process kinetics of the capillary porous bodies.

Vol. 1 1960

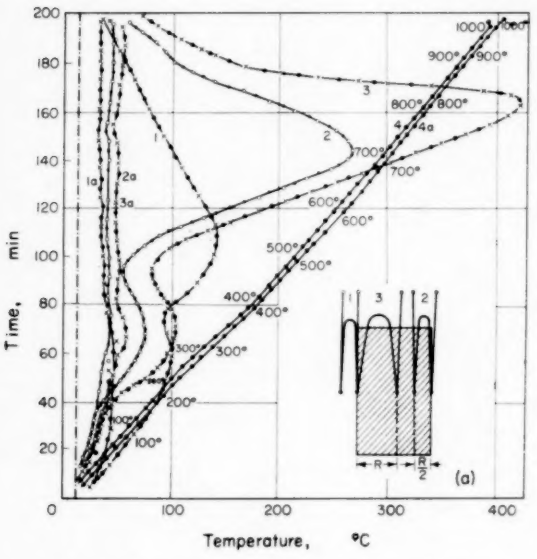

FIG. 2. The heating curves in the process of kilning the cylinder made out of the magnesium hydroxide.

sample. The investigated sample (*a*) may be suspended from the left scale, and by the weight (δ) it is balanced in such a way that the pointer (*b*) has to be placed at the left side of the scale (*c*) and the movable carriage (*e*) has to be at the extreme left position. With the decrease in the sample weight the pointer (*b*) deviates to the left and a screen gate (*e*) attached to the pointer moves together with it thus opening the chink above the photoelectric cell. When the chink is opened the ray from the lighting apparatus (*H*) illuminates the photoelectric cell. The photoelectric current reaches the millivoltmeter of the electronic governor (5), which switches on the electromotor (*g*) through the reductor (*k*) and moves the carriage (*l*) till the screen gate covers the ray from the lighting apparatus. Then the circuit is broken and the carriage stops moving. The photoelectric cell, the lighting apparatus and the slide of the rheostat are mounted on the moving carriage. When the slide moves along the rheostat (*M*) the taken-off voltage changes and comes in the sockets of the automatic multipoint potentiometer. The change of the taken-off voltage from the rheostat is proportional to the shift of the pointer (*c*) and the self-recording potentiometer records a curve which corresponds to the decrease in the weight of the investigated sample. The total weight loss of the sample for the whole kilning process is determined either by making the pointer return to its initial position with the help of a weight, or by weighing the kilned sample after it has been cooled in an desiccator. The rise of the endothermic thermal effect (the heat absorption caused by chemical reactions) at the surface of the sample when the corresponding furnace temperature is obtained is marked on the curves for the sample heating. Thermocouple (1) will show the increase of temperature drop since its hot junction placed at the cylinder surface marks the lag in the surface temperature increase caused by the endothermic effect. At this instant thermocouples (2) and (3) register some decrease in temperature difference between the surface of the sample and the points inside the sample at $x = 0$ and $x = R/2$. The chemical conversions accompanied by the endothermic effect occur at first only at the surface of the sample and not in the whole volume of it. After the termination of the chemical conversions at the surface of the sample the chemical reaction zone will gradually occur deeper in the sample centre. Thermocouple (1) will show then the decrease in temperature drop, while thermocouples (2) and (3) show the increase in it. This drop occurs due to the fact that the temperature at the surface of the sample is continuously rising while the temperature in the deep parts of the sample will be rising more slowly, since the heat entering the sample will be partially absorbed in the region of chemical conversions.

The transition of the point $x = R/2$ where the thermocouple (2) is placed by the deepening front of the endothermic reaction zone is registered on the curve of heating kinetics by abrupt decrease in temperature drop for this sample layer. At the same time thermocouple (3) will continue to show the increase in temperature drop till the endothermic reaction zone reaches the sample centre.

The exothermal effects (chemical conversions, connected with heat evolution) arising in the regions of the thermocouples in the sample are registered in the same way by bends and gaps on the heating kinetics curves.

Synthetic magnesium hydroxide and kaolin

(the Dubrovo deposits) were used for our investigations as mineral substances.

The typical heating kinetics curves in the kilning process are given in Fig. 2 for one of the experiments. The experimental sample is made from synthetic magnesium hydroxide in a form of a cylinder. Curve (4) shows the linear increase of the furnace temperature. Curves (1), (2) and (3) show the presence of chemical conversions with the absorption and evolution of heat. The temperature drop between the surface and the centre of the cylinder ($R = 25$ mm) during kilning reached 420°C by the end of the process.

Curves (1a), (2a) and (3a) correspond to the same thermocouples at the repeated heating of the same sample up to 1,000°C. As can be seen from the heating curves there are no remaining endothermic phenomena left in the sample. All the three curves show the constant temperature difference in the cylinder since it is heated at a constant rate.

Fig. 3 is the heating curve for the process of kilning the kaolin cylinder. A characteristic picture of the superposition of two thermal effects of different nature can be seen from Fig. 3. At the temperature of 480°C the curve $t_1 = f(\tau)$ deviates to the right and this deviation corresponds to the beginning of the endothermic effect at the cylinder surface. An anological course takes place for the curve $t_2 = f(\tau)$, which a bit later will deviate to the left, and this deviation corresponds to the end of the endothermic effect in the cylinder interior at $x = R/2$. The next few gaps in the temperature curves for these thermocouples (at the furnace temperature equal to 960°C) mark the rise of the exothermal effect at the cylinder surface. At this moment of time the endothermic reaction has not yet reached the central layer of the cylinder as can be seen from the course of the temperature curve $t_3 = f(\tau)$, which shows the rapid growth of the temperature difference between the cylinder surface and its centre. The maximum point on the curve $t_3 = f(\tau)$ marks the end of the endothermal reaction in the centre of the cylinder. The end of the exothermal effect in the kaolin cylinder centre is marked by the second series of gaps of all the temperature curves. Their further position on the thermogram corresponds to the

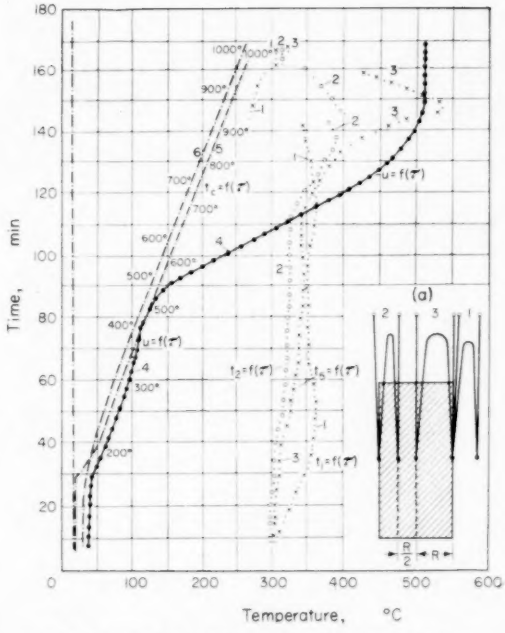

FIG. 3. The curves of heating the cylinder out of kaolin in the kilning process.

process of heating the body which has no internal heat sources.

The curve of the weight loss $u = f(\tau)$ is given in Fig. 3 (curve 4). The changes in time of the medium temperature of two furnaces are represented by the curves $t_m = f(\tau)$ (see curves 5 and 6). The weight-loss curves of the magnesium hydroxide kilned in the form of cylinders of different sizes are given in Fig. 4.

The linear law of furnace heating allows us to determine the thermal diffusivity coefficient $a(\mathrm{m^2/hr})$ and the Biot criterion [1]:

$$a = \frac{bR^2}{\Gamma}\left[\left(\frac{1 - x^2/R^2}{t(R, \tau) - t(x, \tau)}\right)\right] \qquad (1)$$

where b is the heating rate ($b = \mathrm{d}t_m/\mathrm{d}\tau = \mathrm{const}$), Γ is the constant value: for the unlimited plate $\Gamma = 3$ for the cylinder $\Gamma = 4$. The criterion Bi is defined by the formula

$$Bi = \frac{\alpha R}{\lambda} = \frac{2[t(R, \tau) - t(x, \tau)]}{[t_m - t(R, \tau)]\,(1 - x^2/R^2)} \qquad (2)$$

where α is the heat-transfer coefficient

Vol. 1 1960

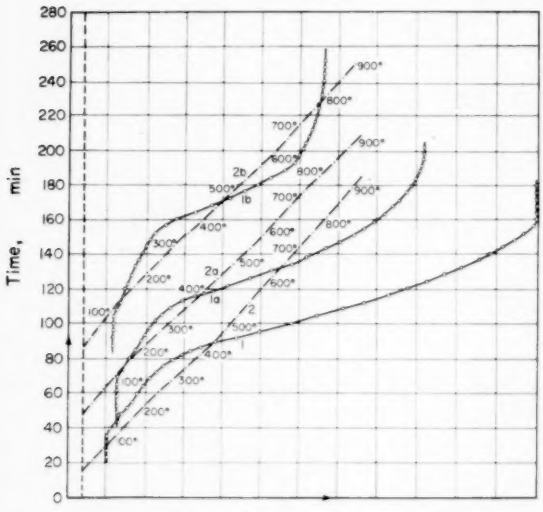

FIG. 4. The curves of weight loss during kilning the cylinders of various sizes, made out of magnesium hydroxide. (1) The weight loss curve (2) The curve of the furnace temperature increase.

(kcal/m² hr °C), λ is the thermal conductivity coefficient (kcal/m hr °C). We can calculate the coefficient a and the criterion Bi from the formulae (1) and (2) for the kilned samples when heating them in a furnace the temperature of which is linearly increasing.

Conditionally we can apply these formulae to the kaolin samples in the process of kilning. In the temperature interval, when the chemical reactions occur, the value of the thermal diffusivity coefficient and the Biot criterion will have the conditional character. Let us define these values through a^* and Bi^*, respectively. The calculation results for the kaolin are given in Table 1. It can be seen from this table that the thermal diffusivity coefficient increases with the temperature rise.

In the temperature interval, where the chemical reactions are negligible, there is almost no difference between the coefficients a and a^*. The Biot criterion is raised with the increase of the temperature t_m, and the Biot criterion in the process of kilning Bi^* is approximately two times smaller than the Biot criterion when the previously kilned samples are heated.

The heater coils, of nichrome wire, were mounted inside of the investigated samples to determine directly the heat-transfer coefficient α, the heat capacity c and the heat of the chemical reaction. Apart from being heated by the furnace the investigated sample could gain additional heat with the help of this coil. The heat of the reaction was determined as follows: a heater coil was mounted inside of the unkilned cylindrical sample along its axis. Two samples were heated simultaneously in the furnace, the unkilned sample with the coil and the kilned one without it. The furnace temperature was increased linearly, the samples were at first heated equally. The mass transfer (the sample weight loss) and the lag in the increase of the temperature, compared with the kilned sample, were observed during the chemical reaction. The rate of heating the unkilned sample was aligned with the kilned one by heating the nichrome wire with an electric current. This process compensated for heat absorbed by the endothermic reaction. It is possible to determine the specific heat of the endothermic reaction through the flow of electric current in the heater coil and through loss of mass by the sample. For the kaolin, for example, the specific heat of the endothermic reaction is equal to 1,230 kcal/kg. The dehydration heat of the magnesium hydroxide is $g = 700$ cal/kg.

Table 1. *The thermophysical characteristics of the kaolin*

t_m(°C)	100	200	300	400	500	600	700	800	900	1000
$a \times 10^5$ (m²/hr)	108	108	101		101	108	108	116		122
$a^* \times 10^5$		138			125	110			125	
Bi		2·70	2·70	2·70	3·75	4·65	5·00	5·75	5·75	6·84
Bi^*		1·5			1·80			2·50		
α (kcal/m² hr °C)	27	40	50	63	90	120	154	170	190	200
$\lambda \times 10^3$(kcal/m hr °C)	292	391	483	580	642	680	686	702	685	650

This method of the sample heating with the help of the heater coil allows the coefficient α to be determined. For this purpose two kilned samples must be used, one of which has a heater coil attached.†

The two samples are placed in the furnace, the temperature of which increases linearly. Only the temperature of the first sample is recorded. The second sample is heated additionally by the coil so that its surface temperature should always be equal to the ambient temperature (the furnace temperature is $t_2(R, \tau) = t_m$). Then the heat supplied to the sample by the additional heating is obviously equal to the amount of heat Q received by the second sample from the surrounding medium. The total heat-transfer coefficient is

$$d\alpha = \frac{0{\cdot}86W}{\Delta t A} = \frac{Q}{\Delta t A} \tag{3}$$

where A is the heat-transfer surface of the samples, W is the output of the nichrome coil, Δt is the temperature drop between the samples at their surfaces equal to the temperature drop between the surrounding medium and the surface of the first sample. Having obtained the value of the heat-transfer coefficient α we can determine the specific heat

$$c = 2\alpha[t_m - t(R, \tau)]/b\gamma R \tag{4}$$

where γ is the sample density (kg/m³).

The thermal conductivity coefficient λ is determined by the formula

$$\lambda = ac\gamma \tag{5}$$

The results of the calculations are given in Table 1. The dependence of the specific heat on temperature is represented in Fig. 5. The dependence of the heat capacity for the unkilned kaolin sample is given in the same Fig. 5 (curve II). The specific heat of the chemical reaction is determined by the total heat capacity and the reaction occurs in the temperature interval from 600° to 800°C.

The analysis of the experimental data shows,

† Usually the coil is joined to the sample before the kilning. The kilning of the sample takes place with the coil attached.

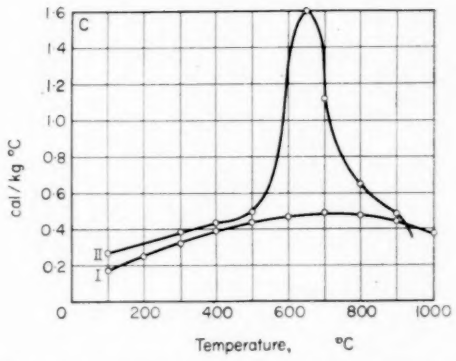

FIG. 5. The dependence of the true (curve I) and the total (curve II) heat capacity of kaolin on temperature.

that the chemical conversions on heating the body occur at first in the surface layer of the body (the chemical reaction zone). This zone will gradually spread into the interior of the body. The displacement mechanism of the chemical conversion zone in the first approximation may be taken as analogous to the mechanism of deepening the evaporation surface when drying wet solid bodies. This process is sketched in Fig. 6 in the case of the infinite plate $2R$ thick. The concentration of the fixed substance at the plate surface is assumed equal to zero, i.e. $\omega(R, \tau) = 0$.

Let the distance between the lower surface of the chemical conversion layer and the plate surface be ξ, and the diffusion coefficient of the

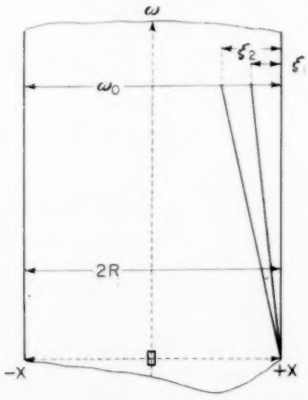

FIG. 6. The scheme for the calculation of the curve of mass-loss kinetics.

Vol. 1 1960

fixed substance through the plate surface layer be k, then we can write

$$-\frac{d\omega}{d\tau}R = \frac{k}{\xi}\omega_0 = \frac{\omega_0}{2}\frac{d\xi}{d\tau} \tag{6}$$

As an approximation we can assume that the decrease in the concentration $\omega(x, \tau)$ in the chemical conversion zone takes place according to the straight-line law (see Fig. 6). From relation (6) we get:

$$\xi = 2\sqrt{(k\tau)} \tag{7}$$

i.e. the conversion surface deepens according to the parabolic law. Moreover, from the relations (6) and (7) we get

$$\frac{\omega}{\omega_0} = 1 - \sqrt{\left(\frac{k\tau}{R^2}\right)} \tag{8}$$

When solving the diffusion problem of fixed substance in a capillary porous body we get an analogous formula with another numerical factor

$$\frac{\omega}{\omega_0} = 1 - \frac{2}{\sqrt{(\pi)}}\sqrt{\left(\frac{k\tau}{R^2}\right)} \tag{9}$$

Using formulae (7) and (8) we can calculate the diffusion coefficient. The following data were marked from the heating kinetics curves for a magnesium hydroxide plate 50 mm thick. ($R = 25$ mm). The dehydration process begins at the average plate temperature equal to 350°C. The time of the displacement of the chemical conversion zone from the surface of the plate to its centre was 40 min. The temperature of the reaction zone was 375°C at the furnace temperature equal to 585°C. Consequently at $\xi = 2{\cdot}5 \times 10^{-2}$ m, $\tau = 0{\cdot}666$ hr. Hence

$$k = \frac{6{\cdot}25}{0{\cdot}666 \times 4} \times 10^{-4} = 2{\cdot}3 \times 10^{-4}\ \text{m}^2/\text{hr}$$

The total mass content was 29·84 g and the weight lost by the plate during 40 min was 16·5 g. Hence we get

$$k = \frac{6{\cdot}25 \times 60(16{\cdot}5)^2}{40 \times (29{\cdot}84)^2} \times 10^{-4} = 2{\cdot}82 \times 10^{-4}\ \text{m}^2/\text{hr}$$

Using the same formula (9) we get

$$k = 2{\cdot}82 \times \frac{\pi}{4} \times 10^{-4} = 2{\cdot}2 \times 10^{-4}\ \text{m}^2/\text{hr}$$

i.e. the two values are quite close.

These calculations prove the established mechanism of the gradual deepening of the zone of chemical reactions in the capillary porous body. The chemical reaction zone is gradually displaced into the interior of the body approximately according to the parabolic law, that coincides with the Stefan law for the freezing of humid bodies.

REFERENCES

1. A. V. Luikov, *Teoria teploprovodnosti*. Gostehizdat, Moscow (1952).
2. A. V. Luikov and J. A. Mihailov, *Teoria perenosa energii i veschestva*. Izdatelstvo Akademii Nauk BSSR, Minsk (1959).
3. A. V. Ralko, *Trudy Energet. Inst. im. Krjijanovskogo Akad. Nauk SSSR; Teplo-i massoobmen v protsesse isparenia*. Izdanie Akademii Nauk SSSR (1958).

Int. J. Heat Mass Transfer. Vol. 1, pp. 280–293. Pergamon Press 1961. Printed in Great Britain.

MIXING AND CHEMICAL REACTION IN AN INITIALLY NON-UNIFORM TEMPERATURE FIELD*

S. I. CHENG and H. H. CHIU
Department of Aeronautical Engineering, Princeton University

(*Received* 10 *November* 1959; *revised* 8 *April* 1960)

Abstract—The development of the velocity, temperature and the concentration profiles in the vicinity of the trailing edge is investigated under the boundary layer approximation for an arbitrary initial temperature profile and an arbitrary value of the parameter B for the chemical kinetics.

A series solution is constructed in terms of a system of "universal functions", from which the initial development of an arbitrary initial temperature profile can be calculated with or without chemical reaction. The first three terms in the series for the temperature have been tabulated previously and are presented here in a diagram.

In the case of no chemical reaction, the analytical results for a given initial temperature distribution predict that the temperature gradient normal to the dividing stream line tends to increase for a limited distance in the downstream direction. This may not be anticipated from the consideration of thermal diffusion alone. Experimental results confirm this qualitative trend. With the three terms in the series solution for the temperature, the agreement between the analytical and the experimental results appears also quite satisfactory.

The analytical results will enable us to calculate the development of the temperature field with chemical reaction. There are as yet no experimental data for comparison.

Résumé—Le développement des profils de concentration, de température et de vitesse, au voisinage du bord de fuite, est étudié à partir d'une approximation de la couche limite pour un profil de température initial arbitraire et une valeur arbitraire du paramètre B de cinétique chimique.

Une solution en forme de série est donnée en fonction d'un système de "fonctions universelles" à partir de laquelle on peut calculer le développement d'un profil de température initial, avec ou sans réaction chimique. Pour la température, les trois premiers termes de la série ont été tabulés précédemment et sont présentés ici sous forme de diagramme.

Dans le cas où il n'y a pas de réaction chimique, les résultats analytiques, trouvés pour une distribution de température initiale, font prévoir un accroissement du gradient de température normal à la ligne de courant, à partir d'une certaine distance dans la direction aval. Ceci ne peut pas s'expliquer uniquement par la diffusion thermique. Les résultats expérimentaux confirment cette tendance qualitative. Avec trois termes de la série solution pour la température, l'accord entre résultats analytiques et expérimentaux semble tout à fait satisfaisant.

Les résultats analytiques nous permettent de calculer le développement du champ de température en présence de réaction chimique. Il n'y a pas encore de données expérimentales pour les comparer.

Zusammenfassung—In dieser Arbeit wird die Entwicklung der Profile der Geschwindigkeit, der Temperatur und der Konzentration in der Nähe der Anströmkante untersucht, wobei die Näherungen der Grenzschichtlehre sowie beliebige anfängliche Temperaturprofile und Werte für die Konstante B der chemischen Kinetik angenommen werden.

Es wird eine Reihenlösung in Ausdrücken eines Systems "universeller Funktionen" aufgestellt, von der aus die anfängliche Entwicklung eines willkürlichen anfänglichen Temperaturprofiles mit oder ohne chemische Reaktion berechnet werden kann. Die ersten drei Ausdrücke in den Reihen für die Temperatur wurden schon früher tabellarisch angegeben und sind hier in einem Diagramm mitgeteilt.

Für den Fall ohne chemische Reaktion zeigt das analytische Ergebnis für eine gegebene anfängliche Temperaturverteilung, dass der Temperaturgradient normal zur trennenden Stromlinie ansteigt für eine begrenzte Entfernung in Strömungsrichtung, was allein aus Betrachtungen über die Wärme

* This research is carried out as part of the work sponsored by the Office of Ordnance Research, U.S. Army under Contract No. OOR DA-36 ORD 2183.

Vol. 1 1960

ausbreitung nicht vorauszusehen war. Experimentelle Ergebnisse bestätigen qualitativ diesen Verlauf. Auch die drei Ausdrücke in der Reihenlösung für die Temperatur stimmen befriedigend mit dem Versuch überein.

Die analytischen Ergebnisse ermöglichen es, die Entwicklung des Temperaturfeldes mit chemischer Reaktion zu berechnen. Experimentelle Daten zum Vergleich liegen noch nicht vor.

Аннотация—Исследуется развитие полей скорости, температуры и концентрации вблизи задней кромки сепаратора при условии аппроксимации начального распределения температуры в пограничном слое и произвольной величины параметра B, характеризующего химическую кинетику.

Решение получено в виде ряда, состоящего из членов системы «универсальных функций», с помощью которого можно вычислить развитие произвольного температурного распределения при наличии химической реакции или без неё. Первые три члена ряда в решении для температурного поля были табулированы ранее и представлены здесь на диаграмме.

При отсутствии химической реакции аналитические результаты для данного начального температурного распределения показывают, что температурный градиент, перпендикулярный к линии, разделяющей потоки, стремится увеличиться на ограниченном расстоянии по направлению потока. Этого нельзя было бы ожидать, исходя из рассмотрения только термодиффузии.

Экспериментальные данные подтверждают этот качественный вывод. Аналитические и экспериментальные результаты также вполне удовлетворительно согласуются для решения, ограниченного тремя членами.

Аналитические результаты позволят вычислить развитие температурного поля при наличии химической реакции. Пока ещё нет экспериментальных данных для сравнения.

I. INTRODUCTION

IGNITION and combustion in the laminar mixing zone between a hot stream consisting of combustion products and a cool, combustible stream was first treated by Marble and Adamson [1] and continued by Dooley [6]. They considered a non-viscous, perfectly insulating, semi-infinite partition separating a cool combustible mixture from its hot combustion products. The velocity, temperature and concentration of combustible are assumed uniform in each half plane at the trailing edge of the partition. Their analysis gives the distribution of the temperature, the concentration of the combustible and the gas velocity in the neighborhood of the trailing edge of the partition. Their results indicate that a local maximum in the temperature profile first occurs, due to heat release by the chemical reaction, in the hot burned gas below the dividing stream line. The problem was reconsidered by Cheng and Kovitz in 1957 [2] to take into account the finite length of the partition and the viscosity of the gas. The initial velocity distribution is taken to be the Blasius flow over a flat plate, but the temperature of each stream is still taken as uniform and discontinuous across the thin partition. The results indicate that the development of the temperature and the velocity field is shortened by an order of magnitude as compared with the results of Marble and Adamson.

The key interest of the problem is to obtain an estimate of the distance of the local temperature maximum downstream of the trailing edge. This distance serves to represent the major coupling between the chemical kinetic and the fluid mechanical aspects in the problem of flame stabilization on a solid body [3]. In any practical system, heat transfer across the partition will give rise to a continuous temperature profile at the trailing edge. The heat transfer, prior to mass and momentum mixing in the wake may adversely affect the rate of chemical reaction and the associated phenomena as is clear from the discussions in [3].

The effect of a nonuniform, continuous initial temperature profile on the development of the wake of a combustible mixture will be considered in the present investigation.

The results of the present analysis brings out an interesting aspect of the heat transfer in a viscous wake layer. This is produced by the convective motion, normal to the partition, of the gases with nonuniform initial temperature profiles. The temperature gradient, normal to the partition, appears to increase in the downstream direction from the trailing edge of the partition for some limited extent. This prediction

from the analysis compares favorably with experimental results.

II. FORMULATION OF THE PROBLEM

The governing equations are the conservation laws of mass, momentum, energy and the concentration of the combustible. Subject to the appropriate assumptions [2], the Howarth transformation is employed to uncouple the continuity and the momentum equations from the energy and the diffusion equations. The momentum equation is then reduced to the incompressible form. In terms of the transformed variables the governing equations can be written as

$$\left.\begin{aligned} u_x + v_y &= 0 \\ uu_x + vu_y &= u_{yy} \end{aligned}\right\} \quad (1)$$

$$\left.\begin{aligned} u\theta_x + v\theta_y &= \frac{1}{Pr}\theta_{yy} + BK\exp\left(-\frac{\theta_a}{\theta}\right) \\ uK_x + vK_y &= \frac{1}{Sc}K_{yy} - CK\exp\left(-\frac{\theta_a}{\theta}\right) \end{aligned}\right\} \quad (2)$$

where Prandtl number $Pr = C_p\lambda/k$ and Schmidt number $Sc = \mu/\rho D$ are assumed to be constant throughout the field. The following notations are adopted from [2].

B $= 4l\Delta H/u_{\mathrm{I}}\gamma\, C_pT_{\mathrm{II}}$
C $= 4l/u_{\mathrm{I}}\tau$
H = heat released per unit mass of combustible
τ = characteristic chemical time constant
R = universal gas constant
A = activation energy
K = relative mass concentration of combustible
T_{II} = heat stream temperature
θ $= T/T_{\mathrm{II}}$
θ_a $= A/RT_{\mathrm{II}}$

u and v are non-dimensional axial and transverse velocity components in the incompressible plane, while χ, y, are the corresponding non-dimensional co-ordinates with the origin at the trailing edge of the flat plate.

The solution for u and v from equations (1) was given by Goldstein [4] for the case of flow near the trailing edge of a flat plate with symmetric Blasius profile at the beginning of mixing.

With $\xi = \chi^{1/3}$ $\eta = y/3\xi$

The solution consists of two forms—one valid for y small and one for y large. For small y:

$$\left.\begin{aligned} u &= \tfrac{1}{3}\sum_{l=0}^{\infty} b_{3l+1}\,\xi^{3l+1} \\ v &= \tfrac{1}{3}\sum_{k=0}^{\infty} C_{3k-1}\,\xi^{3k-1} \end{aligned}\right\} \quad (3)$$

$$b_{3l+1} = f'_{3l}(\eta);\quad C_{3k-1} = \eta f'_{3k}(\eta) - (3k+2)f_{3k}(\eta)$$

The functions f_0, f_3, f_6, and their derivatives have been recalculated for smaller mesh size in [5] and are used in the present calculation.

Let the initial temperature profile be expressed in the power series form, for small y and $\bar{y}$ in the lower and the upper half plane respectively.

$$F(y) = \sum_{r=0}^{\infty}\beta_r\left(\frac{y}{3}\right)^r,\ \bar{F}(\bar{y}) = \sum_{r=0}^{\infty}\bar{\beta}_r\left(\frac{\bar{y}}{3}\right)^r \quad (4)$$

The solution for $\theta(\xi_1\eta)$ will be constructed separately in the upper and lower half-planes. For small y, solutions of the forms

$$\theta(\xi\,.\,\eta) = \sum_{r=0}^{\infty}\theta_r(\eta)\xi^r,\quad K(\xi\,.\,\eta) = \sum_{r=0}^{\infty}K_r(\eta)\xi^r \quad (5)$$

are assumed in each plane. Terms of the type $\xi^r \ln \xi$ will be introduced before the ξ term whenever necessary.

The following limiting process is valid

$$\lim \sum_{r=0}^{\infty}\theta_r(\eta)\xi \to \sum_{r=0}^{\infty}\beta_r\left(\frac{y}{3}\right)^r$$

provided the limiting values

$$\lim_1 \frac{\theta_r(\eta)}{\eta^r} \to \beta_r,\quad \lim_2 \frac{\bar{\theta}_r(\bar{\eta})}{\bar{\eta}^r} = \bar{\beta}_r \quad (6)$$

exist for each θ_r and $\bar{\theta}_r$;

where

$$\lim_1 = \xi \to 0\quad \eta \to \infty\quad y = \text{const.}$$
$$\lim_2 = \xi \to 0\quad \bar{\eta} \to \infty\quad \bar{y} = \text{const.}$$

The constant β_r, $\bar{\beta}_r$ will be considered as given but will not be specified for the present analysis.

Vol. 1 1960

They will be determined from an experimentally measured initial profile.

The initial conditions for the concentration are

$$\lim_1 K(\xi \,.\, \eta) \to 0, \quad \lim_2 \bar{K}(\xi \,.\, \bar{\eta}) \to 1 \tag{7}$$

therefore

$$\left.\begin{aligned} &\lim_1 K_0(\xi \,.\, \eta) \to 0, \quad \lim \bar{K}_0(\xi \,.\, \bar{\eta}) \to 1 \\ &\lim_1 K_r(\xi \,.\, \eta)/\eta_r = \lim_2 \bar{K}_r(\xi \,.\, \bar{\eta})/\bar{\eta}_r \to 0 \end{aligned}\right\} \tag{8}$$

when β_0 is rather close to unity, the equation (4) for the initial temperature profile may be suitable for the expansion of the exponential terms in equation (2). (See Appendix A.) The results are summarized as follows

$$\exp\left(-\frac{\theta_a}{\theta}\right) = \sum_{j=0}^{\infty} D_j(\eta)\xi^j \tag{9}$$

where

$$\left.\begin{aligned} D_0 &= \exp\left(-\frac{\theta_a}{\beta_0}\right) \\ D_1 &= \left(\frac{\theta_a\theta_1}{\beta_0^2} + \frac{\beta_1\theta_a}{\beta_0^2}\,\eta\right)\exp\left(-\frac{\theta_a}{\beta_0}\right) \\ D_2 &= \left\{\left(\frac{\theta_a\theta_2}{\beta_0^2} + \frac{\beta_2\theta_a}{\beta_0^2} - \frac{\theta_a\theta_1^3}{\beta_0^3} + \frac{1}{2}\frac{\theta_a^2\theta_1^4}{\beta_0^4}\right) + \right. \\ &\quad + \left(\frac{\beta_1\theta_a}{\beta_0^4} - \frac{2\beta_1\theta_a}{\beta_0^3}\,\theta_2\right)\eta + \\ &\quad \left. + \left(\frac{1}{2}\frac{\theta_a}{\beta_0} - 1\right)\left(\frac{\theta_a}{\beta_0}\right)\left(\frac{\beta_1^2}{\beta_0}\right)\eta^2\right\}\exp\left(-\frac{\theta_a}{\beta_0}\right) \end{aligned}\right\} \tag{9a}$$

when β_0 is not close to unity, the series (9a) fails to be adequate since only three terms have been carried out for the solution of θ. An alternate expansion of the exponential term should be used. The series has the same form as equation (9) except that D_0, D_1, D_2, are now different from those in (9a). The new coefficients are

$$\left.\begin{aligned} D_0 &= \exp\left(-\frac{\theta_a}{Fm}\right) \\ D_1 &= \left(\frac{\theta_a\theta_1}{Fm^2}\,\alpha_0 + 3\alpha_1\eta\right)\exp\left(-\frac{\theta_a}{Fm}\right) \\ D_2 &= \left\{\alpha_0\theta_a\left[\left(\frac{\theta_a}{Fm^2} - \frac{\theta_1^3}{Fm^3}\right) + \frac{1}{2}\frac{\theta_1}{Fm^2}\right] + \right. \\ &\quad \left. + 3\alpha_1\theta_a\frac{\theta_1}{Fm^2}\,\eta + 3\alpha_2^2\eta^2\right\}\exp\left(-\frac{\theta_a}{Fm}\right) \end{aligned}\right\} \tag{9b}$$

where

$$\left.\begin{aligned} \alpha_0 &= 1 - \frac{\theta_a}{Fm^2}\,Fm'\,\delta m + \\ &\quad \frac{1}{2}\frac{\theta_a}{Fm^2}\left(Fm'' - \frac{2Fm'^2}{Fm} + \frac{\theta_a Fm'}{Fm^2}\right)\delta m^2 \\ \alpha_1 &= \frac{\theta_a}{Fm^2}\,Fm' - \frac{\theta_a}{Fm^2}\left(Fm'' - \right. \\ &\quad \left. - \frac{2Fm'^2}{Fm} + \frac{\theta_a Fm'^2}{Fm^2}\right)\delta m \\ \alpha_2 &= \frac{1}{2}\frac{\theta_a}{Fm^2}\left(Fm'' - \frac{2Fm'^2}{Fm} + \frac{\theta_a Fm'^2}{Fm^2}\right) \end{aligned}\right\} \tag{9c}$$

Substituting (3), (4) and (9) into (2), and equating the coefficients of like powers of ξ, we obtain a series of ordinary differential equations for $\theta_r(\eta)$ and $K_r(\eta)$ as were in [2].

The equations $\theta_r(r = 0, 1, 2, 3, 4)$, and $K_r(r = 0, 1, 2)$ are given as follows

$$\left.\begin{aligned} &\frac{1}{Pr}\,\theta_0'' + 2f_0\,\theta_0' = 0 \\ &\frac{1}{Pr}\,\theta_1'' + 2f_0\,\theta_1' - f_0'\,\theta_0' = 0 \\ &\frac{1}{Pr}\,\theta_2'' + 2f_0\,\theta_2' - 2f_0'\,\theta_2 = -9BD_0K_0 \\ &\frac{1}{Pr}\,\theta_3'' + 2f_0\,\theta_3' - 3f_0'\,\theta_3 = \\ &\quad - 9B(D_0K_1 + D_1K_0) - 5f_3\,\theta_0' \\ &\frac{1}{Pr}\,\theta_4'' + 2f_0\,\theta_4' - 4f_0'\,\theta_4 = -9B(D_0K_2 + \\ &\quad + D_2K_0) - 5f_3\,\theta_1' + f_3'\,\theta_1 + f_0'\,\tilde{\theta}_4 \\ &\frac{1}{Pr}\,\tilde{\theta}_4'' + 2f_0\,\tilde{\theta}_4 - 4f_0'\,\tilde{\theta}_4 = 0 \end{aligned}\right\} \tag{10}$$

$$\left.\begin{aligned} &\frac{1}{Sc}\,K_0'' + 2f_0K_0' = 0 \\ &\frac{1}{Sc}\,K_1'' + 2f_0K_1' - f_0'K_1 = 0 \\ &\frac{1}{Sc}\,K_2'' + 2f_0K_2' - 2f_0'K_2 = 9CD_0K_0 \end{aligned}\right\} \tag{11}$$

III. INTEGRATION OF θ AND K FOR SMALL y

The solution of the differential equations will, in general, depend on the imposed boundary conditions and the governing equation itself. For purposes of practical application of the solution to this problem for a given set of physical quantities and initial conditions, it is desirable to split the equation in several parts so that the individual equation can be freed from any arbitrary constants by suitable scale transformations. Such a splitting is permissible, since the equations for θ_r and K_r are linear. A complete solution can then be obtained by summing up the split equations.

(1) *The splitting of the solution*

There are no physical constants appearing in the homogeneous part of the differential equation except the Prandtl number and the Schmidt number which were assumed to be 0·75 and 1·00 respectively. The value of 0·75 assumed for the Prandtl number is based on the properties of CO_2 at high temperature. The Schmidt number is chosen according to the data of ethylene oxide and CO_2, the two components that will be used in the experiment. The homogeneous solution is split into two linearly independent solutions. Each solution is associated with an undetermined constant. The canonical boundary condition is assigned at $\eta = 0$, for each homogeneous solution. When the equation is non-homogeneous, the forcing function is split into several parts, in such a way that any physical constant, which appears in either part may be adsorbed in the appropriate scale transformations. Proper boundary values are assigned at $\eta = 0$, so that the numerical calculation will not lead to trivial solution.

Each split equation is then integrated separately with the given boundary value at $\eta = 0$, the integration process stops whenever each split equation reaches a substantially stable asymptotic region. The numerical values are tabulated in [7] and given graphically as Fig. 1. The process of splitting requires that an inordinately large number of independent solutions be integrated. For example, θ_3, $\bar{\theta}_3$, requires 6 integrations and θ_4, $\bar{\theta}_4$, requires 24 independent integrations. Only the integrations of θ_1, θ_2 and θ_3 have been carried out. Therefore, the present

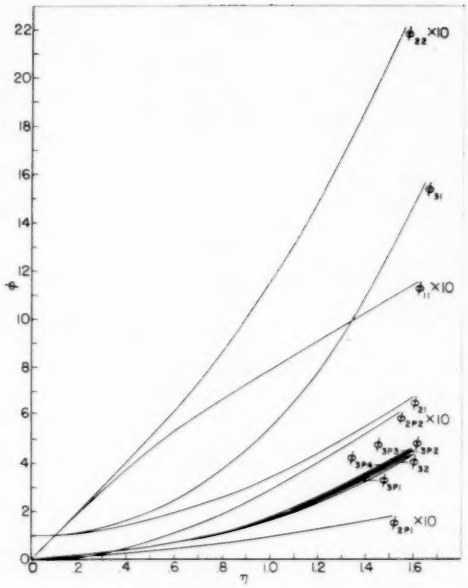

FIG. 1a. Curves of universal temperature function.

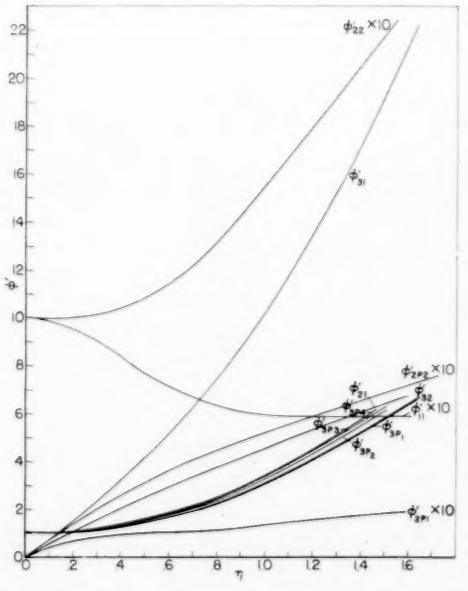

FIG. 1b. Derivative curve of universal temperature function.

Vol. 1 1960

solution cannot be extended to large values of χ and y.

(2) *Determination of the constants*

After each split solution is integrated, all the solutions are summed to construct a complete solution to a given physical problem.

There are four constants to be determined for each pair of $\theta_r, \bar{\theta}_r$. Thus four boundary conditions are required, i.e., those at $\eta = \bar{\eta} = 0$ and $\eta = \bar{\eta} = \infty$. The condition that the temperature profile be smooth at any value of ξ requires that both the function and its first derivative be continuous at $\eta = 0$. At $\eta = \infty$, the temperature profile must approach the initial profile as a limit. This requires that equations (6) must be satisfied for all θ_r's. The asymptotic behaviors of θ_r and K_r, as specified by the differential equations are compatible with those specified in equations (6). The asymptotic behavior of the solution also serves to indicate the cut off point of the numerical integration. The investigation of the asymptotic behavior of θ_r, $(r = 0, 1, 2, 3, 4)$ is presented in Appendix B, and the results are tabulated in Table 1.

Table 1. *Asymptotic behaviour of* θ_r

r	I	$\theta^{(0)}_{\text{asy.}}$	$\theta^{(P)}_{\text{asy.}}$
0	0	η_1^0	
1	0	η_1^1	
2	$\eta_1^{-2} \exp\left(-\frac{P}{3}\eta_1^3\right)$	η_1^2	η_1^2
3	$\eta_1^{-2} \exp\left(-\frac{P}{3}\eta_1^3\right)$	η_1^3	η_1^3
4	η_1^5	η_1^4	$\eta_1 \ln \eta_1$
$\bar{4}$	0	η^4	

Where I is the forcing functions appeared in equation (10). $\theta^{(0)}_{\text{asy.}}$ is the asymptotic behavior of homogeneous solution while $\theta^{(P)}_{\text{asy.}}$ is that of inhomogeneous solution with $\eta_1 = \eta + 0{\cdot}3408$.

The asymptotic behavior of θ_4 is $\eta_1^4 \ln \eta_1$, therefore θ_4 must include a term like $\xi^4 \ln \xi$.

Since the integrations have been carried out only to $r = 3$, the logarithmic term does not appear in the present expansion.

Numerical results for θ_0, θ_1, θ_2 and θ_3 are tabulated in [7] for $Pr = 0{\cdot}75$ and $Sc = 1{\cdot}0$.

The governing equations of K_0 and K_1 as well as their boundary conditions are identical to those in [2] and the solutions are applicable to the present analysis. Since K_2 does not appear in the governing equations for θ_0, θ_1, θ_2, θ_3, it has not been integrated.

(3) *The splitting of* θ_1

For illustrative purposes, the method of splitting and the determination of the constants will be given for the case of θ_1. The equation for θ_1, as given in equation (10) is invariant under the scale transformation,

$$\theta_1 = \beta_1 \Theta_1 \text{ and } \bar{\theta}_1 = \bar{\beta}_1 \bar{\Theta}_1$$

where $\beta_1 = -\bar{\beta}_1$ for the upper and the lower half plane respectively.

We split each of Θ_1 and $\bar{\Theta}_1$ into two independent solutions φ_{11}, and φ_{12} respectively

$$\left.\begin{aligned} \Theta_1 &= A_{11}\varphi_{11} + A_{12}\varphi_{12} \\ \bar{\Theta}_1 &= \bar{A}_{11}\varphi_{11} + \bar{A}_{12}\varphi_{12} \end{aligned}\right\} \tag{12}$$

so that

$$L_1 \varphi_{11} = 0, \quad L_1 \varphi_{12} = 0 \tag{13}$$

where

$$L_1 = \frac{\mathrm{d}}{\mathrm{d}\eta^2} + 2Pr f_0 \frac{\mathrm{d}}{\mathrm{d}\eta} - Pr f_0' \tag{14}$$

Subject to the canonical initial conditions

$$\left.\begin{aligned} \varphi_{11}(0) &= 0 \\ \varphi_{11}'(0) &= 1 \end{aligned}\right\}, \quad \left.\begin{aligned} \varphi_{12}(0) &= 1 \\ \varphi_{12}'(0) &= 0 \end{aligned}\right\} \tag{15}$$

The four unknown constants, A_{11}, A_{12}, $\bar{A}_{11}$ and $\bar{A}_{12}$ are to be determined by

(1) the initial conditions as given in equations (6) and

(2) the smooth matching of the function, and the first derivatives at $\eta = \bar{\eta} = 0$, i.e.

$$\beta_1 \Theta_1(0) = \bar{\beta}_1 \bar{\Theta}_1(0) \tag{16}$$

$$\beta_1 \Theta_1'(0) = -\bar{\beta}_1 \bar{\Theta}_1'(0) \tag{17}$$

These conditions of continuity require $A_{11} = \bar{A}_{11}$ and $A_{12} = -\bar{A}_{12}$. The case of

Table 2(a). *The split solution (when β_0 is close to unity)*
$\theta_r = Nr\ Ari\ \varphi ri + Nrp\ Arpi\ \varphi rp_i$

r		i	N	A	$\varphi(0)$	$\varphi'(0)$
1			β_1	C_{11}	0	1
1		2	β_1	0	0	0
2		1	1	$\{(\beta_2 + \bar{\beta}_2) - N_{2p}(C_{2p1} + C_{2p2})\}/2C_{21}$	1	0
2		2	1	$\{(\beta_2 - \bar{\beta}_2) - N_{2p}(C_{2p1} - C_{2p2})\}/2C_{22}$	0	1
2	p	1	$-9BPr \exp\left(-\frac{\theta_a}{\beta_0}\right)$	1	0	0
2	p	2	$-9BPr \exp\left(-\frac{\theta_a}{\beta_0}\right)$	1	0	0
3		1	1	$\{(\beta_3 + \bar{\beta}_3) - N_{3p}[C_{11}(C_{3p1} - C_{3p3}) - (C_{3p2} - C_{3p4})]\}/2C_{31}$	1	0
3		2	1	$\{(\beta_3 - \bar{\beta}_3) - N_{3p}[C_{11}(C_{3p1} + C_{3p3}) - (C_{3p2} + C_{3p4})]\}/2C_{32}$	0	1
3	p	1	$-9BPr \exp\left(-\frac{\theta_a}{\beta_0}\right) \frac{\theta_a \beta_1}{\beta_0^2}$	C_{11}	0	1
3	p	2	$-9BPr \exp\left(-\frac{\theta_a}{\beta_0}\right) \frac{\theta_a \beta_1}{\beta_0^2}$	1	0	1
3	p	3	$-9BPr \exp\left(-\frac{\theta_a}{\beta_0}\right) \frac{\theta_a \beta_1}{\beta_0^2}$	C_{11}	0	1
3	p	4	$-9BPr \exp\left(-\frac{\theta_a}{\beta_0}\right) \frac{\theta_a \beta_1}{\beta_0^2}$	1	0	1

In which $C_{ri} = \lim_{\eta \to \infty} \varphi_{ri}/\eta_r$
Subscript p indicates particular integral

Nr indicates the scale multiplier for θ_r
β_r the coefficient for the initial temperature profile.

Table 2(b). *The split solution (when β_0 is not close to unity)*

r		i	N	A	$\varphi(0)$	$\varphi'(0)$
1			β_1	C_{11}	0	1
1		2	β_1	0	0	0
2		1	1	$(\beta_2 + \bar{\beta}_2 - N_{2p} C_{2p1})/2C_{21}$	1	0
2		2	1	$(\beta_2 - \bar{\beta}_2 - N_{2p} C_{2p1})/2C_{22}$	0	1
2	p	1	$-9BPr \exp\left(-\frac{\theta_a}{Fm}\right) \alpha_0$		0	0
2		2	0		0	0
3		1	1	$(\beta_3 + \bar{\beta}_3 - N_{3p1} C_{3p1} - N_{3p2} C_{3p2})/2C_{31}$	1	0
3		2	1	$\beta_3 - \bar{\beta}_3 - N_{3p1} C_{3p1} - N_{3p2} C_{3p2})/2C_{32}$	0	1
3	p	1	$-9BPr \exp\left(-\frac{\theta_a}{Fm}\right) \frac{\theta_a A_{11} \alpha_0 \beta_1}{Fm^2}$	C_{11}	0	1
3	p	2	$-9BPr \exp\left(-\frac{\theta_a}{Fm}\right) 3\alpha_1$	1	0	1
3	p	3	0		0	1
3	p	4	0		0	1

Vol. 1 1960

$A_{12} = -\bar{A}_{12}$ is ruled out by the antisymmetricity of θ_1 and $\bar{\theta}_1$. The initial conditions

$$\lim_{\eta\to\infty} \theta_1/\eta \to \beta_1, \quad \lim_{\bar{\eta}\to\infty} \bar{\theta}_1/\bar{\eta} \to \bar{\beta}_1 = -\beta_1 \tag{18}$$

lead to the same result

$$\lim_{\eta\to\infty} A_{11}\varphi_{11}/\eta \to 1 \tag{19}$$

therefore

$$A_{11} = \bar{A}_{11} = 1/\lim_{\eta\to\infty}(\varphi_{11}/\eta) \tag{20}$$

The integration of φ_{11} was carried out up to the point where φ_{11}/η, or φ'_{11} remains essentially constant. The numerical value of A_{11} or $\bar{A}_{11}$ is obtained from (20). The splitting procedure for the independent integrations, and the constants for each split solution are tabulated in Tables 2 (a, b).

IV. RESULTS AND DISCUSSION

(1) *Construction of complete solution of θ for small y and $\bar{y}$*

The complete solution for θ can be written in the following way with all the numerical results inserted:

$$\left.\begin{aligned}
\theta = \beta_0 + 1{\cdot}70\,\beta_1\varphi_{11}\xi + \Big\{\Big[0{\cdot}280\,(\beta_2 + \\
+ \bar{\beta}_2) + 0{\cdot}562\,BPr\exp\left(-\frac{\theta_a}{\beta_0}\right)\Big]\varphi_{21} + \\
+ \Big[0{\cdot}820\,(\beta_2 - \bar{\beta}_2) - 0{\cdot}900\,BPr \\
\exp\left(\frac{-\theta_a}{\beta_0}\right)\Big]\varphi_{22} - 9BPr\exp\left(-\frac{\theta_a}{\beta_0}\right) \\
\varphi_{2p1}\Big\}\xi^2 + \Big\{\Big[0{\cdot}270\,(\beta_3 + \bar{\beta}_3) - 0{\cdot}0453\,BPr \\
\exp\left(-\frac{\theta_a}{\beta_0}\right)\frac{\theta_a\beta_1}{\beta_0^2}\Big]\varphi_{31} + \Big[0{\cdot}904\,(\beta_3 - \\
- \bar{\beta}_3) + 4{\cdot}41\,BPr\exp\left(-\frac{\theta_a}{\beta_0}\right)\frac{\theta_a\beta_1}{\beta_0^2}\Big]\varphi_{32} - \\
- 9BPr\exp\left(-\frac{\theta_a}{\beta_0}\right)\frac{\theta_a\beta_1}{\beta_0^2}(1{\cdot}710\,\varphi_{3p1} + \\
+ \varphi_{3p2})\Big\}\xi^3 + \cdots
\end{aligned}\right\} \tag{21}$$

$\bar{\theta}$ can be written in the same manner except that all the constant β_r must be properly modified and φ_{2p1}, φ_{3p1}, φ_{3p2}, must be replaced by φ_{2p2} φ_{3p3}, and φ_{3p4}. Thus the solutions for θ and $\bar{\theta}$ can be easily calculated at any point ξ, η within the range of validity of the series. Furthermore, the location of the initial bulge can be calculated by substituting the asymptotic solutions of φ_{ij}'s.

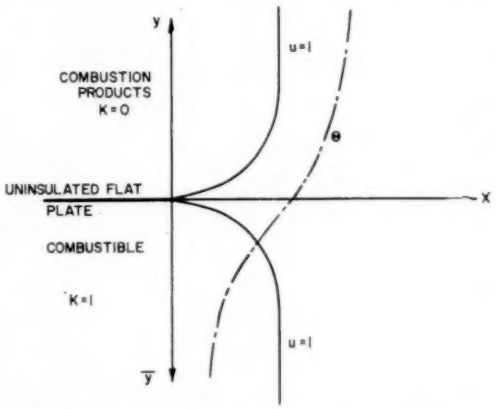

FIG. 2. Schematic of model with co-ordinate system.

(2) *Case of no chemical reaction*

The temperature distribution in the case of the mixing of a heated and a cold air stream, has been calculated for a particular initial temperature profile. The results are compared with the experiment as shown in Figs. 3 and 4.

Fig. 3 shows the initial velocity profile with the free stream velocity of approximately 15·2 ft/sec for both streams. (In Fig. 3 it is seen that the velocity profile is not symmetric with respect to the partition $y = 0$, as in the physical plane.

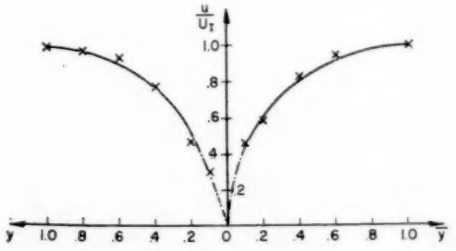

FIG. 3. Initial velocity profile in compressible plane.

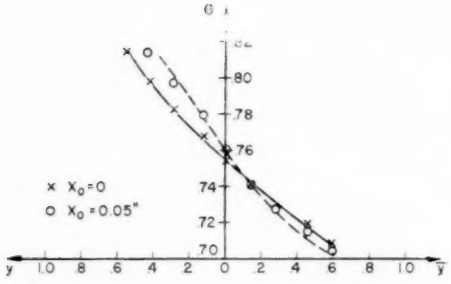

FIG. 4. Temperature profile incompressible plane.

When the y co-ordinates are contracted, according to the Howarth transformation, they will reduce to approximately symmetric Blasius profile as postulated in the analysis. The reduction of the experimental data will be given in Appendix C.) Fig. 4 shows the temperature distribution in the wake near the trailing edge. The free stream temperatures of the hot and the cold streams are 540° and 45°F respectively.

In Fig. 4 the cross represents the initial temperature as measured. The solid curve is the approximation for the initial temperature profile on which the calculation of the downstream flow field is based.

The circle represents the temperature measured at different transverse positions, 0·05 in. downstream of the trailing edge. The broken line is the corresponding temperature distribution as calculated based on equation (21).

It is interesting to note from both the measured and the calculated profile that the downstream temperature is higher than the upstream temperature in the hot stream side, and is lower in the cold stream side along constant y lines when $|y|$ is small. As a result, the temperature profile shows a steeper slope toward the downstream region along the dividing stream line.

This result might be disturbing if one should consider the change of temperature distribution as being carried out by the diffusive process alone as in the ideal case of mixing of two uniform streams.

However, inside the viscous mixing region of two uniform streams, the stream lines must converge toward the dividing stream line immediately downstream of the trailing edge of the partition. This is because the u-velocity component parallel to the dividing stream line, increases toward the downstream direction, i.e. $\partial u/\partial x > 0$. The equation of mass continuity then gives

$$\frac{\partial v}{\partial y} = -\frac{\partial u}{\partial x} + \frac{1}{\rho}\frac{\mathrm{D}\rho}{\mathrm{D}t}.$$

While $\partial u/\partial x$ becomes very large, $-(1/\rho)(\mathrm{D}\rho/\mathrm{D}t)$ is vanishingly small when the trailing edge is approached. Hence $\partial v/\partial y < 0$. With $v = 0$ at $y = 0$ the transverse velocity component v is always negative. The stream lines will therefore converge inside the viscous wake layer, at least immediately downstream of the trailing edge.

The convergence of the stream lines on both sides of the partition toward $y = 0$, upon entering into the wake, tends to increase the temperature gradient across the dividing stream line $y = 0$. This is opposite to the effect of heat diffusion. If the former effect predominates the temperature gradient across the stream line will actually increase toward the downstream region as was found from both the calculated and the measured results. The importance of the non-uniform initial temperature profiles in each stream in determining the temperature field in the wake, especially near the trailing edge of the partition, is then evident even in the absence of chemical reaction.

(3) *Case with chemical reaction*

The rate of chemical reaction in the wake region will be adversely affected because of the lowered effective temperature over the hot side of the wake. However, no definite conclusion could be made concerning the development of the maximum in the temperature profile. The effect of the lowered rate of chemical kinetics is counteracted by the lower rate of heat transfer from the hot stream to the cold stream. Moreover, the maximum temperature point developed deeper in the hot stream when compared with the case with step initial temperature profile. It is difficult to visualize qualitatively how the overall effect will be in the presence of these opposing influences. A detailed investigation will have to depend on the calculated results for specific instances based on equation (21a).

Vol. 1 1960

The criteria of the initial maximum in temperature profile is given as [2]:

$$\theta_\eta = \theta_{\eta\eta} = 0 \tag{22}$$

θ_η and $\theta_{\eta\eta}$ are calculated from the complete solution (21a) by substituting asymptotic approximation in φ_{ipj}. The asymptotic approximation of φ_{ipj} are given in Appendix D. The results are

$$\theta_\eta = (\beta_1 + \tfrac{2}{3}\beta_2 y + a_{22}\chi^{1/3} + \tfrac{1}{3}\beta_3 y^2 + \tfrac{1}{3}a_{32} y\chi^{1/3} + a_{33}\chi^{2/3})(\chi^{1/3}) \tag{23}$$

$$\theta_{\eta\eta} = (\tfrac{2}{3}\beta_2 + \tfrac{2}{3}\beta_3 y + \tfrac{1}{3}a_{32}\chi^{1/3})(3\chi^{2/3}) \tag{24}$$

where

$$\left.\begin{aligned} a_{22} &= 0{\cdot}559\,\beta_2 - 0{\cdot}003\,\bar{\beta}_2 + \\ &\quad + 0{\cdot}009\,BPr\exp\left(-\frac{\theta_a}{Fm}\right)\alpha_0 \\ a_{32} &= 2{\cdot}321\,\beta_3 + 0{\cdot}023\,\bar{\beta}_3 - \\ &\quad - 9BPr\exp\left(-\frac{\theta_a}{Fm}\right)\left(5{\cdot}150\,\frac{\theta_a A_{11}\beta_1}{Fm^2}\alpha_0 + \right. \\ &\quad \left. + (5{\cdot}468)3\alpha_1\right) \\ a_{33} &= 0{\cdot}076\,\beta_3 - 0{\cdot}068\,\bar{\beta}_3 + \\ &\quad + 9BPr\exp\left(-\frac{\theta_a}{Fm}\right)\left(3{\cdot}043\,\frac{\theta_a A_{11}\beta_1}{Fm^2}\alpha_0 + \right. \\ &\quad \left. + (3{\cdot}436)3\alpha_1\right) \end{aligned}\right\} \tag{25}$$

The co-ordinates of the location with the initial maximum in the temperature profile are found from (22–24) as

$$\chi_i^{1/3} = \frac{\{-2(a_{32}\beta_2 - 3a_{22}\beta_3)\,[1 + \sqrt{1 - (\beta_2^2 - 3\beta_1\beta_3)(a_{32}^2 - 12\beta_3 a_{33})/(a_{32}\beta_2 - 3a_{22}\beta_3)^2}]\}}{(a_{32}^2 - 12\beta_3 a_{33})} \tag{26}$$

$$y_i = \frac{-(a_{32}\chi_i^{1/3} + 2\beta_2)}{2\beta_3} \tag{27}$$

After substituting expressions (25) in equation (26) one obtains a general formula for $\chi_i^{1/3}$, which will be extremely complicated. However, it can be expanded in power series of the small parameter $[9BPr\exp(-\theta_a/Fm)]$ provided the following assumptions are satisfied:

(i) $\left|3\frac{a_{22}}{a_{32}}\frac{\beta_3}{\beta_2}\right| < 1$

(ii) $\left|\frac{2[1 - (3\beta_1\beta_3/\beta_2^2)]\beta_2/\beta_1}{a_{32}}\left(a_{22} - 2\frac{a_{33}}{a_{32}}\right)\right| < 1$

These are satisfied under typical conditions. For example, for the case reported in [2] with

$B = 2{\cdot}58 \times 10^{13}$, $\theta_a = 23{\cdot}96$, $Fm = 0(1)$
$\delta m = 0(1)$

The first terms of the expansions are

$$\chi_i^{1/3} = \frac{\beta_2 + \sqrt{(3\beta_1\beta_3)}}{8{\cdot}20\,\alpha_1\,[1 + 0{\cdot}314\,(\theta_a\beta_1/Fm^2)\,(\alpha_0/\alpha_1)]} \times \left\{1 - \frac{0{\cdot}001}{16{\cdot}40\,\alpha_1\,[1 + 0{\cdot}314\,(\theta_a\beta_1/Fm^2)\,(\alpha_0/\alpha_1)]}\right\} \times \frac{1}{9BPr\exp(-\theta_a/Fm)} \tag{28}$$

$$y_i = \sqrt{\frac{3\beta_1}{\beta_3}} \times \left[1 - \frac{0{\cdot}003\,\alpha_0\theta_a}{16{\cdot}40\,\alpha_1}\,\frac{\beta_2 + \sqrt{(3\beta_1\beta_3)}}{1 + 0{\cdot}314\,(\theta_a\beta_1/Fm^2)\,(\alpha_0/\alpha_1)}\right] \tag{29}$$

when the second term in the brackets in equations (28) and (29) is small compared to unity. y_i is approximately equal to $\sqrt{(3\beta_1/\beta_3)}$. $\alpha_0\alpha_1$ etc. will then be evaluated at $\delta m = \sqrt{(3\beta_1/\beta_3)}$. By substituting these values into equations (28) and (29) one obtains a point of the initial maximum in temperature profile.

The increase in temperature at χ_i, y_i due to the chemical heat generation can be calculated from equation (21a) as follows

$$\Delta\theta = 0{\cdot}696\,[\beta_2 + \sqrt{(3\beta_1\beta_3)}]\left(\frac{3\beta_1}{\beta_3}\right)\left\{1 + 0{\cdot}455\,\frac{\theta_a\beta_1}{Fm^2}\frac{\alpha_0}{\alpha_1} + 0\left[\frac{\theta_a\beta_1}{Fm^2}\frac{\alpha_0}{\alpha_1}\right]^2 + \ldots\right\}$$

It is interesting to note that both $\chi_i^{1/3}$, and $\Delta\theta_i$ are proportional to $[\beta_2 + \sqrt{(3\beta_1\beta_3)}]$ which is the second derivative of the initial temperature profile evaluated at $y = \sqrt{(3\beta_1/\beta_3)}$.

This result indicates that for larger negative curvature at y_i the greater is the distance required to develop the temperature maximum in agreement with physical expectations.

Typical values of β's and α's have been estimated from reasonable initial temperature profiles. Both the co-ordinates (χ_i y_i) of the point where temperature maximum occurs are found to be

$$\chi_i^{1/3} = 0{\cdot}0077 \quad . \quad y_i = 0{\cdot}485$$

when the physical constants given in [2] were adopted. Comparison with the values of $\chi_i^{1/3}$ and y_i given in [2] for the step initial temperature profile shows that the temperature maximum develops considerably further away from the dividing stream line and into the hot gas stream when the experimental, smooth initial temperature profile is used. The temperature maximum develops further upstream for the present case.

In conclusion, the present work presents an analytical method for calculating the temperature field with or without chemical reactions in the wake of a flow with nonuniform initial temperature. The importance of the nonuniformity of the initial temperature is illustrated by calling to the attention that the qualitative behavior of the immediate development of the temperature field is opposite to what may be expected if the nonuniformity is ignored. This qualitative analytic prediction is confirmed by experimental data. In view of the importance of the temperature field on the rate of chemical reaction, it is pertinent to emphasize the importance of the temperature nonuniformity in many practical problems, involving chemical reaction. A typical example is presented.

REFERENCES

1. F. E. Marble and T. C. Adamson, *Jet Propulsion* **24**, 85 (1954).
2. S. I. Cheng and A. A. Kovitz, *J. Fluid Mech.* **4**, Part 1, 64 (1958).
3. S. I. Cheng and A. A. Kovitz, *7th Combustion Symposium*, p. 681 (1958).
4. S. Goldstein, *Proc. Camb. Phil. Soc.* **26**, 1 (1930).
5. A. A. Kovitz, *Ignition in the Laminar Wake of a Flat Plate*. Ph.D. Thesis, Department of Aeronautical Engineering, Princeton University (1956).
6. D. A. Dooley, *Combustion in Laminar Mixing Regions and Boundary Layers*. Ph.D. Thesis, California Institute of Technology (1956).
7. S. I. Cheng and H. H. Chiu, *Aerodynamics of Flame Stabilization*. 14th Quarterly Progress Report, Aeronautical Engineering Report No. 335–n, Princeton University.

APPENDIX A

Expansion of $\exp(-\theta_a/\theta)$

Expansion of $\exp(-\theta_a/\theta)$ about $\xi = 0$, holding y constant, can be written as:

$$\exp\left(\frac{-\theta_a}{\theta}\right) = \exp\left(-\frac{\theta_a}{\theta}\right)\Big|_{\xi=0} + \frac{\partial}{\partial\xi}\exp\left(\frac{-\theta_a}{\theta}\right) + \frac{1}{2!}\frac{\partial^2}{\partial\xi^2}\exp\left(-\frac{\theta_a}{\theta}\right)\Big|_{\xi=0}\xi^2 \quad \text{(A1)}$$

where

$$\exp\left(-\frac{\theta_a}{\theta}\right)\Big|_{\xi=0} = \exp\left(-\frac{\theta_a}{F(\eta,\,\xi)}\right)$$

since

$$\theta = F \text{ at } \begin{cases} \xi = 0 \\ \eta \to \infty \\ y = \text{const.} \end{cases}$$

$$\frac{\partial}{\partial\xi}\exp\left(-\frac{\theta_a}{\theta}\right)\Big|_{\xi=0} = \frac{\theta_a}{\theta^2}\theta_\xi \exp\left(-\frac{\theta_a}{\theta}\right)\Big|_{\xi=0} = \frac{\theta_a\theta_1}{F^2}\exp\left(\frac{-\theta_a}{F}\right)$$

Hence equation (1) can be written as

$$\exp\left(-\frac{\theta_a}{\theta}\right) = \exp\left(-\frac{\theta_a}{F}\right)\left\{1 + \xi\frac{\theta_a\theta_1}{F^2} + \xi^2\left[\theta_a\left(\frac{\theta_2}{F^2} - \frac{\theta_1^2}{F^3}\right) + \frac{1}{2!}\left(\frac{\theta_a\theta_1}{F^2}\right)\right] + \ldots\right\} \quad \text{(A2)}$$

$$F = \beta_0 + \beta_1\left(\frac{y}{3}\right) + \beta_2\left(\frac{y}{3}\right)^2 + \beta^3\left(\frac{y}{3}\right)^3 + \ldots$$

when β_0 is close to unity, the expansion of $\exp(-\theta_a/F)$ can be carried out about $y = 0$, with $y = 3\xi\eta$.

$$\left.\begin{aligned} &\exp\left(-\frac{\theta_a}{F}\right) = \exp\left(-\frac{\theta_a}{\beta_0}\right) + \\ &+ \frac{\beta_1\theta_a}{\beta_0^2}\exp\left(-\frac{\theta_a}{\beta_0}\right)\eta\xi + \\ &+ \left\{\frac{\beta_2\theta_a}{\beta_0^2} + \left[\frac{1}{2}\left(\frac{\theta_a\beta_1}{\beta_0^2}\right)^2 - \frac{\theta_a}{\beta_0}\left(\frac{\beta_1}{\beta_0}\right)^2\right]\right\} \times \\ &\times \exp\left(-\frac{\theta_a}{\beta_0}\right)\eta^2\xi^2 + \ldots + \\ &+ \frac{\beta_4\theta_a}{\beta_0^2}\exp\left(-\frac{\theta_a}{\beta_0^2}\right)\eta^4\xi^4 \ln\xi + \ldots \end{aligned}\right\} \quad \text{(A3)}$$

Substitute (A3) into (A2) and rearrange the result in ascending powers of ξ. The following series is obtained:

$$\left.\begin{aligned}
&\exp\left(-\frac{\theta_a}{\theta}\right) = \exp\left(-\frac{\theta_a}{\beta_0}\right) + \left(\frac{\theta_a\beta_1}{\beta_0^2}\eta + \right.\\
&+ \frac{\theta_a\theta_1}{\beta_0^2}\exp\left(\frac{\theta_a}{\beta_0}\right)\xi + \left\{\left(\frac{\theta_a\theta_2}{\beta_0^2} - \frac{\theta_a\theta_1^3}{\beta_0^2} + \right.\right.\\
&+ \frac{1}{2}\frac{\theta_a^2\theta_1}{\beta_0^2} + \left.\frac{\theta_a^1\beta_2}{\beta_0^2}\right) + \left(\frac{\theta_a^2\beta_1}{\beta_0^4} - \frac{2\theta_a\beta_1}{\beta_0^3}\theta_2\right)\eta + \\
&+ \left.\left(\frac{1}{2}\frac{\theta_a}{\beta_0} - 1\right)\left(\frac{\theta_a}{\beta_0}\right)\left(\frac{\beta_1^2}{\beta_0}\right)\eta^2\right\}\\
&\exp\left(-\frac{\theta_a}{\beta_0}\right)\xi^2 + \\
&+ \frac{\theta_a + \beta_4}{\beta_0^2}\exp\left(-\frac{\theta_a}{\beta_0}\right)\eta^4\xi^4\ln\xi + \ldots
\end{aligned}\right\} \quad \text{(A4)}$$

When β_0 is substantially different from unity, say 1/2, the above expansion cannot be used. The expansion of $\exp(-\theta_a/F)$ must be such as to represent with reasonable accuracy this function in the region of y which is important in the development of the temperature maximum. The method of solution of the different equation regimes, on the other hand, $\exp(-\theta_a/F)$ must be expressed in the form of power series of y. Hence assume the following expansion

$$\exp\left(-\frac{\theta_a}{F}\right) = \exp\left(-\frac{\theta_a}{Fm}\right)(a_0 + a_1 y + \\ + a_2 y^2 + \ldots) \qquad \text{(A5)}$$

a_0, a_1, and a_2, are so determined that the truncated polynomial will give the same zeroth. First and second derivatives of $\exp(-\theta_a/F)$ at some important point $y = \delta m$. Hence,

$$a_0 + a_1\delta m + a_2\delta m^2 = 1 \qquad \text{(A6)}$$

$$a_1 + 2a_2\delta m = \left(\frac{\theta_a}{Fm^2}\right)Fm' \qquad \text{(A7)}$$

$$2a_2 = \frac{\theta_a}{Fm^2}Fm'' - \frac{2\theta_a}{Fm^3}(Fm')^2 + \frac{\theta_a^2}{Fm^4}(Fm')^2 \qquad \text{(A8)}$$

From (A6), (A7) and (A8), a_0, a_1, a_2, are calculated, finally (A2) may be written as

$$\exp\left(-\frac{\theta_a}{F}\right) = \exp\left(-\frac{\theta_a}{Fm}\right)_1\left[a_0 + \left(a_0\frac{\theta_a\theta_1}{Fm^2} + \right.\right.$$
$$+ 3a_1\eta\Big)\xi + \left\{a_0\left[\theta_a\left(\frac{\theta_2}{Fm^2} - \frac{\theta^3}{Fm^3}\right) + \right.\right.$$
$$\left.\left.+ \frac{1}{2}\frac{\theta_a\theta_1}{Fm^2}\right] + 3a_1\frac{\theta_a\theta_1}{Fm^2}\eta + 3^2a_2\eta^2\right\}\xi^2 + \ldots\Big]$$

where

$$a_0 = 1 - \frac{\theta_a}{Fm^2}Fm'\delta m + \frac{1}{2}\frac{\theta_a}{Fm^2}\left(Fm'' - \right.$$
$$\left. - \frac{2Fm'^2}{Fm} + \frac{\theta_a Fm'^2}{Fm^2}\right)\delta m^2$$

$$a_1 = \frac{\theta_a}{Fm^2}Fm' - \frac{\theta_a}{Fm^2}\left(Fm'' - \right.$$
$$\left. - \frac{2Fm'^2}{Fm} + \frac{\theta_a Fm'^2}{Fm^2}\right)\delta m$$

$$a_2 = \frac{1}{2}\frac{\theta_a}{Fm^2}\left(Fm'' - \frac{2Fm'^2}{Fm} + \frac{\theta_a Fm'^2}{Fm^2}\right)$$

APPENDIX B

Asymptotic solution of $\theta_r^{(0)}$

The general equation for $\theta_r(\eta)$ can be written in the more convenient form

$$\theta_r'' + \lambda_2 f_0\theta_r' - \lambda_r f_0'\theta_r = Pr\, I_r$$

where

$$\lambda_r = rPr$$

$$I_0 = I_1 = \tilde{I}_4 = 0$$

$$I_2 = -9BD_0K_0$$

$$I_3 = -9B(D_0K_1 + D_1K_0)$$

$$I_4 = -9B(D_0K_2 + D_2K_0) - 5f_3\theta_1' + f_3'\theta_1 + f_0'\theta_4$$

The formal solution for θ_r can be written as

$$\theta_r(\eta) = a_r f_1^{(r)}(\eta) + b_r f_2^{(r)}(\eta) - \\ - Pr\int^\eta I_r \exp\left[-\lambda_2\int^\delta f_0(z)\mathrm{d}z\right]\{f_2^{(r)}(\eta)f_1^{(r)}(\delta) - \\ - f_1^{(r)}(\eta)f_2^{(r)}(\delta)\}\, d\delta$$

where a_r, b_r are the arbitrary constants and $f_1^{(r)}$, $f_2^{(r)}$, are linearly independent solutions to the homogeneous equation. For large η Goldstein shows that f_0 behaves as quadratic function of η

$$f_0(\eta) \sim \tfrac{1}{2}\, a_1\,(\eta + \delta_0)^2 + \mathrm{O}[(\eta+\delta)^{-4} \exp\{-a_1/3\,(\eta+\delta_0)^3\}]$$

$$f_0'(\eta) \sim a_1\,(\eta + \delta_0)$$

Using these forms for f_0, f_0', the homogeneous equation becomes

$$\theta_r^{(0)} + \lambda_2 \tfrac{1}{2}\, a_1\,(\eta+\delta_0)^2\,\theta_r^{(0)} - \lambda_2 a_1(\eta+\delta_0)\,\theta_r^{(0)} = 0$$

The solutions are

$$\theta_r^{(0)} \sim Ar\,\eta_1^{-r-2} \exp\left(-\frac{a}{3}\eta_1^3\right)$$

$$\left\{1 + \sum_{n=1}^{\infty}\left[\frac{1}{36} - \left(\frac{r+1}{3} + \frac{1}{2}\right)^2\right]\left[\frac{1}{36} - \left(\frac{r+1}{3} + \frac{3}{2}\right)^2\right], \left[\frac{1}{36} - \left(\frac{r+1}{3} + n - \frac{1}{2}\right)^2\right] \Big/ \left[n!\left(\frac{a}{3}\eta_1^3\right)^n\right]\right\}$$

$$+ B_r\eta_1^r\left\{1 + \sum_{n=1}^{\infty}\left[\frac{1}{36} - \left(-\frac{r+1}{3} + \frac{1}{2}\right)^2\right]\left[\frac{1}{36} - \left(-\frac{r+1}{3} + \frac{3}{2}\right)^2\right] \cdots \left[\frac{1}{36} - \left(\frac{r+1}{3} - n + \frac{1}{2}\right)^2\right] \Big/ \left[(n!)\,(-1)^n\left(\frac{a}{3}\eta_1^3\right)^n\right]\right\}$$

where

$$\eta_1 = +\eta = \delta_0 + 0{\cdot}3408.$$

APPENDIX C

Reduction of experimental data

The velocity and temperature distribution, as shown in Figs. 3 and 4 are obtained at planes perpendicular to the free stream direction and located at $x = 0$ and $x = 0{\cdot}05$ in., respectively, as measured from the trailing edge of the plate. The hot air was heated by the electric heater to a temperature of 540°F while the cold air was observed to have a temperature of 45°F. Both free stream velocities were 15·2 ft/sec approximately.

The temperature distribution at $x = 0{\cdot}05$ in. was calculated analytically on the basis of equation (21) for a given set of values of β_r, and $\bar{\beta}_r$ which are determined by the initial temperature profile, in the following manner.

Firstly, the physical plane is transformed into the incompressible plane according to the Howarth transformation. For the constant pressure process, the density ratio ρ/ρ_I appearing in the transformation is replaced by the temperature ratio T_I/T. The compressible plane is thus transformed into the incompressible plane. To calculate the spatial variables $\chi = x_1/4l$, $y = \sqrt{(R)}y_1/4l$, as were defined by Goldstein, the effective flat plate length l must be estimated.

It may be obtained on the basis of either the formula of skin friction or of the expression of the change of the centerline velocity given by Goldstein [4]. The Blasius skin friction formula is

$$\left.\frac{\partial u}{\partial y_1}\right|_{y_1=0} = 0{\cdot}664\,\frac{Re^{1/2}}{4l}$$

where Re = Reynolds number $4lu_1/\nu$, l = effective length of the flat plate, u_I = free stream velocity in the direction parallel to the plate, y_1 = transverse distance co-ordinate in the incompressible plane. With $u_I = 15{\cdot}2$ ft/sec, $\nu = 1{\cdot}55 \times 10^{-4}$ ft²/sec., and with

$$\left.\frac{\partial u}{\partial y_1}\right|_{y_1=0} = 26{\cdot}3 \text{ in}^{-1}$$

as was obtained from the velocity profiles in the incompressible plane, l was found to be 1·30 in. Goldstein's formula for the centerline velocity is

$$u = \tfrac{1}{3}\sum_{r=0}^{\infty} \xi^{3r+1} f_{3r}'(0)$$

$f'(0) = 3{\cdot}67896$, $f_3'(0) = 3{\cdot}5415$, $f_6'(0) = 8{\cdot}1190$, with $u_I = 15{\cdot}2$ ft/sec, the centerline velocity distribution was found to fit well with that given with $l = 1{\cdot}25$ in. With $u_I = 15{\cdot}7$ ft/sec, l was found to be 0·8 in., these are shown in Fig. 5.

In the figure circles and crosses indicate the actual velocity distribution along the centerline with $u_I = 15{\cdot}2$ ft/sec and 15·7 ft/sec, respectively. The variation of the center velocity with $l = 1{\cdot}25$ in., 1·0 in., 0·8 in. are plotted. Weighing all the aspects involved, we decide to take $l = 1{\cdot}0$ in. in the calculation. The initial temperature profile in the x–y plane was approximated by

Vol. 1 1960

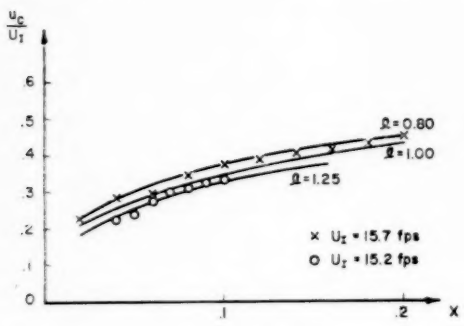

FIG. 5. Centerline velocity profile.

cubic equations for y and $\bar{y}$ smoothly joined at $y = \bar{y} = 0$. By taking 3 points in each y and $\bar{y}$ plane, the 6 unknown constants β_0, β_1, β_2, β_3, $\bar{\beta}_1$, $\bar{\beta}_2$, $\bar{\beta}_3$, are determined, where $\beta_1 = -\bar{\beta}_1$ is imposed as the necessary condition of smooth joining.

At $\chi_0 = 0{\cdot}05$ in., we have $\chi = 0{\cdot}0125$ and $\xi = 0{\cdot}232$. With the values $\beta_0 \ldots \bar{\beta}_3$ determined from the initial temperature profile, the corresponding temperature distribution at $\chi_0 = 0{\cdot}05$ in. is given by equation (21) as

$$\theta = 0{\cdot}7537 + 0{\cdot}0988\varphi_{11} + 0{\cdot}0119\varphi_{21} - \\ -0{\cdot}0301\varphi_{22} - 0{\cdot}004\varphi_{31} + 0{\cdot}0285\varphi_{32}$$

$$\bar{\theta} = 0{\cdot}7537 - 0{\cdot}0988\varphi_{11} + 0{\cdot}0119\varphi_{21} + \\ + 0{\cdot}0301\varphi_{22} - 0{\cdot}004\varphi_{31} - 0{\cdot}0285\varphi_{32}$$

Here φ's are functions of $\eta = y/3\epsilon$. For any given value of y, say $y = 0{\cdot}174$ $\eta = y/3\epsilon = 0{\cdot}25$ the following values are obtained from Table 2(b).

$$\varphi_{11} = 0{\cdot}2436, \quad \varphi_{21} = 1{\cdot}1598, \quad \varphi_{22} = 0{\cdot}2503, \\ \varphi_{31} = 1{\cdot}243, \quad \varphi_{32} = 0{\cdot}2570$$

Thus θ and $\bar{\theta}$ were calculated to be 0·7864, and 0·7387 respectively at the point $\eta = \bar{\eta} = 0{\cdot}25$.

The slope of the temperature profile along the stream line can be calculated easily by differentiating equation (21), with respect to y. With the present data the analytical result gave $\theta_y/\beta_1 = 1{\cdot}625$. While the experimental result is $1{\cdot}61 \pm$ at $\xi = 0{\cdot}232$.

APPENDIX D

Asymptotic approximation of φ_{ipj}

The asymptotic expression of φ_{ipj} are approximated based on the computed values of the temperature function in [7] and are shown in the following:

$$\varphi_{11} = 0{\cdot}587\eta + 0{\cdot}200$$
$$\varphi_{21} = 1{\cdot}800\eta^2 + \eta + 0{\cdot}580$$
$$\varphi_{22} = 0{\cdot}610\eta^2 + 0{\cdot}343\eta + 0{\cdot}193$$
$$\varphi_{2p1} = 0{\cdot}052\eta^2 + 0{\cdot}028\eta + 0{\cdot}019$$
$$\varphi_{2p2} = 0{\cdot}173\eta^2 + 0{\cdot}167\eta - 0{\cdot}052$$
$$\varphi_{31} = 1{\cdot}850\eta^3 + 2{\cdot}170\eta^2 + 0{\cdot}015\eta + 1{\cdot}620$$
$$\varphi_{32} = 0{\cdot}553\eta^3 + 0{\cdot}635\eta^2 + 0{\cdot}080\eta + 0{\cdot}370$$
$$\varphi_{3p1} = 0{\cdot}095\eta^3 + 2{\cdot}680\eta^2 + 3{\cdot}010\eta + 1{\cdot}851$$
$$\varphi_{3p2} = 0{\cdot}100\eta^3 + 2{\cdot}850\eta^2 - 3{\cdot}300\eta + 2{\cdot}041$$
$$\varphi_{3p3} = 0{\cdot}103\eta^3 + 2{\cdot}930\eta^2 - 2{\cdot}847\eta + 1{\cdot}542$$
$$\varphi_{3p4} = 0{\cdot}105\eta^3 + 2{\cdot}979\eta^2 - 2{\cdot}911\eta + 0{\cdot}650$$

The above approximate expressions are justified from the point of view of the behavior of the asymptotic solution as is given in Appendix B.

Int. J. Heat Mass Transfer. Vol. 1, pp. 294–301. Pergamon Press 1961. Printed in Great Britain.

HEAT AND MASS TRANSFER DURING THE DRYING OF MOIST MATERIALS

P. D. LEBEDEV
Moscow Power Institute, U.S.S.R.

(*Received* 9 *May* 1960)

Abstract—This paper deals with heat and mass transfer inside a moist capillary porous body under conditions of an intensive heating process. It was found by the experiments that in the capillaries of a body a pressure of gas and vapour mixture occurs exceeding that of the surrounding air (barometric pressure). One of the main reasons stimulating moisture transfer inside a body in the process of drying is a decrease of this excessive pressure. The coefficients of moisture content are calculated and in analysis the mechanism of drying is given on the basis of the differential equation for heat and mass transfer in dispersed media.

Résumé—Cet article traite du transfert de chaleur et de masse à l'intérieur d'un corps humide à porosité capillaire soumis à un chauffage intensif. Les expériences ont montré que, dans les capillarités du corps la pression du mélange de gaz et de vapeur s'élève au-dessus de la pression ambiante (pression atmosphérique). L'un des principaux facteurs de l'accélération du transport de l'humidité à travers un corps au cours du séchage est la diminution de cette surpression. Les coefficients de teneur en eau sont calculés et une analyse du mécanisme du séchage est donnée, elle est basée sur l'équation différentielle du transport de masse et de chaleur dans un milieu dispersé.

Zusammenfassung—Diese Arbeit beschäftigt sich mit der Wärme- und Stoffübertragung im Inneren eines feuchten, kapillar-porösen Körpers bei intensiver Trocknung. Die Versuche ergaben in den Kapillaren einen Druck des Gas-Dampfgemisches, der über deren Umgebungsdruck (barometrischer Druck) lag. Eine der Hauptursachen für den Feuchtigkeitstransport innerhalb des Körpers während der Trocknung ist ein Abfall dieses Überdrucks. Die Koeffizienten des Feuchtigkeitsgehaltes werden berechnet und eine Analyse des Trocknungsmechanismus gegeben auf der Grundlage der Differentialgleichung für den Wärme- und Stofftransport in dispersen Medien.

Аннотация—В статье рассматривается перенос тепла и вещества внутри влажного капиллярно-пористого тела в процессе интенсивного нагрева. Экспериментами установлено, что в капиллярах тела возникает давление парогазовой смеси, превышающее давление окружающего воздуха (барометрическое давление). Перепад этого избыточного давления является одной из основных причин переноса влаги внутри тела в процессе сушки. На основе дифференциального уравнения тепломассопереноса в дисперсных средах подсчитаны коэффициенты переноса влаги и дан анализ механизма сушки.

Vol. 1 1960

It is known that the process of drying materials consists both of the transfer of moisture within the material and of the evaporation of it from the surface of the material into the surrounding medium. In most cases the rate of drying depends on the intensity of moisture transfer from within the material towards its surface.

In earlier works the heat and mass transfer processes were considered as analogous. Therefore the equation of mass conduction was written analogically to the Fourier heat conduction equation:

$$q' = -a'\gamma_0 \nabla u \qquad (1)$$

where q' is the density of mass flow, kg/m²hr,
∇u is the moisture content gradient,
a' is the moisture potential conductivity coefficient of material,
γ_0 is the density of dry material kg/m^3.

Accordingly the differential equation of mass conduction had the form:

$$\frac{\partial u}{\partial \tau} = a'\nabla^2 u$$

where τ is the time in hr.

1923–30 the American scientists Sherwood and Lewis published their works where analytical dependences for some particular cases of the kinetics of the drying process described by the above equation were given.

The experimental investigations carried out by the Soviet scientists A. M. Fedorov, B. A. Posnov, J. I. Minjovich, I. I. Paleev, A. A. Shumilin and others determined that moisture transfer does not correspond to the molecular diffusion but occurs under the influence of some other causes and that the coefficient a depends on the moisture content of the material.

In 1934, A. V. Luikov discovered the phenomenon of moisture thermal diffusion and established a new factor causing moisture transfer in materials—the temperature gradient and, corresponding to it, the thermal gradient coefficient.

At first this factor was considered insignificant, since it does not influence considerably the low temperature convective drying of various materials. The intensification of heat and mass transfer processes in general and the application of high-frequency to drying material in particular showed the enormous significance of this factor.

In this case the mass transfer equation will be of the following form:

$$q' = -q'_u + q'_t = -a'\gamma_0 \nabla u - a'\gamma_0 \delta \nabla t \quad (3)$$

where δ is the thermal gradient coefficient $1/^\circ C$, q'_u and q'_t are the flows of mass provoked by moisture conductivity and the thermal diffusion of moisture, ∇t is the temperature gradient $^\circ C/m$.

In this case the mass conduction differential equation will be of the following form:

$$\frac{\partial u}{\partial \tau} = a'\nabla^2 u + a'\delta\nabla^2 t \quad (4)$$

and the heat conduction differential equation of the form:

$$\frac{\partial t}{\partial \tau} = a\nabla^2 t + \frac{\epsilon r}{c}\frac{\partial u}{\partial \tau} \quad (5)$$

the second term of which takes into account the influence of the moisture evaporation within the body on the temperature field change. ϵ is the coefficient of moisture internal evaporation; at $\epsilon = 0$ the total mass of moisture is transferred in a liquid form and at $\epsilon = 1$ only in the form of vapour. r is the heat of evaporation, kcal/kg, c is the specific heat of an absolutely dry material, a is the thermal diffusivity coefficient, kcal/kg°C.

The coefficients a' and δ depend on the temperature and moisture content of the material. The coefficient a' remains constant both when the material has a high moisture content and when it is at a constant temperature; in this state a' corresponds to the transfer of osmotically bounded and of capillary moisture in liquid form. On further removal of moisture from the smaller capillaries, it can be transferred not only in the form of liquid but partially also in the vaporous state; in this case the coefficient a' is decreasing. Still greater decrease of a' may be observed when the moisture content of the material is very low. The moisture bound by the polymolecular absorption is then being removed as steam.

The coefficient δ varies in rather a different way with the variation of the moisture content and of the temperature. It decreases with the increase in temperature. The coefficient δ will increase and reach its maximum value with the decrease of the average moisture content of the material, for when there are larger amounts of capillary moisture in the material there is a favourable influence of the trapped air upon the transfer of moisture. Further, a part of the moisture can be transferred as vapour with a decrease of the moisture content (when it approaches the critical moisture level), and δ decreases in consequence of the relative thermal diffusion of vapour and air. When there is only the sorbite moisture in the material, then δ becomes negative since the vapour tends to be transferred in the opposite direction towards the heat flux.

It was established by experiment that an increase in the difference of temperature, moisture concentration and vapour pressure in the interior of the material and at the surface of the material respectively causes an adequate increase in the rate at which it dries.

If the temperature or the moisture content of the surface layers of the material are greater than those of the internal ones, this may either

slow down the transfer of moisture towards the surface of the material or even provoke a reverse transfer of moisture into the internal layers of the material.

Accordingly the moisture, temperature and pressure gradients may have both negative and positive signs. The negative sign shows a lack of agreement between the direction of the moisture-flow vector and the direction of the gradient and corresponds to a transfer of moisture from the internal layers of the material towards its surface.

The application of equation (3) to the analysis of various drying processes shows that the transfer of moisture towards the surface occurs at the convective drying (Fig. 1) owing to the moisture content gradient; on the contrary the temperature gradient makes the transfer of moisture slow down. In this case $q' = q'_u - q'_t$.

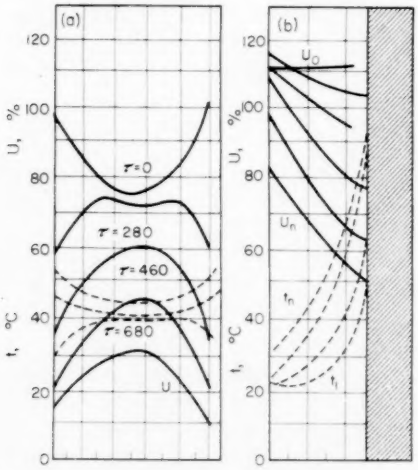

FIG. 1. Typical curves of moisture content and temperature distribution in the material:
(a) For convective drying,
(b) For conductive drying.

The greater the temperature difference between the centre and the surface of a material and the higher the value of the thermal gradient the larger the value of q'_t. The effect of a change of the temperature field on the intensity of the moisture transfer can be neglected only in the case of low-temperature drying. The transfer of moisture towards the surface (Fig. 1(b)) is determined at the contact drying in the same way as in most cases of drying (Fig. 2(b)) i.e. by the temperature gradient; on the contrary the gradient of moisture content slows down the process of drying.

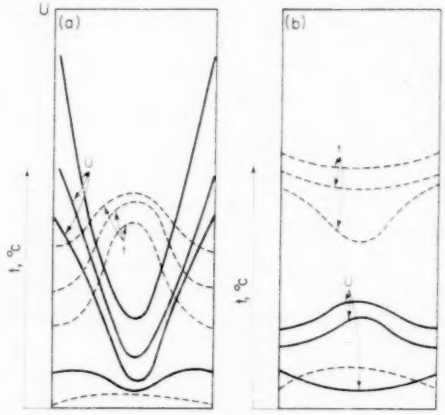

FIG. 2. Curves of moisture content and temperature distributions for high frequency drying of wood.

For instance, forced circulation of air is applied in order to intensify the process of contact fabric drying. In most cases the application of air circulation to the process of high frequency drying also gives positive results. The anomalous fields of temperature and of moisture content can be observed, as shown in Fig. 2(b), at high frequency drying of a piece of wood, the central part of which has a higher moisture content and absorbs more heat. In this case the process of drying goes on sluggishly and an application of the high frequency method makes no sense at all. The main drawback of the convective drying method lies in its duration. All attempts to intensify this method of drying end in failure as they require an increase of the moisture content gradient; this is inadmissible for many materials as it makes them to crack, and thus results in wastage.

Numerous attempts were made, therefore to apply oscillating regimes which allow the influence of the temperature gradient to be operative at least momentarily. The application of high frequency current made it possible to obtain a large temperature gradient. However, this

Vol. 1 1960

method has no utilization in engineering practice because of the low efficiency of the high frequency drying installation.

Still this method of drying may find an economic and rational application in combination with other methods. Posnov and Pershanov suggested a combined high frequency and convective method of wood drying, where electrical energy is spent only to create a negligible decrease of positive temperature in dried boards and the moisture evaporation goes on in a usual way, i.e. with the help of recirculating air heated by the steam air heater. In this case the intensity of the combined drying is double that of the convective one and the expenditure of electrical energy is reduced by ten times compared to pure high frequency drying.

However, the drying processes can be intensified not only by creating a temperature gradient, since some materials are able to endure momentary and sometimes even prolonged heating up to 100°C and higher. In this case the evaporation of moisture can occur within the material. In 1952 a new factor determining the transfer of moisture from within the material towards its surface was discovered and the corresponding coefficient of molar transfer was derived through our investigations on high temperature methods of drying materials using different kinds of heat supply when the material is heated up to 100°C and more, or when the temperature of the material exceeds the saturation temperature at a given pressure. This factor is referred to as the total pressure gradient.

By our preliminary experiments we determined the values of the potential conductivity coefficient and the thermal gradient coefficient at different temperatures and for different moisture contents of the dried material. The corresponding temperature and moisture content gradients were determined directly from the experimental data, by measuring the temperature fields and the moisture content. All this made it possible to build the corresponding mass transfer balances. The analysis of mass transfer balances showed that the law of moisture transfer for a dried material is fully described by equation (3) only for temperatures lower than 100°C.

In cases when the temperature of separate zones within the material exceeds 100°C, one can find a lack of co-ordination in the mass transfer balance calculated on the basis of equation (3) and this divergence is greater, the more the temperature inside the material exceeds 100°C. In these cases a noncompensated field appears in the mass transfer balance. (In Fig. 3 it is shaded in.) It is interesting to note that the intensity of drying and, consequently, the density of moisture flow have extremely high values in some cases of combined high frequency radiative drying in spite of the fact that at some moments there exist extremely small values both for the moisture content and for the temperature gradients (Fig. 4(c)). But the intensity of drying here should be almost equal to zero according to equation (3).

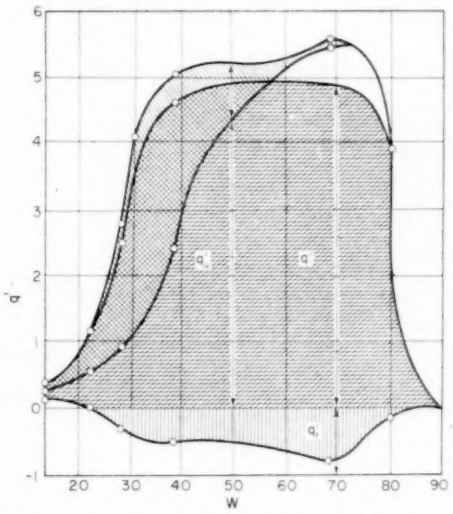

FIG. 3. The dynamics of the flow of moisture for the high radiation frequency method of drying wood. $E = 30$ V/sm; $t = 190$°C.

All this makes it possible to suppose that the gradient of excessive vapour pressure is the main motive force of moisture flow at temperatures exceeding 100°C in the interior of the material.

The nearer the location of a point to the surface, the less the resistance of the whole capillary system through which the vapour passes in its motion towards the surface.

Due to this we had every reason to suppose that

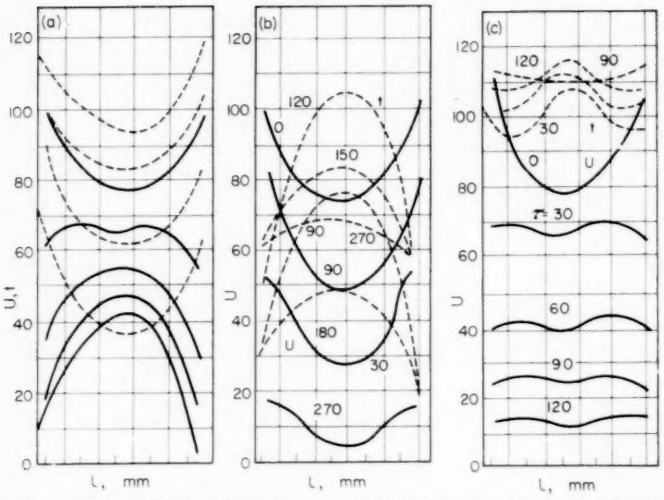

FIG. 4. Curves of moisture content and temperature distributions for different methods of heat supply:
(a) For the radiation method,
(b) For the high frequency method,
(c) For the combined high frequency and radiation method.

in every case the value of the gradient $\partial p_B/\partial x$ has a positive value, i.e. it favours the molar motion of the vapour from the central layers to the periphery. There may exist the possibility that during this motion the vapour carries away the particles of liquid thus increasing the total flow of moisture.

The character of moisture motion under the influence of the excess pressure gradient given $\partial p_B/\partial x$, does not exclude movement under the simultaneous influence both of the moisture content and of the temperature gradients, but the role of moisture transfer owing to the thermal diffusion of moisture is very small because of the small values of δ and can be neglected.

Analysis of the mass transfer balance or of flow dynamics for high temperature drying of different materials (sand, clay, wood, etc.) showed that it is necessary to insert the third term q'_p into equation (3) which takes into account the molar transfer of vapour and moisture at the expense of the excess vapour pressure arising in the material at temperatures exceeding 100°C, i.e.

$$q' = q'_u + q'_t + q'_p = -a'\gamma_0\nabla u - a'\gamma_0\delta\nabla t - a_p\gamma_0\nabla p_B \quad (6)$$

The last term on the right side of the equation represents the density of the moisture flow due to the excess pressure gradient ∇p_B.

The coefficient a_p in equation (6) may be called the coefficient of molar vapour transfer in contrast to a' which is the complex coefficient of vapour diffusion and liquid transfer under the influence of capillary and osmotic forces.

At the beginning of the drying process, when the moisture content of the material is considerable and all the capillaries are filled with moisture, the coefficient of molar vapour transfer a_p remains constant but it decreases when the moisture falls below the hygroscopic one. This coefficient also depends on the structure of the dried material (porosity and capillary radii). Fig. 5 shows the change of the vapour molar-transfer coefficient a_p at high temperature radiative high frequency drying of wood.

The differential mass conduction equation taking into account the excessive pressure gradient may be represented in the following form:

$$\frac{\partial u}{\partial \tau} = a'\nabla^2 u + a'\delta\nabla^2 t + a_p\nabla^2 P_B \quad (7)$$

Vol. 1 1960

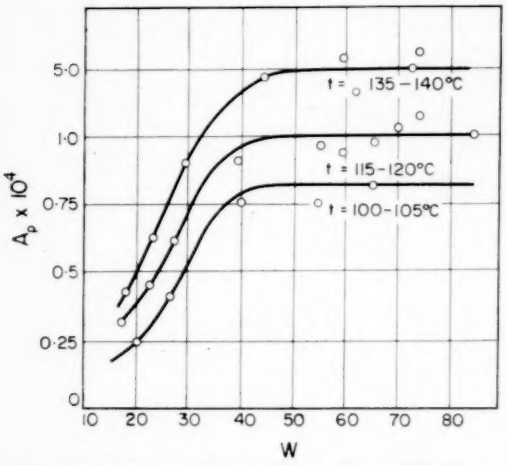

FIG. 5. The change of the molar transfer coefficient a_p for the high frequency radiation method of drying wood depending on the moisture content for different values, given the average temperature of wood.

For internal temperatures below 100°C ($p_B = 0$) or at $\nabla^2 p_B = 0$ equation (9) becomes the ordinary equation (4).

In our previous works the pressure gradient was determined in an indirect manner, but during our further investigations on the processes of wood drying in liquid media we managed to measure the pressure arising inside the wood at different temperatures applying the method of medical needles suggested by G. A. Maximov.

It should be pointed out that in our experiments we measured the excess pressure inside the material. For this purpose two capillary needles were placed at the tested depth. One capillary was soldered and measured the pressure arising from the expansion of the heated air in the capillary, while the second one measured the total pressure including that of the water vapour pressure.

The difference corresponded to the excess pressure of water vapour. It was shown by the experiments that the excess pressure on drying materials in liquid media may be observed only at temperatures above 100°C. In the experiments of Maximov the existence of considerable pressures at temperatures below 100°C was discovered by measurements with the help of unsoldered capillaries by rapid heating with high frequency currents. Maximov explains the existence of excess pressures in some porous materials drying at 70°–80°C by air effusion through the microcapillaries from the surrounding medium into the interior of the material.

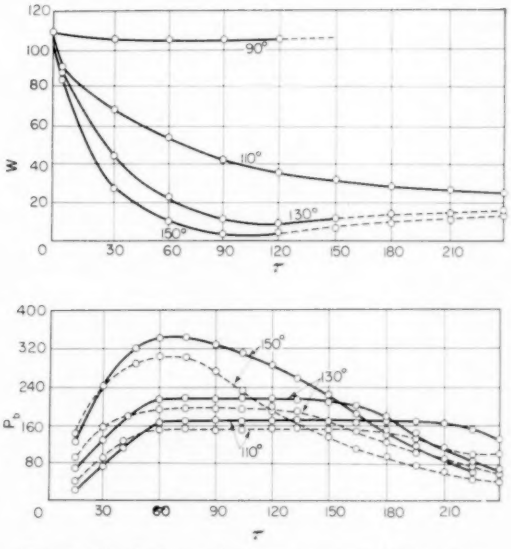

FIG. 6. The drying and pressure curves at the centre and near the surface of a block of wood at different temperatures of a liquid medium (molten paraffin).

Fig. 6 gives the diagrams for wood drying at the initial stage when it has a uniform distribution of moisture in it. The effects were observed at various temperatures of a liquid medium (melted paraffin) into which a wooden cube 50 × 50 × 60 mm was placed.

The direct measurements showed that

$$\nabla p = f(t, \omega, m) \tag{8}$$

where m gives the value of the porosity of the material.

Fig. 7 shows the curves of moisture, temperature and pressure distributions along the thickness of the wood sample at the liquid temperature of 150°C.

The conclusion of some investigators that the excess pressure has to correspond to the saturation temperature is wrong. Thus, when

the moisture content is greater than the hygroscopic one ($\omega = 60$ per cent) the pressure in the centre is only 340 mm of mercury column when the temperature of the material is 150°C (Fig. 7).

The application of the wood drying method in liquids at the expense of ∇p_B gives an acceleration 8–10 times greater than for convective drying.

A more clear understanding of the mechanism of moisture transfer obtained if the complex potential conductivity coefficient a' in the differential transfer equations is replaced by the coefficient of moisture transfer a_l in a liquid phase under the action of the moisture content gradient action provided the molar and molecular transfer of vapour is taken into

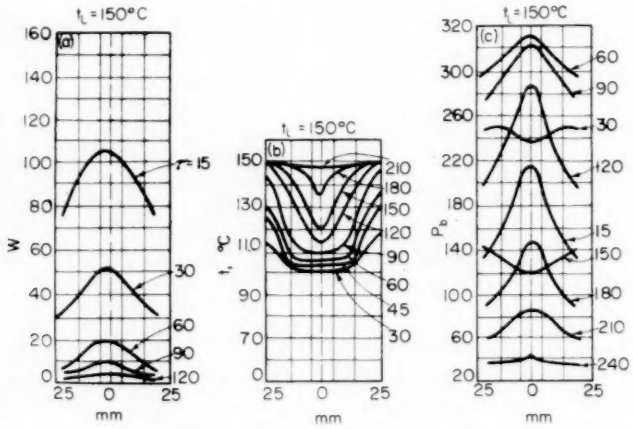

FIG. 7. The moisture, temperature and pressure distribution curves along the thickness of a sample of wood on drying it in molten paraffin at a temperature of 150°C.

The various phenomena and processes associated with materials which are being dried can be explained by the effect of the pressure gradient. Only the action of the pressure gradient can explain in the most simple way, the regularities observed in the drying of materials in organic liquids and in autoclaves with a sharp or gradual decrease of pressure, as well as the sharp increase in volume of particles at high temperature pneumatic drying of materials or of material dried in a boiling layer.

The periodical accelerations and decelerations of pastes drying on a heated surface and many other phenomena inexplicable in any other way can be explained only by the presence of internal pressure. But most important is the fact, that the pressure gradient is a powerful factor which intensifies moisture transfer at the high temperature drying of materials.

We should dwell now upon the interconnexion of the forces of moisture transfer acting within the material.

account separately. In this case the mass conduction differential equations may be presented in the following general form. The condition of drying when there is no excess pressures in the material (at low temperature drying) is

$$\frac{\partial u}{\partial \tau} = a_l' \nabla^2 u + a_l' \delta \nabla^2 t + \epsilon \frac{\partial u}{\partial \tau} \qquad (9)$$

The last term of this equation takes into account molecular vapour transfer; for these conditions it is of the order of 3–5 per cent and therefore may be neglected in engineering calculations. The conditions for drying when there is excess pressure in the material (at high temperature drying) is

$$\frac{\partial u}{\partial \tau} = a_p \nabla^2 u + \epsilon \frac{\partial u}{\partial \tau} \qquad (10)$$

It should be also noted, that moisture can be transferred under the action of the pressure gradient both as vapour and as liquid.

When the temperature of the material is

Vol. 1 1960

above 100°C and evaporation instead of drying is going on, moisture transfer in the liquid phase is small; it is possible only at the beginning when there is a considerable moisture content (higher than the hygroscopic one).

The differential equations given show their complete interconnexion. For example, at low temperature drying the transfer moisture in the material goes on only in the liquid phase and is due to the moisture gradient or the temperature gradient as well as the transfer of moisture in the form of vapour being small. But at high temperature drying the moisture transfer in the material goes on mainly in the form of vapour and the active force is the pressure gradient; the influence both of the moisture content gradient and of the temperature gradient is very small and the moisture transfer in a liquid form is also negligible.

In conclusion we shall give the heat transfer differential equation with the corresponding boundary conditions. The heat conduction differential equation which is valid for the conditions of high and low temperature drying for the various methods of heat supply to the material is:

$$\frac{\partial t}{\partial \tau} = a\nabla^2 t + \frac{\epsilon r}{c}\frac{\partial u}{\partial \tau} + \frac{q}{c\gamma} \qquad (11)$$

and the boundary conditions are

$$-\lambda \nabla t_w + \alpha (t_a - t_w) - r(1 - \epsilon) q' = 0 \qquad (12)$$

For the convective and conductive methods of heat supply the third term of equation (11) is equal to zero, the second term being taken into account only for intensive methods of drying materials.

t_a and t_w are the medium and material surface temperatures respectively.

In conclusion it should be pointed out that the equations given explain the mechanism of moisture transfer and may be applied to analytical calculations and for the establishment of criteria when discussing the experimental results. The rational method of drying has to be determined on the basis of the available technology considerations and economy in drying the material.

REFERENCES

1. P. D. Lebedev, *Sushka infrakrasnymi luchami.* Gosenergoizdat (1955).
2. A. V. Luikov, *Yavlenie perenosa v kapillyarno-poristykh telakh.* Gosizdat tekh-teoret. literatury (1954). A. W. Lykow, Transporterscheinungen in kapillarporösen Körpern. Akademie-Verlag. Berlin (1958).
3. G. K. Filonenko, *Sushilnye ustanovki.* Gosenergoizdat (1952).
4. P. D. Lebedev and A. J. Zuev, *Sushka drevesiny i zhidkikh sredakh.* Gosenergoizdat (1957).

Int. J. Heat Mass Transfer. Vol. 1, pp. 302–305. Pergamon Press 1961. Printed in Great Britain.

HEAT AND MASS TRANSFER BETWEEN MOIST SOLIDS AND AIR

P. D. LEBEDEV

Moscow Power Institute, U.S.S.R.

(*Received* 6 *July* 1960)

Abstract—Heat transfer at the evaporation of a liquid from porous capillary solids differs from heat transfer at the evaporation of a liquid from a free surface. The Nusselt number depends in the process of drying of moist solids not only on the Reynolds number, but also on parametric criteria which characterize the influence of mass transfer on heat transfer. The empirical relations establishing the similarity of criteria for heat and mass transfer are determined on the basis of experimental data.

Résumé—La transmission de chaleur au cours de l'évaporation d'un liquide à partir d'un corps à porosité capillaire diffère de celle qui se produit au cours de l'évaporation d'un liquide à partir d'une surface libre. Le nombre de Nusselt dans le séchage des corps humides ne dépend pas uniquement du nombre de Reynolds mais aussi d'un critère paramétrique qui caractérise l'influence du transport de masse sur le transfert de chaleur. Les relations empiriques, qui établissent la similitude du critère pour les transports de chaleur et de masse, sont déterminées à partir des données expérimentales.

Zusammenfassung—Der Wärmeübergang bei der Verdampfung einer Flüssigkeit an kapillar-porösen Körpern unterscheidet sich von dem an einer freien Oberfläche. Beim Trocknen feuchter Stoffe hängt die Nusseltzahl nicht nur von der Reynoldszahl ab, sondern von Kenngrössen, die den Einfluss der Stoffübertragung auf die Wärmeübertragung charakterisieren. Auf Grund von Versuchswerten werden die entsprechenden Beziehungen aufgestellt.

Аннотация—Теплообмен в процессе испарения жидкости из капиллярно-пористых тел отличается от теплообмена при испарении жидкости со свободной поверхности. Тепловой критерий Нуссельта в процессе сушки влажных тел зависит не только от критерия Рейнольдса, но и от ряда параметрических критериев, характеризующих влияние массообмена на теплообмен.

На основе экспериментальных данных установлены эмпирические соотношения между критериями подобия и тепломассопереноса.

Vol. 1 1960

DURING the process of drying, heat and mass transfer from the surface of a solid into the surrounding moist air is complicated. From a number of previously published works one can see that the drying of moist solids is analogous to the evaporation of liquids from a free surface. However, the identity of heat and mass transfer processes in these two cases did not appear to be corroborated by later works of greater accuracy. The well-known Lewis relation between the heat transfer coefficient α and the coefficient of mass transfer

$$\frac{\alpha}{\beta} = c\gamma \qquad (1)$$

received no confirmation [1]. Here c is the heat capacity of moist air and γ its density.

All attempts to insert some corrections into relation (1) ended in failure, since the rated formulae did not give correct result.

For non-isothermal conditions the total flow of mass is equal to the sum of diffusion, thermodiffusion and molar flows [2].

For the usual conditions evaporation the concentration diffusion is of greatest significance (from 90 to 84 per cent); the magnitude of the molar flow reaches 16 per cent and the portion of the thermodiffusion flow makes up only 1 per cent. In most cases except those when mixtures contain hydrogen it is possible to neglect thermodiffusion.

A model of the molecular mechanism of heat transfer, not complicated by mass transfer, may be presented as follows: near the surface of heat

transfer the laminar layer (laminar sublayer) is observed where the transfer of heat is only caused by molecular thermal conductivity; then there is a transient zone, where heat transfer goes on both by heat conduction and by convection (the laminar layer with slightly expressed turbulence); at last follows the turbulent kernel of the flow, where heat transfer goes on by means of hydrodynamic mixing (molar heat transfer).

In case of heat transfer accompanied by mass transfer the mechanism of the whole process alters somewhat. The presence of the mass flow in a direction normal to the surface from which evaporation proceeds accelerates molecular heat transfer, thus causing an increase in the heat transfer coefficient, other conditions remaining equal.

Besides, at high intensities the process of phase conversion, accompanied by an increase in volume of the substance, considerably influences an increase of the coefficient of heat conduction as well.

The influence of mass transfer on heat transfer may be expressed most precisely by the criterion dependence obtained by the transformation of the system of differential equations describing the law of heat transfer on the surface of a solid and the temperature field of air flowing along the surface.

We shall now consider the mechanism of mass transfer from the surface of a liquid into the surrounding medium (moist air). The moist air may be regarded as a binary vapour–gas mixture, consisting of vapour and dry air.

The vapour diffuses from the surface of a liquid under the influence of the relative concentration gradient $\partial\gamma_{10}/\partial y$, where y is the direction of a normal to the surface of the liquid, γ_{10} is the relative vapour concentration: $\gamma_{10} = \gamma_1/\gamma$, where γ_1 is vapour concentration (vapour mass per unit volume of mixture). The air diffuses in the reverse direction. In a steady state [3] the diffusion flows of vapour and of air are equal, i.e.

$$D_{12}\gamma\frac{\partial\gamma_{10}}{\partial y} = -D_{21}\gamma\frac{\partial\gamma_{20}}{\partial y}; \qquad (2)$$

for the coefficients of the interdependent diffusion of vapour into air and of air into vapour are equal ($D_{12} = D_{21}$), and the gradients of relative concentration of air, $\partial\gamma_{20}/\partial y$, and of vapour. $\partial\gamma_{10}/\partial y$, are equal in magnitude, but opposite in direction ($\gamma_{10} + \gamma_{20} = 1$). Molar motion of moist air (Stefan's flow), with a linear velocity w_c, arises owing to the presence of an obstacle for the diffusion of air, namely, the surface of the liquid at a constant barometric pressure. This molar motion is a convective flow, and increases the vapour transfer by $\gamma_1 w_c$ (the convective component of vapour transfer).

The total specific vapour flow j_1 (kg/m² hr) is equal to

$$j_1 = \gamma\gamma_{10}w_c - D_{12}\gamma\frac{\partial\gamma_{10}}{\partial y} \qquad (3)$$

The resultative air flow is zero ($j_2 = 0$)

$$0 = \gamma\gamma_{20}w_c - D_{21}\gamma\frac{\partial\gamma_{20}}{\partial y} \qquad (4)$$

From the equation (4) w_c can be determined; using formula (2), we obtain

$$w_c = -\frac{D_{12}}{\gamma_{20}}\frac{\partial\gamma_{10}}{\partial y} \qquad (5)$$

On the basis of this equation, formula (3) can be written as:

$$j_1 = \gamma\gamma_{10}w_c + \gamma\gamma_{20}w_c = \gamma w_c; \qquad (6)$$

whence for the linear velocity of convective vapour transfer we obtain the following expression

$$w_c = \frac{j_1}{\gamma} \qquad (7)$$

Usually the hydrodynamics of heat transfer for the forced motion of air are characterized by a Reynolds number, equal to the ratio of the product of the linear velocity of air along the surface w by the characteristic size l to the coefficient of the kinematic viscosity ν:

$$Re = \frac{wl}{\nu}$$

In the case of heat transfer complicated by mass transfer it is necessary to insert the additional criterion K, which characterizes the convective vapour transfer from the surface of a liquid into the surrounding air:

$$K = \frac{w_c l}{\nu} = \frac{j_1 l}{\eta} \qquad (8)$$

where η is the coefficient of dynamic viscosity ($\eta = \nu\gamma$). Then the relation between the Nusselt number Nu and criteria Re and K may be written for moist air as:

$$Nu = ARe^n (1 + K)^m \qquad (9)$$

which leads to the expression $Nu = ARe^n$ at $K = 0$ (the absence of evaporation); i.e. the usual expression of Nu for dry material.

The presence of a unit in the factor $(1 + K)$ gives universality to the formula (9), as at $K = 0$ the factor $(1 + K)$ does not become zero. At the same time K usually has such an order of magnitude (up to 13,500) that a unit is of a negligibly small value. The advantage of the present formula lies in the fact that it holds true for the total duration of all drying processes. From this point of view it may be widely used for thermophysical investigations of the drying process and for an analysis of the operation of working dryers. For designing, the application of this formula should be excluded, as here it is necessary to know beforehand the value of the drying intensity j_1, an unknown quantity.

The members of the Luikov school have suggested in their later works taking into account the influence of the mass transfer process on the heat transfer coefficient for convective drying, using the Guchman criterion, which characterizes the potential of drying. On the basis of experimental work A. V. Nesterenko suggested determining the heat transfer coefficient for the evaporation of water from the open surface according to the formula:

$$Nu_f = Nu_0 + ARe_f^n Pr_f^{0.33} Gu^{0.175} \qquad (10)$$

where Nu_0 is the value of the Nusselt number at $Re = 0$, $Pr = \nu/a$ is the Prandtl number and $Gu = (t_m - t_w)/T_m$ is the Guchman criterion in which t_m and t_w are the temperatures of the medium and of the evaporated water (°C), respectively, T_m is the medium's temperature (°K). The index of f for the criteria in formula (10), shows that their values should be taken for the average temperature of gas flow. A and n are coefficients the values of which, depending on Re, are given in Table 1.

For $Nu > 80$ the value $Nu = 2$ (at $Re = 0$) can be neglected. The criterion equations include not only the criteria obtained from the fundamental equation for connexion and boundary conditions obtained by the method developed by the similarity theory, but may also include parameter criteria, the choice of which may be made according to the physical nature of the process.

Table 1. *The values of A and n in formula* (10)

Re number	*A*	*n*
1–200	1·05	0·50
200–25000	0·385	0·57
25000–70000	0·102	0·73

The application of the parameter criteria may be advantageous both for determining the unknown quantity and for the application of the criterion dependences obtained in engineering.

Proceeding from these considerations we propose a universal equation, suitable for any method of heat supply to the material (convexion, radiation, contact and others) covering the entire drying process (both periods) and including initial values which usually serve in calculations applied to the process of drying:

$$Nu = ARe^n N^m \theta^k \left(\frac{W}{W_{cr}}\right)^{\delta} \qquad (11)$$

In this equation the criterion N, as well as the parameter criterion Gu in equation (10), determines the increase of the heat transfer coefficient at the expense of the turbulization of the air flow by vapours which evaporate from the material surface:

$$N = \frac{T_m}{T_{wt}}$$

where T_m is the absolute temperature of a medium (°K) and T_{wt} is the temperature of the wet thermometer (°K).

The parameter criterion θ in the equation determines the increase of the heat transfer coefficient at the expense of the decrease of the boundary layer thickness with the rise of the irradiator temperature for radiative drying.

The parameter criterion W/W_{cr} is the ratio of the material's moisture content during the period the drop in the rate of drying is observed

Vol. 1 1960

to the critical moisture content of the material; it takes into account the decrease of the heat transfer coefficient with the decrease of the material's moisture content during the drop in the rate of drying.

However, it should be noted that the more correct way is to insert u/u_{cr} instead of W/W_{cr} where u is the moisture content at the surface of the sample in the moment considered (when there is a drop in the rate), u_{cr} is the critical moisture content at the surface of the sample.

What we have stated above follows from these considerations: the ratio of the average moisture content of a sample in the period of time considered characterizes least of all the process of heat and mass transfer going on at the material's surface.

However, for a practical application of formula (11) the criterion W/W_{cr} has a considerable advantage as it is easier and quicker to determine the average moisture content of the material in the process of drying rather than the moisture content at its surface. Moreover for small gradients of moisture content in a sample, i.e. for combined drying by high-frequency currents and by radiation, the difference between W/W_{cr} and u/u_{cr} may be insignificant.

Calculating from experimental data for the whole process of the combined drying of materials the following formulae were derived:

for wood

$$Nu = 0{\cdot}5Re^{0{\cdot}5}\left(\frac{T_m}{T_{wt}}\right)^2\left(\frac{T_r}{T_m}\right)^{0{\cdot}4}\left(\frac{W}{W_{cr}}\right)^{0{\cdot}3} \qquad (12)$$

for clay

$$Nu = 0{\cdot}45Re^{0{\cdot}5}\left(\frac{T_m}{T_{wt}}\right)^2\left(\frac{T.}{T_m}\right)^{0{\cdot}4}\left(\frac{W}{W_{cr}}\right)^{0{\cdot}9} \qquad (13)$$

for sand

$$Nu = 0{\cdot}65Re^{0{\cdot}5}\left(\frac{T_m}{T_{wt}}\right)^2\left(\frac{T_r}{T_{wt}}\right)^{0{\cdot}4}\left(\frac{W}{W_{cr}}\right)^{1{\cdot}8} \qquad (14)$$

The various values for the coefficients A and for the exponents σ of the parameter criterion W/W_{cr} take into account the different ways in which the moisture is associated with the material during the period registering a drop in the rate of drying as well as the difference between the geometric and the real surface of evaporation in some materials as, for example, for sand.

Following this method as indicated in the formulae given below which were obtained by A. P. Bazhenov:

for convective drying of staple fabric:

$$Nu = 0{\cdot}94Re^{0{\cdot}5}\left(\frac{T_m}{T_{wt}}\right)^2\left(\frac{W}{W_{cr}}\right)^{0{\cdot}45} \qquad (15)$$

for radiative–convective drying of staple fabric during the period the rate of drying is constant:

$$Nu = 0{\cdot}9Re^{0{\cdot}5}\left(\frac{T_m}{T_{wt}}\right)^2\left(\frac{T_r}{T_m}\right)^{0{\cdot}42} \qquad (16)$$

On the basis of experimental data B. M. Tcherkinsky obtained the following formula for the drying of a fabric

$$Nu = 0{\cdot}84Re^{0{\cdot}5}\left(\frac{T_m}{T_{wt}}\right)^2\left(\frac{T_r}{T_m}\right)^{0{\cdot}4}\left(\frac{W}{W_{cr}}\right)^{0{\cdot}45} \qquad (17)$$

S. V. Shishkov obtained a formula for the drying of asbestos–rubber rings as follows:

$$Nu = 0{\cdot}68Re^{0{\cdot}5}\left(\frac{T_r}{T_m}\right)^{0{\cdot}4}\left(\frac{W}{W_{cr}}\right)^{0{\cdot}34} \qquad (18)$$

G. A. Grushke obtained a formula for the radiative drying of ceramic plates

$$Nu = 0{\cdot}4Re^{0{\cdot}5}\left(\frac{T_m}{T_{wt}}\right)^2\left(\frac{T_r}{T_m}\right)^{3{\cdot}5}\left(\frac{W}{W_{cr}}\right)^{2{\cdot}9} \qquad (19)$$

Analogous formulae were obtained in the B. I. Pyatachkova experiments on the drying of lump peat, etc., from which one can obtain the formulae calculated for the design of dryers.

REFERENCES

1. P. D. Lebedev, *Sushka Infrakrasnymi Luchami.* Gosenergoizdat (1955).
2. A. V. Luikov, *Yavleniye perenosa v kapilliarno-poristykh telakh.* Gosud. izdat. tekhniko-teoretischeskoii literatury (1954). A. W. Lykow, Transporterscheinungen in kapillarporösen Körpern, Akademie Verlag, Berlin.
3. A. V. Luikov, *Inzhenerno-fizicheskii zhurnal* **2**, No. 11 (1959).
4. I. M. Fedorov, *Teoriya i raschet protsessa sushki.* Gosenergoizdat (1955).
5. B. M. Cherkinskii, K. N. Gorodov and D. Y. Vigdorchik, *Ispolzovaniye gaza dlya intensifikatsii protsessov sushki i termicheskoi obrabotki tkaneii.* Gizlegprom (1959).

Int. J. Heat Mass Transfer. Vol. 1, pp. 306–311. Pergamon Press 1961. Printed in Great Britain.

CONVECTION HEAT TRANSFER COEFFICIENTS FOR TURBULENT FLOW BETWEEN PARALLEL PLATES WITH UNEQUAL HEAT FLUXES

HENRY BARROW

Department of Mechanical Engineering, The University of Liverpool

(*Received* 6 *July* 1960)

Abstract—This paper contains a semi-theoretical analysis of asymmetric heat transfer in fully developed two dimensional turbulent flow between parallel walls.

An extension of the analogy between the transfer of heat and the transfer of momentum (due to Mizushina), is used to determine the heat transfer coefficients for the respective boundaries. The results of the analysis are presented in the form of working formulae from which the relative magnitudes of the heat transfer coefficients may be determined. The formulae may be applied to practical engineering problems, but care is necessary because the assumptions made in the theory impose restrictions on the Prandtl and Reynolds number ranges for which the predictions are acceptable.

It is immediately obvious from the graphical presentation of the results for a particular fluid, that the heat flux ratio is an important additional parameter, and that cognizance of this should be taken in cases of non-uniform heating.

By its nature, the present analysis is preliminary, and an experimental programme has been devised to study the general problem of asymmetric heat transfer and to test the theory.

While channel flow has been considered, the results are thought to be valid for axisymmetric flow in annuli with small outside diameter/inside diameter ratios.

Résumé—Cet article donne une analyse semi-théorique de la transmission de chaleur dans un écoulement turbulent bidimensionnel dissymétrique, pleinement établi, entre deux murs parallèles.

Une extension de l'analogie entre transfert de chaleur et transfert de quantité de mouvement (due à Mizushina) est utilisée pour déterminer les coefficients de transmission de chaleur pour les deux parois. Les résultats de l'analyse sont présentés sous la forme d'une formule pratique à partir de laquelle on peut déterminer les valeurs relatives des coefficients de transmission de chaleur. La formule peut être appliquée à des problèmes techniques réels, mais il faut prendre garde au fait que les hypothèses faites dans la théorie imposent des restrictions dans les domaines de nombres de Reynolds et de Prandtl pour lesquels les résultats sont acceptables.

Il apparait immédiatement sur la présentation graphique des résultats pour un fluide particulier, que le rapport des flux de chaleur est un paramètre supplémentaire important, qu'il faudra connaître dans les cas de chauffage non-uniforme.

Par sa nature, l'étude actuelle est préliminaire, un programme expérimental a été établi pour étudier le problème général d'une transmission de chaleur assymétrique et vérifier la théorie.

Bien que l'écoulement dans un conduit ait été considéré ici, on pense que les résultats sont également valables pour un écoulement à symétrie axiale dans des anneaux, dont les rapports diamètre extérieur sur diamètre intérieur sont petits.

Zusammenfassung—Die Arbeit enthält eine halbtheoretische Untersuchung über den unsymmetrischen Wärmeübergang in vollentwickelter zweidimensionaler turbulenter Strömung zwischen parallelen Wänden.

Eine Erweiterung der Analogie zwischen Wärme- und Impulsübertragung (nach Mizushina) dient zur Ermittlung der Wärmeübergangskoeffizienten an den beiden Wänden, die in Form einer Gebrauchsgleichung für den relativen Wert des Koeffizienten mitgeteilt werden. Bei der Anwendung ist der begrenzte Bereich der Prandtl- und Reynoldszahl zu beachten.

Aus der graphischen Darstellung der Ergebnisse ergibt sich, dass das Verhältnis der Wärmestromdichten bei ungleichförmiger Beheizung von besonderer Bedeutung ist. Zur Prüfung dieser vorläufigen Theorie wird ein Versuchsprogramm angegeben. Die Theorie ist auch auf Ringkanäle mit kleinen Durchmesserverhältnissen anwendbar.

Vol. 1 1960

Аннотация—Эта статья содержит полутеоретический анализ асимметричного теплообмена в полностью развитом двухмерном турбулентном потоке между параллельными стенками. Для определения коэффициентов теплообмена используется (в соответствующих границах) аналогия между теплопереносом и переносом количества движения (по Мизушина).

Результаты анализа представлены в виде расчётных формул, на основании которых можно определить относительные величины коэффициентов теплообмена. Формулы можно применить и к практическим ниженерным задачам, но при этом необходима осторожность, т.к. сделанные в теории предположения налагают ограничения на диапазоны чисел Прандтля и Рейнольдса, для которых эти допущения приемлемы.

Из графического представления результатов для одной жидкости сразу же становится очевидным, что соотношение тепловых потоков является важным дополнительным параметром и что знание этого фактора нужно учитывать в случаях неравномерного нагрева.

Настоящий анализ по своей природе является предварительным. Намечена программа экспериментальных работ для изучения общих проблем асимметричного теплопереноса и проверки теории.

Рассматривался поток по каналу. Предполагается, что эти результаты окажутся справедливыми и для осесимметричного потока в круглых каналах с малыми величинами отношения между наружным и внутренним диаметрами.

NOMENCLATURE

- $d_e = 2s$ = equivalent diameter;
- c = specific heat at constant pressure;
- h = convection heat transfer coefficient;
- ϵ = eddy diffusivity of heat;
- $a = K/c\rho$ = thermal diffusivity;
- K = thermal conductivity;
- ρ = fluid density;
- s = distance between walls;
- q = specific heat flux;
- u, $\bar{u}$, u_τ = local velocity, average velocity, friction velocity;
- y = wall distance;
- μ = viscosity;
- τ = shear stress;
- T = temperature;
- $u^+ = u/u_\tau$ = friction velocity parameter;
- $y^+ = yu_\tau\rho/\mu$ = friction distance parameter;
- x = distance in flow direction;
- γ = a number;
- $Re = d_e\rho\bar{u}/\mu$ = Reynolds number;
- $Pr = c\mu/K$ = Prandtl number;
- $Nu = hd_e/K$ = Nusselt number.

Suffixes

- w = wall;
- 1 = outside boundary of sublayer;
- b = bulk or mixed mean.

INTRODUCTION

THERE are a number of practical applications in which the thermal flux is non-uniform across the flow section. Fig. 1(a) shows two such arrangements which are of immediate interest. For example, thermal insulation may be provided by means of a single coolant flowing in forced convection in ventilation spaces formed by parallel walls or concentric shells adjacent to the heated element [1]. A ventilated space in conjunction with conventional insulating materials is an alternative scheme for reducing heat loss to the surroundings [2]. These arrangements do not necessarily reduce the heat loss from the heated element compared with conventional insulation, but that fraction of the heat which is lost to the coolant is both channelled and controlled. Another practical case involving asymmetric heat flow which might be envisaged is when various coolants are employed in separate flow channels. The coolants employed would depend, amongst other things, on problems of heat removal and heat insulation, and in such a scheme, a sandwiched fluid could provide an additional mechanical shield between two other fluids.

When a fluid (or fluids) which is transparent for thermal radiation is used, heat transfer due to radiation occurs between the hot and cold boundary walls. This depends on the temperature of the walls, the geometry of the flow passage, and the nature of the surfaces employed. In the following analysis thermal radiation is neglected, but its inclusion is simple should

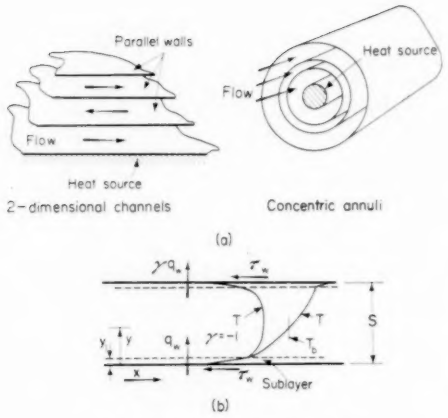

FIG. 1. Asymmetric heat transfer.

conditions make it significant. At sufficiently high coolant flow rates, free convection is swamped and this mechanism of heat transfer is also neglected.

THEORY

The system to be analysed is shown in Fig. 1(b). The fluid is in well developed turbulent flow between two parallel walls distance s apart. At one wall, thermal flux q_w is transferred to the fluid, while γq_w is transferred from the fluid at the opposite boundary. A diagrammatic temperature distribution for the system is shown for the case of $1 > \gamma > 0$; the shape of the profile is discussed in a later section. A heat balance indicates that $q_w(1 - \gamma)$ heat per unit surface area per unit time is channelled with the fluid.

The determination of the two convection heat transfer coefficients requires a knowledge of the temperature distribution in the y direction, and this in turn depends on the velocity distribution when an analogy between the transfer of heat and transfer of momentum is used. For channel flow, Knudsen and Katz [3] suggest that the equation

$$u^+ = 6{\cdot}2 \log_{10} y^+ + 3{\cdot}6$$

correlates the velocity distribution data in the turbulent region.

For the laminar sublayers adjacent the walls, the equation

$$u^+ = y^+$$

may be used, and from these equations the extent of the laminar sublayer, which presents the greater resistance to heat flow, may be determined by solving

$$y_1^+ = 6{\cdot}2 \log_{10} y_1^+ + 3{\cdot}6$$

when,

$$y_1^+ (= u_1^+) = 9{\cdot}74$$

Fig. 2 shows the simplified form of the universal velocity profile for channel flow. No account is taken of the buffer or transition zone.

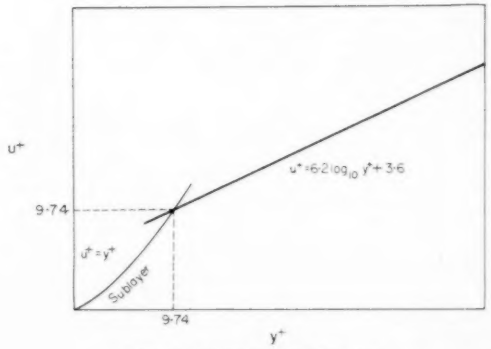

FIG. 2. Velocity distribution.

The convection heat transfer coefficient h which is to be determined, is defined by the equation

$$h = \frac{q_w}{T_w - T_b}$$

(For the other boundary, the appropriate heat flux γq_w and appropriate temperature difference would be used in the definition.)

For terminal conditions with heat fluxes q_w and γq_w uniform lengthwise, and constant heat transfer coefficients, the temperature differences between the fluid and the walls are constant, and furthermore

$$\frac{dT}{dx}\left(= \frac{dT_b}{dx} = \frac{dT_w}{dx}\right)$$

Vol. 1 1960

is constant and independent of position in the channel. The temperature differences between the walls and the fluid are determined by calculating the sublayer and turbulent core temperature drops separately.

Considering first the q_w wall.

In the sublayer, the transfers of heat and momentum are on a molecular scale, when

$$q_w = \frac{K(T_w - T_1)}{y_1}$$

$$\tau_w = \mu \frac{u_1}{y_1}$$

and with

$$u_1^+ = \frac{u_1}{u_\tau} = 9{\cdot}74$$

the temperature drop is

$$(T_w - T_1) = \frac{9{\cdot}74\, q_w\, Pr}{c\rho u_\tau} \qquad (1)$$

Unlike fully developed pipe flow, the distributions of shear stress and heat flux in the turbulent core are not similar functions of the wall distance, in which case, the Reynolds analogy between the transfer of heat and the transfer of momentum does not apply. For the temperature difference $(T_1 - T_b)$, use can be made of Mizushina's [4] extension of the analogy which is outlined in a previous paper [5] dealing with a channel with one wall adiabatic, which is a particular case of asymmetric heat transfer. When $\gamma = -1$, the heating is symmetrical and the velocity and temperature profiles are similar in shape, so that the Reynolds analogy may be used giving the thermal resistance of the turbulent core

$$\frac{T_1 - T_b}{q_w} = \frac{\bar{u} - u_1}{c\tau_w} \qquad (2)$$

This may also be obtained from the heat balance equations

$$-c\rho(\epsilon + \alpha)\frac{\partial T}{\partial y} = \bar{u}c\rho\frac{\partial T}{\partial x}\left(\frac{s}{2} - y\right)$$

and

$$q_w = \bar{u}c\rho\frac{\partial T}{\partial x}\left(\frac{s}{2} - y_1\right)$$

(for unit width of channel, and assuming that the velocity in the core is constant across the flow section and equal to the mean velocity $\bar{u}$). With the assumption that the eddy conductivity $(\epsilon + \alpha)$ is constant, and since $\partial T/\partial x$ is independent of y, these equations may be solved for the temperature, T in the turbulent core.

$$T = T_1 - \frac{q_w}{c\rho(\epsilon + \alpha)}\left\{\frac{sy}{2} - \frac{y^2}{2} - \frac{sy_1}{2} + \frac{y_1^2}{2}\right\}$$

and furthermore, with

$$T_b = \frac{1}{s/2 - y_1}\int_{y_1}^{s/2} T\mathrm{d}y$$

The thermal resistance of the turbulent core is

$$\frac{T_1 - T_b}{q_w} = \frac{2}{c\rho(\epsilon + \alpha)(s - 2y_1)^2}\left\{\frac{s^3}{12} - \frac{s^2y_1}{2} + sy_1^2 - \tfrac{2}{3}y_1^3\right\} \qquad (3)$$

When the laminar sublayer thickness y_1 is small compared with the channel width s, and since the Reynolds analogy is valid for $\epsilon \gg \alpha$ then equations (2) and (3) combined give

$$\left(\frac{T_1 - T_b}{q_w}\right) = \frac{\bar{u} - u_1}{c\tau_w} \doteqdot \frac{s}{6c\rho\epsilon}$$

Now considering the general case of asymmetric heating, with the same assumptions, the heat balance equations are

$$(q_w - \gamma q_w) = \bar{u}c\rho\frac{\partial T}{\partial x}(s - 2y_1)$$

and,

$$-c\rho(\epsilon + \alpha)\frac{\partial T}{\partial y} - \gamma q_w = \bar{u}c\rho\frac{\partial T}{\partial x}(s - y - y_1)$$

Solving, the temperature for this case is given by

$$T = T_1 - \frac{q_w(sy - y^2/2)}{c\rho(\epsilon + \alpha)(s - 2y_1)} - \frac{\gamma q_w y^2/2}{c\rho(\epsilon + \alpha)(s - 2y_1)} \qquad (4)$$

Neglecting the terms in y_1 in the numerators, and with

$$T_b = \frac{1}{s - 2y_1}\int_{y_1}^{s - y_1} T\mathrm{d}y$$

the thermal resistance of the turbulent core for asymmetric heat transfer is

$$\frac{T_1 - T_b}{q_w} \doteqdot \frac{(2+\gamma)s}{6c\rho(\epsilon+\alpha)}$$

or

$$\frac{T_1 - T_b}{q_w} \doteqdot (2+\gamma)\frac{\bar{u}-u_1}{c\tau_w} \qquad (5)$$

Hence the resistance of the turbulent core, referred to the q_w wall for asymmetric heating, is approximately $(2+\gamma)$ times that for symmetrical heating.

By adding equations (1) and (5), the total temperature difference between the q_w wall and the fluid is

$$T_w - T_b = \frac{9{\cdot}74\, q_w Pr}{c\rho u_\tau} + \frac{q_w(2+\gamma)(\bar{u}-u_1)}{cu_\tau^2\rho}$$

Now the Blasius equation

$$\tau_w/\tfrac{1}{2}\rho\bar{u}^2 = 0{\cdot}079\, Re^{-1/4},$$

or

$$u_\tau^2 = 0{\cdot}0395\, Re^{-1/4}\,\bar{u}^2,$$

suitably correlates the wall shear and the Reynolds number of the flow, and since

$$Nu = \frac{Re\, Pr\, q_w}{c\rho\bar{u}(T_w - T_b)} \text{ by definition,}$$

$$Nu = \frac{0{\cdot}1986\, Re^{7/8}\, Pr}{5{\cdot}03(2+\gamma)\, Re^{1/8} + 9{\cdot}74\,[Pr - (2+\gamma)]} \qquad (6)$$

At this point, it should be noted that with $\gamma = -1$, i.e. for symmetrical heating, equation (6) becomes similar in form to the heat transfer equation for pipe flow.

The convection heat transfer coefficient for the γq_w wall may be determined in an identical manner with the heat balance equations

$$(q_w - \gamma q_w) = \bar{u}c\rho\frac{\partial T}{\partial x}(s - 2y_1)$$

and,

$$c\rho(\epsilon+\alpha)\frac{\partial T}{\partial y} - \gamma q_w = \bar{u}c\rho\frac{\partial T}{\partial x}(y - y_1)$$

with y the γq_w wall distance.

The temperature T is given by

$$T = T_1 + \frac{q_w(1-\gamma)y^2/2}{c\rho(\epsilon+\alpha)(s-2y_1)} + \frac{\gamma q_w y}{c\rho(\epsilon+\alpha)} \qquad (7)$$

and the thermal resistance of the turbulent core referred to that wall becomes

$$\frac{T_b - T_1}{\gamma q_w} = (2+1/\gamma)\frac{s}{6c\rho\epsilon} \doteqdot (2+1/\gamma)\frac{\bar{u}-u_1}{c\tau_w}$$

where

$$Nu = \frac{Re\, Pr\, \gamma q_w}{c\rho u(T_b - T_w)} =$$

$$\frac{0{\cdot}1986\, Re^{7/8}\, Pr}{5{\cdot}03(2+1/\gamma)\, Re^{1/8} + 9{\cdot}74\,[Pr - (2+1/\gamma)]} \qquad (8)$$

DISCUSSION

The temperature distribution for asymmetric heat transfer in a two-dimensional channel, has been determined by considering each wall in turn. Equations (4) and (7) for the q_w wall and γq_w respectively, are of the same form as they should be. A typical temperature profile is sketched in Fig. 1(b) showing d^2T/dy^2 to be positive at all points in the turbulent core. This is partly the result of assuming constant eddy diffusivity ϵ [and hence conductive $(\epsilon+\alpha)$] in that region. (The eddy diffusivity ϵ is a function of wall distance and Reynolds number.) In reality, for positive values of γ, a point of contraflexure is to be expected near the centre of the channel. For $\gamma = 1$, the temperature T is linear in y in the core, and the whole thermal flux is transferred from one wall to the other, the fluid bulk temperature remaining constant. Under such conditions, the heat transfer coefficients are the same as indicated by equations (6) and (8) with $\gamma = +1$.

Fig. 3 shows the coefficients plotted in the usual way for a fluid with $Pr = 0{\cdot}7$.

The relative magnitudes are readily obtainable from the curves for a given degree of asymmetry of heat transfer.

For $\gamma = -1$, equations (6) and (8) are identical, and there is good agreement between them and the empirical equation

$$Nu = 0{\cdot}023\, Re^{0{\cdot}8}\, Pr^{0{\cdot}4},$$

Vol. 1 1960

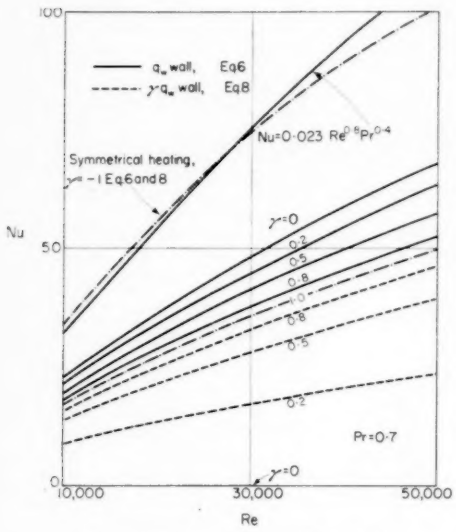

FIG. 3. Heat transfer coefficients.

which is obtained by dimensional analysis and is assumed to apply to channel flow through the hydraulic radius concept.

The use of this empirical equation as it stands, is not warranted for cases of asymmetrical heat transfer, since it does not allow for the additional parameter γ. (A modified form would be $Nu = f(\gamma, Re, Pr)$ where the function f is determined experimentally.) However, comparison of the results of the present analysis for the case of symmetrical heating (i.e. $\gamma = 1$) with the equation $Nu = 0{\cdot}023\ Re^{0{\cdot}8}\ Pr^{0{\cdot}4}$ is valid, and shows that the assumptions made regarding eddy diffusivity, etc., are warranted even over a considerable range of Re, and therefore in the general asymmetrical heating case these assumptions should be acceptable also.

The theory is valid for fluids having Pr greater than about 0·7. For very small values of Pr, the thermal diffusivity a becomes significant in the total conductivity term $(\epsilon + a)$. This limits the use of the present results, which are not valid in cases of heat removal applications where the coolant fluid might have a small Pr number (e.g. liquid metals).

An experimental programme has been devised to test the predictions presented in this paper.

REFERENCES

1. E. P. PEREGRINE and G. ROWLAND, Air flow insulation. in *General Discussion on Heat Transfer*, p. 197. Inst. Mech. Eng., A.S.M.E. (1951).
2. A. L. LONDON and C. R. GARBETT, A ventilated thermal insulation structure for high temperature marine power plants. *Trans. Amer. Soc. Mech. Engrs.* **71**, 817 (1949).
3. J. G. KNUDSEN and D. L. KATZ, Fluid dynamics and heat transfer. *Bull. Institute Engng. Res. Univ. Mich.* No. 37, p. 61 (1953).
4. T. MIZUSHINA, Analogy between fluid friction and heat transfer in annuli. In *General Discussion on Heat Transfer*, p. 191. Inst. Mech. Eng., A.S.M.E. (1951).
5. H. BARROW, *J. Roy. Aero. Soc.* **60**, No. 546, 413 (1956).

Int. J. Heat Mass Transfer. Vol. 1, pp. 312–324. Pergamon Press 1961. Printed in Great Britain.

DECAY OF TEMPERATURE FLUCTUATIONS IN HOMOGENEOUS TURBULENCE BEFORE THE FINAL PERIOD*

A. L. LOEFFLER, Jr.† and R. G. DEISSLER
Lewis Research Center,
National Aeronautics and Space Administration, Cleveland, Ohio

(*Received* 18 *March* 1960)

Abstract—A previous analysis of homogeneous turbulence for times before the final period has been extended to the case of temperature fluctuations in a homogeneous turbulence. The method consists essentially of the solution of the 2- and 3-point Fourier-transformed temperature equations after neglecting the fourth-order correlations in comparison with the second- and third-order correlations. Results are obtained for the convective transfer function, the spectral "energy" function and the total temperature fluctuation "energy". Comparison is made between the analysis and published experimental data obtained using air. The decay law obtained may be written $\overline{T^2} = A(t - t_0)^{-3/2} + B(t - t_0)^{-5}$ where $\overline{T^2}$ is the total "energy" (the mean square of the temperature fluctuations), t is the time and A and t_0 are constants determined by the initial conditions. The constant B depends on both initial conditions and the fluid Prandtl number. For large times the last term becomes negligible, leaving the $-3/2$ power decay law for the final period previously found by Corrsin.

It is shown that the effect of increasing Prandtl number is to extend the spectral "energy" function to larger wave numbers and to reduce the rate of decay of the temperature fluctuations.

Résumé—Une étude précédente de la turbulence homogène, à des instants précédant la période finale, a été étendue au cas des fluctuations de température en turbulence homogène. La méthode consiste essentiellement à résoudre les équations aux transformées de Fourier des températures en deux et trois points, après avoir négligé les corrélations du 4° ordre vis à vis des corrélations du 2° et 3° ordre. Des résultats sont obtenus pour les fonctions de la transmission de chaleur, du spectre d"énergie" et l"énergie" de fluctuation de la température totale. Une comparaison est effectuée entre la présente étude et les résultats expérimentaux publiés pour l'air. La loi de dégradation obtenue peut s'écrire $\overline{T^2} = A(t - t_0)^{-3/2} + B(t - t_0)^{-5}$ où $\overline{T^2}$ est l"énergie" totale (moyenne quadratique des fluctuations de température), t le temps A et t_0 sont des constantes déterminées par les conditions initiales. La constante B dépend à la fois des conditions initiales et du nombre de Prandtl. Pour de grandes périodes, le dernier terme devient négligeable, seule subsiste la loi de dégradation en puissance $-3/2$ pour la période finale précédemment trouvée par Corrsin.

On montre que l'effet de l'augmentation du nombre de Prandtl est d'étendre la fonction du spectre d"énergie" à des nombres d'ondes plus grands et de réduire la vitesse de dégradation des fluctuations de température.

Zusammenfassung—Eine frühere Untersuchung der homogenen Turbulenz für Zeiten vor der Endperiode wurde auf den Fall von Temperaturschwankungen in homogener Turbulenz ausgedehnt. Die Methode besteht im wesentlichen in der Lösung der Fourier-transformierten Temperaturgleichungen für zwei und drei Punkte, unter Vernachlässigung der Korrelationen vierter Ordnung gegen die der zweiten und dritten Ordnung. Man erhält Ergebnisse für die konvektive Übergangsfunktion, die spektrale "Energie"-Funktion und die totale "Energie" der Temperaturschwankungen. Mit Literaturwerten für Luft wird ein Vergleich durchgeführt. Das Abklinggesetz kann in der Form

$$\overline{T^2} = A(t - t_0)^{-3/2} + B(t - t_0)^{-5}$$

geschrieben werden. Hierin bedeuten $\overline{T^2}$ die totale "Energie" (das mittlere Quadrat der Temperatur-

* Presented at the American Physical Society Meeting of the Division of Fluid Dynamics, 23–25 November, 1959, University of Michigan, Ann Arbor, Michigan.

† Present address: Grumman Aircraft Engineering Corporation, Bethpage, N.Y.

Vol. 1 1960

schwankungen), t die Zeit, A und t_0 Konstanten, die aus den Anfangsbedingungen zu bestimmen sind. Die Konstante B hängt sowohl von den Anfangsbedingungen wie von der Prandtlzahl ab. Da für grosse Zeiten der zweite Term zu vernachlässigen ist, bleibt für die Endperiode das Abklinggesetz mit der Potenz-3/2, wie es früher von Corrsin gefunden wurde.

Es zeigt sich ferner, dass bei wachsender Prandtlzahl die spektrale "Energie"-Funktion zu grösseren Wellenzahlen ausgedehnt und das Abklingen der Temperaturschwankungen vermindert wird.

Аннотация—Существующий анализ турбулентности был распространен на случай температурных колебаний в среде с однородной турбулентностью. Метод состоит в решении дифференциальных уравнений переноса тепла с помощью двух-и трёхмерных преобразований Фурье без учёта соотношения преобразований четвертого, второго и третьего порядков. Получены результаты для функций конвективного переноса и спектральной «энергии», а также общей «энергии» температурных колебаний. Сравнивается анализ и опубликованные экспериментальные данные, полученные для воздуха. Закон релаксации может быть записан как

$$\overline{T^2} = A\,(t-t_0)^{-3/2} + B\,(t-t_0)^{-5}$$

где $\overline{T^2}$ — общая «энергия» (среднее квадратичное температурных колебаний), t — время, A и t_0 — постоянные, определяемые начальными условиями. Постоянная B зависит от начальных условий и от критерия Прандтля для жидкости (газа). Для больших промежутков времени последнюю величину не учитываем, оставляя закон релаксации в виде одночлена со степенью — 3/2 для конечного периода, открытого ранее Коррсиным.

Показано, что увеличение критерия Прандтля приводит к распространению спектральной функции «энергии» на большие волновые критерии и к уменьшению скорости затухания температурных колебаний.

INTRODUCTION

A THOROUGH study of the decay of temperature fluctuations in homogeneous turbulence would appear to be one of the initial steps required for understanding the important process of heat transfer in shear turbulence. As pointed out in [1], such a study would also be applicable to concentration fluctuations during the mixing of equi-dense fluids, for the cases of constant mutual diffusion coefficient and no interfacial tension.

Corrsin [1, 2] has already made an analytical attack on the problem of turbulent temperature fluctuations using the approaches employed in the statistical theory of turbulence. His results pertain to the final period of decay, and, for the case of appreciable convective effects, to the "energy" spectral form in specific wave-number ranges. Further work along this same line has more recently been done Ogura [7].

In 1958 Deissler [3] presented a theory of homogeneous turbulence which was valid for times before the final period. Essentially, the theory presented in [3] is valid during the period for which the fourth- and higher-order velocity correlation terms are negligible compared to the second- and third-order correlation terms. In [4] the analysis was extended to still earlier times by neglecting only the fifth- and higher-order correlation terms compared to lower-order correlation terms.

In solving the problem of the decay of temperature fluctuations in homogeneous turbulence before the final period it seems logical to use the approach which has already been employed with success for studying turbulence. In this paper, therefore, the method of [3] is used to study decay of temperature fluctuations in homogeneous turbulence. The results of the analysis are compared to the experimental data of [6].

NOTATION

$C(\kappa)$,	function of κ defined by equation (38);
C_p,	heat capacity at constant pressure;
$F(\eta)$,	function defined by equation (40);
G,	spectral "energy" function;
$H^{\oplus}$,	dimensionless quantity defined by equation (52);
K,	spectral transfer function;
k,	thermal conductivity;
M,	mesh size;
N_0,	constant depending on initial conditions;
Pr,	Prandtl number;
p,	static pressure;

R, dimensionless function of Pr, given by equation (44).
Re_M, Reynolds number, MU/ν;
$\mathbf{r}$, displacement vector from P to P';
$\mathbf{r}'$, displacement vector from P to P'';
$S^{\oplus}$, dimensionless quantity defined by equation (53);
T, temperature fluctuation from time average;
$\bar{T}$, time average value of temperature;
$\tilde{T}$, instantaneous value of temperature;
t, time;
U, time average velocity of fluid in direction perpendicular to grid;
u, velocity fluctuation from time average;
$\bar{u}$, time average value of velocity;
$\tilde{u}$, instantaneous value of velocity;
$\tilde{x}$, distance in flow direction from heated grid;
$\mathbf{x}$, position vector;

Greek symbols

γ, thermal diffusivity;
δ_0, constant depending on initial conditions;
ζ, angle between $\boldsymbol{\varkappa}$ and $\boldsymbol{\varkappa}'$;
η, variable defined by equation (41);
$\boldsymbol{\varkappa}$, $\boldsymbol{\varkappa}'$, wave-number vectors (magnitude in dimensions of 1/length);
λ_T, thermal microscale;
ν, kinematic viscosity;
ρ, fluid density;
$\tau, \phi, \beta, \alpha, \theta$, symbols used in quantities obtained by Fourier transforms.

Subscripts

i, j, k, l, symbol used to indicate direction;
0, indicates initial conditions;
min, minimum value;
norm, normalized quantity.

Superscripts

$'$, indicates quantities at point P';
$''$, indicates quantities at point P'';
$\oplus$, indicates dimensionless quantities.

THEORY

A. Correlation and spectral equations

For an incompressible fluid with constant properties and for negligible frictional heating, the energy equation may be written

$$\rho C_p \left[\frac{\partial \tilde{T}}{\partial t} + \tilde{u}_i \frac{\partial \tilde{T}}{\partial x_i}\right] = k \frac{\partial^2 \tilde{T}}{\partial x_i \partial x_i} \tag{1}$$

where $\tilde{T}$ and $\tilde{u}_i$ are instantaneous values of temperature and velocity. Breaking these instantaneous values into time average and fluctuating components as $\tilde{T} = \bar{T} + T$ and $\tilde{u}_i = \bar{u}_i + u_i$ allows equation (1) to be written

$$\frac{\partial \bar{T}}{\partial t} + \frac{\partial T}{\partial t} + \bar{u}_i \frac{\partial \bar{T}}{\partial x_i} + \bar{u}_i \frac{\partial T}{\partial x_i} + u_i \frac{\partial \bar{T}}{\partial x_i} + u_i \frac{\partial T}{\partial x_i} = \gamma \left[\frac{\partial^2 \bar{T}}{\partial x_i \partial x_i} + \frac{\partial^2 T}{\partial x_i \partial x_i}\right] \tag{2}$$

where $\gamma \equiv k/\rho C_p$. From the condition of homogeneity it follows that $\partial \bar{T}/\partial x_i = 0$, and in addition the usual assumption is made that $\bar{T}$ is independent of time and that $\bar{u}_i = 0$. Thus equation (2) simplifies to

$$\frac{\partial T}{\partial t} + u_i \frac{\partial T}{\partial x_i} = \left(\frac{\nu}{Pr}\right) \frac{\partial^2 T}{\partial x_i \partial x_i} \tag{3}$$

where $Pr = \nu/\gamma$.

Equation (3) is assumed to hold at the arbitrary point P. For point P' the corresponding equation can be written

$$\frac{\partial T'}{\partial t} + u_i' \frac{\partial T'}{\partial x_i'} = \left(\frac{\nu}{Pr}\right) \frac{\partial^2 T'}{\partial x_i' \partial x_i'} \tag{4}$$

Multiplying equation (3) by T', equation (4) by T, time averaging and adding the two equations gives

$$\frac{\partial \overline{TT'}}{\partial t} + \overline{u \frac{\partial (TT')}{\partial x_i}} + \overline{u_i' \frac{\partial (TT')}{\partial x_i'}} = \frac{\nu}{Pr}\left[\frac{\partial^2 (\overline{TT'})}{\partial x_i \partial x_i} + \frac{\partial^2 (\overline{TT'})}{\partial x_i' \partial x_i'}\right] \tag{5}$$

The continuity equation is

$$\frac{\partial u_i}{\partial x_i} = \frac{\partial u_i'}{\partial x_i'} = 0 \tag{6}$$

Vol. 1 1960

Substitution of equation (6) into (5) yields

$$\frac{\partial(\overline{TT'})}{\partial t} + \frac{\partial(\overline{u_i TT'})}{\partial x_i} + \frac{\partial(\overline{u_i' TT'})}{\partial x_i'} = \frac{\nu}{Pr}\left[\frac{\partial^2(\overline{TT'})}{x_i' \partial x_i} + \frac{\partial^2(\overline{TT'})}{\partial x_i' \partial x_i'}\right] \quad (7)$$

By use of a new independent variable,

$$r_i \equiv x_i' - x_i,$$

it is possible to rewrite equation (7) in the form

$$\frac{\partial(\overline{TT'})}{\partial t} - \frac{\partial(\overline{u_i TT'})}{\partial r_i} + \frac{\partial(\overline{u_i' TT'})}{\partial r_i} = \frac{2\nu}{Pr}\frac{\partial^2(\overline{TT'})}{\partial r_i \partial r_i} \quad (8)$$

It is convenient to write this equation in spectral form by use of the following three-dimensional Fourier transforms

$$\overline{TT'}(\mathbf{r}) = \int_{-\infty}^{\infty} \overline{\tau\tau'}(\boldsymbol{\kappa}) \exp(i\boldsymbol{\kappa} \cdot \mathbf{r})\, d\boldsymbol{\kappa} \quad (9)$$

$$\overline{u_i TT'}(\mathbf{r}) = \int_{-\infty}^{\infty} \overline{\phi_i \tau\tau'}(\boldsymbol{\kappa}) \exp(i\boldsymbol{\kappa} \cdot \mathbf{r})\, d\boldsymbol{\kappa} \quad (10)$$

and, since it is obvious by interchanging P and P' that $\overline{u_i' TT'}(\mathbf{r}) = \overline{u_i TT'}(-\mathbf{r})$,

$$\overline{u_i' TT'}(\mathbf{r}) = \int_{-\infty}^{\infty} \overline{\phi_i \tau\tau'}(-\boldsymbol{\kappa}) \exp(i\boldsymbol{\kappa} \cdot \mathbf{r})\, d\boldsymbol{\kappa} \quad (11)$$

Substitution of equations (9)–(11) into equation (8) leads to the spectral equation

$$\frac{\overline{\partial \tau\tau'}(\boldsymbol{\kappa})}{\partial t} + i\kappa_i\left[\overline{\phi_i \tau\tau'}(-\boldsymbol{\kappa}) - \overline{\phi_i \tau\tau'}(\boldsymbol{\kappa})\right] = -\frac{2\nu}{Pr}\kappa^2 \overline{\tau\tau'}(\boldsymbol{\kappa}) \quad (12)$$

Equation (12) is analogous to the two-point spectral equation governing the decay of velocity fluctuations (as pointed out in [1]) and therefore the quantity $\overline{\tau\tau'}(\boldsymbol{\kappa})$ may be interpreted as a temperature fluctuation "energy" contribution of thermal eddies of size $1/\kappa$. Equation (12) expresses the time derivative of this "energy" as a function of the convective transfer to other wave numbers and the "dissipation" due to the action of thermal conductivity. The second term on the left-hand side of equation (12) is the so-called transfer term while the term on the right-hand side is the "dissipation" term.

In order to obtain an additional relation involving the unknown quantities the same general procedure is followed as in [3] and a three-point equation is derived. For this purpose the three points P, P' and P'' together with the indicated position vectors $\mathbf{r}$ and $\mathbf{r}'$ are considered.

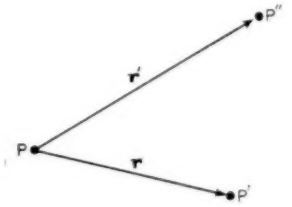

For the two points P' and P'' a relation analogous to equation (7) can be found as

$$\frac{(\partial T'T'')}{\partial t} + \frac{\partial(u_i' T'T'')}{\partial x_i'} + \frac{\partial(u_i'' T'T'')}{\partial x_i''} = \frac{\nu}{Pr}\left\{\frac{\partial^2(T'T'')}{\partial x_i' \partial x_i'} + \frac{\partial^2(T'T'')}{\partial x_i'' \partial x_i''}\right\} \quad (13)$$

If equation (13) is multiplied through by u_j, the jth velocity fluctuation component at point P, the resulting equation can be written in the form

$$\frac{\partial(u_j T'T'')}{\partial t} + \frac{\partial(u_j u_i' T'T'')}{\partial x_i'} + \frac{\partial(u_j u_i'' T'T'')}{\partial x_i''} = \frac{\nu}{Pr}\left\{\frac{\partial^2(u_j T'T'')}{\partial x_i' \partial x_i'} + \frac{\partial^2(u_j T'T'')}{\partial x_i'' \partial x_i''}\right\} + T'T''\frac{\partial u_j}{\partial t} \quad (14)$$

The momentum equation at point P is

$$\frac{\partial u_j}{\partial t} + \frac{\partial(u_j u_i)}{\partial x_i} = -\frac{1}{\rho}\frac{\partial p}{\partial x_j} + \nu\frac{\partial^2 u_j}{\partial x_i \partial x_i} \quad (15)$$

If equation (15) is solved for $\partial u_j/\partial t$ and substituted into equation (14), the result on taking time averages is

$$\left.\begin{aligned} &\frac{\partial(\overline{u_j T'T''})}{\partial t} + \frac{\partial(\overline{u_j u_i' T'T''})}{\partial x_i} + \frac{\partial(\overline{u_j u_i'' T''T'})}{\partial x_i''} = \\ &\frac{\nu}{Pr}\left\{\frac{\partial^2(\overline{u_j T'T''})}{\partial x_i' \partial x_i'} + \frac{\partial^2(\overline{u_j T'T''})}{\partial x_i'' \partial x_i''}\right\} - \\ &- \frac{\partial(\overline{u_j u_i T'T''})}{\partial x_i} - \frac{1}{\rho}\frac{\partial(\overline{pT'T''})}{\partial x_j} + \\ &+ \nu\frac{\partial^2(\overline{u_j T'T''})}{\partial x_i \partial x_i} \end{aligned}\right\} \quad (16)$$

Making use of the relations $r_i = x_i' - x_i$ and $r_i' = x_i'' - x_i$ allows equation (16) to be rewritten as

$$\left.\begin{aligned}&\frac{\partial(\overline{u_jT'T''})}{\partial t} - \frac{\nu}{Pr}\left\{(1+Pr)\frac{\partial^2(\overline{u_jT'T''})}{\partial r_i\partial r_i} + \right.\\ &\left. + 2Pr\,\frac{\partial^2(\overline{u_jT'T''})}{\partial r_i\partial r_i'} + (1+Pr)\frac{\partial^2(\overline{u_jT'T''})}{\partial r_i'\partial r_i'}\right\}\\ &= -\frac{\partial(\overline{u_ju_i'T'T''})}{\partial r_i} - \frac{\partial(\overline{u_ju_i''T''T'})}{\partial r_i'} +\\ &+ \frac{\partial(\overline{u_ju_iT'T''})}{\partial r_i'} + \frac{\partial(\overline{u_ju_iT'T''})}{\partial r_i} +\\ &+ \frac{1}{\rho}\frac{\partial(\overline{pT'T''})}{\partial r_j'} + \frac{1}{\rho}\frac{\partial(\overline{pT'T''})}{\partial r_j}\end{aligned}\right\} \quad (17)$$

Six-dimensional Fourier transforms for quantities in this equation may be defined as

$$\overline{u_jT'T''} = \int_{-\infty}^{\infty}\int_{-\infty}^{\infty}\overline{\beta_j\theta'\theta''}\exp\left[i(\boldsymbol{\kappa}\cdot\mathbf{r} + \boldsymbol{\kappa}'\cdot\mathbf{r}')\right]d\boldsymbol{\kappa}\,d\boldsymbol{\kappa}' \quad (18)$$

$$\overline{u_ju_i'T'T''} = \int_{-\infty}^{\infty}\int_{-\infty}^{\infty}\overline{\beta_j\beta_i'\theta'\theta''}\exp\left[i(\boldsymbol{\kappa}\cdot\mathbf{r} + \boldsymbol{\kappa}'\cdot\mathbf{r}')\right]d\boldsymbol{\kappa}d\boldsymbol{\kappa}' \quad (19)$$

$$\overline{pT'T''} = \int_{-\infty}^{\infty}\int_{-\infty}^{\infty}\overline{\alpha\theta'\theta''}\exp\left[i(\boldsymbol{\kappa}\cdot\mathbf{r} + \boldsymbol{\kappa}'\cdot\mathbf{r}')\right]d\boldsymbol{\kappa}\,d\boldsymbol{\kappa}' \quad (20)$$

Interchanging P' and P'' shows that

$$\overline{u_ju_i''T''T'} = \overline{u_ju_i'T'T''}.$$

By use of this fact and equations (18)–(20), equation (17) may be transformed to

$$\begin{aligned}&\frac{\partial(\overline{\beta_j\theta'\theta''})}{\partial t} + \frac{\nu}{Pr}\left\{(1+Pr)\kappa^2 + 2Pr\,\kappa_i\kappa_i' + \right.\\ &\left. + (1+Pr)\kappa'^2\right\}\overline{\beta_j\theta'\theta''} = -i(\kappa_i+\kappa_i')\overline{\beta_j\beta_i'\theta'\theta''} +\\ &+ i(\kappa_i'+\kappa_i)\overline{\beta_j\beta_i\theta'\theta''} + \frac{1}{\rho}i(\kappa_j+\kappa_j')\overline{\alpha\theta'\theta''} \quad (21)\end{aligned}$$

If the derivative with respect to x_l is taken of the momentum equation for point P, the equation multiplied through by $T'T''$ and time averages taken, the resulting equation is

$$\frac{\partial^2(\overline{u_iu_kT'T''})}{\partial x_l\partial x_k} = -\frac{1}{\rho}\frac{\partial^2(\overline{pT'T''})}{\partial x_l\partial x_l} \quad (22)$$

or, in terms of the displacement vectors $\mathbf{r}$ and $\mathbf{r}'$ this becomes

$$\begin{aligned}&\left[\frac{\partial^2}{\partial r_l'\partial r_k'} + 2\frac{\partial^2}{\partial r_l'\partial r_k} + \frac{\partial^2}{\partial r_l\partial r_k}\right](\overline{u_iu_kT'T''}) =\\ &-\frac{1}{\rho}\left[\frac{\partial^2}{\partial r_l'\partial r_l'} + 2\frac{\partial^2}{\partial r_l'\partial r_l} + \frac{\partial^2}{\partial r_l\partial r_l}\right](\overline{pT'T''}) \quad (23)\end{aligned}$$

Taking the Fourier transform of equation (23) and solving the transformed equation for $\overline{\alpha\theta'\theta''}$ yields

$$\overline{\alpha\theta'\theta''} = \frac{-\rho[\kappa_l'\kappa_k' + 2\kappa_l'\kappa_k + \kappa_l\kappa_k]}{[\kappa_l'\kappa_l' + 2\kappa_l'\kappa_l + \kappa_l\kappa_l]}\overline{\beta_l\beta_k\theta'\theta''} \quad (24)$$

Equation (24) can be used to eliminate $\overline{\alpha\theta'\theta''}$ from equation (21).

B. *Solution for times before the final period*

To obtain the equation for final period decay the third-order fluctuation terms are neglected compared to the second-order terms. Analogously, it would be anticipated that for times before but sufficiently near to the final period the fourth-order fluctuation terms should be negligible in comparison with the third-order terms. If this assumption is made then equation (24) shows that the term $\overline{\alpha\theta'\theta''}$, associated with the pressure fluctuations, should also be neglected. Thus equation (21) simplifies to

$$\begin{aligned}&\frac{\partial\overline{\beta_j\theta'\theta''}}{\partial t} + \frac{\nu}{Pr}\left\{(1+Pr)\kappa^2 + 2Pr\,\kappa_i\kappa_i' + \right.\\ &\left. + (1+Pr)\kappa'^2\right\}\overline{\beta_j\theta'\theta''} = 0 \quad (25)\end{aligned}$$

Inner multiplication of equation (25) by κ_j and integration between t_0 and t gives

$$\begin{aligned}\kappa_j\overline{\beta_j\theta'\theta''} = [\kappa_j\overline{\beta_j\theta'\theta''}]_0\exp\left\{-\frac{\nu}{Pr}[(1+Pr)\kappa^2 + \right.\\ \left. + 2Pr\kappa\kappa'\cos\zeta + (1+Pr)\kappa'^2](t-t_0)\right\} \quad (26)\end{aligned}$$

Letting $\mathbf{r}' = 0$ in equation (18) and comparing the result with equation (10) shows that

$$\kappa_i\overline{\phi_i\tau\tau'}(\boldsymbol{\kappa}) = \int_{-\infty}^{\infty}\kappa_i\overline{\beta_i\theta'\theta''}\,d\boldsymbol{\kappa}' \quad (27)$$

Vol. 1 1960

Substitution of equations (26) and (27) into equation (12) results in

$$\frac{\partial}{\partial t}\overline{\tau\tau'}(\boldsymbol{\kappa}) + \frac{2\nu}{Pr}\kappa^2\overline{\tau\tau'}(\boldsymbol{\kappa}) = \int_{-\infty}^{\infty} i\,[\kappa_i\overline{\beta_i\theta'\theta''} - \kappa_i\overline{\beta_i\theta'(-\boldsymbol{\kappa})\theta''(-\boldsymbol{\kappa}')}]_0 \exp\left\{-\frac{\nu(t-t_0)}{Pr}\left[(1+Pr)\kappa^2 + 2Pr\kappa\kappa'\cos\zeta + (1+Pr)\kappa'^2\right]\right\} d\boldsymbol{\kappa}' \quad (28)$$

Now $d\boldsymbol{\kappa}'(\equiv d\kappa_1' d\kappa_2' d\kappa_3')$ can be expressed in terms of κ' and ζ as

$$d\boldsymbol{\kappa}' = -2\pi\kappa'^2\, d(\cos\zeta)d\kappa' \quad (29)$$

the resulting equation is

$$\frac{\partial G}{\partial t} + \frac{2\nu\kappa^2}{Pr}G = K \quad (33)$$

where

$$K = -\frac{\delta_0}{2\nu(t-t_0)}\int_0^{\infty}(\kappa^3\kappa'^5 - \kappa^5\kappa'^3)\left[\exp\left\{-\frac{\nu(t-t_0)}{Pr}[(1+Pr)\kappa^2 - 2Pr\kappa\kappa' + (1+Pr)\kappa'^2]\right\} - \exp\left\{\frac{-\nu(t-t_0)}{Pr}[(1+Pr)\kappa^2 + 2Pr\kappa\kappa' + (1+Pr)\kappa'^2]\right\}\right] d\kappa' \quad (33a)$$

or, on carrying out the integration,

$$K = \frac{-\sqrt{(\pi)}\,\delta_0 (Pr)^{5/2}\exp\left[-\nu(t-t_0)(1+2Pr)\kappa^2/Pr(1+Pr)\right]}{2\nu^{3/2}(t-t_0)^{3/2}(1+Pr)^{5/2}} \left\{\frac{15Pr\,\kappa^4}{4\nu^2(t-t_0)^2(1+Pr)} + \left[\frac{5Pr^2}{(1+Pr)^2} - \frac{3}{2}\right]\frac{\kappa^6}{\nu(t-t_0)} + \left[\frac{Pr^3}{(1+Pr)^3} - \frac{Pr}{(1+Pr)}\right]\kappa^8\right\} \quad (34)$$

Substitution of equation (29) in equation (28) yields

$$\frac{\partial}{\partial t}\overline{\tau\tau'}(\boldsymbol{\kappa}) + \frac{2\nu}{Pr}\kappa^2\overline{\tau\tau'}(\boldsymbol{\kappa}) = \int_0^{\infty} 2\pi i\kappa_i\,[\overline{\beta_i\theta'\theta''} - \overline{\beta_i\theta'(-\boldsymbol{\kappa})\theta''(-\boldsymbol{\kappa}')}]_0\kappa'^2 \left[\int_{-1}^{1}\exp\left\{\frac{-\nu(t-t_0)}{Pr}[(1+Pr)\kappa^2 + 2Pr\kappa\kappa'\cos\zeta + (1+Pr)\kappa'^2]\right\} d(\cos\zeta)\right] d\kappa' \quad (30)$$

In order to perform the indicated integrations in equations (30) the initial condition,

$$i\kappa_i\,[\overline{\beta_i\theta'\theta''} - \overline{\beta_i\theta'(-\boldsymbol{\kappa})\theta''(-\boldsymbol{\kappa}')}]_0,$$

must be specified. A function which would appear to satisfy all the necessary conditions, as will be seen later, is

$$i\kappa_i\,[\overline{\beta_i\theta'\theta''} - \overline{\beta_i\theta'(-\boldsymbol{\kappa})\theta''(-\boldsymbol{\kappa}')}]_0 = -\frac{\delta_0}{(2\pi)^2}(\kappa^2\kappa'^4 - \kappa^4\kappa'^2) \quad (31)$$

where δ_0 is a constant depending on the initial conditions. Substitution of equation (31) into (30), carrying out the two integrations and defining

$$G(\kappa) = 2\pi\kappa^2\overline{\tau\tau'}(\boldsymbol{\kappa}) \quad (32)$$

(It may be of interest to note that the spectral energy function defined in [1] is larger than that defined in equation (32) by a factor of 4.) Since for low κ values, as shown in [1], a Taylor's series expansion for G begins with the product of a time independent constant and κ^2, equation (33) indicates that K must begin as κ^4 for small κ. This condition of K is fulfilled by equation (34).

It can be shown, using equation (34) that

$$\int_0^{\infty} K\,d\kappa = 0 \quad (35)$$

This was to be expected physically since K is a measure of the transfer of "energy" and the total "energy" transferred to all wave numbers must be zero. The necessity for equation (35) to hold can be shown rigorously as follows: if equation (10) is written for both $\boldsymbol{\kappa}$ and $-\boldsymbol{\kappa}$, and the resulting equations differentiated with respect to r_i and added, the result is, for

$$\mathbf{r} = 0\left(\frac{\partial}{\partial r_i} = -\frac{\partial}{\partial x_i}\right)$$

$$-2\frac{\partial}{\partial x_i}\overline{u_i TT} = \int_{-\infty}^{\infty} i\kappa_i\,[\overline{\phi_i\tau\tau'}(\boldsymbol{\kappa}) - \overline{\phi_i\tau\tau'}(-\kappa)]d\boldsymbol{\kappa}$$

Since according to equations (32), (33) and (12)

$$K \equiv 2\pi i\kappa^2\kappa_i\,[\overline{\phi_i\tau\tau'}\,(-\boldsymbol{\varkappa}) - \overline{\phi_i\tau\tau'}\,(\boldsymbol{\varkappa})]$$

the previous equation can be written

$$-2\frac{\partial}{\partial x_i}\overline{u_iTT} = \int_{-\infty}^{\infty}\frac{K}{2\pi\kappa^2}\mathrm{d}\boldsymbol{\varkappa}$$

Inasmuch as $\mathrm{d}\boldsymbol{\varkappa} = 4\pi\kappa^2\mathrm{d}\kappa$ for $K = K(\kappa, t)$, the last equation becomes

$$\int_0^{\infty} K\,\mathrm{d}\kappa = -\frac{\partial}{\partial x_i}\overline{u_iTT} = 0$$

by homogeneity, Q.E.D.

Since equation (33) is a linear differential equation it can be solved for G as

$$G = \exp\left[-\frac{2\nu\kappa^2(t-t_0)}{Pr}\right]\int K\exp\left[\frac{2\nu\kappa^2(t-t_0)}{Pr}\right]dt + \\ + C(\kappa)\exp\left[\frac{-2\nu\kappa^2(t-t_0)}{Pr}\right] \quad (36)$$

where $C(\kappa)$ is an arbitrary function of κ. For large times, Corrsin [1] has shown the correct form of the expression for G to be

$$G = \frac{N_0}{\pi}\kappa^2\exp\left[\frac{-2\nu\kappa^2(t-t_0)}{Pr}\right] \quad (37)$$

where N_0 is a constant, analogous to the Loitsianskii invariant, which depends on the initial conditions. Using equation (37) to evaluate $C(\kappa)$ in equation (36) yields

$$C(\kappa) = \frac{N_0\kappa^2}{\pi} \quad (38)$$

Substitution of the values of K and $C(\kappa)$ as given by equations (34) and (38) into equation (36) gives the equation

$$G(\kappa, t) = \frac{N_0}{\pi}\kappa^2\exp\left[\frac{-2\nu\kappa^2(t-t_0)}{Pr}\right] + \\ + \frac{\sqrt{(\pi)}\,\delta_0(Pr)^{5/2}\exp\left[-\nu\kappa(t-t_0)(1+2Pr)/Pr\,(1+Pr)\right]}{2\nu^{3/2}(1+Pr)^{7/2}} \\ \left\{\frac{3Pr\,\kappa^4}{2\nu^2(t-t_0)^{5/2}} + \frac{Pr(7Pr-6)\kappa^6}{3\nu(1+Pr)(t-t_0)^{3/2}} - \frac{4(3Pr^2-2Pr+3)\kappa^8}{3(1+Pr)^2(t-t_0)^{1/2}} + \right. \\ \left. + \frac{8\sqrt{(\nu)}\,(3Pr^2-2Pr+3)\kappa^9\,F(\eta)}{3(1+Pr)^{5/2}\sqrt{(Pr)}}\right\} \quad (39)$$

where

$$F(\eta) = \exp(-\eta^2)\int_0^{\eta}\exp(S^2)\,\mathrm{d}S \quad (40)$$

$$\eta = \kappa\sqrt{\left[\frac{\nu(t-t_0)}{Pr(1+Pr)}\right]} \quad (41)$$

The function $F(\eta)$ has been calculated numerically and tabulated in [5]. If in equation (9) $\mathbf{r}$ is set equal to zero and use is made of the definition of G as given by equation (32), the result is

$$\frac{\overline{T^2}}{2} = \int_0^{\infty} G(\kappa)\mathrm{d}\kappa \quad (42)$$

Substituting equation (39) into (42) gives

$$\frac{\overline{T^2}}{2} = \frac{N_0(Pr)^{3/2}}{8\sqrt{(2\pi)}\nu^{3/2}(t-t_0)^{3/2}} + \frac{\delta_0 R}{\nu^6(t-t_0)^5} \quad (43)$$

where R is a function of Prandtl number,

$$R = \frac{\pi(Pr)^6}{2(1+Pr)(1+2Pr)^{5/2}} \\ \left\{\frac{9}{16} + \frac{5Pr(7Pr-6)}{16(1+2Pr)} - \right. \\ - \frac{35Pr(3Pr^2-2Pr+3)}{8(1+2Pr)^2} + \\ + \frac{1{\cdot}5422Pr(3Pr^2-2Pr+3)(1+2Pr)^{5/2}}{\sqrt{(\pi)}(1+Pr)^{11/2}} \\ \left.\left[1 + \sum_{n=1}^{\infty}\frac{(11)\ldots[11+2(n-1)]}{(2n+1)n!(2)^{2n}(1+Pr)^n}\right]\right\} \quad (44)$$

The second term on the right-hand side of equation (43) becomes negligible at large times leaving the final period decay law previously found by Corrsin [1].

Vol. 1 1960

If use is made of the relation $t = \bar{x}/U$ where $\bar{x}$ is the distance from the heated grid and U the mean fluid velocity, equation (43) can be put in the alternative form

$$\frac{\overline{T^2}}{2} = \frac{N_0(Pr)^{3/2}(U/M)^{3/2}}{8\sqrt{(2\pi)}\nu^{3/2}(\bar{x}/M - \bar{x}_0/M)^{3/2}} + \frac{\delta_0(U/M)^5 R}{\nu^6(\bar{x}/M - \bar{x}_0/M)^5} \tag{45}$$

where M is the grid mesh size.

It is convenient to have the equations in dimensionless form. For this purpose the following dimensionless quantities are defined:

$$\kappa^{\oplus} = \sqrt{[\nu(t - t_0)]}\kappa \qquad K^{\oplus} = \frac{\delta_0^{4/7} K}{\nu^{11/7} N_0^{11/7}} \qquad t^{\oplus} = \frac{N_0^{2/7}\nu^{9/7}(t - t_0)}{\delta_0^{2/7}} \qquad G^{\oplus} = \frac{\nu(t - t_0)G}{N_0}$$

$$\overline{T^2}^{\oplus} = \frac{\delta_0^{3/7}\overline{T^2}}{N_0^{10/7}\nu^{3/7}} \tag{46}$$

By making use of relations (46), equations (34), (39) and (43) can be written in dimensionless form as

$$K^{\oplus} = \frac{-\sqrt{(\pi)}(Pr)^{7/2}\exp\left[-\kappa^{\oplus 2}(1 + 2Pr)/Pr(1 + Pr)\right]}{2(1 + Pr)^{5/2} t^{\oplus 11/2}}$$

$$\left\{\frac{15\kappa^{\oplus 4}}{4(1 + Pr)} + \left[\frac{5Pr}{(1 + Pr)^2} - \frac{3}{2Pr}\right]\kappa^{\oplus 6} + \left[\frac{Pr^2}{(1 + Pr)^3} - \frac{1}{(1 + Pr)}\right]\kappa^{\oplus 8}\right\} \tag{47}$$

and

$$G^{\oplus} = \frac{\kappa^{\oplus 2}\exp(-2\kappa^{\oplus 2}/Pr)}{\pi} + \frac{\sqrt{(\pi)}Pr^{7/2}\exp\left[-\kappa^{\oplus 2}(1 + 2Pr)/Pr(1 + Pr)\right]}{2(1 + Pr)^{7/2} t^{\oplus 7/2}}$$

$$\left\{\frac{3\kappa^{\oplus 4}}{2} + \frac{1}{3}\left[\frac{7Pr - 6}{1 + Pr}\right]\kappa^{\oplus 6} - \frac{4(3Pr^2 - 2Pr + 3)\kappa^{\oplus 8}}{3Pr(1 + Pr)^2} + \frac{8(3Pr^2 - 2Pr + 3)\kappa^{\oplus 9}}{3Pr^{3/2}(1 + Pr)^{5/2}} F\left[\sqrt{\left(\frac{\kappa^{\oplus 2}}{Pr(1 + Pr)}\right)}\right]\right\} \tag{48}$$

and

$$\frac{\overline{T^2}^{\oplus}}{2} = \frac{Pr^{3/2}}{8\sqrt{(2\pi)}\, t^{\oplus 3/2}} + \frac{R}{t^{\oplus 5}} \tag{49}$$

Another quantity of interest is the thermal microscale λ_T, which, for the isotropic case, can be defined by the equation

$$\frac{d\overline{T^2}}{dt} = \frac{-12\gamma\overline{T^2}}{\lambda_T^2} \tag{50}$$

Combination of equations (45) and (50) yields

$$\left(\frac{\lambda_T}{M}\right)^2 = \frac{\dfrac{3(-\bar{x}_0/M)^{3/2}}{\sqrt{(2\pi)}\, Re_M Pr[(\bar{x}/M) - (\bar{x}_0/M)^{3/2}]} + \dfrac{24R(Pr)\delta_0^{\oplus}(-\bar{x}_0/M)^5}{(Pr)^{5/2} Re_M[(\bar{x}/M) - (\bar{x}_0/M)]^5}}{\dfrac{3(-\bar{x}_0/M)^{3/2}}{8\sqrt{(2\pi)}\,[(\bar{x}/M) - (\bar{x}_0/M)]^{5/2}} + \dfrac{10R\delta_0^{\oplus}(-\bar{x}_0/M)^5}{Pr^{3/2}[(\bar{x}/M) - (\bar{x}_0/M)]^6}} \tag{51}$$

where Re_M is defined as MU/ν. For large times of decay the second terms in both numerator and denominator become negligibly small and the final period expression for $(\lambda_T/M)^2$ previously derived by Corrsin [2] is obtained.

DISCUSSION AND RESULTS

The experimental data of [6] were obtained behind a heated grid in a wind tunnel using air as fluid. Both temperature and velocity fluctuations were measured with hot wire anemometers. Fig. 1 shows the temperature fluctuation data plotted as $[1/\overline{T^2}]^{2/3}$ against $\bar{x}/M$. The solid line represents the theory as given by equation (45), with the constants $\bar{x}_0/M$, N_0, and δ_0 evaluated as shown. The dotted straight line is the final period curve, as indicated by the first term on the right-hand side of equation (45). The data scatter considerably—it would appear that with present measuring techniques there is less precision in temperature fluctuation measurements than in velocity fluctuation measurements. One of the main reasons for this is that the temperature fluctuations must be kept small to avoid fluid property variations. Comparison of the solid curve with the data indicates that the theory is valid for all $\bar{x}/M$ greater than about 25. None of the data is in the final period.

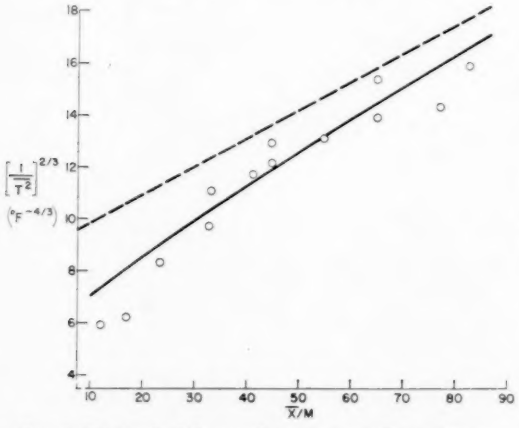

FIG. 1. Theoretical decay of temperature fluctuations compared with experimental data for $Pr = 0{\cdot}72$.
——— Theory, equation (45).
$\bar{X}_0/M = -82{\cdot}6$; $N_0 = 5{\cdot}06 \times 10^{-7}$; $\delta_0 = 5{\cdot}34 \times 10^{-25}$.
— — Theoretical final period.
○ Data of [6].

The effect of the convective terms can be seen in Fig. 2, where the transfer function $K^{\oplus}$ is plotted against $\kappa^{\oplus}$ for various dimensionless times $t^{\oplus}$ for a Prandtl number of 0·72. Since $K^{\oplus}$ is proportional to the net transfer of thermal "energy" into an eddy size, Fig. 2 shows that there is an overall transfer of "energy" from large eddies to small eddies. The integrated transfer term $\int_0^{\infty} K^{\oplus} d\kappa^{\oplus}$, must, however, be zero. The curves indicate that, as expected, the transfer term dies out with increasing time. The results are quite analogous to those found by Deissler [3] for the velocity transfer function.

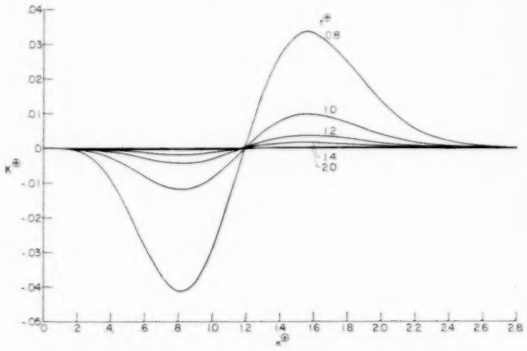

FIG. 2. Dimensionless transfer function $K^{\oplus}$ as a function of wave number and time for $Pr = 0{\cdot}72$.

If a quantity H is defined as the integrand in equation (33a) multiplied by the coefficient before the integral, then a dimensionless quantity $H^{\oplus}$ can be defined by the equation

$$H^{\oplus} \equiv \frac{\nu^5(t-t_0)^5}{\delta_0} H = -\frac{\kappa^{\oplus 8}}{2}\left[\left(\frac{\kappa'}{\kappa}\right)^5 - \left(\frac{\kappa'}{\kappa}\right)^3\right]$$
$$\left\{\exp\left[-\frac{\kappa^{\oplus 2}}{Pr}\left((1+Pr) - 2Pr\frac{\kappa'}{\kappa} + \right.\right.\right.$$
$$\left.\left.\left. + (1+Pr)\left(\frac{\kappa'}{\kappa}\right)^2\right)\right] - \exp\left[-\frac{\kappa^{\oplus 2}}{Pr}\left((1+Pr) + \right.\right.\right.$$
$$\left.\left.\left. + 2Pr\frac{\kappa'}{\kappa} + (1+Pr)\left(\frac{\kappa'}{\kappa}\right)^2\right)\right]\right\} \quad (52)$$

$H^{\oplus}$ is proportional to the amount of thermal "energy" transferred to a wave number κ from the wave number κ'. In Fig. 3 $H^{\oplus}$ is plotted against κ'/κ for three different values of $\kappa^{\oplus}$ and for $Pr = 0{\cdot}72$. The three values of $\kappa^{\oplus}$ chosen

Vol. 1 1960

were such that $K^{\oplus}$ was a minimum, zero and a maximum. As an example of the physical significance of the curves, the curve for $\kappa^{\oplus} = 0{\cdot}814$ represents a minimum for $K^{\oplus}$, so that there is an overall loss by convective transfer. The curve demonstrates this overall loss, since it can be seen that more energy is lost by wave number κ to wave numbers greater than κ than is gained from wave numbers less than κ.

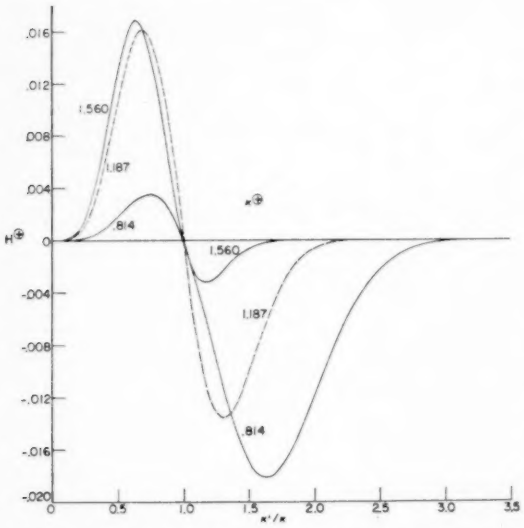

FIG. 3. Variation of dimensionless transfer quantity $H^{\oplus}$ with κ'/κ for three values of $\kappa^{\oplus}$ and $Pr = 0{\cdot}72$.

Fig. 4 is somewhat similar to Fig. 3 except that the effect of κ on the curves has been averaged out by performing an integral of $H^{\oplus}$ from 0 to ∞, obtaining $S^{\oplus}$, or

$$S^{\oplus} = \int_0^{\infty} \{H^{\oplus}\}_{\kappa'/\kappa = \text{const.}} \, \mathrm{d}\kappa^{\oplus} \qquad (53)$$

$S^{\oplus}$ may be interpreted as being proportional to $H^{\oplus}$ for an average value of κ. Thus, on the average, there is a maximum transfer of "energy" to κ from a wave number κ' equal to about $0{\cdot}65\kappa$, while the maximum loss from κ is to a wave number κ' equal to about $1{\cdot}4\kappa$.

The quantities $H^{\oplus}$ and $S^{\oplus}$ are analogous to quantities defined by Deissler [3] in connexion with the velocity inertial transfer, and the trends found here are quite similar to those.

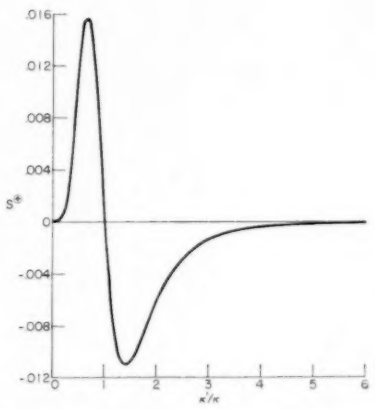

FIG. 4. Variation of averaged transfer quantity $S^{\oplus}$ with κ'/κ for $Pr = 0{\cdot}72$.

In Figs. 5(a), (b) and (c) the transfer function is plotted in the form of $K^{\oplus}t^{\oplus 11/2}$, as found from equation (47), against the dimensionless wave number $\kappa^{\oplus}$ for Prandtl numbers of 0·1, 0·72 and 10·0, respectively. One obvious effect of increasing Prandtl number is to extend the curves out to higher wave numbers. This is to be expected since for higher Prandtl number the thermal conductivity is less and hence there is less tendency for the small thermal eddies to be smeared out.

That changing Prandtl number does not greatly change the shape of the $K^{\oplus}$ curves is shown in Fig. 6, where the ordinates of Fig. 5 have been normalized by division by the absolute value of $[K^{\oplus}t^{\oplus 11/2}]_{\min}$ and the abscissas normalized by division by the value of $\kappa^{\oplus}$ yielding zero ordinate. Thus it would appear that the basic nature of the convective transfer is unaltered by a change in the Prandtl number.

In Figs. 7(a), (b) and (c) curves are presented for the dimensionless spectral function $G^{\oplus}$, as obtained from equation (48). With increasing time the curves approach the final period curve, shown as a dotted line. Physically the $G^{\oplus}$ curves represent the distribution of the total thermal "energy" $\overline{T^2}$ among thermal "eddies" of size $\sim 1/\kappa^{\oplus}$.

Since, as a first approximation theory, the theory presented here is restricted to not-too-

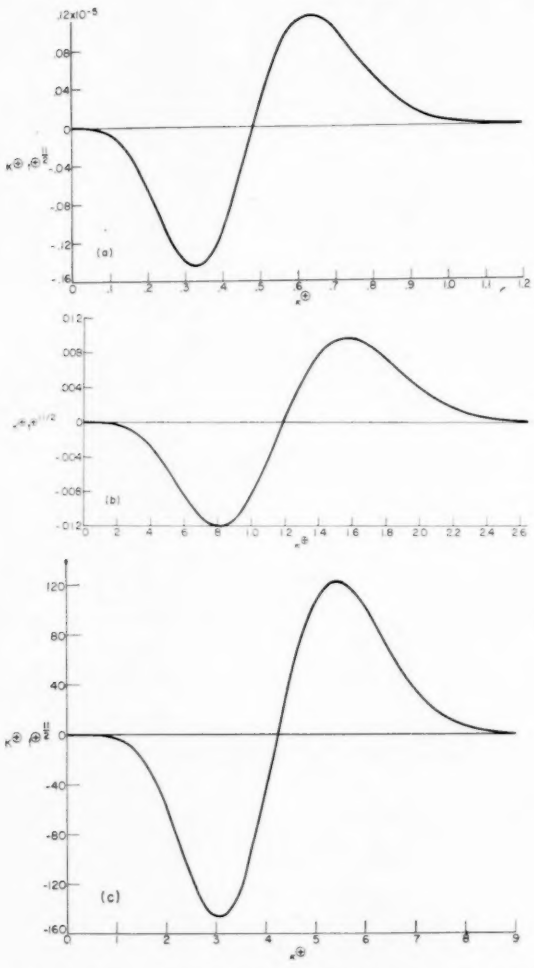

FIG. 5. Variation of $K^{\oplus}t^{\oplus 11/2}$ with wave number. (a) $Pr = 0{\cdot}1$. (b) $Pr = 0{\cdot}72$. (c) $Pr = 10$.

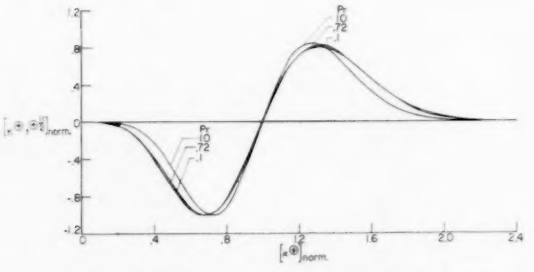

FIG. 6. Same results as in Fig. 5, but with ordinate and abscissa normalized.

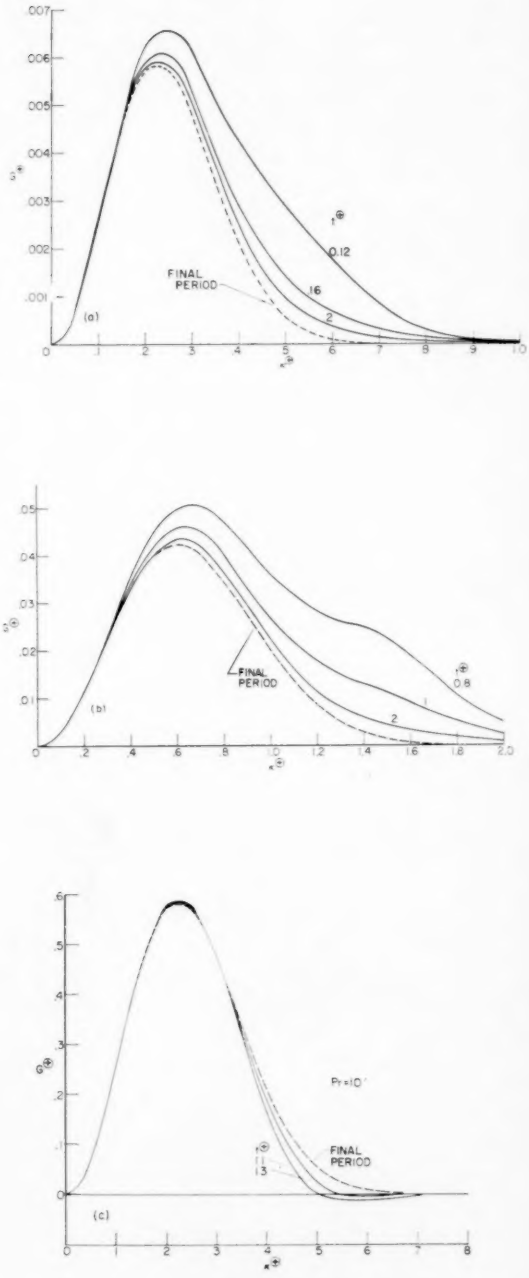

FIG. 7. Dimensionless spectral energy function $G^{\oplus}$ as a function of wave number and time. (a) $Pr = 0{\cdot}1$. (b) $Pr = 0{\cdot}72$. (c) $Pr = 10$.

Vol. 1 1960

large convection/conduction ratios and since (for a given Reynolds number) increasing Prandtl number signifies an increasing value of this ratio, it might be expected that the theory would apply less well for higher values of Prandtl number. Figs. 7(a), (b) and (c) indicate that this is apparently the case: the curves for $Pr = 0{\cdot}1$ are quite smooth, those for $Pr = 0{\cdot}72$ and small values of $t^{\oplus}$ are a little less smooth and for $Pr = 10$ the spectral curves begin to go negative at the smaller values of $t^{\oplus}$.

The reason that the final period curve is approached from below for large $\kappa^{\oplus}$ in Fig. 7(c) is that at such high values of Prandtl number the transfer term supplies thermal "energy" to the high $\kappa^{\oplus}$ range faster than it can be dissipated—hence $[\partial G^{\oplus}/\partial t^{\oplus}]_{\kappa^{\oplus}}$ is positive instead of negative as with the lower Prandtl numbers.

If equation (33) is integrated with respect to κ from 0 to ∞ and use is made of equations (35) and (42), the resulting equation is

$$-\frac{\partial(\overline{T^2}/2)}{\partial t} = \frac{2\nu}{Pr}\int_0^{\infty} \kappa^2 G \, \mathrm{d}\kappa$$

This equation points out the interesting fact that for a given viscosity and temperature fluctuation spectrum the decay rate is inversely proportional to the Prandtl number. The results of this analysis, however, are not comparable on this basis since the manner in which the initial conditions were imposed (equation (31)) precludes comparing two different Prandtl number fluids with the same spectral curve. However, the results of this analysis do show that the decay rate decreases relative to the final period rate with increasing Prandtl number, as can be seen from Figs. 8(a), (b), and (c), where equation (49) has been plotted for values of Prandtl number of 0·1, 0·72 and 10. The rates of decay for $Pr = 0{\cdot}1$ and 0·72 are greater than that predicted by the final period law (dotted line) while that for $Pr = 10$ is less than the final period rate. The Prandtl number function R of equation (49) changes from positive to negative at $Pr = 4{\cdot}7717$ for which $R = 0$ and the decay rate is exactly that for the final period. Although the decay rate for $Pr = 4{\cdot}7717$ is described by the final period equation, the spectral curves are not of the final period shape (except for the final

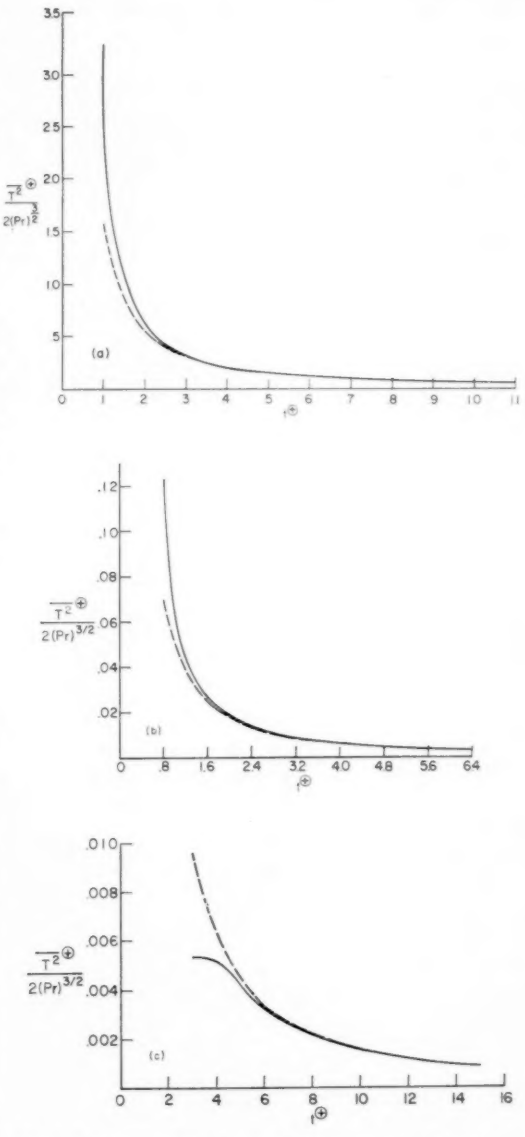

FIG. 8. Dimensionless square of temperature fluctuation as a function of time. ——— Equation (49). — — — — Final period. (a) $Pr = 0{\cdot}1$. (b) $Pr = 0{\cdot}72$. (c) $Pr = 10$.

period). It just happens that each of the spectral curves for this value of Prandtl number lies partly above and partly below the final period curve in such a way that the integral for $\overline{T^2}/2$

indicated by equation (42) is equal to the final period value.

Corrsin [1] has previously pointed out that for the final period, as well as for self-preserving and inertial spectrums at very large Reynolds and Peclet numbers, temperature fluctuations die out more slowly than velocity fluctuations. This analysis indicates that the same is true for times before the final period, as can be seen by comparison of equation (43) for $\overline{T^2}$ with the analogous equation for $\overline{u^2}$ (equation (38) of [3]).

CONCLUSIONS

The principal conclusions to be drawn from the present work appear to be the following:

(1) It was possible to represent the available experimental temperature fluctuation decay data by means of the present theory.

(2) For times before as well as during the final period, the temperature fluctuations decay more slowly than do the velocity fluctuations.

(3) The general effect of increasing Prandtl number is to extend the spectral function to larger wave numbers and to reduce the rate of decay of the temperature fluctuations.

REFERENCES

1. S. Corrsin, *J. Appl. Phys.* **22**, 469–473 (1951).
2. S. Corrsin, *J. Aero. Sci.* **18**, 417–423 (1951).
3. R. G. Deissler, *Phys. Fluids* **1**, 111–121 (1958).
4. R. G. Deissler, *Phys. Fluids* **3**, 176–187 (1960).
5. W. L. Miller and A. R. Gordon, *J. Phys. Chem.* **35**, 2785–2884 (1931).
6. R. R. Mills, Jr., A. L. Kistler, V. O'Brien and S. Corrsin, *Turbulence and Temperature Fluctuations Behind a Heated Grid.* NACA TN 4288 (1958).
7. Yoshimitsu Ogura, *J. Meteorol.* **15**, 539–546 (1958).
8. A. M. Obukhoff, *Izv. Akad. Nauk. SSSR, ser. geogr. i geofiz.* **13**, 58 (1949).
9. G. K. Batchelor, *J. Fluid Mech.* **5**, 1, 113–133 (1959).
10. G. K. Batchelor, I. D. Howells and A. A. Townsend, *J. Fluid Mech.* **5**, 1, 134–139 (1959).

Vol. 1 1960

Int. J. Heat Mass Transfer. Vol. 1, pp. 325–335. Pergamon Press 1961. Printed in Great Britain.

AN ANALYSIS OF LAMINAR FILM BOILING WITH VARIABLE PROPERTIES

P. W. McFADDEN* and R. J. GROSH†
Purdue University, Lafayette, Indiana, U.S.A.

(*Received* 16 *July* 1959)

Abstract—An analysis is made of stable, laminar, free convection, film boiling from isothermal vertical plates and horizontal cylinders surrounded by a saturated liquid. The mathematical techniques of boundary-layer theory are used and the boundary-layer equations are reduced to ordinary differential equations by means of a transformation similar to that used in free convection and condensation. The equations are solved for compressible flow with variable specific heat. Numerical results are presented for near critical water at 2800 and 3100 Lb/in² with wall-to-liquid temperature differences of 250, 500 and 1000°F. Results for heat transfer, velocity distribution and temperature distribution are included and compared to solutions obtained by assuming constant properties.

Résumé—Une analyse est faite du film laminaire, de convection libre en régime stable et à l'ébullition sur des plaques isothermes verticales et des cylindres horizontaux recouverts d'un liquide saturé. Les techniques mathématiques de la théorie de la couche limite sont utilisées et les équations de la couche limite sont réduites à des équations différentielles ordinaires grâce à une transformation analogue à celle utilisée pour la convection libre et la condensation. Les équations sont résolues pour un écoulement compressible avec chaleur spécifique variable. Des résultats numériques sont présentés pour l'eau au voisinage du point critique à 2800 et 3100 lb/in² avec des différences de température entre paroi et liquide de 250, 500, 1000°F. Des résultats sur le transfert de chaleur, la distribuiton des vitesses et des températures sont également donnés et comparés aux solutions obtenues en supposant les propriétés physiques constantes.

Zusammenfassung—Es wird das stabile laminare Filmsieden bei freier Konvektion an einer isothermen senkrechten Wand oder an horizontalen Zylindern, die von gesättigter Flüssigkeit umgeben sind, untersucht. Hierzu werden die Methoden der Grenzschichttheorie angewendet und die Grenzschichtgleichungen in gewöhnliche Differentialgleichungen umgewandelt mit Hilfe einer Transformation, die ähnlich der für freie Konvektion und Kondensation ist. Die Gleichungen werden für kompressible Flüssigkeit mit veränderlicher spezifischer Wärme gelöst. Numerische Ergebnisse werden für Wasser in der Nähe des kritischen Punktes bei 193 und 214 bar mitgeteilt und bei Temperaturdifferenzen zwischen Wand und Flüssigkeit von 139, 278 und 555 grd. Ferner werden die Ergebnisse für den Wärmeübergang, die Geschwindigkeitsverteilung und die Temperaturverteilung angegeben und diese mit den Lösungen für konstante Stoffwerte verglichen.

Аннотация—Даётся анализ устойчивого ламинарного плёночного кипения в условиях свободной конвекции на изотермических вертикальных пластинах и горизонтальных цилиндрах, окруженных насыщенной жидкостью. Используется математический аппарат теории пограничного слоя, а уравнения пограничного сдоя сводятся к обычным дифференциальным уравнениям путём преобразований, аналогичных преобразованиям, применяемым в задачах свободной конвекции и конденсации. Уравнения решаются для сжимаемого потока с переменной удельной теплоёмкостью. Приводятся численные результаты для около критического состояния воды при давлениях, равных 2800 и 3100 фунт/кв. дюйм. и разностях температур между стенкой и жидкостью в 250, 500 и 1000°F. Приведены также результаты по теплообмену, распределению скоростей и температур в сравнении с решениями, полученными в предположении постоянства характеристик.

* Instructor, School of Mechanical Engineering. Purdue University.
† Professor of Mechanical Engineering. Purdue University, Lafayette, Indiana.

NOMENCLATURE

a, b, c, d = dimensionless constants;
c_1 = dimensional constant, $\left[\frac{g(\rho_L - \rho_{sat})\rho_{sat}}{4\mu^2 g_0^2}\right]^{1/4}, \frac{1}{ft^{3/4}}$;
c_2 = dimensionless constant, $\left[\frac{r^3 g(\rho_L - \rho_{sat})\rho_{sat}}{\mu^2 g_0^2}\right]^{1/4}$;
c_p = constant pressure specific heat (B.t.u./lb °F);*
f = function of β defined by equation (27);
g, $\mathbf{g}$ = acceleration or acceleration vector due to gravity, $4{\cdot}17 \times 10^8$ft/hr^2;
g_0 = dimensional constant, $4{\cdot}17 \times 10^8$ftlb/Lb hr^2;
$\mathbf{G}$ = body force per unit volume (Lb/ft^3);*
$\bar{h}$ = function of β defined by equation (27);
h_{fg} = enthalpy of evaporation (B.t.u./lb);
h = local convection heat transfer coefficient (B.t.u./ft^2 hr °F);
k = thermal conductivity (B.t.u./ft hr °F);
L = length of vertical plate (ft);
$N_{Nu,\lambda}$ = Nusselt number based on length λ;
N_{pr} = Prandtl number
p = function of ξ, dimensionless;
P = pressure (Lb/ft^2);
q = local heat transfer rate (B.t.u./hr ft^2);
q''' = heat generation per unit volume (B.t.u./ft^{3}hr);
Q = total heat transferred (B.t.u./hr);
r = cylinder radius (ft);
T = temperature (°F);
T_{sat} = saturation temperature (°F);
T_w = wall temperature (°F);
t = dimensionless temperature defined by equation (27);
u = velocity component in the x-direction (ft/hr);
v = velocity component in the y-direction (ft/hr);
$\mathbf{V}$ = velocity vector (ft/hr);
x = co-ordinate along surface (ft);
y = co-ordinate normal to surface (ft);
β = angular co-ordinate (rad);
δ = thickness of vapor film (ft);
ζ = dimensionless function defined by equation (16);
η = dimensionless independent variable $c_1 y/x^{1/4}$.
θ = dimensionless temperature, $(T - T_{sat})/(T_w - T_{sat})$;
Θ = $(T_w - T_{sat})$ (°F);
μ = viscosity (Lb hr/ft^2);
ξ = dimensionless independent variable defined by equation (27):
ρ = vapor density (lb/ft^3);
ρ_L = liquid density (lb/ft^3);
ρ_{sat} = saturated vapor density (lb/ft^3):
τ = time (hr);
ϕ = dimensionless independent variable, $c_2 y/r$;
ψ = stream function (ft^2/hr);
Ψ = dimensionless stream function defined by equation (24);
∇ = vector operator used for, say, the gradient of a scalar;
∇^2 = Laplace operator.

Subscripts

cp = constant properties;
vp = vertical plate;
c = horizontal cylinder;
x = x-direction.

* The abbreviation for the pound mass is lb, and for pound force is Lb throughout the paper.

INTRODUCTION

ALTHOUGH the first observation of the phenomenon of film boiling was made in 1746, an analytical treatment was not suggested until almost two centuries later. In 1941, Colburn [1] suggested that Nusselt's [2] theory on laminar film condensation could be modified for the case of laminar film boiling. In 1950, Bromley [3] presented a model for the case of stable laminar film boiling on the outside of a horizontal cylinder. By assuming an isothermal wall, a saturated liquid, pure conduction heat transfer across the film and by neglecting inertia in the vapor layer, he derived an expression for the convection coefficient. The free convection heat

Vol. 1 1960

transfer was expressed in terms of a Nusselt number as

$$N_{\mathrm{Nu},D} = c\left[\frac{g(\rho_L - \rho)\,\rho D^3 h_{fg}}{k\mu g_0 \Theta}\right]^{1/4} \tag{1}$$

where the properties were evaluated at an average temperature. The constant c depended upon the boundary conditions at the interface. For zero velocity at the interface c was 0·512, for zero shear stress at the interface c was 0·724. This latter condition is the boundary condition considered in the case of laminar film condensation, the former is usually associated with film boiling. This gives the extremes between which the actual case lies in film boiling and also indicates how liquid movement can influence the results.

In 1952, Bromley [4] modified the theory to take into account the superheating of the vapor film. Cess [5] arrived at an expression similar to equation (1) by assuming a temperature profile in the vapor layer and by considering the effect of the liquid–vapor interfacial shear stress. Chang [6] has presented a wave theory for film boiling. In 1958, Sparrow and Gregg [7] proposed an exact analysis of laminar film condensation with constant properties which is similar to that used in the present paper for laminar film boiling. Both investigations were performed independently of each other.

In the theory presented to date for stable, laminar film boiling on isothermal surfaces, no attempt has been made to consider variable properties. In this paper the writers will show how the severe variations of specific heat and density with temperature near the critical pressure can be exactly considered by treating film boiling with boundary-layer theory. The complete boundary-layer equations will be solved, and the results obtained will be compared with the approximate theories available. Radiation will not be considered in order to investigate only the variable property effects on convection.

FUNDAMENTAL EQUATIONS

The fundamental equations which express the laws of conservation for mass, momentum and energy for stable, laminar, free convection, film boiling were written as follows:

$$\frac{\partial \rho}{\partial \tau} + \nabla(\rho \mathbf{V}) = 0 \tag{2}$$

$$\frac{\rho}{g_0}\frac{\mathrm{d}\mathbf{V}}{\mathrm{d}\tau} = \mu\nabla^2\mathbf{V} - \nabla P + \mathbf{G} + \frac{\mu}{3}\nabla(\nabla \cdot \mathbf{V}) \tag{3}$$

$$\rho c_p \frac{\mathrm{d}T}{\mathrm{d}\tau} = k\nabla^2 T + q''' \tag{4}$$

Equations (2) through (4) were valid for compressible flow with variable specific heat. Viscosity and thermal conductivity were assumed constant since their variation was one-half order of magnitude, or more, less than the variation in density and specific heat for the situations considered in this paper.

In order to solve these equations, some additional assumptions were necessary. Only steady, two-dimensional boundary-layer flow was considered as shown in Fig. 1A; thus equations (2) through (4) became

$$\frac{\partial(\rho u)}{\partial x} + \frac{\partial(\rho v)}{\partial y} = 0 \tag{5}$$

$$\frac{\rho}{g_0}\left(u\frac{\partial u}{\partial x} + v\frac{\partial u}{\partial y}\right) = u\frac{\partial^2 u}{\partial y^2} - [\nabla P]_x + [\mathbf{G}]_x \tag{6}$$

$$\rho c_p\left(u\frac{\partial T}{\partial x} + v\frac{\partial T}{\partial y}\right) = k\frac{\partial^2 T}{\partial y^2} \tag{7}$$

where the heat generation per unit volume was assumed to be zero. Schlichting [8] shows that these equations are also valid for the case of a cylinder, as shown in Fig. 1B, if the boundary layer thickness is small compared to the cylinder radius.

An isothermal wall was assumed as well as a saturated liquid which was everywhere at rest; thus, the boundary conditions for the above equations became

$$\left.\begin{aligned} u = v = 0,\ T = T_w \qquad & y = 0 \\ u = 0,\ T = T_{\mathrm{sat}} \qquad & y = \delta \end{aligned}\right\} \tag{8}$$

An additional condition was required because the film thickness δ was not known *a priori*. This was obtained by noting that all the heat transferred by conduction at the liquid–vapor interface was used to vaporize liquid; that is

$$q = \rho_{\mathrm{sat}}\, h_{fg}\, v = -k\frac{\partial T}{\partial y} \qquad y = \delta \tag{9}$$

Equations (5) through (7) with conditions given by equations (8) and (9) are the simplified equations which were solved for the case of film boiling from a vertical plate and a horizontal cylinder.

The first step in the solution of equations (5) through (9) was the introduction of a stream function; that is

$$\rho u = \rho_{\text{sat}} \frac{\partial \psi}{\partial y}, \quad \rho v = -\rho_{\text{sat}} \frac{\partial \psi}{\partial x} \tag{10}$$

This substitution eliminated equation (5) and equations (6) and (7) became

$$\left.\begin{aligned} &\frac{\partial \psi}{\partial y}\frac{\partial^2 \psi}{\partial x \partial y} - \frac{\partial \psi}{\partial x}\frac{\partial^2 \psi}{\partial y^2} - \frac{\rho g_0}{\rho^2_{\text{sat}}}\{[\nabla P]_x - [\mathbf{G}]_x\} \\ &\quad - \frac{\mu g_0}{\rho_{\text{sat}}}\frac{\partial^3 \psi}{\partial y^3} \\ &\quad = \frac{1}{\rho}\frac{\partial \rho}{\partial x}\left(\frac{\partial \psi}{\partial y}\right)^2 - \frac{1}{\rho}\frac{\partial \psi}{\partial x}\frac{\partial \psi}{\partial y}\frac{\partial \rho}{\partial y} \\ &\quad - \frac{2\mu g_0}{\rho\,\rho_{\text{sat}}}\frac{\partial \rho}{\partial y}\frac{\partial^2 \psi}{\partial y^2} \\ &\quad - \frac{\mu g_0}{\rho \rho_{\text{sat}}}\frac{\partial \psi}{\partial y}\left\{\frac{\partial^2 \rho}{\partial y^2} - \frac{2}{\rho}\left(\frac{\partial \rho}{\partial y}\right)^2\right\} \end{aligned}\right\} \tag{11}$$

and

$$\frac{\partial \psi}{\partial y}\frac{\partial T}{\partial x} - \frac{\partial \psi}{\partial x}\frac{\partial T}{\partial y} = \frac{k}{\rho_{\text{sat}} c_p}\frac{\partial^2 T}{\partial y^2} \tag{12}$$

The boundary conditions in equation (8) became

$$\left.\begin{aligned} &\frac{\partial \psi}{\partial y} = \frac{\partial \psi}{\partial x} = 0,\ T = T_w && y = 0 \\ &\frac{\partial \psi}{\partial y} = 0,\ T = T_{\text{sat}},\ \frac{\partial T}{\partial y} = \frac{h_{fg}}{k}\rho_{\text{sat}}\frac{\partial \psi}{\partial x}, && y = \delta \end{aligned}\right\} \tag{13}$$

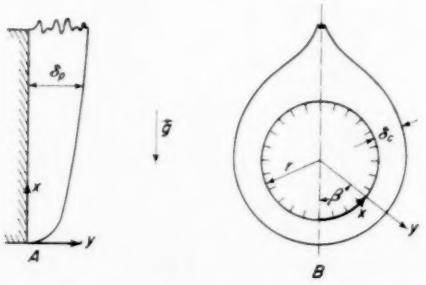

FIG. 1. Physical model and co-ordinate system for: A, plane wall and B, horizontal cylinder

It remained to reduce these to ordinary differential equations to facilitate solution.

REDUCTION OF EQUATIONS

Equations (11), (12) and (13) were simplified by expressing the pressure gradient and body force in terms of specific weights and by introducing a similarity transformation which reduced the partial to ordinary differential equations. These steps will now be described.

Plane vertical wall

The pressure gradient in the x-direction was the hydrostatic pressure gradient

$$[\nabla P]_x = -\frac{g}{g_0}\rho_L \tag{14}$$

and body force in the x-direction was the gravity force on the vapor,

$$[\mathbf{G}]_x = -\frac{g}{g_0}\rho \tag{15}$$

The sum of the pressure gradient and body force

$$\frac{g(\rho_L - \rho)}{g_0}$$

gave the bouyant force. By introducing a similarity transformation, equations (11) and (12) were made ordinary. To this end

$$\left.\begin{aligned} \eta &= c_1 \frac{y}{x^{1/4}} \\ \psi &= 4\frac{\mu g_0}{\rho_{\text{sat}}} c_1 x^{3/4}\zeta(\eta) \end{aligned}\right\} \tag{16}$$

where

$$c_1 = \left[\frac{g(\rho_L - \rho_{\text{sat}})\,\rho_{\text{sat}}}{4\mu^2 g_0^2}\right]^{1/4} \tag{17}$$

were introduced where η was a new independent variable. Also, at a given pressure, density was a function only of temperature thus

$$\frac{\partial \rho}{\partial x} = \frac{d\rho}{dT}\frac{\partial T}{\partial x}, \quad \frac{\partial \rho}{\partial y} = \frac{d\rho}{dT}\frac{\partial T}{\partial y} \tag{18}$$

Introducing the above in equations (11) and (12) there resulted

Vol. 1 1960

$$\left.\begin{aligned}\zeta''' + 3\zeta\zeta'' - 2(\zeta')^2 + \frac{(\rho_L - \rho)\,\rho}{(\rho_L - \rho_{sat})\,\rho_{sat}} = \\ = \frac{1}{\rho}\frac{d\rho}{d\theta}\theta'[3\zeta\zeta' + 2\zeta''] + \\ + \frac{1}{\rho}\zeta'(\theta')^2\left[\frac{d^2\rho}{d\theta^2} - \frac{2}{\rho}\left(\frac{d\rho}{d\theta}\right)^2\right] + \frac{1}{\rho}\frac{d\rho}{d\theta}\zeta'\theta''\end{aligned}\right\} \quad (19)$$

$$\theta'' + 3\frac{\mu g_0}{k} c_p \zeta\theta' = 0 \quad (20)$$

where the primes on ζ and θ represent differentiation with respect to η. The boundary conditions on this set of equations were obtained from equations (9) and (13) as:

$$\left.\begin{aligned}\zeta = \zeta' = 0,\ \theta = 1 \qquad \eta = 0 \\ \zeta' = 0,\ \theta = 0,\ \theta' = -3\frac{\mu g_0}{k}\frac{h_{fg}}{\Theta}\zeta \quad \eta = \eta_\delta\end{aligned}\right\} \quad (21)$$

The simultaneous solution of equations (19) and (20) with the boundary conditions above, completely described the temperature and velocity distributions and also the heat transfer for stable, laminar free convection film boiling where radiation is not important.

It should be noted that the results for the vertical plate can also be applied to the vertical cylinder if δ/r is less than 0·03. This should introduce an error of about 1 per cent in the film thickness according to Greenburg [9].

Horizontal cylinder

The pressure gradient in the x-direction was the hydrostatic pressure gradient again

$$[\nabla P]_x = -\frac{g}{g_0}\rho_L \sin\frac{x}{r} \quad (22)$$

and the body force in the x-direction

$$[G]_x = -\frac{g}{g_0}\rho \sin\frac{x}{r} \quad (23)$$

was the gravity force on the vapor.

The first step in reducing equations (11) and (12) to ordinary differential equations was to introduce the following

$$\left.\begin{aligned}\beta &= \frac{x}{r} \\ \phi &= c_2\frac{y}{r} \\ \Psi &= \frac{\psi}{c_2}\frac{\rho_{sat}}{\mu g_0} \\ c_2 &= \left[\frac{r^3 g(\rho_L - \rho_{sat})\,\rho_{sat}}{\mu^2 g_0^2}\right]^{1/4}\end{aligned}\right\} \quad (24)$$

In this way, equations (11) and (12) became

$$\left.\begin{aligned}\frac{\partial\Psi}{\partial\phi}\frac{\partial^2\Psi}{\partial\beta\partial\phi} - \frac{\partial\Psi}{\partial\beta}\frac{\partial^2\Psi}{\partial\phi^2} - \\ \frac{(\rho_L - \rho)\,\rho}{(\rho_L - \rho_{sat})\,\rho_{sat}}\sin\beta - \frac{\partial^3\Psi}{\partial\phi^3} \\ = \frac{1}{\rho}\left(\frac{\partial\Psi}{\partial\phi}\right)^2\frac{\partial\rho}{\partial\beta} - \frac{1}{\rho}\frac{\partial\Psi}{\partial\phi}\frac{\partial\Psi}{\partial\beta}\frac{\partial\rho}{\partial\phi} \\ - \frac{2}{\rho}\frac{\partial\rho}{\partial\phi}\frac{\partial^2\Psi}{\partial\phi^2} \\ - \frac{1}{\rho}\frac{\partial\Psi}{\partial\phi}\left[\frac{\partial^2\rho}{\partial\phi^2} - \frac{2}{\rho}\left(\frac{\partial\rho}{\partial\phi}\right)^2\right]\end{aligned}\right\} \quad (25)$$

$$\frac{\partial\Psi}{\partial\phi}\frac{\partial\theta}{\partial\beta} - \frac{\partial\Psi}{\partial\beta}\frac{\partial\theta}{\partial\phi} = \frac{k}{\mu g_0 c_p}\frac{\partial^2\theta}{\partial\phi^2} \quad (26)$$

To simplify these, the following substitutions were used

$$\left.\begin{aligned}\xi &= \phi\,\hbar(\beta) \\ \Psi(\beta,\phi) &= p(\xi)\,f(\beta) \\ \theta(\beta,\phi) &= t(\xi)\end{aligned}\right\} \quad (27)$$

and then equations (25) and (26) became

$$\left.\begin{aligned}p'''\{f\hbar^3\} + pp''\{ff'\hbar^2\} - (p')^2\{f^2\hbar'\hbar + \\ + \hbar^2 f'f\} + \frac{(\rho_L - \rho)\,\rho}{(\rho_L - \rho_{sat})\,\rho_{sat}}\sin\beta = \\ = \frac{1}{\rho}\frac{\partial\rho}{\rho\xi}\{\hbar^2 f'fpp' + 2\hbar^3 fp''\} + \\ + \left[\frac{\partial^2\rho}{\partial\xi^2} - \frac{2}{\rho}\left(\frac{\partial\rho}{\partial\xi}\right)^2\right]\frac{1}{\rho}\hbar^3 fp'\end{aligned}\right\} \quad (28)$$

and

$$t''\hbar + \frac{\mu g_0}{k} c_p\, pt'f' = 0 \quad (29)$$

where primes on t and p represent differentiation with respect to ξ and primes on f and h represent differentiation with respect to β. Now, when

$$\left.\begin{aligned} f'(\beta) &= a\hbar(\beta) \\ f^2(\beta)\hbar(\beta)\hbar'(\beta) &= b\sin\beta \\ f(\beta)\hbar^2(\beta)f'(\beta) &= c\sin\beta \\ f(\beta)\hbar^3(\beta) &= d\sin\beta \end{aligned}\right\} \quad (30)$$

equations (28) and (29) could be written as

$$\left.\begin{aligned} &p'''d + pp''c - (p')^2\{b + c\} + \\ &+ \frac{(\rho_L - \rho)\,\rho}{(\rho_L - \rho_{sat})\,\rho_{sat}} = \\ &= \frac{1}{\rho}\frac{\partial\rho}{\partial\xi}\{cpp' + 2p''d\} + \\ &+ \frac{1}{\rho}p'd\left[\frac{\partial^2\rho}{\partial\xi^2} - \frac{2}{\rho}\left(\frac{\partial\rho}{\partial\xi}\right)^2\right] \end{aligned}\right\} \quad (31)$$

$$t'' + a\frac{\mu g_0}{k}c_p\,pt' = 0 \quad (32)$$

Fortunately, equations (30) were solved by Hermann [10] who gives graphs of $\hbar$ and $f\hbar$ vs. β, and values for the constants as follows: $a = 3$, $b = -1$, $c = 3$ and $d = 1$.

Finally, using values for the constants a through d, equations (31) and (32) became

$$\left.\begin{aligned} &p''' + 3pp'' - 2(p')^2 + \frac{(\rho_L - \rho)\,\rho}{(\rho_L - \rho_{sat})\,\rho_{sat}} = \\ &= \frac{1}{\rho}\frac{\mathrm{d}\rho}{\mathrm{d}t}t'[3pp' + 2p''] + \frac{1}{\rho}p'\frac{\mathrm{d}\rho}{\mathrm{d}t}t'' + \\ &+ \frac{1}{\rho}p'(t')^2\left[\frac{\mathrm{d}^2\rho}{\mathrm{d}t^2} - \frac{2}{\rho}\left(\frac{d\rho}{dt}\right)^2\right] \end{aligned}\right\} \quad (33)$$

$$t'' + 3\frac{\mu g_0}{k}c_p\,pt' = 0 \quad (34)$$

The boundary conditions on equations (33) and (34) were

$$\left.\begin{aligned} &p = p' = 0,\ t = 1 && \xi = 0 \\ &p' = 0,\ t = 0,\ t' = -3\frac{\mu g_0}{k}\frac{h_{fg}}{\Theta}p && \xi = \xi_\delta \end{aligned}\right\} \quad (35)$$

Thus it is seen that these are the same differential equations and boundary conditions which were set up for the case of the flat plate.

Relation between heat transfer on cylinder and on plate

Since the reduced differential equations were the same for the plate and cylinder, it was expected that the heat transfer for each was related.

For the vertical plate the local wall heat transfer could be expressed as

$$q_w = -k\left(\frac{\partial T}{\partial y}\right)_w = -k\,\Theta\,c_1x^{-1/4}\left(\frac{\mathrm{d}\theta}{\mathrm{d}\eta}\right)_w = \\ = -h_{vp}\Theta \quad (36)$$

and an average heat-transfer coefficient was found by integrating the local coefficient over the entire plate. Thus

$$(h_{vp})_{avg} = \frac{1}{\Theta L}\int_0^L k\,\Theta\,c_1\left(\frac{\mathrm{d}\theta}{\mathrm{d}\eta}\right)_w x^{-1/4}\,\mathrm{d}x = \\ = k\,c_1\left(\frac{\mathrm{d}\theta}{\mathrm{d}\eta}\right)_w\frac{4}{3L^{1/4}} \quad (37)$$

The heat transfer may also be expressed in terms of an average Nusselt number as

$$N_{Nu,L} = \frac{4}{3}L^{3/4}c_1\left(\frac{\mathrm{d}\theta}{\mathrm{d}\eta}\right)_w \quad (38)$$

We now consider the horizontal cylinder. In the case of the horizontal cylinder the wall heat flux could be expressed as

$$q_w = -k\left(\frac{\partial T}{\partial y}\right)_w = -k\Theta\frac{c_2}{r}\left(\frac{\partial\theta}{\partial\phi}\right)_w \\ = -k\,\Theta\frac{c_2}{r}\hbar(\beta)\left(\frac{\mathrm{d}t}{\mathrm{d}\xi}\right)_w = -h_c\,\Theta \quad (39)$$

and an average heat-transfer coefficient was found by integrating the local coefficient over the entire cylinder. Thus

$$(h_c)_{avg} = \frac{1}{\Theta\pi}\int_0^\pi k\Theta\frac{c_2}{r}\left(\frac{\mathrm{d}t}{\mathrm{d}\xi}\right)_w\hbar(\beta)\,\mathrm{d}\beta \\ = \frac{(1{\cdot}91)k\,c_2}{\pi r}\left(\frac{\mathrm{d}t}{\mathrm{d}\xi}\right)_w \quad (40)$$

which followed from Hermann's [10] graphical integration where

$$\int_0^\pi\hbar(\beta)\,\mathrm{d}\beta = 1{\cdot}91 \quad (41)$$

Vol. 1 1960

The heat transfer was expressed in terms of an average Nusselt number as

$$N_{Nu,D} = 1{\cdot}025\, c_2 \left(\frac{dt}{d\xi}\right)_w \tag{42}$$

The similarity between equations (38) and (42) is now apparent.

For a given fluid surrounding a plate or cylinder at the same pressure and with the same wall to fluid temperature difference it followed that

$$\left(\frac{d\theta}{d\eta}\right)_w = \left(\frac{dt}{d\xi}\right)_w \tag{43}$$

Therefore, for identical characteristic lengths

$$\frac{(h_c)_{avg}}{(h_{vp})_{avg}} = 0{\cdot}77 \tag{44}$$

and

$$\frac{Q_c}{Q_{vp}} = 2{\cdot}42 \tag{45}$$

Thus, once the vertical flat plate problem was solved, heat transfer results were transferred directly to the horizontal cylinder or vice versa.

SOLUTION OF EQUATIONS

The reduced differential equations for the plate and cylinder, equations (19) and (20) were identical. They were solved numerically by the Runge–Kutta [11] method on a Datatron 204 digital computer for the cases where: (a) properties were constant, (b) specific heat and bouyant force were variable, and (c) specific heat and density were variable. Equations for the two former cases were easily derived from equations (19) and (20). The calculations were performed for water at two different pressure levels, 2800 and 3100 lb/in². The critical pressure for water is thought to be slightly above 3200 lb/in².

The increments in the independent variable used in the Runge–Kutta method were 0·01 and 0·05 at the low- and high-pressure levels, respectively. It was observed that decreasing the interval from 0·1 to 0·01 changed the results for θ' at η equal to zero by less than 5 per cent.

Initial conditions on velocity and temperature and their derivatives with respect to η were required for the computer. Since the boundary conditions in this problem were mixed, that is, three were given at η equal to zero and three at η_δ, as indicated in equation (21), it was necessary to estimate ζ'' and θ' initially. The initial estimate was then refined until ζ' and θ went to zero at η equal to η_δ and at the same time equation (21) was satisfied. It was considered adequate to satisfy the last of equations (21) within ± 5 per cent; since, this introduced at most an error of from 1 to 2 per cent in θ' at η equal to zero.

Variable properties and their first and second derivatives with respect to temperature were tabulated and stored in the computer for each 0·01 interval of the dimensionless temperature excess. A linear interpolation was used for values between those stored.

Saturation and density data were obtained from Keenan and Keyes [12]. For densities at temperatures higher than the tabulated values, the data from Keenan and Keyes was faired into the ideal-gas equation of state. This would introduce at most an error of about 3 per cent excluding the inaccuracy of values in the table to which values were faired. Values for $d\rho/d\theta$ and $d^2\rho/d\theta^2$ were obtained numerically from a plot of ρ vs. θ. Values of $d\rho/d\theta$ and $d^2\rho/d\theta^2$ at $\theta = 0{\cdot}00$ and $\theta = 1{\cdot}00$ were extrapolated. Numerical evaluation such as this was not highly accurate, but gave a good approximation. The specific heat was also taken from Keenan and Keyes [12], and data for temperatures beyond those given in the reference were extrapolated according to the curves given in the reference. The viscosity and thermal conductivity were taken from Dsrjinskogo [13], and data for temperatures beyond those listed in the tables were extrapolated according to the curves given in the reference. At all times, interpolations between given points were taken linearly. In those cases where properties were considered constant they were evaluated at the arithmetic mean wall and saturation temperature.

RESULTS

The effects of considering variable properties at pressures approaching the critical pressure were illustrated by the results obtained from the solution of equations (19) and (20) for the three specified cases. The significant results are presented in Table 1. Table 2 presents a comparison of results obtained considering: (1) all

Table 1. *Significant results*

		Compressible			Incompressible			All properties constant				
P (lb/in^2)	Θ (°F)	η_δ	$\zeta'_{\max}$	$\left(\frac{d\theta}{d\eta}\right)_w$	η_δ	$\zeta'_{\max}$	$\left(\frac{d\theta}{d\eta}\right)_w$	$\frac{c_p\Theta}{h_{fg}}$	N_{Pr}	η_δ	$\zeta'_{\max}$	$\left(\frac{d\theta}{d\eta}\right)_w$
2800	250	1·39	0·17	0·76	0·96	0·25	1·14	0·92	1·26	1·27	0·181	0·88
	500	1·64	0·19	0·67	1·04	0·35	1·09	1·32	1·0	1·43	0·233	0·79
	1000	1·84	0·21	0·62	1·14	0·47	1·04	2·3	0·90	1·60	0·285	0·73
3100	250	2·35	0·093	0·48				1·8	1·45	1·37	0·214	0·84
	500	2·83	0·103	0·41				2·3	1·0	1·56	0·271	0·75
	1000	3·15	0·113	0·39				3·8	0·88	1·69	0·302	0·71

properties constant; (2) variable specific heat with density variations considered only in the evaluation of the bouyant force, and (3) compressible flow with variable specific heat. The comparisons of heat transfer, maximum velocity and film thickness were made according to the following. Since

$$q = -k\frac{\partial T}{\partial y} = -k\Theta c_1 x^{-1/4}\frac{\mathrm{d}\theta}{\mathrm{d}\eta} \tag{46}$$

for the same wall to liquid temperature difference and the same value of x,

$$\frac{q}{q_{cp}} = \frac{\{c_1(\mathrm{d}\theta/\mathrm{d}\eta)\}}{\{c(\mathrm{d}\theta/\mathrm{d}\eta)\}_{cp}} \tag{47}$$

was used to compare the heat transfer as calculated by constant property and variable property analyses. Also since

$$u = 4\frac{\mu g_0}{\rho_{\mathrm{sat}}} c_1^2 \zeta' \tag{48}$$

and

$$\eta_\delta = c_1\frac{y}{x^{1/4}} \tag{49}$$

for the same wall-to-liquid temperature difference and the same value of x,

$$\frac{u_{\max}}{(u_{\max})_{cp}} = \frac{\rho_{cp}}{\rho_{\mathrm{sat}}}\left(\frac{c_1}{c_{cp}}\right)^2\frac{\zeta'_{\max}}{(\zeta'_{\max})_{cp}} \tag{50}$$

and

$$\frac{\delta}{\delta_{cp}} = \frac{c_{cp}}{c_1}\frac{\eta_\delta}{(\eta_\delta)_{cp}} \tag{51}$$

were used to compare the maximum velocity and film thickness, respectively, as calculated by the three methods.

It was of interest to note that if at a given pressure $u/u_{\max}$ was plotted against y/δ, the data fell very close to a single curve no matter what the wall temperature, as shown in Fig. 2. If data for different pressures were compared in this matter, the position of the maximum velocity was seen to vary as shown in Fig. 3. For constant properties the maximum velocity occurs at $y/\delta = 1/2$. The shifting of the velocity maximum was not easily explained. However, if inertia terms were neglected in equation (6), $(\rho_L - \rho)/\rho$ was assumed to decrease linearly from the wall to the liquid–vapor interface, and other properties were considered constant, it was seen that the velocity maximum should be shifted in the direction indicated.

Table 2. *A comparison of results*

		Compressible			Incompressible	
P (lb/in^2)	Θ (°F)	$\frac{q}{q_{cp}}$	$\frac{u_{\max}}{u(\max cp)}$	$\frac{\delta}{\delta_{cp}}$	$\frac{q}{q_{cp}}$	$\frac{\delta}{\delta_{cp}}$
2800	250	0·96	0·61	0·98	1·66	0·66
	500	0·98	0·47	0·99	1·6	0·62
	1000	1·04	0·37	0·94	1·63	0·59
3100	250	0·65	0·23	1·55		
	500	0·64	0·17	1·57		
	1000	0·63	0·145	1·53		

As seen in Table 2, the effect of considering compressible flow was to decrease the maximum

Vol. 1 1960

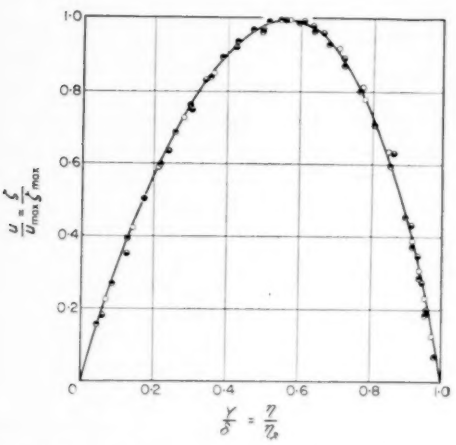

FIG. 2. Dimensionless velocity distribution for water vapor, $P = 3100$ lb/in²

- $\Theta = 250$°F
- $\Theta = 500$°F
- $\Theta = 1000$°F

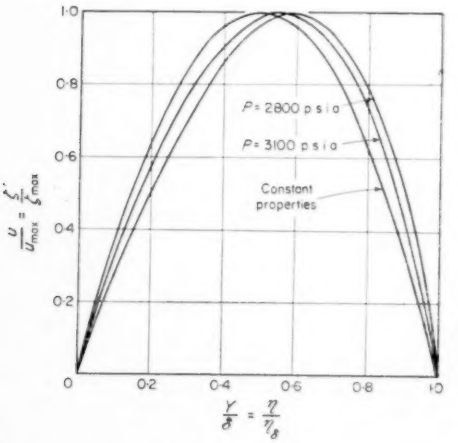

FIG. 3. Comparison of dimensionless velocity distributions

velocity in the film. This would tend to offset the increase in shear stress at the liquid–vapor interface caused by the shifting of the maximum velocity.

The temperature profiles at three different wall-to-liquid temperature differences at 2800 and 3100 lb/in² are shown in Figs. 4 and 5, respectively. Note that if the compressible-flow temperature profiles for the same value of $c_p\Theta/h_{fg}$ are plotted against y/δ, the curves are identical as shown in Fig. 6.

The effect on the temperature profile of considering a variable specific heat and bouyant force but otherwise incompressible flow is shown in Fig. 7. The profiles for only one wall-to-liquid temperature difference are shown, the effect being the same for all other cases investigated.

The effect of considering the vapor as incompressible while taking into account the variation

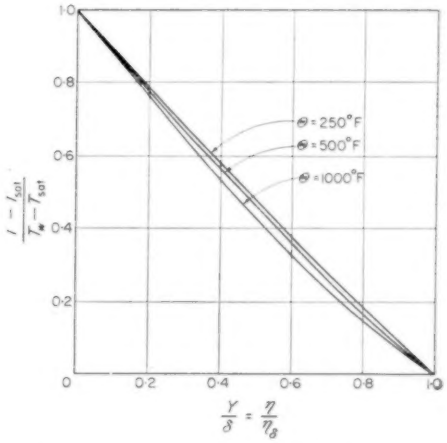

FIG. 4. Dimensionless temperature distribution in the vapor layer considering variable properties, water at 2800 lb/in².

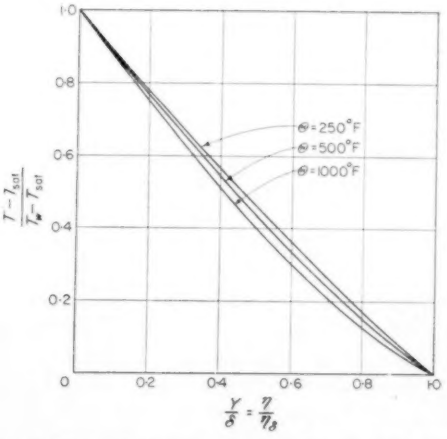

FIG. 5. Dimensionless temperature distribution in the vapor layer considering variable properties, water at 3100 lb/in².

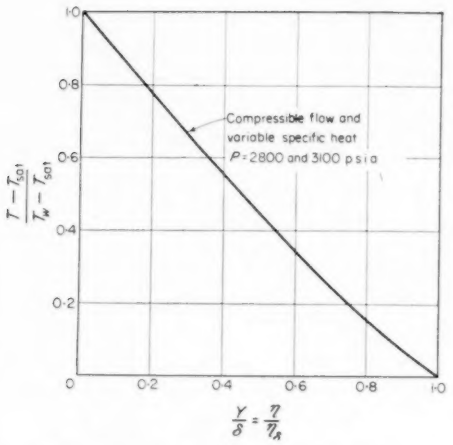

FIG. 6. Comparison of temperature distributions for $cp\Theta/h_{fg} = 2{\cdot}3$

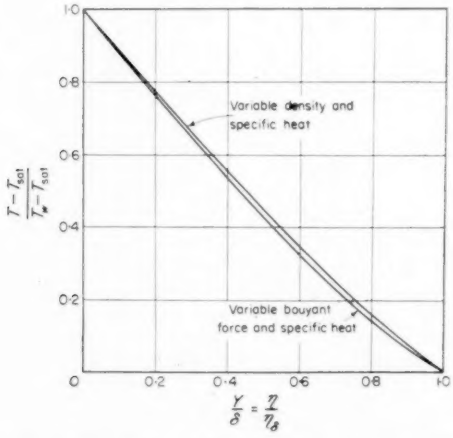

FIG. 7. The effect of an incompressible fluid with variable bouyant force and specific heat on temperature distribution, water at 2800 lb/in², $\Theta = 1000°F$

of specific heat and bouyant force was to increase the heat transfer by about 60 per cent at 2800 lb/in², as shown in Table 2. When compressible flow as well was considered, the variable-property analysis gave no significantly different results than the constant-property analysis at 2800 lb/in², provided the properties were evaluated at the mean temperature.

At 3100 lb/in² the decrease in film velocity due to considering compressible flow increased the film thickness appreciably. The effect was to decrease the heat transfer compared to that expected with a constant-property analysis.

CONCLUSION

The results of this investigation showed that the heat transfer as calculated by the constant-property method did not always agree with the heat transfer as calculated by the variable-property methods. For water at 2800 lb/in² the consideration of compressible flow and variable specific heat did not appreciably change the heat transfer from that calculated by assuming constant properties, provided the constant properties were evaluated at the arithmetic mean film temperature. At 3100 lb/in², however, the heat transfer as calculated by assuming constant properties was from 54 to 59 per cent greater than the heat transfer as calculated by considering compressible flow and variable specific heat.

The method of considering variable specific heat while density variations were used only in the evaluation of the bouyant force was not valid. The variable specific heat tends to increase the wall heat transfer; the variable density thickens the vapor layer and thus tends to decrease the heat transfer.

At 2800 and 3100 lb/in² radiation plays a more important role in film boiling than does the consideration of variable properties.

Actually, 3100 lb/in² is still very far from the critical pressure. It is felt that as the critical pressure is approached even more closely, the role that variable properties play in film-boiling heat transfer will become increasingly important. The work required near the critical pressure can not be completed, however, until more accurate property values in this region are available.

ACKNOWLEDGEMENT

The writers wish to thank Argonne National Laboratory, and ultimately the Atomic Energy Commission for making this work possible through Argonne National Laboratory Subcontract 31–109–38–704. We particularly wish to thank Dr. P. Lottes of Argonne National Laboratory for his advice and encouragement throughout this work.

REFERENCES

1. J. W. WESTWATER, Boiling of Liquids in *Advances in Chemical Engineering* (Edited by T. B. DREW and J. W. HOOPES, JR.), Vol. II. Academic Press, New York (1958).

Vol. 1 1960

2. W. NUSSELT, *Z. Ver. dtsch. Ing.* **60**, 541 and 569 (1916).
3. L. A. BROMLEY, *Chem. Engng. Progr.* **46**, 221 (1950).
4. L. A. BROMLEY, *Industr. Engng. Chem.* **44**, 2966 (1952).
5. R. D. CESS, A personal communication concerning unpublished work.
6. V. P. CHANG, *J. Heat Transfer* 1 (1959).
7. E. M. SPARROW and J. L. GREGG, *J. Heat Transfer* 13 (1959).
8. H. SCHLICHTING, *Boundary Layer Theory* (Translated by J. KESTIN) McGraw-Hill, New York (1955).
9. A. B. GREENBURG, *Mechanics of Film Flow on a Vertical Surface*. Ph.D. Thesis, Purdue University (1956).
10. R. HERMANN, *Heat Transfer by Free Convection from Horizontal Cylinders in Diatomic Gases*. NACA TM 1366.
11. F. B. HILDEBRAND, *Introduction to Numerical Analysis*. McGraw-Hill, New York (1956).
12. J. H. KEENAN and F. G. KEYES, *Thermodynamic Properties of Steam* (1st Ed.). John Wiley, New York (1951).
13. F. E. DSRJINSKOGO, *Tables of Thermodynamic Properties of Water and Water Vapor Based on Experimental Data*. Governmental Energetical Publishing House, Moscow (1952).

Int. J. Heat Mass Transfer. Vol. 1, pp. 336–356. Pergamon Press 1961. Printed in Great Britain.

HEAT TRANSFER BIBLIOGRAPHY

E. R. G. ECKERT, J. P. HARTNETT and E. M. SPARROW

Department of Mechanical Engineering, Institute of Technology, University of Minnesota, Minneapolis 14, Minnesota, U.S.A.

(*Received* 8 *August* 1960)

APPLICATIONS

GRAY BROOKS and GOUG-JEN SU, Heat transfer in agitated kettles. *Chem. Engng. Progr.* **55,** 54 (1955).

A. P. BUTHOD, How to estimate heat exchangers. *Oil Gas J.* **58,** No. 3, 67 (1960).

A. CHARNES and S. RAYNOR, Solar heating of a rotating cylindrical space vehicle. *J. Amer. Rocket Soc.* **30,** No. 5, 479 (1960).

S. V. DONSKOV, Heat transfer from tube bundles into a flowing granular material. *Teploenergetika* No. 11, 76 (1958). (In Russian.)

L. K. DORAISWAMY and N. B. PATEL, Performance of a pulsed heat exchanger. *J. Sci. Industr. Res. A* **18,** 522 (1959).

R. H. EDWARDS and G. S. CAMPBELL, Prediction of peak temperature for satellite entries with lift. *J. Amer. Rocket Soc.* **30,** No. 5, 496 (1960).

JAMES R. FAIR, What you need to design thermosiphon reboilers. *Petrol. Engr.* **32,** 105 (1960).

S. N. FAYNZIL'BERG, Investigation of the influence of the coefficient of heat conductivity of a rib on the heat delivery of a bank of melting tubes (Issledovaniye vliyaniya koeffitsiyenta teploprovodnosti rebra na teplootdachu puchkov iz plavnikovykh trub). *Izv. Kiyevsk. Politekh. Inst.* **17,** 122 (1956).

K. A. GARDNER, Heat-exchanger tube-sheet design-3. U-tube and bayonet-tube sheets. *J. Appl. Mech. E* **27,** No. 1, 25 (1960).

C. GAZLEY, W. W. KELLOGG and E. H. VESTINA, *Space Vehicle Environment.* Rand Corporation, Report P-1335 (Rev.), 15 June (1959).

VON GUNTER GRASS and PETER FRANZ COENEN, Systematische Untersuchungen über den Wärmeübergang und Strömungswiderstand von Rippenrohren, ein Beitrag zur Verwendung von Spezialrohren bei Gasgekuhlten Reaktoren. *Atomkernenergie* **4,** 2 (1959).

L. G. GREEN, Experiments on porous-wall cooling and flow separation control in a supersonic nozzle. *J. Aero. Space Sci.* **26,** No. 11, 689 (1959).

GERHARD HELLE, Thermal control of the explorer satellites. *J. Amer. Rocket Soc.* **30,** No. 4, 344 (1960).

ERICH HENSEL, Senkung der Wandtemperaturen von Wärmeübertragern durch Langsrippenrohre. *Chem.-Ing.-Tech.* **32,** No. 4, 258 (1960).

EVERETT D. HOWE, Solar distillation experiments at the University of California. *Solar Energy* **3,** No. 3, 31 (1959).

W. M. KAYS, The basic heat transfer and flow friction characteristics of six compact high-performance heat transfer surfaces. *J. Engng. Power A* **82,** No. 1, 27 (1960).

ROBERT KERN, How to design heat exchanger piping. *Petrol. Refiner* **39,** 137 (1960).

M. D. KHASKIND (Odessa), Heat transfer in the ground under the insulation of refrigerators (Teploperedacha v grunte pod izolyatsiyey kholodinikov). *Izv. Akad. Nauk SSSR, otdel. tekh. nauk* No. 10, 51 (1958).

JOHN L. KRAMER, HERMAN H. LOWELL and WILLIAM H. ROUDEBUSH, *Numerical Computation of Aerodynamic Heating of Liquid Propellants.* NASA TN D–273 (1960).

RICHARD B. LANCASHIRE, ERWIN A. LEZBERG and JAMES F. MORRIS, *Experimental Results of a Heat-Transfer Study from a Full-Scale Pebble-Bed Heater.* NASA TN D–265 (1960).

CURT H. LIEBERT, JAMES E. HATCH and RONALD W. GRANT, *Application of Various Techniques for Determining Local Heat-Transfer Coefficients in a Rocket Engine From Transient Experiment Data.* NASA TN D–277 (1960).

A. L. LONDON, The transient response of gas-turbine-plant heat exchangers-regeneration,

Vol. 1 1960

intercoolers, precoolers and ducting. *J. Engng. Power A* **81,** No. 4, 433 (1959).

E. L. LUSTENADER, The use of think films for increasing evaporation and condensation rates in process equipment. *J. Heat Transfer* C **81,** No. 4, 297 (1959).

GUNTHER MUESMANN, Messungen und Grenzschichtbeobachtungen an affin Verdickten Geblaseprofilen in Abhängigkeit von der Reynoldszahl. (Reprint.) *Z. Flugwissen.* **7,** 9, 253 (1959).

KIYOSHI MURAKAWA and SHIZUYO MIZUNO HASHIMOTO, Measurement of plasma temperature and electron density. *J. Phys. Soc., Japan* **14,** 1235 (1959).

HOWARD MYERS, Aerodynamically heated surfaces—A chemical analysis. *J. Aero. Space Engng.* **19,** 34 (1960).

M. F. NAGIYEV and P. V. KARAMZIN, Development of a method for the compilation and correlation of experimental data on the heat transfer in heat exchangers having odd-shaped spaces downstream of the tubes, and its practical application. *Izv. Akad. Nauk Azerbaidzhan SSR* No. 4, 33 (1956).

C. B. NEEL, *Cooling of Structures in High-Speed Flight.* AGARD Report No. 210 (1958).

KURT PAWLIK, Air as cooling agent in condensing systems in stream power stations and in process plants. *Z. Ver. dtsch. Ing.* **102,** No. 1 (1960).

W. S. PELLINI, Flight in the thermosphere—I. Material requirements for thermal protection systems. *Metal Progr.* **77,** No. 3, 69 (1960).

S. PETTERSSEN, Heat exchange and weather forecasting. *Proc. Nat. Acad. Sci., Wash.* **45,** No. 12, 1655 (1959).

R. D. PIERCE, O. E. DWYER and J. J. MARTIN, Heat transfer and fluid dynamics in mercury-water spray columns. *J. Amer. Inst. Chem. Engrs.* **5,** No. 2, 257 (1959).

A. A. PUTNAM, Flow-induced noise in heat exchangers. *J. Engng. Power* **81,** No. 4, 417 (1959).

G. RATIANI, R. KHUNTSARIIA and O. TURKESTANISHVILI, The use of solar energy as heat source for a heat pump. *Kholodil'naia Tekh.* **36,** No. 6, 17 (1959).

WILLIAM H. RICHARDSON and FRANCIS STRACHWITZ, *Sandia Corporation Bibliography. Gas-Cooled Reactors.* Office of Technical Services, Dept. of Commerce, Washington (ZTK9203. G2 Un3. 1g Ref.)

RICHARD J. ROSA, *Magnetohydrodynamic Power Generation Using Nuclear Fuel.* AVCO Everett Research Laboratory, Research Report 87 (1960).

M. W. RUBESIN, *Influence of Aerodynamic Heating on Structural Design of Aircraft.* AGARD Report, No. 207 (1958).

P. RUCKENSTEIN, On heat transfer in reactors. Translation of *Acad. Rep. Populare Romine, Studii Cercetari Fiz.* **7,** No. 1, 63 (1956).

W. RUHLE, Der Wärme-und Stoffübergang im Stromtrockner. *Chem.-Ing.-Tech. Verfahrenstechnik und Apparatewessen* **32,** No. 2, 73 (1960).

C. M. SCHMIDT and A. J. HANAWALT, Skin temperatures of satellite. *Jet Propulsion* **27,** No. 10, 1079 (1957).

WOLFGANG SCHWADERER, Temperature increases and cooling procedures in concrete structural elements. *Z. Ver. dtsch. Ing. Z.* **102,** No. 7, 271 (1960).

M. C. SLIN'KO, The use of a pseudo-liquid layer for heating and cooling in laboratory investigations (Primeneiye psevdoozhizhennoge sloya dlya obogrici i okhlazhdeniya pri laboratornykh issledovaniyakh). *Fiz. Khim.* **32,** No. 12, 2841 (1958).

WILLIAM A. STRAUSS and RUDOLPH EDSE, *Adiabatic Flame Temperatures, Combustion Gas Compositions, and Expansion Ratios of Combustible Gas Mixtures at Various Pressures.* U.S. Air Force, Wright Air Development Center, WADC TN 59–49 (1959).

(The structural effects of kinetic heating. *J. Roy Aero. Soc.* **63,** 615 (1959).

BYRON L. SWENSON, *A Study of Methods for Stimulating the Atmosphere Entry of Vehicles with Small-Scale Models.* NASA TN D–90 (1960).

M. W. THRING, Compact calorimeter for measuring the overall thermal efficiency of freestanding fires and stoves for room warming. *J. Sci. Instrum.* **36,** No. 12, 488 (1959).

M. W. THRING, Flames and furnaces. Heat transfer as a thermodynamic problem. *Iron & Steel* **32,** No. 12, 508 (1959).

ROBERT A. TIDBALL, Liquid-metal heat exchangers. *Power* **104,** 82 (1960).

H. A. VODDEN, Simple method of temperature control. *J. Sci. Instrum.* **37,** No. 2, 69 (1960).

B. A. ZENKEVICH, On the generalization of the experimental data on critical heat loads in forced flowing of under-heated water (K obobshcheniyu opytnykh dannykh po kriticheskim teplovym nagruzkam pri vynuzhdennom dvizhenii nedogretoy vody). *Atomnaia Energiia* **6,** No. 2, 169 (1959).

BOOKS

California Institute of Technology, *Astronautics Information*. Open Literature Survey, Vol. I, Part D, Entries 13, 166–13, 888.

California Institute of Technology, *Astronautics Information*. Abstracts, Vol. II, Nos. 1–3 (1960).

ALAN J. CHAPMAN, *Heat Transfer*. Macmillan, New York (1960).

FRANCIS J. CLAUSS (Editor), *First Symposium on the Surface Effects on Spacecraft Materials*. Transactions of the symposium co-sponsored by the Missiles and Space Division of Lockheed Aircraft Corporation and the Air Research and Development Command of the U.S. Air Force, California (1959). Wiley, New York (1960).

R. W. DETRA and H. HIDALGO, *Generalized Heat Transfer Formulae and Graphs*. AVCO Everett Research Laboratory, AVCO Corporation, Everett, Mass. Research Report 72 (1960).

E. ECKERT, *Introduction to Heat and Mass Transfer* (2nd Ed.). Springer, Berlin (1959).

S. FLUGGE and C. TRUESDELL (Editors), *Encyclopedia of Physics. I. Fluid Dynamics* (*Strömungsmechanik*). Vol. 8, Springer, Berlin (1959).

WALLACE D. HAYES and RONALD F. PROBSTEIN, *Hypersonic Flow Theory*, Vol. 5. Academic Press, New York (1959).

G. HORVAY, Review of book by A. V. LIKOV and YU. A. MIKHAILOV, *Theory of Energy and Material Transfer*. Metallurgy and Ceramics Research Dept., General Electric Research Laboratory, Schenectady, N.Y. (1960).

G. K. KULLBERG and H. B. KENDALL, Improve heat transfer coefficients. With silicone resin coatings. *Chem. Engng. Progr.* **56,** 82 (1960).

G. A. SLACK, *Conduction of Heat in Solids, Experiment and Theory. Heat Transfer Measurement Conductivity*. 59RL2172 (1959).

BOUNDARY LAYERS

J. L. ABBOTT, *Investigation of Thermal Insulation Materials*. U.S. Dept. of the Navy, Bureau of Ordnance NAVORD Report 6545 (1959).

ANDREAS ACRIVOS, A rapid method foı estimating the shear stress and the separation point in laminar incompressible boundary-layer flows. *J. Aero. Space Sci.* **27,** No. 4, 314 (1960).

T. C. ADAMSON, JR., Estimation of nonequilibrium reaction flight regimes for blunt bodies at hypersonic speeds. *J. Amer. Rocket Soc.* **30,** No. 4, 358 (1960).

VON W. ALBRING, Transformation der Impulsgleichung für turbulente Grenzschicht von Rotationskorpern auf ebene Korper. *Z. angew. Math. Mech.* **40,** 1/3, 38 (1960).

V. S. ARPACI, Dynamic response of heat exchangers having internal heat sources—III. *J. Heat Transfer* C **81,** No. 4, 253 (1959).

P. D. ARTHUR, Maximum turbulent boundary layer heating rates on a hemispherical nose. *J. Amer Rocket Soc.* **30,** No. 2, 207 (1960).

A. M. BAIN, High-temperature research in Europe and Asia: Staff report welding a pressure vessel for a Canadian test reactor. *Metal Progr.* **77,** No. 1, 96 (1960).

BARRETT S. BALDWIN, *An Optimization Study of Effects on Aircraft Performance of Various Forms of Heat Addition*. NASA TN D–74 (1960).

A. C. BAXTER and W. C. REYNOLDS, Fundamental solutions for heat transfer from non-isothermal flat plates. *J. Aero. Sci.* **25,** No. 6, 403 (1958).

JOHN V. BECKER, Heating penalty associated with modulated entry into earth's atmosphere. *J. Amer. Rocket Soc.* **30,** No. 5, 504 (1960).

MITCHEL H. BERTRAM, *Boundary-Layer Displacement Effects in Air at Mach Numbers of* 6·8 *and* 9·6. NASA TR R–22, supersedes NACA TN 4133.

JOHN H. BONIN, CHANNON F. PRICE and DONALD E. TAYLOR, *Determination of Factors Governing Selection and Application of Materials for Ablation Cooling of Hypervelocity Vehicles*. U.S. Air Force, Wright Air Development Center, WADC TR 59–87 (1959).

Vol. 1 1960

D. B. BREWSTER, P. GROSBERG and A. H. NISSAN, The stability of viscous flow between horizontal concentric cylinders. *Proc. Roy. Soc.* A **251,** No. 1264 (1959). (No. 2348.)

O. B. BRON, Problems of liquid cooling in electrical equipment. *Electric Technology, USSR* **4,** 503 (1959).

P. B. BURBANK and B. L. HODGE, *Distribution of Heat Transfer on a* 10° *Cone at Angles of Attack from* 0° *to* 15° *for Mach Numbers of* 2·49 *to* 4·65 *and a Solution to the Heat Transfer Equation that Permits Complete Machine Calculations.* NASA Memo. 6–4–59L (1959).

N. B. COHEN, *A Method for Computing Turbulent Heat Transfer in the Presence of a Streamwise Pressure Gradient for Bodies in High-Speed* Flow. NASA Memo. 1–2–69L (1959).

L. F. CRABTREE, Hypersonic boundary layers with special reference to heat transfer. *J. Roy. Aero. Soc.* **63,** No. 585, 513 (1959).

L. J. CRANE, A note on Stewartson's paper "On asymptotic expansions in the theory of boundary layers". *J. Math. Phys.* **38,** No. 3, 172 (1959).

JERRY GREY (submitted by Project Leader), *Heat Transfer from an Ionized Gas to a Gaseous Coolant.* Princeton University, Dept. of Aeronautical Engineering, Princeton, New Jersey (1959).

R. J. GRIBBEN, Laminar boundary layer with suction and injection. *Phys. Fluids* **2,** No. 3, 305 (1959). (No. 2404.)

J. P. HARTNETT, E. R. G. ECKERT and R. BIRKEBAK, Determination of convective heat transfer to nonisothermal surfaces including the effect of pressure gradient. *Proceedings of the Sixth Midwest Conference on Fluid Mechanics, Austin, Texas* 1959, pp. 47–70. Austin University Press (1959).

WALLACE D. HAYES and RONALD F. PROBSTEIN, Viscous hypersonic similitude. *J. Aero. Space Sci.* **26,** 815 (1959).

F. K. HILL, Turbulent boundary layer measurements at Mach numbers from 8 to 10. *Phys. Fluids* **2,** No. 6, 668 (1959).

SHIH-KUNG KAO, Turbulent transfer in the boundary layer of a stratified fluid. *J. Meteorol.* **16,** No. 5, 497 (1959).

JACK L. KERREBROCK, *Electrode Boundary Layers in Direct Current Plasma Accelerators.* California Institute of Technology, Daniel and Florence Guggenheim Jet Propulsion Center, Pasadena, California, AFOSR TN 60–287 (1960).

S. J. KLINE, A. V. LISIN and B. A. WAITMAN, *Preliminary Experimental Investigation of Effect of Free-Stream Turbulence on Turbulent Boundary-Layer Growth.* Stanford University, NASA TN D–368 (1960).

A. M. KUETHE, Stagnation point fluctuations on a body of revolution. *Phys. Fluids* **2,** No. 6, 714 (1959).

G. A. KULONEN, Shockwave-boundary layer interaction in the neighborhood of the leading edge of a flat plate at hypersonic speeds taking radiant energy into account. Translation of *Vestnik Leningrad Univ. ser. mat. mekh. i astron.* No. 2, 172 (1958).

B. LE FUR, Heat transfer and recovery factor in a laminar boundary layer with arbitrary pressure gradient and wall temperature distribution. *J. Aero. Space Sci.* **26,** No. 10, 682 (1959). (Readers Forum.) (No. 2512.)

C. C. LIN, *Turbulent Flows and Heat Transfer.* Princeton University Press, Princeton, N.J. (TL709H53) (1959).

MICHELL LITT and S. K. FRIEDLANDER, An experimental study of diffusion-controlled reactions in a laminar boundary layer. *J. Amer. Chem. Engrs.* **5,** No. 4, 483 (1959).

B. H. LOCHTENBERG, Transition in a separated laminar boundary layer. *J. Aero. Space Sci.* **27,** 91 (1960).

R. E. LUXTON and A. D. YOUNG, *A Generalized Method for the Calculation of the Laminar Compressible Boundary Layer with Heat Transfer and Non-Uniform Pressure Distribution.* Aeronautical Research Council (Gt. Brit.) (1960).

LESLIE M. MACK, *Numerical Calculation of the Stability of the Compressible, Laminar Boundary Layer.* Jet Propulsion Laboratory, California Institute of Technology, Pasadena, California, Report No. 20–122 (1960).

DAVID MEKSYN, Plate thermometer. *Z. angew. Math. Phys.* **11,** 63 (1960).

ADRIAN PALLONE, *Non-Similar Solutions of the Compressible Laminar Boundary Layer Equations with Applications to the Upstream Transpiration Cooling Problem.* Research and

Advanced Development Division, AVCO Corp., Wilmington, Mass., Technical Report RAD–TR–9–60–8 (1960).

J. LEITH POTTER and JACK D. WHITFIELD, *Effects of Unit Reynolds Number, Nose Bluntness and Roughness on Boundary Layer Transition*. Arnold Engineering Center, Air Research and Development Command, AEDC–TR–60–5 (1960).

W. C. RAGSDALE, Heat transfer in nozzles. *Chem. Engng. Sci.* **11,** No. 4, 242 (1960).

S. M. SCALA and G. W. SUTTON, Energy transfer at a chemically reacting or slip interface. *J. Amer. Rocket Soc.* **29,** No. 2, 141, Tech. Notes (1959).

H. SCHLICHTING, Some developments in boundary layer research in the past thirty years. *J. Roy. Aero. Soc.* **64,** No. 590, 63 (1960).

W. R. SCHOWALTER, The application of boundary-layer theory to power-law pseudoplastic fluids: similar solutions. *J. Amer. Inst. Chem. Engrs.* **6,** No. 1, 24 (1960).

J. F. SCHMIDT, *Laminar Skin-Friction and Heat-Transfer Parameters for Flat Plate at Hypersonic Speeds in Terms of Free-Steam Flow Properties*. NASA TN D–8 (1959).

T. SCHULTZ-GRUNOW, Turbulent heat transmission in the centrifugal field. Translation of *Forsch. IngWes.* **17,** No. 3, 65 (1951).

M. A. SINBEL, Boundary-layer solution for a flow in a diverging passage having a swirl component. *J. Appl. Mech.* E **26,** No. 4, 477 (1959).

JAMES C. SIVELLS and ROBERT G. PAYNE, *A Method of Calculating Turbulent-Boundary Layer Growth at Hypersonic Mach Numbers*. Arnold Engineering Development Center, Air Research and Development Command, USAF, AEDC–TR–59–3, ASTIA Document No. AD–208774 (1959).

M. B. SKOPETS, Approximate method for integrating the equations of a laminar boundary layer in an incompressible gas in the presence of heat transfer. *J. Tech. Phys., Moscow*. Translation of *Zk. Tekh. Fiz.* **4,** No. 4, 411 (1959).

DONALD W. SMITH and JOHN H. WALKER, *Skin-Friction Measurements in Incompressible Flow*. NASA Technical Report R–36; supersedes NACA TN 4231.

H. H. SOGIN, Laminar transfer from isothermal spanwise strips on a flat plate. *J. Heat Transfer* C **82,** No. 1, 53 (1960).

D. A. SPENCE, *Distributions of Velocity, Enthalpy and Shear Stress in the Compressible Turbulent Boundary Layer on a Flat Plate*. Roy. Aircraft Establishment (Gt. Brit.), RAE Report Aero 2631 (1959).

KENNETH F. STETSON, Boundary-layer transition on blunt bodies with highly cooled boundary layers. *J. Aero Space Sci.* **27,** 81 (1960).

THORVAL TENDELAND, *Effects of Mach Number and Wall-Temperature Ratio on Turbulent Heat Transfer at Mach Numbers from* 3 *to* 5. NASA TR R–16; supersedes NACA TN 4236 (1959).

L. TING, On the mixing of two parallel streams. *J. Math. Phys.* **38,** No. 3, 153 (1959).

ROBERTO VAGLIO-LAURIN, Turbulent heat transfer on blunt-nosed bodies in two-dimensional and general three-dimensional hypersonic flow. *J. Aero. Space Sci.* **27,** 27 (1960).

H. C. VETTER, Note on the calculation of equilibrium skin temperatures. *J. Aero. Space Sci.* **26,** No. 11 757 (1959). (Reader's Forum.) (No. 2515.)

A. WALZ, Compressible turbulent boundary layers with heat transfer and pressure gradient in flow direction. *J. Res. Nat. Bur. Stand.* B **63,** No. 1, 53 (1959). (No. 2397.)

PETER P. WEGENER, Experiments on the departure from chemical equilibrium in a supersonic flow. *J. Amer. Rocket Soc.* **30,** No. 4, 322 (1960).

J. G. WOODLEY, *Measurements of the Effect of Surface Cooling on Boundary Layer Transition on a* 15 *Degree Cone—II. Tests at* $M=4$ *in the* 5 *inc. no.* 5. Wind tunnel at RAE Farnborough, Aero. Res. Council (Gt. Brit.) C.P. 479.

K. T. YANG, Unsteady laminar compressible boundary layers on infinite plate with suction or injection. *J. Aero. Space Sci.* **26,** No. 10, 653 (1959).

L. M. ZYSINA-MOLOZHEN, An approximate method for calculating the thermal boundary layer. *J. Tech. Phys., Moscow*. Translation of *Zh. Tekh. Fiz.* **4,** No. 5, 564 (1959).

L. M. ZYSINA-MOLOZHEN, The calculation of heat transfer in a cascade of blades. *J. Tech.*

Vol. 1 1960

Phys., Moscow. Translation of *Zh. Tekh. Fiz.* **4**, No. 5, 558 (1959).

L. M. ZYSINA-MOLOZHEN, A study of the effect of a longitudinal pressure gradient on the development of a boundary layer. *J. Tech. Phys., Moscow*. Translation of *Zh. Tekh. Fiz.* **4**, No. 4 (1959).

CHANGE OF PHASE

DONALD W. BELL, Correlation of burnout heat-flux data at 2,000 pisa. *Nuc. Sci. Engng.* **7**, No. 3, 245 (1960).

PAUL J. BERENSON, *Transition Boiling Heat Transfer from a Horizontal Surface*. Division of Sponsored Research, Mass. Institute of Tech., Cambridge, Mass., TR No. 17 (1960).

D. C. P. BIRT, J. J. BRUNT, J. T. SHELTON and R. G. H. WATSON, Methods of improving heat transfer from condensing steam and their application to condensers and evaporators. *Trans. Inst. Chem. Engrs.* **37**, No. 5, 289 (1959).

V. M. BORISHANSKIY, The coefficients of the transfer of heat to boiling water at excessive pressures. Translation of *Energomashinostroyeniye* **4**, No. 7, 5 (1958).

EDMOND A. BRUN and GERARD DONNADIEU, Transmission de chaleur d'un lit de particules solides en etat de fluidisation. *C.R. Acad. Sci., Paris* **250**, 1605 (1960). Centre National de la Recherche Scientifique Laboratoire d'Aerothermique Publication No. 128.

D. H. CHARLESWORTH and W. R. MARSHALL, Evaporation from drops containing dissolved solids. *J. Amer. Inst. Chem. Engrs.* **6**, No. 1, 9 (1960).

MOHAN J. CHAWLA, Die Abkuhlung von Wasser am Berieselungsverdampfer (Cooling of water flowing film-like over evaporator tubes). *Kaltetechnik*. **4**, 96 (1960).

C. DEVIN, JR., Survey of thermal, radiation and viscous damping of pulsating air bubbles in water. *J. Acoust. Soc. Amer.* **31**, No. 12, 1654 (1959).

K. FORSTER, *Calculation of Heat Flux in Superheated Liquids*. Dept. of Engng., University of California, Los Angeles, California, Report No. 59–63 (1959).

KURT FORSTER, *Heat Conduction in a Liquid with Evaporation on a Boundary*. Dept. of Engng., University of California, Los Angeles, Calif., Report No. 59–63 (this is part 2 of a Progress Report).

A. FRANK, Wärme- und Stoffaustausch Zwischen Dampfbase und Flussigkeit bei Stickstoff/Sauerstoff-Gemischen. *Chem.-Ing.-Tech.* **32**, No. 5, 330 (1960).

N. A. FUKS, On the theory of evaporation of fine droplets. *Zh. Tekh. Fiz.* **28**, 1, 159 (1958); *Ref. Zh. Mekh.* No. 10, Rev. 11265 (1958). (In Russian.)

P. GRASSMAN, Mass and heat transfer between two fluid phases. Translation of *Chem.-Ing.-Teck*. **31**, No. 3, 148 (1959).

H. GROOTHUIS, Heat transfer in two-phase flow. *Chem. Engng. Sci.* **11**, No. 3, 212 (1959).

W. GUTH, Cinematographic photographs of water vapour bubbles. Translation of *Acustica* No. 1, 445 (1954).

G. E. HARBECK, JR. and G. E. KOBERG, A method of evaluating the effect of a monomolecular film in suppressing reservoir evaporation. *J. Geophys. Res.* **64**, No. 1, 89 (1959).

FUJIO HIRANO and KANEYASU NISHIKAWA, Time variation of nucleate boiling heat transfer of water. *Bull. Japan. Soc. Mech. Engrs.* **2**, No. 7 (1959).

WALTER JAMES and EDWARD SILBERMAN, *Two-Phase Flow Studies in Horizontal Pipes with Special Reference to Bubbly Mixtures*. University of Minnesota, St. Anthony Falls Hydraulic Laboratory, Technical Paper No. 26, Series B (1958).

A. I. JOHNSON and A. E. HAMIELEC, Mass transfer inside drops. *J. Amer. Inst. Chem. Engrs.* **6**, No. 1, 145 (1960).

P. D. JONTZ and MYERS, The effect of dynamic surface tension on nucleate boiling coefficients. *J. Amer. Inst. Chem. Engrs.* **6**, No. 1, 34 (1960).

H. KOLBEL, ERHARD BORCHERS and JOHANNES MARTINS, Wärmeübergang in Blasensaulen—III. Messungen an Gasdurchstromten Suspensionen. *Chem.-Ing.-Tech.* **32**, No. 2, 84 (1960).

S. I. KOSTERIN, B. I. SHEYNIR and A. K. KATARZHIS, Experimental characteristics of stratified flow in a steam-water mixture in a straight, horizontal pipe. Translation of *Teploenergetika* **3**, No. 1, 22 (1956).

H. M. KURIHARA and MYERS, The effects of superheat and surface roughness on boiling

coefficients. *J. Amer. Inst. Chem. Engrs.* **6,** No. 1, 83 (1960).

A. V. LYKOV, Heat and mass transfer in disperse media with phase changes. Translation of *Inzh. Fiz. Zh.* **1,** No. 6, 12 (1958).

A. J. MADDEN and F. J. HALFEN, *Temperature Depressions for Evaporating Spheres at Low Pressures.* University of Minnesota.

SIMON OSTRACH, ARTHUR W. GOLDSTEIN and JESSE HAMMAN, *The Effect of a Deceleration Force on a Melting Boundary Layer.* NASA Lewis Research Center, Cleveland, Ohio (Prepared for *J. Aero. Sci.*).

L. ROBERTS, *Approximate Analysis of Unsteady Vaporization Near Stagnation Point of Blunt Bodies.* NASA TN D–41 (1959).

S. L. SOO, Effect of the wall on two-phase turbulent motion. *J. Appl. Mech.* E **27,** No. 1, 5 (1960).

V. YA. STAPRENS, Capillary condensation. *Trudy Lab. Gidrogeol. Problem Akad. Nauk. SSSR* **12,** 89 (1955). *Ref. Zh. Mekh.* No. 10, Rev. 11264 (1958). (In Russian.)

G. G. TRESCHOV, An experimental investigation of heat exchange mechanism at a boiling water surface. *Teploenergetika* No. 5, 44 (1957). (In Russian.)

V. V. VYSHENSKII, Investigation of heat emission of particles in a straight flow by the analogy method with diffusion. *Izv. Akad. Nauk Kazakh. SSR ser. energet.* No. 1 (12), 75 (1957); *Ref. Zh. Mekh.* No. 1, Rev. 533 (1959). (No. 2525.) (In Russian.)

B. A. ZENKEVICH, Use of the principle of similarity for the critical thermal loading during the constrained motion of liquid. *Atomnaia Energiia* **4** (1), 74 (1958); *Ref. Zh. Mekh.* No. 1, Rev. 548 (1959). (No. 2526.) (In Russian.)

V. I. ZUBKOV, On the evaporation of solid globules in a gas flow. *J. Tech. Phys., Moscow* **3,** No. 6, 1121 (1959).

CHANNEL FLOW

A. D. AL'TSHUL' (Moscow), Hydraulic models for uniform turbulent flow in pipes and channels (O gidravlicheskom modeltrovanii ravnomernykh turbulentnykh potokov v truboprovodakh i kanalakh). *Izv. Akad. Nauk SSSR, otdel. tekh. nauk. energetika i avtomatika* No. 1, 121 (1959).

H. C. AGRAWAL, Heat transfer in laminar flow between parallel plates at small Peclet numbers. *Appl. Sci. Res., Hague* A **9,** Nos. 2–3, 177 (1960).

R. ARIS, The longitudinal diffusion coefficient in flow through a tube with stagnant pockets. *Chem. Engng. Sci.* **11,** No. 3, 194 (1959).

A. V. ARSEYEV (Candidate of Tech. Sci.), The heat transfer and resistance of tubes during high temperature heating of air (Teplootdacha i soprotivleniye v trubakh pri vysokotemperaturnom nagreve vozdukha). *Teploenergetika* No. 6, 67 (1959).

H. D. BAEHR, Gleichungen für den Wärmeübergang bei Hydrodynamisch Nicht Augebildeter Laminarströmung in Rohren. *Chem.-Ing.-Tech.* **32,** No. 2, 89 (1960).

HANS DIETER BAEHR and WOLFGANG STREWE, The temperature curve in twin flow reactor cooling channels. *Atomkernergie* **4,** 345 (1959).

R. B. BIRD and C. F. CURTISS (I), R. B. BIRD, C. F. CURTISS and W. E. STEWART (II), Tangential Newtonian flow in annuli (I). Unsteady state velocity profiles (II). *Chem. Engng. Sci.* **11,** No. 2, 108 (1959).

RICHARD S. BROKAW, *Correlation of Turbulent Heat Transfer in a Tube for the Dissociating System* $N_2O_4 \rightleftarrows 2NO_2$. NACA RM E57K19a (1958).

PIERRE CALVET and DIETRICH FAULMANN, Exploitation de la veine a section circulaire de la soufflerie hypersonique. *J. Recherches Centre Nat. Recherche Sci. Laks Belle Vue (Paris),* No. 49, 359 (1959). (Centre National de la Recherche Scientifique Laboratoire d'Aerothermique Publication No. 125.)

R. D. CESS and E. C. SHAFFER, Laminar heat transfer between parallel plates with an unsymmetrically prescribed heat flux at the walls. *Appl. Sci. Res., Hague* A **9,** No. 1, 64 (1959).

PAUL L. CHAMBRE, On chemical reactions in internal flow systems. *Appl. Sci. Res., Hague* A **9,** Nos. 2–3, 157 (1960).

SIN-I CHENG and RICHARD H. LEVY, *The Boundary Layer in a Corner.* Dept. of Aeronautical Engineering, Princeton University, Report 485, AFOSR TN 59–1165 (1959).

Vol. 1 1960

JESSE COATES and BERNARD S. PRESSBURG, Heat transfer to moving fluids. *Chem. Engng. Progr.* **66,** 67 (1959).

ROBERT G. DEISSLER and MAYNARD F. TAYLOR, *Analysis of Turbulent Flow and Heat Transfer in Noncircular Passages.* NASA TR R–31 (1959).

E. R. G. ECKERT, *Analysis of Laminar Heat Transfer in Wedge-Shaped Passages.* Wright Air Development Center TR 56–98 (1956).

P. P. FEDOSKO, Convective heat exchange and resistance during motion of air in short tubes at low Reynolds number. *Trudy Leningrad. Inst. Inzh. Vodn. Transp.* No. 24, 162 (1957); *Ref. Zh. Mekh.* No. 10, Rev. 11251 (1958). (In Russian.)

J. M. FOWLER and C. F. WARNER, Measurements of the heat transfer coefficients for hydrogen flowing in a heated tube. *J. Amer. Rocket Soc.* **30,** No. 3, 266 (1960).

F. A. GAYDON and H. NUTTALL, Viscous flow through tubes of multipy connected cross sections. *Trans. Amer. Soc. Mech. Engrs., J. Appl. Mech.* E **26,** No. 4, 573 (1959).

GUNTHER GRASS, The improvement of heat transfer to water derivable from the artificial roughening of surfaces in reactors or in heat exchangers. Translation of *Atomkerneregie* **3,** 328 (1958).

H. W. HAHNEMANN, Pressure loss and heat transfer with swirled flow. *Z. Ver. dtsch. Ing.* **101,** No. 31, 1431 (1959).

Heat transfer at high gas pressures—II. *Engineering* **188,** 317 (1959).

B. L. HICKS, An exact calculation of some steady, diabatic two-dimensional fields of compressible flow. *J. Aero. Space Sci.* **27,** No. 2, 142 (1960).

R. M. INMAN, Heat transfer for laminar flow in an annulus with porous walls. *J. Aero. Space Sci.* **26,** No. 8, 532 (1959). (Readers' Forum.)

S. I. KOSTERIN and A. D. MAGOMEDOV, A study of viscous liquid motion in the presence of heat transfer in the region of large Prandtl numbers. *Izv. Akad. Nauk SSSR, otdel. tekh. nauk* No. 10, 155 (1958). (In Russian.)

S. I. KOSTERIN and B. I. SHEYNIN, The hydraulic frictional resistances to the flow of a mixture of steam and water in a straight horizontal tube. Translation of *Teploenergetika* **5,** No. 6, 71 (1958).

F. KREITH, Heat transfer and friction in turbulent vortex flow. *Appl. Sci. Res., Hague* A **8,** No. 6, 457 (1959).

L. I. KUDRYASHEV L. A. VVEDENSKAYA, Controlled and a controlled within limits; temperature regime and their applications to the experimental determination of the coefficient of heat emission and resistance when bodies of arbitrary form are heated. *Sbornik. Nauch. Trudy Kuibyshevsk. Indust. Inst.* No. 7, 47 (1957); *Ref. Zh. Mekh.* No. 1, Rev. 534 (1959). (In Russian.)

M. E. LAPIDES and M. B. GOLDSTEIN, *Heat Transfer Source File Data.* G. E. Co. Atomic Products Div., Aircraft Nuclear Propulsion Dept., APEX 425 (1958).

E. E. LEMEKHOV, On the length of the mixing path at turbulent motion of incompressible fluid in pipes. *Vestnik. Leningrad. Univ.* **14,** No. 19, 130 (1959).

J. R. MCCARTHY and H. WOLF, Forced convection heat transfer to gaseous hydrogen at high heat flux and high pressure in a smooth, round, electrically heated tube. *J. Amer. Rocket Soc.* **30,** No. 4, 423 (1960).

B. R. MORTON, Laminar convection in uniformly heated horizontal pipes at low Rayleigh numbers. *Quart. J. Mech. Appl. Math.* **12,** Part 4, 410 (1959).

A. H. NISSAN and F. C. HAAS, The hydrodynamics of flow between horizontal concentric cylinders—II. Generalized criteria and correlations of heat transfer data. *Chem. Engng. Sci.* **11,** No. 3, 207 (1959).

R. H. NORRIS, *Comments and Bibliography on Heat Transfer for Turbulent Flow between Parallel Walls Having Asymmetric Wall-Temperatures or Heat Fluxes* (1960).

MORRIS PERLMUTTER and ROBERT SIEGEL, *Unsteady Laminar Flow in a Duct with Unsteady Heat Addition.* NASA Lewis Research Center (undated), E–880. (Prepared for ASME Meeting Dec. 1960 and *J. Heat Transfer.*)

KARL STEPHAN, Heat-transfer and pressure drop on undeveloped laminar flow in pipes and in smooth slits. *Chem.-Ing.-Tech.* **21,** 773 (1960).

M. A. STYRIKOVICH (Corresponding Member,

AS USSR) and L. YE. FAKTOROVICH (Engineer), The influence of the length of a heated section of tube on the magnitude of critical rates of heat transfer during forced motion of a steam-water mixture (Vliyaniye dliny obogrevyemogo uchastka truby na velichinu kriticheskikh teplovykh potokov pri vynuzhdennom dvizhenii parovodyanoy smesi). *Teploenergetika* No. 2, 83 (1959).

A. G. TEMKIN, Heat exchange in laminar flow through noncircular tubes. *J. Tech. Phys., Moscow*. Translation of *Zh. Tech. Phys.* **4,** No. 4, 383 (1959).

P. H. WANG, On the convective heat transfer for turbulent flow of single-phase fluid through concentric annuli. *Sci. Sinica* **8,** No. 1 98 (1959). (In English.)

PETER J. WESTERVELT, Effect of sound waves on heat transfer. *J. Acoust. Soc. Amer.* **32,** No. 3, 337 (1960).

S. W. YUAN, Turbulent flow in channels with porous walls. *J. Math. Phys.* **38,** No. 3, 166 (1959).

A. YA. YUSHIN, Experimental investigation of local heat convection in a mixed motion of liquid in a round tube. (In Russian.) *Sbornib Statei Nauch. Stud. O-va Mosk. Energ. Inst.* No. 10, 164 (1957); *Ref. Zh. Mekh.* No. 10 (1958), Rev.

V. ZAKKAY, Heat transfer at a corner. *J. Aero. Space Sci.* **27,** No. 2, 157 (1960).

CONDUCTION

W. D. BAINES, *On the Transfer of Heat From a River to an Ice Sheet*. NRC Mechanical Engineering Report MH–93.

D. C. BAXTER, *The Freezing and Melting Times of Slabs and Cylinders*. Nat. Res. Council Canada, Div. Mech. Engng., Rep. MK–1 (1959).

J. V. BECK, Effect of thermocouple cavity onheat sink temperature. *J. Heat Transfer* C **82,** No. 1, 27 (1960).

S. BORBELY, Investigation in connection with nonlinear heat conduction. *Magyar Tud. Akad. Musz. Tud. Oszt. Kozl.* **23,** 3/4, 261 (1959). (In Hungarian.)

L. BROGLIO, *Heat Conduction in Solids at Hypersonic Speeds*. AGARD Report 209 (1958).

STEPHEN J. CITRON, Heat conduction in a melting slab. *J. Aero Space Sci.* **27,** No. 3, 219, (1960).

STEPHEN J. CITRON, A note on the relation of Blot's method in heat conduction to a least-squares procedure. *J. Aero Space Sci.* **27,** No. 4, 317 (1960).

I. N. DANILOVA, Temperature changes in an infinite hollow cylinder when the temperature of the external medium changes in step form (O temperaturnom pole v negranichennom polom tsilindre, kogda temperatura vneshney sredy menyayetsya po zakonu lomanoy). *Izv. Akad. Nauk SSSR, otdel. tekh. nauk energetika i avtomatika* No. 1, 131 (1959).

W. DAVIES, Thermal transients in graphite–copper contacts. *Brit. J. Appl. Phys.* **10,** No. 12, 516 (1959).

H. FIEBER, About the temperature field in domains moving along one direction and periodically variable. Translation of *Osterr. Ing.-Arch.* **10,** Nos. 2/3, 155 (1956).

C. FORBES, DEWEY, JR., STEWART I. SCHLESINGER and LAWRENCE SASHKIN, Temperature profiles in a finite solid with moving boundary. *J. Aero. Space Sci.* **27,** 59 (1960).

H. GOLDENBERG, Transient temperature rise due to a line source in a semi-infinite medium, with a radiation boundary condition at the interface. *Brit. J. Appl. Phys.* **10,** No. 7, 314 (1959).

I. GRANET, An approach to the calculation of the temperature distribution in cylindrical reactor vessels. *J. Amer. Soc. Naval Engrs.* **71,** No. 3, 465 (1959).

W. W. GRANNEMANN, Transient junction temperatures in power transistors. *Elect. Engng.* **79,** No. 1, 53 (1960).

W. T. GUY, JR., L. B. LESEM and G. W. CRAWFOR, Laplace transformation solution of simultaneous linear flow in two regions separated by a fixed boundary. *Proceedings of the Sixth Midwestern Conference on Fluid Mechanics, Austin, Texas* 1959, pp. 218–231. Austin University Press (1959).

N. E. HAGER, Thin-heater thermal conductivity apparatus. *Rev. Sci. Instrum.* **31,** No. 2, 177 (1960).

Vol. 1 1960

H. W. HAHNEMANN, Wärmeübertragung und Wärmespannung bei Rippenrohren. *Z. Ver. dtsch. Ing.* **102,** No. 11, 423 (1960).

J. E. HATCH, R. L. SCHACHT, L. U. ALBERS and P. G. SAPER, *Graphical Presentation of Difference Solutions for Transient Radial Heat Conduction in Hollow Cylinders with Heat Tranfser at Inner Radius and Finite Slabs with Heat Transfer at One Boundary*. NASA TR R–56 (1960).

G. HORVAY, *Priblishennii Raschet Protesessov Teploprovodnosti* (*Approximate Calculation of Heat Conduction Processes*). Metallurgy and Ceramics Research Dept., G.E. Co. Research Lab., Schenectady, N.Y., Memo. Rept. No. ME–102 (1960).

M. IRIARTE, JR., An accurate transfer function for the dynamic analysis of temperature and heat release in cylindrical fuel elements. *Nucl. Sci. Engng.* **7,** No. 1, 26 (1960).

W. D. KINGERY, Thermal conductivity—XLV. Conductivity of multicomponent systems. *J. Amer. Ceram. Soc.* **42,** No. 12, 617 (1959).

DAIZO KUNII and J. M. SMITH, Heat transfer characteristics of porous rocks. *J. Amer. Inst. Chem. Engrs.* **6,** No. 1, 71–78 (1960).

S. P. KUZNETSOV, Investigation of the nonstationary fields of temperature and humidity in an unbound plate with no humidity evaporation. *Izv. Tomskogo Politekh. Inst.* **89,** 8 (1958); *Ref. Zh. Mekh.* No. 10, Rev. 11270 (1958). (In Russian.)

W. T. KYNER, On a free boundary value problem for the heat equation. *Quart. Appl. Math.* **17,** No. 3, 305 (1959).

I. A. LOFFE, Plane nonstationary heat conduction problem for a semi-infinite body with an internal isothermal cylindrical source of heat. *J. Tech. Phys., Moscow* **4,** No. 3, 369 (1959). Translation of *Zh. Tekh. Fiz.* **29,** No. 3, 417 (1959).

MARK LOTKIN, The calculation of heat flow in melting solids. *Quart. Appl. Math.* **28,** No. 1, 79 (1960).

C. S. LOWTHIAN, Transient temperatures in a uranium rod. *J. Nucl. Energy* A **10,** Nos. 3/4, 95 (1959).

T. J. MIRSEPASSI, Steady-state temperature distribution in solids undergoing certain change of property. *Brit. J. Appl. Phys.* **10,** No. 12, 538 (1959).

T. P. NEWCOMB, Flow of heat in a composite solid. *Brit. J. Appl. Phys.* **10,** No. 5, 204 (1959).

J. R. PHILIP, General method of exact solution of the concentration-dependent diffusion equation. *Aust. J. Phys.* **13,** No. 1, 1 (1960).

L. A. PIPES, Matrix analysis of heat transfer problems. *J. Franklin Inst.* **263,** No. 3, 195 (1957).

G. RIBAUD, Thermal conductivity of porous and pulverulent materials: A theoretical study. Translation of *Chaleur et Ind.* **18,** No. 201, 36 (1937).

J. J. SHEA, The melting of finite slabs. *J. Appl. Mech.* E **27,** No. 1, 16 (1960).

M. H. THEYS, Integral transport theory of thermal utilization factor of infinite slab geometry. *Nucl. Sci. Engng.* **7,** No. 1, 58 (1960).

N. B. VARGAFTIK and O. N. OLESHCHUK, Experimental investigation of the heat conduction of water. Translation of *Teploenergetika* **6,** No. 10, 70 (1959).

VACLAV VODICKA, Steady temperature field in a semi-infinite composite plate. *Appl. Sci. Res., Hague* A **9,** Nos. 2–3, 190 (1960).

J. E. WILKINS, JR., Conduction of heat in an insulated spherical shell with arbitrary spherically symmetric sources. *SIAM Rev.* **1,** No. 2, 149 (1959).

K. L. WRAY, thermal conductivity of clear fused silica at high temperature. *J. Appl. Phys.* **30,** No. 11, 1702 (1959).

L. S. ZAITSEVA, An experimental investigation of the heat conductivity of monatomic gases over wide temperature intervals. *J. Tech. Phys., Moscow*. Translation of the *Zh. Tekh. Fiz.* **4,** No. 4, 444 (1959).

V. S. ZARUBIN, One problem in nonstationary heat conduction. *J. Amer. Rocket Soc.* No. 10, 773 (1959). (Russian supplement.)

YA. P. ZINGERMAN, The thermal conductivity of an oxide cathode (Pro teploprovidnist' oksiydonoho katoda). RTS No .1030 (1959). Translation of *Ukraïn. Fiz. Zh.* **1,** No. 3, 308 (1956).

FLOW WITH SEPARATED REGIONS

J. ACKERET, *On Temperature Distribution Behind Cylinders in Flow*. NASA Tech. Translation TT–n F–2 (1959).

A. A. ANDREEVSKII, Heat transfer to a single pipe in a transverse flow of fluid with small Prandtl number. *Inzh. Fiz. Zh.* **2,** No. 10, 46 (1959).

M. H. BLOOM, Shroud tests of pressure and heat transfer over short afterbodies with separated wakes. *J. Aero. Space Sci.* **26,** No. 10, 626, 662 (1959).

PIERRE CALVET and GERARD DONNADIEU, Une methode de mesure des coefficients de convection dans un lit poreux. *C.R. Acad. Sci., Paris* **250,** 2324 (1960).

J. DON GRAY, *Boundary Layer Separation Effects on the Static Stability of a Flared-Tail Missile Configuration*. Arnold Engineering Development Center, Air Research and Development Command, Arnold Air Force Station, Tennessee, AEDC TN 60–103 (1960).

A. KLINKENBERG, Unsteady state heat transfer in stationary packed beds. *Chem. Engng. Sci.* **11,** No. 4, 260 (1960).

L. C. NAPOLITANO, On an exact solution of laminar mixing of two different gases. *J. Aero. Space Sci.* **27,** No. 2, 144 (1960).

H. H. PEARCEY, *The Occurrence and Development of Boundary-Layer Separations at High Incidences and High Speeds*. Aero. Res. Council (Gt. Brit.) (1960), ARC R & M 3109; supersedes ARC 17,901; ARC FM 2302; ARC Perf. 1387.

H. THOMNN, Measurements of heat transfer and recovery temperature in regions of separated flow at a Mach number of 1·8. *Flygtekn. Forsoksaast. Medd.* **82** (1958). (In English.)

H. A. VREEDENBERG, Heat transfer between a fluidized bed and a vertical tube. *Chem. Engng. Sci.* **11,** No. 4, 274 (1960).

J. WADSWORTH, *The Experimental Examination of the Local Heat Transfer on the Surface of a Sphere When Subjected to Forced Convective Cooling*. Nat. Res. Council of Canada, Ottawa, Canada, Rept. No. MT–39 (1958).

SAKAE YAGI and DAIZO KUNII, Studies on heat transfer near wall surface in packed beds. *J. Amer. Inst. Chem. Engrs.* **6,** No. 1, 97 (1960).

O. V. YAKOVLEVSKIY (Moscow), On the thickness of the zone of turbulent mixing on the boundary between two currents of gas of different velocity and density (Otolschine zony turbulentnogo peremeshivaniya na granitse dvukh potokov gza raznoy skorosti i plotnosti). *Izv. Akad. Nauk SSSR, otdel. tekh. nauk* No. 10, 153 (1958).

VICTOR ZAKKAY, Heat transfer at a corner. *J. Aero. Space Sci.* **27,** No. 2, 157 (1960).

RAREFIED GASES

H. J. BOMELBURG, Heat loss from very thick heated wires in rarefied gases. *Phys. Fluids* **2,** No. 6, 717 (1959).

EDMOND BRUN, Considerations generale sur l'aerothermique des gaz rarefies. Reprint from *Rarefied Gas Dynamics* (volume and year not indicated), pp. 367–382. Pergamon Press. (Centre National de la Recherche Scientifique Laboratoire d'Aerothermique Publication No. 124.)

H. HOSHIZAKI, The effect of shick-generated vorticity, surface slip and temperature jump on stagnation-point heat-transfer rates. *J. Aero. Space Sci.* **27,** No. 2, 135 (1960).

LESTER LEES, *A Kinetic Theory Description of Rarefied Gas Flows*. Guggenheim Aeronautical Laboratory, California Institute of Technology, Memo. No. 51 (1959).

RONALD F. PROBSTEIN, Aerodynamics of rarefied gases. Reprint from *Rarefied Gas Dynamics*, pp. 258–275. Pergamon Press, London, Oxford, New York, Paris (1960).

RONALD F. PROBSTEIN, Continuum theory and rarefied hypersonic aerodynamics. Reprint from *Rarefied Gas Dynamics*, pp. 416–431. Pergamon Press, London, Oxford, New York, Paris (1960).

R. F. PROBSTEIN, Viscous aerodynamic characteristics in hypersonic rarefied gas flow. *J. Aero. Space Sci.* **27,** No. 3, 174 (1960).

S. A. SCHAAF, Recent progress in rarefied gas dynamics. *J. Amer. Rocket Soc.* **30,** No. 5, 443 (1960).

RUTH N. WELTMANN and PERRY W. KUHNS, *Heat Transfer to Cylinders in Crossflow in Hypersonic Rarefied Gas Streams*. NASA TN D–267 (1960).

Vol. 1 1960

MAGNETHYDRODYNAMICS

JOHN H. BOYNTON, Experimental study of an ablating sphere with hydromagnetic effect included. *J. Aero. Space Sci.* **27,** No. 4, 306 (1960).

WILLIAM B. BUSH, Compressible flat-plate boundary-layer flow with an applied magnetic field. *J. Aero. Space Sci.* **27,** 49 (1960).

S. CHANDRASEKHAR, The stability of non-dissipative Couette flow in hydromagnetics. *Proc. Nat. Acad. Sci., Wash.* **46,** No. 2, 253 (1960).

C. C. CHANG and T. S. LUNDGREN, Flow of an incompressible fluid in a hydromagnetic capacitor. *Phys. Fluids* **2,** No. 6, 627 (1959).

E. E. COVERT and K. KERNEY, *A Review of the Literature of Plasma Physics.* WADC TR 59–486, Mass. Inst. Technol., Naval Supersonic Lab. TR 373 (1959).

M. D. COWLEY, A magnetogasdynamic analogy. *J. Amer. Rocket Soc.* **30,** No. 3, 271 (1960).

P. J. DICKERMAN and V. J. RAELSON, *Investigation of the Effects of an Axial Magnetic Field on the Flow of an Ionized Gas.* Laboratories for Applied Sciences, The University of Chicago, LAS–QR–M175–3 (1960).

JAMES A. FAY, *Hall Effects in a Laminar Boundary Layer of the Hartmann Type.* AVCO Everett Research Laboratory, Everett, Mass., AFOSR TN 60–291, Research Report 81 (1959).

FRANK FISHMAN, *End Effects in Magnetohydrodynamic Channel Flow.* AVCO Everett Research Laboratory, AFBMD TN 59–5, Research Report 78 (1959).

S. GLOBE, Laminar steady-state magnetohydrodynamic flow in an annular channel. *Phys. Fluids* **2,** No. 4, 404 (1959).

MEREDITH C. GOURDINE, *On the Role of Viscosity and Conductivity in Magnetohydrodynamics.* Jet Propulsion Laboratory, California Institute of Technology, Pasadena, Calif., Tech. Report No. 32–3 (1960).

MEREDITH C. GOURDINE, *Power Generation by Means of the "Electric Wind".* Jet Propulsion Laboratory, Calif. Institute of Technology, Pasadena, Calif., Tech. Report No. 72–6 (1960).

A. S. GUPTA, Flow of an electrically conducted fluid past a porous flat plate in the presence of a transverse magnetic field. *Z. angew. Math. Phys.* **11,** No. 1, 43 (1960).

J. L. KERREBROCK, Similar solutions for boundary layers in constant-temperature magnetogasdynamic channel flow. *J. Aero. Space Sci.* **27,** No. 2, 156 (1960).

M. N. KOGAN, On highly thermoconductive flows. *Dokl. Akad. Nauk SSSR* **120,** No. 3, 488 (1959).

J. E. MCCUNE and W. R. SEARS, On magnetohydrodynamic channel flow. *J. Aero. Space Sci.* **27,** No. 2, 139 (1960).

J. E. MCCUNE and W. R. SEARS, On the concepts of moving electric and magnetic fields in magnetohydrodynamics. *J. Aero. Space Sci.* **26,** No. 10, 674 (1959). (Readers' Forum.)

R. X. MEYER, Magnetohydrodynamics and aerodynamic heating. *J. Amer. Rocket Soc.* **29,** No. 3, 187 (1959).

HAKURO OGUCHI, *The Blunt Body Viscous Layer Problem With and Without an Applied Magnetic Field.* Division of Engng., Brown University, Providence, R.I., WADD TN 60–57 (1960).

VERNON J. ROSSOW, *Boundary-Layer Stability Diagrams for Electrically Conducting Fluids in the Presence of a Magnetic Field.* NASA TR R–37; supersedes NACA TN 4282 (1959).

V. J. ROSSOW, *On Series Expansions in Magnetic Reynolds Number.* NASA TN D–10 (1959).

SHENG WU CHING, *On the Energy Equation in Magnetogasdynamics.* Jet Propulsion Laboratory, Calif. Institute of Technology, Tech. Report 32–2 (1960).

J. A. SHERCLIFF, Magnetogasdynamics and its possible aeronautical applications. *J. Roy. Aero. Soc.* **63,** No. 585, 518 (Discussion), 528 (1959).

S. I. SYROVATSKIY, Magnetohydrodynamics. Translation of *Usp. Fiz. Nauk SSSR* **62,** No. 3, 247 (1957).

C. S. WU and W. D. HAYES, *Axisymmetric Stagnant Flow of a Viscous and Electrically Conducting Fluid near the Blunt Nose of a Spinning Body with Presence of Magnetic Field—I. Exact Solution of Incompressible and Constant Properties Model.* AFOSR TN 58–405; Princeton University, Dept. of Aero. Engng., Report 431; ASTIA AD 159 208 (1958).

C. S. Wu, *Axisymmetric Stagnant Flow of a Viscous and Electrically Conducting Fluid Near the Blunt Nose of a Spinning Body with Presence of Magnetic Viscous Layer and Small Magnetic Reynolds Number*. AFOSR TN 58–711; Princeton University, Dept. Aero. Engng., Report 431; ASTIA AD 162 246 (1958).

Ching-Sheng Wu, *On the Energy Equation in Magnetogasdynamics*. Jet Propulsion Laboratory, California Institute of Technology, Pasadena, Calif., Tech Report No. 32–2 (1960).

R. W. Ziemer, Experimental investigation in magneto-aerodynamics. *J. Amer. Rocket Soc.* **29,** No. 9, 642 (1959).

MEASUREMENT TECHNIQUES

W. G. Agnew, *End-Gas Temperature Measurement by a Two-Wave Length Infrared Radiation Method*. Society of Automotive Engineers, New York, Preprint 201D (1960).

Richard J. Allen, Surface insulation for cryogenic fluids. *Rev. Sci. Instrum.* **31,** No. 2, 203 (1960).

R. M. Atkins, Temperature measurement with thermistors. *Instrum. & Control Syst.* **33,** No. 1, 86 (1960).

A. S. Balchan and H. G. Drickamer, High pressure high temperature optical device. *Rev. Sci. Instrum.* **31,** No. 5, 511 (1960).

D. L. Burk, The ratio pyrometer. *Instrum. & Control Syst.* **33,** No. 1, 64 (1960).

J. G. Burns, W. H. Childs, A. A. Nicol and M. A. S. Ross, Development and use of a vane device for boundary-layer measurements. *Appl. Mech. Rev.* **13,** No. 5, 354 (1960). (No. 2407.)

M. C. Burrows, S. Shimizu, P. S. Myers and O. A. Uyehara, *The Measurement of Unburned-Gas Temperatures in an Engine by an Infrared Radiation Pyrometer*. Society of Automotive Engineers, New York, Preprint 201E (1960).

K. A. Chykayev, The thermodynamic method of determining the average mass temperature in gas streams (Termodinamicheskiy metod opredeleniya srednemassovoy temperatury v gazovykh potokakh). *Izmeritel'naya Tekh.* No. 5, 37 (1958).

Joseph D. Clem, Jr., Development of a special thermocouple for measuring transient temperatures. *Rev. Sci. Instrum.* **31,** No. 3, 334 (1960).

P. L. Clemens and R. L. Ledford, *A Transistorized Galvanometer Current Limiter*. Arnold Engineering Development Center, Air Research and Development Command, USAF, AEDC TN 59–110 (1959). (For additional copies write ASTIA (TISVV), Arlington Hall Station, Arlington 12, Virginia.)

Julius Cohen, Resistance-heated high vacuum furnace for temperature to 1400°C. *Rev. Sci. Instrum.* **31,** No. 3, 267 (1960).

The convection chamber—a new instrument for the observation of charged particle tracks. *Pribory i Tekh. Eksp.* No. 4, 49 (1959).

S. Corrsin, *Directional Sensitivity for a Finite Hot-Wire Anemometer*. Mech. Engng. Dept. the John Hopkins University (undated): AFOSR TN 60–171.

S. G. Datar, *Temperature Response of a Hot-Wire Anemometer to Shock and Rarefaction Waves*. Toronto University, Institute of Aerophysics; UTIA TN No. 28. (1959); TL 570 T64.84t Vis.

I. G. Donaldson, Temperature errors introduced by temperature measuring probes. *Brit. J. Appl. Phys.* **10,** No. 6, 252 (1959).

A. J. Dyer, Heat transport anemometer of high stability. *J. Sci. Instrum.* **37,** No. 5, 166 (1960).

R. L. Eisner, Apparatus for accurate measurement of thermoelectric power. *Rev. Sci. Instrum.* **31,** No. 4, 462 (1960).

J. Ergalant, The measuring of temperatures. *Chaleur & Ind.* No. 410, 263 (1959).

Hans Friedlingsdorf, Messung der Temperaturleitzahl Thermoplastischer Kunststoffe im Berich von 20 bis 200°C. *Chem.-Ing.-Tech.* **32,** No. 4, 291 (1960).

K. M. Greenland, Resistance thermometry. *Control* **3,** No. 20, 113 (1960).

S. P. Gvozdov (Deceased) and A. A. Yerunova, Chemical temperature indicators (Khimicheskiye indikatory temperatury). *Izv. vysshikh Uchebnykh Zavedeniy, khim. i khimich. Tekh.* No. 5, 154 (1958).

Nathaniel E. Hager, Jr., Thin-heater thermal conductivity apparatus. *Rev. Sci. Instrum.* **31,** No. 2, 177 (1960).

T. C. Harman, J. H. Cahn and M. J. Logan,

Vol. 1 1960

Measurement of thermal conductivity by utilization of the Peltier effect. *J. Appl. Phys.* **30,** 9, 1351 (1959).

WALTER HUNSINGER, La mesure des temperatures avec les thermoelements—II. L'influence de la temperature de comparison et la facon d'en tenir compte. Translation in French of *Arch. Messen* **267,** 77 (1958).

D. S. JOHNSON, Velocity and temperature fluctuation measurements in a turbulent boundary layer. *J. Appl. Mech.* E **81,** No. 3, 325 (1959).

M. A. KAGANOV, A theoretical analysis of the method of measuring thermal conductivity of semiconductors proposed by A. V. Loffe and A. F. Loffe. *J. Tech. Phys., Moscow* **3,** No. 11, 2169 (1959).

A. B. KAUFMAN, How accurate are your temperature transducer calibrations? *Instrum. & Control Syst.* **32,** No. 11, 1682 (1959).

A. B. KAUFMAN, Using thermocouples with non-standard reference temperature. *Instrum. & Control Syst.* **33,** No. 1, 106 (1960).

D. KELLY, Thermocouple temperature measurement without special instruments. *Instrum. & Control Syst.* **33,** No. 1, 76 (1960).

M. K. KINGERY, *Preliminary Development of Telemetry for Aeroballistic Ranges.* Arnold Engineering Development Center, Air Research and Development Command USAF, AEDC TN 59–7, ASTIA Document No. AD–208692 (1959).

Y. KOBASHI, N. KONO and T. NISHI, Improvements of a pressure pickup for the measurements of turbulence characteristics. *J. Aero. Space Sci.* **27,** No. 2, 149 (1960).

YE. A. KOLENKO and V. G. YUR'YEV, A hygrometer with thermoelectric cooling. *Pribory i Tekh. Eksp.* No. 4, 137 (1959).

N. D. KOSOV and O. V. RIVIN (Alma-Ata), Determination of the heat amount by the method of heat-current measurement (Opredeleniye kolichestv tepla metodom izmereniya teplovogo potoka). *Zh. Fiz. Khim.* **33,** No. 1, 83 (1959).

ROY C. KURTZROCK, Quick connector for multipoint thermocouple assemblies. *Rev. Sci. Instrum.* **31,** No. 4, 457 (1960).

A. V. LOFFE and A. F. LOFFE, Measurement of the thermal conductivity of semiconductors in the vicinity of room temperatures. *J. Tech. Phys., Moscow* **3,** No. 11, 2163 (1959).

Low-temperature characteristics of chromel–alumel thermocouples. *Instrum. & Control Syst.* **33,** No. 1, 90 (1960).

G. C. LOWENTHAL and A. F. A. HARPER, Resistance–temperature relationship of platinum at low temperatures and its influence on precision thermometry. *Brit. J. Appl. Phys.* **11,** No. 5, 205 (1960).

J. H. MCGUIRE and H. WRAIGHT, Radiometer for field use. *J. Sci. Instrum.* **37,** No. 4, 128 (1960).

J. G. MCTIGUE, J. D. OVERTON and G. PETTY, JR., *Two Techniques for Detecting Boundary-Layer Transition in Flight at Supersonic Speeds and at Altitudes above* 20,000 *Feet.* NASA TN D–18 (1959).

M. P. MADAN, Simple bridge method for measurement of thermal conductivity of gases and gas mixtures. *J. Franklin Inst.* **263,** No. 3, 207 (1957).

P. V. MARONE, Thin-film–thermometer measurements in partially ionized shock-tube flows. *Phys. Fluids* **2,** No. 6, 719 (1959).

D. MEKSYN, Plate thermometer. *Z. angew. Math. Phys.* **11,** 1, 63 (1960).

W. K. MOEN, Surface temperature measurement. *Instrum. & Control Syst.* **33,** No. 1, 70 (1960).

V. D. NIKIFOROV, Checking thermoelements and pyrometric equipment (O poverkakh termopar i pirometricheskikh priborov). *Izmeritel'naya Tekh.* No. 5, 43 (1958).

M. P. ORLOVA, How to attain the boiling temperature of oxygen. *Izmeritel'naya Tekh.* No. 5, 23 (1959).

V. M. PETROV, Recording of thermal conditions in calorimeters by means of photo-compensation amplifier. *Pribory i Tekh. Eksp.* No. 4, 143 (1959).

H. D. SCHULZ-METHKE, New means for brightness measurement. Tranlation of *Metall* **12,** No. 6, 625 (1958).

V. G. SHAW, High temperature measurement. *Instrum. & Control Syst.* **33,** No. 1, 58 (1960).

W. W. SHORT and B. H. SAGE, Temperature measurements in a spherical field: transfer coefficients and corrections for thermocouples

in boundary flows. *J. Amer. Inst. Chem. Engrs.* **6,** No. 1, 163 (1960).

A. M. SHIROTA and B. K. MAL'TSEV, On a gold–platinum thermocouple. Translation of *Izmeritel'naya Tekh.* No. 8, 27 (1959).

D. B. SLEATOR and M. R. LEWIS, *A Direct Method of Measuring Density Behind Shock Waves.* Ballistic Research Laboratories, Aberdeen Proving Ground, Maryland, BRL Report No. 1087 (1959).

SHIZAN SOMA and TU. TAKEUCHI, A new type of thermal conductivity gas detector—I. *J. Phys. Soc., Japan* **15,** No. 2, 333 (1960).

H. M. STRONG and F. P. BUNDY, Flat panel vacuum thermal insulation (P-zero). *J. Appl. Phys.* 39 (1960).

JAY W. STUART, JR., The pitot and static tubes–condensed sources of general fundamentals and applications. *J. Aero. Space Sci.* **27,** No. 2, 136 (1960).

H. E. STUBBS, High speed bolometer. *Rev. Sci. Instrum.* **31,** No. 2, 115 (1960).

L. H. TANNER, *The Design and Use of Interferometers in Aerodynamics.* Aero. Res. Council (Gt. Brit.) (1959).

B. W. TAYLOR, *Development of a Thin Film Heat-Transfer Gauge for Shock-Tube Flows.* Toronto University, Inst. of Aerophysics, UTIA TN No. 27 (1959).

H. A. VODDEN, Simple method of temperature control. *J. Sci. Instrum.* **37,** No. 2, 69 (1960).

W. B. WILSON, Device for ultra-high-pressure high temperature research. *Rev. Sci. Instrum.* **31,** No. 3, 331 (1960).

C. T. ZAHN, Dewar system for low temperature experiments. *Rev. Sci. Instrum.* **31,** No. 3, 328 (1960).

NATURAL CONVECTION

R. C. L. BOSWORTH, Attempts to measure the inductive element associated with the natural convection of heat. *Aust. J. Phys.* **13,** No. 1, 84 (1960).

R. C. L. BOSWORTH and C. M. GRODEN, Thermal transients associated with natural convection. *Aust. J. Phys.* **13,** No. 1, 73 (1960).

WILLIS BRAUN, SIMON OSTRACH and JOHN E. HEIGHWAY, *Free-Convection Similarity Flows about Two-Dimensional and Axisymmetric Bodies with Closed Lower Ends.* Lewis Research Center, NASA, Cleveland, Ohio, E–817. (Prepared for *Int. J. Heat & Mass Transfer.*)

N. L. BYZOVA, On the theory of self-excited oscillations in a thermal convection flow (K teorii samovozbuzhadayushchikhsya kolebaniy potoka teplovoy konvektsii). *Trudy Morskogo Gidrofiz. Inst. Akad. Nauk SSSR* **6,** 80 (1955).

I. N. DANILOVA (Moscow). The temperature distribution in an infinite hollow cylinder with heat exchange at the boundaries with media at variable and constant temperature (Raspredele niye temperatury v neogranichennom polom tsilindre pri teploobmene na granitsakh so sredami peremennoy i postoyannoy temperatury). *Izv. Akad. Nauk, otdel. tekh. nauk* No. 2, 148 (1958).

M. M. FARZETDINOV, On the uniqueness of the solutions of the equation of weak convection in the steady state. *Prikl. Mat. i Mekh.* **22,** No. 2, 393 (1958).

J. D. GRIFFITH and R. H. SABERSKY, Convection in a fluid at supercritical pressures. *J. Amer. Rocket Soc.* **30,** No. 3 (1960).

J. P. HOLMAN, H. E. GARTRELL and E. E. SOEHNGEN, *A Study of Free Convection Boundary Layer Oscillations and Their Effects on Heat Transfer.* The American Society of Mechanical Engineers, New York, Paper No. 60–SA–25 (1960).

V. T. KHOZIANINOV, Heat transfer between the normal and superfluid phases of liquid helium. *J. Tech. Phys., Moscow* **3,** No. 6, 1219 (1958).

L. I. KOMAROVA, The role of natural convection in the kinetics of the dissolution of benzoic acid in sodium hydroxide solution (Rol' yestestvennoy konvektsii v kinetike rastvoreniya benzoynoy kisloty v rastvore yedkoga natra). *Zh. Fiz. Khim.* **32,** No. 12, 2748 (1958).

A. N. KOZLOVA, Temperature distribution inside an inclined tube filled with air in the presence of free convection. *J. Tech. Phys., Moscow* **4,** No. 3, 285 (1959). Translation of *Zh. Tekh. Fiz.* **29,** No. 3, 319 (1959).

L. I. KUDRYASHEV and A. YA. IPATENKO, Effect of free motion on the heat transfer coefficient for flow around a sphere in the region of

Vol. 1 1960

small Reynolds numbers. *J. Tech. Phys., Moscow* **4,** No. 3, 275 (1959). Translation of *Zh. Tekh. Fiz.* **29,** No. 3, 309 (1959).

A. B. METZNER and W. L. FRIEND, Theoretical analogies between heat, mass and momentum transfer and modifications for fluids of high Prandtl or Schmidt numbers. *Canad. J. Chem. Engng.* **36,** No. 6, 235 (1958).

Y. NAKAGAWA, Theoretical and experimental study of heat transfer by cellular convection in the presence of impressed magnetic field. *Proceedings of the Sixth Midwestern Conference on Fluid Mechanics, Austin* 1959, pp. 417–426, Austin University Press (1959).

L. V. MESINA, Influence of temperature stratification on heat exchange in water. Translation of *Glavnaya Geofiz Icheskaya., Observ. Atoriya, Leningrad. Trudy* **59,** No. 121, 37 (1956).

S. P. PUSTOVOYT (Perm'), On the nonsteady heat convection in a spherical cavity (O nestatsionarnoy teplovoy konvektsii v sfericheskoy polosti). *Prikl. Mat. i Mekh.* **22,** No. 4, 568 (1958).

V. B. SHEIN, Experimental investigation of concentration–convection processes in vertical or slightly inclined circular tubes. *J. Tech. Phys., Moscow* **4,** No. 9, 1060 (1960).

K. P. SINGH and H. A. HAVEMANN, Heat transport by liquids enclosed in vertical tubes. *Proceedings of the Second Congress Theor. Appl. Mech., New Delhi* pp. 221–236. Indian Society Theor. Appl. Mech., Kharagpur (1956).

K. P. SINGH and H. A. HAVEMANN, Transport of heat by convection and boiling in liquids enclosed in vertical tubes. *Proceedings of the Third Congress Theor. Appl. Mech. Bagalore* pp. 277–292. Indian Soc. Theor. Appl. Mech., Kharagpur (1957).

ARTHUR L. SPROTT, JACK P. HOLMAN and FREDERICK L. DURAND, *An Experimental Study of the Interaction of Strong Sound Fields with Free Convection Boundary Layers.* Wright Air Development Center, Air Research and Development Command, U.S. Air Force, Wright-Patterson Air Force Base, Ohio, WADC TR 59–717 (1959).

J. VAN DER BURGH, Thermal convection at a melting benzene. *Appl. Sci. Res., Hague* A **9,** No. 4, 293 (1960).

E. I. YANTOVSKII, An estimate of the influence of free convection upon turbulent flow. *J. Tech. Phys., Moscow* **4,** No. 2, 1280 (1960).

PROPERTIES

Additive improves UO_2 thermal conductivity. *Nucleonics* **17,** No. 11, 156 (1959).

E. BAUER, Transport coefficients of air to 8000K. *J. Amer. Rocket Soc.* **29,** No. 10, Part I, 721 (1959).

A. F. BEGUNKOVA, Use of the generalized theory of regular thermal conditions for extrapolation of temperature during thermal-physical experiments (Primeneniye obobschennoy teorii regulyarnogo teplovogo rezhim dlya ekstrapolyatsii temperatur pri teplofizicheskikh eksperimentakh). *Teploenergetika* 75 (1959).

J. A. BIRCH, W. R. G. KEMP, P. G. KLEMENS and R. J. TAINSH, The lattice thermal conductivity of some gold alloys. *Aust. J. Phys.* **12,** No. 4, 455 (1959).

RICHARD S. BROKAW, Thermal conductivity of gas mixtures in chemical equilibrium—II. (Proposed Paper for the *J. Chem. Phys.*)

G. F. BUTENKO and M. I. RADCHENKO, The calculation of the thermal conductivity of molten metals (O raschete teploprovodnosti rasplavlennykh metallov). *Atomnaia Energiia* **6,** No. 2, 205 (1959).

KENNETH P. COFFIN, Effect of argon and helium on the thermal conductivity of the $N_2O_4 \rightleftarrows 2NO_2$ system. Reprint from the *J. Chem. Phys.* **31,** No. 5, 1290 (1959).

F. C. EVERSTEIN, The viscosity of liquids as a function of temperature. *Chem. Engng. Sci.* **11,** No. 4, 267 (1960).

KENNETH P. COFFIN and CLEVELAND O'NEAL, JR., NASA TN 4209 (1958).

WAYNE D. ERICKSON and HELEN S. CREEKMORE, *A Study of Equilibrium Real-Gas Effects in Hypersonic Air Nozzles, Including Charts of Thermodynamic Properties for Equilibrium Air.* NASA TN D–231 (1960).

J. D. FLEMING, J. W. JOHNSON and H. V. GRUBB, Diffusivities by tracer techniques. *Chem. Engng. Progress* **56,** No. 3, 69 (1960).

WALLACE R. GAMBILL, How to estimate liquid densities. *Chem. Engng.* **66,** 193 (1959).

A. GOLDSMITH and T. E. WATERMAN, *Thermophysical Properties of Solid Materials*. WADC TR 58–476 (1959).

MARTIN GRABAU, *A Method of Forming Continuous Empirical Equations for the Thermodynamic Properties of Air From Ambient Temperatures to* 15,000°*K with Applications*. Arnold Engineering Development Center, Air Research and Development Command, USAF (1959). AEDC–TN–59–102, ASTIA (TISVV).

H. R. HASSE and W. R. COOK, *The Determination of Molecular Forces from the Viscosity of a Gas* pp. 196–221. Verifaxed.

FREDERICK C. HAUSEN, RICHARD A. EARLY, FREDERICK E. ALLZOFON and FRED C. WITTEBORN, *Theoretical and Experimental Including Effects of Oxygen Dissociation*. U.S. Nat. Aero. and Space Ad., Tech. Report NASA TR R–27 (1959).

R. A. HORD, *Approximate Composition and Thermodynamic Properties of Nonionized Nitrogen–Oxygen Mixtures*. NASA TN D–2 (1959).

J. KESTIN and W. LEIDENFROST, An absolute determination of the viscosity of eleven gases over a range of pressures. *Physica* **25**, 1033 (1959).

J. KESTIN, On relative measurements of the viscosity of gases by the oscillating disks method. *Z. angew. Math. Mech.* **10**, 6, 558 (1959).

CHARLES R. KING, *Compilation of Thermodynamic Properties, Transport Properties, and Theoretical Rocket Performances of Gaseous Hydrogen*. NASA TN D–275 (1960).

J. D. MCCLELLAND, Thermal conductivity of magnesia from 1030° to 1880°C. *J. Amer. Ceram. Soc.* **43**, No. 1, 54 (1960).

D. B. MANN, Thermodynamic properties of helium at low temperatures and high pressures. *J. Heat Transfer* C **81**, No. 4, 323 (1959).

E. A. MASON, Transport properties of high-temperature multi component gas collision integrals for the exponential repulsive potential. *Phys. Fluids* **2**, No. 6, 688 (1959).

V. A. MEDVEDEV, V. V. KOROBOV and V. F. BAYBUZ (Moscow), Investigation of the thermodynamic properties of substances according to the method of the explosion in a spherical bomb—II. Hydroxyl (Issledovaniye termodinamiches-kikh svoystv veshchestv meodom vzryva v sfericheskoy bombe—II. Gidroksil). *Zh. Fiz. Khim.* **33**, No. 1, 58 (1959).

L. MONCHICK, Collision integrals for the exponential repulsive potential. *Phys. Fluids* **2**, No. 6, 695 (1959).

L. MOWER, Conductivity of a warm plasma. *Phys. Rev.* **116**, No. 1, 2nd ser., 16 (1959).

N. A. NIKOL'SKIY (Candidate of Technical Sciences), N. A. KALAKUTSKAYA (Candidate of Technical Sciences), I. M. PCHELKIN (Engineer), T. V. KLASSEN (Engineer) and V. A. VEL'TISHCHEVA (Engineer), The thermal physical properties of molten metals (Teplofizicheskiye svoystva rasplavlennykh metallov). *Teploenergetika* No. 2, 92 (1959).

R. E. PATTLE, Diffusion from an instantaneous point source with a concentration-dependent coefficient. *Quart. J. Mech. Appl. Math.* **12**, Part 4, 407 (1959).

K. F. ROGERS, *Some Thermal Properties of Durestos Type Materials*—II. Roy. Aircraft Est. (Gt. Brit.) (1959), RAE TN Chem. 1358. (Ask for N-81737.)

S. C. SAXENA and E. A. MASON, Diffusion coefficients of gases from the rate of approach to the steady state in thermal diffusion. *Mol. Phys.* **2**, No. 3, 264 (1959).

SINCLAIRE M. SCALA and CHARLES W. BAULKNIGHT, Transport and thermodynamic properties in a hypersonic laminar boundary layer—2. Applications. *J. Amer. Rocket Soc.* **30**, No. 4, 329 (1960).

WILLIAM SCHOTTE, Thermal conductivity of packed beds. *J. Amer. Inst. Chem. Engrs.* **6**, No. 1, 63 (1960).

D. B. SPALDING, Conserved property diagrams for rate process calculations—II. *Chem. Engng. Sci.* **11**, No. 4, 225 (1960).

A. N. SPENCER, Viscosity and thermal conductivity of liquid boron trifluoride. *Brit. J. Appl. Phys.* **11**, No. 2, 60 (1960).

B. N. SRIVASTAVA and R. C. SRIVASTAVA, Thermal conductivity and Eucken correction for diatomic gases and binary gas mixtures. *Appl. Mech. Rev.* **13**, No. 3 (1960).

D. E. STOGRYN and J. O. HIRSCHFELDER, *The Initial Pressure Dependence of Thermal Conductivity and Viscosity*. University of Wisconsin,

Vol. 1 1960

Naval Research Lab., Dept. of Chemistry, WISONR–36 (1959).

E. V. STUPOCHENKO, I. P. STAKHANOV, E. V. SAMUILOV, A. S. PLESHANOV and I. B. ROZHDESTVENSKII, Thermodynamic properties of air in the temperature interval from 1000 to 12,000 K and the pressure intervals from 0·001 to 1000 atm. *J. Amer. Rocket Soc.* **30,** 98 (1960).

Thermal Insulation Group Formed. NIMA (1960).

Thermal Conductivity of Silicon Carbide Powder. U.S. Atomic Energy Commission APEX–516 (1959).

K. L. WRAY, Thermal conductivity of clear fused silica at high temperatures. *J. Appl. Phys.* **30,** No. 11, 1702 (1959).

R. G. VINES, Measurement of the thermal conductivities of gases at high temperatures. *J. Heat Transfer* C **82,** No. 1, 48 (1960).

TRANSFER MECHANISMS

STANLEY CORRSIN, Outline of some topics in homogeneous turbulent flow. Reprint from *J. Geophys. Res.* **64,** No. 12, 2134 (1959).

S. R. M. ELLIS and B. GAY, The parallel flow of two fluid streams: Interfacial shear and fluid interaction. *Trans. Inst. Chem. Engrs.* **37,** No. 4, 206 (1959).

S. FELDMAN, On the instability theory of the melted surface of an ablating body when entering the atmosphere. *J. Fluid Mech.* **6,** 1, 131 (1959).

A. W. GOLDSTEIN, *Stability of Horizontal Fluid Layer with Unsteady Heating From Below and Time-Dependent Body Force.* NASA TR NR–4 (1959).

HENRY GORTLER, Einige neuere Ergebnisse zur Hydrodynamischen Stabilitatstheorie. *Z. Flugwiss.* **8,** No. 1, 1 (1960).

DAVID T. HARRJE and E. J. CROKE (Prepared by), *Heat Transfer in Oscillating Flow.* Princeton University, Dept. of Aero. Engng., Princeton, New Jersey, Aeronautical Engineering Report No. 483 (1959).

A. L. KISTLER, Fluctuation measurements in supersonic turbulent boundary layer. *Phys. Fluids* **2,** No. 3, 290 (1959).

LESLIE S. G. KOVASZNAY, *Plasma Turbulence.* Physical Research Lab., Space Tech. Lab., Los Angeles, Calif. (1960); STL/TR–60–0000–AE038.

BERNARD M. LEADON and ROY E. BARTLE, Pitot-probe measurement of local skin-friction reduction due to transpiration in a low-speed turbulent boundary layer. *J. Aero. Space Sci.* **27,** No. 3, 235 (1960).

J. C. MCMULLEN, *Boundary Layer Transition on the NOL Standard Cone in the Ballistic Research Laboratories' Supersonic Wind Tunnels (U).* BRL TN No. 1303 (1960).

J. MENKES, *On the Stability of a Heterogeneous Shear Layer Subject to a Body Force.* Jet Propulsion Lab., Calif. Institute of Tech., Pasadena, Calif., Tech Report No. 32–12 (1960).

WILLIAM R. MICKELSEN, Measurements of the effect of molecular diffusivity in turbulent diffusion. *J. Fluid Mech.* **7,** Part 3, 397 (1960).

SIMON OSTRACH and STEPHEN H. MASLEN, NASA Lewis Research Center, Cleveland, Ohio. E–957 (undated). (Prepared for *J. Fluid Mech.*)

J. LEITH POTTER, JACK D. WHITFIELD and WM. T. STRIKE, *Transition Measurements and the Correlation of Transition Sensitive Data.* Arnold Engineering Development Center, Air Research and Development Command, USAF, AEDC TR 59–4. ASTIA Document co. AD–208775 (1959); ASTIA (TISVV).

ELI RESHOTKO, *Stability of the Compressible Laminar Boundary Layer.* Guggenheim Aeronautical Laboratory, Calif. Institute of Technology, Memo. No. 52. (1960).

F. M. RICHARDSON, Patterns in turbulent flow in the wall-adjacent region. *Phys. Fluids* **2,** No. 6, 718 (1959).

N. W. RYAN and M. M. JOHNSON, Transition from laminar to turbulent flow in pipes. *J. Amer. Inst. Chem. Engrs.* **5,** No. 4, 433 (1959).

TRANSPIRATION AND MASS TRANSFER COOLING

M. C. ADAMS, Recent advances in ablation. *J. Amer. Rocket Soc.* **29,** No. 9, 625 (1959).

H. A. BETHE and M. C. ADAMS, A theory for the ablation of glassy materials. *J. Aero. Space Sci.* **26,** No. 6, 321 (1959).

PAUL M. CHUNG and AEMER D. ANDERSON, *Dissociative Relaxation of Oxygen over an Adiabatic Flat Plate at Hypersonic Mach Numbers*. NASA TN D–140 (1960).

PAUL M. CHUNG and AEMER D. ANDERSON, Surface recombination in the frozen compressible flow of a dissociated diatomic gas past a catalytic flat plate. *J. Amer. Rocket Soc.* **30,** No. 3, 262 (1960).

JAN DLOUGHY and W. H. GAUVIN, Heat and mass transfer in spray drying. *J. Amer. Inst. Chem. Engrs.* **6,** No. 1, 29 (1960).

R. G. FLEDDERMANN and HURWICZ, *Transient Ablation and Heat-Conduction Phenomena at a Vaporizing Surface*. Air Force Ballistic Missile Div., Air Research and Development Command, USAF, Inglewood, Calif. (1960).

S. K. FRIEDLANDER, Rapid chemical reaction in a laminar boundary layer. *Appl. Sci. Res., Hague* **8,** No. 6, 403 (1959).

V. KOLAR, Contribution to the theory of mass and heat transfer in a turbulent medium. *Collection Czechoslov. Chem. Commun.* **24,** No. 12, 3811 (1959).

A. V. LYKOV, An investigation of heat and mass transfer in binary gas mixtures. *Inzh. Fiz. Zh.* **2,** No. 11, 20 (1959).

A. J. MADDEN and EDGAR L. PIRET, Evaporation rates of liquids to flowing gas streams. *J. Amer. Inst. Chem. Engrs.* **5,** No. 4, 413 (1959).

V. P. MOTULEVICH (Moscow), Calculation on heat transfer and friction of a flat plate in supersonic flow in the presence of pore gas and sublimation in the laminar boundary layer (Raschet teploobena i treniya ploskoy plastiny, obduvayemoy sverkhzvukovym potokom, pri nalichii poristogo podvoda gaza i sublimatsii v usloviyakh laminarnogo pogranichnoga sloya). *Izv. Akad. Nauk SSSR, otdel. tekh. nauk, energetika i avtomatika* No. 1, 33 (1959).

A. P. PRUDNIKOV (Moscow), Analytical study of processes of heat and mass exchange during convective drying (Analiticheskoye issledovaniye protesessov teplo—I. Massoobmena pri konvektivnoy sushke). *Izv. Akad. Nauk SSSR, otdel. tekh. nauk* No. 10, 63 (1958).

W. E. RANZ, Some experiments on the dynamics of liquid films. *J. Appl. Phys.* **30,** No. 12, 1950 (1959).

LEONARD ROBERTS, *An Analysis of Nose Ablation for Ballistic Vehicles*. NASA TN D–254 (1960).

LEONARD ROBERTS, *Mass Transfer Cooling Near the Stagnation Point*. NASA TR R–8; supersedes NACA TN 4391 (1959).

LEONARD ROBERTS, *A Theoretical Study of Stagnation-Point Ablation*. NASA TR R–9; supersedes NACA TN 4392 (1959).

T. K. SHERWOOD, Mass transfer to a turbulent fluid with and without chemical reaction. *Chem. Engng. Sci.* **11,** No. 2, 81 (1959).

D. B. SPALDING, Berechnung von Massenubertragungs-Geschwindigkeiten bei Gleichzeitiger Chemischer Reaktion und Warmeubertragung. *Chem.-Ing.-Tech.* **32,** No. 2, 91 (1960).

D. B. SPALDING, Theory of particle combustion at high pressures. *J. Amer. Rocket Soc.* **29,** No. 11, 828 (1959).

ROTATING

T. V. DAVIES, On the forced motion due to hearing of a deep rotating liquid in an annulus. *J. Fluid Mech.* **5,** No. 4, 593 (1959).

J. P. HARTNETT, Heat transfer from a nonisothermal disk. *J. Appl. Mech.* E **26,** No. 4, 672 (1959).

JACK P. HOLMAN and GEORGE D. MOORE, *An Experimental Study of Vortex Chamber Flow*. Wright Air Development Center, WADC TN 59–388 (1959).

R. P. KANWAL, Slow rotatory motion of a circular disk about one of its diameters in a viscous fluid. *J. Appl. Mech.* E **26,** No. 4, 485 (1959).

JOSEPH M. SAVINO and ROBERT G. RAGSDALE, *Some Temperature and Pressure Measurements in Confined Vortex Fields*. Lewis Research Center, NASA, Cleveland, Ohio, ASME Paper No. 60–SA–4.

S. N. SINGH, Heat transfer by laminar flow from a rotating sphere. *Appl. Sci. Res.* A **9,** No. 2–3, 197 (1960).

RADIATION

V. N. ADRIANOV (Moscow), Electrical analogues applied to solving radiative heat transfer problems (Primeneniye metoda elektroanalogii k resheniyu zadach luchistogo teploobmena). *Izv. Akad. Nauk SSSR, otdel. tekh. nauk, energetika i avtomatika.* No. 1, 20 (1959).

S. G. AGABABOV, Emissivity of boiler furnace

slags. Translation of *Teploenergetika* **5,** No. 8, 56 (1958).

ROGER A. ANDERSON and WILLIAM A. BROOKS, JR., Effectiveness of radiation as a structural cooling technique for hypersonic vehicles. *J. Aero. Space Sci.* **27,** 41 (1960).

J. G. BARTAS, Radiation fin effectiveness. *J. Heat Transfer* C **82,** No. 1, 73 (1960).

J. A. BASTIN, Use of an integrating sphere to distinguish between absorption and scattering in solids. *Brit. J. Appl. Phys.* **10,** No. 9, 412 (1959).

R. N. BAYLOR and F. C. SMITH, The redistribution of hypersonic thermal loads due to structural cross-radiation. *Proceedings of the Fourth Midwestern Conference on Solid. Mech., Austin, Texas,* 1959, pp. 298–317. Austin University Press (1959).

J. R. BEATTIE, Spectral emission of radiation by glass. *Brit. J. Appl. Phys.* **2,** No. 4, 151 (1960).

J. T. BEVANS, *Correlation of the Total Emissivity of Carbon Dioxide and Water Vapor.* Shell Development Company, A division of Shell Oil Co., Emeryville, Calif.

J. T. BEVANS, Radiant interchange within an enclosure. *J. Heat Transfer* C **82,** No. 1, 1 (1960).

J. H. CAIRNS, Apparatus for investigating total hemispherical emissivity. *J. Sci. Instrum.* **37,** No. 3, 84 (1960).

J. P. CALLINAN and W. P. BERGGREN, Some radiator design criteria for space vehicles. *Trans. Amer. Soc. Mech. Engrs.* C **81,** *J. Heat Transfer* 237 (1959).

R. L. CHAMBERS, Radiation fin efficiency for one-dimensional heat flow in a circular fin. *J. Heat Transfer* C **81,** No. 4, 327 (1959).

JIN H. CHIN and STUART W. CHURCHILL, Incorporation of error function absorption coefficient in transport equation. *Quart. Appl. Math.* **28,** No. 1, 93 (1960).

K. L. COULSON, Characteristics of the radiation emerging from the top of a Rayleigh atmosphere—I. *Planet. Space Sci.* **1,** No. 4, 265 (1959).

R. V. DUNKLE, Spectral characteristics of fabrics from 1 to 23 microns. *J. Heat Transfer* C **82,** No. 1, 64 (1960).

G. FARKAS and P. VARGA, Determination of the emissivity of a radiating cavity. *Magyar Fiz. Foly.* **7,** No. 1, 37 (1959). (In Hungarian.)

A. FEDOR, New charts provide quick way to radiant heat transfer. *Chem. Engng.* **66,** No. 2, 101.

G. M. GARIBYAN, Radiation of a charged particle traversing a layered medium. Translation of *Zh. Eksp. Teor. Fiz.* **35,** No. 6 (12), 1435 (1958).

J. D. S. GOULDEN, Infra-red spectroscopy of aqueous solutions. *Spectrochim. Acta* No. 8, 657 (1959).

B. A. GRIGOR'EV, Problems concerning the heating of an unbounded plate by an unsteady flow of radiative energy (in Russian). *Izv. Akad. Nauk SSSR, otdel. tekh. nauk,* No. 1, 86 (1958).

E. H. HUBBARD, Flame emissivity and radiation effects from adding carbon black to liquid fuels. *Combustion* **31,** No. 5, 34 (1959).

R. C. JORDAN, What future for solar heating? *ASHRAE J.* **2,** 74 (1960).

FRANK KREITH, *Radiation Heat Transfer and Thermal Control of Spacecraft.* Oklahoma Engineering Experiment Station, Oklahoma State University, Stillwater, Oklahoma, Publication No. 112 (1960).

SEYMOUR LIEBLEIN, *Analysis of Temperature Distribution and Radiant Heat Transfer along a Rectangular Fin of Constant Thickness.* U.S. Nat. Aeronautics and Space Administration Tech. Note 196 (1959).

R. C. LORD, Infrared emission spectra of ammonia-oxygen and hydrazine flames. *Spectrochim. Acta* No. 8, 605 (1959).

K. N. MATHUR, M. L. KHANNA, T. N. DAVEY and S. P. SURI, Domestic solar water heater. *J. Sci. Indust. Res., India* A **18,** No. 2, 51 (1959).

EDWIN N. NILSON and RICHARD CURRY, The minimum-weight straight fin triangular profile radiating to space. *J. Aero. Space Sci.* **27,** No. 2, 146 (1960).

V. A. PROKOF'YEV, Absorption and dispersion of weak forced waves of very small and very large frequency under the action of radiational heat transfer (Pogloshcheniye i dispersiya slabykh vynuzhdennykh voln ochen' maloy i ochen' bol'shoy pod vliyaniyem radiatsion-

nogo perenosa tepla). *Izv. Akad. Nauk, otdel. tekh. nauk* No. 12, 15 (1958).

J. C. RICHMOND, Spectral emittance of ceramic-coated and uncoated specimens of inconel and stainless steel. *J. Amer. Ceram. Soc.* **42,** No. 12, 633 (1959).

S. N. SHORIN, Radiant heat exchange in an absorbing medium. Translation of *Izv. Akad. Nauk SSSR, otdel. tekh. nauk* No. 3, 389 (1951).

H. TABOR, Radiation convection and conduction coefficients in solar collectors. *Bull. Res. Council, Israel* 6C, **3,** 155 (1958).

Transfer of Heat by Radiation. Radiant Heat Transfer of the Shock Layer and Measurement of Emission Factors of Metals. Presented at the eighth meeting of AGARD Structures and Materials Panel, Copenhagen, Denmark, 20–25 October 1958. AGARD Report 211, CN–80075 (1958).

W. R. WADE and F. W. CASEY, JR., *Measurements of Total Hemispherical Emissivity of Several Stably Oxidized Nickeltitanium Carbide Cemented Hard Metals from* 600°*F to* 1,600°*F.* NASA Memo. 5–13–59L (1959).

RODGER C. WEATHERSTON and WILLIAM E. SMITH, A method for heat rejection from space powerplants. *J. Amer. Rocket Soc.* **30,** No. 3, 268 (1960).

J. ERNEST WILKINS, JR., Minimizing the mass of thin radiating fins. *J. Aero. Space Sci.* **27,** No. 2, 145 (1960).

Vol. 1 1960

ol.
1
960